A FRAMEWORK FOR FORMALIZING SCIENCE BASED COMPOSITES MANUFACTURING PRACTICE

by

Janna Noemi Fabris

BE(Hons)/BCS, The University of Melbourne, 2004

A THESIS SUBMITTED IN PARTIAL FULFILLMENT OF

THE REQUIREMENTS FOR THE DEGREE OF

DOCTOR OF PHILOSOPHY

in

THE FACULTY OF GRADUATE AND POSTDOCTORAL STUDIES

(Materials Engineering)

THE UNIVERSITY OF BRITISH COLUMBIA

(Vancouver)

October 2018

The following individuals certify that they have read, and recommend to the Faculty of Graduate and Postdoctoral Studies for acceptance, the dissertation entitled:

A framework for formalizing science based composites manufacturing practice

submitted by Janna Fabris in partial fulfillment of the requirements for

the degree of Doctor of Philosophy

in Materials Engineering

Examining Committee:

Anoush Poursartip, Materials Engineering

Supervisor

Reza Vaziri, Civil Engineering

Supervisory Committee Member

Warren Poole, Materials Engineering

University Examiner

Scott Dunbar, Mining Engineering

University Examiner

Additional Supervisory Committee Members:

Elicia Maine, Beedie School of Business, Simon Fraser University

Supervisory Committee Member

Chad Sinclair, Materials Engineering

Supervisory Committee Member

Abstract

Advanced composites are materials growing in importance. In recent years, all major aerospace original equipment manufacturers (OEMs) have invested significantly in this technology, and its use in automotive, alternative energy and industrial applications is rapidly growing. Increases in product size and production scaling, given radically larger and more complex structures and the sheer volume of composites manufacturing, are leading to challenging problems concerning manufacturing risk, such as increasing development time frames and program costs.

The use of manufacturing science to address these problems has always been a rational and promising strategy with most research efforts focusing on automation to improve production efficiencies, the development of multiphysics based models exercised in manufacturing simulation software, and the promise of production 'big data' analytics given improvements in sensor technologies and machine based learning algorithms. However, it is no longer sufficient to keep adding to this science base without explicitly addressing how manufacturing practice should be changed.

In this thesis, qualitative research analysis of two industrial small and medium sized enterprises (SMEs) based in Western Canada is first performed to investigate the use of the composites manufacturing science base to manage technological and market uncertainty, and how the needs and receptor capabilities of OEMs and SMEs differ. Next, a manufacturing outcomes taxonomy explicitly linking the *science–technology–practice* levels of activity and a hierarchical knowledge model (Equipment–Tool–Part–Material factory ontology) that defines a common

nomenclature for organizing composites manufacturing domain knowledge are introduced. A series of high-level manufacturing scenarios are presented to demonstrate this developed framework. Finally, case studies based on the thermal analysis of thick thermoset composites data sets using manufacturing simulation are presented. These case studies represent a starting point for how science based approaches can be used to directly support manufacturing decisions at *all* stages of the development design cycle.

This work represents efforts to introduce a new translational research strategy aimed at both the composites manufacturing research community and the composites industry. Its focus is to encourage the systematic *use* of composites manufacturing science to transform manufacturing practice, and to support the effective management of increasing manufacturing risk.

Lay Summary

There is no doubt that advanced manufacturing enables highly sophisticated end products that underpin and transform our society – think Boeing 787 Dreamliner or BMW I3.

Traditionally, empirically based practices (‘know-how’) have been used to deal with increasing manufacturing risk. These practices rely strongly on engineering judgement, experience, methods of ‘trial and error’, and lack standardization. While the research community has mastered knowledge creation (‘know-why’) in key areas of automation, manufacturing simulation and the promise of production analytics, further progress is needed to position this knowledge so that it can be adopted more readily by industry to manage manufacturing risk effectively. This suggests that we should look carefully at how research is used in practice.

This research aims to establish a framework that encourages the systematic *use* of the composites manufacturing science base. The goal is to formalize knowledge use so that the composites industry can create value from manufacturing science.

Preface

This thesis presents research performed by Janna Fabris. This research was supervised by Dr. Anoush Poursartip at The University of British Columbia and co-supervised by supervisory committee member Dr. Elicia Maine at Simon Fraser University Beedie School of Business.

It should be noted that technical and other important terms used in this work are specified in the Glossary. Figure 1-2 is courtesy of the Composites Research Network (CRN).

The work presented in Chapter 3 was performed by Janna Fabris under the co-supervision of Dr. Anoush Poursartip and Dr. Elicia Maine. The outcomes taxonomy and case study analysis of an aerospace OEM presented in Sections 3.1.2 and 3.2.1 were developed under the supervision of Dr. Anoush Poursartip. The formulation of a research protocol, data collection, and qualitative analysis of the industrial composites SME case studies presented in Sections 3.2.2, 3.2.3 and 3.3 were performed under the supervision of Dr. Elicia Maine. This work was granted approval from Simon Fraser University Office of Research Ethics and harmonized with The University of British Columbia Behavioural Research Ethics Board (SFU ORE certificate: 2016s0142). Figure 3-3 is adapted from work performed by Dr. Christophe Mobuchon and Dr. Navid Zobeiry.

All framework concepts presented in Chapter 4 were developed by Janna Fabris under the supervision of Dr. Anoush Poursartip. Workflow examples presented in Section 4.1.2 were co-developed by Janna Fabris in collaboration with Dr. Christophe Mobuchon and Dr. Navid Zobeiry. The high-level case study presented in Section 4.3.4 was developed by Janna Fabris,

based on original work performed by Dr. Goran Fernlund and Dr. Christophe Mobuchon. Figure 4-4 and Figure 5-13 are adapted from work performed by Dr. Christophe Mobuchon and Dr. Navid Zobeiry.

All simulation modelling work and analysis for the thick composites laminate data sets presented in Chapter 5 and Appendix D was performed by Janna Fabris under the supervision of Dr. Anoush Poursartip. The experimental work for the Johnston and Hubert data set was performed by former PhD students, Dr. Andrew Johnston and Dr. Pascal Hubert. Figure 5-7, Figure 5-12 (b) and Figure D-1 are from Johnston (1997). The experimental work for the Kotlik and Shimizu data set was performed by former student, Mr. James Kotlik. The method for back-calculating effective heat transfer boundary conditions was originally developed by visiting researcher, Mr. Takayuki Shimizu, from Mitsubishi Heavy Industries Ltd. Figure D-9 is from Shimizu *et al* (2008). The experimental work for the Slesinger data set was performed by former MASc student, Mr. Nathan Slesinger. Figure D-21 is from Slesinger (2010). The experimental work for the CCMRD9.2 data set was provided by Mr. Alastair McKee, from Convergent Manufacturing Technologies Inc. (CMT Inc.), on behalf of The Canadian Composites Manufacturing R&D Inc. (CCMRD) Project 9.2. The release of data was granted by Mr. Gene Manchur, CCMRD. Figure 5-15 and Figure D-25 are courtesy of CCMRD. Figure D-30 is courtesy of CRN. Figure D-33 and Figure D-34 are courtesy of MASc student Mr. John Park. The experimental work for the Boeing-UW data set was performed by University of Washington MSE310 students supervised by Dr. Karl Nelson, from The Boeing Company. This data was provided by Dr. Karl Nelson. Figure D-35 (a) and Figure D-35 (c) are courtesy of Dr. Karl Nelson. Work performed by Dr. Navid Zobeiry is discussed in Section D.5.6.

The Hexcel 8552 NCAMP experimental work presented in Appendix E.2 was provided by Dr. Anthony Floyd, from CMT Inc., on behalf of the National Institute for Aviation Research (NIAR) based at Wichita State University. The release of this data was granted by Dr. John Tomblin, NIAR. The analysis of this data was performed by Janna Fabris under the supervision of Dr. Anoush Poursartip to establish a baseline for comparison to the preliminary Hexcel 8552-1 material characterization work presented in this thesis.

A manuscript based on sections of Chapter 3 has been published. **J. Fabris**, D. Roughley, A. Poursartip and E. Maine (2017) *Managing the Technological and Market Uncertainty of Composites Innovation: A Case Study of Composites Manufacturers in Western Canada and Interventions by a Translational Research Centre.* Translational Materials Research, 4 046001. Most parts of this manuscript were written by Janna Fabris, under the supervision of Dr. Elicia Maine and Dr. Anoush Poursartip.

A manuscript based on sections of Chapter 4 and Appendix D.4 has been published. **J. Fabris**, N. Zobeiry, J. Park and A. Poursartip (2018) *Effect of Tool Design on Thermal Management in Composites Processing*. SAMPE Journal, Vol. 54 (4). Parts of this manuscript were written by Janna Fabris, under the supervision of Dr. Anoush Poursartip.

A manuscript based on sections of Chapter 3 and Chapter 4 has been submitted for publication. **J. Fabris**, G. Fernlund and A. Poursartip (2018) *A Framework for Formalizing Science Based Composites Manufacturing Practice.* All parts of this manuscript were written by Janna Fabris, under the supervision of Dr. Anoush Poursartip.

Sections of Chapter 3 and Chapter 4 were presented in 10th Canada-Japan Workshop on Composites, Vancouver, Canada. A paper was published in the conference proceedings. **J. Fabris** and A. Poursartip (2014) *Knowledge in Practice: The Next step in Reducing Risk in Composites Manufacturing and Design.* All parts of this paper were written by Janna Fabris, under the supervision of Dr. Anoush Poursartip.

A version of Section 4.1.2 was presented in SAMPE Technical Conference, Baltimore, US. A paper was published in the conference proceedings. **J. Fabris**, C. Mobuchon, N. Zobeiry, D. Lussier, G. Fernlund and A. Poursartip (2015) *Introducing Thermal History Producibility Assessment at Conceptual Design.* All parts of this paper were written by Janna Fabris, under the supervision of Dr. Anoush Poursartip.

A version of Section 5.2 and Appendix D.1 was presented in SAMPE Technical Conference, Seattle, US. A paper was published in the conference proceedings. **J. Fabris**, D. Lussier, N. Zobeiry, C. Mobuchon, and A. Poursartip (2014) *Development of Standardized Approaches to Thermal Management in Composites Manufacturing.* Most parts of this paper were written by Janna Fabris, under the supervision of Dr. Anoush Poursartip.

A version of Section 5.3 and Appendix D.4 was presented in SAMPE Technical Conference, Long Beach, US. A paper was published in the conference proceedings. **J. Fabris**, C. Mobuchon, N. Zobeiry, and A. Poursartip (2016) *Understanding the Consequences of Tooling Design Choices on Thermal History in Composites Processing.* All parts of this paper were written by Janna Fabris, under the supervision of Dr. Anoush Poursartip.

A version of Section 5.3, Appendix D.2 and Appendix D.4 was presented in SAMPE Technical Conference, Seattle, US. A paper was published in the conference proceedings. **J. Fabris** and A. Poursartip (2017) *Using Process Modelling as a Job-aid to Reduce Composites Manufacturing Risk*. All parts of this paper were written by Janna Fabris, under the supervision of Dr. Anoush Poursartip.

Table of Contents

Abstract ..... **iii**

Lay Summary ..... **v**

Preface ..... **vi**

Table of Contents ..... **xi**

List of Tables ..... **xvii**

List of Figures ..... **xx**

List of Symbols ..... **xxxv**

List of Abbreviations ..... **xxxviii**

Glossary ..... **xlii**

Acknowledgements ..... **xlix**

Dedication ..... **xlxi**

Chapter 1: Introduction **1**

1.1 The Growth of Advanced Composites Materials 1

1.2 Challenges Facing the Composites Industry 3

1.3 Translational Research Efforts in Composites Manufacturing 6

1.4 Summary 11

Chapter 2: Literature Review and Research Objectives **13**

2.1 Innovation Management Theory for Science Based Innovations 14

2.1.1 Commercializing advanced materials technologies 14

2.1.2 Attributes of technological and market uncertainty 16

2.1.3 Strategies for accelerating the commercialization process 17

2.2 Development and Applications of Knowledge Systems 18

2.2.1 Conceptual frameworks 19

2.2.2 Domain applications 21

2.3 Trends in Composites Manufacturing Research for Thermal Management 22

2.3.1 Mastering the manufacturing science 22

2.3.1.1 Heat transfer models 26

2.3.1.2 Cure kinetics models 28

2.3.1.3 Boundary conditions 30

2.3.2 Harnessing manufacturing science in simulation 32

2.3.3 Studies representative of industrial processing conditions 36

2.4 Research Objectives and Scope of Thesis Work 40

2.4.1 Synthesis of literature 40

2.4.2 Research objectives and scope 41

Chapter 3: Managing Uncertainty in Composites Manufacturing 46

3.1 Current Practice 47

3.1.1 Manufacturing quality control and oversight 47

3.1.2 Manufacturing outcomes 50

3.1.2.1 Causal relationships 52

3.1.2.2 Sources and sinks 54

3.1.3 Current practice represents high risk 57

3.2 Creating Value from Science Based Practice 59

3.2.1 Case 1: Aerospace OEM 60

3.2.2 Case 2: Industrial SME #1 (Structural GFRP component manufacturer) 61

3.2.3 Case 3: Industrial SME #2 (High performance CFRP component manufacturer) . 65

3.3 Analysis 69

3.3.1 Technological uncertainty 70

3.3.2 Market uncertainty 72

3.3.3 Conclusions 75

3.4 Summary and Discussion 77

Chapter 4: Conceptual Theory Building and Framework Development 79

4.1 Formalizing Science Based Practice 79

4.1.1 Knowledge translation 80

4.1.1.1 Participants 81

4.1.1.2 Determinants 81

4.1.2 Transforming manufacturing practice 84

4.1.2.1 Protect 86

4.1.2.2 Advance 87

4.1.2.3 Disrupt 89

4.2 Equipment–Tool–Part–Material Factory Ontology 91

4.2.1 Concept definition 91

4.2.2 Attributes 92

4.2.3 Relations 95

4.2.4 Instances 96

4.2.5 Workflows 100

4.3 Case Studies 101

4.3.1 Case 1: Large composites part development involving a Tier 1 supplier 103

4.3.2 Case 2: Large composites part development with developmental autoclave..... 107

4.3.3 Case 3: Bid for a small composites part work package 109

4.3.4 Case 4: Process improvement for a high-volume composites part 111

4.3.5 Case 5: Capturing knowledge for reuse in future programs 114

4.4 Summary and Discussion 117

Chapter 5: Applications of Science Based Practice for Thermal Management.....120

5.1 Case 1: Managing Thermal Modelling Uncertainty 124

5.1.1 Heat transfer models 128

5.1.2 Cure kinetics models 131

5.1.3 Boundary conditions 134

5.1.4 Summary 137

5.2 Case 2: Cure Cycle Development and Evaluation 139

5.2.1 ETPM definition 141

5.2.2 Cure cycle development and evaluation 146

5.2.3 Experimental measurements 151

5.2.4 Summary 153

5.3 Case 3: Experimental Thermal Profile Validation 155

5.3.1 ETPM definition 157

5.3.2 Experimental measurements 160

5.3.3 Thermal profile validation 163

5.3.4 Summary 166

5.4 Summary and Discussion 167

Chapter 6: Summary and Future Work **169**

6.1 Summary 169

6.2 Contributions 175

6.3 Future Work 176

6.3.1 Developed framework 176

6.3.2 Thermal management data sets 178

References **181**

Appendices **197**

Appendix A Thermal Management Studies of Thick Thermoset Composites 197

A.1 Definition of thick composites 197

A.2 Summary of thick laminate studies reported in the scientific literature 199

Appendix B SME Qualitative Research Study Documentation 215

B.1 Research study interview questions 215

B.2 Informed consent form 216

Appendix C Proposed Thermal Management Knowledge in Practice Document Topics 219

C.1 Positioning science based knowledge 219

C.2 ETPM factory ontology scratchpad 228

Appendix D Thick Thermoset Composites Data Sets 229

D.1 Johnston and Hubert data set 230

D.2 Kotlik and Shimizu data set 239

D.3 Slesinger data set 256

D.4 CCMRD9.2 data set 261

D.5 Boeing-UW data set 277

Appendix E Material Properties and Material Database Input Parameters 297

E.1 Properties of Hexcel AS4/8552 unidirectional prepreg 297

E.2 Properties of Hexcel AS4/8552-1 unidirectional prepreg..... 299

E.3 Properties of Toray T800H/3900-2 unidirectional prepreg 312

E.4 Thermophysical material properties..... 315

Appendix F Effective Heat Transfer Coefficient Back-calculation Method 316

F.1 Closed-form solution with asymmetric boundary conditions 316

F.2 Equivalent-1D heat transfer boundary conditions 317

F.3 Equivalent-3D heat transfer boundary conditions (no tool substructure modelled) 320

List of Tables

Table 1-1: Comparison of typical value creation attributes for large and small composites manufacturers[a]. 5

Table 1-2: High-level assessment of the current science base for composites manufacturing processes. 8

Table 1-3: Examples of composites translational research centres (CTRCs) in North America and Europe. 10

Table 2-1: Thermal management examples highlighting trends in moving from knowledge creation to knowledge use in composites manufacturing[a]. Note: Manufacturing simulation is shown as an example of an enabling technology. 23

Table 2-2. The value of manufacturing simulation. Boeing 767-400ER wingtip front spar analysis shown as an example. Adapted from [126] (Hahn *et al*, 2001) and [183] (Floyd, 2017). 33

Table 2-3: Subset of studies identified in the scientific literature that are representative of industrial composites processing scenarios[a,b]. 39

Table 2-4: Scope of thesis work presented. 42

Table 3-1: Examples of studies in the scientific literature that use the 'sources and sinks' framework to describe trends in composites manufacturing outcomes. 55

Table 3-2: Attributes of technological uncertainty[a] experienced by SME #1 and SME #2. 72

Table 3-3: Attributes of market uncertainty, value creation and evolution/experimentation[a] experienced by SME #1 and SME#2. 74

Table 4-1: Workflow examples of current typical practice and future better practice. Note: Thermal management examples are shown. 89

Table 4-2: ETPM[a] factory ontology attribute nomenclature. Note: Classes are denoted in uppercase and angle brackets denote collections of classes or attributes. 94

Table 4-3: ETPM[a] factory ontology instance nomenclature and suggested design-gate index definitions. Thermal management examples are shown. Note: Instances are denoted in lowercase, shorthand notation is denoted in italics and angle brackets indicate collections of instances. 99

Table 5-1: Summary of the thick thermoset composites data sets analyzed..... 122

Table 5-2: Effective heat transfer coefficients for the thick thermoset composites data sets analyzed[a]. 123

Table 5-3: Identifcation and classification of modelling uncertainty and error for the thermal modelling of cure processes[a,b]. Adapted from [125] (Hahn *et al*, 2004). 126

Table 5-4: ETPM[a] attribute definition for a 28.2 mm thick panel with tapered core. 144

Table 5-5: Process requirements and acceptance criteria for a 28.2 mm thick panel with tapered core. Note: These requirements and criteria are shown as examples for the purposes of this case study. 146

Table 5-6: Overall summary of RAVEN-1D analyses for a 28.2 mm thick panel with tapered core. Note: Cure cycle acceptance criteria are summarized in Table 5-5. 148

Table 5-7: ETPM[a] attribute definition for a 12.4 mm thick C-shaped laminate. 159

Table A-1: Overview of studies reported from literature review of thick thermoset composites. 200

Table A-2: Overview of studies reported from literature review of thick thermoset composites with respect to thermal management science base[a,b]. 202

Table A-3: Cure kinetics models reported from literature review of thick thermoset composites (see Table A-2). 204

Table A-4: Overview of studies reported from literature review of thick thermoset composites with respect to thermal management technology base. 208

Table A-5: Overview of thermal management studies of thick thermoset composites in the scientific literature based on ETPM factory ontology. 210

Table A-6: Overview of studies of thick thermoset composites in the scientific literature based on the ETPM factory ontology with respect to thermal management. 212

Table C-1: Proposed science based knowledge topics for thermal management. 221

Table C-2: Proposed design practice topics for thermal management. 223

Table C-3: Material screening and characterization science based practice example. 225

Table C-4: Cure cycle development and evaluation science based practice example. 226

Table C-5: Manufacturer recommended cure cycle[a] for Hexcel AS4/552 and Toray T800H/3900-2. 227

Table D-1: Effective heat transfer coefficients for the Johnston and Hubert data set. 231

Table D-2: ETPM[a] attribute definition for the Johnston and Hubert data set. 231

Table D-3: Effective heat transfer coefficients for the Kotlik and Shimizu data set[a]. 240

Table D-4: ETPM[a] attribute definition for the Kotlik and Shimizu data set (TEST-A, TEST-B). 241

Table D-5: ETPM[a] attribute definition for the Kotlik and Shimizu data set (TEST-C, TEST-D, TEST-E). 241

Table D-6: Heat transfer boundary condition sensitivity due to a reduction of experimental measurement points for a 38.4 mm thick laminate[a,b,c]. Note: TEST-A experienced a cure cycle interruption during the initial ramp segment and an unintentional bag leak was introduced prior to TEST-C. 248

Table D-7: ETPM[a] attribute definition for the Slesinger data set. 257

Table D-8: Effective heat transfer coefficients for the CCMRD9.2 data set (12.4 mm thick C-shaped laminate)[a]. 262

Table D-9: ETPM[a] attribute definition for the CCMRD9.2 data set (3.1 mm thick C-shaped laminate). 262

Table D-10: ETPM[a] attribute definition for a family of nominally geometrically identical small-scale tools. 270

Table D-11: Effective heat transfer coefficients for the Boeing-UW data set[a]. 279

Table D-12: ETPM[a] attribute definition for the Boeing-UW data set (Experiment 20151028-001). 280

Table D-13: ETPM[a] attribute definition for the Boeing-UW data set (Experiment 20151109-002). 280

Table D-14: ETPM[a] attribute definition for the Boeing-UW data set (Experiment 20161017-001). 281

Table E-1: Hexcel AS4/8552 materials database input parameters used for the Johnston and Hubert data set (refer to Appendix D.1). 298

Table E-2: AS4/8552-1 preliminary materials database input parameters for the Kotlik and Shimizu (refer Appendix D.2) and Slesinger (refer Appendix D.3) data sets. 300

Table E-3: Summary of DSC tests used in the preliminary cure kinetics characterization of Hexcel 8552-1. 303

Table E-4: T800H/3900-2 materials database input parameters used for the Slesinger (refer to Appendix D.3), CCMRD9.2 (refer to Appendix D.4) and Boeing-UW (refer to Appendix D.5) data sets. 313

Table E-5: Thermophysical material property input parameters used in the thick composite laminate data sets (refer to Appendix D). 315

List of Figures

Figure 1-1: The growth in market demand for carbon fibre compared to the growth of composites research: (a) market growth of carbon fibre and (b) publication rate of scientific literature. Annual market data is adapted from references [1–6]. Annual publication rate is determined by using a keyword search of the UBC-Summon database [11] as a proxy, with search terms: "CFRP", "carbon fibre reinforced polymer" and "carbon fibre reinforced plastic". Note: Closed symbols represent actual market data and open symbols represent estimated market data. 2

Figure 1-2: *Knowledge in Practice* conceptual workflow (figure courtesy of CRN). TRL: Technology Readiness Level. 11

Figure 2-1: Thick thermoset composites studies identified in the scientific literature[a]. CFRP: Carbon Fibre Reinforced Polymer; GFRP: Glass Fibre Reinforced Polymer. Note: Subset of studies that consider tool thermal effects and convective heat transfer boundary conditions are shown in bold (N = 13). 25

Figure 3-1: Typical aerospace composites manufacturing practice. Adapted from [192] (CMH-17, 2012): (a) high-level design workflow and (b) the problems associated with this approach. MRCC: Manufacturer Recommended Cure Cycle; M&P: Material & Process. .. 49

Figure 3-2: Preliminary outcomes taxonomy for composites processing. Extension of approaches from [127,128] (Griffith *et al*, 2002) and [187–189] (Potter *et al*, 2007). Note: Manufacturing outcomes are classified by theme (left to right), material equivalency (top to bottom) and outcome type (process parameter (red), material structure (green) and material performance (blue)), where intermediate outcomes shown in italics and final outcomes are shown in plain text. 51

Figure 3-3: Thermal management sources and sinks[a,b] for autoclave cure are shown. Adapted from Mobuchon and Zobeiry (2014). HTC: Heat Transfer Coefficient; $\dot{T}$(t): applied heating rate; T(t): applied temperature; P_A: applied pressure; P_V: applied vacuum pressure. Note: Minimum/maximum temperatures are classified as process parameter outcomes. 56

Figure 3-4: Program development cost-risk relationship for complex engineering systems. Adapted from [16] (NDIA, 2011). M&S: modelling and simulation. 57

Figure 3-5: Structural glass fibre component manufacturer (SME #1). 62

Figure 3-6: High performance carbon fibre component manufacturer (SME #2). CFRP: Carbon Fibre Reinforced Polymer. 66

Figure 4-1: A framework for explicitly addressing the practice of manufacturing science. 80

Figure 4-2: The determinants of knowledge translation. Adapted from [59,60] (Graham et al, 2006) and [61] (Hicks et al, 2002). ICME: Integrated Computational Materials Engineering; MDO: Multidisciplinary Design Optimization; KBE: Knowledge Based Engineering; WWFE: World-wide Failure Exercise; CK: Cure Kinetics; cdmHUB: Composites Design and Manufacturing HUB; ETPM: Equipment–Tool–Part–Material..... 82

Figure 4-3: Transforming composites manufacturing practice (*protect–advance–disrupt*). Extension of approach from [39] (Ashby, 2011). ICME: Integrated Computational Materials Engineering; MGI: Materials Genome Initiative; EMMC: European Materials Modelling Council; VMAP: Virtual Material Modelling in Manufacturing; MDO: Multidisciplinary Design Optimization. 85

Figure 4-4: Experimental thermal profiling workflow. Adapted from Mobuchon and Zobeiry (2014). ETPM: Equipment–Tool–Part–Material; w, x, y, z: design-gate indices; M&P: Material & Process; TC: Thermocouple. Note: Current typical practice (protect) is to empirically measure the thermal response of parts and tools and future better practice (advance) is to perform thermal assessments using manufacturing simulation. 88

Figure 4-5: A high-level representation of the ETPM factory ontology. This hierarchical knowledge model represents manufacturing problems relating to building up the capability of the factory (Factory) and the acceptability of parts as they move through the factory (Producibility). ETPM: Equipment–Tool–Part–Material; *fn:* function. Note: Classes are denoted in uppercase. Angle brackets denote a collection of classes. 92

Figure 4-6: ETPM factory ontology class hierarchy and attributes for thermal management. Examples for autoclave and oven cure processes are shown. ETPM: Equipment–Tool–Part–Material; tm: thermal management; TC: Thermocouple; req: requirement; htc: heat transfer coefficient; IML: Inner Mould Line; OML: Outer Mould Line; ρ: density; C_p: specific heat capacity; k: thermal conductivity; $\dot{T}$(t): temperature rate; T(t): hold temperature. Note: Instances are denoted in lowercase. Variable attributes are shown in plain text and constraint attributes are shown in bold. Arrows indicate interactions between ETPM classes. 95

Figure 4-7: The ETPM factory ontology can be used to directly support manufacturing practice and effective decision making at *all* stages of the development design cycle and production. ETPM: Equipment–Tool–Part–Material; $((e)_w, (t)_x, (p)_y, (m)_z)$: a considered collection of manufacturing choices; $[(e)_w, (t)_x, (p)_y, (m)_z]$: a collection of manufacturing choices that has passed validation; w, x, y, z: design-gate indices. Note: Italics indicate the use of shorthand notation. While the questions posed at each stage are essentially the same, it is the definition of the factory system that changes. 101

Figure 4-8: Large composites part development. This scenario demonstrates the complex sequence of manufacturing decisions involving an OEM and Tier 1 supplier and is represented using the ETPM factory ontology as: (a) decision tree highlighting all possible design states that could be evaluated and (b) flowchart showing the details of the manufacturing choices made. ETPM: Equipment–Tool–Part–Material; w, x, y, z: design-gate indices; ℓ: material instance identifier; OEM: Original Equipment Manufacturer; req: manufacturing requirement. Note: Instances are denoted in lowercase. An alternative design path is shown in grey. Solid double lines indicate where responsibility is transferred between the OEM and the Tier 1 supplier. 106

Figure 4-9: Large composites part development. This scenario shows the concurrent sequence of manufacturing decisions made by an OEM who has access to a developmental autoclave and is represented using the ETPM factory ontology as: (a) decision tree highlighting all possible design states that could be evaluated and (b) flowchart showing the details of the manufacturing choices made. ETPM: Equipment–Tool–Part–Material; w, x, y, z: design-gate indices; *i*: equipment instance identifier; OEM: Original Equipment Manufacturer; req: manufacturing requirement. Note: Instances are denoted in lowercase. Horizontal dashed lines indicate concurrent design steps. 108

Figure 4-10: Bid for a small composites part work package. This scenario highlights the limited number of manufacturing choices available to an existing 'build to print' parts supplier and is represented using the ETPM factory ontology as: (a) decision tree highlighting all possible design states that could be evaluated and (b) flowchart showing the details of the manufacturing choices made. ETPM: Equipment–Tool–Part–Material; w, x, y, z: design-gate indices; *j*: tool instance identifier; req: manufacturing requirement; tm: thermal management; htc: heat transfer coefficient. Note: Instances are denoted in lowercase. Unavailable design states are shown in grey. 110

Figure 4-11: Process improvement for a high-volume composites part. Based on original work by Fernlund and Mobuchon (2015). This scenario demonstrates how science based practice can be used for efficient process optimization and is represented using the ETPM factory ontology as: (a) decision tree highlighting all possible design states that could be evaluated and (b) flowchart showing the details of the manufacturing choices made. ETPM: Equipment–Tool–Part–Material; w, x, y, z: design-gate indices; *i*: equipment instance identifier; ℓ: material instance identifier; α: degree of cure; *t*: time; *T:* temperature; H_R: resin heat of reaction. Note: Instances are denoted in lowercase. An alternative design path is shown in grey. Solid wavy lines indicate that the precise design path is unknown. 113

Figure 4-12: Knowledge reuse. This scenario highlights the value in systematically capturing knowledge, in the form of expert opinion, experience, test and analysis, for reuse in future programs and is represented using the ETPM factory ontology as: (a) decision tree highlighting all possible design states that could be evaluated and (b) flowchart showing the details of the manufacturing choices made. ETPM: Equipment–Tool–Part–Material; w, x, y, z: design-gate indices; *n*: program instance identifier; HTC: Heat Transfer Coefficient. Arbitrary design states are specified in this scenario. Solid wavy lines indicate that the precise design path is unknown. 116

Figure 4-13: New product development. These scenarios show how different parts of the ETPM decision tree can be used depending on the type of manufacturing-innovation relationship involved: (a) 'Process-driven innovation', or a Material focused sequence of manufacturing decisions, appear on the left side of the decision tree and (b) 'Pure product innovation', or an Equipment focused sequence of manufacturing decisions, appear on the right side of the decision tree. ETPM: Equipment–Tool–Part–Material; w, x, y, z: design-gate indices; NPD: New Product Development. Note: The manufacturing-innovation relationships shown are based on the modularity-maturity matrix [49] (Pisano & Shih, 2012). Solid wavy lines indicate that the precise design path is unknown. 118

Figure 5-1: Thermal modelling workflow. Extension of approaches from [194] (Ashby, 1992) and [195] (Advani *et al*, 2011). CK: Cure Kinetics; BCs: Boundary Conditions; TC: Thermocouple. 124

Figure 5-2: Confidence in partially reliable data. Using a combination of data sources can increase confidence in making effective manufacturing decisions. Based on [186] (Fernlund, 2010). *p*: Probability of reliability. Note: Arbitrary probabilities are assigned in the matrix shown. 127

Figure 5-3: Comparison of experimentally measured and predicted modelling results for a 38.4 mm thick laminate (experiment ID: TEST-A) at mid-laminate (TC-21) and at the part/tool interface (TC-0) to investigate the benefits and trade-offs in thermal modelling complexity. Temperature profiles (T v t) of: (a) RAVEN-1D drill point analysis with part and tool plate modelled and (b) COMPRO-3D analysis with part and tool plate (no tool substructure modelled). Experimental data from [145] (Shimizu *et al*, 2008). ETPM: Equipment–Tool–Part–Material; TC: Thermocouple; UD: Unidirectional. Note: Temperature overshoot in the RAVEN-1D prediction at the part/tool interface at point A. 130

Figure 5-4: Comparison of experimentally measured and predicted RAVEN-1D modelling results for material system derivatives Hexcel AS4/8552 and AS4/8552-1. Temperature profiles (T v t) of: (a) 14.7 mm thick laminate (experiment ID: 20100225-80) and (b) 38.4 mm thick laminate (experiment ID: TEST-A). Experimental data from [150] (Slesinger, 2010) and [145] (Shimizu *et al*, 2008). ETPM: Equipment–Tool–Part–Material; TC: Thermocouple; UD: Unidirectional; DOC: Degree of Cure. Note: Premature temperature overshoot in the AS4/8552 prediction at point A. 133

Figure 5-5: Comparison of experimentally measured and predicted RAVEN-1D modelling results for back-to-back experiments to investigate the validity of HTC boundary condition inputs. Temperature profiles (T v t) of: (a) 19.1 mm thick laminate (experiment ID: 20151028-001) and (b) 38.4 mm thick laminate (experiment ID: TEST-A and TEST-B). Experimental data from [237] (Boeing-UW, 2017) and [145] (Shimizu *et al*, 2008). ETPM: Equipment–Tool–Part–Material; TC: Thermocouple; UD: Unidirectional. Note: TEST-B is offset by 12 minutes due to the cure cycle interruption observed in TEST-A at point A. Vertical lines indicate heat up, hold and cool down cure cycle segments. 136

Figure 5-6: Cure cycle development and evaluation workflow. Extension of approach from [129,130] (Nelson *et al*, 2002). ETPM: Equipment–Tool–Part–Material; w, x, y, z: design-gate indices; MRCC: Manufacturer Recommended Cure Cycle; z: through-thickness coordinate; $\dot{T}$: temperature rate; ΔT: temperature difference; α_{gel}: gelation; μ_{min}: minimum viscosity; $T_g > T$: vitrification. 140

Figure 5-7: Geometery for a 28.2 mm thick panel with tapered core (schematic from [100] (Johnston, 1997)). 142

Figure 5-8: Cure cycle evaluation. This scenario demonstrates the use of manufacturing simulation to recommend a cure cycle for a 28.2 mm thick panel with tapered core. This problem is depicted as: (a) development workflow at design state $((e)_1, (t)_1, (p)_1, (m)_2)$ = (1, 1, 1, 2) with a manufacturing trial performed at $((e)_2, (t)_2, (p)_2, (m)_2)$ = (2, 2, 2, 2) and (b) ETPM thermal management attributes. Experimental data from [100] (Johnston, 1997). ETPM: Equipment–Tool–Part–Material; w, x, y, z: design-gate indices; TC: Thermocouple; HTC: Heat Transfer Coefficient; TBD: To Be Determined; *z*: through-thickness coordinate; DOC: Degree of Cure; UD: Unidirectional; req: manufacturing requirement; MRCC: Manufacturer Recommended Cure Cycle. Note: Instances are denoted in lowercase, shorthand notation is denoted in italics. A typical material qualification design path is shown in black. Solid wavy lines indicate that the precise design path is unknown. 143

Figure 5-9: Processing scenarios considered for a 28.2 mm thick panel with tapered core: (a) Case I: 25.4 mm thick Invar tool with open substructure (thick tool), (b) Case II: 25.4 mm thick Invar tool with closed substructure ('cold' tool strategy to mitigate exotherm) and (c) Case III: 9.5 mm thick Invar tool with open substructure (thin tool). TC: Thermocouple; HTC: Heat Transfer Coefficient. Note: A high toolside HTC represents an open tool substructure, whereas a low toolside HTC represents a closed tool substructure. 144

Figure 5-10: Predicted RAVEN-1D modelling results for Case I (processing scenario: 25.4 mm thick Invar tool with open substructure). Temperature profile (T v t) and temperature rate versus temperature ($\dot{T}$ v T) plots for: (a) nominal MRCC (overall outcome: fail) and (b) slow MRCC (overall outcome: fail). MRCC: Manufacturer Recommended Cure Cycle; TC: Thermocouple; DOC: Degree of Cure. Note: Cure cycle acceptance criteria are summarized in Table 5-5 (pass (unshaded), marginal (yellow), fail (red)). 149

Figure 5-11: Predicted RAVEN-1D modelling results for Case I (processing scenario: 25.4 mm thick Invar tool with open substructure). Temperature profile (T v t) and temperature rate versus temperature ($\dot{T}$ v T) plots for: (a) extending the 110 °C hold (overall outcome: fail) and (b) introducing an intermediate 150 °C hold (overall outcome: marginal). TC: Thermocouple; DOC: Degree of Cure. Note: Cure cycle acceptance criteria are summarized in Table 5-5 (pass (unshaded), marginal (yellow), fail (red)). 150

Figure 5-12: Comparison of experimentally measured and predicted modelling results for a 28.2 mm thick panel with tapered core. Temperature profiles (T v t) of: (a) RAVEN-1D analysis using the AS4/8552 NCAMP material model (Case I) and (b) original COMPRO-2D analysis using the AS4/8552 open literature material model (figure from [100] (Johnston, 1997)). Experimental data from [100] (Johnston, 1997). ETPM: Equipment–Tool–Part–Material; HTC: Heat Transfer Coefficient; BCs: Boundary Conditions; TC: Thermocouple; UD: Unidirectional. Note: Predicted autoclave air temperature is based on the cure cycle development and evaluation performed in this case study. Temperature overshoot overpredicted at point A and temperature overshoot underpredicted in the original prediction at point B. 152

Figure 5-13: Experimental thermal profiling workflow. Troubleshooting apparent and real thermocouple failures. Adapted from Mobuchon and Zobeiry (2014). ETPM: Equipment–Tool–Part–Material; w, x, y, z: design-gate indices; M&P: Material & Process; TC: Thermocouple; CFD: Computational Fluid Dynamics; HTC: Heat Transfer Coefficient. .. 156

Figure 5-14: Experimental thermal profile validation. This scenario demonstrates the use of manufacturing simulation to investigate a real thermocouple failure in a 12.4 mm thick C-shaped laminate (part ID: CCM9.2-077). This problem is depicted as: (a) troubleshooting workflow at design state $((e)_2, (t)_2, (p)_2, (m)_3) = (2, 2, 2, 3)$ and could be considered as representative production scenario at $((e)_3, (t)_3, (p)_3, (m)_3) = (3, 3, 3, 3)$ and (b) ETPM thermal management attributes. Experimental data from [236] (Arafath *et al*, 2015). ETPM: Equipment–Tool–Part–Material; w, x, y, z: design-gate indices; TC: Thermocouple; req: manufacturing requirement; HTC: Heat Transfer Coefficient; *z*: through-thickness coordinate; UD: Unidirectional. Note: Instances are denoted in lowercase, shorthand notation is denoted in italics. Solid wavy lines indicate that the precise design path is unknown. 158

Figure 5-15: Instrumented 12.4 mm thick T800H/3900-2 C-shaped laminate (part ID: CCM9.2-077) prior to bagging (photo courtesy of CCMRD [236]). 160

Figure 5-16: Experimentally measured results for a 12.4 mm thick C-shaped laminate (part ID: CCM9.2-077) comparing thermocouples located at the part surface (TC33), part/tool interface (TC5) and tool underside surface (TC22): (a) temperature profile (T v t) and (b) temperature difference with respect to the autoclave air temperature (ΔT v t). Experimental data from [236] (Arafath *et al*, 2015). ETPM: Equipment–Tool–Part–Material; TC: Thermocouple; UD: Unidirectional. Note: Reduction in temperature difference observed (> 1.5 °C TC limit of error at the part surface and part/tool interface) at approximately t = 30 min at point A due to autoclave pressurization. Vertical lines indicate heat up, hold and cool down cure cycle segments. 162

Figure 5-17: Experimentally measured and predicted RAVEN-1D modelling results for a 12.4 mm thick C-shaped laminate (part ID: CCM9.2-077). The effect of low and high heat transfer due to autoclave pressurization (low HTC back-calculated at t = 30 min and high HTC back-calculated at $70 < t < 90$ min): (a) temperature profile (T v t) and (b) temperature difference with respect to the autoclave air temperature (ΔT v t). Experimental data from [236] (Arafath *et al*, 2015). ETPM: Equipment–Tool–Part–Material; HTC: Heat Transfer Coefficient; TC: Thermocouple; UD: Unidirectional. Note: Temperature difference overpredicted at the part surface at point A (> 1.5 °C TC limit of error at the part surface for the low HTC case) and temperature overshoot predicted at point B. Vertical lines indicate heat up, hold and cool down cure cycle segments. 164

Figure 6-1: A framework for formalizing science based composites manufacturing practice was introduced in this work to support the effective management of increasing manufacturing risk. The developed framework includes: (a) a manufacturing outcomes taxonomy to systematically link the *science–technology–practice* levels of activity and ETPM factory ontology to organize composites manufacturing domain knowledge and (b) ETPM decision tree that represents *all* stages of the development design cycle (the entire manufacturing design space). ETPM: Equipment–Tool–Part–Material; GI: Design-gate index; TRL: Technology Readiness Level. 172

Figure A-1: General types of cure kinetics models developed for the thermal modelling of thermoset composites. Adapted from [100] (Johnston, 1997), [144] (Dykeman, 2008) and [181] (CMT Inc., 2017). CK: Cure Kinetics; $\dot{\alpha}$: cure rate; $f(\alpha)$: functional form. 207

Figure C-1: The *Knowledge in Practice* framework is intended to act as an interface between open literature and industrial specifications and design methods. ETPM: Equipment–Tool–Part–Material; *fn:* function. 220

Figure C-2: Comparison of predicted RAVEN-1D MRCC processing envelopes. Temperature profile (T v t) and glass transition temperature versus cure advancement (T_g v α) plots shown for: (a) Hexcel AS4/8552 (example of a two phase material system) and (b) Toray T800H/3900-2 (example of a multiple phase material system). MRCC: Manufacturer Recommended Cure Cycle; α: Degree of Cure. Note: Evaluation performed using AS4/8552 NCAMP [135,238] and T800H/3900-2 open literature [144,238] material models. 227

Figure C-3: ETPM decision tree and attribute canvas. These tools can be used to systematically capture manufacturing scenarios with simulation based thinking. GI: Design-gate Index. 228

Figure D-1: Johnston and Hubert data set: (a) experimental setup prior to bagging[a] and (b) schematic of part and thermocouple locations (photo and schematic from [100] (Johnston, 1997)). 230

Figure D-2: Comparison of experimentally measured and predicted RAVEN-1D modelling results for the Johnston and Hubert data set (ATCAS: 28.2 mm thick panel with tapered core): (a) temperature profile (T v t) and (b) temperature difference with respect to the autoclave air temperature (ΔT v t). Experimental data from [100] (Johnston, 1997). ETPM: Equipment–Tool–Part–Material; TC: Thermocouple; UD: Unidirectional. Note: Vertical lines indicate heat up, hold and cool down cure cycle segments. 232

Figure D-3: Comparison of experimentally measured and predicted RAVEN-1D modelling results for the Johnston and Hubert data set (ATCAS: 28.2 mm thick panel with tapered core). The effect of low and high heat transfer: (a) low autoclave pressure (170 kPa/10 psig) and (b) high autoclave pressure (375 kPa/40 psig). Experimental data from [100] (Johnston, 1997). ETPM: Equipment–Tool–Part–Material; TC: Thermocouple; UD: Unidirectional; HTC: Heat Transfer Coefficient. Note: Revised effective HTCs are back-calculated from the experimental data and summarized in Table D-1. 233

Figure D-4: Comparison of experimentally measured and predicted RAVEN-1D modelling results for the Johnston and Hubert data set (ATCAS: 28.2 mm thick panel with tapered core). AS4/8552 NCAMP material model initial DOC sensitivity: (a) $\alpha_i = 0.001$ (default as per 8552 NCAMP CK model [135]) and (b) $\alpha_i = 0.05$ (default as per the open literature 8552 CK model characterized by Johnston [100]). Experimental data from [100] (Johnston, 1997). ETPM: Equipment–Tool–Part–Material; TC: Thermocouple; UD: Unidirectional; DOC: Degree of Cure; α_i: initial degree of cure; CK: Cure Kinetics. 234

Figure D-5: Predicted RAVEN-1D modelling results for Case II (processing scenario: 25.4 mm thick Invar tool with closed substructure). Temperature profile (T v t) and temperature rate versus temperature ($\dot{T}$ v T) plots for: (a) nominal MRCC (overall outcome: fail) and (b) slow MRCC (overall outcome: fail). MRCC: Manufacturer Recommended Cure Cycle; TC: Thermocouple; DOC: Degree of Cure. Note: Cure cycle acceptance criteria are summarized in Table 5-5 (pass (unshaded), marginal (yellow), fail (red)). 235

Figure D-6: Predicted RAVEN-1D modelling results for Case II (processing scenario: 25.4 mm thick Invar tool with closed substructure). Temperature profile (T v t) and temperature rate versus temperature ($\dot{T}$ v T) plots for: (a) extending the 110 °C hold (overall outcome: fail) and (b) introducing an intermediate 150 °C hold (overall outcome: fail). TC: Thermocouple; DOC: Degree of Cure. Note: Cure cycle acceptance criteria are summarized in Table 5-5 (pass (unshaded), marginal (yellow), fail (red)). 236

Figure D-7: Predicted RAVEN-1D modelling results for Case III (processing scenario: 9.5 mm thick Invar tool with open substructure). Temperature profile (T v t) and temperature rate versus temperature ($\dot{T}$ v T) plots for: (a) nominal MRCC (overall outcome: fail) and (b) slow MRCC (overall outcome: fail). MRCC: Manufacturer Recommended Cure Cycle; TC: Thermocouple; DOC: Degree of Cure. Note: Cure cycle acceptance criteria are summarized in Table 5-5 (pass (unshaded), marginal (yellow), fail (red)). 237

Figure D-8: Predicted RAVEN-1D modelling results for Case III (processing scenario: 9.5 mm thick Invar tool with open substructure). Temperature profile (T v t) and temperature rate versus temperature ($\dot{T}$ v T) plots for: (a) extending the 110 °C hold (overall outcome: marginal) and (b) introducing an intermediate 150 °C hold (overall outcome: marginal). TC: Thermocouple; DOC: Degree of Cure. Note: Cure cycle acceptance criteria are summarized in Table 5-5 (pass (unshaded), marginal (yellow), fail (red)). 238

Figure D-9: Kotlik and Shimizu data set: (a) experimental setup and (b) schematic of thermocouple locations (photo and schematic from [145] (Shimizu *et al*, 2008)). 239

Figure D-10: Comparison of experimentally measured and predicted RAVEN-1D and COMPRO-3D modelling results for the Kotlik and Shimizu data set (TEST-A: 38.4 mm thick laminate, curing 2-hold cycle): (a) temperature profile (T v t) and (b) temperature difference with respect to the autoclave air temperature (ΔT v t). Experimental data from [145] (Shimizu *et al*, 2008). ETPM: Equipment–Tool–Part–Material; TC: Thermocouple; UD: Unidirectional. Note: Vertical lines indicate heat up, hold and cool down cure cycle segments. 242

Figure D-11: Comparison of experimentally measured and predicted RAVEN-1D modelling results for the Kotlik and Shimizu data set (TEST-B: 38.4 mm thick laminate, cured 2-hold cycle): (a) temperature profile (T v t) and (b) temperature difference with respect to the autoclave air temperature (ΔT v t). Experimental data from [145] (Shimizu *et al*, 2008). ETPM: Equipment–Tool–Part–Material; TC: Thermocouple; UD: Unidirectional. Note: Vertical lines indicate heat up, hold and cool down cure cycle segments. 243

Figure D-12: Comparison of experimentally measured and predicted RAVEN-1D modelling results for the Kotlik and Shimizu data set (TEST-C: 38.4 mm thick laminate, cured 1-hold cycle at 2.8 °C /min): (a) temperature profile (T v t) and (b) temperature difference with respect to the autoclave air temperature (ΔT v t). Experimental data from [145] (Shimizu et al, 2008). ETPM: Equipment–Tool–Part–Material; TC: Thermocouple; UD: Unidirectional. Note: Unintentional bag leak introduced into experimental test setup. Vertical lines indicate heat up, hold and cool down cure cycle segments. 244

Figure D-13: Comparison of experimentally measured and predicted RAVEN-1D modelling results for the Kotlik and Shimizu data set (TEST-D: 38.4 mm thick laminate, cured 1-hold cycle at 1.7 °C /min): (a) temperature profile (*T* v *t*) and (b) temperature difference with respect to the autoclave air temperature (Δ*T* v *t*). Experimental data from [145] (Shimizu *et al*, 2008). ETPM: Equipment–Tool–Part–Material; TC: Thermocouple; UD: Unidirectional. Note: Unintentional bag leak introduced into experimental test setup. Vertical lines indicate heat up, hold and cool down cure cycle segments. 245

Figure D-14: Comparison of experimentally measured and predicted RAVEN-1D modelling results for the Kotlik and Shimizu data set (TEST-E: 38.4 mm thick laminate, cured 1-hold cycle at 0.6 °C /min): (a) temperature profile (*T* v *t*) and (b) temperature difference with respect to the autoclave air temperature (Δ*T* v *t*). Experimental data from [145] (Shimizu *et al*, 2008). ETPM: Equipment–Tool–Part–Material; TC: Thermocouple; UD: Unidirectional. Note: Unintentional bag leak introduced into experimental test setup. Vertical lines indicate heat up, hold and cool down cure cycle segments. 246

Figure D-15: Comparison of experimentally measured and predicted RAVEN-1D modelling results for a 38.4 mm thick laminate[a] (part TCs: TC-0 (interface, *z* = 0 mm), TC-6 to TC-36, TC-42 (surface, *z* = 38.4 mm). Through-thickness temperature profiles (*z* v *T*) of: (a) curing and cured laminate (experiment ID: TEST-A and TEST-B) and (b) laminate without bag leak and with bag leak (experiment ID: TEST-B and TEST-C). Experimental data from [145] (Shimizu *et al*, 2008). ETPM: Equipment–Tool–Part–Material; TC: Thermocouple; UD: Unidirectional. Note: Temperature profiles shown when the autoclave air temperature reaches 110 °C (initial ramp). Effective HTCs back calculated from 33 measurement points (spaced every six plies). 250

Figure D-16: Comparison of experimentally measured and predicted RAVEN-1D modelling results for a 38.4 mm thick laminate[a] (part TCs: TC-0 (interface, *z* = 0 mm), TC-21, TC-42 (surface, *z* = 38.4 mm). Through-thickness temperature profiles (*z* v *T*) of: (a) curing and cured laminate (experiment ID: TEST-A and TEST-B) and (b) laminate without bag leak and with bag leak (experiment ID: TEST-B and TEST-C). Experimental data from [145] (Shimizu *et al*, 2008). ETPM: Equipment–Tool–Part–Material; TC: Thermocouple; UD: Unidirectional. Note: Temperature profiles shown when the autoclave air temperature reaches 110 °C (initial ramp). Effective HTCs back calculated from two measurement points (top/bottom). 251

Figure D-17: Comparison of experimentally measured and predicted RAVEN-1D modelling results for a 38.4 mm thick laminate[a] (part TCs: TC-0 (interface, *z* = 0 mm), TC-6 to TC-36, TC-42 (surface, *z* = 38.4 mm). Through-thickness temperature profiles (*z* v *T*) of: (a) curing and cured laminate (experiment ID: TEST-A and TEST-B) and (b) laminate without bag leak and with bag leak (experiment ID: TEST-B and TEST-C). Experimental data from [145] (Shimizu *et al*, 2008). ETPM: Equipment–Tool–Part–Material; TC: Thermocouple; UD: Unidirectional. Note: Temperature profiles shown when the autoclave air temperature reaches 60 °C (cool down). Effective HTCs back calculated from 33 measurement points (spaced every six plies). 252

Figure D-18: Comparison of experimentally measured and predicted RAVEN-1D modelling results for a 38.4 mm thick laminate[a] (part TCs: TC-0 (interface, z = 0 mm), TC-21, TC-42 (surface, z = 38.4 mm). Through-thickness temperature profiles (z v T) of: (a) curing and cured laminate (experiment ID: TEST-A and TEST-B) and (b) laminate without bag leak and with bag leak (experiment ID: TEST-B and TEST-C). Experimental data from [145] (Shimizu *et al*, 2008). ETPM: Equipment–Tool–Part–Material; TC: Thermocouple; UD: Unidirectional. Note: Temperature profiles shown when the autoclave air temperature reaches 60 °C (cool down). Effective HTCs back calculated from two measurement points (top/bottom). 253

Figure D-19: Comparison of five measurement points (spaced every 48 plies) and quadratic data fit results from 33 measurement points (spaced every six plies) for a 38.4 mm thick laminate[a] (part TCs: TC-0 (interface, z = 0 mm), TC-13, TC-21, TC-29, TC-42 (surface, z = 38.4 mm). Through-thickness temperature profiles (z v T) of curing and cured laminate (experiment ID: TEST-A and TEST-B). Experimental data from [145] (Shimizu *et al*, 2008). ETPM: Equipment–Tool–Part–Material; TC: Thermocouple; UD: Unidirectional. Note: Temperature profiles shown when the autoclave air temperature reaches 110 °C (initial ramp). Adjacent TCs to TC-13 shown to highlight apparent TC failure at point A. 254

Figure D-20: Comparison of three measurement points (spaced every 96 plies) and quadratic data fit results from 33 measurement points (spaced every six plies) for a 38.4 mm thick laminate[a] (part TCs: TC-0 (interface, z = 0 mm), TC-21, TC-42 (surface, z = 38.4 mm). Through-thickness temperature profiles (z v T) of laminate without bag leak and with bag leak (experiment ID: TEST-B and TEST-C). Experimental data from [145] (Shimizu *et al*, 2008). ETPM: Equipment–Tool–Part–Material; TC: Thermocouple; UD: Unidirectional. Note: Temperature profiles shown when the autoclave air temperature reaches 110 °C (initial ramp). Adjacent TCs to TC-21 shown to highlight apparent TC failure at point A. 255

Figure D-21: Slesinger data set: (a) experimental setup prior to bagging and (b) schematic of thermocouple locations (photo and schematic from [150] (Slesinger, 2010)). 256

Figure D-22: Comparison of experimentally measured and predicted RAVEN-1D modelling results for the Slesinger data set (AS4/8552-1, 11.7 mm thick laminate): (a) temperature profile (T v t) and (b) temperature difference with respect to the autoclave air temperature (ΔT v t). Experimental data from [150] (Slesinger, 2010). ETPM: Equipment–Tool–Part–Material; TC: Thermocouple; UD: Unidirectional. Note: Vertical lines indicate heat up, hold and cool down cure cycle segments. 258

Figure D-23: Comparison of experimentally measured and predicted RAVEN-1D modelling results for the Slesinger data set (AS4/8552-1, 14.7 mm thick laminate): (a) temperature profile (T v t) and (b) temperature difference with respect to the autoclave air temperature (ΔT v t). Experimental data from [150] (Slesinger, 2010). ETPM: Equipment–Tool–Part–Material; TC: Thermocouple; UD: Unidirectional. Note: Vertical lines indicate heat up, hold and cool down cure cycle segments. 259

Figure D-24: Comparison of experimentally measured and predicted RAVEN-1D modelling results for the Slesinger data set (T800H/3900-2, 7.5 mm thick laminate): (a) temperature profile (T v t) and (b) temperature difference with respect to the autoclave air temperature (ΔT v t). Experimental data from [150] (Slesinger, 2010). ETPM: Equipment–Tool–Part–Material; TC: Thermocouple; UD: Unidirectional. Note: Vertical lines indicate heat up, hold and cool down cure cycle segments. 260

Figure D-25: CCMRD9.2 data set: (a) representative experimental setup and (b) schematic of thermocouple locations for 12.4 mm thick C-shaped laminate (photo and schematic courtesy of CCMRD [236]). 261

Figure D-26: Experimentally measured results for the CCMRD9.2 data set (3.1 mm thick C-shaped laminate, Invar tool (part ID: CCM9.2-043)): (a) temperature profile (T v t) and (b) temperature difference with respect to the autoclave air temperature (ΔT v t). Experimental data from [236] (Arafath *et al*, 2015). ETPM: Equipment–Tool–Part–Material; TC: Thermocouple; UD: Unidirectional. Note: Perturbation in temperature difference (< 1.5 °C TC limit of error) observed at approximately t = 30 min at point A due to autoclave pressurization (inferred from other experiments). Vertical lines indicate heat up, hold and cool down cure cycle segments. 263

Figure D-27: Experimentally measured results for the CCMRD9.2 data set (3.1 mm thick C-shaped laminate, Invar tool (part ID: CCM9.2-052)): (a) temperature profile (T v t) and (b) temperature difference with respect to the autoclave air temperature (ΔT v t). Experimental data from [236] (Arafath *et al*, 2015). ETPM: Equipment–Tool–Part–Material; TC: Thermocouple; UD: Unidirectional. Note: Perturbation in temperature difference not observed at approximately t = 30 min at point A due to autoclave pressurization. Vertical lines indicate heat up, hold and cool down cure cycle segments. 264

Figure D-28: Experimentally measured results for the CCMRD9.2 data set (3.1 mm thick C-shaped laminate, Al-alloy tool (part ID: CCM9.2-028)): (a) temperature profile (T v t) and (b) temperature difference with respect to the autoclave air temperature (ΔT v t). Experimental data from [236] (Arafath *et al*, 2015). ETPM: Equipment–Tool–Part–Material; TC: Thermocouple; UD: Unidirectional. Note: Perturbation in temperature difference (< 1.5 °C TC limit of error at the tool underside surface) observed at approximately t = 30 min at point A due to autoclave pressurization. Vertical lines indicate heat up, hold and cool down cure cycle segments. 265

Figure D-29: Experimentally measured results for the CCMRD9.2 data set (3.1 mm thick C-shaped laminate, CFRP tool (part ID: CCM9.2-031)): (a) temperature profile (T v t) and (b) temperature difference with respect to the autoclave air temperature (ΔT v t). Experimental data from [236] (Arafath *et al*, 2015). ETPM: Equipment–Tool–Part–Material; TC: Thermocouple; UD: Unidirectional. Note: Perturbation in temperature difference (> 1.5 °C TC limit of error at the part surface) observed at approximately t = 30 min at point A due to autoclave pressurization (inferred from other experiments). Vertical lines indicate heat up, hold and cool down cure cycle segments. 266

Figure D-30: Family of small-scale tools fabricated from: (a) Invar 36 (Invar), (b) 6061-T6 aluminum alloy (Al-alloy) and (c) composite (CFRP) (photo courtesy of CRN). Note: These tools are nominally geometrically identical (overall dimensions: 1200 mm (length), 800 mm (width), 480 mm (height)) 270

Figure D-31: Estimated temperature difference at the tool surface with respect to the autoclave air temperature (ΔT v h) for small-scale Invar, Al-alloy and CFRP tools[a,b]. h: heat transfer coefficient; ΔT: temperature difference. Note: Vertical line indicates typical upper heat transfer limit for autoclave cure (very high impinging airflow). Temperature difference values shown in grey are unlikely to be achieved in autoclave cure. 271

Figure D-32: Experimentally measured results for a family of small-scale tools comparing thermocouples located on the tool topside (TC15) and underside (TC31) surfaces. Temperature profiles (T v t) of: (a) Invar tool (experiment ID: CCM9.2-042-043-044), (b) Al-alloy tool (experiment ID: CCM9.2-033-034-035) and (c) CFRP tool (experiment ID: CCM9.2-030-031-032). Experimental data from [236] (Arafath *et al*, 2015). ETPM: Equipment–Tool–Part–Material; TC: Thermocouple; ΔT: temperature difference. Note: Apparent thermocouple failures observed in Invar and CFRP tools in heat up at point A... 273

Figure D-33: HTC distribution and location for the CCMRD9.2 data set (12.4 mm thick C-shaped laminate, Invar tool (part ID: CCM9.2-077)). Experimental data from [236] (Arafath *et al*, 2015) and predicted CFD data from [178] Park (2018). TC: Thermocouple; HTC: Heat Transfer Coefficient. Note: HTC distribution based on CFD analysis that does not consider thermal resistances due to consumables/bagging. 274

Figure D-34: Experimentally measured and predicted COMPRO-3D modelling results for a 12.4 mm thick C-shaped laminate (part ID: CCM9.2-077) comparing part thermocouples TC33 (surface) and TC5 (interface): (a) temperature profile (T v t) and (b) temperature difference with respect to the autoclave air temperature (ΔT v t). Experimental data from [236] (Arafath *et al*, 2015) and predicted modelling data from [178] Park (2018). ETPM: Equipment–Tool–Part–Material; TC: Thermocouple; UD: Unidirectional. Note: Temperature difference in heat up underpredicted at the part surface at point A. HTC distribution based on CFD analysis that does not consider thermal resistances due to consumables/bagging. Vertical lines indicate heat up, hold and cool down cure cycle segments. 275

Figure D-35: Boeing-UW data set. MSE-2015 (experiments 20151028-001 & 20151109-002): (a) representative experimental setup and (b) schematic of thermocouple locations and MSE-2016 (experiment 20161017-001): (c) experimental setup and (d) schematic of thermocouple locations (photos courtesy of Karl Nelson [237]). 278

Figure D-36: Comparison of experimentally measured and predicted RAVEN-1D modelling results for the Boeing-UW data set (Experiment 20151028-001: 19.1 mm thick laminate): (a) temperature profile (T v t) and (b) temperature difference with respect to the autoclave air temperature (ΔT v t). Experimental data from [237] (Boeing-UW, 2017). ETPM: Equipment–Tool–Part–Material; TC: Thermocouple; UD: Unidirectional. Note: Experiments run back-to-back in autoclave. Vertical lines indicate heat up, hold and cool down cure cycle segments. 282

Figure D-37: Comparison of experimentally measured and predicted RAVEN-1D and COMPRO-3D modelling results for the Boeing-UW data set (Experiment 20151109-002: 6.4 mm thick laminate): (a) temperature profile (T v t) and (b) temperature difference with respect to the autoclave air temperature (ΔT v t). Experimental data from [237] (Boeing-UW, 2017). ETPM: Equipment–Tool–Part–Material; TC: Thermocouple; UD: Unidirectional. Note: Vertical lines indicate heat up, hold and cool down cure cycle segments. 283

Figure D-38: Comparison of experimentally measured and predicted RAVEN-1D and COMPRO-3D modelling results for the Boeing-UW data set (Experiment 20151109-002: 19.1 mm thick laminate): (a) temperature profile (T v t) and (b) temperature difference with respect to the autoclave air temperature (ΔT v t). Experimental data from [237] (Boeing-UW, 2017). ETPM: Equipment–Tool–Part–Material; TC: Thermocouple; UD: Unidirectional. Note: Vertical lines indicate heat up, hold and cool down cure cycle segments. 284

Figure D-39: Comparison of experimentally measured and predicted RAVEN-1D and COMPRO-3D modelling results for the Boeing-UW data set (Experiment 20161017-001: 12.7 mm thick laminate): (a) temperature profile (T v t) and (b) temperature difference with respect to the autoclave air temperature (ΔT v t). Experimental data from [237] (Boeing-UW, 2017). ETPM: Equipment–Tool–Part–Material; TC: Thermocouple; UD: Unidirectional. Note: Autoclave pressurized to 410 kPa/45 psig to prevent ‘core crush’. Vertical lines indicate heat up, hold and cool down cure cycle segments. 285

Figure D-40: Comparison of experimentally measured and predicted RAVEN-1D and COMPRO-3D modelling results for the Boeing-UW data set (Experiment 20161017-001: 25.4 mm thick laminate): (a) temperature profile (T v t) and (b) temperature difference with respect to the autoclave air temperature (ΔT v t). Experimental data from [237] (Boeing-UW, 2017). ETPM: Equipment–Tool–Part–Material; TC: Thermocouple; UD: Unidirectional. Note: Autoclave pressurized to 410 kPa/45 psig to prevent ‘core crush’. Vertical lines indicate heat up, hold and cool down cure cycle segments. 286

Figure D-41: Comparison of experimentally measured and predicted RAVEN-1D and COMPRO-3D modelling results for the Boeing-UW data set (Experiment 20161017-001: 33.0 mm thick panel with septum): (a) temperature profile (T v t) and (b) temperature difference with respect to the autoclave air temperature (ΔT v t). Experimental data from [237] (Boeing-UW, 2017). ETPM: Equipment–Tool–Part–Material; TC: Thermocouple; UD: Unidirectional. Note: Autoclave pressurized to 410 kPa/45 psig to prevent ‘core crush’. Vertical lines indicate heat up, hold and cool down cure cycle segments. 287

Figure D-42: Comparison of experimentally measured and predicted RAVEN-1D modelling results for a 12.7 mm thick laminate (experiment ID: 20161017-001): (a) temperature profile (T v t) and (b) temperature difference with respect to the autoclave air temperature (ΔT v t). Experimental data from [237] (Boeing-UW, 2017). ETPM: Equipment–Tool–Part–Material; TC: Thermocouple; UD: Unidirectional. Note: Tool size effects are significant for this experiment. The resin thermal conductivity sensitivity study is a comparative analysis. Autoclave pressurized to 410 kPa/45 psig to prevent ‘core crush’. Vertical lines indicate heat up, hold and cool down cure cycle segments. 291

Figure D-43: Comparison of experimentally measured and predicted RAVEN-1D modelling results for a 25.4 mm thick laminate (experiment ID: 20161017-001): (a) temperature profile (T v t) and (b) temperature difference with respect to the autoclave air temperature (ΔT v t). Experimental data from [237] (Boeing-UW, 2017). ETPM: Equipment–Tool–Part–Material; TC: Thermocouple; UD: Unidirectional. Note: Temperature difference in heat up and cool down overpredicted at point A and temperature overshoot overpredicted at point B. Tool size effects are significant to a lesser extent in this experiment. The resin thermal conductivity sensitivity study is a comparative analysis. Autoclave pressurized to 410 kPa/45 psig to prevent 'core crush'. Vertical lines indicate heat up, hold and cool down cure cycle segments. 292

Figure D-44: Experimentally measured results for a 19.1 mm thick laminate comparing mid-laminate thermocouples located at the centre (TC-C4) and edge (TC-C5). Curing laminate in industrial autoclave B (experiment ID: 20151028-001-1): (a) temperature profile (T v t) and (b) temperature difference with respect to the autoclave air temperature (ΔT v t). Experimental data from [237] (Boeing-UW, 2017). ETPM: Equipment–Tool–Part–Material; TC: Thermocouple; UD: Unidirectional. Note: Vertical lines indicate heat up, hold and cool down cure cycle segments. 295

Figure D-45: Experimentally measured results for a 19.1 mm thick laminate comparing mid-laminate thermocouples located at the centre (TC-C4) and edge (TC-C5). Curing laminate in industrial autoclave C (experiment ID: 20151109-002): (a) temperature profile (T v t) and (b) temperature difference (ΔT v t). Experimental data from [237] (Boeing-UW, 2017). ETPM: Equipment–Tool–Part–Material; TC: Thermocouple; UD: Unidirectional. Note: Vertical lines indicate heat up, hold and cool down cure cycle segments. 296

Figure E-1: Linear baseline examples for DSC tests: (a) baseline for nonisothermal DSC test and residual scans of isothermal tests (4 °C/ min nonisothermal scan) and (b) baseline for isothermal DSC tests (110 °C isothermal scan). Experimental data from Hexcel 8552-1 preliminary cure kinetics characterization. 304

Figure E-2: Comparison of heat of reaction for nonisothermal DSC tests: (a) experimental data, used with permission, from Hexcel 8552 NCAMP material model database [135] (Van Ee *et al*, 2009) and (b) experimental data from Hexcel 8552-1 preliminary cure kinetics characterization. Note: Linear baselines were used for the cases shown. 305

Figure E-3: Comparison of heat of reaction for isothermal DSC tests: (a) experimental data from the Hexcel 8552 NCAMP material model database [135] (Van Ee *et al*, 2009) and (b) experimental data from Hexcel 8552-1 preliminary cure kinetics characterization. Note: NCAMP DSC data used with permission (NIAR, 2016). Linear baselines were used for the cases shown. 306

Figure E-4: Comparison of T_g versus α and the DiBenedetto model fit based on nonisothermal, isothermal and interrupted isothermal DSC tests: (a) experimental T_g data and model from Hexcel 8552 NCAMP material model database [135] (Van Ee *et al*, 2009) and (b) experimental T_g data and model from Hexcel 8552-1 preliminary cure kinetics characterization. Note: NCAMP DSC data used with permission (NIAR, 2016). Linear baselines were used for the cases shown. 309

Figure E-5: Comparisons of DOC and cure rate from experimental data and model predictions for Hexcel 8552-1 preliminary cure kinetics characterization: (a) DOC for isothermal DSC tests, (b) cure rate for isothermal DSC tests, (c) DOC for nonisothermal DSC tests and (d) cure rate for nonisothermal DSC tests. 310

Figure E-6: RAVEN generated cure versus temperature (α v T) process maps for Hexcel AS4/8552 (NCAMP material model) with isochronals shown as solid lines and Hexcel AS4/8552-1 (preliminary material model) with isochronals shown as dashed lines. Note: The glass transition temperature (T_g) is shown in black. 311

Figure F-1: Calculation of equivalent-1D heat transfer coefficient. Adapted from [145] (Shimizu *et al*, 2008)..... 317

Figure F-2: Calculation of equivalent-3D heat transfer coefficient (no tool substructure modelled). 320

List of Symbols

a	Thermal diffusivity ($k/\rho C_p$)
A	Heat transfer area
$A_{t\text{-bot}}$	Tool plate bottom surface heat transfer area
A_{top}	Bagside surface heat transfer area
$A_{t\text{-top}}$	Tool plate top surface heat transfer area
Bi	Biot number (hL/k)
Bi_e	Effective Biot number
C_p	Specific heat capacity
$d\alpha/dt$, $\dot{\alpha}$	Cure rate
Da	Damköhler number (K_0L^2/a)
e, t, p, m	Equipment–Tool–Part–Material instances (ETPM factory ontology)
E, T, P, M	Equipment–Tool–Part–Material classes (ETPM factory ontology)
$f(\alpha)$	Cure dependence of cure rate
f	Factory instance or design state (ETPM factory ontology)
F	Factory concept or factory system (ETPM factory ontology)
Fo	Fourier number (at/L^2) (conduction time scale)
h	Heat transfer coefficient
h_{bot}	Effective toolside heat transfer coefficient
$h_{t\text{-bot}}$	Effective tool plate bottom surface heat transfer coefficient
h_{top}	Effective bagside heat transfer coefficient
$h_{t\text{-top}}$	Effective tool plate top surface heat transfer coefficient
H_R	Total heat generated during a complete resin reaction
HR_{AVE}	Averaged heat of reaction for all nonisothermal and isothermal DSC tests
$HR_{DYN\text{-}AVE}$	Averaged nonisothermal heat of reaction
HR_{hold}	Heat released during an isothermal segment of a DSC test
$HR_{ISO\text{-}AVE}$	Averaged isothermal heat of reaction
HR_{ramp}	Heat released during a nonisothermal segment of a DSC test
$\dot{H}$	Specific rate of heat generation due to the exothermic resin reaction
$\dot{H}_{max}$	Maximum specific rate of heat generation due to the exothermic resin reaction

i, j, k, l, n	Number of variable attributes or instance identifiers (ETPM factory ontology)
i, n	Number of measurement points (determination of effective heat transfer coefficient)
k	Thermal conductivity
k_f	Fibre thermal conductivity
k_r	Resin thermal conductivity
k_x, k_y	In-plane thermal conductivity
k_z	Through-thickness thermal conductivity
K_0	Pre-exponential factor (reaction time scale)
L	Slab half-thickness
L_p	Laminate slab half-thickness
L_t	Tool plate slab half-thickness
L_e	Effective slab half-thickness
$L_{e\text{-}p}$	Effective laminate half-thickness
$L_{e\text{-}t}$	Effective tool plate half-thickness
m	Mass
$m.C_p$	Thermal mass
n	Number of reactions (‘semi model-free’ CK model)
o	Producibility instance or design state outcome (ETPM factory ontology)
O	Producibility concept or factory system response (ETPM factory ontology)
p	Probability of reliability
P	Pressure
P_A	Autoclave pressure
P_V	Vacuum pressure
t	Time
T	Temperature
T_g	Glass transition temperature
$T_g > T$	Vitrification
T_{g0}	Initial glass transition temperature of curing material
$T_{g\infty}$	Glass transition temperature of fully cured material
T_m	Melt temperature
T_{max}	Maximum lead temperature
T_s	Slab surface temperature

T_∞	Autoclave or oven air temperature
$\dot{T}$	Temperature rate
u	Number of constraint attributes (ETPM factory ontology)
v	Number of objective indices (ETPM factory ontology)
V_f	Fibre volume fraction
V_r	Resin volume fraction
w, x, y, z	Design-gate indices (ETPM factory ontology)
x, y	In-plane coordinates
z	Through-thickness coordinate
α	Degree of cure
α_f	Final degree of cure
α_gel	Gelation
α_i	Initial degree of cure
δ	Non-dimensional location of the adiabatic line with respect to the midplane
ΔQ	Heat gained/lost
Δt	Time step
ΔT	Temperature difference
ΔT_s	Temperature difference between the slab surface and autoclave/oven air temperature
ΔT_{ss}	Steady-state temperature difference between the slab surface and autoclave/oven air temperature
Δz	Distance between adjacent through-thickness measurement points
$\Delta\zeta$	Distance between adjacent through-thickness measurement points (non-dimensional)
λ	DiBenedetto equation material constant
μ_min	Minimum viscosity
ρ	Density
ρ_f	Fibre density
ρ_r	Resin density
ζ	Non-dimensional through-thickness coordinate
ζ_e	Effective non-dimensional through-thickness coordinate

List of Abbreviations

0D	Material point (simulation based) or measurement point (sensor based)
1D	One-dimensional
2D	Two-dimensional
3D	Three-dimensional
ACEE	NASA Aircraft Energy Efficiency Program
ACMA	American Composites Manufacturers Association
ACP	NASA Advanced Composites Project
AFP	Automated Fibre Placement
AI	Artificial Intelligence
AIM-C	DARPA Accelerated Insertion of Materials – Composites
ASTM	American Society for Testing and Materials
ATCAS	NASA Advanced Technology Composites Aircraft Structures
BC	Boundary Condition
BIM	Building Information Model (Architectual, engineering and construction domain)
BSI	Bubble Severity Index
CAD/FEA	Computer Aided Design / Finite Element Analysis
CAHCD	Computer Aided Heating Cycle Design
CCA	Canadian Composites Alliance
CCA	Common Component Architecture (COMPRO Simulation Software)
CCM	Continuous Cure Method
CCM9.2	CCMRD Project 9.2
CCMRD	The Canadian Composites Manufacturing R&D Inc.
cdmHUB	Composites Design and Manufacturing HUB (Purdue University)
CDSS	Clinical Decision Support System (Health sciences domain)
CFD	Computation Fluid Dynamics
CFRP	Carbon Fibre Reinforced Polymer
CHILE	Cure Hardening Instantaneous Linear Elastic
CK	Cure Kinetics
CMH-17	Composites Material Handbook-17

CMT Inc.	Convergent Manufacturing Technologies Inc.
CPA-TA	Composites Producibility Assessment – Thermal Assessment (plug-in)
CPT	Cured Ply Thickness
CRN	Composites Research Network
CTRC	Composites Translational Research Centre
DARPA	Defense Advanced Research Projects Agency
DFM	Design for Manufacturing
DDM	Direct Differentiation Method
DOC	Degree of Cure
DOE	Design of Experiments
DoIC	Degree of Intimate Contact
DOT	Design Optimization Tool
DOX	Degree of Crystallization
DP	Drill point
DSC	Differential Scanning Calorimetry
EBM	Evidence Based Medicine (Health sciences domain)
EC	Expected Cost (ETPM factory ontology)
EMMC	European Materials Modelling Council
EMMO	European Materials Modelling Ontology framework
ETPM	Equipment–Tool–Part–Material (ETPM factory ontology)
FAA	Federal Aviation Authority
FD	Finite Difference
FE	Finite Element
FEP	Foundational Engineering Problem
FERUM	Finite Element Reliability Using Matlab
FI	Flow Index
FPQ	First Part Qualification
GA	Genetic Algorithm
GFRP	Glass Fibre Reinforced Polymer
GI	Design-gate Index (ETPM factory ontology)
HR	Heat of Reaction
HTC	Heat Transfer Coefficient

IACMI	Institute for Advanced Composites Manufacturing Innovation
ICM2	USAF Integrated Computational Methods for Composites Materials
ICME	Integrated Computational Materials Engineering
IIOT	Industrial Internet of Things
IP	Intellectual Property
IR	Infrared
ISED	Ministry of Innovation, Science and Economic Development Canada (Government of Canada)
KBE	Knowledge Based Engineering
KPC	Knowledge in Practice Centre
KPD	Knowledge in Practice Document
KTA	Knowledge to Action (Health sciences domain)
M&P	Material and Process
M&S	Modelling and Simulation
MC	Monte Carlo approach
MDM	Material Deposition Management
MDO	Multidisciplinary Design Optimization
MGI	Materials Genome Initiative
MRCC	Manufacturer Recommended Cure Cycle
MRL	Manufacturing Readiness Level
NASA	National Aeronautics and Space Administration
NCAMP	NIAR National Center for Advanced Materials Performance
NCC	National Composites Centre (University of Bristol)
NDA	Non-Disclosure Agreement
NIAR	National Institute for Aviation Research (Wichita State University)
NIST	National Institute of Standards and Technology
NPD	New Product Development
NRC-IRAP	Industrial Research Assistance Program of the National Research Council Canada
NSERC	Natural Science and Engineering Research Council of Canada
OOA	Out-of-Autoclave
PCM	Probablistic Collocation Method
PDC	USAF Processing for Dimensional Control
PPV	Pre-production Verification

QM	Quality Management
QPA	Qualitative Process Automation
R&D	Research and Development
RDCS	Robust Design Computational System
RI	Risk Index (ETPM factory ontology)
RSDM	Residual Stress and Dimensional Control Management
RTM	Resin Transfer Moulding
SAMPE	Society for the Advancement of Material and Process Engineering
SCAI	Fraunhofer Institute for Algorithms and Scientific Computing
SFU	Simon Fraser University
SHMPC	Shrinking Horizon Model Predictive Control
SME	Small and Medium sized Enterprise
TBD	To Be Determined
TC	Thermocouple
TM	Thermal Management
TRL	Technology Readiness Level
TRUST	DARPA Transition Reliable Unitized STructure
UBC	The University of British Columbia
UD	Unidirectional
USAF	US Air Force
USD	US Dollar
USPTO	US Patent and Trademark Office
VARTM	Vacuum Assisted Resin Transfer Moulding
VMAP	Virtual Material Modelling in Manufacturing
WD	Western Economic Diversification Canada (a federal department of ISED, Government of Canada)

Glossary

Advanced manufacturing	Refers to the development and adoption of emerging innovation/ technology that establishes new ways to: • Manufacture existing products and enhance existing processes • Manufacture new products from new advanced technologies • Develop cost-efficient ways of working (eg. new business models, integrating all parts of the value chain)
'Building block' approach	In this approach, risk is incrementally assessed in the scale-up of part size and complexity. Material and process (M&P) variabilities are evaluated at lower scales (eg. coupon level). While at higher scales (eg. production scale structures), load paths and structural designs are verified. This approach involves three complementary engineering design activities: • Material qualification • Structural certification • Production approval
Computational thinking (simulation based thinking)	A problem solving process where computational skills (eg. thinking logically, algorithmically, and recursively), can be used to express solutions in a manner than can be actioned effectively by human intervention or machine.
Cure window (manufacturing cycle)	The allowable range of temperature, pressure, and vacuum values. These limits are usually defined as process requirements.
Development design cycle	The key design phases in new product development (NPD), particularly for complex engineering systems, including: • Conceptual design • Preliminary design (trade study) • Detail design • Production
Effective heat transfer coefficient	The heat transfer coefficient applied to surface boundaries that include lumped bagside and/or toolside effects. These effects include: bagging and consumables, tool size effects, tool substructure and heat transfer due to convection (eg. autoclave airflow) and radiation (eg. autoclave wall, rack effects).

Equivalent heat transfer coefficient

The effective heat transfer coefficient applied to surface boundaries that include deconvoluted bagside and/or toolside effects.

In this thesis, the reported equivalent heat transfer coefficients refer to the tool surface boundaries. These boundary condition inputs have been deconvoluted to account for tool size effects:

- *Equivalent-1D*: the effective heat transfer coefficients applied as boundary condition inputs for RAVEN-1D thermal analyses
- *Equivalent-3D*: the effective heat transfer coefficients applied as boundary conditions inputs for COMPRO-3D thermal analyses where no tool substructure has been modelled

ETPM factory ontology (*Knowledge in Practice*)

A systems level description of manufacturing problems relating to the physical factory and part producibility. The ETPM factory ontology consists of four classes and two concepts:

- Equipment (E)
- Tool and consumables (T)
- Part (P)
- Material and process (M)

- *Factory*: F = <E, T, P, M>
- *Producibility*: O = *fn*<E, T, P, M>

Note: Angle brackets denote a collection of classes.

Generic technology (innovation management)

Refers to the breadth of impact in terms of the potential economic and/or societal benefits across multiple industrial sectors.

Knowledge (*Knowledge in Practice*)

In this thesis, a distinction between experience based knowledge and science based knowledge is made:

- *Experience based knowledge* ('know-how'): an understanding of potential outcomes and their relationships that is founded on pragmatism and experience accumulated over time in individual programs, companies and in the industry more broadly
- *Science based knowledge* ('know-why'): an understanding of potential outcomes and their relationships, based on the important processing physics, that is mature enough to be codified using the appropriate governing laws and constitutive equations

In the context of *Knowledge in Practice*, knowledge refers to the systematic use of science based knowledge in composites manufacturing practice.

Knowledge in Practice

A framework for formalizing effective and low risk science based composites manufacturing practice and the process of knowledge translation.

It should be noted that the implementation of this framework, as in the development of a knowledge management/decision support tool, is beyond the scope of the research work presented in this thesis.

Manufacturing outcomes (*Knowledge in Practice*)

Outcomes represent the range of response/sensitivity to factory system attributes. Those that fail to satisfy manufacturing requirements are known as defects.

In this thesis, manufacturing outcomes are defined as:

- Process parameter outcomes
- Material structure outcomes
- Material performance outcomes

Current practice appears to track an *ad hoc* mix of these outcome types to link material properties to the state of a material and to ensure acceptable part quality.

Material deposition management

This theme deals with the steps primarily involved in moving material into the correct position on the tool or with combining fibre, resin and other constituents in-situ on tools.

Material equivalency

The commonality of material level properties at all scales of the 'building block' (eg. coupon level to production scale structures) in terms of *chemical–physical–mechanical* states (eg. DOC/DOX, fibre volume fraction, residual stresses).

Material qualification

An engineering design activity that relates to the determination of material level properties that will be used in the structural design and certification.

Modelling & simulation

The use of multiphysics models. A common perception is that simulation validity is related to complexity (Poursartip's law: the validity of a computational model is directly proportional to the size of the screen and number of colours). The essence of modelling is simplication, but without the loss of the important processing physics.

The development of these *enabling* software tools, that are good enough to capture (eg. codify knowledge) and exercise the science base, is currently seen as the ultimate level of translational research.

Ontology (knowledge engineering/ information science)

An ontology is a formal representation of knowledge within a domain of interest. Relationships are expressed as '*has-a*' or '*use-a*' (eg. the ontological description of a tiger may be that it *has a* relationship with Asia, the continent in which it lives).

In this thesis, an object-oriented approach is used to define the types, properties, and relationships of the objects (entities) of interest that exist for composites manufacturing domain knowledge. The following terms, related to object-oriented programming, are used:

- *Class/concept*: definition for creating an object
- *Attributes*: characteristics or properties that describe an object
- *Relations*: connections or constraints between objects
- *Instance*: an object that is created from a class/concept
- *Collection*: a set of classes/concepts or objects

Outcomes taxonomy (*Knowledge in Practice*)	A structured approach to classify a hierarchy of manufacturing outcomes for any given manufacturing cycle, or to capture a lack of knowledge. In this thesis, the outcomes taxonomy presented extends prior work to systematically identify imperfect composites manufacturing knowledge (eg. epistemic uncertainty), using defect taxonomies.
Part producibility (design for manufacturing)	Design for manufacturing (DFM) is the general engineering practice of designing products with manufacturing in mind, in terms of cost and the ease in which the products are made. In this thesis, part producibility refers to the capability of the manufacturing process to produce parts of acceptable quality (eg. meet engineering, manufacturing, regulatory requirements), repeatably and robustly. A robust process is where outcomes are insensitive to variabilities of manufacturing choices selected (eg. equipment, tool, material, part).
Practice (*Knowledge in Practice*)	In this thesis, practice refers to any manufacturing and/or decision making activity that occurs during *any* stage of the development design cycle (eg. conceptual design to production). Two types of manufacturing problems are identified: • *Factory*: building up the capability of the physical factory • *Part Producibility*: acceptable part quality In the context of *Knowledge in Practice*, practice refers to the systematic use of science based knowledge to reduce composites manufacturing risk, cost, and development time.
Production approval	An engineering design activity that ensures that the material qualification and structural certification steps are properly linked once the structure enters production.
Quality management	This theme concerned with managing changes in the physical response of parts/tools when the resin is predominantly in a liquid phase (eg. pre-gelation, pre-solidification) and the prevention of manufacturing defects.
Radical innovation/technology (innovation management)	Refers to the depth of impact in terms of the potential for very substantial improvements to product performance (eg. 5 – 10 times) and/or production costs (eg. 30 – 50%).
Residual stress & dimensional control management	This theme relates to management of internal stresses that occur as the material undergoes differential thermal and physical phase change volume changes and viscoelastic property development.

Risk (manufacturing)

The probability (chance) and/or cost of undesirable outcomes or an inability to manage uncertainty effectively. Manufacturing risk can lead to:

- Technical issues
- Program/schedule delays
- Cost overruns

Science based ventures (innovation management)

Ventures that seek to profit from the participation in both the creation and advancement of science (eg. advanced materials, bio/nanotechnology). Science based ventures face high commercialization barriers/challenges given the prolonged periods of technological and market uncertainty experienced.

Structural certification

An engineering design activity that relates to the acceptance of the *as manufactured* structure as being able to sustain the necessary loads and other service conditions determined by engineering, manufacturing, and regulatory requirements.

Taxonomy (knowledge engineering/ information science)

A hierarchical system of classification that captures simple superclass/subclass (eg. parent/child) relationships of the objects (entities) of interest. Relationships are expressed as '*is-a*' (eg. the taxonomy of a tiger is that it *is a* subtype of cat).

Technology-market matching (innovation management)

A process of matching/prioritizing promising technologies for a given market application and/or an appropriate target market for a given technology. Technology performance, market viability and the innovation ecosystem are factors that may be considered in this matching process.

Technology modularity-maturity (innovation management)

As defined in relation to manufacturing strategy/sourcing decisions:

- *Technology modularity*: refers to the ease in which research and development (R&D), and production activities can be separated
- *Technology maturity*: relates to the evolution of a technology in terms of further opportunities to significantly enhance product performance attributes

There are four types of manufacturing-innovation relationships:

- Process-driven innovation (low modularity, low maturity)
- Process-embedded innovation (low modularity, high maturity)
- Pure process innovation (high modularity, low maturity)
- Pure product innovation (high modularity, high maturity)

Themes (*Knowledge in Practice*)

Describe the key components of all composites manufacturing processes. Themes represent the *time–temperature–pressure–vacuum* history, which is traditionally is used to define a manufacturing cycle. There are four processing themes:

- Thermal management
- Material deposition management
- Quality management
- Residual stress and dimensional control management

Thermal management	This theme is concerned with managing the thermal response of materials in storage/handling or parts/tools when they are subsequently heated.
Thermal profiling	Experimental thermal profiling is a current typical practice in composite manufacturing where part/tool temperatures and temperature rates are empirically measured using thermocouples. This activity is performed to ensure that all material points in the part of interest satisfy the cure window with respect to: • Minimum/maximum heat up and cool down rates • Length (duration) of temperature holds
Thermocouple failures (sensor)	Thermocouple failures in experimental thermal profiling are common. In this thesis, a distinction between apparent and real failures is made: • *Apparent failure*: failure to satisfy process specifications that can be attributed to sensors that provide invalid measurements • *Real failure*: true deviation from process specifications that results in manufacturing defects and the decision to scrap parts
Uncertainty (modelling & simulation)	In this thesis, a distinction between uncertainty and error is made: • *Aleatory uncertainty*: associated with inherent variability • *Epistemic uncertainty*: unknowns due to a lack of knowledge • *Acknowledged errors*: explicit assumptions and/or simplifications (eg. modelling practices) • *Unacknowledged errors*: mistakes and/or blunders (eg. using the wrong material model) Process requirements, such as material and process specifications, are typically used to manage *aleatory uncertainty*. Imperfect knowledge or *epistemic uncertainty* can be managed by increasing the understanding of manufacturing outcomes and their interactions (eg. *process–structure–performance* relationships).
Uncertainty (innovation management)	As defined in terms of commercialization opportunities/risks: • *Technological uncertainty*: relates to the feasibility of an innovation idea and/or the economic viability of scaling (eg. from primary research to production) • *Market uncertainty*: exists if the innovation idea cannot sufficiently meet market needs, where the market opportunity is not obvious/cannot be guaranteed, or where competitors are working on alternative solutions

Uncertainty quantification (modelling & simulation)

An emerging discipline that relates to the characterization of modelling and simulation uncertainties. There are four key aspects of uncertainty quantification (UQ) that can be used to manage uncertainty to establish an 'evidence of credibility' in a computational model:

- Identification and classification
- Ranking
- Propagation (probablistics or uncertainty analysis)
- Management

It should be noted that uncertainty propagation is beyond the scope of the research work presented in this thesis.

Value chain position

Relates to where an innovation idea contributes value within the activities between the raw material supplier and the end consumer:

- *Upstream position*: many intermediaries exist between the innovation idea and the end consumer (eg. further away)
- *Downstream position*: few/none intermediaries exist between the innovation idea and the end consumer

Value creation/capture

Relates to the actions pursued by ventures in seeking to profit from an innovation idea:

- *Value creation*: enhancing the market attractiveness of an innovation idea (eg. making products/services more valuable)
- *Value capture*: appropriating value from an innovation idea (eg. generating revenue and/or profit)

Verification & validation (modelling & simulation)

In this thesis, a distinction between computational model verification and validation is made:

- *Verification*: confirms the implementation of a computational model to ensure that it represents the mathematical model and equations used to describe it (requirements are met)
- *Validation*: demonstrates the accuracy of a computational model, in the context of its intended use, to check that it represents the physics of the problem and the 'reality of interest' (needs are satisfied)

Workflows (*Knowledge in Practice*)

A set of steps/procedures that are intended to provide to guidance in manufacturing and/or decision making activities:

- *Standard workflows*: are intended to formalize practices where the manufacturing science base exists, the focus is to provide guidance using manufacturing simulation as an enabling tool (eg. design activities/decisions relating to thermal management)
- *Complex workflows*: are intended to reduce the level of effort in practices where the existing manufacturing science base is not sufficiently mature to support production scale problems, the focus is to provide guidance using simulation based thinking and/or checklists (eg. design activities/decisions relating to porosity management)

Acknowledgements

This work would not have been possible without the support of my family, friends, and colleagues to whom I wish to express my heartfelt thanks.

I am sincerely grateful to my supervisor, Dr. Anoush Poursartip, for his enthusiasm, technical guidance and insights, support for this project and my growth as a researcher. I would also wish to express my gratitude to Dr. Elicia Maine for her energy, passion, and academic support over the course of my PhD. Working with you both has been an absolute privilege and I thank you both for the tremendous opportunities you have provided me and have encouraged me to pursue. I also wish to acknowledge Dr. Karl Nelson, from The Boeing Company, for his mentorship, technical guidance, and persistent encouragement for which I am indebted.

I would like to thank Dr. Anoush Poursartip, Dr. Goran Fernlund and Dr. Reza Vaziri for the opportunity to be a member of the Composites Research Network. I have truly appreciated the support and friendships with current and past members of the group. Special thanks to my colleagues Ms. Suzana Topic, Dr. Navid Zobeiry, Dr. Christophe Mobuchon, Dr. Casey Keulen, Mr. David Roughley, Dr. Kamyar Gordnian, Dr. Leyla Farhang, Dr. Sanjukta Chatterjee, Dr. Mina Shahbazi, Dr. Dan Lussier, Ms. Chao Li, Mr. Andrew Stewart, Mr. Bryn Crawford, and Mr. John Park.

I would like to acknowledge all members and financial sponsors of the Composites Research Network. My PhD experience has also been greatly enhanced by the financial support of The University of British Columbia Four Year Fellowship and Public Scholars Initiative.

For industrial guidance and feedback, I would like to thank Dr. Bill Lyons, Dr. Karl Nelson, Mr. Kurtis Wilden, Mr. Mike Thompson, Mr. Geoff Butler, Mr. Robert Courdji, Ms. Amy Bahe and others from The Boeing Company, and my former colleagues from Boeing Australia. Additionally, I am extremely appreciative of the prompt technical support and helpful discussions from Dr. Anthony Floyd, Dr. Alireza Forghani, Mr. Alastair McKee, Mr. Martin Roy, Mr. David Van Ee, and the late Corey Lynam, from Convergent Manufacturing Technologies Inc. A special note of appreciation to the SMEs, particularly the three technical experts, who graciously gave their time for the preparation of the case studies presented in Sections 3.2.2 and 3.2.3 of this thesis.

Many thanks are owed to my supportive friends, both near and far. Thank you especially to Karl and Mary Nelson, Geoff Butler and Lin Chen, Brenda Wilson, Amy Walker, Breanna Mitchell, Jessica Bilkey, my GCSTC 2015 cohort peers, Ssu Yuan (Chua) Nolan, Lil Cheong, Rebecca Wu, and Carla Cher. And finally, I would like to thank my wonderful parents, Gus and Margaret, my sister Giulia and my brothers David and Michael, for their unconditional love and support.

Dedication

To my parents

'*Knowing in part may make a fine tale,*
but wisdom comes from seeing the whole.'

-*Ed Young* (*Seven Blind Mice*)

Chapter 1: Introduction

There is an unprecedented use of advanced composites materials, particularly fibre reinforced polymers, in increasingly more sophisticated end products at higher production volumes [1–6]. For example, the aerospace industry is considered an early adopter of advanced composites materials and in recent years, all major aerospace original equipment manufacturers (OEMs) have invested significantly in this technology. Large and complex primary fuselage and wing structures of modern commercial aircraft, such as the Boeing 787 Dreamliner and 777X, Airbus A350 XWB and Bombardier CSeries, are now fabricated from carbon fibre reinforced polymers (CFRP) [7–10]. The use of advanced composites materials in structural applications is also rapidly growing in other mass market industries, such as automotive, alternative energy and energy storage, as well as high performance consumer products [6].

1.1 The Growth of Advanced Composites Materials

A good measure of the growth of advanced composites materials is in the demand for CFRP since the commercialization of carbon fibre in the mid 1960s. Since then, the US composites industry has grown 25 times larger, compared with the steel and aluminum industries which have grown only 1.5 times and three times over the same period respectively [5]. From 2000 to 2017, the global market growth of carbon fibre has risen from 15.5 metric kilotons to 70 metric kilotons as shown in Figure 1-1 (a) [1–6]. The demand for carbon fibre is expected to reach 95 metric kilotons by 2019 [6]. Innovation is driving this growth, with the demand for composites end products expected to reach $113.2 billion (USD) by 2022 [6].

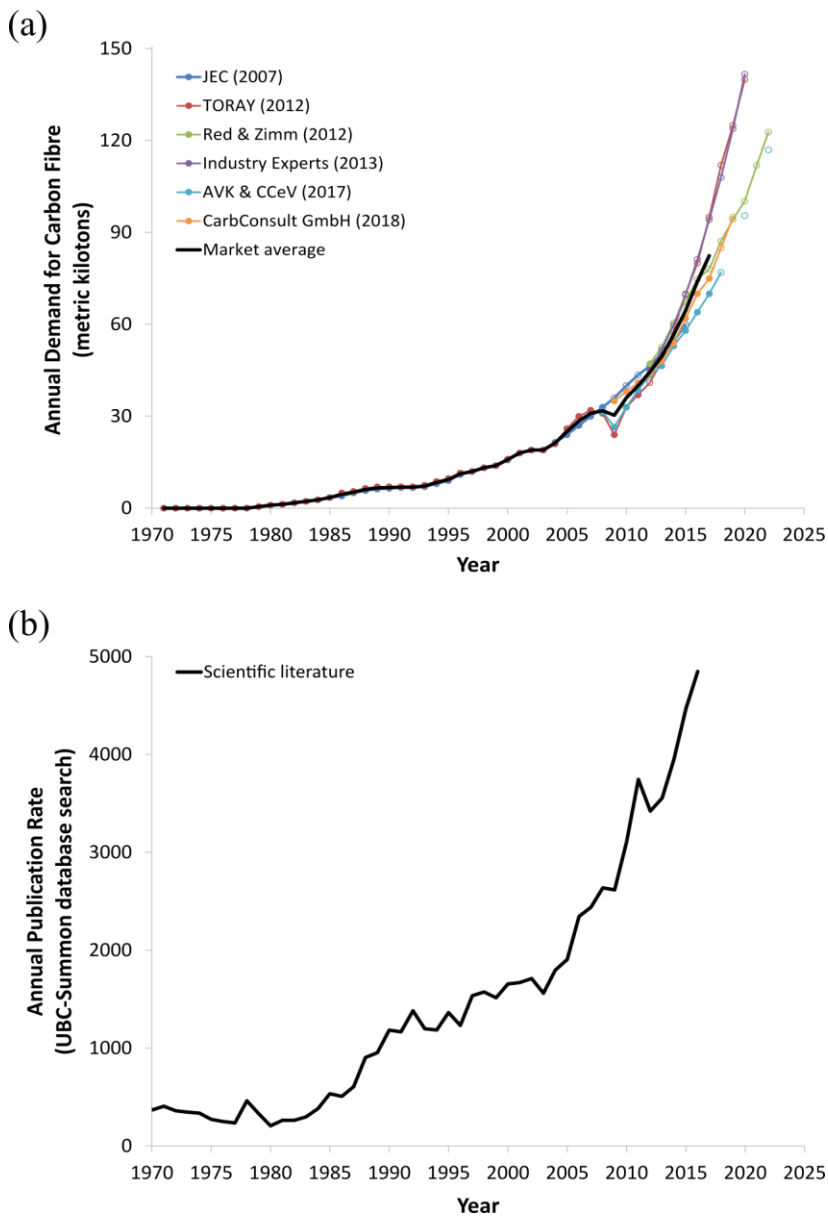

Figure 1-1: The growth in market demand for carbon fibre compared to the growth of composites research: (a) market growth of carbon fibre and (b) publication rate of scientific literature. Annual market data is adapted from references [1–6]. Annual publication rate is determined by using a keyword search of the UBC-Summon database [11] as a proxy, with search terms: "CFRP", "carbon fibre reinforced polymer" and "carbon fibre reinforced plastic". Note: Closed symbols represent actual market data and open symbols represent estimated market data.

Significant opportunities exist to improve the quality, cost and yield of composites end products given the growth of scientific research in composites manufacturing. The number of scientific papers published between 1968 and 2015 is presented in Figure 1-1 (b)[1] and shows that the rate of primary scientific research appears to be keeping pace with the growth of the composites industry. The rate of new papers published has increased by over 10 times within the past 35 years, equating to over 250 new papers per month. With a current backlog of over 60, 000 papers, this data also highlights the increasing difficulty to keep up with all advances in the state of the art.

1.2 Challenges Facing the Composites Industry

There are many challenging problems when dealing with the increasing composites manufacturing risk associated with increasing product size and complexity, and production scaling [12–14]. Issues concerning unanticipated manufacturing difficulties, late engineering design changes, program delays in bringing products to market and significant cost overruns can be traced back to an inability to appropriately identify this risk upfront in the program development design cycle, such as conceptual design [15–17]. Traditionally, empirically based practices or 'know-how' have been used to deal with this risk and uncertainty. These practices rely strongly on engineering judgement, experience, and methods of 'trial and error'. Additionally, with many composites experts now approaching retirement, even the largest and most experienced manufacturers are facing daunting technology transfer, knowledge management, and workforce development challenges within their own organizations and across their supplier networks.

[1] This figure was compiled based on a basic keyword search, using the Summon meta-search tool [11] via The University of British Columbia (UBC) library as a proxy, with search terms: 'carbon fibre reinforced polymer', 'carbon fibre reinforced plastic' and 'CFRP'.

While the use of manufacturing science to create value and manage risk is recognized as a promising strategy by large composites manufactuers, key barriers for its widespread adoption exist. Namely, the perception is that composites manufacturing science is a niche discipline, and the enabling technologies available are too complex for non-experts to use fast and effectively [18]. For composites SMEs, there are additional challenges: 1) knowing that the manufacturing science base exists; 2) having the research and development (R&D) resources and funding to be able to access this science; and 3) accepting and managing the uncertainty associated with such innovations.

For instance, the composites industry in Western Canada predominantly consists of small and medium sized enterprises (SMEs), with a small but significant group of larger companies [19]. Many of these SMEs lack the resources to undertake R&D, thus greatly limiting their ability to grow through innovation. Survey work conducted in 2012 by Roughley [19] found that over 50% of the surveyed companies in Western Canada undertake little or no R&D activities (eg. < 5% of revenue is reinvested)[2].

A comparison of typical value creation attributes for large and small composites manufacturers (eg. aerospace OEM and supplier network vs. industrial SME), based on the value creation model by Maine and Garnsey [20], is presented in Table 1-1.

[2] In the context of the survey work conducted, the definition of R&D is any activity that is not overhead or contributing directly to production. SMEs may consider materials testing and characterization or the introduction of a new piece of equipment as an R&D activity.

Table 1-1: Comparison of typical value creation attributes for large and small composites manufacturers[a].

	Aerospace systems integrator[b] (eg. OEM, Tier 1)	**Aerospace supplier network[b] (eg. Tier 2, material supplier)**	**Non-aerospace[c] (eg. industrial SME)**
Size of firm			
Size (employees)	Multinational (~85,000 employees)	Large (< 500 employees)	Small (~50 employees)
Size (R&D[d] spend)	High	Mid	Low/None
Current/Target markets			
Number of markets	Single (commercial jetliner)	Single (commercial jetliner)	Multiple
Product size & complexity (proxy for cost & performance)	Large primary structure (eg. fuselage, wing) Prepreg CFRP[e]/epoxy (autoclave cure) AFP[e]/forming	Small primary/secondary structures (eg. wing spars, floor beams) Prepreg CFRP[e]/epoxy (autoclave cure) Hand layup	Semi-complex structures (eg. sandwich structures) GFRP[e]/vinyl ester (room temp. cure) Wet (spray) layup
Production volume (proxy for size of market)	5 models/19 variants (~10 shipsets/month)	N/A	37 models/48 variants (production rate unknown)
NPD[f] time frames	Slow (210+ months)	N/A ('build to print')	Moderate/Fast (12 – 24 months)
Market uncertainty			
Position in value chain	Downstream	Midstream	Midstream/Downstream
Negotiating power within value chain	High	Low	Low
Regional/National support (within Canada)	N/A	Yes	Yes
Technological uncertainty			
Risk tolerance for M&P[g] substitution	Low (certification costs)	N/A	Mid/High
Regulatory requirements	High	High	Mid
Access to manufacturing science	High (early adopter)	Mid	Low (prior to partnering with CRN)

[a] These attributes are based on the value creation model [20] (Maine & Garnsey, 2006).
[b] OEM: Original Equipment Manufacturer; From case studies & reports: [21] (Tang & Zimmerman, 2009), [22] (CSRT, 2014), [23] (Slayton & Spinardi, 2015).
[c] SME: Small & Medium sized Enterprise; From reports: [19] (Roughley, 2013), [24] (CRN, 2016)
[d] R&D: Research & Development. The definition of R&D is any activity that is not overhead or contributing directly to production.
While large companies may make distinctions in terms of R&D spend for NPD or for product/process improvements, small companies are less likely to do so.
[e] CFRP: Carbon Fibre Reinforced Polymer; GFRP: Glass Fibre Reinforced Polymer; AFP: Automated Fibre Placement
[f] NPD: New Product Development
[g] M&P: Material & Process

1.3 Translational Research Efforts in Composites Manufacturing

Over the past 30 years, there have been tremendous advances in composites manufacturing research and the opportunities for innovation are continuing to develop. Most efforts to reduce risk in composites manufacturing practice and enhance the competitiveness of composites end products have focused on the emergence of three key research thrusts:

- *Automation*: The use of automated equipment and robots to reduce touch labour costs, improve repeatability and achieve production efficiencies.

- *Simulation*: The use of multiphysics based models, as exercised in software, to describe the response of the manufacturing system, such as virtual manufacturing, process modelling and Integrated Computational Materials Engineering (ICME).

- *Production analytics*: The promise of 'big data' given improvements in enabling sensor technologies and machine based learning algorithms, and the acquisition and synthesis of vast amounts of production data, such as the Industrial Internet of Things (IIOT).

For the purposes of defining a common framework, it is convenient to consider all composites manufacturing processes in terms of four broad themes. These themes describe the key components or phases of the *time–temperature–pressure–vacuum* history, which is traditionally used to define the upper and lower limits of a manufacturing cycle, also known as the cure window.

A brief description of these themes is given here:

- *Thermal management* covers the thermochemical management of materials in storage or handling and the subsequent thermal response of parts and tools during cure[3].

- *Material deposition management* deals with the steps primarily concerned with moving material into the correct position on a tool (eg. automated robotic placed prepreg tape on a tool, resin infusion of a fabric preform draped on a tool).

- *Quality management* is concerned with managing changes in the physical response of parts and tools during the pre-gelation and pre-solidification stages of the process cycle (eg. the prevention of manufacturing defects, such as wrinkling and porosity).

- *Residual stress and dimensional control management* relates to controlling the changes in the mechanical response of parts and subsequent geometric changes when removed from tools or when parts are post cured (eg. due to the development of internal stress as the material undergoes differential thermal and phase change volume changes, and the matrix gains elastic memory due to viscoelastic property development).

Numerous research teams are working on advancing the manufacturing science or 'know-why' underlying each of these themes, as summarized in Table 1-2, and it is noted that a greater depth of fundamental understanding of the science base exists in some themes compared to others.

[3] For thermoplastic matrices, the concept of cure management is replaced with crystallization/melt management.

Table 1-2: High-level assessment of the current science base for composites manufacturing processes.

Theme	Theme description	Sub-theme example	Knowledge maturity[a]	Remarks	Ref.
Thermal management	Managing the thermochemical & thermophysical evolution of material properties & the thermal response of parts/tools	Cure	*Excellent*	Multiscale modelling capability exists to predict outcomes, such as the thermal response of thermoset epoxy prepreg materials (eg. process maps to complex numerical models). Practical prediction heat transfer boundary conditions for autoclaves/ovens is yet to be realized and remains the greatest source of uncertainty. Fundamental research attention now focuses on the development & characterization of next generation material systems.	[25–29]
Material deposition management	Managing the placement of a combination of fibre, resin & other constituents on tools	AFP[b] Forming RTM[b] VARTM[b]	*Poor* *Poor* *Very good* *Good*	Regained fundamental research attention due to a focus on rapid & automated deposition of material for large structures. Some significant process modelling capability exists to predict outcomes, such as drape & resin fill-time.	[30–34]
Quality management	Managing changes in the physical response of parts/tools	Wrinkling Porosity	*Good* *Good*	Regained fundamental research attention due to a focus on large structures & out-of-autoclave materials. The capability to predict/quantify outcomes, such as wrinkling & porosity is an active area of research.	[31,35]
Residual stress & dimensional control management	Managing the development of internal stresses in materials & the mechanical response when parts are removed from tools or are post cured		*Very good*	Robust multiscale modelling/manufacturing simulation capability exists to predict outcomes, such as process-induced residual stress & spring-in angle (eg. complex 3D numerical analyses). Complex cycles involving coupled flow/stress, viscoelastic effects & part/tool interaction are not fully understood. Fundamental research attention now focuses on above, as well as methods to reduce computational cost.	[36–38]

[a] Our depth of understanding is classified as follows:
Excellent: The knowledge base is codified by manufacturing science ('know-why') and robust manufacturing simulation capabilities exist.
Very good: The knowledge base is codified, with a focus on maturing existing manufacturing simulation capabilities.
Good: The knowledge base is maturing, with significant advances in codifying the manufacturing science.
Poor: The knowledge base is dominated by manufacturing experience ('know-how'), with a focus on developing the manufacturing science.

[b] AFP: Automated Fibre Placement; RTM: Resin Transfer Moulding; VARTM: Vacuum Assisted Resin Transfer Moulding

Composites translational research centres (CTRCs) have been developed in composites manufacturing clusters around the world to support regional and national competencies in composites innovation. Table 1-3 compares leading CTRCs located in North America and Europe, highlighting differences in their respective research governance models. All centres share competencies in composites manufacturing science, although these specific competencies differ in translating primary research and technological advances into production scale manufacturing processes. Most involve a tier-membership model from industrial partners and are also supported by government funding. The Canadian, US and UK CTRCs are typically based in leading universities and government research centres, while the German CTRC is an independent not-for-profit organization with strong industrial funding and connection to affiliated universities.

One of the key roles of the Composites Research Network (CRN), a CTRC based at The University of British Columbia (UBC), is to support and develop the innovation capabilities of composites SMEs based in Western Canada. It does so by promoting composites manufacturing practices based on the most rigorous science. In recognizing that the production scale problems faced by large and experienced OEMs and small composites SMEs can be solved using the same underlying science base, CRN has sought to initiate and establish a framework known as *Knowledge in Practice*. This framework is positioned to bridge the gap between scientific research and the needs of industry (see Figure 1-2). It is noted that the goals of this approach are a logical progression of the maturity in this domain. For example, the formalization of the use of materials science in design, pioneered by Ashby [39], has led to an effective revolution in how engineers learn how to systematically select materials for mechanical design.

Table 1-3: Examples of composites translational research centres (CTRCs) in North America and Europe.

	Composites Research Network (CRN) [40]	**Institute for Advanced Composites Manufacturing Innovation (IACMI)** [41]	**National Composites Centre (NCC)** [42]	**Fraunhofer Institute for Chemical Technology (ICT)**[a] [43]
Geographic location	Canada (British Columbia)	US (Tennessee)	UK (Bristol)	Germany (Pfinztal)
Research governance	Academic research network with industrial advisory board Network of 8 universities & research centres, hosted by UBC Nodes at: UBC, U Victoria, U Alberta, U Lethbridge, McGill, Camosun College, CIC[b], CLS[b]	Not-for-profit organization with industrial leadership & academic hubs Network of 7 universities & research centres, hosted by Oakridge National Laboratory	Independent research centre with industrial leadership & academic cross-appointments at below director level Hosted by U Bristol Partnerships with other UK centres of excellence & organizations (eg. ACCIS[c], AMRC[c], CIMComp[c])	Not-for-profit organization with academic cross-appointments at institute director level Collaborations with KIT[d] (Germany) & Project Centres based at UWO[d] (Canada) & UNIST[d] (South Korea)
Established	2012	2015	2009	1994 (polymer engineering group)
Competencies	• Materials characterization • Process simulation • Structural failure & impact • Science based practice	• Composites materials & process • Compressed gas storage • Design, modelling & simulation • Vehicles • Wind turbines	• Advanced composites manufacture • Design & simulation • Digital manufacturing, automation & tooling • Materials & processes	• High performance fibre composites • Nanocomposites • Thermoplastic/thermoset processing • Foam technologies • Compounding & extrusion • Testing
Niche	Advancing manufacturing science & application while simultaneously addressing needs of Western Canada	Automotive, wind energy & energy storage markets Strategic presence in key states: TN, MI, OH, IN, KY (vehicles & compressed gas) & CO (wind energy)	Linking activities across all industrial sectors in research education and training Pilot scale facilities	Application-orientated R&D of products to pilot scale levels Research services are offered to partners (eg. product ideation, M&P development, prototype manufacture)
Key influencers/ funding sources	Western Economic Diversification Canada (WD), NSERC[e]/NRC-IRAP[e] Tier-membership model	Department of Energy (DOE) Tier-membership model	HVM CATAPULT[f], HCA[g]/ERDF[g]/BIS[g] Tier-membership model	Fraunhofer-Gesellschaft Basic research: 100% public grants Contract research: 70% private sector & 30% public sector funding

[a] The Fraunhofer ICT is one of 67 current Fraunhofer-Gesellschaft institutes and is an example of the many Fraunhofer institutes focused on composites technology.

[b] CIC: Composites Innovation Centre; CLS: Canadian Light Source

[c] ACCIS: Bristol Composites Institute (formally Advanced Composites Collaboration for Innovation and Science); AMRC: Advanced Manufacturing Research Centre; CIMComp: Centre for Innovative Manufacturing in Composites

[d] KIT: Karlsrhue Institute of Technology; UWO: University of Western Ontario; UNIST: Ulsan National Institute of Science and Technology

[e] NSERC: Natural Sciences and Engineering Research Council of Canada; NRC-IRAP: Industrial Research Assistance Program of the National Research Council Canada

[f] HVM CATAPULT: High Value Manufacturing CATAPULT

[g] HCA: Homes and Communities Agency; ERDF: European Regional Development Fund; BIS: Department of Business, Innovation and Skills

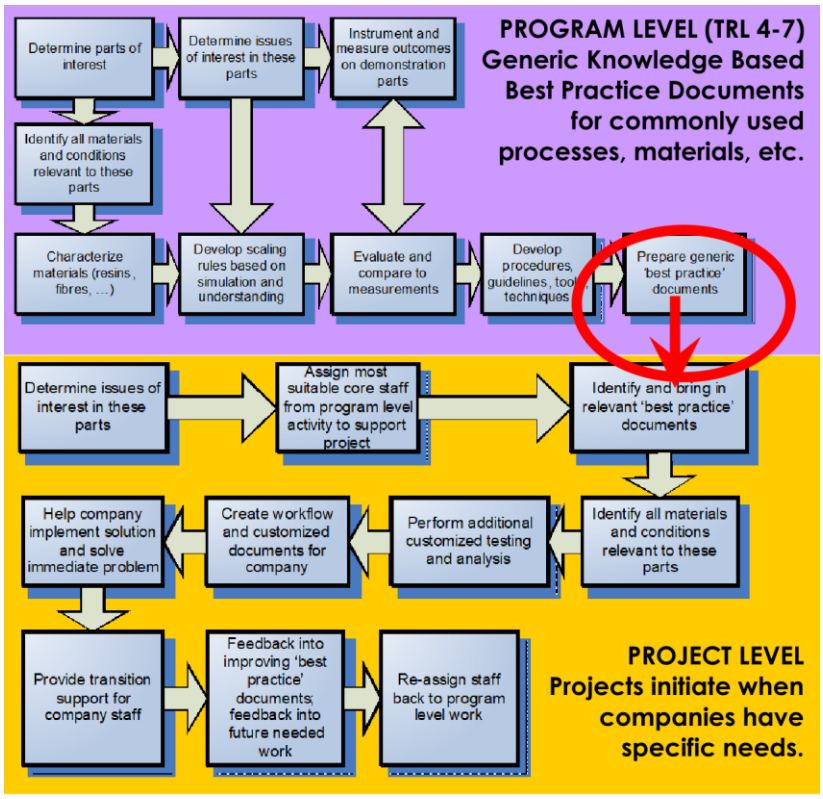

Figure 1-2: *Knowledge in Practice* conceptual workflow (figure courtesy of CRN). TRL: Technology Readiness Level.

1.4 Summary

Despite the growth of the composites industry, most manufacturing practices used to produce increasingly sophisticated composites end products at higher production volumes are empirically based and lack standardization. Issues relating to first-time quality, cost reductions and yield improvements affect both large experienced OEMs and small composites SMEs alike. While there have been tremendous advances in fundamental composites manufacturing research, as more scientific knowledge is created, its use is less obvious. It is no longer sustainable to keep adding to the science base without explicitly addressing how manufacturing practice should be changed. This suggests that a new translational research strategy is needed.

The goal of the work presented in this thesis is to develop a framework that encourages the adoption of composites manufacturing science in industrial practice to effectively manage increasing manufacturing risk. This work is initially aimed at both the composites manufacturing research community and the composites industry, including composites OEMs and SMEs, and the supplier network.

In the next chapter, a brief literature review is presented relating to: 1) strategies for overcoming commercialization barriers in science based innovations; 2) simulation based approaches for organizing domain knowledge; and 3) trends in composites manufacturing research for the thermal management of autoclave and oven cured thermoset composites to illustrate the distinction between knowledge creation and knowledge use. The research objectives and scope for the work presented in this thesis are then outlined at the end of Chapter 2.

Chapter 2: Literature Review and Research Objectives

As discussed in Chapter 1, although composites manufacturing science is recognized as a promising strategy to minimize manufacturing risk, the rate of adoption in industry has been slow and *ad hoc*. The perception is that composites manufacturing science is still a niche discipline despite the tremendous advances in scientific research.

In this chapter, first a brief review of innovation management literature relating to the unique challenges in commercializing science based innovations and the strategies to support the adoption of innovation related to advanced manufacturing is presented. This is followed by a discussion of simulation based approaches to organize domain knowledge. Application examples of conceptual frameworks that have been developed in the health sciences and engineering design domains are briefly reviewed. Next, a synthesis of previous works relating to the thermal management of autoclave and oven cured laminates is presented to demonstrate shifts in composites manufacturing research from knowledge creation to knowledge use. Thick thermoset composites studies identified in the scientific literature are introduced and discussed in terms of the underlying manufacturing science and technology bases. A subset of these studies, representative of industrial processing scenarios, are briefly reviewed. Finally, the research objectives and scope are outlined at the end of this chapter.

2.1 Innovation Management Theory for Science Based Innovations

The innovation management literature is reviewed to provide an overview of the challenges relating to the commercialization of advanced materials technologies. The key attributes of technological and market uncertainty that critically influence the ability to innovate as well as strategies to accelerate the commercialization process for this type of science based innovation are discussed.

2.1.1 Commercializing advanced materials technologies

Companies commercializing advanced materials technologies are often ventures that are attempting to profit from the development of science based innovations [20,44–46]. These ventures typically focus on the commercialization of radical generic technologies that are initiated mid-to-upstream in multiple industrial value chains [20,45]. In this context, radical innovation relates to potential ability to provide very substantial improvements in product performance (eg. 5 – 10 times) and/or the production costs (eg. 30 – 50%), and generic innovation is the potential economic and/or societal benefit across multiple industrial sectors [20,45].

Compared to high-technology innovations, such as software, science-based innovations, such as advanced materials and bio/nanotechnology, experience prolonged periods of technological and market uncertainty [46,47]. For advanced materials technologies, additional constraints exist given that product and process innovation is highly interdependent [20,47]. While established innovation management literature on the commercialization of advanced materials technologies exists, it is recent works by Slayton and Spinardi [23], and Chatzimichali and Potter [48] that have begun to rigorously discuss the implications of the interaction of product and process innovation with regard to advanced composites materials and composites manufacturing technologies.

Pisano and Shih [49] developed a technology modularity-maturity matrix to classify four types of manufacturing-innovation relationships, where technology modularity is defined as the ease in which R&D and production can be separated, and technology maturity as the evolution of a technology in terms of the opportunity to improve product performance attributes. The four relationships are: 'process-driven innovation' (low modularity, low maturity), 'process-embedded innovation' (low modularity, high maturity), 'pure process innovation' (high modularity, low maturity), and 'pure product innovation' (high modularity, high maturity). They posit that 'advanced materials fabrication' is a form of process-embedded innovation [49]. While there is a perception that advanced materials technologies are mature, this is not necessarily true in terms of their use to produce sophisticated end products at increasingly higher production volumes. In such cases, the uncertainty associated with the manufacturing technologies or process innovations required is often underestimated in the product development process [23,48–50].

Typically composites manufacturing processes are difficult to codify and thus a tremendous amount of experience based knowledge and a lack of standardization exists [23,48]. Process innovation is not easy to replicate, and subtle changes to production processes can result in unintended changes to end product attributes. The impacts of these changes to the size and complexity of end products and production scaling are not yet well understood [12–14]. Since R&D and production cannot be easily separated, the manufacturing strategy adopted can detrimentally affect the ability to innovate. According to Fuchs [51], the decision to do production offshore not only shifts the locus of knowledge but increases the likelihood that R&D will also be offshored. Once the innovation ecosystem is disrupted, it is often very difficult to reclaim and rebuild.

2.1.2 Attributes of technological and market uncertainty

Based on a value creation model developed by Maine and Garnsey [20], the attributes of technological and market uncertainty that critically influence the potential for ventures to successfully commercialize radical generic technologies are as follows:

- *Technological uncertainty* is a function of technical readiness and the difficulty in performing R&D development. Influencing factors that impact value creation include: attempting to outperform established substitute products, matching existing end product performance attributes at a lower cost, or meeting market needs when introducing a technology to a new market.

- *Market uncertainty* exists when the market opportunity is not obvious, and it cannot be guaranteed that a market can be created, or whether a technology sufficiently addresses market needs. Market perceptions and customer utility for the technology, a lack of continuity, observability and trialability of the final product during the development process, value chain positioning (eg. upstream, downstream), and the ability to identify the right application in the right market or multiple markets are influencing factors that can impact value creation. The Porter five-forces model [52] is often used to understand how a venture's value chain position and relative negotiating power can affect the ability to capture value and profit from the innovations they seek to commercialize.

The perception of risk and uncertainty has been identified as a key innovation barrier for Canadian firms [53,54].

2.1.3 Strategies for accelerating the commercialization process

Maine and Seegopaul [46] recommend the timely validation of technology readiness, market prioritization through technology-market matching, value chain positioning to maximize value capture potential, and establishing effective alliance partnerships as strategies to accelerate the commercialization process for advanced material technologies. Companies commercializing advanced materials technologies have successfully created value using a market pull strategy in cases where the market is prepared to pay a premium [46]. Typically with the commercialization of radical generic technologies, companies are more likely to create value using a technology push or technology-market matching strategy [20,46]. The technology-market matching process, as proposed by Maine and Garnsey [20], prioritizes promising technologies for a given market application and/or the appropriate target markets for a given technology.

Effective alliance partnerships can be beneficial for companies commercializing advanced materials technologies to: 1) access complementary assess, such as design and distribution capabilities; and 2) establish influence downstream in the value chain. However, these collaborations must be strategically managed [46]. For instance, when advanced materials technology is developed within a university research laboratory, an 'innovation orchard' or other type of accelerator, such as a CTRC, may be needed to get the technology to a stage where it can be usable and useful to industry [46,55]. The work undertaken by CRN to support the composites industry is an example where such an innovation ecosystem exists. Open innovation is one such approach proposed by Chesbrough [56] that fosters a willingness to access and exploit outside knowledge, and Pisano and Shih [49] recommend 'building up capabilities in manufacturing sciences' as a strategy to support innovation related to advanced manufacturing.

2.2 Development and Applications of Knowledge Systems

Design for manufacturing (DFM) and concurrent engineering have gained wide acceptance in industry. In its current form, the practice of design for manufacturing has broadened to include the 'simultaneous development of a design and supporting life cycle processes', such as product quality and perfomance, ease of manufacturing or producibility, cost and environmental design considerations [57,58]. Although design for manufacturing has streamlined the process of designing complex systems, knowledge exchange and the communication between interdisciplinary product development teams are cited as barriers to its effective use [58].

A 2011 National Defense Industrial Association (NDIA) white paper that investigated the modelling and simulation (M&S) capability needs for complex engineering systems, such as aerospace and defense, concluded that 'the impact of producibility on life cycle cost is often neglected due to the lack of validated modelling and simulation based DFM tools for manufacturing' [16]. This white paper highlighted that 'design for manufacturing needs to become a science'.

In the remainder of this section, several conceptual frameworks and simulation based approaches for organizing domain knowledge are presented. Selected application examples from the health sciences and engineering design domains are briefly reviewed.

2.2.1 Conceptual frameworks

Conceptual frameworks are analytical tools that are developed to facilitate the comprehension and organization of ideas and knowledge. Two conceptual frameworks that relate to the process of moving knowledge into action are discussed. Simulation based approaches and concepts for organizing domain knowledge are also presented.

The knowledge-to-action framework proposed by Graham *et al* [59,60] provides a model to promote the use of 'best available' evidence from clinical research in the health sciences domain. In this context, knowledge translation refers to the process of integrating the roles of 'knowledge creation and knowledge application'. On the other hand, knowledge exchange is the use of relevant and applicable knowledge to make informed decisions in health care. These works highlight the importance in defining a common nomenclature for the process of formalizing knowledge translation.

In an engineering context, Hicks *et al* [61] noted the lack of formal and consistent definitions for information and knowledge in engineering design. As a first step towards effective knowledge capture and reuse, they formalized the relationships between data, information, and knowledge and the transformation processes for decision making. This work also acknowledged that the competitive advantage of organizational knowledge is gained through 'making individual knowledge available to the entire organization' rather than based on a handful of experts or 'strategically positioned' individuals.

An ontology, based on knowledge engineering and information science, is a formal representation of knowledge within a domain of interest. Object-oriented ontologies make use of terms common in object-oriented programming. For example, classes and concepts define the attributes and relations for creating objects. Where attributes are characteristics, or properties, that describe an object, and relations describe the connections, or constraints, between objects. An instance is an object that is created from a class, and a collection is a set of classes or objects.

Gruber [62] defines an ontology as 'the specification of conceptualisations, used to help programs and humans share knowledge'. Where the conceptualization is a hierarchical decomposition of the knowledge domain of interest defined in terms of attributes and relations, and the specification formalizes the representation of this conceptualization.

In the absence of a science based understanding, simulation based thinking can be used to solve problems in a systematic and structured manner. In recent years, the term 'computational thinking' has been popularized in articles by Wing [63,64] as a fundamental skill that uses heuristic reasoning to solve problems, design systems and understand human behaviour.

2.2.2 Domain applications

Object-oriented ontologies have been used to represent domain knowledge in a range of scientific and industrial disciplines, such as health sciences and engineering design. Selected works from these domains are briefly reviewed:

- *Health sciences*: Evidence Based Medicine (EBM) refers to the practice of medicine based on the best scientific evidence and clinical experience [65]. The promise of clinical decision support systems (CDSS) to facilitate the use of evidence based medicine and improve the quality of health care quality and efficiency have been reviewed in works, such as Sim *et al* [65] and Kung *et al* [66].

- *Architectural, engineering and construction*: Building Information Modelling (BIM) is most commonly accepted as the digital representation of the physical and functional characteristics of a building and a shared knowledge resource during its life cycle. Notable works in this emerging field include Succar [67], and Taylor and Bernstein [68].

- *Engineering design*: Knowledge Based Engineering (KBE) is a research discipline concerned with the capture and reuse of knowledge in product and process engineering. Recent examples of DFM tools developed for the life cycle management of advanced composites include works by Verhagen *et al* [69–71] and Premkumar *et al* [72].

2.3 Trends in Composites Manufacturing Research for Thermal Management

A science based understanding of thermal management problems in composites manufacturing is relatively mature, as summarized in Chapter 1 (see Table 1-2). These types of problems are discussed in this section to highlight trends in composites manufacturing research in moving from knowledge creation to knowledge use. Thick thermoset composites studies identified in the literature are introduced in terms of mastering the science base for the thermal management of curing laminates and harnessing this manufacturing science in the form of simulation based DFM tools, exercised as software. A brief review of a subset of these studies, representative of industrial production scenarios, is also presented.

2.3.1 Mastering the manufacturing science

Since the mid-late 1970s, composites manufacturing research has evolved from a scientific curiosity. Early programs, such as the NASA Aircraft Energy Efficiency (ACEE) program (1975 – 1986) and the US Air Force (USAF) Processing Science for Epoxy Resin Composites program (1980 – 1984), focused on evaluating the promise of advanced composites in aerospace applications [73]. This early work established the processing science of composites as a research discipline.

Foundational work by Loos and Springer [74–76], relating to heat transfer and resin cure kinetics, has led to a comprehensive science based understanding of the thermal response of autoclave and oven cured thermoset composites. Although not exhaustive, Table 2-1 highlights contributions to this area of research that show shifts in our understanding from science based knowledge to the use of this science base in practice.

Table 2-1: Thermal management examples highlighting trends in moving from knowledge creation to knowledge use in composites manufacturing[a].
Note: Manufacturing simulation is shown as an example of an enabling technology.

Year	Contributors	Knowledge (creation) Manufacturing science	Technology Manufacturing simulation	Practice (use) Manufacturing decision making	Ref.
1983	Loos & Springer	Heat transfer/cure kinetics	CURE code		[75,76]
1980 – 1984	USAF	Processing science			[77,78]
1986 –	Campbell *et al*	Processing science			[79,80]
1989	Maffezzoli *et al*	Melt kinetics			[81]
1990	Bogetti & Gillespie	Heat transfer/cure kinetics	TGCURE code		[83–85]
1992	Mantell & Springer	Crystallization kinetics			[87]
1993	Smith & Poursartip	Heat transfer	LAMCURE code		[91]
1994	Hojjati & Hoa	Heat transfer/cure kinetics	user FD[b] method		[93,94]
1997 1994 – 1997	Johnston *et al* NASA ATCAS	Heat transfer/cure kinetics	COMPRO-2D (V1)		[99–101] [102,103]
2001	Li *et al*	Heat transfer/cure kinetics	Probabilistic analysis user FE[d]/DOT[c] software		[120,121]
2001	Antonucci *et al*	Heat transfer			[122,123]
2000 – 2004	DARPA AIM-C		Probabilistic analysis COMPRO-2D (V1)/RDCS[d]		[125–130]
2004 – 2007	Boeing		COMPRO-2D (V1)/RDCS[d]	787 Dreamliner fuselage barrel cure cycle development & optimization	[134]
2005 –	FAA/NIAR NCAMP		Hexcel 8552 characterization binder/ material models made available (2009)		[135]
2005	Ersoy *et al*	Cure kinetics			[136,137]
2007	Rasekh *et al*	Heat transfer/closed-form equations (1D)			[141,142]
2008	Dykeman & Poursartip	Cure kinetics/process maps (0D)			[143,144]
2008	Shimizu *et al*	Heat transfer	Back-calculating effective HTCs[e]		[145]

Table continued on next page

Table 2-1 continued

Year	Contributors	Knowledge (creation) Manufacturing science	Technology Manufacturing simulation	Practice (use) Manufacturing decision making	Ref.
2009	Bebamzadeh *et al*	Heat transfer	Probabilistic analysis user DDM[f] method/FERUM[f] (Matlab)		[146,147]
2010	Slesinger *et al*	Heat transfer/cure kinetics	Laminate level CK model validation methods		[148–150]
2012 –	USAF ICM2 (MGI)		COMPRO CCA[g] (V2)	GE Aviation: engine FEPs[h] Lockheed Martin: airframe FEPs[h]	[152–158]
2012 –	DARPA TRUST		Cytec (Solvay) 5320-1 characterization/ material models made available (2017)		[159]
2015 –	CMT Inc.		CPA-TA[j] for CAD[j] environments		[160]
2015	Mesogitis *et al*	Heat transfer/cure kinetics	Probabilistic analysis user subroutines/MC[k] & PCM[k] (MSC.MARC)		[161–163]
2016	Weber *et al*	Heat transfer	Fast methods for generating HTCs[e]		[167]
2016	Hunt *et al*	Cure kinetics			[168]
2017	Gordnian *et al*	Crystallization/melt kinetics			[169,170]
2017	EMMC Fraunhofer SCAI		Materials modelling/EMMO[l] Interoperability and integration (eg. VMAP[l])		[175] [176]
2018	Park *et al*	Heat transfer	Experimental/CFD[m] zone based HTCs[e]		[177–179]

[a] The work summarized in this table is not exhaustive. The contributions shown are to highlight trends in moving from science based knowledge creation to knowledge use.
[b] FD: Finite Difference method
[c] FE: Finite Element; DOT: Design Optimization Tool
[d] RDCS: Robust Design Computational System
[e] HTC: Heat Transfer Coefficient
[f] DDM: Direct Differentiation Method; FERUM: Finite Element Reliability Using Matlab
[g] CCA: Common Component Architecture
[h] FEP: Foundational Engineering Problem
[i] KPC: Knowledge in Practice Centre
[j] CPA-TA: Composites Producibility Assessment – Thermal Assessment; CAD: Computer Aided Design
[k] MC: Monte Carlo approach; PCM: Probabilistic Collocation Method
[l] EMMO: European Materials Modelling Ontology framework; VMAP: Virtual Material Modelling in Manufacturing
[m] CFD: Computational Fluid Dynamics

A modest number of works (N = 39) have been reported in the scientific literature relating to the thermal management of thick thermoset composites[4] (see Figure 2-1). Many of these studies were performed to investigate the difficulties associated with processing thick thermoset composites. Further details and synthesis of these studies is provided in Appendix A (see Table A-1). These studies are introduced to discuss the existing manufacturing science and technology bases for the thermal management of curing laminates.

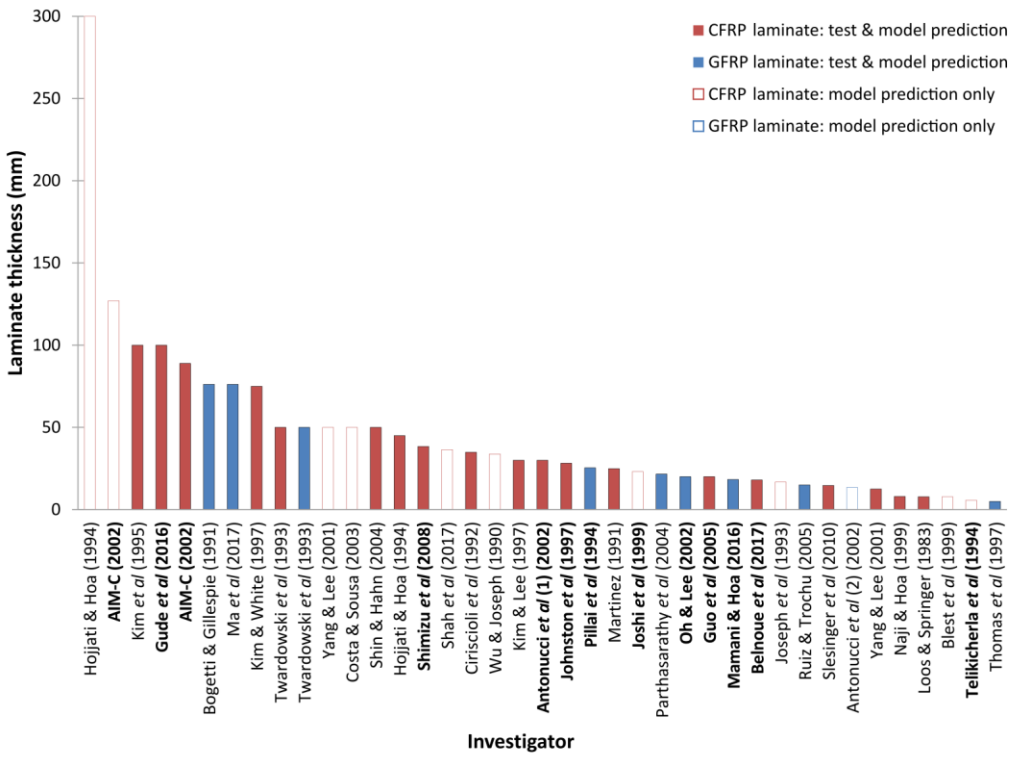

Figure 2-1: Thick thermoset composites studies identified in the scientific literature[a]. CFRP: Carbon Fibre Reinforced Polymer; GFRP: Glass Fibre Reinforced Polymer. Note: Subset of studies that consider tool thermal effects and convective heat transfer boundary conditions are shown in bold (N = 13).

[a] Studies that investigated thermoset laminates ≥ 5 mm thick are included in this survey, even though there is no consensus in the scientific literature relating to what constitutes a 'thick' laminate (refer to Appendix A.1).

[4] These studies have been identified based on a keyword search of terms 'thick laminate', 'thick-sectioned composite' and 'thick thermoset composite laminate'.

A thermochemical model is a multiphysics model that can be used to predict the internal temperature and cure advancement (degree of cure) of curing thermoset composites. There are three main components of thermochemical models for autoclave and oven processing: 1) the conduction heat transfer model; 2) the cure kinetics model; and 3) convective heat transfer boundary condition inputs. The components are briefly discussed in the following sections.

2.3.1.1 Heat transfer models

The governing heat transfer equation for autoclave and oven processing is the Fourier heat conduction equation with a heat generation rate term for the resin cure reaction, given by [180]:

$$\frac{\partial}{\partial t}\left(\rho C_{\mathrm{p}} T\right) = \frac{\partial}{\partial x}\left(k_{\mathrm{x}} \frac{\partial T}{\partial x}\right) + \frac{\partial}{\partial y}\left(k_{\mathrm{y}} \frac{\partial T}{\partial y}\right) + \frac{\partial}{\partial z}\left(k_{\mathrm{z}} \frac{\partial T}{\partial z}\right) + \rho_{\mathrm{r}} V_{\mathrm{r}} \dot{H} \tag{2-1}$$

where in Equation (2-1), ρ is the density, C_{p} is the specific heat capacity, k_{x}, k_{y}, k_{z} are the thermal conductivities, ρ_{r} is the resin density, V_{r} is the volume fraction of resin, $\dot{H}$ is the specific rate of heat generation due to the exothermic resin reaction.

The rate of heat generation can be determined from Equation (2-2):

$$\dot{H} = \frac{d\alpha}{dt} H_{\mathrm{R}} \tag{2-2}$$

where, $d\alpha/dt$ is the cure rate and H_{R} is the total amount of heat generated during a complete resin reaction.

From Table A-2, most composites thermal models consider one-dimensional (1D) heat flow in the through-thickness direction. More sophisticated two- and three-dimensional (2D, 3D) models have also been reported in the literature, such as works by Bogetti and Gillespie [83–85], Johnston *et al* [99,100], Joshi [111] and Shah *et al* [173]. It is noted that the development of these models has progressed from the use of specialized finite difference (FD) schemes and finite element (FE) codes, to user subroutines defined in general purpose FE software packages and, more recently, the use of commercialized manufacturing software.

Simpler analytical closed-form solutions have been developed by Raskeh *et al* [141,142] to evaluate the transient steady state behaviours of curing laminates at various stages of the cure cycle. For a single slab material, and assuming symmetric heat transfer boundary conditions, Equation (2-3) describes the maximum thermal lag mid-slab during a cure cycle ramp segment and Equation (2-4) describes the maximum temperature rise mid-slab during an exotherm event during a cure cycle hold:

$$\Delta T_{\mathrm{ss}} = -\left(T_{\infty} - T_{\mathrm{s}}\right) = -\dot{T}\,\frac{L^2}{a}\left(\frac{1}{2} + \frac{1}{Bi}\right) \tag{2-3}$$

$$\Delta T_{\mathrm{ss}} = -\left(T_{\infty} - T_{\mathrm{s}}\right) = \left(\frac{\rho_{\mathrm{r}} V_{\mathrm{r}} \dot{H}_{\max}}{\rho C_{\mathrm{p}}} - \dot{T}\right)\frac{L^2}{a}\left(\frac{1}{2} + \frac{1}{Bi}\right) \tag{2-4}$$

where T_{∞} is the autoclave air temperature, $\dot{T}$ is the temperature rate, a is the thermal diffusivity ($k/\rho C_{\mathrm{p}}$) of the slab, L is the slab half-thickness, Bi is the Biot number (hL/k), h is the convective heat transfer coefficient, k is the thermal conductivity and $\dot{H}_{\max}$ is the maximum specific rate of heat generation due to the exothermic resin reaction.

2.3.1.2 Cure kinetics models

Many different cure kinetics (CK) models have been proposed for predicting the cure rate for a large number of resin systems [28,29]. The cure rate is often expressed as:

$$\frac{d\alpha}{dt} = K_0 f(\alpha) \tag{2-5}$$

where in Equation (2-5), K_0 is a pre-exponential factor and $f(\alpha)$ is the cure dependence of the cure rate. A common approach in characterizing the cure kinetics model is to find the functional form for $f(\alpha)$. Some typical reaction models include: the *n*th order reaction equation, the autocatalytic equation, and the combination of these two equations [100,144,181]. Another characterization approach is a 'semi model-free' cure kinetics model where the prediction of cure rate is provided as a lookup table for a given combination of temperature and degree of cure [181]. The 'model-free' approach was originally proposed by Vyazovkin and Wight [182].

The remainder of this section briefly describes examples of cure kinetics models that are available in the scientific literature to highlight the increasing sophistication, complexity, and range of the models. The cure kinetics models used in the thick thermoset composites studies identified in this literature review are summarized in Table A-3.

The Hercules (Hexcel) 3501-6 CK model developed by Lee *et al* [74] represents early work in the characterization of epoxy based resin systems for the process modelling of thermoset composites. This cure kinetics model separates *n*th order and autocatalytic kinetic reaction terms but does not consider diffusion control regimes (see Table A-3).

Van Ee *et al* [135] developed a Hexcel 8552 CK model for the NIAR National Center for Advanced Materials Performance (NCAMP) program, with the cure rate defined as an inverse summation of kinetic and diffusion reaction terms. The glass transition temperature is defined using the empirical DiBenedetto relationship (see Table A-3 and Appendix E.1).

Dykeman [144] developed a Toray 3900-2 CK model that also defines the cure rate as an inverse summation of kinetic and diffusion reaction terms. However, the glass transition temperature is defined with a modified form of the empirical DiBenedetto relationship to account for phase separation (see Table A-3 and Appendix E.3).

A Cytec (Solvay) 5320-1 CK model developed by Thorpe *et al* [159] for the DARPA Transition Reliable Unitized STructure (TRUST) program is an example of a 'semi model-free' cure kinetics model. The cure rate is defined by an inverse sum of $n = 2$ reactions. The glass transition temperature is defined by the empirical DiBenedetto relationship. It should be noted that the model form used in this CK model represents a generalized form of the model used for the 8552 NCAMP CK model.

2.3.1.3 Boundary conditions

The most appropriate heat transfer boundary condition is to use a convective heat transfer coefficient (HTC) since the dominant source of heat transfer in autoclave and oven processing is forced convection heat transfer. Equation (2-6) gives the basic definition of the convective heat transfer coefficient [180]:

$$h = \frac{\Delta Q}{A \cdot \left(T_\infty - T_s\right) \cdot \Delta t} \tag{2-6}$$

where ΔQ is the heat gained/lost, A is the heat transfer area, T_∞ is the autoclave and oven air temperature, T_s is the slab surface temperature and Δt is the time step.

The factors that make predicting these boundary conditions difficult include [80]: 1) variations in autoclave or oven (equipment) airflow, temperature and pressure; 2) variations in loading environments, such as tool nesting and part shadowing; and 3) equipment and tool design, such as the airflow system and tooling substructure. Thus, few studies have investigated autoclave or oven heat transfer boundary conditions. The boundary conditions applied to the thick thermoset composites studies identified in this literature review are summarized in Table A-2.

Early work by Johnston *et al* [100,101] established a basic relationship describing the effect of autoclave pressure on heat transfer coefficient for fully developed turbulent flows:

$$h \propto \left(\frac{P}{T}\right)^{4/5} \tag{2-7}$$

where in Equation (2-7), P is absolute pressure and T is absolute temperature.

More recent works have focused on the robust development of autoclave or oven airflow and heat transfer coefficient characterization methods.

Shimizu *et al* [145] proposed several practical methods for the back-calculation of effective heat transfer coefficients. Effective heat transfer coefficients consider effects, such as thermal resistances due to bagging and consumables and tool size effects, at the bagside (top) and/or toolside (bottom) surface boundaries. These approaches differ depending on how the governing heat equation is approximated and how the adiabatic line, taken from the part/tool interface, is computed. The accuracy of these methods is dependent on the availability of through-thickness measurement points. The effective heat transfer coefficient can be back-calculated by discretizing Equation (2-6):

$$h = \frac{\sum_{i=1}^{n} \rho C_{\mathrm{p}} L \Delta T_{\mathrm{i}} \Delta z_{\mathrm{i}}}{\Delta T_{\mathrm{s}} \cdot \Delta t} \tag{2-8}$$

where in Equation (2-8), the subscript i represents a measurement point from the slab surface (i = 1) to the adiabatic line ($i = n$), ΔT_{i} is the change in temperature at the measurement point, Δz_{i} is the distance between adjacent measurement points, z is the through-thickness coordinate, ΔT_s is the temperature difference between the slab surface and the autoclave or oven air temperature, and Δt is the time step. Further details of this method are given in Appendix F.

Slesinger *et al* [148,150] investigated methods to characterize autoclave or oven airflow and heat transfer coefficients using visual methods, calorimetry and computational fluid dynamics (CFD) analysis. This work recommended that autoclave and oven qualification be performed based on heat transfer coefficient distributions rather than temperature or airflow uniformities.

Weber *et al* [167] proposed a semi-empirical method for estimating heat transfer boundary conditions, involving the generation of a 'catalog of boundary condition shift factors'. Experimental verification of this method was performed using multiple processing scenarios: tooling configurations, loading scenarios and three different autoclaves.

Studies by Park *et al* [177–179] have focused on the determination of zone based heat transfer coefficient distributions using CFD analysis in empty and loaded autoclave and oven processing scenarios. Verification of this work was performed using a novel infrared (IR) thermography technique along with conventional experimental thermal profiling studies of parts and tools.

2.3.2 Harnessing manufacturing science in simulation

By the mid 1990s, three research thrusts in areas of automation, simulation and production data analytics have emerged in efforts to address composites affordability, as discussed in Section 1.3. Key programs, such as the NASA Advanced Technology Composite Aircraft Structures (ATCAS) program (1994 – 1997) [99–103] and DARPA Accelerated Insertion of Materials – Composites (AIM-C) program (2000 – 2004) [125–130] represented efforts in the first use of first generation process modelling tools, and the use of these enabling DFM tools by manufacturing experts to manage composites manufacturing risk, cost and development time.

For thermal management problems, these DFM tools can evaluate cure cycles and predict the thermal response of composite laminates *a priori*. A multiscale modelling 'building block' approach now exists. Based on the studies identified in this literature review, Table A-4 summarizes the contributions to the composites manufacturing technology base.

An industrial survey conducted by the USAF in 2006 [18] revealed the key barriers in using simulation to support effective manufacturing decisions. The issues identified included: timing, the ability to standardize material models and the unreasonable inputs and test data required to create these models, the trade-off between model and computational complexity, and the demands on the expertise of the user. Table 2-2 is an example of efforts to improve material models and simulation efficiencies with the integration of these tools into commercial computer aided design (CAD) software packages for use by non-experts [126,183].

Table 2-2. The value of manufacturing simulation. Boeing 767-400ER wingtip front spar analysis shown as an example. Adapted from [126] (Hahn *et al*, 2001) and [183] (Floyd, 2017).

Conventional approach	Using simulation (~2001)	Current & future vision
• 32 runs for simple DOE[a] • 4 months to setup & solve • Intensive data reduction • 216 hours actual labour to complete	• 127 runs for sensitivity analysis & design scan • 1-2 weeks to setup & solve • Intensive user-interaction with multiple codes avoided • Automated data reduction • 28 hours actual labour to complete	ADVANCES: • Semi-automated workflow guided model setup & analysis • Integration into commercial CAD/FEA[b] software packages • Many short runtime simplified analyses guiding the analyst to a few long runtime detailed analyses (multiscale modelling) • Higher fidelity material constitutive models & characterization GOAL: • Non-expert analyst solves this problem in fewer than 8 hours

[a] DOE: Design of Experiments
[b] CAD: Computer Aided Design; FEA: Finite Element Analysis

In describing the key computational issues for ICME, Panchal *et al* [152] suggest that uncertainty in modelling and simulation is a 'first order concern' that is often overlooked. It is assumed that suitable management practices exist. Based on the work by Oberkampf *et al* [184,185], the accepted definitions of uncertainty and error in simulation based design contexts are:

- *Aleatory uncertainty* is a form of irreducible uncertainty that is associated inherent variability, such as material and process (M&P) variability. This type of uncertainty can be quantified using probability theory or estimated as distributions if sufficient data exists.

- *Epistemic uncertainty* relates to the uncertainty due to a lack of knowledge, such as the incomplete information about a material or process, or the fidelity of physical models. As a form of reducible uncertainty, epistemic uncertainty can be quantified and reduced by gaining additional information from expert opinion, experience, test, or analysis. Errors are inaccuracies that are cannot be attributed to a lack of knowledge.

- *Acknowledged errors* are known assumptions or simplifications that are explicitly made, such as using a material model beyond its range of validity.

- *Unacknowledged errors* are mistakes, such as using the wrong material model.

Confidence in using modelling and simulation can be achieved by appropriately dealing with potential sources of modelling uncertainty and error.

Two strategies to develop an 'evidence of credibility' in simulation are [125,152,184,185]:

- *Uncertainty quantification* is an emerging discipline that refers to the characterization and quantification of modelling uncertainties. Approaches, such as Bayesian based methods (eg. [125,186]), can be used to combine the results of model predictions with other sources of data, and probabilistic[5] methods, such as the use of multidisciplinary design optimization (MDO) tools (see Table 2-1), can be used to understand the propagation of modelling uncertainty or the sensitivity of model input uncertainties on model output uncertainties.

- *Validation* is assessment of model accuracy by comparison of the model predictions to experimental data. Model validation can be performed at different scales. For example, works by Dykeman [144] and Slesinger *et al* [149,150] have contributed to establishing validation methods for cure kinetics models at DSC test and laminate level scales.

To capture imperfect composites manufacturing knowledge, works by Griffith *et al* [127,128], as part of the DARPA AIM-C program, and Potter *et al* [187–189] attempted to systematically identify composites manufacturing uncertainties and their relationships using defect taxonomies. These initial efforts focused on M&P variabilities for autoclave cure and resin transfer moulding (RTM) processes, respectively. It should be noted that structured approaches formalizing *process–structure–performance* relationships have been developed in other materials disciplines, such as the 'flow block diagrams' by Olson *et al* [190,191] for high performance metal alloys.

---

[5] Uncertainty propagation is acknowledged here as an important aspect of dealing with modelling uncertainty, but is beyond the scope of the research presented in this thesis.

Works by Hahn *et al* [125], as part of the DARPA AIM-C program, and Fernlund [186] have attempted to quantify and formalize methods for addressing composites manufacturing risk using Bayesian based approaches.

In recent years, 'materials innovation ecosystems', such as the Materials Genome Initiative (MGI) (2011 –) [152,153] and the European Materials Modelling Council (EMMC) (2015 –) [175], have been established. These leading initiatives are focused on aspects of model standardization and interoperability within hierarchical multiscale modelling schemes. Within these initatives, programs, such as the USAF Integrated Computational Methods for Composite Materials (ICM2) (2012 –) [154–158] and Faunhofer Institute for Alogrithms and Scientific Computing (SCAI) Virtual Material Modelling in Manufactuirng (VMAP) (2017 –) [176], are focused on developing mature ICME digital frameworks (technology base) for composites manufacturing.

2.3.3 Studies representative of industrial processing conditions

In practice, the typical thermal response of curing laminates is dependent on the interaction of: 1) the internal heat generation of parts (reactivity of the material); 2) the thermophysical properties of parts and tools; and 3) the airflow around and between parts, tools, and equipment. Of the 39 thick laminate composites studies identified in this literature review, a third (N = 13) chose to consider tool thermal effects and convective heat transfer boundary conditions representative of industrial processing conditions. These works are summarized in Table 2-3. Approximately half (N= 6) of these studies arbitrarily defined heat transfer boundary condition values. The remaining works are briefly described in this section.

Work by Johnston *et al* [99–101] contributed to the development of first-generation process modelling tools (COMPRO-2D). The study of a 28.2 mm thick panel with tapered core, as part of the NASA ATCAS program, validated the 'virtual autoclave' modelling concept.
The observed effects of autoclave pressure on heat transfer coefficient were also first described in this work (see Equation (2-7) and Appendix D.1).

Michaud *et al* [117,118] investigated the process optimization for RTM cure composites using methods originally developed for autoclave processing. Modifications to the TGCURE code, originally developed by Bogetti and Gillespie [83–85], were made to account for the thermal diffusivity of the tool. Experimental validation was performed with 25.4 mm thick laminates using heat flux sensors. This study highlighted 'the need to include the tool in the simulation of thick-sectioned RTM composite laminates'.

Antonucci *et al* [123] proposed a simplified thermal model where the thermal resistances of tools and consumables are lumped as effective heat transfer boundary conditions. This approach was experimentally validated with 30 mm thick laminates cured in an industrial autoclave.

As part of the DARPA AIM-C program, Nelson *et al* [129,130] investigated the curing of thick laminates using simulation to 'develop a robust cure cycles given inherent variability due to heat transfer'. Based on COMPRO-2D model predictions, cure cycles were recommended for 89 mm and 127 mm thick laminates. The 89 mm thick laminate cure cycle was validated by experimental test. This study highlighted the use of first-generation process modelling tools by an expert user.

Shimizu *et al* [145] studied the effects of autoclave pressure, temperature heating rate, tool size effects and bagging conditions for a 38.4 mm thick laminate. This study also demonstrated simple methods to back-calculate effective heat transfer coefficients for parts and tools (see Equation (2-8) and Appendix D.2).

Gude *et al* [166] devised an 'experimental-numerical' validation strategy for the systematic analysis of curing processes for complex-shaped RTM laminates. Experimental verification of this proposed approach was performed on a large complex-shaped turbine fan blade.

Work by Belnoue *et al* [174] investigated the formation of fibre path defects in automated fiber placement (AFP) manufactured composites during cure. Based on the work by Johnston *et al* [99–101], a cure kinetics validation study on an 18 mm thick laminate was performed to validate a novel multiphysics modelling framework, coupling heat transfer and hyper-viscoelastic consolidation models.

Table 2-3: Subset of studies identified in the scientific literature that are representative of industrial composites processing scenarios[a,b].

Principal investigators	Material system	Part geometry & max. thickness (mm)	Tool geometry & thickness (mm)	Remarks	Ref.
Telikicherla *et al*	AS/3501-6	flat (5.7 mm)	tool plate	HTC arbitrarily specified as effective Biot number	[92]
Johnston *et al*	AS4/8552 glass/phenolic core	panel with tapered core (28.2 mm)	Invar tool plate (25.4 mm)		[99–101]
Joshi *et al*	AS4/3501-6	flat (23.1 mm)	Al-alloy tool plate (13 mm)	HTC from Vodicka (1994)	[111]
Michaud *et al*	E-glass/411-C50	flat (25.4 mm)	Al-alloy matched tool (12.7 mm)		[117,118]
Oh & Lee	UGN150 prepreg	flat (20 mm)	Al-alloy tool plate (15 mm)	HTC from 3D FE model based on Joshi (1999)	[119]
Antonucci *et al*	carbon/epoxy	flat (30 mm)	Al-alloy RTM mould		[123]
AIM-C	IM7/977-3	flat (89 mm, 127 mm)	Invar tool plate (12.7 mm)		[129,130]
Guo *et al*	T300/HD03	flat (20 mm)	Al-alloy tool plate (35 mm)	HTC from Lee (2002)	[140]
Shimizu *et a*l	AS4/8552-1	flat (38.4 mm)	Al-alloy tool plate (25.4 mm)		[145]
Mamani & Hoa	S2-glass/E773	flat (18.3 mm)	Al-alloy tool plate (50 mm)	HTC taken from Lee (2002)	[164]
Gude *et al*	GV300TFX/RTM6	flat (100 mm)	Al-alloy RTM mould		[166]
Belnoue *et al*	IM7/8552	flat (18 mm)	Al-alloy tool plate (10 mm)	CK validation study based on Johnston (1997)	[174]

[a] Thermal management studies that consider tool thermal effects and convective heat transfer boundary conditions.
[b] Additional thick thermoset composites data sets are presented in Chapter 5 & Appendix D.

2.4 Research Objectives and Scope of Thesis Work

2.4.1 Synthesis of literature

Based on the literature survey presented, the following research gaps have been identified:

- **A misconception of composites manufacturing exists in the innovation management literature.** Using the modularity-maturity matrix proposed by Pisano and Shih [49], the production of sophisticated composites products should be classified as 'process-driven innovation', or low modularity and low maturity technology. Composites product and process innovations are highly coupled, and the manufacturing strategy pursued detrimentally impacts the ability for composites manufacturers to innovate. Although there is work reported in the literature that investigates how large composites companies manage technological and market uncertainty, how composites SMEs overcome these commercialization challenges is less understood.

- **It is no longer sufficient to keep adding to the science base without explicitly addressing how manufacturing practice can adopt or change.** The use of the manufacturing science base to reduce risk is considered a promising strategy. However, the *ad hoc* use of this knowledge is no longer a sustainable approach for effective risk management in practice. As the composites industry collectively moves towards science based manufacturing, it becomes increasingly more important to: 1) ensure that the manufacturing science base is open, correct, usable and useful; 2) mature the technology base so that these enabling DFM tools can create value in *all* stages of the development design cycle; and 3) standardize routine workflows to allow manufacturing experts to become more efficient and enable non-experts to develop expertise quickly.

- **Few thermal management studies for thick thermoset composites exist in the scientific literature**. A modest number of thick thermoset composites studies (N = 39), spanning over 35 years of composites manufacturing research, were identified. Of these studies, a third (N = 13) chose to consider tooling effects and heat transfer boundary conditions representative of industrial processing scenarios in the thermal management problem investigated. Approximately half of this subset (N = 6) arbitrarily defined these boundary conditions or were found to be replicating earlier prior work. This suggests that: 1) the research community has mastered the proficiency to create and codify the composites manufacturing science base for these types of problems; 2) we are past the point now where we need to demonstrate that the manufacturing simulation for thermal management problems works; and 3) work to demonstrate and document how the use of this knowledge can directly support effective manufacturing decisions is now needed.

2.4.2 Research objectives and scope

The work presented in this thesis aims to initiate efforts for a new translational research strategy, focusing on the use of the composites manufacturing science base to manage manufacturing risk more effectively. The initial emphasis and scope of the work presented is the science based practice for thermal management problems in composites manufacturing and the use of manufacturing simulation to support effective decision making. The scope of this thesis work is summarized in Table 2-4.

Table 2-4: Scope of thesis work presented.

Theme / Level	Thermal management (TM)	Material deposition management (MDM)	Quality management (QM)	Residual stress & dimensional control management (RSDM)
	Excellent understanding ('know-why')	Poor understanding ('know-how')	Good understanding ('know-how')	Very good understanding ('know-why')
Science	• Heat transfer • Resin cure kinetics • Boundary conditions	Science (creating knowledge) • Fundamental understanding of the important processing physics • Characterizing complex relationships with appropriate governing laws & constitutive equations		
Technology	Simulation: • Using simulation to manage risk effectively	Technology (codifying knowledge) • Developing robust enabling tools that capture the science base • Key research thrusts: automation, simulation, & 'big data' analytics		
Practice	Model: • Formalizing good thermal modelling practice Measure: • Knowing what to look for in production data	Practice (systematic use of knowledge) • Fast & effective science based manufacturing decision making – intended to complement not displace existing design workflows – routinize standard workflows – reduce effort in complex workflows • Coping better with uncertainty – product size/complexity & production scaling • Right-sizing approach for different industries & receptor capacity – aerospace OEMs to industrial SMEs		

There are three research objectives. Firstly, to investigate current manufacturing practices and design activities, and gather case based evidence showing how composites manufacturers can create value from using the science base to minimize manufacturing risk. Secondly, to develop and introduce a framework that formalizes science based composites manufacturing practice and the process of knowledge translation. The developed framework is intended to systematically integrate and aggregate the manufacturing science base in open, usable, and useful form. It should be noted that the implementation of this framework, as in the development of a knowledge management and decision support tool, is beyond the scope of this work. Thirdly, to demonstrate the application of science based composites manufacturing practice where the manufacturing science base is relatively mature. The development of three thermal management case studies, based on the analysis of five thick thermoset composites data sets, is presented.

An interdisciplinary research approach, that integrates relevant theory and prior work from the innovation managegment, computer science and engineering domains, is adopted to address the research gaps and objectives identified. Technical and other important terms used in this work are specified in the Glossary.

The research presented in this thesis is organized as follows:

- *Chapter 3: Managing Uncertainty in Composites Manufacturing* – A synthesis of current composites manufacturing practice is presented. Included is a discussion of the key design activities and structured approaches used in the aerospace sector to manage manufacturing risk. Direct observation and evaluation of an aerospace OEM and qualitative case based analysis of two composites SMEs is presented and discussed to show how the use of the manufacturing science base creates value.

- *Chapter 4: Conceptual Theory Building and Framework Development* – The development of a framework to encourage the use of composites manufacturing science in industrial practice is presented. Structured approaches for formalizing the process of knowledge translation and transforming manufacturing practice are outlined. A hierarchical knowledge model, organizing composites manufacturing domain knowledge, is proposed.

- *Chapter 5: Applications of Science Based Practice for Thermal Management* – Five data sets, representative of realistic production scenarios for processing thick thermoset composites, are presented in demonstrating the application of science based practice for thermal management problems in composites manufacturing. The development of case studies formalizing thermal modelling practice, cure cycle development and evaluation and the assessment of apparent and real failures in experimental thermal profiling are outlined.

- *Chapter 6: Summary and Future Work* – A discussion of the significance of formalizing a framework for science based composites manufacturing practice is provided. Future improvements and extensions to this research are also presented.

- *Appendix A: Thermal Management Studies of Thick Thermoset Composites* – Presents additional details and synthesis of the thick thermoset composites studies reviewed in the scientific literature.

- *Appendix B: SME Qualitative Research Study Documentation* – Documents the research study protocol and methods, and participant consent form for the qualitative SME case based analysis.

- *Appendix C: Proposed Thermal Management Knowledge in Practice Document Topics* – Outlines proposed science based knowledge and design practice document topics for thermal management. Tools to systematically capture manufacturing scenarios are presented.

- *Appendix D: Thick Thermoset Composites Data Sets* – Summarizes details of the five thick thermoset composites data sets analyzed, including reported effective heat transfer coefficients, test set-up and numerical modelling parameters, and temperature plots showing experimental and predicted thermal responses.

- *Appendix E: Material Properties and Material Database Input Parameters* – Presents the material properties and material models used in the data sets analyzed, including details of the preliminary characterization of the Hexcel AS4/8552-1 prepreg material system.

- *Appendix F: Effective Heat Transfer Coefficient Back-calculation Method* – Outlines the methodologies used to back-calculate the effective heat transfer coefficients used in the data sets analyzed.

The work described in this thesis represents a continuation of 30+ years of composites manufacturing research in the UBC Composites Group/CRN to advance the science base and enhance the capabilities nowadays embedded in the commercial manufacturing simulation technology base. The contribution of the author to the *Knowledge in Practice* framework consists of the justification for science based manufacturing practice (Chapter 3), conceptual theory building and framework development (Chapter 4) and initial efforts to develop and document science based practices for thermal management (Chapter 5). Colleagues at CRN are actively using the principles and concepts proposed by the author in ongoing translational research activities with industrial partners, and collaborative projects with composites SMEs based in Western Canada.

Chapter 3: Managing Uncertainty in Composites Manufacturing

One challenge facing the composites industry, discussed in Sections 1.2 and 2.1.1, is the increasing manufacturing risk and uncertainty associated with increasing product and production scaling [12–14]. Composites manufacturers are likely to experience prolonged periods of technological and market uncertainty, and this can hinder efforts to innovate [53,54]. Thus, the management of technological and market uncertainty is key to enabling innovation [46].

To justify the need for formalizing science based practice, current typical practices used by the composites manufacturing industry to manage increasing manufacturing risk and uncertainty are outlined and discussed in this chapter, including a description of the key design activities that represent the most structured approach in composites manufacturing practice and the cost-risk relationships typically encountered in the development of complex engineering systems. An outcomes taxonomy, based on a science based understanding and simulation based thinking, is introduced to capture imperfect composites manufacturing knowledge and to explicitly link *science–technology–practice* levels of activity.

The direct observation and evaluation of a large and experienced aerospace OEM, along with qualitative analysis of two composites SMEs who chose to collaborate with a CTRC are presented. These case studies demonstrate how using the composites manufacturing science base can contribute to reducing technological uncertainty and enable potential market opportunities for further innovation.

3.1 Current Practice

In this section, the practices typically used by the composites industry are outlined to highlight the need to transform these approaches from a world of empirical 'know-how' to science based 'know-why' to better deal with increasing manufacturing risk.

3.1.1 Manufacturing quality control and oversight

Typical current aerospace practice is based on a structured 'building block' approach, where there is incremental scale-up in size and complexity from small coupons up to the actual structure of interest. This approach represents the most structured workflow in composites manufacturing. There are three complementary design activities: material qualification, structural certification and production approval [192,193] (see Figure 3-1 (a)). Although these design activities refer to typical aerospace practice, the same or similar approaches are likely in all industrial sectors, albeit perhaps more implicit and less regulated:

- *Material qualification* relates to the determination of the material level properties that will be used in the structural design and certification. Given that the properties of a composite material are a function of its chemical (eg. degree of cure), physical (eg. fibre orientation and volume fraction, void fraction) and mechanical state (eg. residual stresses), a key consideration in material qualification is the linkage of the material properties to the material state. This is a non-trivial problem given the current state of the art and thus typical current practice uses a mixture of process parameter outcomes (eg. temperature history as seen in the material), material structure outcomes (eg. cured ply thickness, void fraction) and material performance outcomes (eg. mechanical tests on

trim or traveller coupons). Exactly what, how and why different tests are done appears to be based on a mix of science, pragmatism and experience accumulated over time in individual programs, companies and in the composites industry more broadly. This is the essence of 'know-how'.

- *Structural certification* relates to the acceptance of the structure as being able to safely carry the loads and other service conditions according to the necessary engineering and manufacturing requirements and regulations. Since many tests are done at the lower scales of the 'building block' approach, this philosophy is based on the commonality of the material at all levels of the 'building block'. This is otherwise known as material equivalency. A key assumption and requirement in this structural certification step is that the material in the final structure be equivalent to the material that was qualified in the material qualification step.

- *Production approval* is the step that ensures that the material qualification and structural certification steps are properly linked once the structure enters production. With production approval, one ensures that the necessary quality control and oversight protocols for acceptable part producibility, that is the ability to produce parts repeatably and robustly, are in place. A robust process is where the manufacturing outcomes of interest are as insensitive as possible to the manufacturing choices selected. A manufacturing outcome is considered a defect if it falls outside of specified limits, as determined by the previous two steps.

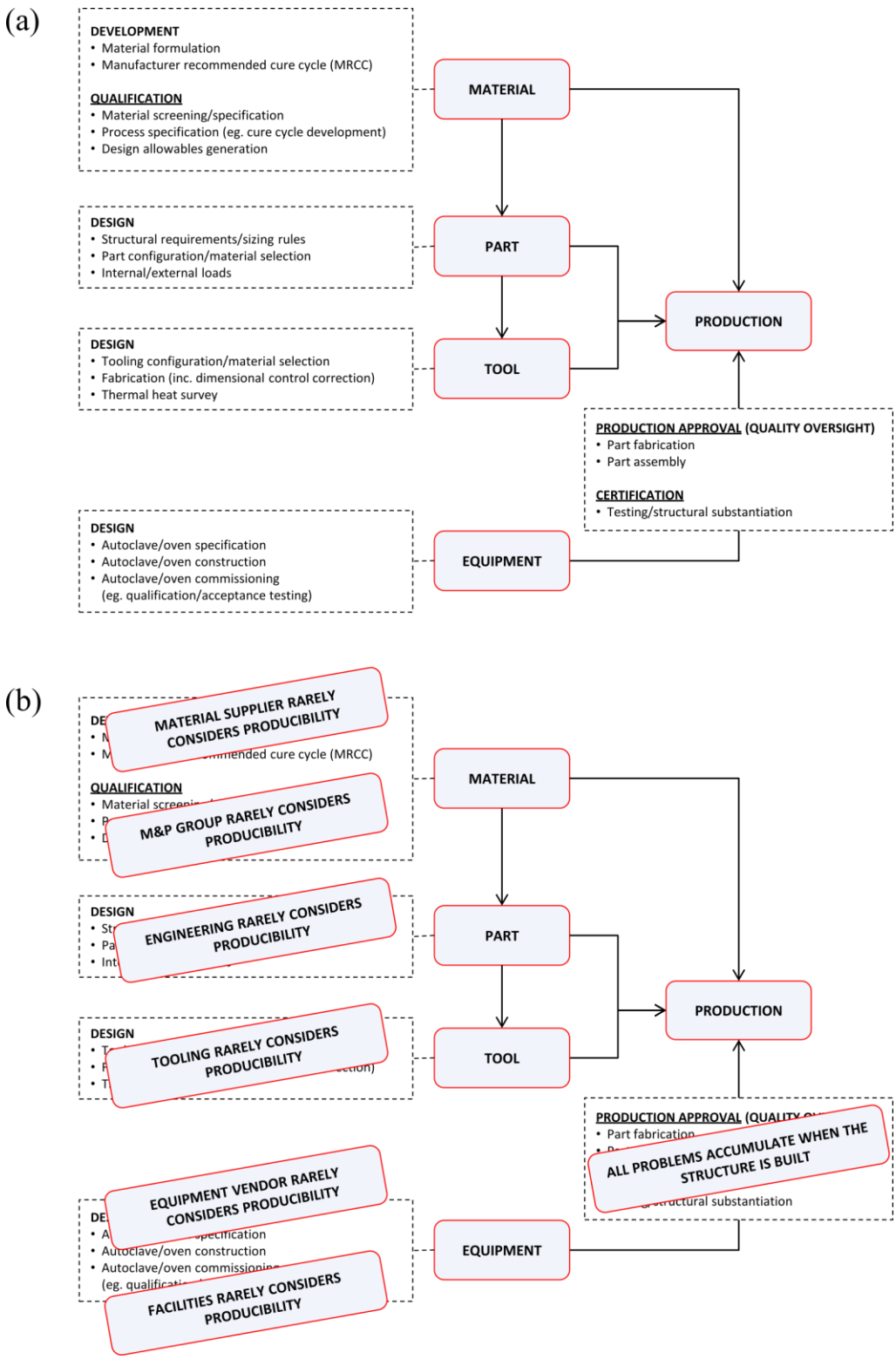

Figure 3-1: Typical aerospace composites manufacturing practice. Adapted from [192] (CMH-17, 2012): (a) high-level design workflow and (b) the problems associated with this approach. MRCC: Manufacturer Recommended Cure Cycle; M&P: Material & Process.

3.1.2 Manufacturing outcomes

Manufacturing outcomes are tracked to ensure the acceptable quality of the composites end product. While the *process–structure−performance* relationships may not be known in all cases, most manufacturers know that they must control the variability of their processes. In extending prior work by Griffith *et al* [127,128] and Potter *et al* [187–189] to capture imperfect composites knowledge using defect taxonomies, as discussed in Section 2.3.2, a preliminary outcomes taxonomy is introduced in this work that is philosophically founded on science based understanding and simulation based thinking (eg. [63,190,191,194,195]). As with past efforts, the development of this taxonomy, shown in Figure 3-2, is a useful and necessary guide to consider which outcomes matter, and when, for any given manufacturing cycle.

This taxonomy has been developed using an approach analogous to the sub-model framework originally proposed by Loos and Springer [75,76]. This same approach has underpinned the development of several simulation based frameworks for process modelling in composites manufacturing (eg. [99–101,195]). For example, given our understanding of the manufacturing science, temperature and degree of cure are considered state variables of the composite material [99–101]. These manufacturing outcomes, along with resin viscosity, represent the thermochemical model, and thus are classified as thermal management and chemical equivalency outcomes in Figure 3-2. Where our understanding of the manufacturing science is less mature this outcomes taxonomy can be populated with placeholders. In such cases, this highlights gaps within the existing science base that could be considered for future research.

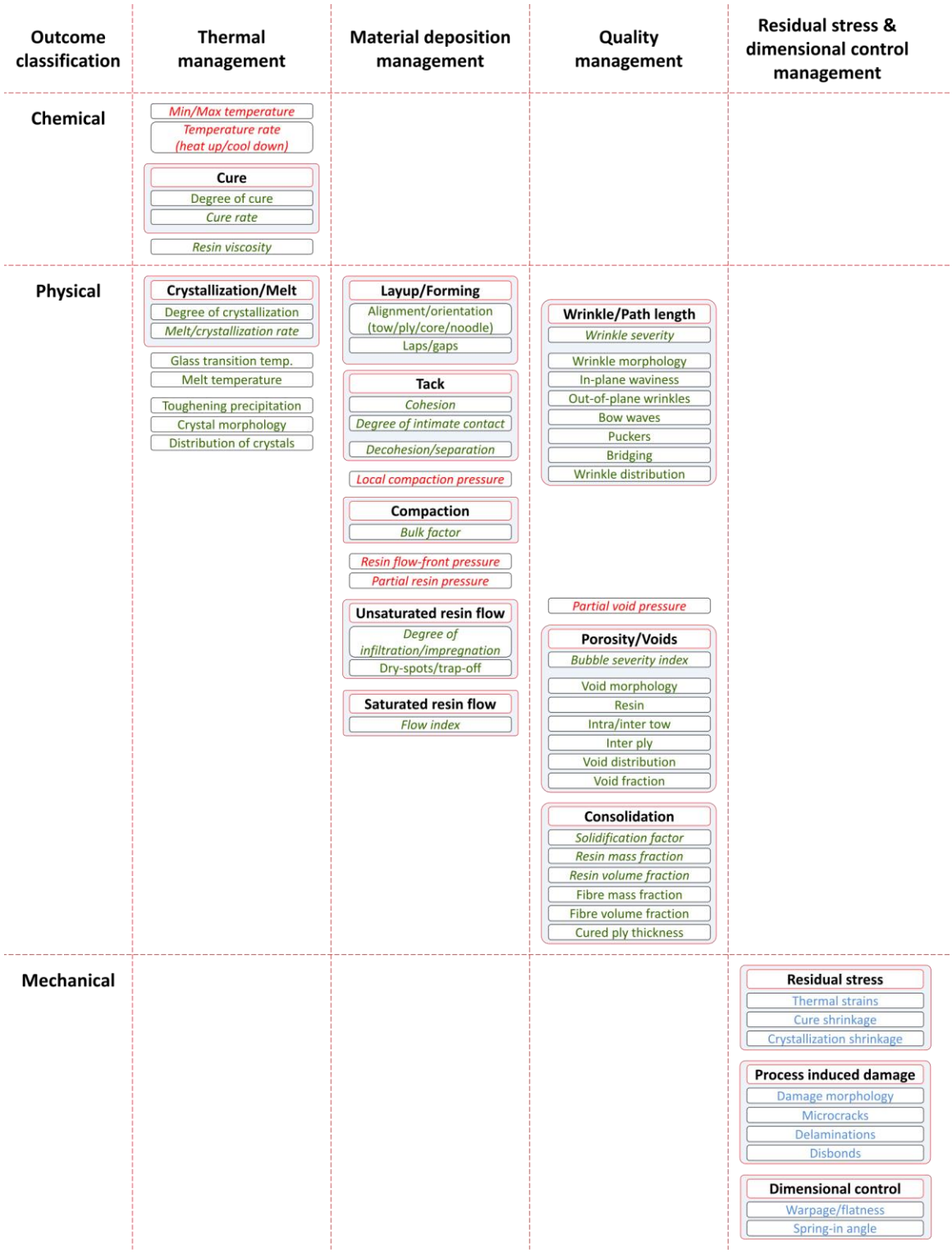

Figure 3-2: Preliminary outcomes taxonomy for composites processing. Extension of approaches from [127,128] (Griffith *et al*, 2002) and [187–189] (Potter *et al*, 2007). Note: Manufacturing outcomes are classified by theme (left to right), material equivalency (top to bottom) and outcome type (process parameter (red), material structure (green) and material performance (blue)), where intermediate outcomes shown in italics and final outcomes are shown in plain text.

3.1.2.1 Causal relationships

It is convenient to consider manufacturing outcomes in terms of the range of response at a given material point in a structure of interest. Outcome types are classified according to the fundamental *process–structure–performance* paradigm of materials science [196], where:

- *Process parameter outcomes* (shown in red in Figure 3-2) are proxies that infer the state of the material (eg. the temperature history as seen in the material, partial resin pressure). It should be noted that these outcomes are *actual* quantities as seen by the material, rather than *applied* quantities or external stimuli[6] that are imposed on the material.

- *Material structure outcomes* (shown in green in Figure 3-2) describe the changes in the internal arrangement of components within the material. In terms of morphology, the distribution and severity of these outcomes occurs at multiple length scales (eg. wrinkle wavelength, void size).

- *Material performance outcomes* (shown in blue in Figure 3-2) directly relate to the in-service behaviour of the material. In a manufacturing context, these outcomes may contribute to a reduction of the allowable stress/strain used in the structural design (eg. locked in residual stresses, process-induced damage, geometric changes).

[6] Six characteristic types of stimuli are: temperature (thermal), load or force (mechanical), electric field (electrical), magnetic field (magnetic), electromagnetic or light radiation (optical), and chemical (deteriorative) [196].

Additionally, and based on terminology proposed by Griffith *et al* [127,128], outcomes can be characterized in terms of when they are measured or tracked in the manufacturing cycle as:

- *Intermediate outcomes* (shown in italics) refer to time and spatially varying reductions in actual value, integral or differential forms of indirectly measurable or theoretically measurable changes of the material during a process step (eg. the temperature as seen in the material, DOC at gelation, the resin flow index).

- *Final outcomes* (show in plain text) are often measured at the end of a process step. These outcomes are directly measurable or theoretically measurable, independent of any knowledge of the process history (eg. the final DOC, cured ply thickness, spring-in angle).

The organization of manufacturing outcomes by: 1) processing theme (*time–temperature–pressure–vacuum* history); 2) material equivalency (*chemical–physical–mechanical* transformations of the material); and 3) outcome type (*process–structure−performance* relationships) results in the formation of a banded matrix (see Figure 3-2). For a given manufacturing outcome of interest, upstream dependencies (to the left and above) can be described as potential root causes and downstream dependencies (to the right and below) as possible 'knock-on' effects. For example, a high degree of cure, greater than the degree of cure at gelation, at the start of a final cure cycle hold (outcome: thermal management, chemical equivalency), might indicate the likely possibility of 'knock-on' effects, such as a reduction in resin flow (outcome: material deposition management, physical equivalency) and the development of unacceptable residual stresses (outcome: residual stress and dimensional control management, mechanical equivalency).

3.1.2.2 Sources and sinks

The outcomes taxonomy proposed in this work represents a high-level hierarchical representation of manufacturing outcomes that we choose to track for any given manufacturing cycle. While the causal relationships between outcomes can be described in terms of the classification of outcomes at this scale, as described in the previous section, the relationships between manufacturing choices and manufacturing outcomes requires an understanding the precise nature of these interactions at a lower scale. In this context, the outcomes taxonomy can serve as an entry point to systematically identify and capture these relationships.

One approach that describes these interactions at a lower scale is the 'sources and sinks' framework initially developed by Arafath *et al* [197] and Lane *et al* [198] for void growth and dissipation in out-of-autoclave (OOA) material systems. In general, 'sources' contribute to the generation of manufacturing outcomes and 'sinks' contribute to the reduction, or mitigation, of manufacturing outcomes. Take for example porosity/voids (outcome: quality management, physical equivalency). The 'sources' identified for void growth include entrapped air, volatiles and off-gassing, and bag/tool leaks and the 'sinks' identified for void dissipation include resin and gas transport for the removal of air and volatiles, elevated resin pressure to promote void shrinkage and collapse and resin infiltration [197,198].

It is worth noting that current work relating to porosity/void focuses on: 1) broadening our understanding of the physics and time scales of these individual mechanisms (science) (eg. [35,197–203]); 2) linking together our understanding of these mechanisms to develop efficient physics based methods for porosity prediction in production scale structures

(technology) (eg. [204]); and 3) strategies proposing improvements to the design of processes using science based approaches (practice) (eg. [205–207]). The use of this 'sources and sinks' framework for other composites manufacturing outcomes is summarized in Table 3-1.

Pragmatically, an effective strategy for the management of any manufacturing outcome is to balance sources and sinks [197,198,207]. The relative importance of outcome sources and sinks, or overall outcome severity, is dependent on equipment, tool, part and material attributes [197,207]. For example, Mobuchon and Zobeiry (2014) performed a simulation based parametric study to examine trends in manufacturing attribute variations on minimum/maximum temperature outcomes, as shown in Figure 3-3. Future work aims to confirm these relationships using production data analytics, analogous to recent work reported in the literature relating to data science based approaches for materials development in additive manufacturing (eg. [208,209]).

Table 3-1: Examples of studies in the scientific literature that use the 'sources and sinks' framework to describe trends in composites manufacturing outcomes.

Theme[a]	Contributors	Outcome	Remarks	Ref.
TM	Mobuchon & Zobeiry (2014)	Min/max temp.	See Figure 3-3	
MDM	Forghani *et al* (2017)	Tack	Degree of intimate contact (DoIC)	[210]
QM	Arafath *et al* (2009)	Void/porosity	Incorporation of gas transport time scales	[197]
	Lane *et al* (2010)			[198]
	Farhang (2014)			[202]
	Mobuchon *et al* (2014)			[205]
	Fernlund *et al* (2016)			[207]
	Bedayat *et al* (2017)		Bubble severity index (BSI)	[204]
RSDM	Zobeiry & Poursartip (2015)	Residual stress		[36]
	Fernlund *et al* (2007)	Spring-in angle		[211]

[a] TM: Thermal management; MDM: Material deposition management; QM: Quality management; RSDM: Residual stress & dimensional control management

	Attribute			Min temp.	Max temp.
Equipment	top HTC	↑		↓	↓
Tool	bottom HTC (tool substructure)	↑	thin tools thick tools	↓	↓ ↑
	tool material		CFRP Al-alloy Steel Invar	↑	↓
	tool plate thickness	↑		↑	↓
Part	laminate thickness	↑		↑	↑
Material	heating rate	↑		↑	↑

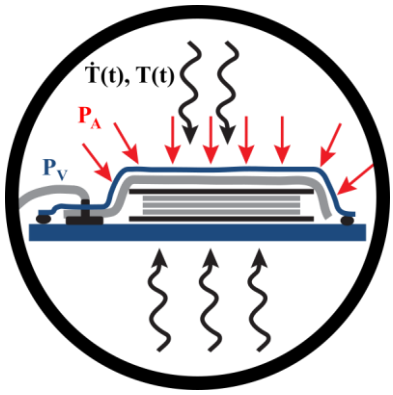

Figure 3-3: Thermal management sources and sinks[a,b] for autoclave cure are shown. Adapted from Mobuchon and Zobeiry (2014). HTC: Heat Transfer Coefficient; $\dot{T}$(t): applied heating rate; T(t): applied temperature; P_A: applied pressure; P_V: applied vacuum pressure. Note: Minimum/maximum temperatures are classified as process parameter outcomes.

[a] 'Sources' are attributes that contribute to increasing the min/max temperature (red arrow) and 'sinks' are attributes that contribute to reducing the min/max temperature (blue arrow) in parts. Based on original work relating to void generation and dissipation [197] (Arafath *et al*, 2009) and [198] (Lane *et al*, 2010).

[b] Trends shown due to changes in Equipment, Tool and Part variable attributes, and Material constraint attributes. An explanation of variable and constraint attribute types is given in Section 4.2.2.

In choosing to deconstruct composites manufacturing problems in this manner, the outcomes taxonomy introduced in this work can be used to identify relationships that are consistent with work to: 1) characterize and identify the appropriate constitutive equations and models (science) (eg. wrinkling management [212–218], porosity management [197–203]); 2) advance the sophistication and maturity of manufacturing simulation frameworks (technology) (eg. hyper-viscoelastic constitutive model [174], three-phase integrated flow-stress model [219,220]); and 3) confirm, in the ideal case, what composites manufacturing experts know from experience given the mix of manufacturing outcomes that are tracked as 'know-how' or, in the other extreme, reveal contradictions in existing assumptions established in industry (practice).

3.1.3 Current practice represents high risk

In any new product development (NPD) program, the greatest portion of program costs are committed very early, as shown in Figure 3-4. At the end of conceptual design, for example, while only 8% of actual program costs have been spent, as much as 70% of costs have already been committed based on the decisions made [15,16]. These decisions, in terms of the manufacturing strategy to be pursued, are significant considering the high costs and long lead times for materials development, tool design, and equipment purchase and aquisition. Committed costs such as these are non-recoverable if the program fails, or is cancelled [15–17]. By the time the program reaches the production phase, materials development has been completed, and tools and equipment physically exist. The consequences of these early decisions can potentially lead to considerably high risk, such as schedule delays and cost overruns, if parts of acceptable quality cannot be produced. The cost to make design changes significantly increases over the life of the program.

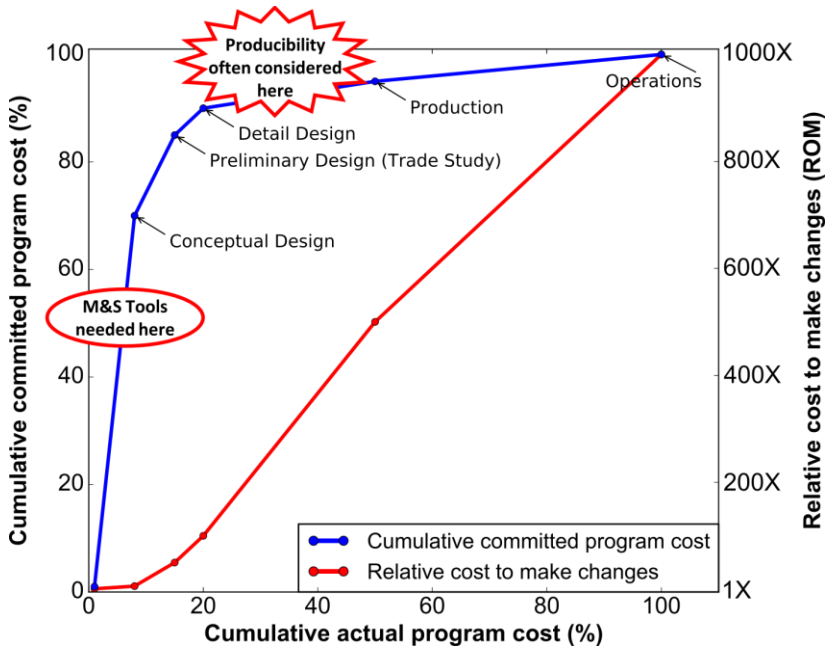

Figure 3-4: Program development cost-risk relationship for complex engineering systems. Adapted from [16] (NDIA, 2011). M&S: modelling and simulation.

As depicted in Figure 3-4, producibility is typically considered in the late stages of the development design cycle. 'Hidden costs' are often incurred to overcome manufacturing problems and production inefficiencies unintentionally engineered into products and supply chains [16] (see Figure 3-1 (b)). Producibility is often neglected in the earlier stages of the development design cycle, as discussed in Section 2.2, due to a lack of validated DFM tools for manufacturing.

An early example of composites manufacturing risk, during the late 1960s and early 1970s, was the use of CFRP fan blades in the Rolls Royce RB211 engines. While engineers at the time understood the basic *structure–performance* relationships at laminate scales, numerous issues were encountered, including inadequate resistance to bird strike and manufacturing repeatability [221][7]. An over confidence in the use of advanced composites materials at this early stage significantly contributed to events that ultimately resulted in leading Rolls Royce into crisis, receivership and bankruptcy [221–223].

Another indicator of increasing risk is the time and cost to develop and certify next generation aircraft. Current forecasts indicate development time frames greater than 210 months to develop and certify next generation aircraft, compared to the 60 month time frames in the 1960s and 150 month time frames in the 1990s [224–226]. Interestingly, similarly challenging industries, such as integrated circuits and automotive, are reversing these trends with regard to their complexity and uncertainty management practices.

[7] Although it is commonly known that bird strike was a major technical barrier, manufacturing control was also a major issue.

3.2 Creating Value from Science Based Practice

Large composites manufacturers are more likely to use the practices discussed in Section 3.1 to manage manufacturing risk. These typically empirical practices, based on a structured 'building block' approach, are used to control and oversee the acceptable quality of the composites end product [192,193]. Case study evidence is presented in this section to highlight the use of science based composites manufacturing practice to make effective manufacturing decisions and minimize manufacturing risk. The direct observation and evaluation of a large composites manufacturer is given in Section 3.2.1.

While the challenges in managing technological and market uncertainty have been described in the literature for large composites manufacturers (eg. [23]), how composites SMEs manage these challenges is much less understood. Two composites SMEs based in Western Canada who chose to collaborate with a CTRC are investigated, with case study descriptions in Sections 3.2.2 and 3.2.3, and analysis in Section 3.3. Of the 120 SME interventions conducted by the CTRC involved in these studies at the time that this analysis was performed, approximately half of these cases focused on resolving issues in existing process innovations. All of these interventions faced broadly similar challenges. The two case studies selected are representative of these approximately 60 manufacturing science interventions.

These cases are used to compare how small composites manufacturers address technological and market uncertainty, and how choosing to partner with a CTRC enabled technological and market uncertainties to be reduced and possible opportunities to be exploited using science based approaches. While these selected cases demonstrate the successful use of the composites

manufacturing science to address technological uncertainty, they also highlight mixed outcomes in terms of managing market uncertainty and contributing to the success of the SME, and the regional innovation ecosystem in Western Canada.

Semi-structured primary interviews were conducted with three technical experts from the two composites SMEs[8]. The questions asked in these interviews can be found in Appendix B. Information from these interviews was supplemented with secondary data gathered from CRN project reports, US Patent and Trademark Office (USPTO) patent database searches, company websites, publicly available records, and news releases. To enable the integration of data gathered from these sources, timelines were constructed to capture important events and factors affecting technological and market uncertainty. Tables summarizing key technological and market uncertainty attributes were also generated. The categorization of these attributes and criteria was informed by prior work by Maine *et al* [20,45], in advanced materials and nanotechnology.

3.2.1 Case 1: Aerospace OEM

A good example that demonstrates the success in scaling up the science base is the value that manufacturing simulation provided The Boeing Company during the development of the 787 Dreamliner. Boeing engineers gained an early confidence in the software they used, initially developed by Johnston *et al* [99–101] in the mid 1990s, resulting from the lessons learned from participation in research programs, such as NASA ATCAS, USAF Processing for Dimensional Control (PDC) (1998 – 2000) and DARPA AIM-C. In the hands of these experts, this software

[8] The identities of these SMEs and technical experts have been anonymized at the request of the interviewees.

was used to determine the autoclave cure cycle for the one-piece fuselage barrel sections. The cure cycle selected was named 'Cycle 297' in reference to being the 297th cycle iteration evaluated [134]. Manufacturing simulation was also used to establish tooling compensation strategies for the complex wing spar structures. In using manufacturing simulation, this meant that Boeing could reduce risk, cost and development time within existing specifications and requirements. Fewer manufacturing trials were needed to ensure that all fuselage barrels passed thermal compliance requirements and for wing spars to meet geometric tolerances. Additionally, Boeing was able to transfer technology and knowledge to its supply chain partners of these major components efficiently. These partners also benefitted from using science based practice [14].

3.2.2 Case 2: Industrial SME #1 (Structural GFRP component manufacturer)[9]

SME #1 was established in the early 1980s as the exclusive in-house manufacturing division of its parent company for its primary market, and by the mid-1990s the company formed a partnership with its initial customer in a secondary market. SME #1 is an innovative company that creates competitive advantage through new technologies, products, and materials. Technology development initially focused on an incumbent opaque open moulding glass fibre reinforced polymer (GFRP) processing technology to produce their products. From 2002 to 2003, the company developed and introduced a novel opaque RTM processing technology to address environmental regulations, improve product quality and open-up new product offerings within its primary market. This is characterized as a 'technology opportunity' on the timeline depicted in Figure 3-5.

[9] This case study was compiled from primary and secondary sources, including interviews with a technical expert from SME #1 conducted on June 1st and June 23rd, 2016.

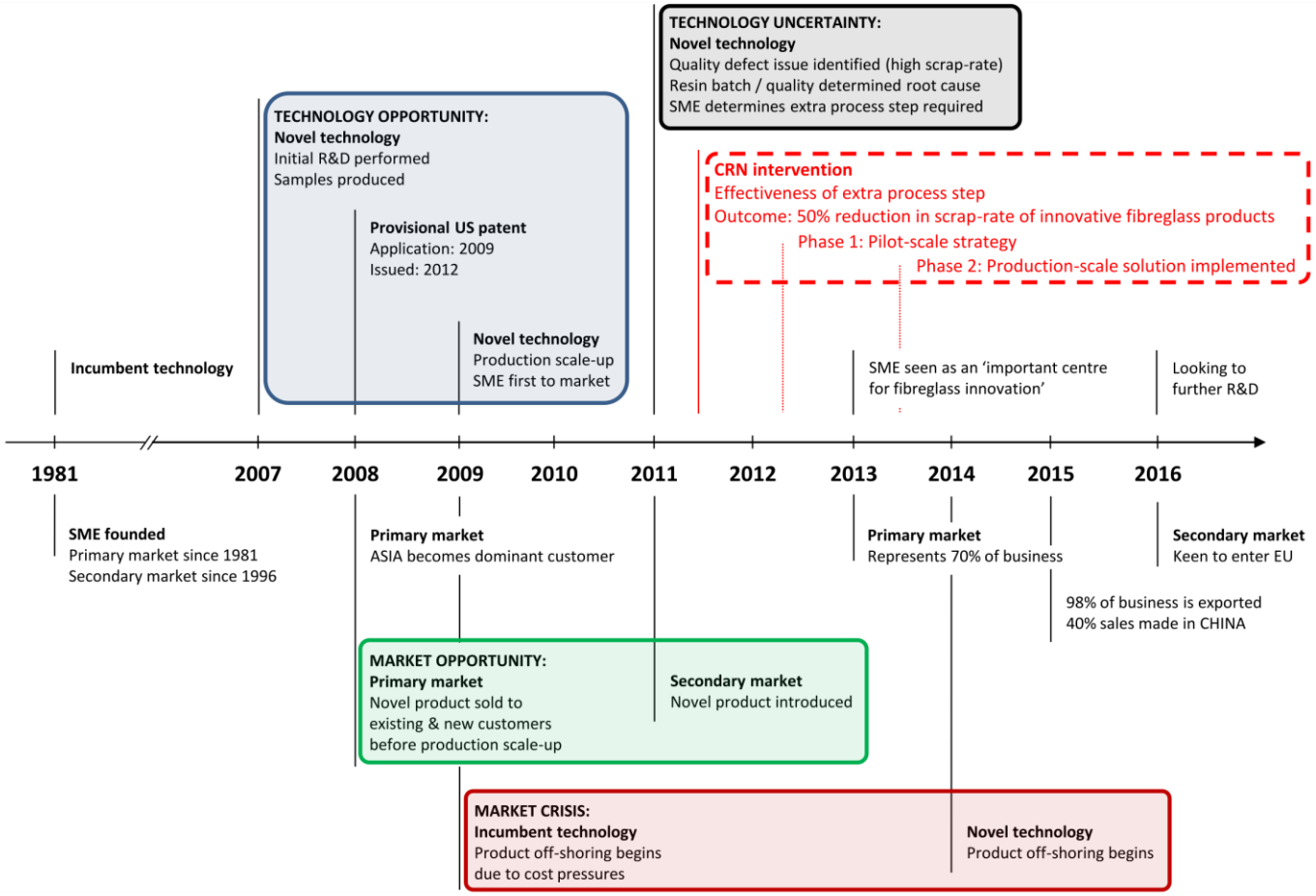

Figure 3-5: Structural glass fibre component manufacturer (SME #1).

In 2009, the in-house manufacturing business model changed, and SME #1 was no longer exclusively fabricating products for its parent company in its primary market. Shifts in the dominant customer base in the early-mid 2000s and high production costs contributed to the decision to offshore their incumbent GFRP processing technology. This is characterized as a 'market crisis' on the timeline depicted in Figure 3-5. This offshoring decision forced SME #1 to enhance its competitiveness in high margin products and high value technologies in order to survive. As a result, they become an important centre for glass fibre innovations.

SME #1 created market demand amongst existing and new customers in the primary market with the concept and development of a novel translucent RTM processing technology to enable innovative glass fibre products with both structural and functional attributes. This is characterized as a 'market opportunity' on the timeline depicted in Figure 3-5. In-house R&D resulted in the production of product samples which were functionally and aesthetically valued by customers. This product created such demand that it was sold to customers prior to production scale-up. R&D development of this new product resulted in the filing of a provisional patent in 2008 that was issued in 2012. Commercial production began in 2009. While there were initial concerns regarding product quality relating to porosity management, which greatly affects translucency and thus aesthetic value, customers were still keen to accept the product. These quality issues were not apparent in the samples originally produced.

In 2011, quality issues in this product became more apparent given the introduction of this new product in their secondary market. Porosity acceptance limits for the primary market were not acceptable for the secondary market application. Given the nature of the translucent RTM process and, unlike the opaque products produced, this quality issue could not be resolved by repairing the product. This production defect alone contributed to a significant increase in production cost and scrap rates. The reason for the defects was unknown and the defects did not appear in the small, flat product samples. This is characterized as 'technology uncertainty' on the timeline depicted Figure 3-5. SME #1 undertook extensive in-house R&D to determine the root cause and established, through systematic and time intensive isolation of process variables, that resin batch variability was the contributing factor. It was determined that an extra processing step to degas the resin was necessary to mitigate the problem.

By mid-2011 a partnership with CRN was formed to investigate the effectiveness of this additional processing step, with an initial strategy proposed at pilot scale and the implementation of a production scale solution. The outcome of this project was very successful, with scrap rates of products fabricated using the novel translucent RTM processing technology falling by 50%, and a significant production cost reduction achieved. SME #1 acknowledges that they benefitted from CRN's contribution and work, which over an 18-month period, involved: technical staff at CRN establishing a science based understanding of problems in the production process when fabricating large and geometrically complex parts, predicting the processing conditions for high product quality, performing trials on site with the company's manufacturing equipment, and collaborating with SME #1 to adapt their manufacturing practices. Through greater process

control, SME #1 was also able to improve their acceptance criteria for porosity across all their products, and thus technology uncertainty was greatly reduced.

Despite the successful technology outcome achieved with CRN, the outlook for SME #1 is mixed. The company is vulnerable to high labour costs and fluctuations in raw material costs and faces significant challenges to remain quality and cost competitive. Nevertheless, and even with a decline in market share in their primary market, SME #1 remains optimistic in relation to future innovation and development of high-margin products within its novel translucent product range, and is seeking out new opportunities, particularly new customers, and products, within their secondary market and alternative new markets.

3.2.3 Case 3: Industrial SME #2 (High performance CFRP component manufacturer)[10]

Originally SME #2 was established as an in-house component division prior to being spun-off in the early 1990s to cater for the needs of progressive customers in the boutique aftermarket in its primary market (see Figure 3-6). This company is internationally recognized for its CFRP technology and high performance CFRP products for OEM customers, and boutique aftermarket in its primary market.

[10] This case study was compiled from primary and secondary sources, including an interview with technical experts from SME #2 conducted on July 12th, 2016.

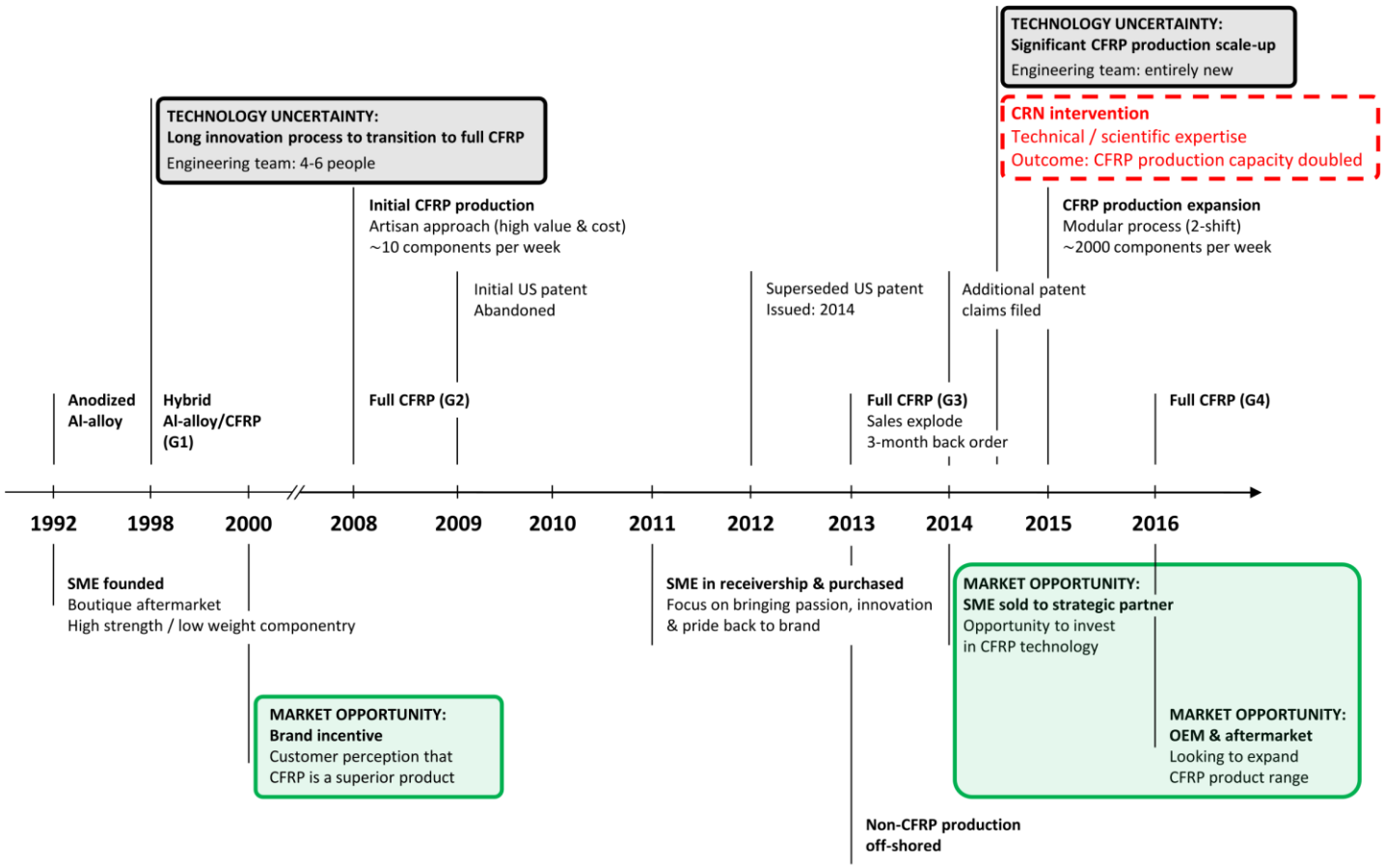

Figure 3-6: High performance carbon fibre component manufacturer (SME #2). CFRP: Carbon Fibre Reinforced Polymer.

Shifts towards CFRP in this primary market occurred in the 2000s, driven by the desire to improve performance and functional attributes, but also to signal top quality, differentiated product to customers. Customer perception was at the time, as it is now, that CFRP enables a superior premium product, and thus there was a brand incentive for SME #2 to get into CFRP technology and to understand it early. This 'market opportunity' is depicted on the timeline in Figure 3-6. SME #2 initially experimented with CFRP to develop a first-generation hybrid Al-alloy/CFRP product (G1). The company undertook a lengthy period of product, process, and equipment innovation to bring its first full-CFRP product, considered the second-generation CFRP product (G2) to market in 2008. This is characterized on the timeline depicted in Figure 3-6 as 'technology uncertainty'. A combination of true innovation, 'eureka moments', 'trial and error' and lack of industry perception were factors that led to the development of a unique yet unconventional production process in which a patent application was filed in 2009 and issued in 2014. This initial CFRP process resembled more of an artisan/hobby approach with high value, low volume (in the order of ~10 components per week), long lead times and was reflected in the high cost of the product.

By early 2011, new management of SME #2 recognized the need to protect their CFRP technology through patents, trade secrets, and non-disclosure agreements (NDAs), and had the entrepreneurial vision to want to reposition themselves in their value chain. This is characterized as 'market opportunity' on the timeline depicted in Figure 3-6. By 2013, SME #2 had offshored all non-CFRP products and technology, moved to a new production facility and launched their third-generation full-CFRP product (G3). By late 2014, SME #2 was purchased by a parent company. This decision appears strategic as the partnership was formed to win market share for

OEM customers over its competitors in the primary market. SME #2 brings its CFRP technology and expanded product range to the table, whereas the parent company provides necessary distribution channels to potential OEM customers.

Amid the success of its G3 product, SME #2 collaborated with CRN in mid-2014. The company was experiencing a backlog in orders and was suddenly faced with a completely new engineering team. Despite additional investment in equipment and a two-shift operation, the current production process could not keep up with demand. While it was evident that changes to the production process were necessary, the engineering team was extremely cautious about implementing changes without completely understanding why or, more importantly, detrimentally affecting product quality or productivity. This is characterized as 'technology uncertainty' on the timeline depicted in Figure 3-6.

CRN's technical expertise in understanding the manufacturing science for thermal management problems and resources provided the engineering team with the confidence to identify production bottlenecks that may have not been obvious or identified as rapidly had a traditional 'trial and error' approach been adopted. This six-month project involved: CRN technical staff performing materials characterization at UBC, the use of modelling and simulation to optimize the manufacturing process, trials on site at the company, and collaborating with SME #2 employees to adapt their manufacturing practices. The outcome of this project resulted in a doubling of production capacity and an increased utilization of existing production equipment with no detrimental impact on product quality or structural integrity, and with minimal capital cost.

This partnership also provided the engineering team at SME #2 with a better understanding of their process, and these insights enable them to be creative and approach future R&D differently.

Since this project concluded in mid-2015, SME #2 has now implemented a production system capable of meeting the demand for their CFRP products (in the order of ~2000 components per week). Additionally, SME #2 has managed to retain its autonomy despite its status as a subsidiary to its parent company. At a time when many in the primary market are offshoring all technology, SME #2 and its CFRP technology has remained in Canada. The company recognizes many benefits in doing so: 1) with geographic isolation, it is easier to protect the CFRP technology and the knowledge regarding the technology and process; 2) with the collocation of engineering and production, it is easier and more efficient to troubleshoot problems and rapidly develop future R&D; and 3) taking advantage of its regional innovation ecosystem, established due the introduction of the Boeing 787 Dreamliner, with its world-class material supplier locally located nearby in the US, and with its interaction with CRN.

3.3 Analysis

The case studies of the two composites manufacturers, SME #1 and SME #2, are compared and contrasted along the attributes which led to technological and market uncertainty, and the role of collaborating with a CTRC to resolve technological uncertainty and create market opportunity is assessed. The attributes of technological and market uncertainty are drawn from a value creation model developed by Maine and Garnsey [20] and discussed in Section 2.1.2.

3.3.1 Technological uncertainty

Both SME #1 and SME #2 experienced high technological uncertainty in developing radical technology to enable higher margin products with improved performance attributes. SME #1's novel technology is classified as radical as it enabled an entirely new performance attribute, and SME #2's novel CFRP processing technology is classified as radical as it enabled significantly enhanced existing performance attributes and cost reductions through increased production volume. To achieve these outcomes, both SMEs required complementary innovations. While SME #1 relied on both upstream (material supplier) and downstream (product design) value chain partners to enable the development of their novel GFRP processing technology, SME #2 relied on concurrent in-house product development.

Process innovation was key for both SME #1 and SME #2 to scale-up production. Both SMEs successfully pursued strategies to develop and patent their high value composite materials processing technologies in-house. This required customized R&D, expertise and skilled teams, and long time frames. For SME #1, development of their novel GFRP processing technology took several years and enabled them to claim 'first-to-market' status. On the other hand, original process innovation took much longer for SME #2, but resulted in a unique CFRP technology which has since become an integral element of the company's image and brand.

Given the high amount of tacit knowledge generated, both SMEs demonstrated development of low modularity process innovation. Although the upside of a low modularity technology can create a significant competitive advantage [49], both SMEs experienced additional downside effects. For SME #1, this has meant offshoring their 'know-how' given that they are no longer

operating an exclusive in-house manufacturing business model. With significant and sudden changes to their engineering team, for SME #2 this meant that they became extremely cautious about making changes to their process for fear of unanticipated consequences.

In both cases, the science based intervention by CRN to reduce technological uncertainty focused on existing process technology scale-up, albeit in different stages in the commercialization process. SME #1 had experienced technical problems in scaling up their novel GFRP processing technology, leading to production disruptions as they attempted to identify the root cause and a suitable corrective action. During this troubleshooting period, SME #1 was unable to deliver products to their customers. CRN's intervention with SME #1 focused on examining the effectiveness of introducing an extra processing step to reduce quality defects. In contrast, SME #2 engaged CRN at a far earlier stage of the commercialization process. Thus, they were able to reduce both technological and market uncertainty by taking advantage of CRN expertise in scaling up their process innovation. CRN's intervention with SME #2 focused on process optimization giving SME #2 the confidence to make decisions about their manufacturing process more efficiently and effectively than had traditional 'trial and error' methods been used. Technological uncertainty was successfully addressed in both cases. However, as summarized in Table 3-2, with CRN intervention occurring sooner in the commercialization process SME #2 could reduce a broader range of uncertainty attributes compared to SME #1. SME #2 was able to create value from using manufacturing science base to exploit market opportunities without production disruptions. On the other hand, SME #1 experienced continuity, observability and trialability problems, which are typically experienced in the scaling up of most advanced materials technologies [20].

Table 3-2: Attributes of technological uncertainty[a] experienced by SME #1 and SME #2.

	SME #1[b]	SME #2[c]
Radical technology (product)	High (new performance attribute enabled)	High (significantly improved performance attributes, significant reduction in manufacturing cost)
Process innovation needed	Yes (process driven)	Yes (process driven)
Modularity	Low	Low
Maturity	Low (quality)	Low (yield, cost)
Customized R&D needed	Yes (in-house)	Yes (in-house)
Complementary innovations needed	Yes (material, product design)	Yes (product design)
CRN intervention (access to science)		
Technological risk	Reduced (process scaling, quality)	Reduced (yield, cost)
Technological opportunity	N/A	Enabled
Time frame	24 months (2-phase project)	6 months
Outcome	50% reduction in scrap rate of innovative product	Production capacity doubled

[a] These attributes and criteria are based on the value creation model [20] (Maine & Garnsey, 2006) and the modularity-maturity matrix [49] (Pisano & Shih, 2012).
[b] Novel GFRP processing technology.
[c] Novel CFRP processing technology.

3.3.2 Market uncertainty

Both SME #1 and SME #2 experienced moderately high market uncertainty, and both responded to perceived market opportunity. However, the motivation to pursue composite materials technology differed in each case. With the development of new innovative translucent GFRP products, SME #1 demonstrated attributes of a technology push strategy in both their primary and secondary markets, but also assessed market opportunity through offering samples to existing and desired customers (see Figure 3-5). SME #2 demonstrated elements of a technology-market matching strategy to adopt CFRP technology early for their primary market (see Figure 3-6), this market opportunity was motivated by industry shifts and market perceptions of quality.

As summarized in Table 3-3, SME #1 has chosen to target multiple markets, and has been able to occupy a downstream value chain position within each of these markets to enable easier prediction of market trends and customer needs. While SME #2 has chosen to focus on multiple applications within a single target market and has strengthened its value chain position with the decision to forward integrate to increase market share and access to OEM customers. Both SMEs lowered market uncertainty in targeting substitution applications. However, in needing complementary innovations, in materials and product design, to commercialize their products this increased market uncertainty in both cases

The perception of composite materials technology as high value innovation differs greatly within SME #1 and SME #2 target markets. While product cost is a dominant factor in SME #1 target markets, superior product performance, aesthetics and branding are dominant factors within the SME #2 target market. Consequently, industrial customers in SME #1 markets are less likely to value the process innovation developed as highly as the predominantly end-consumer customers in SME #2 markets. This difference is evident in the business models and innovation strategies that these composites SMEs have adopted. For instance, SME #1 has chosen to become a centre for glass fibre innovation rather than continue to operate as an exclusive in-house manufacturer for their novel glass fibre products. While process innovation continues to occur in Canada, some production capability and oversight has been offshored. In contrast, innovation and technology protection is vitally important to SME #2. Thus, SME #2 has strategically retained their unique CFRP technology in-house with future scope to consider reclaiming products and capabilities that are currently manufactured offshore.

Table 3-3: Attributes of market uncertainty, value creation and evolution/experimentation[a] experienced by SME #1 and SME#2.

	SME #1[b]	**SME #2[c]**
Number of markets	Multiple	Single
Target	Primary market (emergent) Secondary market (substitution)	Primary market (substitution)
Value chain position	Downstream	Midstream → Forward integration
Negotiating power within value chain	Low (downstream, high buyer power)	Low (upstream) Mid (downstream, moderate buyer power)
Complementary innovations needed	Yes (material, product design)	Yes (product design)
Lack of continuity, observability, trialability	Mid	Low
Change in leadership	No	Yes (2011)
Business / revenue model	In-house manufacturing → Offshoring	In-house manufacturing
Demonstrated value		
Patents issued	Yes	Yes
Importance of IP[d]	Mid (patent)	High (patent, trade secret, NDA[d])
Access to complementary assets	Low (none identified)	Mid (parent company)
Access to finance	Mid (SR&ED[e])	High (SR&ED[e], corporate investment)
CRN intervention (access to science)		
Market risk	N/A	N/A
Market opportunity	N/A	Enabled
National/regional support	Yes (NSERC[f])	Yes (NSERC[f], NRC-IRAP[f])

[a] These attributes and criteria are based on the value creation model [20] (Maine & Garnsey, 2006) and the five-forces model [52] (Porter, 1985).
[b] Incumbent GFRP and novel GFRP processing technology.
[c] Novel CFRP processing technology.
[d] IP: Intellectual Property; NDA: Non-Disclosure Agreement
[e] SR&ED: Scientific Research and Experimental Development Program
[f] NSERC: Natural Sciences and Engineering Research Council of Canada; NRC-IRAP: Industrial Research Assistance Program of the National Research Council Canada

Market uncertainty in the composites industry is compounded by the high integration of product and process innovation [20,45]. The dependence on process innovation to enable product innovation is most challenging, particularly in low modularity technologies [49]. In this respect, a technology push strategy impeded the ability for SME #1 to perform technology-market matching successfully, whereas SME #2 had the autonomy and capability to do so. Although CRN's intervention in both cases did reduce technological uncertainty, market uncertainty was more compellingly addressed with SME #2 than with SME #1. SME #1 is vulnerable to fluctuations in raw material costs and labour, the loss of market share, and risks being completely squeezed-out of the value chain. In contrast, SME #2 is facing greater market opportunity with strong demand for its CFRP products in its primary market and is further increasing its product range.

3.3.3 Conclusions

In the SME case studies selected for analysis in Sections 3.2.2 and 3.2.3, it was shown that the science based interventions performed by CRN did contribute to reducing technological uncertainties, but that this approach resulted in mixed outcomes in terms of enabling new market opportunities and retaining composites manufacturing competencies in Canada. This study demonstrated both the potential benefits of SMEs choosing to collaborate with a CTRC, and the rationale for doing so upfront in the commercialization process. The factors contributing to value creation observed in this study included: 1) the customer utility for composites end products; 2) the freedom to influence both product and process innovation; and 3) intellectual property protection.

Typically, in working with OEMs and large composites suppliers, CTRCs provide no more than technical expertise in supporting the development of new products and recognizing potential market opportunities. It is important to consider that the receptor capabilities for large composites manufacturers and SMEs are different in terms of resources and expertise. To be most effective, CTRCs need to understand what motivates SMEs outside of seeking technical advice on the immediate problem, and thus may choose to develop technology-market matching capabilities to broaden the spectrum of advice and support provided. This may involve partnering with 'innovation benefactors' [56], such as government organizations or accelerators (eg. Canadian NSERC ENGAGE or NRC-IRAP programs, UK Knowledge Transfer Partnerships) which focus on technology brokering and identifying market needs.

The data and case studies presented are based on composites SMEs located in Western Canada, and set in the context of extant innovation management literature and a broader survey of composites SMEs. Thus, this analysis may be generalized to other regions around the world. The outcomes of this study suggest that composites SMEs can create and capture value using science based manufacturing practices through choosing to collaborate with CTRCs. In turn, CTRCs can play an important role in enhancing the strength of their innovation ecosystem to help retain and enhance composites manufacturing capabilities using science based approaches.

3.4 Summary and Discussion

Composites manufacturers are likely to experience high technological and market uncertainty in seeking to bring innovative products to market. The current typical practices for managing composites manufacturing risk and uncertainty were discussed in this chapter. These empirical practices represent high risk since part producibility is often considered after significant program costs have been committed. An outcomes taxonomy was introduced to classify manufacturing outcomes for composites processing based on science based understanding and simulation based thinking. It was shown that this taxonomy can be used to link the manufacturing science base with industrial practice in a structured manner. Finally, through direct observation and case study analysis of large and small composites manufacturers, the value of using composites manufacturing science to reduce technological uncertainty and enable potential market opportunities was demonstrated.

While the value of using the manufacturing science base to manage uncertainty is recognized by large composites manufacturers, as discussed in Section 3.2.1, key barriers for its widespread adoption exist. The perception in industry is that composites manufacturing science is still a niche discipline, and the enabling DFM tools that are available are too complex for non-experts to use quickly and effectively [18]. For composites SMEs, additional challenges for applying science based practice are: 1) knowing that the manufacturing science exists; 2) having the R&D resources and funding to be able to access this knowledge; and 3) accepting and managing the uncertainty involved in such innovations.

In the next chapter, concepts for knowledge translation and transforming manufacturing practice, initially aimed at the composites manufacturing research community and the composites industry, are introduced, along with a hierarchical knowledge model that is intended to organize composites manufacturing domain knowledge and enable effective decision making at *all* stages of the development design cycle.

Chapter 4: Conceptual Theory Building and Framework Development

This chapter introduces philosophical elements of a framework developed to encourage the systematic use of manufacturing science in composites manufacturing practice (see Figure 4-1). Firstly, a rationale for prompting the composites manufacturing research community to consider the steps beyond knowledge creation (knowledge translation), and the composites industry to transform manufacturing practice (*protect–advance–disrupt*) is introduced. Secondly, a hierarchical knowledge model that defines a common nomenclature for representing composites manufacturing problems, in terms of building up the capability of the factory and part producibility (Equipment–Tool–Part–Material factory ontology) is developed. Finally, a series of high-level thermal management manufacturing scenarios are presented to illustrate these concepts and, more importantly, to demonstrate the value of formalizing science based practice. It should be noted that the implementation of the framework introduced in this chapter, as in the development of a knowledge management and decision support tool, is considered future work.

4.1 Formalizing Science Based Practice

Despite the ongoing primary research and resulting volume of scientific literature produced, as discussed in Section 1.1, the uptake of composites manufacturing science in industry has been rather slow and *ad hoc*. This suggests that a new translational research strategy is needed to address this issue. Within such a strategy, the development of a usable framework that combines the manufacturing science base and industrial practice is a necessary first step for formalizing science based composites manufacturing practice (see Figure 4-1).

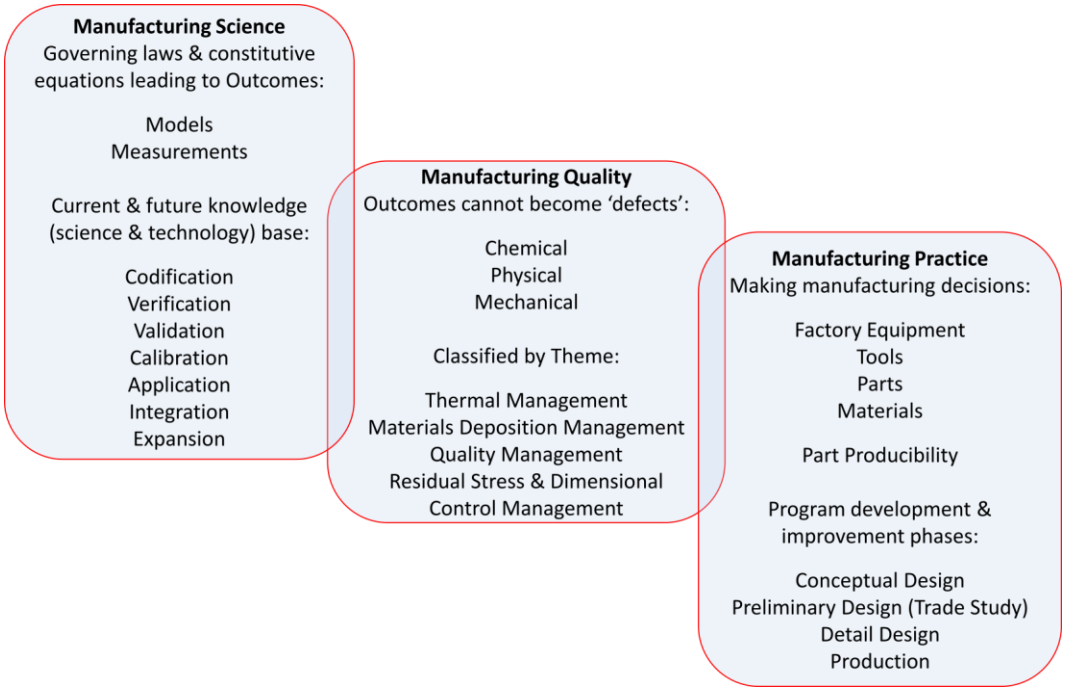

Figure 4-1: A framework for explicitly addressing the practice of manufacturing science.

4.1.1 Knowledge translation

In the context of this research, knowledge translation is the transfer and appropriate size scaling of the manufacturing science base to support effective decision making. This concept is founded on conceptual frameworks, as discussed in Section 2.2.1, such as the knowledge-to-action framework by Graham *et al* [59,60] in the health sciences domain and the relationships between data, information, knowledge and decision making described by Hicks *et al* [61] in engineering design. While the terms technology transfer and knowledge translation are complementary, they are not interchangeable. Technology transfer may be used to describe the scale-up and commercialization activities associated with product and process innovations, whereas knowledge translation refers to the practice of using knowledge, founded on scientific research, for effective decision making.

4.1.1.1 Participants

Knowledge translation is a challenging undertaking that requires a collaborative effort from the composites community. Terms originally defined for the Building Information Modelling framework proposed by Succar [67] in the construction engineering domain are used. In this work, these terms describe the breadth and depth of the composites community:

- *Fields* refer to the breadth of participants across the domain. These include research groups (eg. university based, not-for-profit organizations, institutes), technology vendors, the composites industry (eg. aerospace, automotive, industrial), certifying authorities, standards organizations (eg. CMH-17, ASTM, SAE) and funding agencies (eg. NASA, DARPA, USAF) and industrial associations (eg. SAMPE, ACMA, CCA).

- *Lenses* describe the depth of participants within the domain. These include enterprise (eg. OEMs, SMEs, composites supply chain), facility (eg. new site, existing site), program (eg. NPD, legacy), department (eg. technical: M&P, manufacturing, engineering, tooling, non-technical: management, procurement) and individual (eg. manufacturing expert, new engineer, non-technical decision maker, student).

4.1.1.2 Determinants

Knowledge translation can be divided into two key concepts: knowledge creation and knowledge use, with each comprising idealized phases (see Figure 4-2). The reality, given the complex, dynamic and iterative process of knowledge translation, is that the relationships between these concepts and phases is ambiguous. These phases are adapted from the knowledge-to-action framework by Graham *et al* [59,60] and the hierarchical model by Hicks *et al* [61].

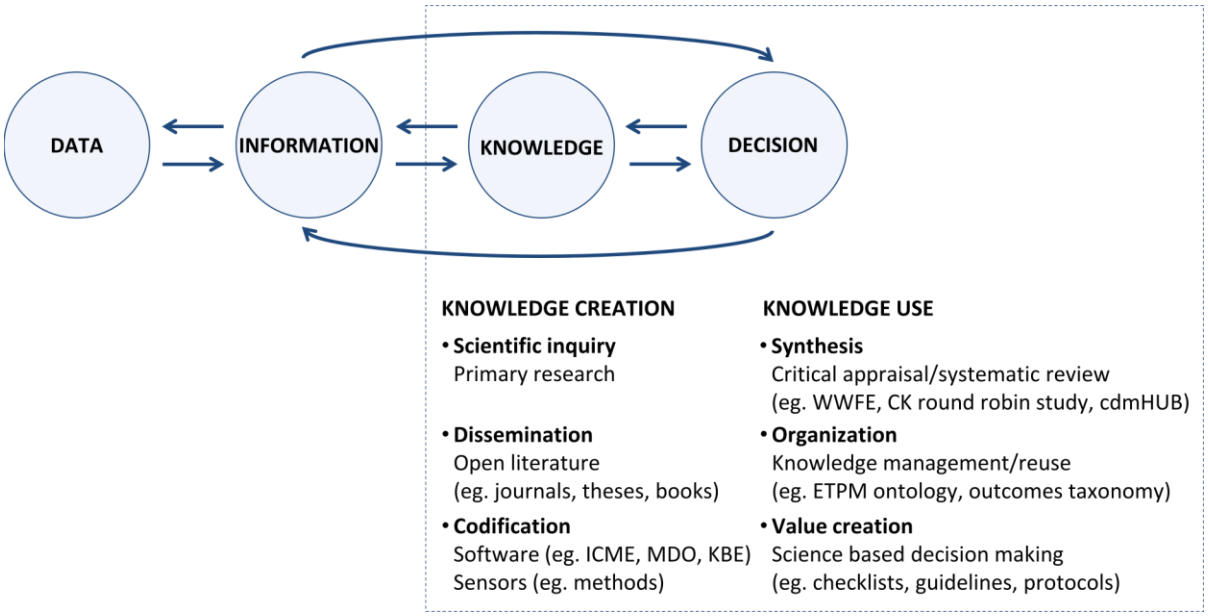

Figure 4-2: The determinants of knowledge translation. Adapted from [59,60] (Graham et al, 2006) and [61] (Hicks et al, 2002). ICME: Integrated Computational Materials Engineering; MDO: Multidisciplinary Design Optimization; KBE: Knowledge Based Engineering; WWFE: World-wide Failure Exercise; CK: Cure Kinetics; cdmHUB: Composites Design and Manufacturing HUB; ETPM: Equipment–Tool–Part–Material.

The three phases of knowledge creation are:

- *Scientific inquiry* includes the completion of primary research in the form of: 1) models, such as the characterization of governing laws and constitutive equations; or 2) measurements, such as the development of discriminator tests or experimental protocols.

- *Dissemination* refers to the efforts to make research findings available in the open literature, such as in journal publications, conference proceedings and doctoral theses.

- *Codification* is the development of the technology base that is good enough to exercise the science. For example, multiscale modelling (eg. ICME: MGI [152,153], EMMC [175]), multidisciplinary design optimization (eg. [120,121]) and the development of knowledge based engineering software tools (eg. [71,72]). Currently, this phase is widely viewed as the ultimate level of translational research.

While the research community has mastered knowledge creation, attention is now needed to address knowledge use. As with knowledge creation, knowledge use is also composed of three phases. These phases are necessary to facilitate the uptake and reuse of the science base by the composites industry and elicit change in manufacturing practice:

- *Synthesis* is the need for sustained critical appraisal and systematic review of all relevant research literature to ensure that the manufacturing science base remains open, correct, usable and useful. This phase positions new knowledge relative to what is known, across length scales and time scales, and shares lessons learned. Efforts in terms of: 1) the science base, such as the World-wide Failure Exercise (WWFE) [227] and cure kinetics round robin study by Dykeman [144]; and 2) the technology base, such as the NCAMP program [228] and Composites Design and Manufacturing HUB (cdmHUB) [229] are excellent examples. Proposed knowledge synthesis topics for thermal management are given in Appendix C.1.

- *Organization* refers to the knowledge management of the manufacturing science base. A formal description of the domain knowledge establishes a common nomenclature between: 1) people, for knowledge exchange and reuse; and 2) systems, for the integration of the technology base. This phase can assist with highlighting gaps within the existing science base, allow new knowledge to be created, permit the implementation of incomplete knowledge (eg. the simple but effective Cure Hardening Instantaneous Linear Elastic (CHILE) constitutive model [100]), promote the interoperability of the technology base (eg. AIM-C [125–130], ICM2 [154–158], VMAP [176]), or be used as a debriefing tool for composites manufacturing experts as they retire.

- *Value creation* is the systematic and targeted development of science based interventions that can directly support standardizing routine workflows and reducing effort in complex workflows. The focus of this phase is to scale the science base relative to the candidate application, or receptor capacity of the knowledge user, and to transform practice without introducing significant risk.

The organization and value creation phases of knowledge use are discussed in Section 4.2. Thermal management case studies, demonstrating the use of manufacturing simulation to support effective decision making and initial efforts to formalize science based workfows are presented in Chapter 5.

4.1.2 Transforming manufacturing practice

In terms of the modularity-maturity matrix proposed by Pisano and Shih [49], and discussed in Section 2.1.1, the production of large-scale composites structures should be considered as as 'process-driven innovation', or low modularity and low maturity technology. The incremental introduction of science based practice will enable composites manufacturing to be transformed from a low modularity and maturity technology, to 'pure product innovation', or a high modularity and high maturity technology (see Figure 4-3).

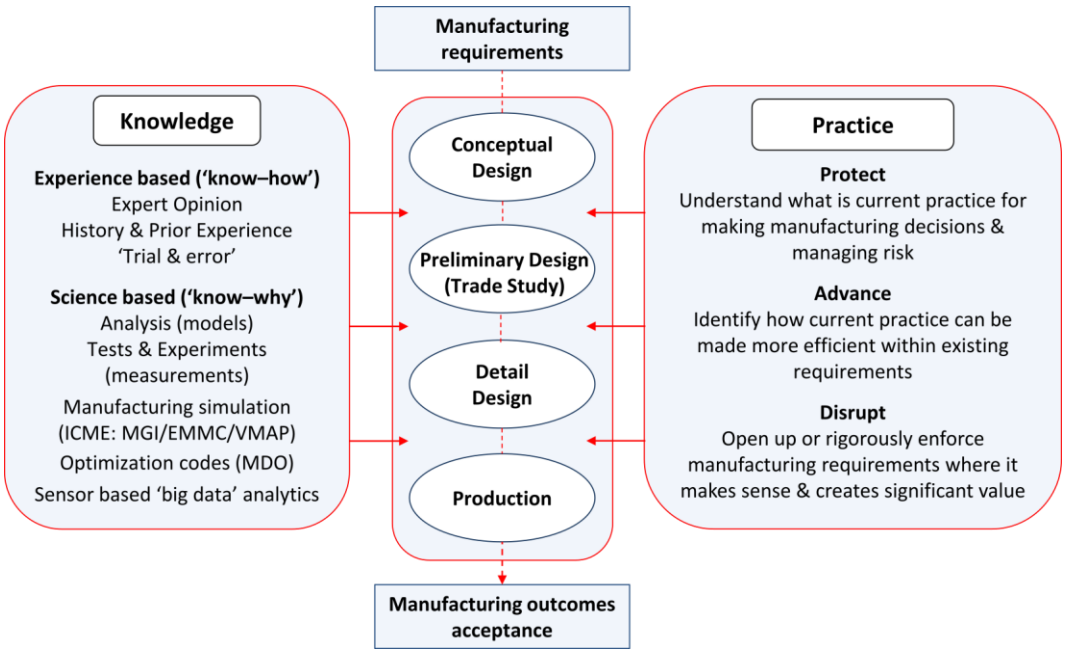

Figure 4-3: Transforming composites manufacturing practice (*protect–advance–disrupt*). Extension of approach from [39] (Ashby, 2011). ICME: Integrated Computational Materials Engineering; MGI: Materials Genome Initiative; EMMC: European Materials Modelling Council; VMAP: Virtual Material Modelling in Manufacturing; MDO: Multidisciplinary Design Optimization.

The following steps to achieve this change sustainably are proposed:

- *Protect* describes current typical practice. Capturing the best current knowledge available for making manufacturing decisions and managing risk, be it of the form of expert opinion, experience, test, or analysis.

- *Advance* refers to future better practice. Using the science base to identify how current practice can be made more efficient, within existing manufacturing requirements. In some ways, this can be considered as back filling the manufacturing practice dominated by 'know-how' with 'know-why'.

- *Disrupt* relates to developing future best practice. This last step requires a deep understanding of the local facts and global science at meaningful production scales to create significant improvements in efficiency, effectiveness, and robustness. This requires understanding as to when it makes sense to either open-up or conversely rigorously enforce manufacturing requirements, thus creating significant value.

An end-to-end thermal management example is used to briefly illustrate these steps, where experimental thermal profiling is defined as current typical practice, and performing a thermal assessment using manufacturing simulation as future better practice (see Figure 4-4). A basic description of these respective workflows is given in Table 4-1.

4.1.2.1 Protect

Typically, the cure window links the materials database generated at the coupon and test panel scale to the material in the part at the production scale. Experimental thermal profiling is a current typical practice in composites manufacturing that involves the empirical measurement of the temperature and temperature rates of parts and tools to ensure that every material point in the part is within this window. Thermocouples (TCs), measuring maximum (lead) and minimum (lag) temperatures, are used to ensure that the temperature profiles of all material points satisfy the respective upper and lower limits of the cure window.

Experimental thermal profiling is often performed late in the development process where by this stage: 1) the part design is well advanced; 2) tooling exists that has most likely been designed and built using legacy approaches; and 3) the autoclave or oven has been commissioned and is functioning or, if new, has been specified and purchased based on legacy approaches. Problems can arise when an experimental thermal profile fails since the cost to make changes at this late stage is significant, as discussed in Section 3.1.3. Typically, each of the basic steps in the experimental thermal profiling workflow, depicted in Figure 4-4 and shown in Table 4-1, are based on empirical approaches. For instance, the determination of representative parts and part families, the location of lead and lag thermocouples, and the troubleshooting strategies to overcome thermal profiling failures, have typically been selected and/or performed based on experience and 'trial and error'.

4.1.2.2 Advance

As an immediate first step towards science based practice, manufacturing simulation can be introduced into this current workflow as an enabling tool. However, the intention would not be to change accepted practice with this science based intervention. Documentation, acceptance, and certification are performed in the same way, however done much faster and cheaper. An incremental transition, such as this, can: 1) build confidence in the use of simulation; 2) shows immediate short-term value; and 3) prepares M&P and manufacturing engineers for greater and more effective change. All decisions can be made using a judicious mix of sensor based test and simulation based analysis.

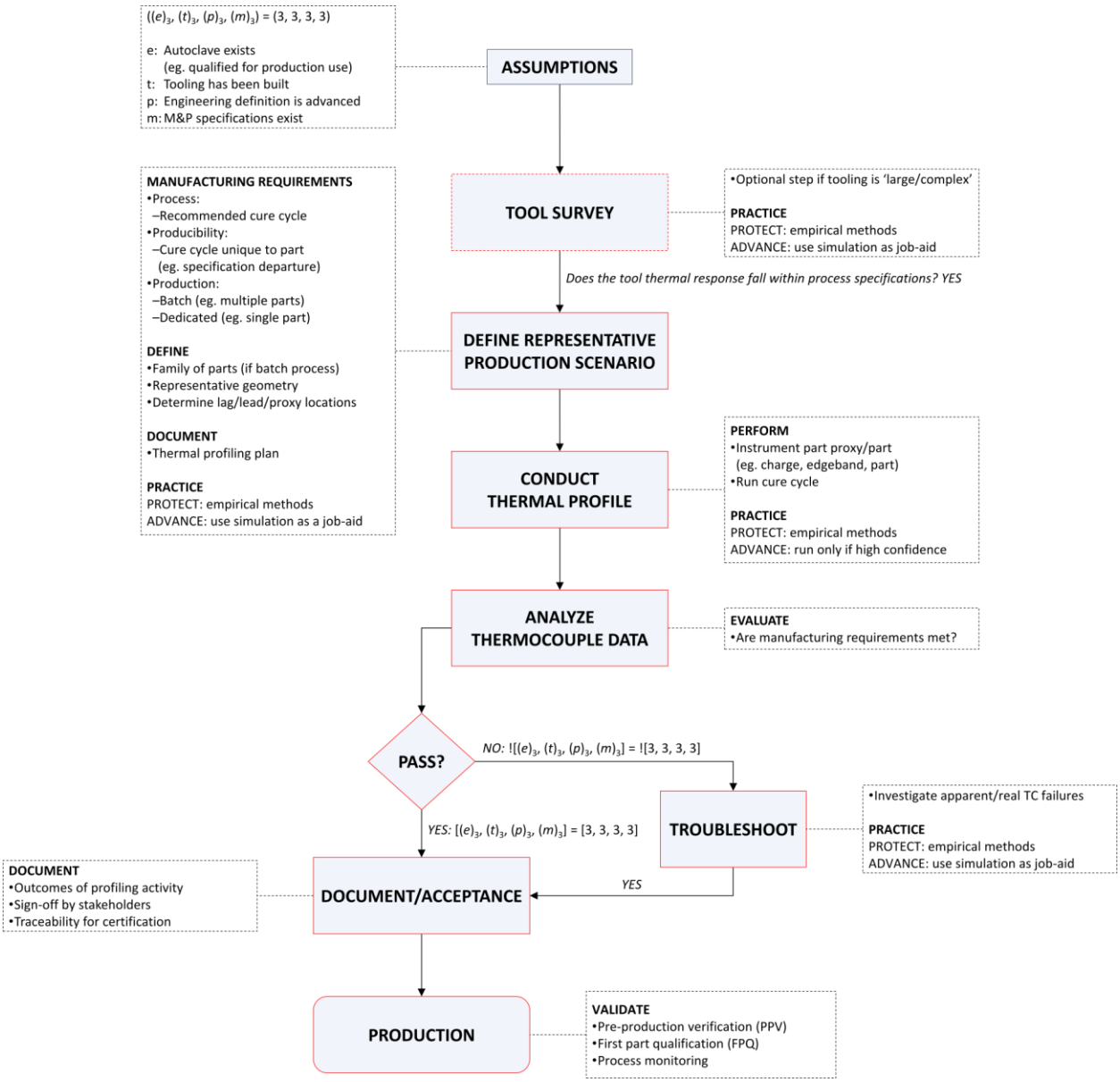

Figure 4-4: Experimental thermal profiling workflow. Adapted from Mobuchon and Zobeiry (2014). ETPM: Equipment–Tool–Part–Material; w, x, y, z: design-gate indices; M&P: Material & Process; TC: Thermocouple. Note: Current typical practice (protect) is to empirically measure the thermal response of parts and tools and future better practice (advance) is to perform thermal assessments using manufacturing simulation.

Table 4-1: Workflow examples of current typical practice and future better practice. Note: Thermal management examples are shown.

Workflow steps	PROTECT: Current typical practice Thermal profiling	ADVANCE: Future better practice Thermal assessment
Define	Production scale part or representative part? Production or developmental facility? (eg. equipment, tools) Determine location of sensors (eg. lead, lag, slowest heat up rate TCs[a])	Determine the attributes to analyze (eg. range of likely HTCs[a], preferred tool concepts, candidate materials, cure cycles) Identify the critical zones/features using manufacturing simulation (eg. 1D drill points)
Perform	Create thermal profiling plan for trial or tool survey (eg. sampling frequency, redundant TCs[a])	Create models & run
Evaluate	Analyze the results for apparent or real failures (eg. faulty TCs[a] vs. true deviation from process specifications)	How robust is my cure window[b]? What is my proximity to 'design cliffs'?
Validate	Are thermal management outcomes acceptable? Perform multiple thermal profiles until success	Perform thermal profile to confirm analysis

[a] TC: Thermocouple; [b] HTC: Heat Transfer Coefficient

[b] A cure window is the allowable range of temperature, pressure, and vacuum values. These limits are typically defined in a process specification.

For instance, as shown in Figure 4-4 and summarized in Table 4-1, the best representative parts and part families can be selected, and the decision to proceed with running an experimental thermal profile can be made if a high confidence in its success exists. Science based methods can be used to evaluate apparent failures to support the justifiable means for rejecting experimental data and ensuring sufficient thermocouple redundancy so that an experimental thermal profile is still valid even if one or more thermocouples are neglected. In terms of troubleshooting real failures, these can be minimized in terms of the effort needed to reduce risk, cost, and time.

4.1.2.3 Disrupt

Enabling significant improvements in efficiency, effectiveness and robustness in composites manufacturing requires thinking beyond accepted practice. Once we are confident in understanding what happens when making production scale structures, these insights can be used

to assess how we could do things differently. Take for example current process specifications used in the aerospace industry. These requirements define the cure window: the upper and lower limits of a cure cycle as a series of ramps and holds. However, what is the rationale for this? Efforts to uncover the origins of this approach suggests a pragmatic and *ad hoc* evolution in the early days of the industry and are best exemplified by the comments of an industry expert who provided their thoughts for why these limits are defined as they are:

> *"… some thoughts for setting limits on max–min cure rates might be:*
> 1. *We have always set these limits*
> 2. *We used XX/min last time on our datasheets*
> 3. *Our test lab can only test at XX/min to YY/min rates*
> 4. *Why do we really need information outside of old limits?*
> 5. *Isn't XX/min standard within the industry?*
> 6. *Don't ASTM/SACMA methods say we only need these rates?*
> 7. *Our competitors use XX/min and YY/min, so our datasheets should mirror theirs*
> 8. *Who cares – just specify some limits!*
>
> …
>
> *Science??? Wow – something new to think about.*" (Industry Expert, [230])

It is instructive to try to justify these limits based on manufacturing science. Typically process specifications have no timing requirements. All material points in a part of interest are deemed to meet the specification independently of one another, regardless of timing. However, the thermal response at all material points in a structure are linked via a nominal air temperature (eg. autoclave air temperature). Thus, to minimize thermal gradients it does make sense to specify lower temperature rate limits. However, upper temperature rate limits cannot be justified other than for the controlling the occurrence of an uncontrolled exotherm on the final hold. In the future, by understanding the best way to achieve material equivalency, we can turn practice from a prescriptive driven to a performance driven process, based on knowing how the part of interest behaves.

4.2 Equipment–Tool–Part–Material Factory Ontology

An object-oriented programming approach, as discussed in Section 2.2.1, is used to develop a hierarchical knowledge model that defines a common nomenclature for: 1) organizing composites manufacturing domain knowledge, as in the current and future science and technology bases (knowledge); and 2) enabling effective decision making at *all* stages of the development design cycle (practice). The details of this ontology, known as the Equipment–Tool–Part–Material (ETPM) factory ontology, are described in the following sections.

4.2.1 Concept definition

Composites manufacturing problems can be described as a systems level problem composed of four classes: 'Equipment' (E), 'Tool and consumables' (T), 'Part' (P) and 'Material and process' (M). Classes are denoted in uppercase. This Equipment–Tool–Part–Material (ETPM) factory system enables manufacturing uncertainty to be deconvoluted systematically and can be used to represent two orthogonal types of manufacturing problems that are encountered in practice (see Figure 4-5), where:

- *Factory* (F) is the aggregation of individual components of the factory, or the building up of the capability of the factory system (F = <E, T, P, M>). Angle brackets denote a collection of classes.

- *Producibility* (O) refers to the acceptability of parts as they move through the factory, or the combined response of the factory system (O = *fn*<E, T, P, M>)[11].

[11] Although the producibility concept is introduced in this work in terms of part quality acceptance, this concept can also be considered as a definition of manufacturing risk or cost.

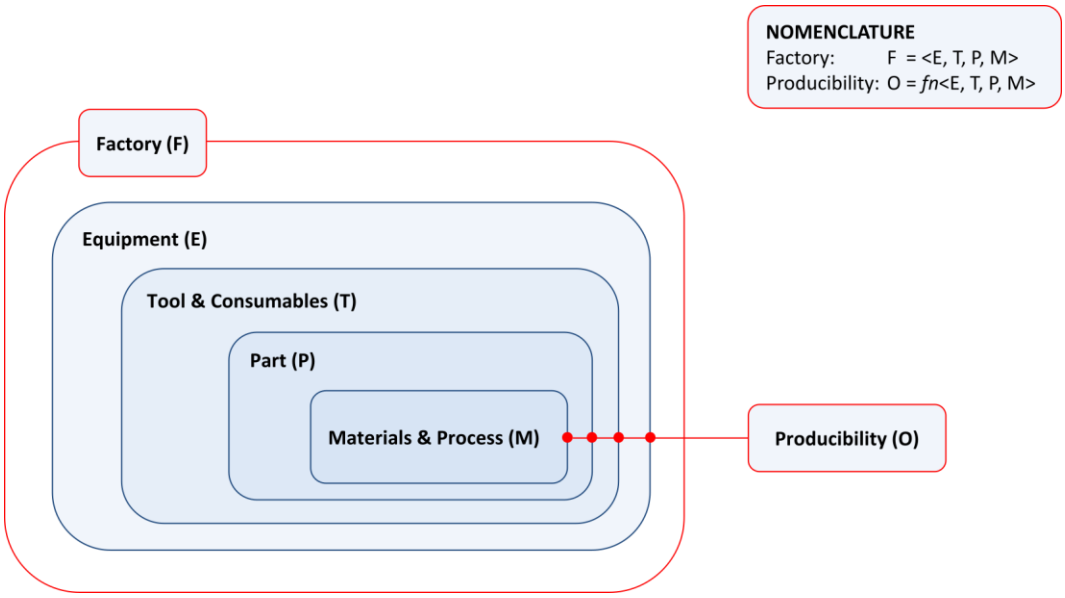

Figure 4-5: A high-level representation of the ETPM factory ontology. This hierarchical knowledge model represents manufacturing problems relating to building up the capability of the factory (Factory) and the acceptability of parts as they move through the factory (Producibility). ETPM: Equipment–Tool–Part–Material; *fn:* function. Note: Classes are denoted in uppercase. Angle brackets denote a collection of classes.

4.2.2 Attributes

The attributes of factory and producibility types of manufacturing problems are defined in Table 4-2. In categorizing these attributes, terms first proposed by Ashby [39] for systematic materials selection in mechanical design are adopted:

- *Variables* are parameters of the factory system that are grouped in terms of the thermal management, material deposition management, quality management and residual stress and dimensional control management processing themes. For problems relating to the capability of the factory, these attributes are the physical characteristics or properties of the respective ETPM classes (see Figure 4-6), for example autoclave heat transfer coefficients, or the tool plate thickness. In terms of part producibility, these attributes are referred to as manufacturing outcomes (see Figure 3-2), for example the *achieved* porosity level or fibre volume fraction.

- *Constraints* set the acceptable limits or requirements imposed on the factory system. For convenience these attributes are tracked in the appropriate ETPM class. Manufacturing requirements can be considered in terms of process, producibility and production. Process requirements define the global specification of a material system, for example the *acceptable* fibre volume fraction or porosity level and are attributes of the Material class. Modifications made to these requirements for a given material system affect *all* subsequent parts produced with this specification. As an aside, this approach differs from work relating to defect taxonomies in composites manufacturing that choose to breakout defects in terms of process, rather than by transformations of the material (eg. [187–189]). Producibility requirements are a local specification that are uniquely applied to parts or part families, for example the use of an intermediate hold or low pressure cure to prevent 'core crush' (eg. collapse of the honeycomb core cell walls). These requirements are attributes of the Part class. Finally, production requirements are another type of local specification applied to support changes to production, for example fast cycles to support production rate increases or batch style cycles to support the fabrication of many different parts in a batch and are thus attributes of the Equipment class. This ontological approach adopted here reflects the industrial practice of using producibility and production requirements to open-up baseline process specifications. This is also known as a specification departure.

- *Objective indices* refer to assessment metrics that are tracked explicitly as attributes. These metrics are the results of screening and ranking activities performed on the factory system. The concepts of a design-gate index (GI) is introduced as a measure of the design freedom or the penalty to make design changes to the factory system, is introduced. The GI index is

an attribute of the respective ETPM classes and is assigned one of three levels [1–2–3]. This index will be described further in Section 4.2.3. The risk index (RI) is a measure of our confidence in the factory system, where a pass (green), marginal (yellow) or fail (red) criterion [G–Y–R] is assigned and enumerated across all manufacturing outcomes considered. In future, an expected cost metric (EC) can be used to track the expected cost of the factory system. While the initial focus here is to describe the metrics rather than approaches used to perform the assessment, it is noted that work relating to the use of Bayesian approaches to manage manufacturing risk (eg. [125,186]), and the development of composites manufacturing cost models (eg. [70,231]) exists in the scientific literature.

Table 4-2: ETPM[a] factory ontology attribute nomenclature. Note: Classes are denoted in uppercase and angle brackets denote collections of classes or attributes.

ETPM[a] factory ontology attribute nomenclature
Factory[b,c,d]
$\mathrm{F} = \langle \mathrm{E, T, P, M} \rangle = \Big\{ \underbrace{\langle \mathrm{a}^{\mathrm{TM}} \rangle, \langle \mathrm{a}^{\mathrm{MDM}} \rangle, \langle \mathrm{a}^{\mathrm{QM}} \rangle, \langle \mathrm{a}^{\mathrm{RSDM}} \rangle}_{\textit{variable attributes (chracteristic)}}, \overbrace{\langle \mathrm{a}^{\mathrm{REQ}} \rangle}^{\textit{constraint attributes}}, \underbrace{\mathrm{a}^{\mathrm{GI}}}_{\textit{objective index}} \Big\}$
$\Big(\text{eg. } \mathrm{E} = \Big\{ \mathrm{a}_1^{\mathrm{TM}}, \mathrm{a}_2^{\mathrm{TM}} \ldots \mathrm{a}_i^{\mathrm{TM}}, \mathrm{a}_1^{\mathrm{MDM}}, \mathrm{a}_2^{\mathrm{MDM}} \ldots \mathrm{a}_j^{\mathrm{MDM}}, \mathrm{a}_1^{\mathrm{QM}}, \mathrm{a}_2^{\mathrm{QM}} \ldots \mathrm{a}_k^{\mathrm{QM}}, \mathrm{a}_1^{\mathrm{RSDM}}, \mathrm{a}_2^{\mathrm{RSDM}} \ldots \mathrm{a}_l^{\mathrm{RSDM}}, \mathrm{a}_1^{\mathrm{REQ}}, \mathrm{a}_2^{\mathrm{REQ}} \ldots \mathrm{a}_u^{\mathrm{REQ}}, \mathrm{a}^{\mathrm{GI}} \Big\} \Big)$
Producibility[b,c,e]
$\mathrm{O} = fn\langle \mathrm{E, T, P, M} \rangle = \Big\{ \underbrace{\langle \mathrm{a}^{\mathrm{TM}} \rangle, \langle \mathrm{a}^{\mathrm{MDM}} \rangle, \langle \mathrm{a}^{\mathrm{QM}} \rangle, \langle \mathrm{a}^{\mathrm{RSDM}} \rangle}_{\textit{variable attributes (outcome)}}, \overbrace{\langle \mathrm{a}^{\mathrm{RI}} \rangle, \mathrm{a}^{\mathrm{EC}}}^{\textit{objective indices}} \Big\}$
$\Big(\text{eg. } \mathrm{O} = \Big\{ \mathrm{a}_1^{\mathrm{TM}}, \mathrm{a}_2^{\mathrm{TM}} \ldots \mathrm{a}_i^{\mathrm{TM}}, \mathrm{a}_1^{\mathrm{MDM}}, \mathrm{a}_2^{\mathrm{MDM}} \ldots \mathrm{a}_j^{\mathrm{MDM}}, \mathrm{a}_1^{\mathrm{QM}}, \mathrm{a}_2^{\mathrm{QM}} \ldots \mathrm{a}_k^{\mathrm{QM}}, \mathrm{a}_1^{\mathrm{RSDM}}, \mathrm{a}_2^{\mathrm{RSDM}} \ldots \mathrm{a}_l^{\mathrm{RSDM}}, \mathrm{a}_1^{\mathrm{RI}}, \mathrm{a}_2^{\mathrm{RI}} \ldots \mathrm{a}_v^{\mathrm{RI}}, \mathrm{a}^{\mathrm{EC}} \Big\} \Big)$

[a] ETPM: Equipment–Tool–Part–Material
[b] *i*, *j*, *k*, *l*: number of variable attributes; *u*: number of constraint attributes; *v*: number of objective indices
[c] Variable attributes for: thermal management (a^{TM}); material deposition management ($\mathrm{a}^{\mathrm{MDM}}$); quality management ($\mathrm{a}^{\mathrm{QM}}$); residual stress & dimensional control management ($\mathrm{a}^{\mathrm{RSDM}}$)
[d] Constraint attributes for manufacturing requirements ($\mathrm{a}^{\mathrm{REQ}}$) (eg. process requirements ($\mathrm{M.a}^{\mathrm{REQ}}$), producibility requirements ($\mathrm{P.a}^{\mathrm{REQ}}$), production requirements ($\mathrm{E.a}^{\mathrm{REQ}}$)); GI: Design-gate Index
[e] *fn*: function; RI: Risk Index; EC: Expected Cost

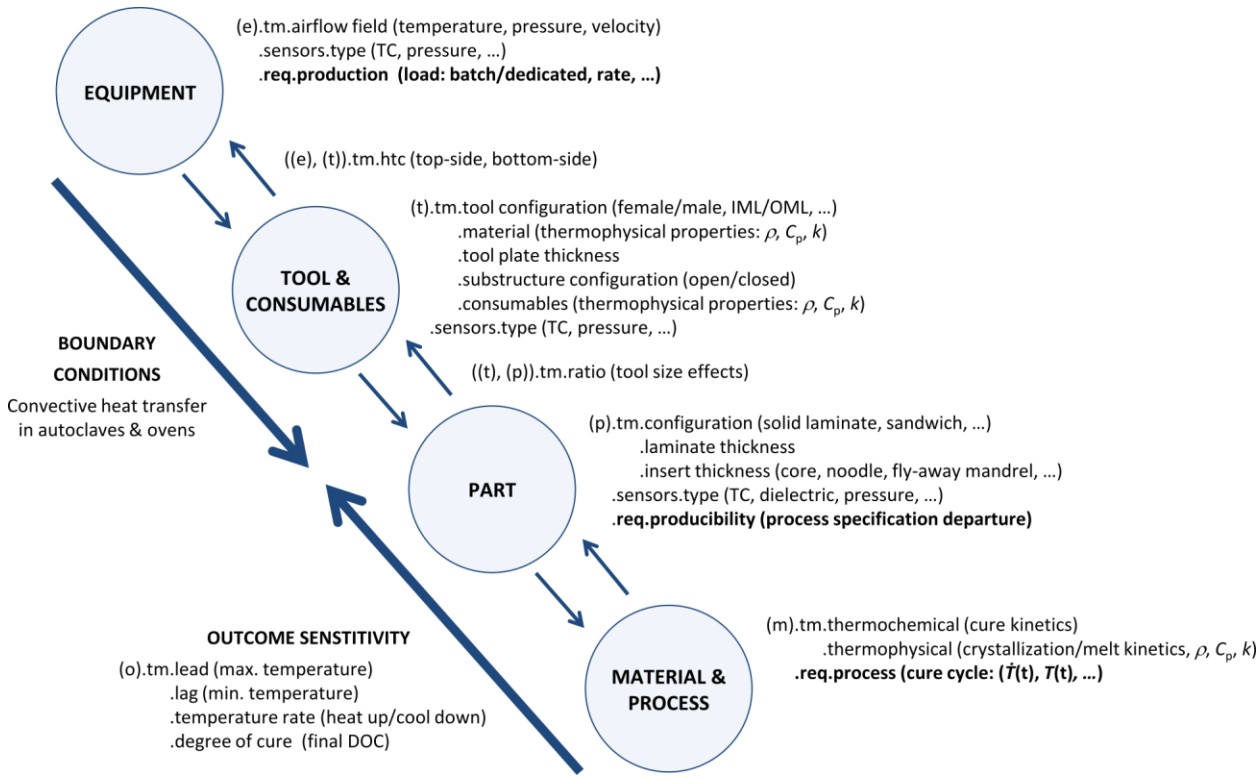

Figure 4-6: ETPM factory ontology class hierarchy and attributes for thermal management. Examples for autoclave and oven cure processes are shown. ETPM: Equipment–Tool–Part–Material; tm: thermal management; TC: Thermocouple; req: requirement; htc: heat transfer coefficient; IML: Inner Mould Line; OML: Outer Mould Line; ρ: density; C_p: specific heat capacity; k: thermal conductivity; $\dot{T}$(t): temperature rate; T(t): hold temperature. Note: Instances are denoted in lowercase. Variable attributes are shown in plain text and constraint attributes are shown in bold. Arrows indicate interactions between ETPM classes.

4.2.3 Relations

From a science based perspective, a hierarchy within the factory system exists. This hierarchy explains the interactions between respective ETPM classes. While the Equipment and Tool classes represent the boundary conditions of the factory system, the Part and Material classes represent the outcome sensitivity of the factory system response (see Figure 4-6). Process requirements are often confused with the applied equipment boundary conditions. Thus, it must be emphasized that it is the capability of the equipment that represents the best case for the factory system to satisfy the process requirements of the material. For example, an empty autoclave or oven airflow field

(eg. temperature, pressure, velocity) represents the best case to achieve the required heating rates and hold temperatures. The subsequent addition of tools and parts introduces thermal resistances into the factory system. Ultimately, the goal is to ensure that the thermal response of all material points within the structure of interest satisfy process requirements. As discussed in Section 3.1.2.2, an effective strategy is to balance thermal management sources and sinks (see Figure 3-3).

4.2.4 Instances

ETPM instances represent physical objects of the factory, either as a specific individual or as collections of the four respective ETPM classes. Instances are denoted in lowercase. For example, the three autoclaves compared by Johnston *et al* [100,101], industrial autoclaves A and B, as well as the UBC autoclave, can all be considered thermal management instances that belong to the Equipment class, as children of the HeatingSystem and HorizontalAirflow subclasses. As specific individuals, these instances are denoted as (e_1) = industrial autoclave A, (e_2) = industrial autoclave B and (e_3) = UBC autoclave. As a collection, these instances are denoted as (e) = (e_1, e_2, e_3). The use of italics indicates shorthand notation.

The design-gate index (GI) is used to determine where we are in the development design cycle, from conceptual design to production. For convenience, this index is explicitly tracked as an attribute of the respective ETPM classes and is assigned one of three levels [1–2–3]. When the GI level changes a new ETPM instance is created. For example, $(e)_3 = (e_1, e_2)_3$ indicates that industrial autoclaves A and B are at GI level = 3, meaning that both physically exist and are ready for production use. It should be noted that the UBC autoclave is omitted from the collection $(e)_3$ as it is a research autoclave that has not been qualified for production use.

GI levels can be incremented (eg. level 1 to 2) or rolled back (eg. level 3 to 2), where the need to downgrade indicates that some form of troubleshooting of an ETPM instance is required.

The suggested GI level definitions, outlined in Table 4-3, are based on accepted engineering design frameworks, such as the 'building block' approach [192,193], gated design and program life cycle, and technology and manufacturing readiness levels (TRLs/MRLs) [17,132]. However, it is noted that for each of these existing paradigms, these definitions may be interpreted differently in practice. Typical technology readiness level ranges are given as guidance. A brief description of the GI levels is summarized here:

- *GI level 1* (conceptual design or TRL1–TRL3) represents the early stages of the development design cycle and the highest design freedom. Typically, this is where significant program decisions and costs are committed, particularly with regard to the material and equipment components of the factory system.

- *GI level 2* (preliminary design/trade study or TRL4–TRL6) is where manufacturing choices are down selected, and the details of the factory system are specified. At this stage, components of the factory system may physically exist or exist as proxies that are not intended for production implementation (eg. developmental autoclaves and tools, pre-production parts). In a research context, this is the highest GI level that can be attained.

- *GI level 3* (detailed design or TRL7–TRL9) relates to the final stages of the development design cycle and finalizing the factory system for production readiness. Components of the factory system must physically exist, thus the penalty to make design changes at this stage is significant.

ETPM design states are super collections of ETPM instances or realizations of the factory system. They are denoted as $((e)_w, (t)_x, (p)_y, (m)_z)$, where w, x, y, z are design-gate indices, taking on values [1–2–3]. This nomenclature is also summarized in Table 4-3. A total of 81 ($N = 3^4$) unique design states exist, if it is assumed that the GI index of each of the four ETPM classes can change by one level. These design states allow us to systematically consider all possible manufacturing choices at *all* stages of the development design cycle and production. In the idealized case, and either by a sequence of sequential or concurrent design steps, manufacturing decisions might begin at $((e)_1, (t)_1, (p)_1, (m)_1) = (1, 1, 1, 1)$ and end at $[(e)_3, (t)_3, (p)_3, (m)_3] = [3, 3, 3, 3]$ (see Figure 4-7). It should be noted that using three GI levels provides a sufficient level of resolution of the problem complexity. For instance, using two GI levels would result in 16 ($N = 2^4$) unique design states. Conversely, using nine GI levels, directly representing the nine TRL levels typically used in practice, would result in 6561 ($N = 9^4$) unique design states.

Depending on the nature of the manufacturing problem, not all design states may be admissible. ETPM design states may additionally represent 'bad' or high-risk design states, and thus are undesirable. For example, $((e)_1, (t)_1, (p)_3, (m)_2) = (1, 1, 3, 2)$ represents a design state where the engineering definition of the part has matured in advance of the material design allowables. This design state would be highly undesirable, and thus might be considered inadmissible.

Table 4-3: ETPM[a] factory ontology instance nomenclature and suggested design-gate index definitions. Thermal management examples are shown. Note: Instances are denoted in lowercase, shorthand notation is denoted in italics and angle brackets indicate collections of instances.

ETPM[a] instance nomenclature
Factory[b]
$(\mathrm{f}) = \left\langle (\mathrm{e}_1, \mathrm{e}_2 \ldots \mathrm{e}_i)_\mathrm{w}, (\mathrm{t}_1, \mathrm{t}_2 \ldots \mathrm{t}_j)_\mathrm{x}, (\mathrm{p}_1, \mathrm{p}_2 \ldots \mathrm{p}_k)_\mathrm{y}, (\mathrm{m}_1, \mathrm{m}_2 \ldots \mathrm{m}_l)_\mathrm{z} \right\rangle$
$(\mathrm{f}) = \left\langle (e)_\mathrm{w}, (t)_\mathrm{x}, (p)_\mathrm{y}, (m)_\mathrm{z} \right\rangle$ where w, x, y, z = 1, 2, 3
$\left(\text{eg. } (e)_1 = (\mathrm{e}_1, \mathrm{e}_2 \ldots \mathrm{e}_{i1})_1,\ (e)_2 = (\mathrm{e}_1, \mathrm{e}_2 \ldots \mathrm{e}_{i2})_2,\ (e)_3 = (\mathrm{e}_1, \mathrm{e}_2 \ldots \mathrm{e}_{i3})_3 \quad \text{where } i_3 \le i_2 \le i_1\right)$
Producibility[b,c,d]
$(\mathrm{o}) = fn\left\langle (\mathrm{e}_1, \mathrm{e}_2 \ldots \mathrm{e}_i)_\mathrm{w}, (\mathrm{t}_1, \mathrm{t}_2 \ldots \mathrm{t}_j)_\mathrm{x}, (\mathrm{p}_1, \mathrm{p}_2 \ldots \mathrm{p}_k)_\mathrm{y}, (\mathrm{m}_1, \mathrm{m}_2 \ldots \mathrm{m}_l)_\mathrm{z} \right\rangle$ where w, x, y, z = 1, 2, 3
$(\mathrm{o}) = \left((e)_\mathrm{w}, (t)_\mathrm{x}, (p)_\mathrm{y}, (m)_\mathrm{z}\right) = (\mathrm{w, x, y, z})$
$[\mathrm{o}] = \left[(e)_\mathrm{w}, (t)_\mathrm{x}, (p)_\mathrm{y}, (m)_\mathrm{z}\right] = [\mathrm{w, x, y, z}]$
$![\mathrm{o}] = ![(e)_\mathrm{w}, (t)_\mathrm{x}, (p)_\mathrm{y}, (m)_\mathrm{z}] = ![\mathrm{w, x, y, z}]$
Suggested design-gate index definitions[e]
GI level 1 (conceptual design or TRL1–TRL3)
$(\mathrm{e})_1$: Equipment selection (eg. represented as a range of HTCs for autoclave/oven cure)
$(\mathrm{t})_1$: Tool concepts (eg. represented as a lumped response/thermal mass)
$(\mathrm{p})_1$: Part concepts (eg. preliminary structural layouts)
$(\mathrm{m})_1$: Material selection & characterization of coupon level laminate properties Initial process cycle evaluation & development
GI level 2 (preliminary design/trade study or TRL4–TRL6)
$(\mathrm{e})_2$: Equipment specifications are defined if equipment is new Existing equipment or developmental equipment[f] may be used in manufacturing trials
$(\mathrm{t})_2$: Engineering definition of the tool is specified if tooling is new (eg. material selection & detail design) Existing tools or developmental tools[f] may be used in manufacturing trials
$(\mathrm{p})_2$: Engineering definition of the part is specified (eg. detail design)
$(\mathrm{m})_2$: Broader characterization of laminate properties at configured coupon & element levels Process cycle finalized for the generation of the material allowables database & manufacturing trials
GI level 3 (detailed design or TRL7–TRL9)
$(\mathrm{e})_3$: Equipment is commissioned for production use (eg. legacy equipment or new equipment has been built)
$(\mathrm{t})_3$: Tools physically exist for production use (eg. legacy tools or new tools have been built)
$(\mathrm{p})_3$: Engineering drawings released
$(\mathrm{m})_3$: Material allowables database exists, material & process specification documents released

[a] ETPM: Equipment–Tool–Part–Material
[b] *i*, *j*, *k*, *l*: number of instances; w, x, y, z: design-gate indices
[c] *fn*: function
[d] (w, x, y, z): collection of manufacturing choices under consideration; [w, x, y, z]: validated collection of manufacturing choices; ![w, x, y, z]: collection of manufacturing choices that have failed validation.
[e] GI: Design-gate Index; TRL: Technology Readiness Level
[f] Not intended for production use but used as a physical proxy.

4.2.5 Workflows

Workflows are a set of tasks or actions that allow us to systematically move from one design state to the next. As you enter a design state, the collection of manufacturing choices that have been chosen are evaluated. This is denoted as $((e)_w, (t)_x, (p)_y, (m)_z) = (w, x, y, z)$. As you exit a design state, some form of validation is needed to determine whether the manufacturing choices satisfy manufacturing requirements. The design state $[(e)_w, (t)_x, (p)_y, (m)_z] = [w, x, y, z]$ represents a collection that has passed some form of validation and $![(e)_w, (t)_x, (p)_y, (m)_z] = ![w, x, y, z]$ is a collection that has failed validation. This nomenclature is summarized in Table 4-3.

At each stage in the development design cycle and in production, the questions we ask and the steps we take to resolve these questions are essentially the same (see Figure 4-7). 'How can we reduce risk in every step?' How do we cope with inevitable design changes as the program progresses?' 'How do we cope with problems as we encounter them?' These workflows can be considered a starting point for the development of science based guidelines and checklists. On one hand, standard workflows can be performed with the use of the existing manufacturing science base. For instance, it could be the use of manufacturing simulation to support cure cycle evaluation and development as an activity associated with material qualification at $((e)_1, (t)_1, (p)_1, (m)_2) = (1, 1, 1, 2)$; or alternatively to support experimental thermal profiling activities as part of structural certification at $((e)_3, (t)_3, (p)_3, (m)_3) = (3, 3, 3, 3)$, as previously outlined in Table 4-1. For complex workflows, while the existing manufacturing science base may not be sufficiently mature, the same structured approaches, or simulation based thinking, as disussed in Section 2.2.1, can be applied to manage manufacturing risk effectively.

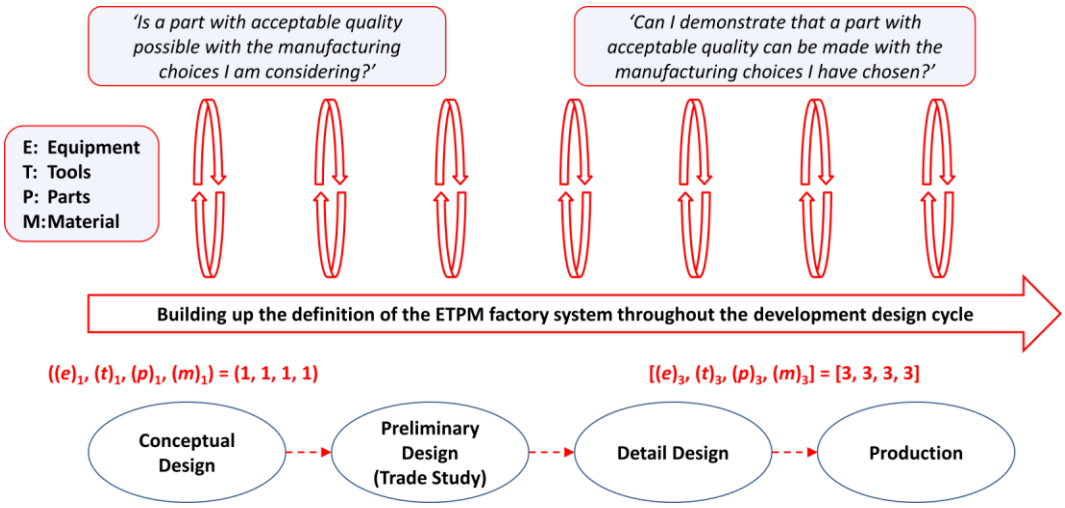

Figure 4-7: The ETPM factory ontology can be used to directly support manufacturing practice and effective decision making at *all* stages of the development design cycle and production. ETPM: Equipment–Tool–Part–Material; $((e)_w, (t)_x, (p)_y, (m)_z)$: a considered collection of manufacturing choices; $[(e)_w, (t)_x, (p)_y, (m)_z]$: a collection of manufacturing choices that has passed validation; w, x, y, z: design-gate indices. Note: Italics indicate the use of shorthand notation. While the questions posed at each stage are essentially the same, it is the definition of the factory system that changes.

ETPM factory ontology scratchpad tools, including a decision tree and attribute canvas, are given in Appendix C.2. These tools can be used to systematically capture manufacturing scenarios. High-level thermal management examples are presented in the next section and in Chapter 5.

4.3 Case Studies

The framework outlined in the previous section is intended to link the manufacturing science base to industrial practice. The capabilities of this developed framework are illustrated with five high-level thermal management manufacturing scenarios that are representative of typical problems faced by composites manufacturers. These case studies are presented in order of the key stages in the development design cycle as follows:

- *Case 1*: *Large composites part development* (conceptual design) – Demonstrates the complex end-to-end sequence of manufacturing decisions involving an OEM and Tier 1 supplier (Figure 4-8).

- *Case 2: Large composites part development* (preliminary design/trade study) – Shows the concurrent manufacturing decisions that an OEM, with access to a developmental autoclave, might pursue (Figure 4-9).

- *Case 3*: *Bid for a small composites part work package* (detail design) – Highlights the limited number of manufacturing choices available to an existing composites supplier (Figure 4-10).

- *Case 4*: *Process improvement* (production) – Demonstrates how science based practice can be used to support the implementation of a new production process for a high-volume composites part (Figure 4-11).

- *Case 5*: *Capturing knowledge for reuse* (future programs) – Highlights the value in systematically capturing knowledge, in the form of expert opinion, experience, test and analysis, for use in future programs (Figure 4-12).

In each case study, the ETPM factory ontology is laid out as a decision tree to show how the manufacturing design space can be systematically traversed with the details of the manufacturing choices made shown in a complementary flowchart. These scenarios demonstrate that there is a pattern to how knowledge use can be formalized.

4.3.1 Case 1: Large composites part development involving a Tier 1 supplier

This case study demonstrates the complex sequence of manufacturing decisions involving an OEM[12] and Tier 1 supplier for the design and build of a large composites part. This part under consideration is assumed to be a primary structure, such as a section of the fuselage or wing. An end-to-end design path is shown in black in Figure 4-8 (a), with an alternative design path shown in grey. Solid double lines indicate where responsibility is transferred between the OEM and Tier 1 supplier. The details of the manufacturing choices made are shown in Figure 4-8 (b).

This scenario begins at $((e)_1, (t)_1, (p)_1, (m)_1) = (1, 1, 1, 1)$, where the OEM is initially presented with a set of four choices (N = 4, see Figure 4-8 (a)). Typically, at this initial stage, the focus is on the Material. Consider what might occur in the qualification of a new material in the following steps. At $[(e)_1, (t)_1, (p)_1, (m_\ell)_1] = [1, 1, 1, 1]$, the coupon level properties of a collection of materials would have been screened and candidate material m_ℓ has been selected for further development. It should be noted that at this early stage, the selection of a material implicitly means that the process broadly associated with this material has also been selected. At the next stage, $[(e)_1, (t)_1, (p)_1, (m_\ell)_2] = [1, 1, 1, 2]$, the element level or configured laminate properties of the candidate material are characterized, and a preliminary process cycle is developed for the generation of the material allowables database. By stage $[(e)_1, (t)_1, (p)_1, (m_\ell)_3] = [1, 1, 1, 3]$, the candidate material is considered qualified for production use. The material allowables database exists and the documents specifying the process requirements have been

[12] For instance, Boeing, Airbus and Bombardier are examples of aerospace OEMs.

released. Typically, the OEM is the custodian of these requirements. This design state also represents an alternative entry point for the OEM if an *existing* material system been chosen.

In preparation for handover from the OEM to the Tier 1 supplier, at stage $[(e)_1, (t)_1, (p)_2, (m_\ell)_3]$ = [1, 1, 2, 3], the OEM might choose to lay out the preliminary engineering definition of the part. This may include defining geometric features, such as laminate thicknesses and ply drops. Moving to the next design state $((e)_2, (t)_1, (p)_2, (m_\ell)_3)$ = (2, 1, 2, 3), represents an entry point for the Tier 1 supplier who is seeking the design and build responsibility for this work package. At this stage, the supplier faces the largest set of choices (N = 19, see Figure 4-8 (a)) for the task of proposing a manufacturing strategy to secure the work. Given that the part of interest is large, it is likely the supplier will focus on the Equipment. Conceivably, this decision is pursued in preference to all other manufacturing choices at this stage due to the long lead times required to commission a new production autoclave. The design state $[(e)_2, (t)_1, (p)_2, (m_\ell)_3]$ = [2, 1, 2, 3], indicates that the manufacturing strategy proposed for this work package has been agreed to by the OEM, and that design and manufacturing authority has been awarded to the supplier. By $[(e)_3, (t)_1, (p)_2, (m_\ell)_3]$ = [3, 1, 2, 3], the production autoclave has been built.

Fewer choices are now available (N = 16, see Figure 4-8 (a)) in moving to the next design state where the focus now shifts from the Equipment to the Tool. At this stage, the supplier might be contemplating preferred tooling concepts, in terms of tool materials, tool plate thicknesses and substructure configurations. The response $![(e)_3, (t)_2, (p)_2, (m_\ell)_3]$ = ![3, 2, 2, 3] might indicate that manufacturing trials at this point are failing to satisfy process requirements.

The troubleshooting strategy assumed in this case study is that the supplier chooses to work with the OEM to requalify material m_ℓ. This non-trivial decision to redefine the constraint attributes by opening up the process requirements is represented by $((e)_3, (t)_2, (p)_2, (m)_2) = (3, 2, 2, 2)$. The design state $[(e)_3, (t)_2, (p)_2, (m_{\ell+1})_2] = [3, 2, 2, 2]$ indicates that modified process cycle $m_{\ell+1}$ has been developed, and by stage $[(e)_3, (t)_2, (p)_2, (m_{\ell+1})_3] = [3, 2, 2, 3]$ a modified material allowables database and revised specification documents have been made available to the supplier. Other possible troubleshooting strategies that the supplier might have pursued at this stage include modifications to: 1) Part constraint attributes (eg. $(e)_3, (t)_2, (p)_1, (m)_3) = (3, 2, 1, 3)$), such as defining producibility requirements allowing for a specification departure to open-up the process requirements; 2) Tool variable attributes (eg. $(e)_3, (t)_1, (p)_2, (m)_3) = (3, 1, 2, 3)$), such as revising the tool plate thickness or substructure configuration; or 3) Equipment variable attributes (eg. $(e)_2, (t)_2, (p)_2, (m)_3) = (2, 2, 2, 3)$), such as redirecting the airflow in the autoclave (eg. [232,233]). Manufacturing trials re-run by the supplier at this stage now pass these new process requirements. With this troubleshooting loop complete, the supplier is able to reach production implementation at $[(e)_3, (t)_3, (p)_3, (m_{\ell+1})_3] = [3, 3, 3, 3]$.

An alternative design path is shown in Figure 4-8 where the supplier may have chosen to concurrently mature the tooling strategy. In this sequence, the design state $![(e)_2, (t)_2, (p)_2, (m_\ell)_3] = ![2, 2, 2, 3]$ indicates that manufacturing trials are again failing to satisfy process requirements. The same troubleshooting strategy to requalify material m_ℓ is assumed and is represented by $((e)_2, (t)_2, (p)_2, (m)_2) = (2, 2, 2, 2)$.

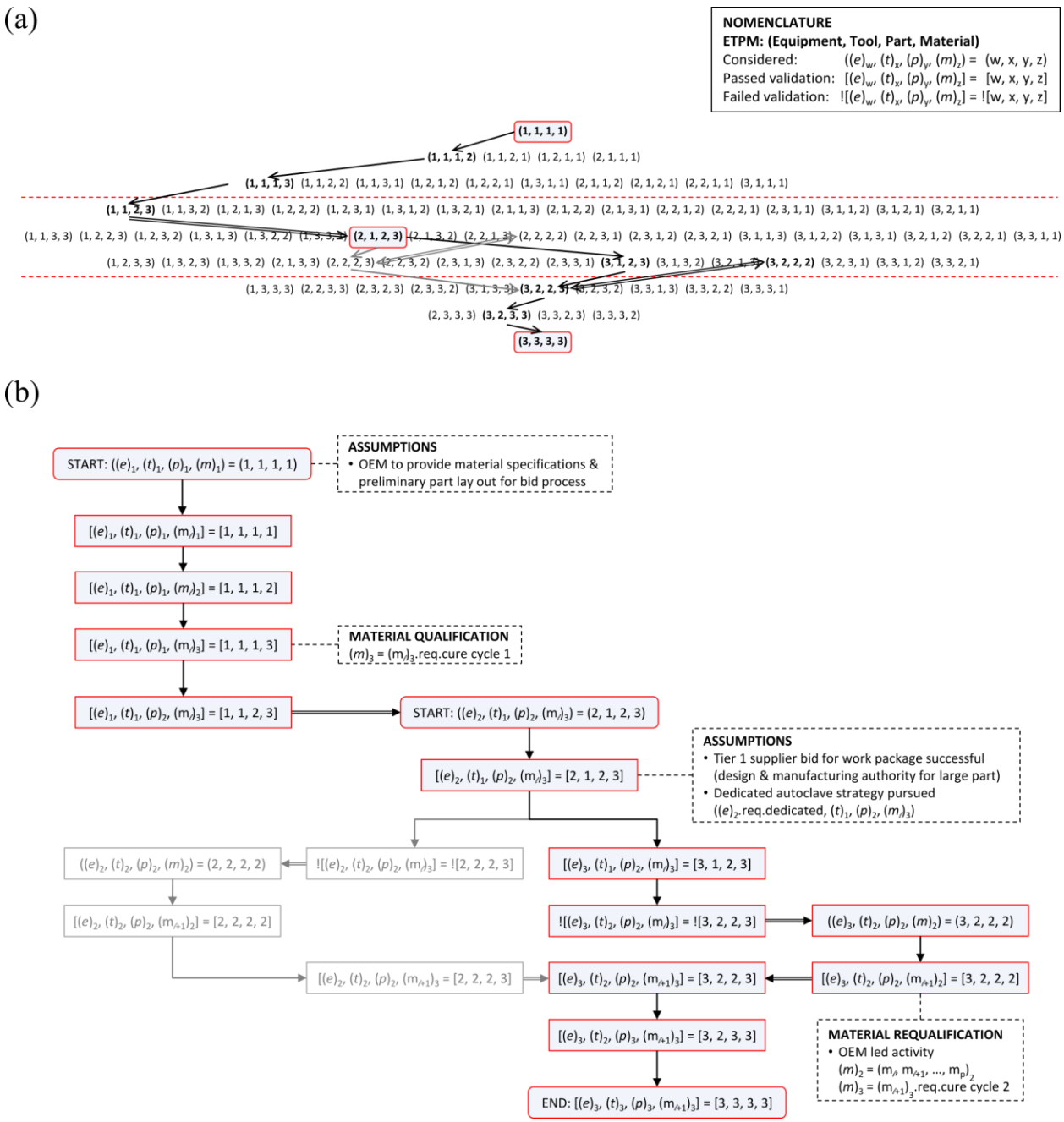

Figure 4-8: Large composites part development. This scenario demonstrates the complex sequence of manufacturing decisions involving an OEM and Tier 1 supplier and is represented using the ETPM factory ontology as: (a) decision tree highlighting all possible design states that could be evaluated and (b) flowchart showing the details of the manufacturing choices made. ETPM: Equipment–Tool–Part–Material; w, x, y, z: design-gate indices; ℓ: material instance identifier; OEM: Original Equipment Manufacturer; req: manufacturing requirement. Note: Instances are denoted in lowercase. An alternative design path is shown in grey. Solid double lines indicate where responsibility is transferred between the OEM and the Tier 1 supplier.

4.3.2 Case 2: Large composites part development with developmental autoclave

As with the first scenario, this case study relates to the design and build of a large composites part. In this example, the focus is on the concurrent sequence of manufacturing decisions that an OEM, with access to a developmental autoclave, might consider pursuing. Using a developmental autoclave means that manufacturing trials can proceed without having to wait until a production autoclave is commissioned. A typical design path is shown in Figure 4-9 (a), and a concurrent design path, involving the use of a developmental autoclave, is indicated with horizontal dashed lines.

As shown in Figure 4-9 (b), a proxy design path forks from the primary design path at $((e)_2, (t)_1, (p)_2, (m)_3) = (2, 1, 2, 3)$. The outcome of design state, $[(e_i)_2, (t)_1, (p)_2, (m)_3] = [2, 1, 2, 3]$ might represent a decision to use developmental autoclave e_i to focus on the development of a tooling strategy for the part of interest while a new production autoclave, e_{i+1}, has been commissioned, represented by design state $[(e_{i+1})_2, (t)_1, (p)_2, (m)_3] = [2, 1, 2, 3]$. By $[(e_{i+1})_3, (t)_1, (p)_2, (m)_3] = [3, 1, 2, 3]$, this production autoclave physically exists. The proxy and primary design paths are then combined at the next stage, $[(e_{i+1})_3, (t)_2, (p)_2, (m)_3] = [3, 2, 2, 3]$, meaning that the final stages of development for this large part is transferred from developmental autoclave e_i to production autoclave e_{i+1} in preparation for production implementation at $[(e_{i+1})_3, (t)_3, (p)_3, (m)_3] = [3, 3, 3, 3]$.

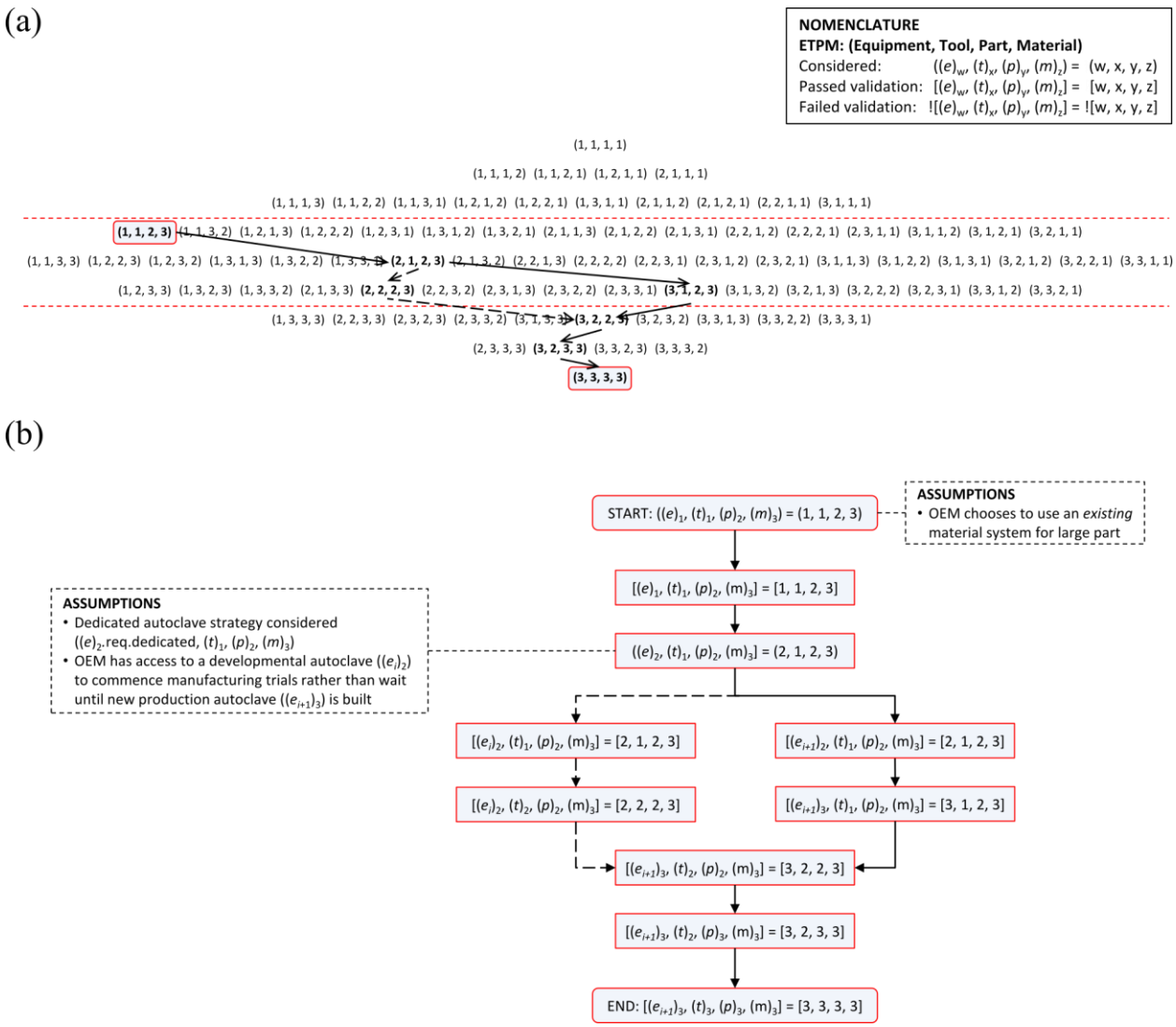

Figure 4-9: Large composites part development. This scenario shows the concurrent sequence of manufacturing decisions made by an OEM who has access to a developmental autoclave and is represented using the ETPM factory ontology as: (a) decision tree highlighting all possible design states that could be evaluated and (b) flowchart showing the details of the manufacturing choices made. ETPM: Equipment–Tool–Part–Material; w, x, y, z: design-gate indices; *i*: equipment instance identifier; OEM: Original Equipment Manufacturer; req: manufacturing requirement. Note: Instances are denoted in lowercase. Horizontal dashed lines indicate concurrent design steps.

4.3.3 Case 3: Bid for a small composites part work package

In contrast to the previous two scenarios presented, this case study highlights the limited number of manufacturing choices available to a 'build to print' supplier who is deciding whether to bid for a small composites part work package. A 'build to print' supplier is typically given manufacturing responsibility while the OEM maintains ownership of the part design. For this example, the work package is assumed to be a family of parts with similar geometric complexity and thickness, such as fuselage frames or wing skin stringer stiffening elements. Although the design path in Figure 4-10 (a) may appear straightforward, the manufacturing decisions made by composites suppliers are far from trivial. The process of bidding for a work package represents great risk. Overbidding may result in the work being awarded to a competitor, whereas underbidding can lead to significant financial loss in attempting to satisfy the contract.

The choices for a 'build to print' supplier are typically limited to defining the variable attributes of the Equipment and Tool, meaning that few design states are available. This reduction in the manufacturing design space is evident in the decision tree in Figure 4-10 (a), with unavailable design states shown in grey. As shown in Figure 4-10 (b), the entry point $((e)_3, (t)_1, (p)_3, (m)_3)$ = (3, 1, 3, 3) might represent an existing supplier who is seeking additional work for an existing autoclave 'bus stop' or batch process. The decision to bid on the work package, in this example, essentially becomes a capability assessment question 'Can we make this work if we find a suitable tooling strategy?' If the result, based on preferred tooling concepts, is $![(e)_3, (t)_1, (p)_3, (m)_3]$ = ![3, 1, 3, 3], this may indicate that the best option is to *not* bid for the work. Otherwise if the bid is successful, then the subsequent steps that supplier follows are intended to mature a tooling strategy for production implementation at $[(e)_3, (t)_3, (p)_3, (m)_3]$ = [3, 3, 3, 3].

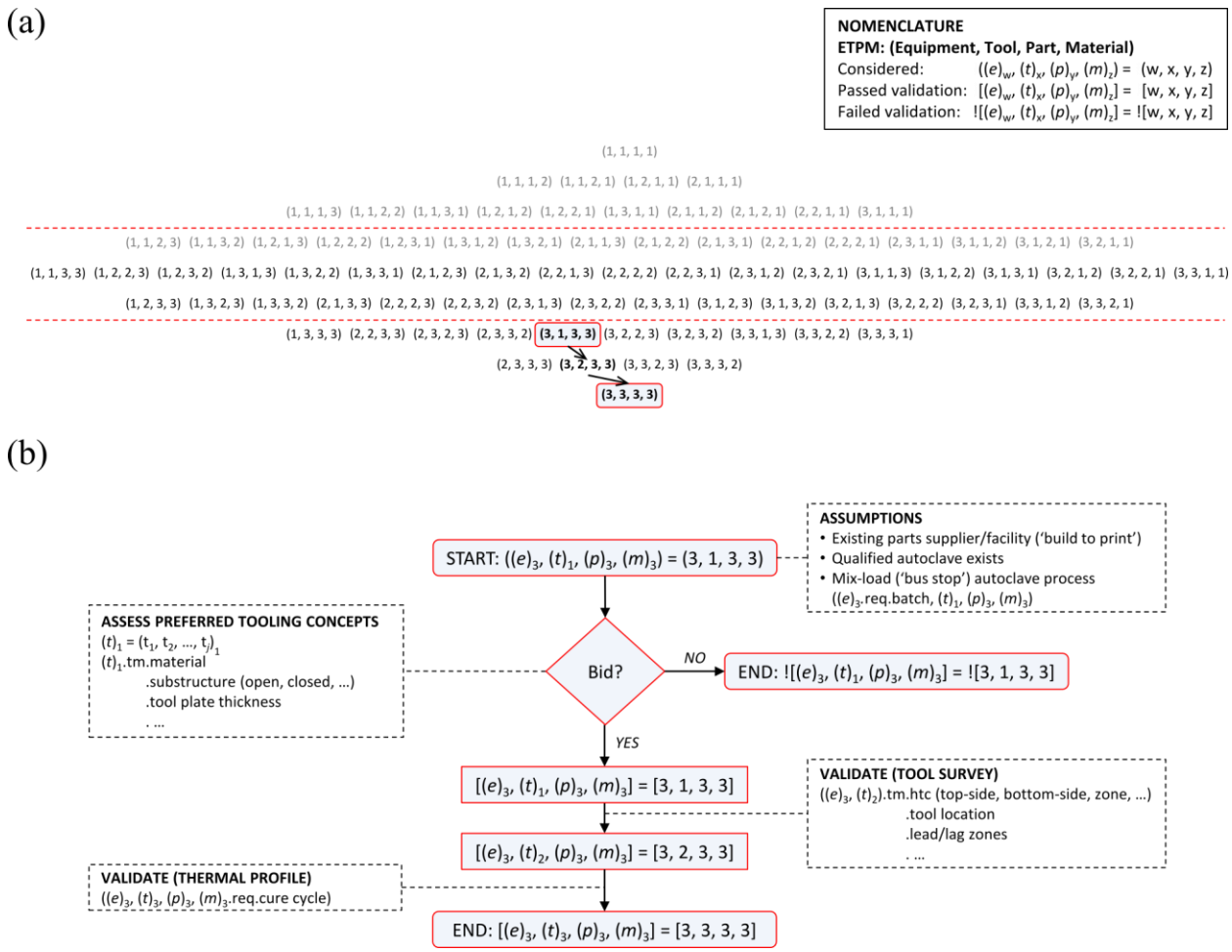

Figure 4-10: Bid for a small composites part work package. This scenario highlights the limited number of manufacturing choices available to an existing 'build to print' parts supplier and is represented using the ETPM factory ontology as: (a) decision tree highlighting all possible design states that could be evaluated and (b) flowchart showing the details of the manufacturing choices made. ETPM: Equipment–Tool–Part–Material; w, x, y, z: design-gate indices; *j*: tool instance identifier; req: manufacturing requirement; tm: thermal management; htc: heat transfer coefficient. Note: Instances are denoted in lowercase. Unavailable design states are shown in grey.

4.3.4 Case 4: Process improvement for a high-volume composites part

This case study demonstrates how science based practice can be introduced for the efficient process optimization of a high-volume composites part[13]. The science based intervention discussed in this scenario is shown in black in Figure 4-11 (a), with an alternative approach shown in grey. Solid wavy lines indicate the precise design path is not known. The production process under investigation, represented by $[(e_i)_3, (t)_3, (p)_3, (m_\ell)_3] = [3, 3, 3, 3]$ and shown in Figure 4-11 (b), involves the use of hot-press e_i to consolidate parts produced with material m_ℓ in a single step. Although a rate increase is necessary to keep up with demand, the composites manufacturer is hesitant to make changes to this current production process without understanding why and, more importantly, without detrimentally impacting part producibility. Production delays or interruptions could be disastrous given that there is already a significant backlog in orders for these parts. Initially, the production capacity is increased by $N \times [(e_i)_3, (t)_3, (p)_3, (m_\ell)_3] = N \times [3, 3, 3, 3]$ without the benefit of scientific insight and at the highest possible capital cost. The investment in additional equipment and tooling, and the introduction of a second shift does not sufficiently address the problem.

A science based approach, requiring an understanding of heat transfer and resin cure kinetics, is then considered to identify possible production bottlenecks that are not immediately apparent. At $((e_i)_3, (t)_3, (p)_3, (m_\ell)_2) = (3, 3, 3, 2)$, a cure kinetics model is developed to survey this current production process by simulation. Based on this preliminary analysis, it is identified that the consolidation time in the hot-press is not optimal, indicating that this problem is related to cure

[13] Based on original work by Fernlund and Mobuchon (2015).

cycle management. Production targets are set to reduce the overall process time by 20% and to match or exceed existing part quality and performance requirements. At a minimum, any new process introduced must achieve the same final DOC as the current production process.

Two process improvements strategies are considered that involve changes to: 1) Material variable attributes (eg. $((e_i)_3, (t)_3, (p)_2, (m)_1) = (3, 3, 2, 1)$), such as introducing a new material system; or 2) Material constraint attributes (eg. $((e_i)_3, (t)_3, (p)_3, (m_{\ell+1})_2) = (3, 3, 3, 2)$), such as modifying the existing cure cycle, now $m_{\ell+1}$. Of these two options, a focus on redefining the process requirements represents lower manufacturing risk since the introduction of a new material would require an immediate reassessment of the part design and material allowables. At stage $[(e_i)_3, (t)_3, (p)_3, (m_{\ell+1})_2] = [3, 3, 3, 2]$, a modified cure cycle with an optimized consolidation temperature has been developed with the potential to reduce the process time in the hot-press by a factor of two.

While modifications to the cure cycle result in exceeding the production targets, the focus now shifts to investigating the utilization of the hot-press. At $((e)_2, (t)_3, (p)_3, (m_{\ell+1})_2) = (2, 3, 3, 2)$, a two-step process involving partial part consolidation in the hot-press press followed by a secondary post-curing step, now e_{i+1}, is considered. Based on a parametric heat transfer analysis, this proposed manufacturing strategy has the potential to reduce the process time in the hot-press by a factor of four. At $[(e_{i+1})_2, (t)_3, (p)_3, (m_{\ell+1})_2] = [2, 3, 3, 2]$, this strategy is validated with manufacturing trials, and visual inspection and mechanical testing of pre-production parts. With minimal capital investment and at no penalty to part quality and performance, the opportunity to double the production capacity is possible. This new production process, $N \times [(e_{i+1})_3, (t)_3, (p)_3, (m_{\ell+1})_3] = N \times [3, 3, 3, 3]$, developed with manufacturing science, is successfully implemented.

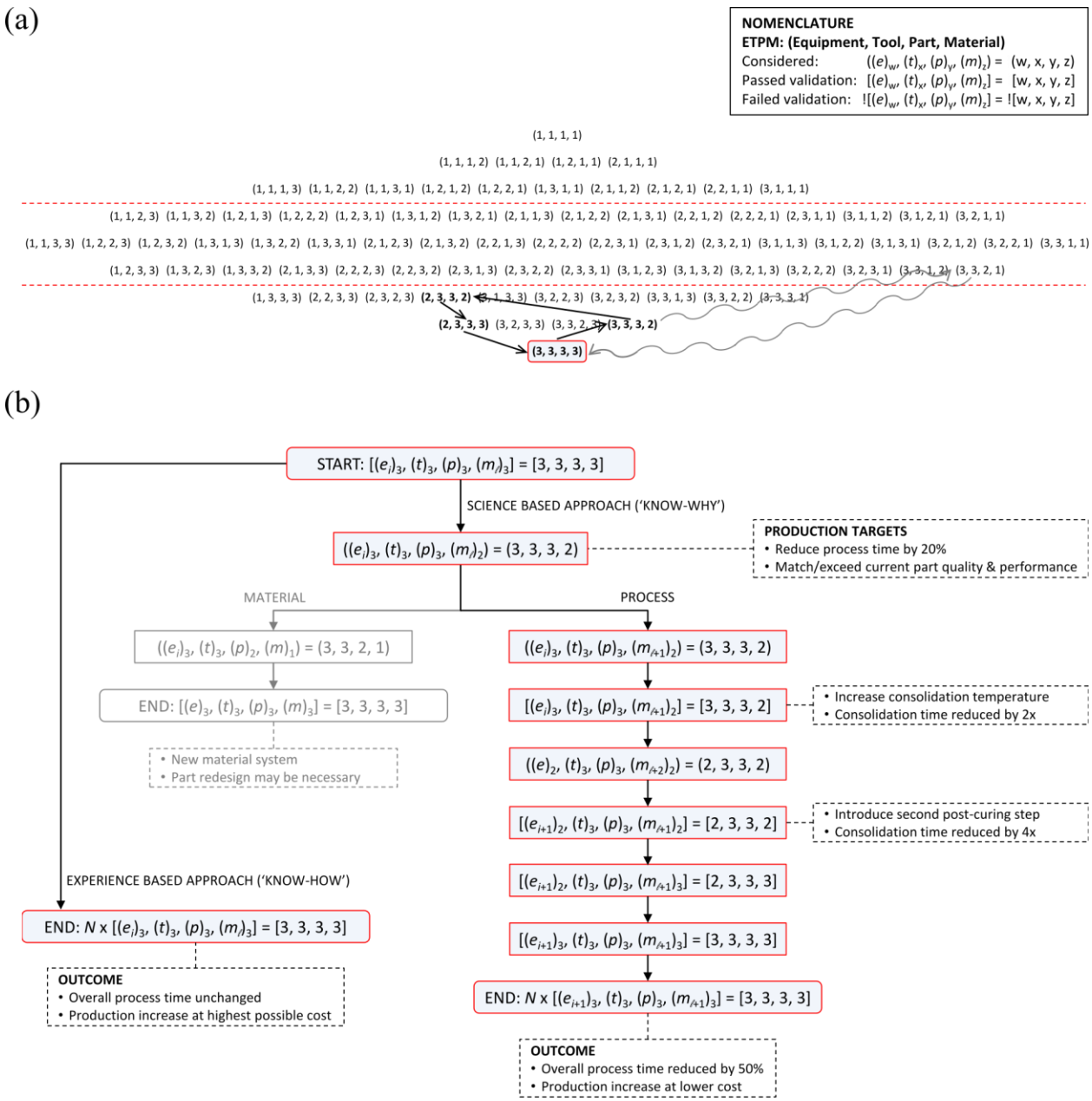

Figure 4-11: Process improvement for a high-volume composites part. Based on original work by Fernlund and Mobuchon (2015). This scenario demonstrates how science based practice can be used for efficient process optimization and is represented using the ETPM factory ontology as: (a) decision tree highlighting all possible design states that could be evaluated and (b) flowchart showing the details of the manufacturing choices made. ETPM: Equipment–Tool–Part–Material; w, x, y, z: design-gate indices; *i*: equipment instance identifier; *ℓ*: material instance identifier; *α*: degree of cure; *t*: time; *T*: temperature; H_R: resin heat of reaction. Note: Instances are denoted in lowercase. An alternative design path is shown in grey. Solid wavy lines indicate that the precise design path is unknown.

4.3.5 Case 5: Capturing knowledge for reuse in future programs

Over time, manufacturers accumulate an enormous amount of knowledge, in the form of expert opinion, experience, test and analysis. In this final case study, the ETPM factory ontology is used to highlight the value in systematically capturing this knowledge for reuse in future programs. An idealized design path is shown in Figure 4-12 (a). Using terminology introduced in Section 4.1.1, this acquired knowledge can be viewed with multiple lenses (eg. wide lens at the enterprise level, narrow lens at the product level) that are depicted in Figure 4-12 (b).

Consider the knowledge gained in program *n*. At the enterprise level, respresented by design state $[(e)_1, (t)_1, (p)_1, (m)_3]_n = [1, 1, 1, 3]$, the focus of the knowledge aquired relates to the Material. Composites manufacturers invest significantly in qualifying and maintaining material systems over long time frames. For instance, Toray T800H/3900-2 is a CFRP prepreg system that is extensively used in commercial aerospace applications. This material was first commercialized in the early 1990s (eg. [234,235]). For manufacturers who choose to use manufacturing simulation as an intrinsic part of their manufacturing and certification strategies, the characterization, validation, and upkeep of the associated material models is as equally important as the generation and maintenance of the process specification documents and material allowables databases.

The next design state, $[(e)_3, (t)_2, (p)_2, (m)_3]_n = [3, 2, 2, 3]$, represents the business unit or factory level. This design state may represent the supplier network depending on the business model pursued (eg. in-house manufacturing, awarding suppliers with design and build authority, ‘build to print’ suppliers). The focus of knowledge gained at this level relates to the Equipment.

For example, composites manufacturers who choose to transition from autoclave to OOA cure processing (thermal management) or from hand layup to AFP and forming (material deposition management) demonstrate that they have sufficient confidence in their knowledge base to make such changes.

At the program level, design state $[(e)_3, (t)_3, (p)_2, (m)_3]_n = [3, 3, 2, 3]$, the focus of knowledge acquired relates to the Tool and the Part. At this level, the design details can affect the manufacturing system at global and local scales. Take for example the role of tool design on thermal outcomes in autoclave and oven processes. At the global scale, tool substructure design can affect the airflow, and thus heat transfer boundary conditions. At the local scale, tool material selection and geometric effects, such as tool plate thickness and its construction, can affect the thermal response of parts, and thus the ability to satisfy process requirements. Composites manufacturers can choose to use the science based methods, such as IR thermography and CFD analysis (eg. [177–179]), to understand these effects for robust and effective tool design.

Finally, the design state $[(e)_3, (t)_3, (p)_3, (m)_3]_n = [3, 3, 3, 3]$ represents the product level where the focus of the knowledge gained relates to Part producibility. Validation of the manufacturing system is performed at this stage, such as experimental thermal profiling or the use of manufacturing simulation as an enabling tool as discussed in Section 4.1.2. Ideally, in pursuing the next program, n+1, composites manufacturers can reuse the knowledge accumulated at all levels.

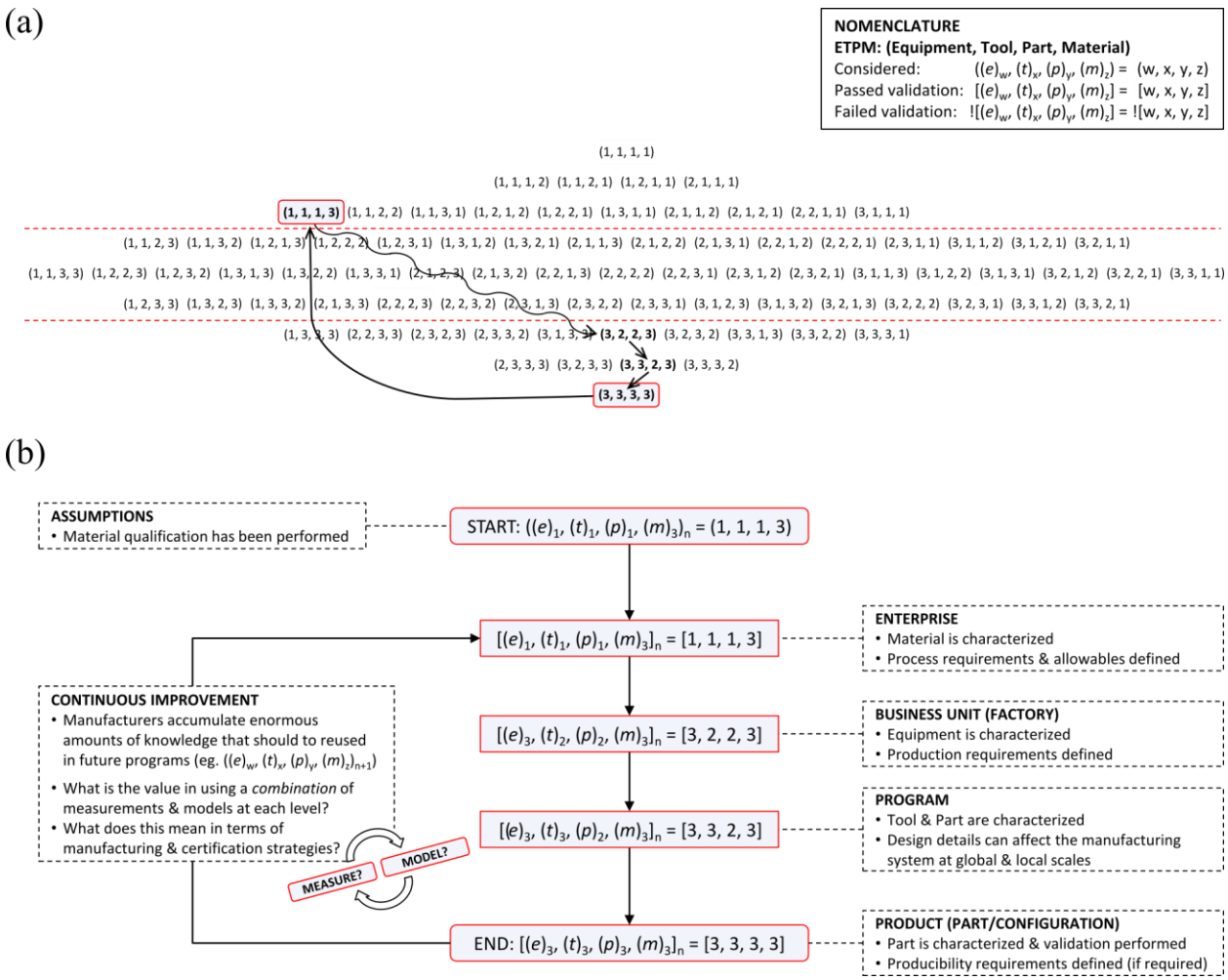

Figure 4-12: Knowledge reuse. This scenario highlights the value in systematically capturing knowledge, in the form of expert opinion, experience, test and analysis, for reuse in future programs and is represented using the ETPM factory ontology as: (a) decision tree highlighting all possible design states that could be evaluated and (b) flowchart showing the details of the manufacturing choices made. ETPM: Equipment–Tool–Part–Material; w, x, y, z: design-gate indices; *n*: program instance identifier; HTC: Heat Transfer Coefficient. Arbitrary design states are specified in this scenario. Solid wavy lines indicate that the precise design path is unknown.

4.4 Summary and Discussion

A usable framework that combines composites manufacturing science and industrial practice has been developed based on conceptual frameworks discussed in Section 2.2. The conceptual elements introduced in this chapter included: 1) steps for formalizing the manufacturing science base (knowledge translation) and transforming practice (*protect–advance–disrupt*); and 2) an ontology defining a common nomenclature for organizing composites manufacturing domain knowledge (ETPM factory ontology). Proposed science based knowledge and design practice topics for thermal management, and tools to systematically capture manufacturing scenarios with simulation based thinking are presented in Appendix C.2.

High-level thermal management manufacturing scenarios were presented to demonstrate the value of formalizing science based practice for composites manufacturing. Although there was no explicit requirement to make use of the manufacturing science base in the case studies shown, it is apparent that as we systematically traverse the manufacturing design space using the ETPM factory ontology, this knowledge, in the form of simulation, could be applied to directly support manufacturing decisions at *all* stages of the development design cycle, from conceptual design to production (eg. material qualification, structural certification, production approval).

These case studies also represent a Material focused approach to new product development, where the sequence of design steps appears on the left of the ETPM decision tree (see Figure 4-13 (a)). As discussed in Section 2.1.1, this is considered a form of ‘process-driven innovation’, or low modularity and low maturity technology, in terms of the modularity-maturity matrix proposed by Pisano and Shih [49].

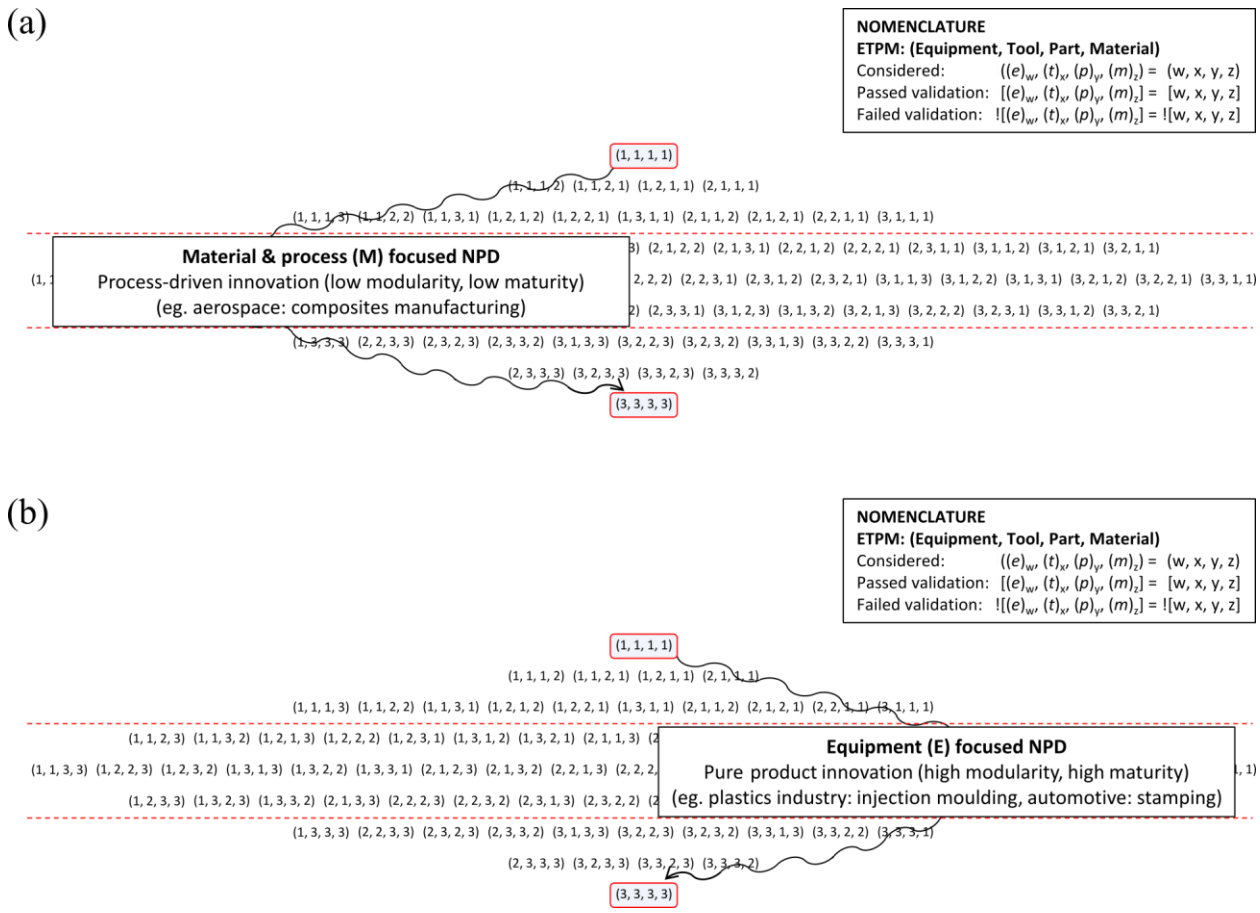

Figure 4-13: New product development. These scenarios show how different parts of the ETPM decision tree can be used depending on the type of manufacturing-innovation relationship involved: (a) 'Process-driven innovation', or a Material focused sequence of manufacturing decisions, appear on the left side of the decision tree and (b) 'Pure product innovation', or an Equipment focused sequence of manufacturing decisions, appear on the right side of the decision tree. ETPM: Equipment–Tool–Part–Material; w, x, y, z: design-gate indices; NPD: New Product Development. Note: The manufacturing-innovation relationships shown are based on the modularity-maturity matrix [49] (Pisano & Shih, 2012). Solid wavy lines indicate that the precise design path is unknown.

Manufacturing scenarios may also appear on the right of the ETPM decision tree (see Figure 4-13 (b)). These cases represent an Equipment focused approach to new product development. Take for example injection moulding technologies in the plastics industry, and sheet metal stamping technologies in the automotive industry. These high volume technologies are classified as 'pure product innovation', or high modularity and high maturity technologies [49].

The ETPM factory ontology can be applied retrospectively to industrial cases to identify the steps taken as current practice (protect). Having defined practice in terms of this framework, manufacturing simulation can then be introduced as an enabling tool to make these decisions more efficiently (advance). Ultimately, using this same structured approach, the manufacturing science underlying each step can be used to open-up the manufacturing requirements, and thus remove any unnecessary constraints unduly imposed on the problem (disrupt). These steps are depicted in Figure 4-3.

The systematic use of the ETPM factory ontology and composites manufacturing science based will be demonstrated in Chapter 5. The case studies presented in this next chapter focus on the thermal management of curing laminates since the manufacturing science for these types of problems is relatively mature. Thus, a logical starting point for formalizing science based composites manufacturing practices is for these types of problems.

The use of this framework to formalize science based practices in other advanced manufacturing disciplines is suggested as future work.

Chapter 5: Applications of Science Based Practice for Thermal Management

In this chapter, thermal management case studies are presented to demonstrate the systematic *use* of the ETPM factory ontology and the compostites manufacturing science base. In each case study, manufacturing simulation is used to: 1) manage experimental and modelling uncertainty and partially reliable data; 2) minimize manufacturing risk; and 3) enable effective use of production data. These case studies are as follows:

- *Case 1: Managing thermal modelling uncertainty* – Establish confidence in using simulation based data (predictive modelling results), identify key sources of thermal modelling uncertainty and the importance of model validation (Figure 5-1).

- *Case 2: Cure cycle development and evaluation* (development) – Investigate and recommend a cure cycle for a part with intermediate complexity (Figure 5-6).

- *Case 3: Experimental thermal profile validation* (troubleshooting) – Interpret experimentally measured temperature data to investigate apparent and real thermocouple failures in small-scale parts and tools (Figure 5-13).

Thermal analysis of five thick thermoset composites data sets, based on experimental work by Johnston and Hubert (ATCAS) [100], Shimizu *et al* [145], Slesinger [150], CCMRD Project 9.2 [236] and Boeing-UW MSE310 students [237], was performed and are presented as examples in this chapter. These data sets are summarized in Table 5-1, with back-calculated effective heat transfer coefficients for each data set reported in Table 5-2.

These data sets represent real production scenarios, such as cure cycle aborts, unintentional bag leaks and mislabeled thermocouples. In some cases, the experiments performed were not carefully controlled, thus some thermal management attributes were estimated or unknown, such as autoclave airflow characteristics, tool substructure details and through-thickness temperature profiles of parts given the number of thermocouples used. In terms of the ETPM factory ontology, introduced in Section 4.2, these data sets represent a range of thermal management attributes: 1) Equipment, such as autoclave airflow characteristics and loading scenarios; 2) Tool, such as tooling materials, tool plate thicknesses and substructure complexity; 3) Part, such as part complexity and thickness; and 4) Material, such as the material systems used, applied cure cycles and the fidelity of available material models for thermal modelling. Thick thermoset composites studies reported in the scientific literature, and discussed in Section 2.3.1, are also summarized in terms of the ETPM factory ontology and thermal management attributes in Appendix A (see Table A-5 and Table A-6).

All five data sets were analyzed assuming 1D heat flow in the through-thickness direction and using RAVEN simulation software V3.9.2 [238] (RAVEN-1D) drill point analysis. Additional thermal modelling was performed using ABAQUS-COMPRO CCA V1.12 [239] (COMPRO-3D) in some cases to investigate the validity and limitations of the 1D approach. Further experimental details and experimentally measured and predicted modelling results for these data sets is provided in Appendix D. The details of the material models and properties used to analyze these data sets is given in Appendix E. It should be noted that as part of this work, a preliminary thermal model for Hexcel AS4/8552-1 unidirectional prepreg was characterized (refer to Appendix E.2). The method for back-calculating the reported effective heat transfer coefficients is presented in Appendix F.

Table 5-1: Summary of the thick thermoset composites data sets analyzed.

Data set	Experiment	Equipment (E)	Tool & consumables (T)		Part (P)		Material & process (M)				
		autoclave	geometry & thickness (mm)	tool material	geometry	thickness (mm)	material system	condition	cycle	hold temperature	heating rate
Johnston & Hubert[a]	ATCAS	Industrial-A	tool	Invar	panel (tapered core)	28.2 mm	AS4/8552 phenolic core	curing	3-hold	110 °C, 150 °C, 180 °C	1.1 °C/ min
Kotlik & Shimizu[b]	TEST-A	UBC	tool plate (24.5 mm)	Al-alloy	flat	38.4 mm	AS4/8552-1	curing	2-hold	110 °C, 180 °C	2.8 °C/ min
	TEST-B							cured			1.1 °C/ min
	TEST-C							cured	1-hold	120 °C	2.8 °C/ min
	TEST-D										1.7 °C/ min
	TEST-E										0.6 °C/ min
Slesinger[c]	20100225-60	UBC	insulating bricks (16 mm)	Silicone	flat	11.7 mm	AS4/8552-1	curing	1-hold	180 °C	1.25 °C/ min
	20100226-60							cured			
	20100225-80					14.7 mm		curing	1-hold	180 °C	
	20100226-80							cured			
	20100304-40					7.5 mm	T800H/3900-2	curing	1-hold	180 °C	5.0 °C/ min
	20100305-40							cured			
CCMRD9.2[d]	CCM9.2-077	UBC	small-scale tool	Invar	C-shaped laminate	12.4 mm	T800H/3900-2	curing	1-hold	180 °C	nominal
Boeing-UW[e]	20151028-001-1	Industrial-B	tool plate (12.7 mm)	Al-alloy	flat	6.4 mm	T800H/3900-2	curing	1-hold	180 °C	nominal
	20151028-001-2					19.1 mm		cured			
	20151109-002	Industrial-C				6.4 mm		curing	1-hold	180 °C	nominal
						19.1 mm					
	20161017-001	Industrial-D	tool plate (9.5 mm)	Al-alloy	flat	12.7 mm	T800H/3900-2	curing	1-hold	180 °C	nominal
						25.4 mm					
					panel (core/septum)	33.0 mm	T800H/3900-2 aramid core				

[a] Experimental data from [100] (Johnston, 1997), refer to Appendix D.1.
[b] Experimental data from [145] (Shimizu *et al*, 2008), refer to Appendix D.2.
[c] Experimental data from [150] (Slesinger, 2010), refer to Appendix D.3.
[d] Experimental data from [236] (Arafath *et al*, 2015), refer to Appendix D.4.
[e] Experimental data from [237] (Boeing-UW, 2017), refer to Appendix D.5.

Table 5-2: Effective heat transfer coefficients for the thick thermoset composites data sets analyzed[a].

Data set	Experiment	Equipment (E)	Tool & consumables (T)	Equivalent-1D HTC		Equivalent-3D HTC (no tool substructure modelled)		
		autoclave	geometry & thickness (mm)	top W/ (m^2K)	bottom W/ (m^2K)	top W/ (m^2K)	tool top W/ (m^2K)	tool bottom W/ (m^2K)
Johnston & Hubert[b,c]	ATCAS	Industrial-A	Invar tool plate (25.4 mm)	15	55			
Kotlik & Shimizu[b,d]	TEST-A	UBC	Al-alloy tool plate (25.4 mm)	75	160	75	70	50
	TEST-B			65	160	65	70	55
	TEST-C			15	100			
	TEST-D			15	95			
	TEST-E			15	95			
Slesinger[e]	20100225 20100226 20100304 20100305	UBC	KE1204 RTV silicone insulating bricks (16 mm)	prescribed temperature				
CCMRD9.2[b,f]	CCM9.2-077	UBC	Invar small-scale tool (12.7 mm face plate)	40 (50)	80 (75)			
Boeing-UW[g]	20151028-001-1	Industrial-B	Al-alloy tool plate (12.7 mm)	35	150	35	85	75
	20151028-001-2			40	170	40	95	85
	20151109-002	Industrial-C		30	95	30	50	45
	20161017-001	Industrial-D	Al-alloy tool plate (9.5 mm)	40	100	40	35	30

[a] The method for back-calculating effective HTCs is described in Appendix F.
[b] HTCs from revised analyses (2018) are reported.
[c] Experimental data from [100] (Johnston, 1997), refer to Appendix D.1. ATCAS: 28.2 mm thick panel with tapered core.
[d] Experimental data from [145] (Shimizu *et al*, 2008), refer to Appendix D.2. TEST-A (curing, 2-hold cycle); TEST-B (cured, 2-hold cycle); TEST-C (cured, 1-hold cycle at 2.8 °C/ min); TEST-D (cured, 1-hold cycle at 1.7 °C/ min); TEST-E (cured, 1-hold cycle at 0.6 °C/ min).
[e] Experimental data from [150] (Slesinger, 2010), refer to Appendix D.3. Set temperature boundary conditions are applied to the respective surface boundaries of the top and bottom insulating bricks. AS4/8552-1 laminates: 20100225 (curing); 20100226 (cured); T800H/3900-2 laminate: 20100304 (curing); 20100305 (cured).
[f] Experimental data from [236] (Arafath *et al*, 2015), refer to Appendix D.4. CCM9.2-077: 12.4 mm thick C-shaped laminate. Low autoclave HTC value (unpressurized). High autoclave HTC value (pressurized) shown in parentheses.
[g] Experimental data from [237] (Boeing-UW, 2017), refer to Appendix D.5. MSE-2015: 20151028-001-1 (curing); 200151028-001-2 (cured); 20151109-002: (curing); MSE-2016: 20161017-001 (curing).

5.1 Case 1: Managing Thermal Modelling Uncertainty

As discussed in Sections 2.3.1 and 4.2.3, the thermal management of curing laminates is a manufacturing system problem. The science base for these types of problems is relatively mature and can be represented using manufacturing simulation. For the thermal modelling of cure processes, there are three main components of the thermochemical model: the conduction heat transfer model, the cure kinetics model and convective heat transfer boundary conditions. A workflow for the development, validation and use of thermal models for cure processes is shown in Figure 5-1.

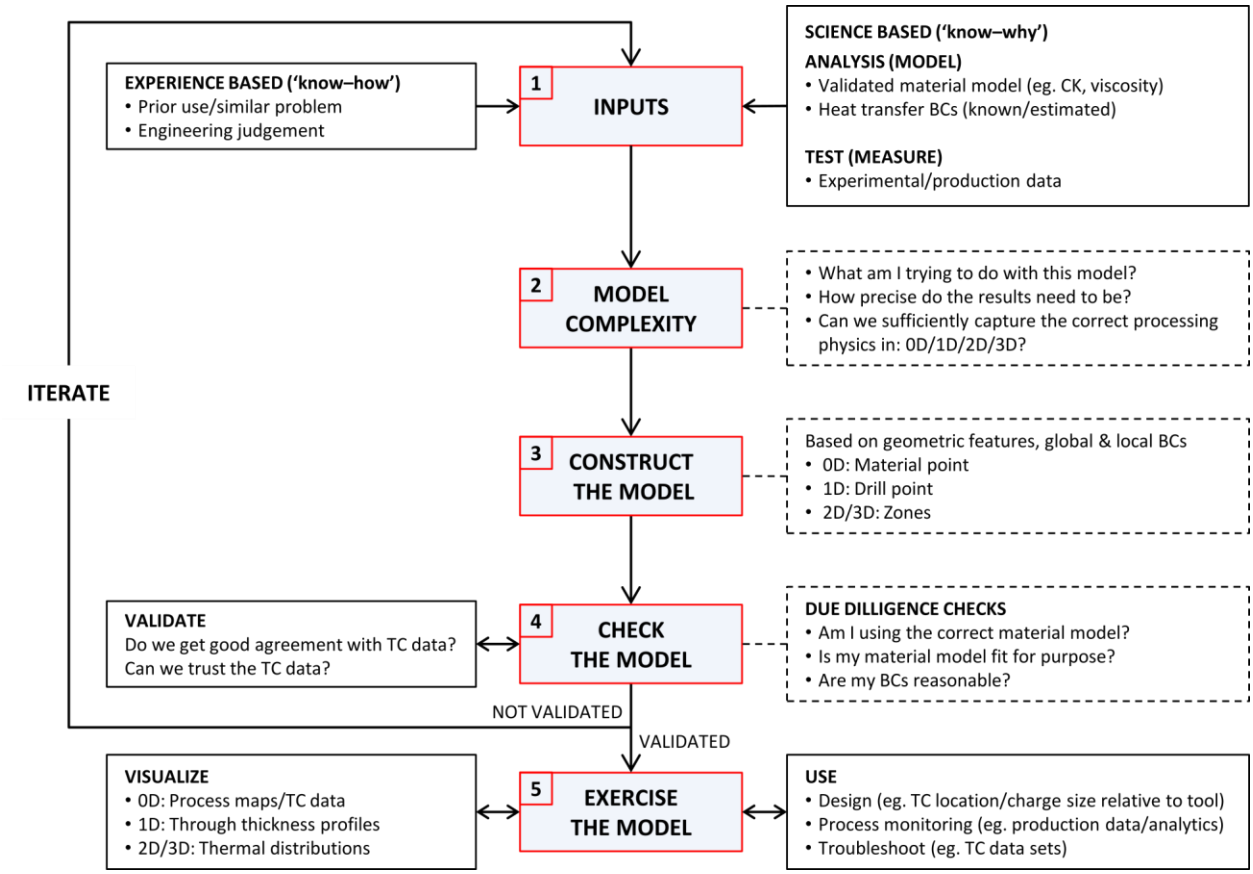

Figure 5-1: Thermal modelling workflow. Extension of approaches from [194] (Ashby, 1992) and [195] (Advani *et al*, 2011). CK: Cure Kinetics; BCs: Boundary Conditions; TC: Thermocouple.

Manufacturing simulation can provide guidance and useful insights in aspects of process development, production monitoring and troublehooting [194,195]. However, as discussed in Section 2.3.2, modelling uncertainty and establishing a confidence in model predictions are primary issues in using simulation to support decision making in design [152]. This first case study is intended to establish confidence in the thermal modelling of cure processes and the use of manufacturing simulation as an enabling tool.

Based on the accepted classification of uncertainty and error in modelling and simulation defined by Oberkampf *et al* [184,185], the key sources of uncertainty and error for the thermal modelling of cure processes have been identified and are summarized in Table 5-3.

Aleatory uncertainty is typically managed using material and process specifications, whereas an awareness of epistemic uncertainty can contribute to reducing the missteps, false-starts, and duplication of effort based on experience. A strategy to reduce epistemic uncertainty is to use a combination of data sources. Even with partially reliable data, using a combination of data sources can increase our confidence in making effective composites manufacturing decisions. For instance, and as shown in Figure 5-2, assuming we had access to both simulation based data (predictive modelling results) and sensor based data (experimentally measured results), and the probability of either data source being correct is 80%, then confidence in using either source of data to support decision making is 80%. However, in using a combination of both sources of data, this confidence increases to 94%.

Table 5-3: Identifcation and classification of modelling uncertainty and error for the thermal modelling of cure processes[a,b]. Adapted from [125] (Hahn *et al*, 2004).

	Aleatory uncertainty	Epistemic uncertainty	Acknowledged errors	Unacknowledged errors
	• M&P[f] variations	• lack of knowledge/ignorance • fidelity of physical models • incomplete information	• known errors • assumptions/simplifications • modelling practices	• error in inputs/outputs • mistakes
Heat transfer models (eg. conduction)	• initial conditions	• governing energy equation (eg. 1D/2D/3D heat flow) • contact resistances at interfaces (eg. part/consumables & part/tool, air gaps: bag leaks, parts lifting off tools during cure) • in-plane part/tool interactions (eg. edge, tool size effects)	• solution method (eg. analytical, numerical) • representation (eg. drill point vs. zone) • geometric simplifications (eg. parts & tools) • mesh sensitivities	• model implementation (eg. error in FE[g] code, 'bugs')
Material models (eg. cure kinetics)[c,d]	• batch-to-variation (eg. initial DOC[h], ageing) • sample size • test matrix/randomization	• form of the model (eg. mechanistic, semi-empirical) • understanding material behaviours (eg. material system derivatives)	• using model beyond its range of validity (eg. nonisothermal temp. & heating rates, isothermal temp.)	• DSC[h] measurement (eg. calibration) • data-fit (eg. baselines) • model-fit (eg. data reduction) • model implementation (eg. error in FE[g] code, 'bugs') • using wrong model
Boundary conditions[d,e]	• temperature variations • airflow variations • HTC[i] distribution (eg. loading environment: positioning of part & tools in autoclave/oven)	• HTC[i] modelling (eg. includes pressure effects, consumables, tool substructure, but does not account for part shielding/shadowing)	• using prescribed temp. vs. HTCs[i] (eg. constant, varying/distributions) • HTC[i] representation (eg. neglected, lumped: effective/ equivalent, explicitly defined: convective, radiation)	• characterization (eg. calorimeters, CFD[i]) • data reduction (eg. back-calculation) • BCs[i] incorrectly applied to system boundaries

[a] Definitions of modelling uncertainty & error from [184,185] (Oberkampf *et al*, 2002).
[b] The sources of modelling uncertainty & error summarized in this table are not exhaustive.
[c] Refer to Table 6.1 to Table 6.6 [144] (Dykeman, 2008) for recommended practices for minimizing cure modelling uncertainties.
[d] Refer to [148–150] (Slesinger *et al*, 2010) for recommended practices for cure model validation at the laminate level & autoclave airflow/HTC characterization.
[e] Refer to [177–179] (Park *et al*, 2017) for recommended practices for experimental/CFD zone based HTC characterization.
[f] M&P: Material & Process
[g] FE: Finite Element
[h] DOC: Degree of Cure; DSC: Differential Scanning Calorimetry;
[i] HTC: Heat Transfer Coefficient; CFD: Computational Fluid Dynamics; BC: Boundary Condition

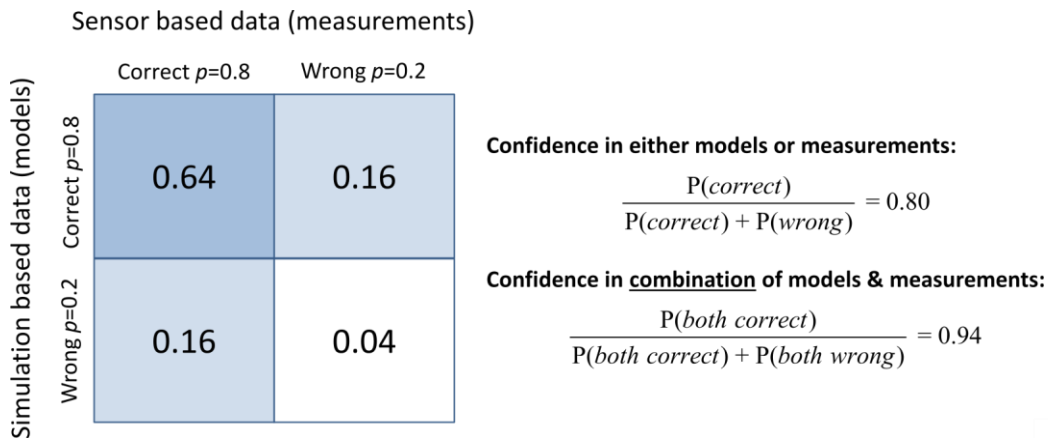

Figure 5-2: Confidence in partially reliable data. Using a combination of data sources can increase confidence in making effective manufacturing decisions. Based on [186] (Fernlund, 2010). *p*: Probability of reliability. Note: Arbitrary probabilities are assigned in the matrix shown.

Confidence in using manufacturing simulation can be achieved by appropriately dealing with potential sources of modelling uncertainty and error. Two strategies to develop an 'evidence of credibility' in simulation are uncertainty quantification and model validation [152,184,185]. Where uncertainty quantification relates to identifying and characterizing modelling uncertainties, and model validation relates to the assessment of model accuracy by way of comparing model predictions to experimental data.

Selected modelling uncertainties from Table 5-3 are briefly discussed in the following sections: 1) the complexity of the solution method (conduction heat transfer model); 2) understanding the thermal behaviours of material systems and their derivatives (cure kinetics model); and 3) effective heat transfer coefficient validation (convective boundary conditions).

5.1.1 Heat transfer models

The essence of modelling and simulation is simplification, but without the loss of the important processing physics [194,195]. However, a common perception is that the validity of a model is related to its solution complexity[14]. Knowledge of how to 'right size' a problem requires an understanding of similar problems at all levels of complexity, ranging from simple 1D analytical solutions to complex 3D numerical models. A multiscale simulation capability exists for the prediction of thermal management outcomes, as disussed in Section 2.3.2.

In this first example, the benefits and trade-offs in using different levels of thermal model complexity are briefly examined. RAVEN-1D and COMPRO-3D models are used to analyze experimental results for a 38.4 mm thick laminate (in-plane dimensions: 152 mm x 152 mm) cured on a 25.4 mm thick Al-alloy tool (in-plane dimensions: 535 mm x 305 mm). Experimentally measured and predicted modelling results are shown in Figure 5-3. The details these analyses are given in Appendix D.2 (experiment ID: TEST-A). It should be noted that this work extends the original analysis and observations reported by Shimizu *et al* [145].

For the RAVEN-1D model (see Figure 5-3 (a)), reasonable agreement is observed at the mid-laminate. However, the model (T0) overpredicts the experimental results (TC-0) by more than 10 °C at the part/tool interface (point A).

[14] Poursartip's law (facetiously) states that the validity of a computational model is directly proportional to the size of the screen and the number of colours (Poursartip, 2018).

For the COMPRO-3D model (see Figure 5-3 (b)), the temperature profile is also reasonably predicted at the mid-laminate. An improvement in the model prediction is also observed at the part/tool interface, with the predicted temperature at T0 within 3.0 °C of the experimental results at TC-0.

A number of conclusions can be drawn in comparing the RAVEN-1D and COMPRO-3D model predictions. Firstly, the difference in the predicted temperature profiles at the part/tool interface is attributed to tool size effects. This observation was also reported by Shimizu *et al* [145]. Secondly, with comparable temperature profiles predicted at the mid-laminate for both RAVEN-1D and COMPRO-3D models this suggests that the tool size effect could be considered a 'non-local' effect. In other words, material points located further away from the part/tool interface are less sensitive to the influence of the tool acting as a heat sink than material points located closer to the part/tool interface. Finally, it is observed in both RAVEN-1D and COMPRO-3D models that the predicted temperature profiles lag the experimental results after the exotherm at 250 min < t < 300 min. This difference could be attributed to the change in the heat transfer coefficient due to the consumables/bagging collapsing and filling with resin. The effect of the consumables on heat transfer was also reported by Shimizu *et al* [145]. It is also suspected that, like the tool size effect, the effect of consumables could be described as a 'non-local' effect. Changes in effective heat transfer coefficient during cure were not accounted for in the RAVEN-1D and COMPRO-3D models used in this work. Further investigation is suggested as future work.

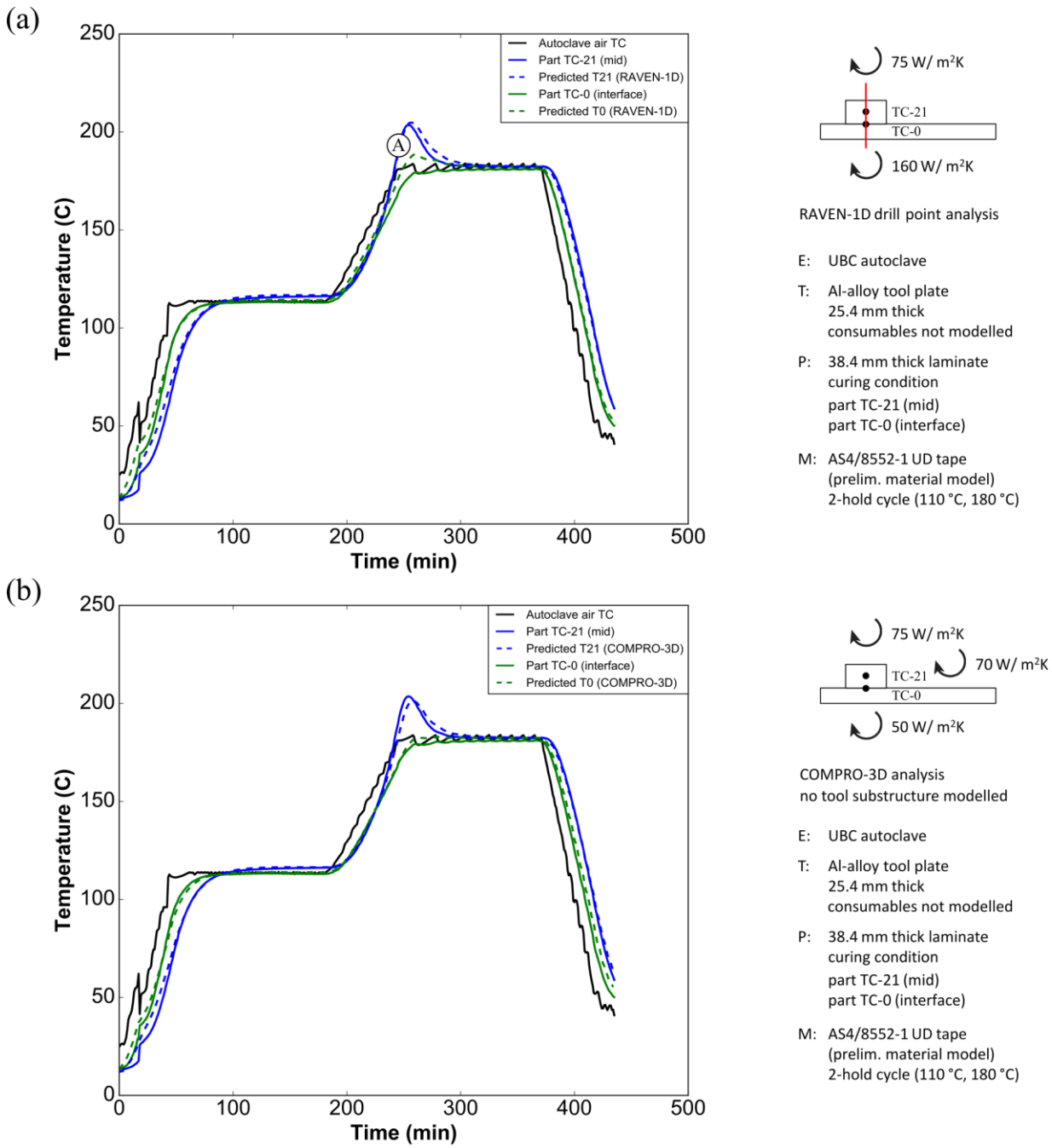

Figure 5-3: Comparison of experimentally measured and predicted modelling results for a 38.4 mm thick laminate (experiment ID: TEST-A) at mid-laminate (TC-21) and at the part/tool interface (TC-0) to investigate the benefits and trade-offs in thermal modelling complexity. Temperature profiles (*T* v *t*) of: (a) RAVEN-1D drill point analysis with part and tool plate modelled and (b) COMPRO-3D analysis with part and tool plate (no tool substructure modelled). Experimental data from [145] (Shimizu *et al*, 2008). ETPM: Equipment–Tool–Part–Material; TC: Thermocouple; UD: Unidirectional. Note: Temperature overshoot in the RAVEN-1D prediction at the part/tool interface at point A.

5.1.2 Cure kinetics models

The knowledge associated with understanding the material properties and processing behaviours of material systems can be considered a form of epistemic uncertainty. For instance, works by Dykeman [144] and Slesinger *et al* [149,150] have contributed to reducing the uncertainties related to first-order material property effects in cure modelling, such as cure kinetics characterization and validation.

In this next example, the processing behaviours of Hexcel AS4/8552 (baseline) and Hexcel AS4/8552-1 (derivative) material systems are briefly investigated to highlight subtle, but important differences in terms of the thermal management of these material systems. Although there is limited public information about the processing behaviour of the AS4/8552-1 material system, it is understood that this material derivative exhibits improved out-time and extended mechanical life compared to the baseline AS4/8552 material system [240].

For this study, the AS4/8552 NCAMP material model and a preliminary AS4/8552-1 material model, characterized as part of this work, are used. The 8552 NCAMP CK model is a 'model fitted' cure kinetics model that is validated within the range of temperatures: 100 °C < T < 190 °C (isothermal), -90 °C < T < 275 °C (dynamic) and 1 °C/ min < $\dot{T}$ < 10 °C/ min [135]. This model is considered a 'gold standard' model. On the other hand, the 8552-1 CK model is a preliminary 'semi model-free' cure kinetics model that is validated within the range of temperatures: 110 °C < T < 180 °C (isothermal), -90 °C < T < 275 °C (dynamic) and 1 °C/ min < $\dot{T}$ < 5 °C/ min. Further details of these respective models are given in Appendix E.1 and Appendix E.2.

Both material models are exercised using 1-hold and 2-hold cure cycles, with the experimentally measured and predicted RAVEN-1D modelling results shown in Figure 5-4. The details of these respective analyses are given in Appendix D.3 (experiment ID: 2010225-80) and Appendix D.2 (experiment ID: TEST-A).

For the 1-hold cycle (see Figure 5-4 (a)), the experimentally measured peak exotherm temperature at the mid-laminate (TC80-40) is 202 °C at t = 159 min. Both models exhibit almost identical temperature profiles, with predicted peak exotherm temperatures (T80-40) occuring within 1 °C of the experiment, but with the timing of this peak temperature occurring 5 min earlier in the AS4/8552 prediction and lagging by 7 min in the AS4/8552-1 prediction. For the 2-hold cycle (see Figure 5-4 (b)), differences in the predicted mid-laminate temperature profiles at lower temperatures are observed. At the end of the initial 110 °C hold at t = 180 min (point A), the AS4/8552 model overpredicts the temperature at material point T21 = 122 °C and DOC21 = 0.27. In comparison, the AS4/8552-1 model exhibits lower cure advancement with T21 = 116 °C and DOC21 = 0.16. Due to the premature exotherm, the AS4/8552 model significantly underpredicts the peak exotherm temperature at the final 180 °C hold by more than 10 °C. The AS4/8552-1 model, on the other hand, predicts the peak exotherm temperature (T21) within 1.2 °C and two minutes of the experimentally measured peak exotherm temperature (TC-21).

These results show that manufacturing simulation can be used to provide useful insights about how the cure cycle can be used to control cure advancement. A study that highlights a need to reconsider second-order material property effects, such as resin thermal conductivity, is presented in Appendix D.5.5.

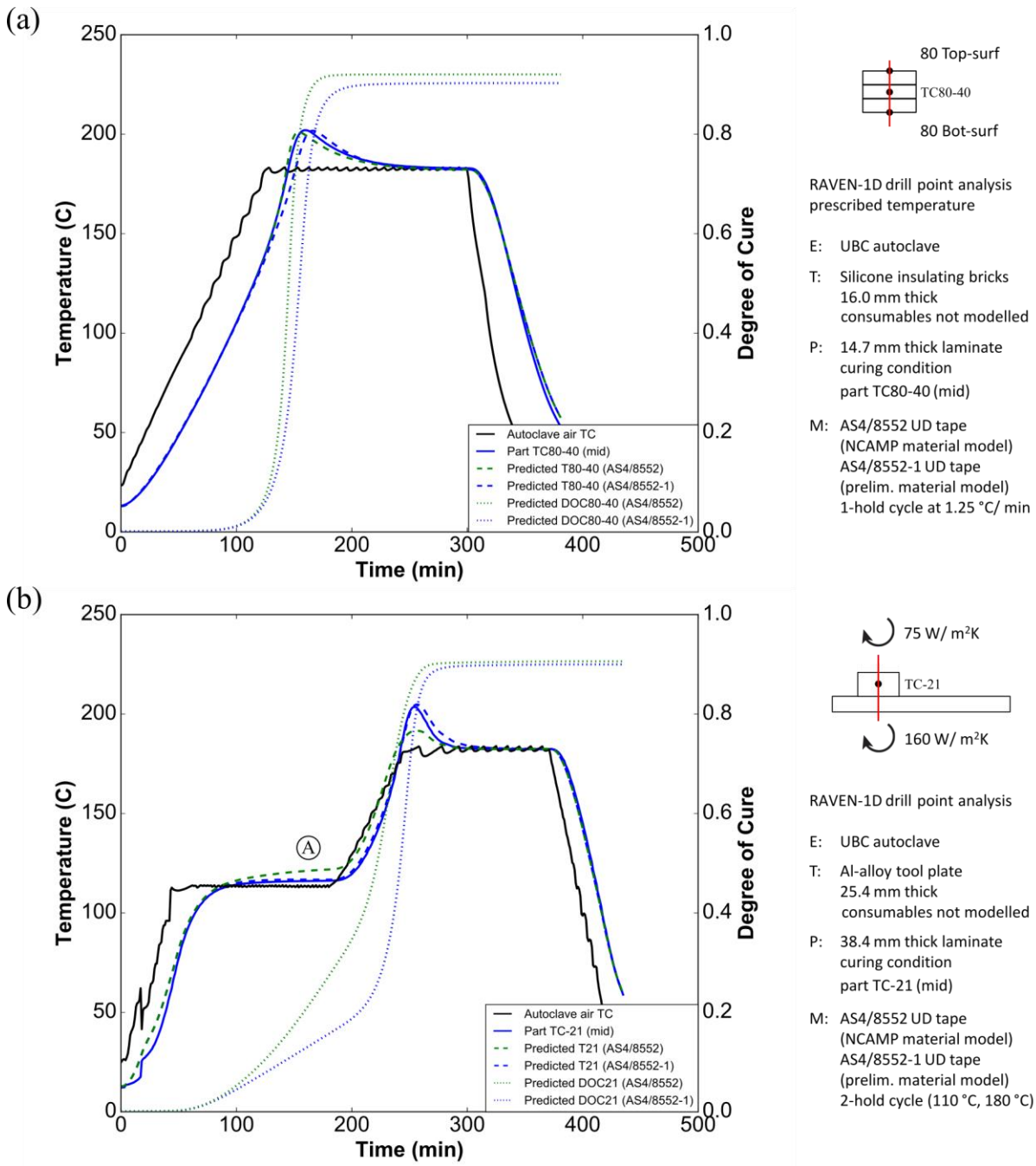

Figure 5-4: Comparison of experimentally measured and predicted RAVEN-1D modelling results for material system derivatives Hexcel AS4/8552 and AS4/8552-1. Temperature profiles (*T* v *t*) of: (a) 14.7 mm thick laminate (experiment ID: 20100225-80) and (b) 38.4 mm thick laminate (experiment ID: TEST-A). Experimental data from [150] (Slesinger, 2010) and [145] (Shimizu *et al*, 2008). ETPM: Equipment–Tool–Part–Material; TC: Thermocouple; UD: Unidirectional; DOC: Degree of Cure. Note: Premature temperature overshoot in the AS4/8552 prediction at point A.

5.1.3 Boundary conditions

The determination of convective heat transfer boundary condition inputs remains the greatest source of uncertainty for the thermal modelling of cure processes given variations in autoclave and oven temperature, airflow and loading conditions. Current typical practice is to 'calibrate' heat transfer boundary condition inputs with experimental thermocouple data.

In this final example, the thermochemical validation method proposed by Slesinger *et al* [149,150] is used to assess the goodness of the back-calculated effective heat transfer boundary condition inputs. Equivalent-1D and equivalent-3D values have been back-calculated using methods originally proposed by Shimizu *et al* [145]. The details of this approach are given in Appendix F, with a sensitivity study assessing its accuracy presented in Appendix D.2.5. Complementary work by Park [178] investigates experimental and simulation based approaches for the determination of zone based convective heat transfer coefficient distributions.

In terms of the ETPM factory ontology, discussed in Section 4.2.3, the Equipment and Tool classes contribute to the boundary conditions of the factory system. The following effects are observed in the back-calculated effective heat transfer coefficient values for the data sets shown in Table 5-2:

- *Autoclave pressure* (equipment): The effect of autoclave pressure on heat transfer coefficient (see Equation (2-7)). For example, the high pressure cure (720 kPa/90 psig) run in industrial autoclave B compared to the low pressure cure (410 kPa/45 psig) run in industrial autoclave D to prevent 'core crush'.

- *Consumables and condition of bagging* (tool): A significant drop in the effective top heat transfer coefficient value due to the presence of a bag leak. The effective bottom heat transfer coefficient can also be effected due to a change in the heat transfer area of the tool plate surface [145]. For example, TEST-B (without bag leak: h_{top} = 65 W/ (m^2 K)) compared with TEST-C (with bag leak: h_{top} = 15 W/ (m^2 K)).

- *Tool size effects* (tool): An artificially high effective bottom heat transfer coefficient value due to in-plane heat flow effects, such as tool size effects (eg. the size of the part relative to the tool) [145]. For example, TEST-A (h_{top} = 75 W/ (m^2 K) and h_{bot} = 160 W/ (m^2 K)).

Experimental data from back-to-back experiments, run in two different autoclaves: industrial autoclave B and the UBC autoclave, are analyzed. Experimentally measured and predicted RAVEN-1D modelling results are shown in Figure 5-5. The details of these respective analyses are given in Appendix D.5 (experiment ID: 20151028-001) and Appendix D.2 (experiment ID: TEST-A and TEST-B), with the effective heat transfer boundary condition inputs applied to the RAVEN-1D models reported in Table 5-2.

For the cured T800H/3900-2 laminate processed in industrial autoclave B (see Figure 5-5 (a)), the predicted mid-laminate temperature profile (TC4), lags the experimental results (TC-C4) by approximately 4.0 °C during heat up and 2.4 °C during the cool down. This difference is attributed to the material model (refer to Appendix D.5.5). In the curing case, the prediction at TC4 lags the experimental mid-laminate temperature profile at TC-C4, and overpredicts the peak exotherm temperature by more than 5.0 °C.

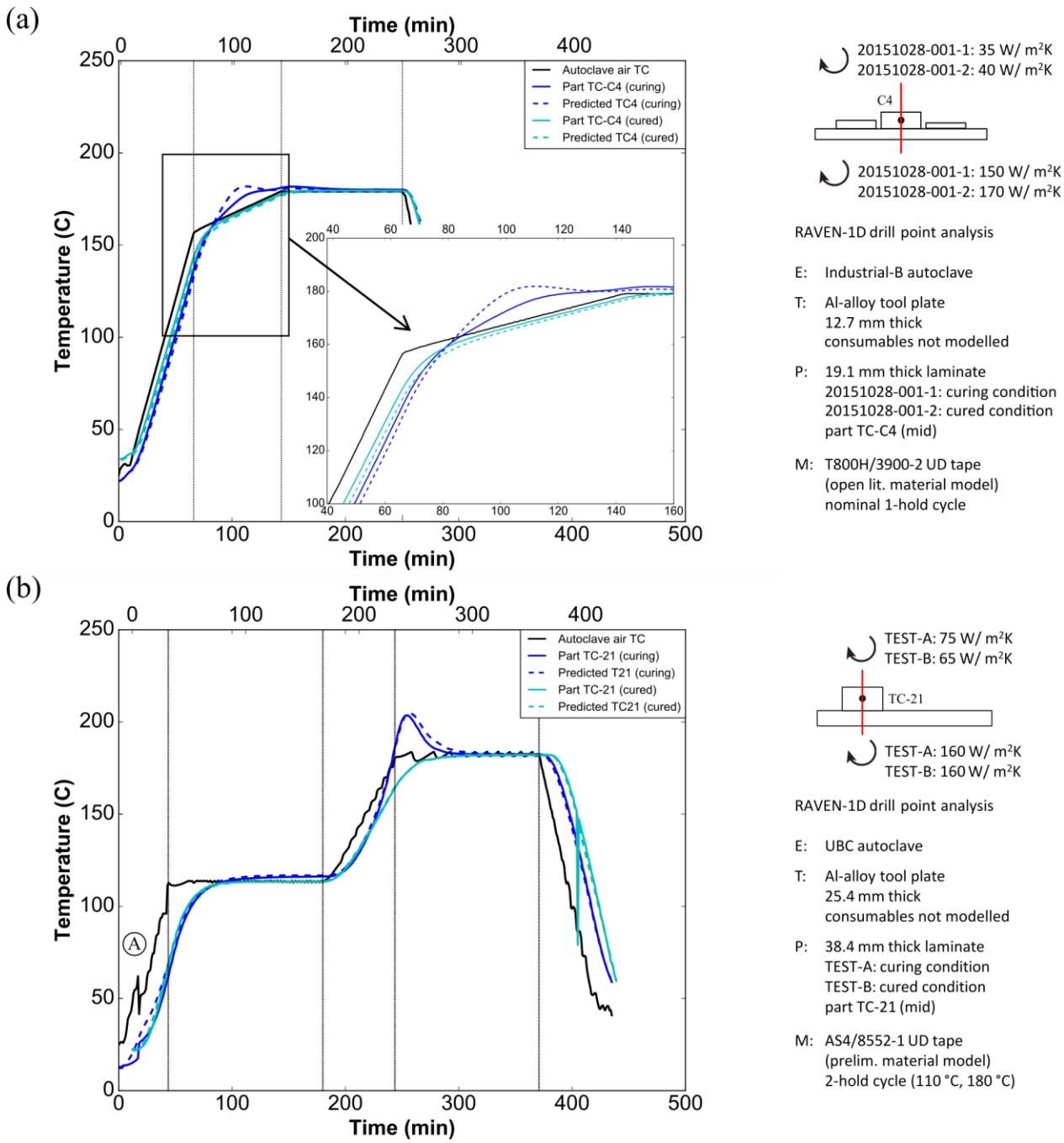

Figure 5-5: Comparison of experimentally measured and predicted RAVEN-1D modelling results for back-to-back experiments to investigate the validity of HTC boundary condition inputs. Temperature profiles (*T* v *t*) of: (a) 19.1 mm thick laminate (experiment ID: 20151028-001) and (b) 38.4 mm thick laminate (experiment ID: TEST-A and TEST-B). Experimental data from [237] (Boeing-UW, 2017) and [145] (Shimizu *et al*, 2008). ETPM: Equipment–Tool–Part–Material; TC: Thermocouple; UD: Unidirectional. Note: TEST-B is offset by 12 minutes due to the cure cycle interruption observed in TEST-A at point A. Vertical lines indicate heat up, hold and cool down cure cycle segments.

For the cured AS4/8552-1 laminate processed in the UBC autoclave (see Figure 5-5 (b)), no apparent differences in the predicted (T21) and measured (TC-21) mid-laminate temperature profiles are observed. In the curing case, and as reported in Section 5.1.2, the predicted peak exotherm temperature at T21 is within 1.2 °C and two minutes of the experimentally measured temperature data at TC-21. It should be noted that due to the cure cycle interruption observed in TEST-A (curing condition), TEST-B (cured condition) is offset by 12 minutes (point A).

These results show that reasonable effective heat transfer boundary conditions inputs have been applied to the thermal models. Accounting for the fact that curing and cured laminates have slightly different thermophysical properties, the validation strategy proposed by Slesinger *et al* [149,150] could be extended to validate heat transfer boundary condition inputs. The validation of effective heat transfer coefficients using simulation based 'synthetic' temperature profile data is presented in Appendix D.5.2.

5.1.4 Summary

As discussed in Section 2.3.2, the management of uncertainty in modelling and simulation is often overlooked since it is assumed that suitable practices exist. In this first case study, a structured approach for managing the uncertainty associated with the thermal modelling of cure processes and gaining confidence in the predicted modelling results was presented. The key sources of thermal modelling uncertainty were identified according to the accepted classification of modelling uncertainty and error defined by Oberkampf *et al* [184,185] and the main components of the thermochemical model (see Table 5-3).

The steps for gaining confidence in the predicted thermal modeling results are depicted in the workflow shown in Figure 5-1, and include: 1) validating material model and heat transfer boundary condition inputs for the intended problem that the thermal model will be applied to; 2) understanding the implications of modelling simplications to determine the most appropriate solution method, given that for thermal management problems a multiscale modelling 'building block' approach exists; and 3) validating the thermal model against experimentally measured data to assess its accuracy.

Three examples were presented, in terms of the main components of the thermochemical model, to demonstrate these important steps using data sets that represent real production scenarios. These examples showed that a high confidence in the predicted modelling results can be achieved.

Having outlined a structured approach for managing the uncertainty associated with the thermal modelling of cure processes, two contrasting case studies are presented in the following sections to show how modelling and simulation can be used as an enabling tool to support manufacturing decisions. The first case study, relating to material qualification, is an example of a development workflow that is typically performed in the early stages of the development design cycle. The second case study, on the other hand, represents a troubleshooting workflow relating to structural certification that is typically performed in the late stages of the development design cycle. Both of these cases represent a starting point for formalizing science based practices for thermal management in composites manufacturing.

5.2 Case 2: Cure Cycle Development and Evaluation

Material qualification relates to the determination of material level properties that are used in the structural design and certification, as discussed in Sections 3.1.1 and 4.1.2. One of the main steps in qualifying a material, whether a new material system or an existing material system for a new application, is the development and evaluation of a cure cycle suitable for the generation of the material allowables database, and scaling to production processes. This cure cycle is defined within a broader cure window: the allowable range of temperature, pressure, and vacuum values. One the key issues identified[15], particularly with defining the cure window, is failing to consider the full range of future applications and processing scenarios (eg. transitioning from autoclave to OOA cure processes or from hand layup to AFP/forming, see Section 4.3.5).

The manufacturing science base can be used in defining the cure window and in recommending a cure cycle for the qualification of a material. For instance, manufacturing simulation can be used to assess the effects of cure cycle variations on equipment, tool, and part attributes (eg. $((e)_1, (t)_1, (p)_1, (m)_2) = (1, 1, 1, 2)$), as shown in Figure 5-6. While analysis can provide information on managing outcomes, such as temperature, DOC, viscosity (flow index), consolidation and the relative effects of residual stress, the evaluation of process effects on mechanical properties, such as the 'effect of defects', must be performed primarily by test [125]. However, as discussed in Section 2.3.2, a science based understanding of process-induced defects is an active area of research.

[15] Based on a survey of composites manufacturing experts by Mobuchon and Zobeiry (2014).

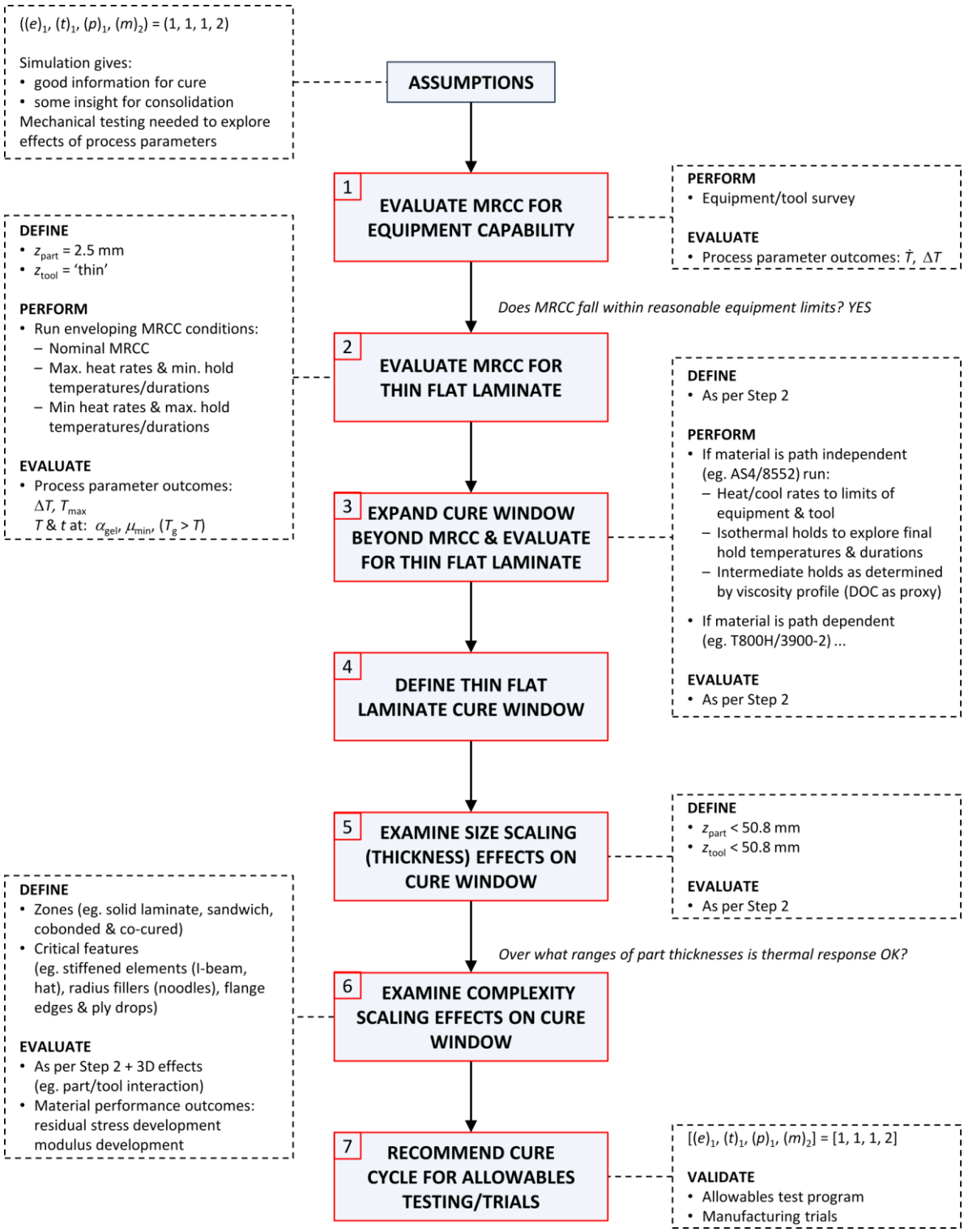

Figure 5-6: Cure cycle development and evaluation workflow. Extension of approach from [129,130] **(Nelson *et al*, 2002). ETPM: Equipment–Tool–Part–Material; w, x, y, z: design-gate indices; MRCC: Manufacturer Recommended Cure Cycle; *z*: through-thickness coordinate; $\dot{T}$: temperature rate; ΔT: temperature difference; α_{gel}: gelation; μ_{min}: minimum viscosity; $T_g > T$: vitrification.**

This second case study highlights the benefits of using manufacturing simulation to evaluate candidate cure cycles for a 28.2 mm thick AS4/8552 panel with tapered core. The work presented is based on development activities performed at the time of the NASA ATCAS program for fuselage structures [100,103].

5.2.1 ETPM definition

The part considered in this case study is a 28.2 mm thick AS4/8552 panel with tapered core that was processed on a very large Invar tool. This part has intermediate complexity due to the transition from a 28.2 mm thick solid laminate ('solid' zone) to a 23.7 mm thick 130 kg/ m^3 glass/phenolic honeycomb core with 2.2 mm thick facesheets ('sandwich' zone), as shown in Figure 5-7. This part was manufactured as part of the NASA ATCAS program to develop optimized cure cycles for structures of similar complexity [100,103]. It should be noted that it took a team of composites manufacturing experts many months to devise a cure cycle capable of producing high quality parts with adequate consolidation, low porosity while preventing 'core crush' [100].

The ATCAS program represented the first use of first-generation process modelling tools. Since then, manufacturing simulation has become robust, fast, and more widely available in commercial software packages that range in complexity and sophistication. There have also been improvements in the material models used to predict the thermal response of curing laminates.

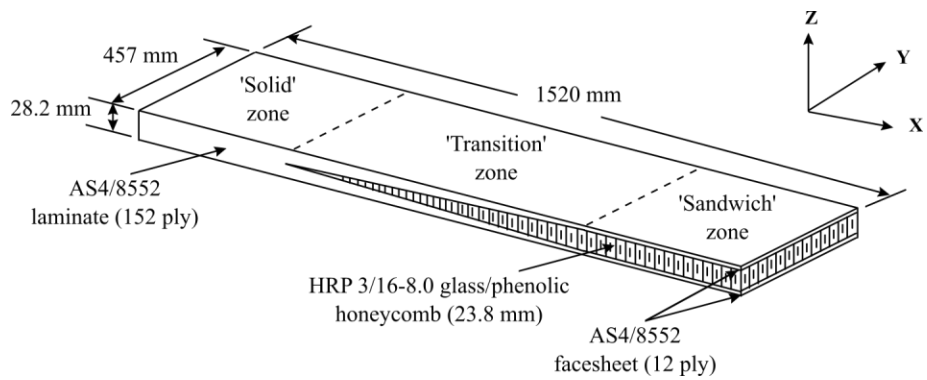

Figure 5-7: Geometery for a 28.2 mm thick panel with tapered core (schematic from [100] (Johnston, 1997)).

This case study is depicted as a development workflow at design state $((e)_1, (t)_1, (p)_1, (m)_2)$ = (1, 1, 1, 2) in the ETPM decision tree shown in Figure 5-8 (a) and is a subset of the material qualification design path shown in black. A solid wavy line indicates that a manufacturing trial is performed at $((e)_2, (t)_2, (p)_2, (m)_2)$ = (2, 2, 2, 2). Refer to Table 4-3 for definitions of the ETPM design-gate indices. This manufacturing trial refers to an experimental thermal profile performed as part of the ATCAS program [100] (refer to Appendix D.1).

The cure cycle evaluation performed in this case study uses preferred equipment and tooling concepts, shown as ETPM thermal management attributes, in Figure 5-8 (b). Experimental setup and modelling inputs are summarized in Table 5-4. Effective heat transfer coefficient values for low pressure cure (375 kPa/40 psig) are estimated based on the autoclave characterization work conducted on industrial autoclave A at the time of the ATCAS program [100]. Invar tool plate thickness and substructure configuration are investigated as three processing scenarios shown in Figure 5-9. The effect of open and closed substructure is modelled using high and low effective bottom heat transfer coefficient values. This case study also makes use of the AS4/8552 NCAMP material model [135,238]. This validity of this model is specified in Section 5.1.2.

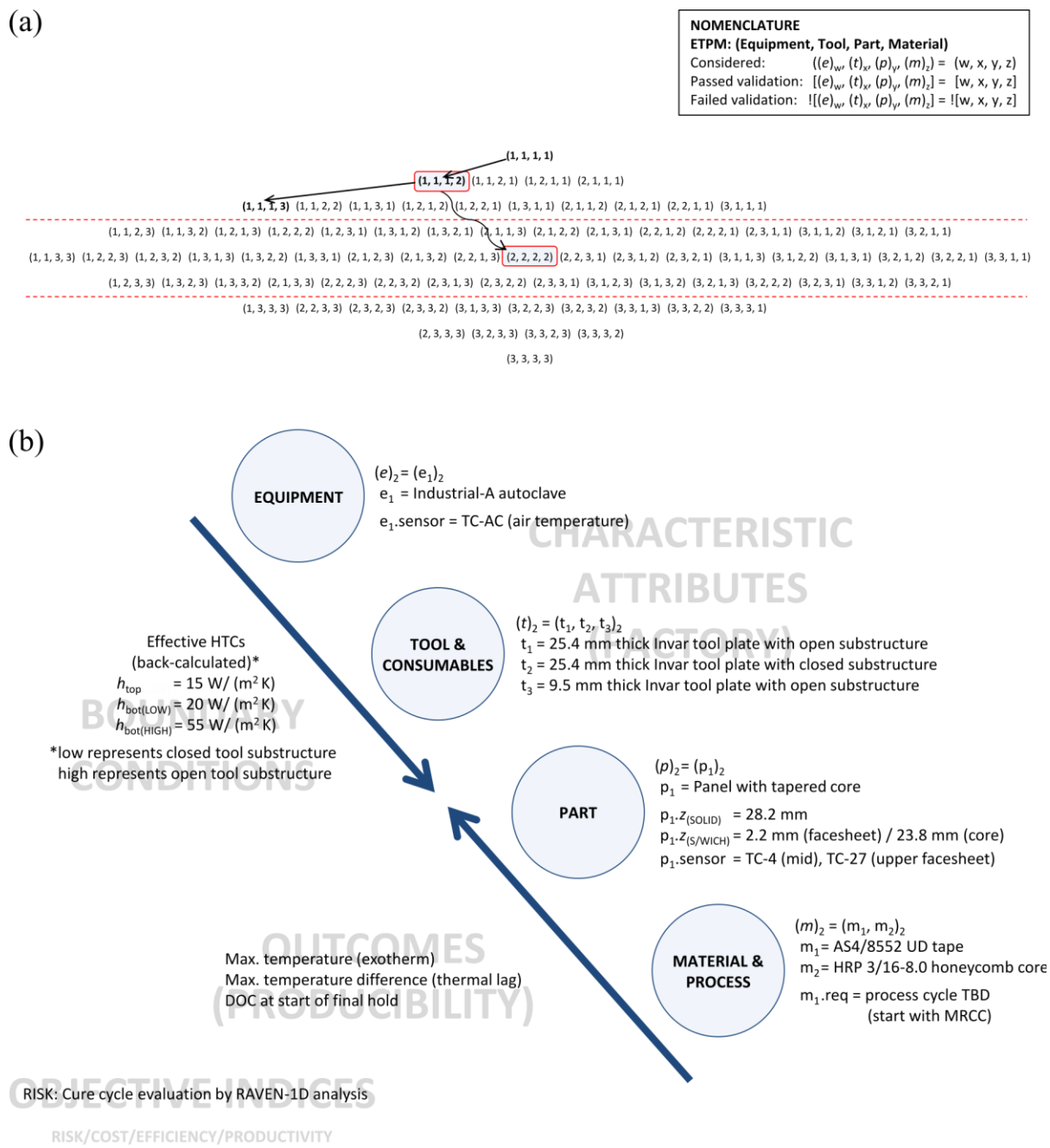

Figure 5-8: Cure cycle evaluation. This scenario demonstrates the use of manufacturing simulation to recommend a cure cycle for a 28.2 mm thick panel with tapered core. This problem is depicted as: (a) development workflow at design state $((e)_1, (t)_1, (p)_1, (m)_2)$ = (1, 1, 1, 2) with a manufacturing trial performed at $((e)_2, (t)_2, (p)_2, (m)_2)$ = (2, 2, 2, 2) and (b) ETPM thermal management attributes. Experimental data from [100] (Johnston, 1997). ETPM: Equipment–Tool–Part–Material; w, x, y, z: design-gate indices; TC: Thermocouple; HTC: Heat Transfer Coefficient; TBD: To Be Determined; *z*: through-thickness coordinate; DOC: Degree of Cure; UD: Unidirectional; req: manufacturing requirement; MRCC: Manufacturer Recommended Cure Cycle. Note: Instances are denoted in lowercase, shorthand notation is denoted in italics. A typical material qualification design path is shown in black. Solid wavy lines indicate that the precise design path is unknown.

Table 5-4: ETPM[a] attribute definition for a 28.2 mm thick panel with tapered core.

		Test[b]	Analysis
Equipment	**(E)**	Autoclave: Industrial-A TC-AC (air temperature)	$h_{top\ (HIGH)}$ = 15 W/ (m^2 K)
Tool	**(T)**	Invar tool z_{tool} = 25.4 mm	$h_{bot\ (LOW)}$ = 20 W/ (m^2 K) $h_{bot\ (HIGH)}$ = 55 W/ (m^2 K) $z_{tool\ (THIN)}$ = 9.5 mm $z_{tool\ (THICK)}$ = 25.4 mm
Part	**(P)**	Panel with tapered core (1524 mm x 457 mm) $z_{part\ (SOLID)}$ = 28.2 mm (152 ply) $z_{part\ (S/WICH)}$ = 2.2 mm (12 ply) / 23.8 mm (core) TC-4 (mid-laminate) TC-27 (upper facesheet)	RAVEN-1D drill point analysis [238] T4: mid (solid zone) T27: upper f/sheet (sandwich zone)
Material	**(M)**	AS4/8552 UD tape Glass/phenolic honeycomb core HRP (3/16-8.0) Cure cycle development and evaluation (see Table 5-5 for process requirements)	AS4/8552 NCAMP material model Nominal aramid honeycomb (thermal only)

[a] ETPM: Equipment–Tool–Part–Material
[b] Based on experimental data from [100] (Johnston, 1997), refer to Appendix D.1.

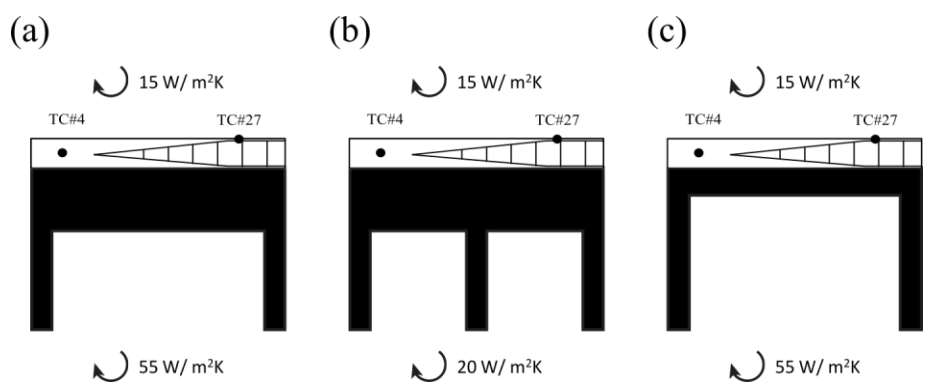

Figure 5-9: Processing scenarios considered for a 28.2 mm thick panel with tapered core: (a) Case I: 25.4 mm thick Invar tool with open substructure (thick tool), (b) Case II: 25.4 mm thick Invar tool with closed substructure ('cold' tool strategy to mitigate exotherm) and (c) Case III: 9.5 mm thick Invar tool with open substructure (thin tool). TC: Thermocouple; HTC: Heat Transfer Coefficient. Note: A high toolside HTC represents an open tool substructure, whereas a low toolside HTC represents a closed tool substructure.

Process requirements for this case study are derived from the Hexcel HexPly 8552 manufacturer recommended cure cycle (MRCC) [241]. It should be noted that the requirements specified here are shown as examples for the purposes of this case study. In practice, material suppliers may recommend requirements based on their knowledge of the resin chemistry and/or other unusual characteristics of their materials. Additionally, composites manufacturers may also define requirements based on their knowledge of the materials they use.

To guide cure cycle evaluation, acceptance criteria are defined to assess thermal outcomes relative to the process requirements. These criteria could be considered the definition of the cure window for this case study. Three criteria are specified:

- *Maximum hold temperature*: The maximum hold temperature must not be exceeded by more than a certain value (eg. to prevent degradation of the material).

- *Thermal lag*: Regardless of timing, different material points in a structure are deemed to meet the thermal lag criterion independently of each other. However, the temperature profile at all material points in a structure is linked via the air temperature. It is therefore convenient to consider temperature rate requirements in terms of the temperature at which this requirement is violated when approaching any hold segment during cure.

- *Resin gelation timing*: Gelation is required at the final hold temperature. Premature gelation may adversely affect downstream outcomes (eg. porosity due to insufficient resin flow, process-induced delaminations due to the development of residual streses).

Both the process requirements and cure cycle acceptance criteria are listed in Table 5-5.

Table 5-5: Process requirements and acceptance criteria for a 28.2 mm thick panel with tapered core. Note: These requirements and criteria are shown as examples for the purposes of this case study.

Outcome	Requirement	Acceptance criteria	
Process parameter			
Hold temperature	± 5 °C on all holds		
Maximum temperature (at final 180 °C hold)		T < 185 °C T < 190 °C T > 190 °C	pass marginal fail
Heat & cool rates	Ignore thermal lag for T < 50 °C Cool down at 2–5 °C/ min Heat up at 0.3–3 °C/ min		
Thermal lag (transition to any hold)		ΔT within 5 °C ΔT within 15 °C ΔT not within 15 °C	pass (unshaded) marginal (yellow) fail (red)
Material structucture			
Resin gelation[a] timing (at start of final 180 °C hold)		DOC < 0.45 0.45 < DOC < 0.55 DOC > 0.55	pass marginal fail

[a] Estimated DOC at gelation for Hexcel AS4/8552. DOC: Degree of Cure

Manufacturing simulation, or manufacturing trials guided by simulation, should be used to: 1) define a cure window that is favourable to a broad range of foreseeable processing scenarios; and 2) challenge process requirements, particularly in cases where they do not make sense.

5.2.2 Cure cycle development and evaluation

For each processing scenario, two drill points are selected to represent the critical zones in the thick panel with tapered core. At each drill point, a RAVEN-1D analysis is performed. The first drill point represents a section in the ‘solid’ zone, with a material point (T4) located mid-laminate. The second drill point represents a section in the ‘sandwich’ zone, with a material point (T27) located in the upper facesheet. These selected material points correspond to part TCs (TC-4 and TC-27) from the experimental thermal profile performed during the ATCAS program [100] (see Figure D-1 (b)).

The baseline processing scenario considered in this case study is Case I (see Figure 5-9 (a)). Predicted RAVEN-1D modelling results for this case are shown as temperature profile (T v t) and temperature rate versus temperature ($\dot{T}$ v T) plots in Figure 5-10 and Figure 5-11. Temperature profile plots are commonly used to visualize the thermal reponse of parts and tools. These plots can be used to identify whether the maximum temperature and DOC thermal outcomes satisfy process requirements. The temperature rate plot can be used to evaluate the thermal lag outcome by explictly revealing the thermal rate response of parts and tools. The cure cycle acceptance criteria are included directly in these plots as pass (unshaded), marginal (yellow) and fail (red).

Based on the 'sources and sinks' relationships identified for thermal management (see Figure 3-3), the following modifcations to the cure cycle are made:

- *Nominal MRCC*: The initial cure cycle is the nominal MRCC [241], with a heating rate of 2.0 °C/ min. From Figure 5-10 (a), the overall result from material points T4 and T27 is a fail. The predicted peak exotherm temperature in the 'solid' zone is T4 = 223 °C and occurs 16 minutes after the predicted autoclave air temperature reaches the final 180 °C hold. The first modification to the cure cycle is to reduce the heating rate.

- *Slow MRCC*: The heating rate is reduced to 1.1 °C/ min. From Figure 5-10 (b), the overall result from material points T4 and T27 remains unchanged. The predicted peak exotherm temperature is T4 = 213 °C and occurs earlier in the cycle at 12 minutes after the predicted autoclave air temperature reaches the final 180 °C hold. The next cure cycle iteration is to extend the initial hold dwell time to shift the timing of the predicted peak exotherm temperature into the ramp (transition to the final 180 °C hold).

- *Extend 110 °C hold*: The initial 110°C hold is extended by 120 minutes. From Figure 5-11 (a), the overall result from material points T4 and T27 is a fail. While maximum temperature and thermal lag criteria are acceptable and marginally acceptable for both material points respectively, the DOC is high at the start of the final 180 °C hold, with predicted DOC4 = 0.66 in the 'solid' zone and predicted DOC27 = 0.71 in the 'sandwich' zone. The next modification to the cure cycle is to introduce an intermediate hold to reduce 'knock-on' effects to downstream outcomes due to premature gelation.

- *Introduce 150 °C hold*: Finally, an intermediate 150 °C hold is introduced. From Figure 5-11 (b), the overall result from material points T4 and T27 is marginally acceptable. The resin gelation timing criterion is satisfied for both material points, with predicted DOC4 = 0.38 and predicted DOC27 = 0.42 at the start of the final 180 °C hold. Based on the results of this evaluation, this cure cycle is recommended for manufacturing trials.

A summary of overall results for this case study is given in Table 5-6. The predicted modelling results for Case II (see Figure 5-9 (b)) and III (see Figure 5-9 (c)) are presented in Appendix D.1.5.

Table 5-6: Overall summary of RAVEN-1D analyses for a 28.2 mm thick panel with tapered core. Note: Cure cycle acceptance criteria are summarized in Table 5-5.

Design iteration	Case I Thick tool (25.4 mm) Open substructure	Case II[a] Thick tool (25.4 mm) Closed substructure	Case III[a] Thin tool (9.5 mm) Open substructure
Nominal MRCC[b]	fail	fail	fail
Slow MRCC[b]	fail	fail	fail
Extend 110 °C hold	fail	fail	fail
Introduce 150 °C hold	marginal[c]	fail	marginal[c]

[a] The results for Cases II & III are presented in Appendix D.1.5.
[b] MRCC: Manufacturer Recommended Cure Cycle
[c] The resin gelation timing criterion is acceptable for Case I & marginally acceptable for Case III.

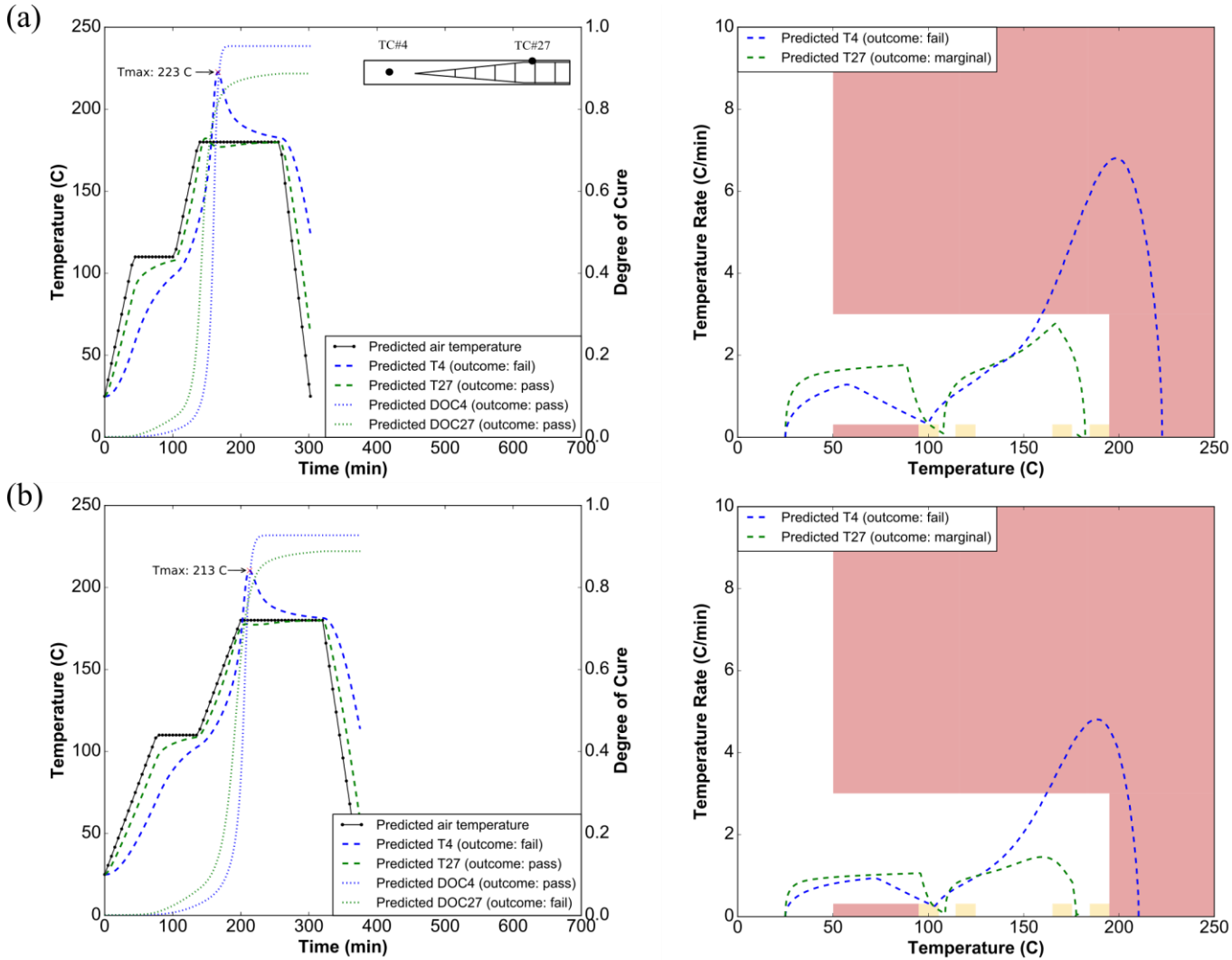

Figure 5-10: Predicted RAVEN-1D modelling results for Case I (processing scenario: 25.4 mm thick Invar tool with open substructure). Temperature profile (T v t) and temperature rate versus temperature ($\dot{T}$ v T) plots for: (a) nominal MRCC (overall outcome: fail) and (b) slow MRCC (overall outcome: fail). MRCC: Manufacturer Recommended Cure Cycle; TC: Thermocouple; DOC: Degree of Cure. Note: Cure cycle acceptance criteria are summarized in Table 5-5 (pass (unshaded), marginal (yellow), fail (red)).

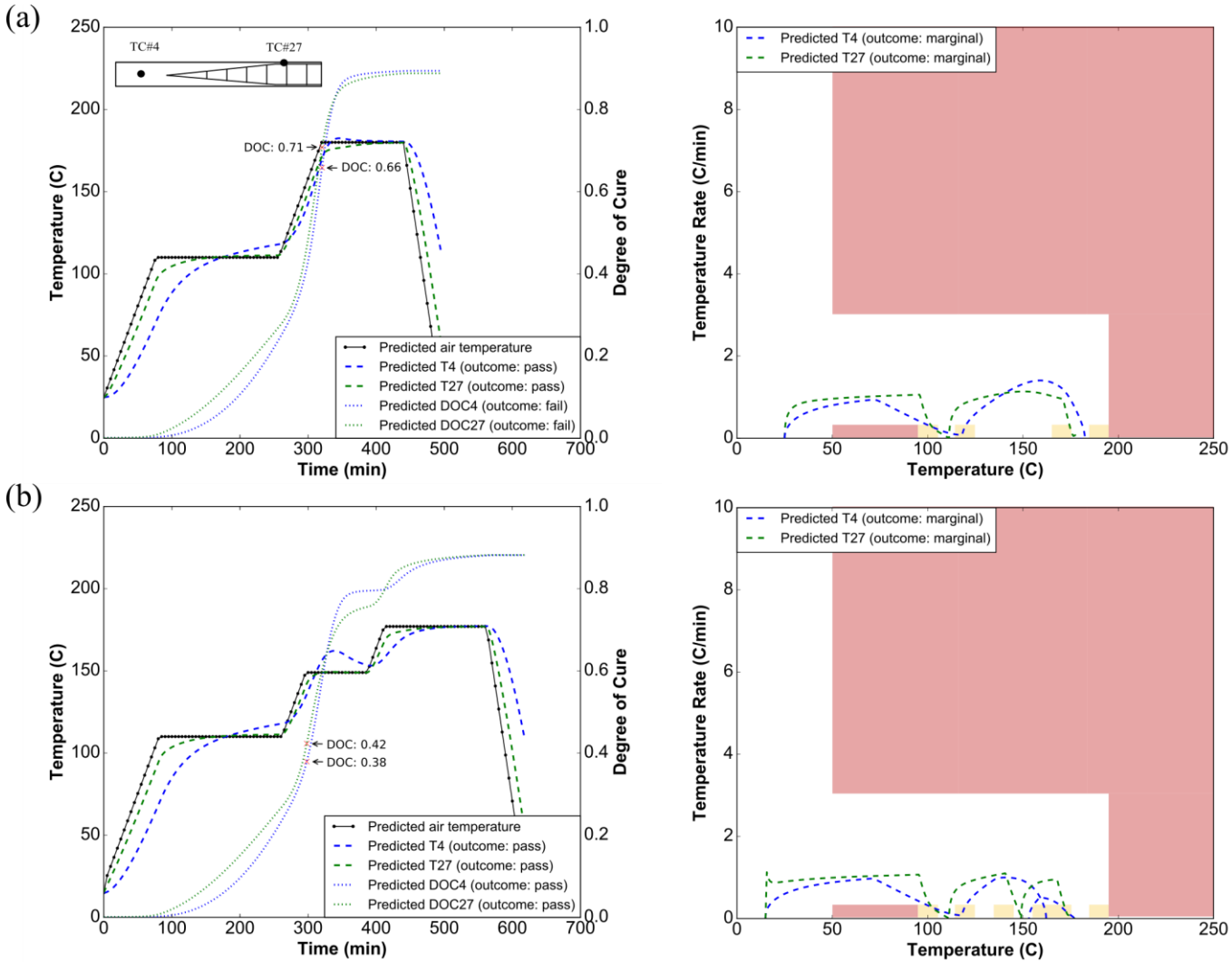

Figure 5-11: Predicted RAVEN-1D modelling results for Case I (processing scenario: 25.4 mm thick Invar tool with open substructure). Temperature profile (T v t) and temperature rate versus temperature ($\dot{T}$ v T) plots for: (a) extending the 110 °C hold (overall outcome: fail) and (b) introducing an intermediate 150 °C hold (overall outcome: marginal). TC: Thermocouple; DOC: Degree of Cure. Note: Cure cycle acceptance criteria are summarized in Table 5-5 (pass (unshaded), marginal (yellow), fail (red)).

5.2.3 Experimental measurements

The results of a manufacturing trial performed at the time of the ATCAS program are compared to RAVEN-1D model predictions based on the 3-hold cure cycle developed in Section 5.2.2 and original COMPRO-2D model predictions performed by Johnston [100] in Figure 5-12. It should be noted that the experimental temperature data is from [100] (Johnston, 1997).

As reported in the original analysis [100], differences in experimental temperature profiles at the mid-laminate in the 'solid' zone (TC-4) and upper facesheet in the 'sandwich' zone (TC-27) are observed. Firstly, the relative thermal lag in the 'solid' zone at TC-4 compared to the 'sandwich' zone at TC-27 due to the respective thermal mass of these zones (eg. difference due to laminate thickness). Secondly, an observable exotherm at TC-4 occurs during the intermediate 150 °C hold at t = 339 min (point A). No exotherm is observed at TC-27 given the thin facesheet thickness.

Reasonable agreement between the experimentally measured and predicted RAVEN-1D modelling results is shown in Figure 5-12 (a). Compared with the experimental data, the RAVEN-1D model: 1) underpredicts the thermal lag at material point T4 in the 'solid' zone during the initial heat up segment of the cure cycle; and 2) overpredicts the peak exotherm temperature at material point T4 by 5°C during the intermediate 150 °C hold at t = 340 min (point A). These discrepancies are the likely result of the constant heat transfer boundary conditions applied to the RAVEN-1D model compared with actual heat transfer variations within industrial autoclave A and the initial conditions specified in the thermal model.

(a)

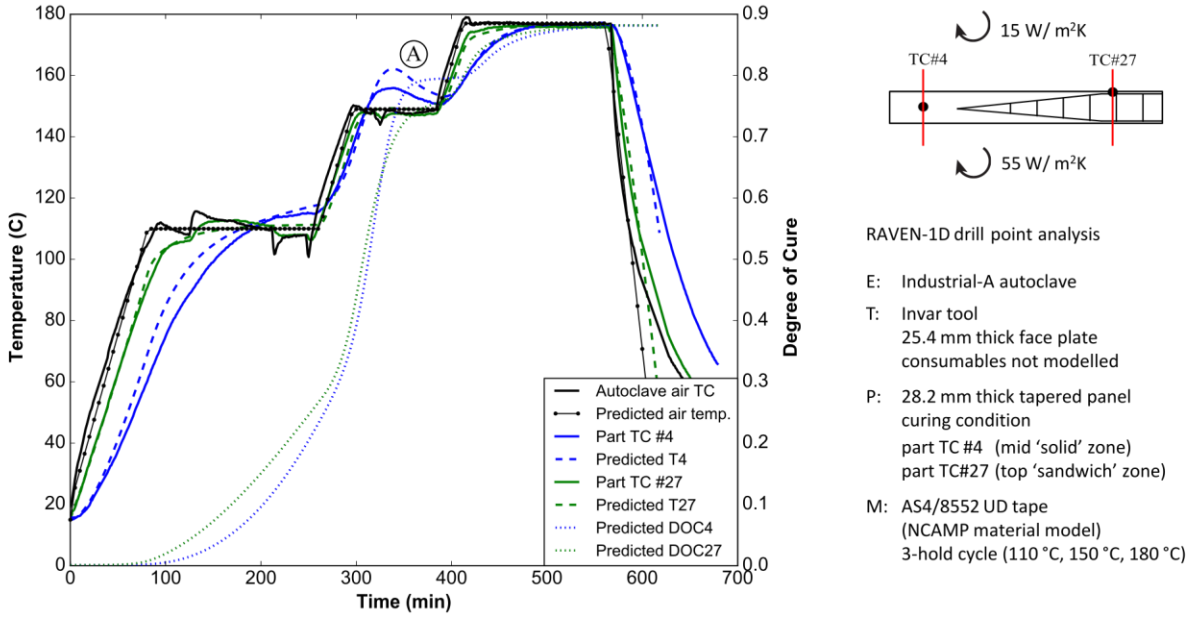

(b)

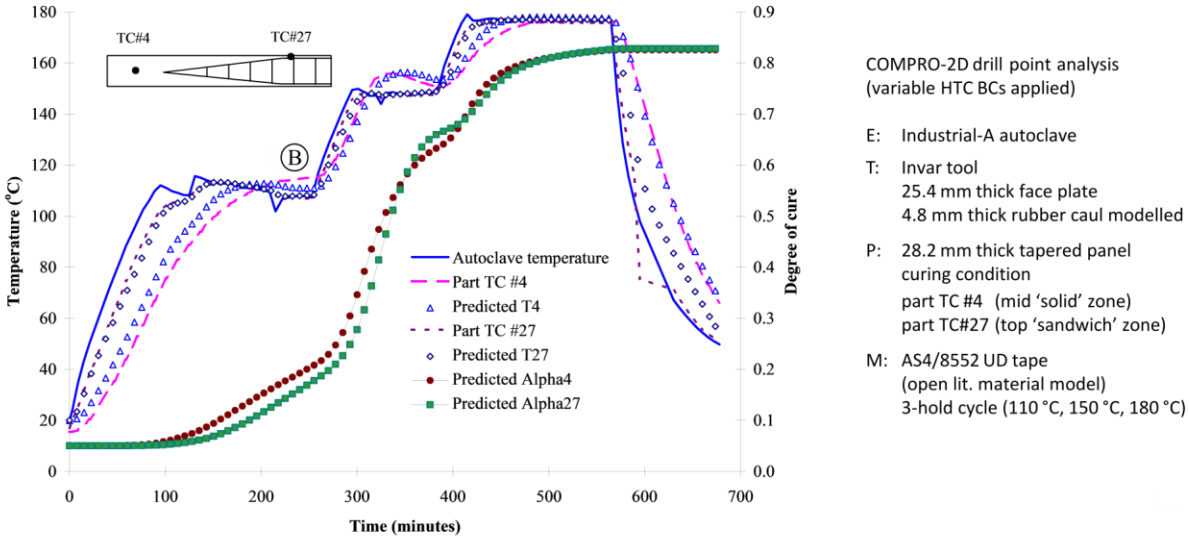

Figure 5-12: Comparison of experimentally measured and predicted modelling results for a 28.2 mm thick panel with tapered core. Temperature profiles (*T* v *t*) of: (a) RAVEN-1D analysis using the AS4/8552 NCAMP material model (Case I) and (b) original COMPRO-2D analysis using the AS4/8552 open literature material model (figure from [100] (Johnston, 1997)). Experimental data from [100] (Johnston, 1997). ETPM: Equipment–Tool–Part–Material; HTC: Heat Transfer Coefficient; BCs: Boundary Conditions; TC: Thermocouple; UD: Unidirectional. Note: Predicted autoclave air temperature is based on the cure cycle development and evaluation performed in this case study. Temperature overshoot overpredicted at point A and temperature overshoot underpredicted in the original prediction at point B.

The original COMPRO-2D analysis performed by Johnston [100] is shown in Figure 5-12 (b). While this model underpredicts the overshoot in the material point T4 at the end of the initial 110 °C hold at t = 215 min (point B), this overshoot is predicted in the revised RAVEN-1D analysis. The improvement in the revised model prediction is attributed to improvements in the AS4/8552 NCAMP material model. As previously mentioned, constant heat transfer boundary conditions are applied to the revised RAVEN-1D model. The effect of low and high heat transfer, due to changes in autoclave pressurization, on the predicted RAVEN-1D modelling results are shown in Figure D-3. A comparative analysis showing the AS4/8552 NCAMP material model initial degree of cure sensitivity is shown in Figure D-4.

5.2.4 Summary

RAVEN-1D thermal models were used to rapidly iterate and systematically evaluate proposed cure cycle modifications for a part with intermediate complexity (eg. $((e)_1, (t)_1, (p)_1, (m)_2) = (1, 1, 1, 2)$). Based on this analysis, a 3-hold cure cycle was recommended for manufacturing trials, an experimental thermal profile performed at the time of the ATCAS program (eg. $((e)_2, (t)_2, (p)_2, (m)_2) = (2, 2, 2, 2)$). Compared with the experimental data, the predicted modelling results underpredicted the thermal lag during the initial heat up and overpredicted the peak exotherm temperature during the intermediate hold. These discrepancies were attributed to the heat transfer boundary conditions applied to the model. Compared with the original COMPRO-2D analysis, improvements in the revised RAVEN-1D model predictions were observed that were attributed to improvements in material model characterization.

From this case study, several conclusions can be made. Firstly, that it is possible to systematically evaluate manufacturing concepts without the need to run complex 3D thermal models. Not only does this reduce the computational requirements needed for the analysis, but it can also lower the necessary training requirements needed to enable non-experts with these tools. Secondly, manufacturing simulation can be used to assess manufacturing concepts in the early stages of the development design cycle *before* significant costs are committed (eg. conceptual design). More importantly, this can allow M&P and manufacturing engineers to be engaged in the decision making processes earlier in the development design cycle. For instance, knowing whether an existing or standard cure cycle is feasible could mean the difference between being able to manufacture parts in a 'bus stop' or batch production run, or whether a dedicated cure cycle in existing or new facilities is required. In terms of the cure window, manufacturing simulation can be used to define sufficiently broad processing limits to account for a wide range of foreseeable processing scenarios. Additionally, these same scientific insights could be used to assess the capabilities of the supplier network. Finally, this case study showed that the practice of developing and evaluating cure cycles can be standardized as a routine thermal management workflow, given that the manufacturing science base exists.

Future work is recommended to document science based practices for workflows associated with material qualification. Preliminary topics for material screening and characterization, and cure cycle development and evaluation are proposed in Appendix C.1.

5.3 Case 3: Experimental Thermal Profile Validation

Experimental thermal profiling is an important structural certification and process monitoring activity in composites manufacturing, as discussed in Sections 3.1.1 and 4.1.2. Typically, thermocouples are used to empirically measure the thermal response of parts and tools to ensure that process specifications are satisfied, and material equivalency is acheived. Another important result from the experimental thermal profile is to identify the locations of thermocouples for production monitoring. In practice, part TCs are typically located in regions of the part that will subsequently be trimmed (eg. edgeband) or insulated tool TCs that are intended to measure the lagging temperature.

Thermal profiling failures occur frequently and can be very costly, especially if the failure is identified at some time after parts have entered service[16]. There are two types of failures:

- *Apparent failures* are caused by faulty sensors or sensors that provide invalid measurements, such as a poorly insulated thermocouple or improper thermocouple calibration (refer to Appendix D.4.5).
- *Real failures* are actual variations from process specifications.

The manufacturing science base can be used to analyze, validate, and troubleshoot thermal profiling failures (eg. ![$(e)_3$, $(t)_3$, $(p)_3$, $(m)_3$] = ![3, 3, 3, 3]), as shown in Figure 5-13.

[16] Based on a survey of composites manufacturing experts by Mobuchon and Zobeiry (2014).

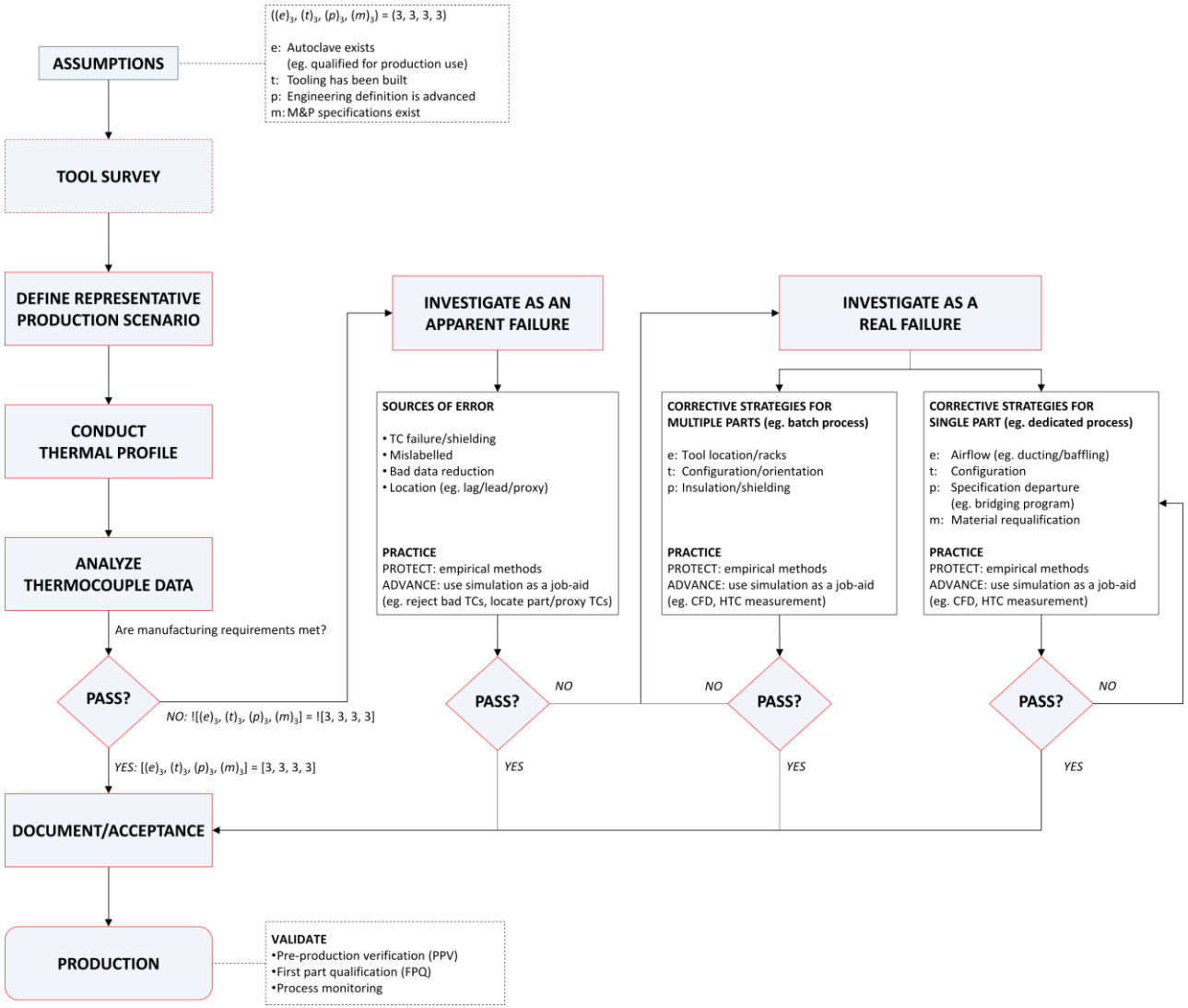

Figure 5-13: Experimental thermal profiling workflow. Troubleshooting apparent and real thermocouple failures. Adapted from Mobuchon and Zobeiry (2014). ETPM: Equipment–Tool–Part–Material; w, x, y, z: design-gate indices; M&P: Material & Process; TC: Thermocouple; CFD: Computational Fluid Dynamics; HTC: Heat Transfer Coefficient.

This final case study demonstrates how science based knowledge, in the form of simulation, can be used to investigate and interpret experimentally measured thermocouple data for a 12.4 mm thick T800H/3900-2 C-shaped laminate. The outcome of this analysis suggests that the experimental temperature data may be indicating a 'false-pass', meaning that the experimental thermal profile may be providing a false confidence in the ability to satisfy process requirements. This is an example of a real failure. Other case studies, presented in Appendix D.2.5 and Appendix D.4.5, show how science based approaches can be used to investigate apparent failures.

5.3.1 ETPM definition

A 12.4 mm thick T800H/3900-2 C-shaped laminate (Part ID: CCM9.2-077) was processed on a male Invar tool in a 'bus stop' or batch process autoclave loading scenario. This part was manufactured as part of CCMRD Project 9.2 (CCM9.2) to investigate and extend the current state of the art in the prediction of dimensional change for autoclave cured laminates [236]. It should be noted that while the parts and tool were extensively instrumented with thermocouples to observe in-plane and through-thickness temperature gradients, this original work was not intended as a thermal management study.

This case study is depicted as a troubleshooting workflow at design state $((e)_2, (t)_2, (p)_2, (m)_3)$ = (2, 2, 2, 3) in the ETPM decision tree shown in Figure 5-14 (a). A solid wavy line indicates that this scenario could be considered as a representative thermal profile for the production scenario at $((e)_3, (t)_3, (p)_3, (m)_3)$ = (3, 3, 3, 3). Refer to Table 4-3 for definitions of the ETPM design-gate indices. ETPM thermal management attributes for this case study are shown in Figure 5-14 (b), with the experimental setup and modelling inputs summarized in Table 5-7.

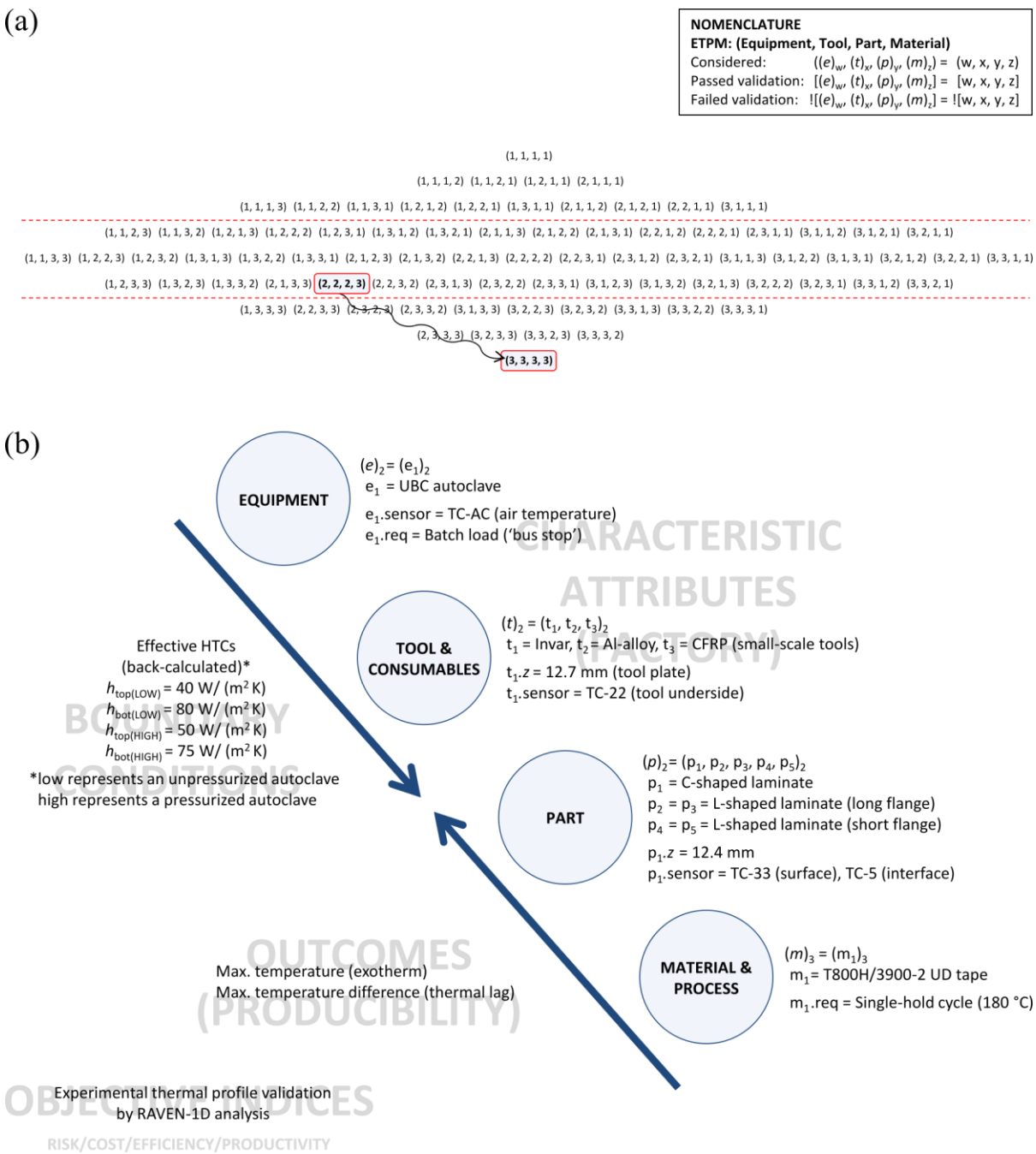

Figure 5-14: Experimental thermal profile validation. This scenario demonstrates the use of manufacturing simulation to investigate a real thermocouple failure in a 12.4 mm thick C-shaped laminate (part ID: CCM9.2-077). This problem is depicted as: (a) troubleshooting workflow at design state (($(e)_2$, $(t)_2$, $(p)_2$, $(m)_3$) = (2, 2, 2, 3) and could be considered as representative production scenario at (($(e)_3$, $(t)_3$, $(p)_3$, $(m)_3$) = (3, 3, 3, 3) and (b) ETPM thermal management attributes. Experimental data from [236] (Arafath *et al*, 2015). ETPM: Equipment–Tool–Part–Material; w, x, y, z: design-gate indices; TC: Thermocouple; req: manufacturing requirement; HTC: Heat Transfer Coefficient; *z*: through-thickness coordinate; UD: Unidirectional. Note: Instances are denoted in lowercase, shorthand notation is denoted in italics. Solid wavy lines indicate that the precise design path is unknown.

Table 5-7: ETPM[a] attribute definition for a 12.4 mm thick C-shaped laminate.

		Test[b]	Analysis[c]
Equipment	**(E)**	Autoclave: UBC TC-AC (air temperature)	$h_{top\ (LOW)}$ = 40 W/ (m^2 K) $h_{top\ (HIGH)}$ = 50 W/ (m^2 K)
Tool	**(T)**	Invar (small-scale tool) z_{tool} = 12.7 mm TC-22 (tool underside)	$h_{bot\ (LOW)}$ = 80 W/ (m^2 K) $h_{bot\ (HIGH)}$ = 75 W/ (m^2 K)
Part	**(P)**	C-shaped laminate (300 mm (web) x 80 mm (flange) x 100 mm) 20 mm (fillet radius) z_{part} = 12.4 mm (64 ply) TC-33 (surface) TC-5 (interface)	RAVEN-1D drill point analysis [238] T33: part/bag (surface) T5: part/tool (interface)
Material	**(M)**	T800H/3900-2 UD tape Single-hold cycle (180 °C)	T800H/3900-2 open lit. material model

[a] ETPM: Equipment–Tool–Part–Material
[b] Experimental data from [236] (Arafath *et al*, 2015), refer to Appendix D.4. Part ID: CCM9.2-077.
[c] Effective HTCs: Low HTC value (unpressurized) back-calculated at t = 30 min. High HTC value (pressurized) back-calculated at 70 min < t < 90 min.

The UBC autoclave used in this case study has been extensively characterized [150]. Modulation of the autoclave air temperature (TC-AC) in this autoclave is caused by the autoclave controller. The Invar tool, with a nominal tool plate thickness z_{tool} = 12.7 mm, belongs to a family of small-scale tools (see Figure D-30 (a)). The C-shaped laminate was cured using a nominal 180 °C single-hold cure cycle. A Toray T800H/3900-2 open literature material model is used where cure kinetics and specific heat capacity models have been characterized. The 3900-2 CK model is a 'model fitted' cure kinetics model, validated within the range of temperatures: 130 °C < T < 230 °C (isothermal), -40 °C < T < 275 °C (dynamic) and 0.2 °C/ min < $\dot{T}$ < 10 °C/ min [144]. Further details about this material model are given in Appendix E.3.

As shown in Figure 5-15, two part TCs (TC33 and TC5) were installed on the edge of the part at the web centre. An insulated tool TC (TC22) was installed on the underside tool surface.

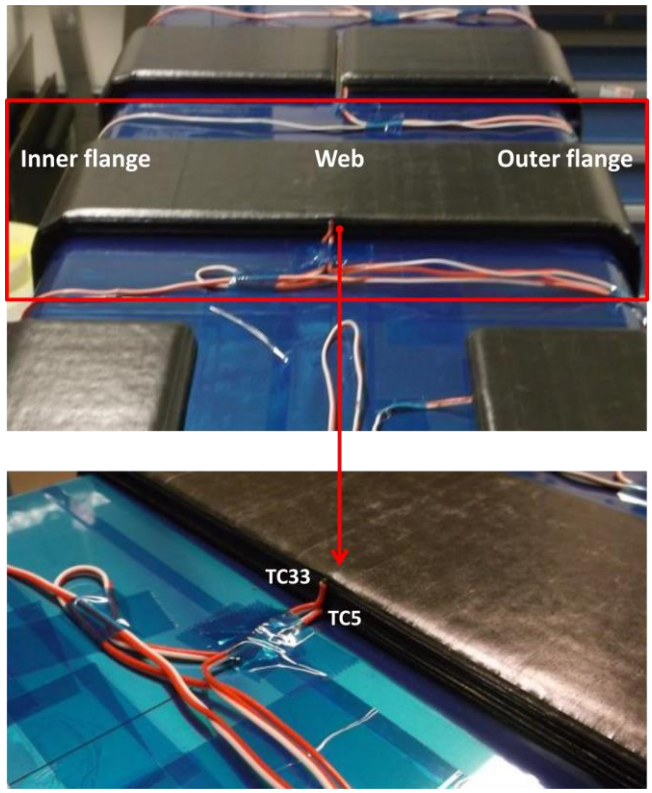

Figure 5-15: Instrumented 12.4 mm thick T800H/3900-2 C-shaped laminate (part ID: CCM9.2-077) prior to bagging (photo courtesy of CCMRD [236]).

5.3.2 Experimental measurements

Temperature profile (T v t) and temperature difference with respect to the autoclave air temperature (ΔT v t) plots of the experimentally measured temperature data are shown in Figure 5-16. It should be noted that the experimental temperature data is from [236] (Arafath *et al*, 2015). The temperature difference plot, based on work by Rasekh *et al* [141,142], shows when parts and tools reach a transient steady-state condition on ramp segments during cure. Thermal lag is denoted as a negative value, where for heat up cure segments $\Delta T = -(T_\infty - T)$ and for cool down cure segments $\Delta T = (T_\infty - T)$. A positive value, or temperature overshoot, is permissible only within the bounds of the specified cure window.

In the idealized case, once parts and tools reach a transient steady-state condition, the temperature difference remains constant (see Figure D-27 (b) for example). However, in practice, the autoclave heat transfer can change during cure (eg. [101,148,178]). This can be indicated as a perturbation or decrease/increase in the thermal lag in the temperature difference plot. For instance, a reduction in the temperature difference during heat up may occur due to: 1) decreasing gas density due to increasing temperature; 2) increasing gas density due to autoclave pressurization or the effect of pressurizing the autoclave while heating; and 3) the response of the autoclave airflow system to changes in gas density (eg. autoclave fan speed).

For this experiment, a reduction in thermal lag is observed in the experimental temperature profiles at the part surface (TC33), part/tool interface (TC5) and tool underside surface (TC22) during heat up segment of the cure cycle at point A (see Figure 5-16 (b)). This change appears to correspond with autoclave pressurization at approximately t = 30 min. Part T33 and TC5 respond to this change with a reduction in thermal lag of 2.9 °C and 2.6 °C, respectively. While tool TC22 appears insensitive to this effect, given a change in temperature difference that is within the typical limits of themocouple accuracy. Once the transient steady-state condition is reached at t = 50 min, and given the overall mass of the Invar tool, the temperature difference between part TC33 and tool TC22 is about 6.2 °C. These plots also show that no exotherm is observed on the 180 °C hold (see Figure 5-16 (a)).

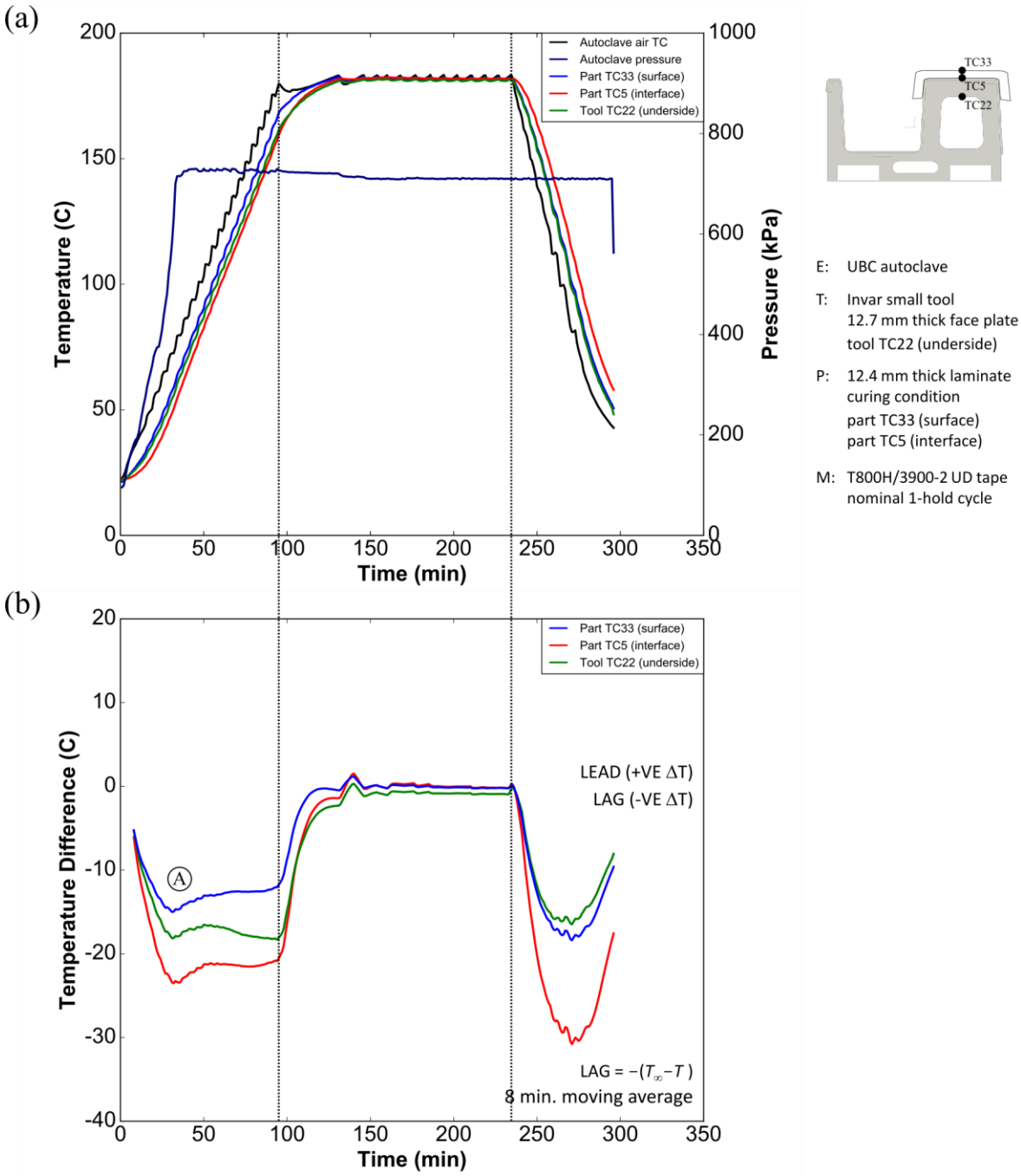

Figure 5-16: Experimentally measured results for a 12.4 mm thick C-shaped laminate (part ID: CCM9.2-077) comparing thermocouples located at the part surface (TC33), part/tool interface (TC5) and tool underside surface (TC22): (a) temperature profile (*T* v *t*) and (b) temperature difference with respect to the autoclave air temperature (Δ*T* v *t*). Experimental data from [236] (Arafath *et al*, 2015). ETPM: Equipment–Tool–Part–Material; TC: Thermocouple; UD: Unidirectional. Note: Reduction in temperature difference observed (> 1.5 °C TC limit of error at the part surface and part/tool interface) at approximately *t* = 30 min at point A due to autoclave pressurization. Vertical lines indicate heat up, hold and cool down cure cycle segments.

5.3.3 Thermal profile validation

An initial RAVEN-1D drill point analysis is performed to validate the experimental temperature data. This analysis assumes a nominal laminate thickness of z_{part} = 12.4 mm and tool thickness z_{tool} = 12.7 mm. Two cases are run to investigate the effect of low and high heat transfer due to autoclave pressurization during heat up. The measured autoclave air temperature profile and back-calculated effective heat transfer coefficients are used as boundary condition inputs. For the unpressurized case, effective heat transfer coefficients are back-calculated from t = 30 min, with $h_{\text{top (LOW)}}$ = 40 W/ (m^2 K) and $h_{\text{bot (LOW)}}$ = 80 W/ (m^2 K). For the pressurized case, effective heat transfer coefficients are back-calculated from 70 min < t < 90 min, with $h_{\text{top (HIGH)}}$ = 50 W/ (m^2 K) and $h_{\text{bot (HIGH)}}$ = 75 W/ (m^2 K). These values were computed using the method described in Appendix F.2 based on tool TC22. The results are shown in Figure 5-17.

Two observations can be made in comparing the experimentally measured and predicted modelling results. The RAVEN-1D model: 1) overpredicts the thermal lag at the part surface (T33) during the heat up segment of the cure cycle at t = 50 min (point A) for the unpressurized case. This result is expected since the model is not able to account for the change in autoclave heat transfer. The thermal lag at T33 is reasonably predicted for the pressurized case. The prediction at the part/tool interface (T5) appears insensitive to this effect, with no apparent differences in the unpressurized and pressurized model predictions and excellent agreement to the experimental data; and 2) predicts an observable exotherm at t = 130 min (point B) for both unpressurized and pressurized cases, with the predicted peak temperature at T33 exceeding typical process requirements (typically ± 5 °C on hold segments). This second observation is inconsistent with the experimentally measured results.

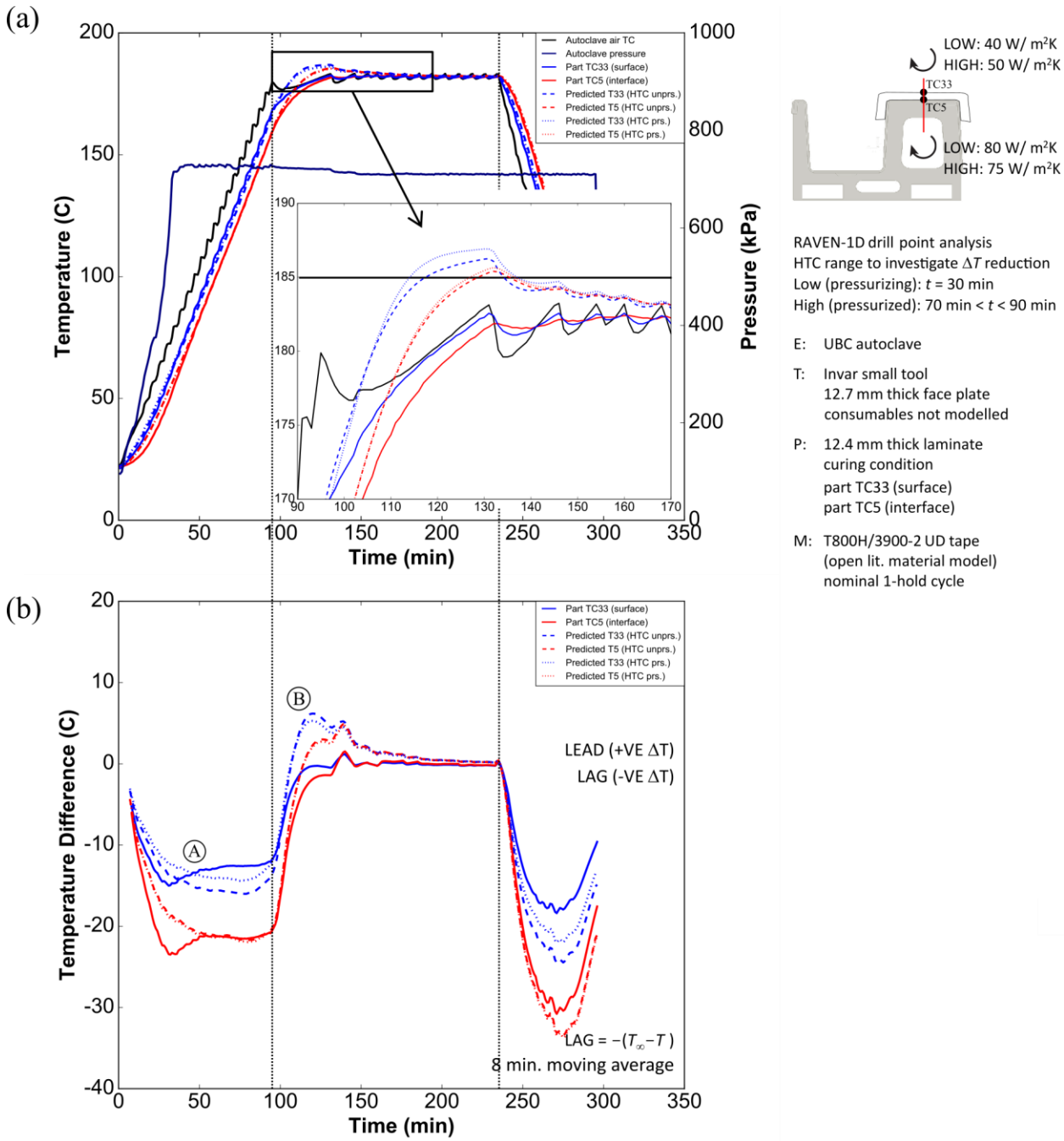

Figure 5-17: Experimentally measured and predicted RAVEN-1D modelling results for a 12.4 mm thick C-shaped laminate (part ID: CCM9.2-077). The effect of low and high heat transfer due to autoclave pressurization (low HTC back-calculated at t = 30 min and high HTC back-calculated at 70 < t < 90 min): (a) temperature profile (T v t) and (b) temperature difference with respect to the autoclave air temperature (ΔT v t). Experimental data from [236] (Arafath *et al*, 2015). ETPM: Equipment–Tool–Part–Material; HTC: Heat Transfer Coefficient; TC: Thermocouple; UD: Unidirectional. Note: Temperature difference overpredicted at the part surface at point A (> 1.5 °C TC limit of error at the part surface for the low HTC case) and temperature overshoot predicted at point B. Vertical lines indicate heat up, hold and cool down cure cycle segments.

One possible explanation for this discrepancy is that the RAVEN-1D model is not able to account for in-plane heat flow effects, such as edge and tool size effects. Complementary modelling work performed by Park [178], and presented in Appendix D.4.6, confirms this hypothesis, with the COMPRO-3D model showing excellent agreement with the experimental temperature data. However, interrogation of this model also suggests that 1D heat flow in the thickness direction is not achieved, as one might expect or as is typically assumed. This indicates that, relative to the tool, the part is not sufficiently wide enough to eliminate any edge effects. These effects are discussed further in Appendix D.5.6.

While the results of the thermal profile for this experiment have been validated by COMPRO-3D analysis (eg. $[(e)_2, (t)_2, (p)_2, (m)_3] = [2, 2, 2, 3]$), consider the scenario where this experimental data had been intended as a representative thermal profile for a production scale part (eg. $((e)_3, (t)_3, (p)_3, (m)_3) = (3, 3, 3, 3)$). As a proxy, this experimental thermal profile is presenting a 'false pass'. In other words, this representative part is not correctly capturing the intended processing physics. Thus, the experimentally measured data is giving a false indication with regard to satisfying the process specifications. If this representative part had been suitably sized to enable the recovery of 1D heat flow in the thickness direction, then the RAVEN-1D analysis shown in Figure 5-17 would more accurately represent the experiment. As previously discussed, this model predicts a peak exotherm temperature that would result in the failure to meet process requirements. This is an example of a real failure (eg. $![(e)_2, (t)_2, (p)_2, (m)_3] = ![2, 2, 2, 3]$).

Achieving high confidence in the results of an experimental thermal profile is a key factor in deciding whether to perform an experimental thermal profile on representative parts versus production scale parts. Mistakes at this late stage in the development design cycle are costly, such as having to scrap parts that fail to meet process specifications or make modifications to the manufacturing process. As this case study highlights, manufacturing simulation can be used to assess whether to perform an experimental thermal profile on a representative part, or whether one should consider the thermal profiling of parts based on the actual build to ensure that the intended processing physics is captured.

5.3.4 Summary

RAVEN-1D and COMPRO-3D models were used to validate the results of an experimental thermal profile performed on a 12.4 mm thick C-shaped laminate. This study showed that the RAVEN-1D analysis was not able to account for in-plane heat flow effects, and thus overpredicted the peak exotherm on the 180 °C hold. On the other hand, the COMPRO-3D model showed excellent agreement with the experimental temperature data, and thus validated the results (eg. $[(e)_2, (t)_2, (p)_2, (m)_3] = [2, 2, 2, 3]$). Interrogation of this model showed that the part was not sufficiently sized to eliminate edge effects. As a representative thermal profile of a production part (eg. $((e)_3, (t)_3, (p)_3, (m)_3) = (3, 3, 3, 3)$), this experimental data presenting a ‘false pass’, or a false confidence in the ability to satisfy the process requirements. Based on the RAVEN-1D results presented, had a more representative part been used, it is likely that the experimental thermal profile would have resulted in a real failure (eg. $![(e)_3, (t)_3, (p)_3, (m)_3] = ![3, 3, 3, 3]$).

Guidelines for the placement of part thermocouples and for defining representative parts for thermal profiling should consider both edge and tool size scaling effects. Preliminary science based guidance for the placement of part thermocouples is given in Appendix D.2.5 and Appendix D.5.6. Further investigation is suggested as future work.

5.4 Summary and Discussion

Three case studies were presented in this chapter to demonstrate the use of the ETPM factory ontology and the composites manufacturing science base for the thermal management of thick thermoset composites.

The first case study focused on gaining confidence in using manufacturing science, exercised in simulation software. The key sources of modelling uncertainty were identified based on the accepted classification of modelling uncertainty and error defined by Oberkampf *et al* [184,185] (see Table 5-3). Strategies to develop an 'evidence of credibility' in simulation, such as uncertainty quanitification and model validation were briefly discussed. Selected modelling uncertainties were presented, in terms of the main components of the thermochemical model, to demonstrate that a high confidence in the predicted modelling results can be achieved provided the appropriate material model and heat transfer boundary condition inputs are applied to the thermal model.

The remaining two case studies showed the systematic use of the ETPM factory ontology and manufacturing simulation to enable the effective management of manufacturing risk in industrially relevant production scenarios. The second case study showed the use of manufacturing simulation, in terms of a development workflow relating to material qualification, for the evauation and recommendation of a suitable cure cycle for a part of intermediate complexity. This case study showed that it is possible to use manufacturing simulation *before* significant costs are committed in the early stages of the development design cycle. The final case study demonstrated the use of manufacturing simulation, in terms of a troubleshooting workflow typically performed as part of structural certification, to validate the results of an experimental thermal profile. This case study highlighted how manufacturing simulation can be used to identify and *prevent* costly mistakes, such as incorrectly interpreting the results of an experimental thermal profile. Science based approaches for investigating apparent and real thermocouple failures and locating part thermocouples were discussed.

These case studies represent a starting point for formalizing science based practices as standard workflows in composites manufacturing to reduce risk, cost, and development time frames.

Chapter 6: Summary and Future Work

In this thesis, a framework for formalizing science based composites manufacturing practice has been developed. Its focus is to encourage the systematic *use* of composites manufacturing science to transform manufacturing practice, and to support the effective management of increasing manufacturing risk. This work is aimed at both the composites manufacturing research community (knowledge translation) and the composites industry (transforming practice).

In the following sections, a summary and main contributions of this work are presented, as well as potential areas for future work.

6.1 Summary

Composites manufacturing is a form of 'process-driven innovation', or low modularity and low maturity technology, given that product and process innovations are highly coupled and the manufacturing strategy pursued detrimentally affects the ability to innovate. Composites manufacturers are likely to experience high technological and market uncertainty in seeking to bring innovative products to market. The current typical practices for managing composites manufacturing risk, based on a 'building block' approach, were discussed in Chapter 3. These empirical practices represent high risk since part producibility is often considered after significant program costs have been committed. Producibility is often neglected in the earlier stages of the development design cycle (eg. conceptual design) due to a lack of validated DFM tools for manufacturing.

The direct observation of an aerospace OEM and qualitative case based analysis of two industrial SMEs based in Western Canada who chose to work with a CTRC was performed. This work, drawn on extant innovation mangagement literature, investigated the challenges and successes in using manufacturing science to manage technological and market uncertainty and enable potential market opportunities. For the two industrial SME case studies selected for analysis, the factors contributing to the success of the SME included: 1) the customer utility for composites end products; 2) the freedom to influence both product and process innovation; and 3) intellectual property (IP) protection. The use of composites manufacturing science successfully addressed technological uncertainty in both cases, with SME #1 achieving a 50% reduction in the scrap rate of their products, and SME #2 doubling their production capacity with minimal capital investment or impact to product quality and performance. However, these cases also highlighted mixed outcomes in terms of managing market uncertainty and contributing to the success of the SME, and the regional innovation ecosystem in Western Canada.

It is important to consider that the receptor capabilities for composites OEMs and SMEs are different in terms of R&D resources and funding, and experience. Large composites manufacturers recognize the value of using manufacturing science to manage uncertainty and have the in-house expertise to use this knowledge effectively. Yet key barriers for its widespread adoption exist. The perception is that composites manufacturing science is still a niche discipline, and the enabling DFM tools that are available are too complex for non-experts to use quickly and effectively. For composites SMEs, the additional challenges for applying science based practice are: 1) knowing that the manufacturing science exists; 2) having the receptor capacity to be able to access this knowledge; and 3) accepting and managing the uncertainty involved in such innovations.

A framework for formalizing science based composites manufacturing practice, as shown in Figure 6-1, was introduced in Chapter 4. This proposed approach is called *Knowledge in Practice*. The main conceptual elements of this framework include:

- *Outcomes taxonomy* is an extension of prior work to capture imperfect composites manufacturing knowledge using defect taxonomies. A simulation based approach was used to establish a consistent linkage between the *science–technology–practice* levels of activity (see Figure 6-1 (a)). Manufacturing outcomes, considered in terms of the range of response in the part of interest at a given material point, are grouped by theme (the key phases of the manufacturing cycle), material equivalency (transformations of the material) and outcome type (*process–structure–performance* relationships). A preliminary outcomes taxonomy for composites processing was presented.

- *ETPM factory ontology* is a hierarchical knowledge model that is used to represent manufacturing problems in terms of building up the factory and the acceptable quality of parts as they move through the factory. This ontology can be used to organize composites manufacturing domain knowledge, and to support the use of manufacturing science to manage increasing manufacturing risk at *all* stages of the development design cycle. The entire manufacturing design space is represented by 81 unique ETPM design states (see Figure 6-1 (b)). Five high-level thermal management manufacturing scenarios were presented to highlight the value of formalizing science based practice. These case studies exercised several capabilities of this developed framework, including the ability to capture: development and troubleshooting workflows, sequential and concurrent design steps, and inadmissible ETPM design states.

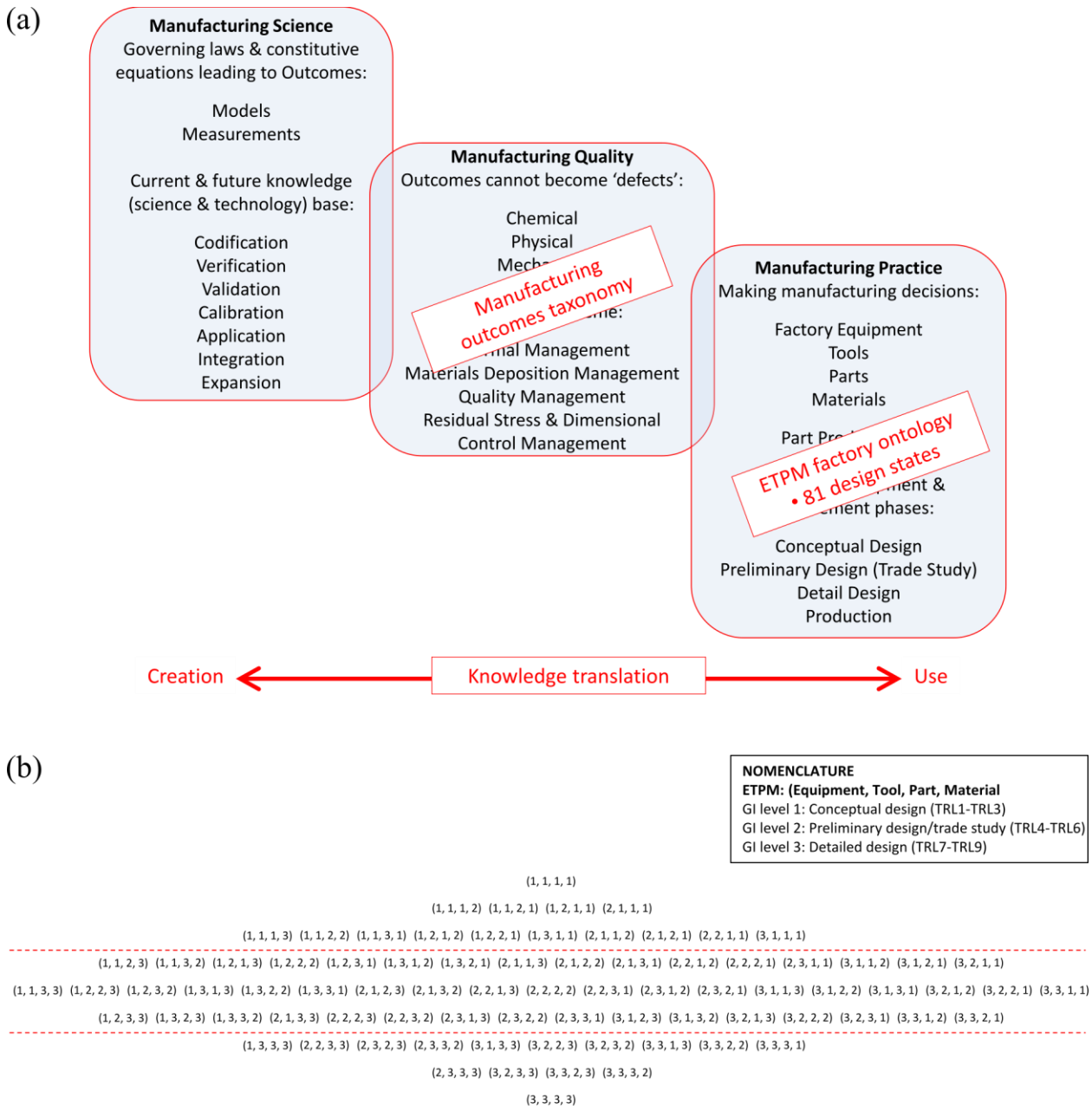

Figure 6-1: A framework for formalizing science based composites manufacturing practice was introduced in this work to support the effective management of increasing manufacturing risk. The developed framework includes: (a) a manufacturing outcomes taxonomy to systematically link the *science–technology–practice* levels of activity and ETPM factory ontology to organize composites manufacturing domain knowledge and (b) ETPM decision tree that represents *all* stages of the development design cycle (the entire manufacturing design space). ETPM: Equipment–Tool–Part–Material; GI: Design-gate index; TRL: Technology Readiness Level.

Thermal management case studies were presented in Chapter 5 to demonstrate the use of the developed framework and the composites manufacturing science base. These case studies were developed based on the thermal analysis of five thick thermoset composites data sets given that the science base for thermal management problems is relatively mature. The data sets selected for analysis represent real production scenarios and a range of ETPM thermal management attributes, including: autoclave airflow characteristics, tooling materials and substructure complexity, part complexity and thickness, and material systems and the fidelity of the material models available for thermal modelling.

The first case study outlined an structured approach to establish confidence in the thermal modelling of cure processes, and the use of partially reliable simulation based data (predicted modelling results) and sensor based data (experimentally measured results). The key sources of thermal modelling uncertainty were identified in terms of the accepted classification of modelling uncertainty and error, and the main components of the thermochemical model (see Table 5-3). Selected thermal modelling uncertainties relating to: 1) the complexity of solution method (conduction heat transfer model); 2) understanding the thermal behaviours of material systems and their derivatives (cure kinetics model); and effective heat transfer coefficient validation (convective boundary conditions) were presented. These examples showed that a high confidence in the model predictions can be achieved provided the appropriate material model and heat transfer boundary condition inputs are applied to the thermal model.

The second case study showed the use of manufacturing simulation for the evaluation and recommendation of a suitable cure cycle for a 28.2 mm thick AS4/8552 panel with tapered core (eg. $((e)_1, (t)_1, (p)_1, (m)_2) = (1, 1, 1, 2)$). RAVEN-1D thermal models were used to rapidly iterate and systematically evaluate cure cycles for three processing scenarios (see Table 5-6). Based on this analysis, a 3-hold cure cycle was recommended for manufacturing trials (eg. $((e)_2, (t)_2, (p)_2, (m)_2) = (2, 2, 2, 2)$). This case study showed that it is possible to systematically evaluate manufacturing concepts using manufacturing simulation *before* significant costs are committed in the early stages of the development design cycle.

The final case study demonstrated the use of manufacturing simulation to validate the results of an experimental thermal profile for a 12.4 mm thick T800H/3900-2 C-shaped laminate (eg. $((e)_2, (t)_2, (p)_2, (m)_3) = (2, 2, 2, 3)$). The predicted RAVEN-1D modelling results showed that the experimental data was presenting a ‘false pass’ or a false confidence in satisfying the process specifications. As a representative thermal profile of a production part, this experimental data that would have otherwise indicated in a real failure (eg. $![(e)_3, (t)_3, (p)_3, (m)_3] = ![3, 3, 3, 3]$). This case study highlighted how manufacturing simulation can be used to identify and *prevent* costly mistakes, such as incorrectly interpreting the results of an experimental thermal profile.

The thermal management manufacturing scenrios and case studies presented in this work represent a starting point for developing standard composites manufacturing science based workflows.

6.2 Contributions

The main contributions of this work are briefly summarized as:

- Investigation of the use of manufacturing science by large and small composites manufacturers to reduce technological uncertainty and enable potential market opportunities, and how the needs and receptor capabilities of OEMs and SMEs differ.

- Development of an outcomes taxonomy to classify manufacturing outcomes based on a science based understanding and simulation based thinking, and to systematically link the *science–technology–practice* levels of activity.

- Outline the steps for formalizing science based practice, including the determinants of knowledge translation and the transformation manufacturing practice.

- Development of the ETPM factory ontology to organize composites manufacturing domain knowledge, and to enable the effective management of increasing manufacturing risk. The entire manufacturing design space is represented with 81 unique ETPM design states. Scratchpad tools, such as the ETPM decision tree and attribute canvas, can be used to systematically capture and evaluate manufacturing scenarios using simulation based thinking.

- Thermal analysis of five thick thermoset composites data sets that represent real production scenarios. This work involved the preliminary material characterization of the Hexcel AS4/8552-1 material system, and the back-calculation of effective heat transfer coefficient values for RAVEN-1D and COMPRO-3D thermal models.

- Demonstration of the systematic *use* of the ETPM factory ontology and composites manufacturing science base. This work represents a starting point for developing standard thermal management workflows, such as cure cycle development and evaluation, and experimental thermal profile validation and troubleshooting.

6.3 Future Work

Some areas of future work are proposed in terms of the developed framework and the data sets analyzed for the thermal management case studies presented in this thesis.

6.3.1 Developed framework

- **Application to composites manufacturing problems where the science base is less mature.** The ETPM factory onotology has been exercised with case study examples for thermal management, where the science base is relatively mature. The generality and robustness of this proposed ontology should be investigated. A first step would be to develop case study examples with manufacturing problems relating to wrinkling and porosity management.

- **Development of hierarchical ETPM subclass taxonomies.** The description of the design-gate index in this work is very basic. It might be useful to visualize ETPM class characteristic attributes using subclass taxonomies to philosophically resolve what it means to mature from GI level 1 to level 3. These taxonomies could then be used to systematically evaluate changes made to the factory system, and the associated design penalties, within a subclass versus across a subclass.

- **Incorporation of outcomes for composites assembly and repair.** The development of the outcomes taxonomy in this research focused on manufacturing outcomes for composites processing, it might be useful to extend this proposed approach to capture manufacturing outcomes relating to composites assembly and in-service repair.

- **Development of enabling assessment tools for efficient exploration of the composites manufacturing design space.** The development of the manufacturing technology base, such as ICME, the use of MDO and Bayesian approaches to assess manufacturing risk, and cost models for composites manufacturing, was beyond the scope of this work. However, the ETPM factory ontology could be used to prompt further development of these tools. Integration of this technology base could be accomplished using the objective indices, such as the risk index and effective cost metric. This should be investigated.

- **Development of practice document guidelines for documenting and maintaining science based practices.** Topics for thermal management *Knowledge in Practice Documents* (KPDs) were proposed in Appendix C. Guidelines for overseeing the creation these documents would enhance the quality of the content created and the processes by which they are appraised and maintained. The development of a standard format is needed to facilitate the delivery these documents for improved decision making. It might be worthwhile to understand the lessons learned in the health sciences domain in relation to the set of standards proposed for the development of clinical practice guidelines and the challenges associated with their implementation.

- **Implementation of an online knowledge management and decision support tool.** The development of an online KPD repository and decision support system, based on the implementation of the ETPM factory ontology, is the subject of future work. This tool is called the *Knowledge in Practice Centre* (KPC).

- **Investigation of the use of the ETPM factory ontology for other advanced manufacturing disciplines.** The composites manufacturing scenarios presented in this work highlighted the typical sequence of design steps pursued for 'process-driven innovation' (low modularity, low maturity). Future work should consider the new product development approach typically pursued for other advanced manufacturing technologies defined by Pisano and Shih [49] as: 'process-embedded innovation' (low modularity, high maturity), 'pure process innovation' (high modularity, low maturity), and 'pure product innovation' (high modularity, high maturity) (see Figure 4-13).

6.3.2 Thermal management data sets

- **Increasing the sophistication of 3D thermal models.** The tool substructure was not explicitly modelled in the 3D thermal analysis work presented in this thesis. The details of the tool, other than the tool material and tool plate thickness, were unknown for many of the data sets analyzed. Future work should investigate the trade-off in model complexity, with the inclusion of tool substructure and consumables, versus the results obtained from 1D and simple 3D thermal models.

- **Development of data and model fitting protocols to upgrade existing cure kinetics models.** Based on the analysis work performed it is recommended that the Toray 3900-2 open literature CK model, characterized by Dykeman [144], be upgraded. A suggested approach is to refit the original DSC data gathered to a 'semi model-free' cure kinetics model. The Hexcel 8552-1 preliminary CK model, characterized in this work, should also be validated to ensure that it is 'fit for general purpose'.

- **Investigation of resin and composite thermal conductivity development in the pre-gelation phase of processing.** Although it is accepted that resin thermal conductivity is a function of the degree of cure, temperature and volume fraction, the insights obtained from the data sets analyzed suggests that prior work should be reinvestigated to examine thermal conductivity sensitivities during pre-gelation, and to determine whether improved thermal conductivity models are needed (refer to Appendix D.5.5).

- **Further investigation of practical methods to determine heat transfer coefficients.** Boundary conditions are considered the greatest source of uncertainty in thermal modelling. Practical methods to determine heat transfer coefficients *a priori* are still needed, including the effect of contact resistances during processing, such as bag leaks or parts lifting off tools.

- **Determination of experimental discriminator tests for path dependent effects.** Increased understanding of cure path dependent effects, such as phase separation in multiple phase material systems, would result in improved practices for the material qualification of new materials systems and the modification of existing composites manufacturing process requirements. This should be investigated to improve the cure cycle development and evaluation thermal management workflow outlined in this thesis (see Figure 5-6).

- **Further investigation of thermal edge and tool size effects.** Based on the workflow presented for experimental thermal profile validation (see Figure 5-13), and in extending the preliminary 2D heat transfer work by Rasekh [142] and Zobeiry (2017), the development of science based guidelines for the placement of part thermocouples, and the selection of representative parts and tools for experimental thermal profiling should be pursued (refer to Appendix D.2.5 and Appendix D.5.6).

References

[1] JEC, "The global market for PAN-based carbon fibre," *JEC Composites Magazine*,pp. 18–19, Dec-2007.

[2] S.-J. Park, *Carbon Fibers*, vol. 210. Dordrecht: Springer Netherlands, 2015.

[3] S. Das, J. Warren, D. West, and S. M. Schexnayder, "Global Carbon Fiber Composites Supply Chain Competitiveness Analysis. Report No. ORNL/SR-2016/100 - NREL/TP-6A50-66071," Clean Energy Manufacturing Analysis Center, Golden, CO, 2016.

[4] E. Witten, M. Sauer, and M. Kuhnel, "Composites Market Report 2017: Market developments, trends, outlook and challenges," AVK & CCeV, 2017.

[5] S. Mazumdar, D. Karthikeyan, D. Pichler, M. Benevento, and R. Frassine, "2017 State of the Industry Report: A look at five key areas in the composites industry," *Composites Manufacturing*, vol. 33, no. 1, Arlington, VA, pp. 22–27, 2017.

[6] S. Mazumdar, M. Benevento, D. Pichler, J. Hinirchsen, and E. Witten, "2018 State of the Industry Report: A global outlook at materials and markets for composites," *Composites Manufacturing*, vol. 34, no. 1, pp. 18–23, 2018.

[7] "Boeing 787 Dreamliner." Available: http://www.boeing.com/commercial/787/. [Accessed: 04-Apr-2017].

[8] "Boeing 777X." Available: http://www.boeing.com/commercial/777x/. [Accessed: 04-Apr-2017].

[9] "Airbus A350 XWB." Available: http://www.a350xwb.com/. [Accessed: 04-Apr-2017].

[10] "Bombardier CSeries." Available: http://commercialaircraft.bombardier.com/en/cseries.html. [Accessed: 04-Apr-2017].

[11] ProQuest, "Products & Services - The Summon Service." Available: http://www.proquest.com/products-services/The-Summon-Service.html. [Accessed: 06-Feb-2018].

[12] L. B. Ilcewicz, "Scaling crucial to integrated product development of composite aerospace structures. Part 1," *Composites Part A: Applied Science and Manufacturing*, vol. 30, no. 3, pp. 385–393, 1999.

[13] L. B. Ilcewicz, D. J. Hoffman, and A. J. Fawcett, "Composite Applications in Commercial Airframe Structures," in *Comprehensive Composite Materials*, A. Kelly and C. Zweben, Eds. Elsevier Science Ltd., 2000, pp. 87–119.

[14] L. Ilcewicz and C. Ashforth, "Scaling Crucial to Integrated Product Development of Composite Airframe Stuctures," in *Comprehensive Composite Materials II*, Vol. 3., A. Poursartip, Ed. Elsevier Science Ltd., 2018, pp. 26–90.

[15] F. Phillips and R. Srivastava, "Committed Costs vs. Uncertainty in New Product Development. Working Paper WP-1993-02-01," 1993.

[16] NDIA Manufacturing Division Whitepaper, "21st Century Manufacturing Modeling & Simulation Research and Investment Needs," 2011. Available: http://www.ndia.org/Divisions/Divisions/Manufacturing/Documents/NDIAAMECMS.pdf. [Accessed: 11-Jan-2014].

[17] M. Sullivan, “Best Practices: DOD Can Achieve Better Outcomes by Standardizing the Way Manufacturing Risks Are Managed. Report No. GAO-10-439,” Government Accountability Office, Washington, D.C., 2010.

[18] T. Storage, Private Communication. AFRL, 2006.

[19] D. J. Roughley, “Industry and Market Analysis: 2012 Survey,” Composites Research Network, Vancouver, Canada, 2013.

[20] E. Maine and E. Garnsey, “Commercializing generic technology: The case of advanced materials ventures,” *Research Policy*, vol. 35, no. 3, pp. 375–393, 2006.

[21] C. S. Tang and J. D. Zimmerman, “Managing New Product Development and Supply Chain Risks: The Boeing 787 Case,” *Supply Chain Forum*, vol. 10, no. 2, pp. 74–86, 2009.

[22] Boeing 787-8 CSRT Team, “Boeing 787-8 Design, Certification, and Manufacturing Systems Review. Report prepared for the FAA,” 2014. Available: http://www.faa.gov/about/plans_reports/media/787_report_final.pdf. [Accessed: 18-May-2014].

[23] R. Slayton and G. Spinardi, “Radical innovation in scaling up: Boeing’s Dreamliner and the challenge of socio-technical transitions,” *Technovation*, vol. 47, pp. 47–58, 2015.

[24] Composites Research Network, “SME Project Summaries.” Available: http://crn.ubc.ca/. [Accessed: 02-Oct-2016].

[25] L. Berglund and J. Kenny, “Processing Science for High Performance Thermoset Composites,” *SAMPE Journal*, vol. 27, no. 2, pp. 27–37, 1991.

[26] D. Hunston, W. McDonough, B. Fanconi, F. Mopsik, F. Wang, F. Phelan, and M. Chiang, “Assessment of the State-Of-The-Art for Process Monitoring Sensors for Polymer Composites. Report No. NISTIR 4514,” National Institute of Standards and Technology, Washington, D.C., 1991.

[27] A. Mallow and F. Campbell, “Autoclave Processing,” in *Processing of Composites*, R. S. Dave and A. C. Loos, Eds. Munich, Germany: Hanser Publishers, 2000, pp. 293–316.

[28] P. Hubert, G. Fernlund, and A. Poursartip, “Autoclave processing for composites,” in *Manufacturing Techniques for Polymer Matrix Composites*, S. G. Advani and K.-T. Hsiao, Eds. Cambridge, UK: Woodhead Publishing, 2012, pp. 414–434.

[29] G. Fernlund, C. Mobuchon, and N. Zobeiry, “Autoclave Processing,” in *Comprehensive Composite Materials II*, Vol 2., R. Talreja, Ed. Elsevier Science Ltd., 2018, pp. 42–62.

[30] D. H.-J. A. Lukaszewicz, C. Ward, and K. D. Potter, “The engineering aspects of automated prepreg layup: History, present and future,” *Composites Part B: Engineering*, vol. 43, no. 3, pp. 997–1009, 2012.

[31] P. Boisse, N. Hamila, and A. Madeo, “Analysis of Defect Development in Composite Forming,” in *The Structural Integrity of Carbon Fiber Composites*, P. W. R. Beaumont and C. Soutis, Eds. Cham, Switzerland: Springer International Publishing, 2017, pp. 319–337.

[32] P. Simacek and S. G. Advani, “Desirable features in mold filling simulations for liquid composite molding processes,” *Polymer Composites*, vol. 25, no. 4, pp. 355–367, Aug. 2004.

[33] F. Trochu, E. Ruiz, V. Achim, and S. Soukane, “Advanced numerical simulation of liquid composite molding for process analysis and optimization,” *Composites Part A: Applied Science and Manufacturing*, vol. 37, no. 6, pp. 890–902, Jun. 2006.

[34] S. G. Advani and P. Simacek, “Liquid Composite Molding: Role of Modeling and Simulation in Process Advancement,” in *Proceedings of ICCM-20 Conference*, 2015, p. 12.

[35] T. Centea, L. K. Grunenfelder, and S. R. Nutt, “A review of out-of-autoclave prepregs – Material properties, process phenomena, and manufacturing considerations,” *Composites Part A: Applied Science and Manufacturing*, vol. 70, pp. 132–154, 2014.

[36] N. Zobeiry and A. Poursartip, “The origins of residual stress and its evaluation in composite materials,” in *Structural Integrity and Durability of Advanced Composites*, Elsevier, 2015, pp. 43–72.

[37] N. Zobeiry, A. Forghani, C. Li, K. Gordnian, R. Thorpe, R. Vaziri, G. Fernlund, and A. Poursartip, “Multiscale characterization and representation of composite materials during processing,” *Philosophical Transactions of the Royal Society of London A: Mathematical, Physical and Engineering Sciences*, vol. 374, no. 2071, 2016.

[38] I. Baran, K. Cinar, N. Ersoy, R. Akkerman, and J. H. Hattel, “A Review on the Mechanical Modeling of Composite Manufacturing Processes,” *Archives of Computational Methods in Engineering*, vol. 24, no. 2, pp. 365–395, 2017.

[39] M. F. Ashby, *Material Selection in Mechanical Design*, 4th ed. Oxford, UK: Elsevier Ltd., 2011.

[40] “Composites Research Network (CRN).” Available: http://crn.ubc.ca/. [Accessed: 31-May-2017].

[41] “Institute for Advanced Composites Manufacturing Innovation (IACMI).” Available: http://iacmi.org/. [Accessed: 31-May-2017].

[42] “National Composites Centre (NCC).” Available: http://nccuk.com/. [Accessed: 31-May-2017].

[43] “Fraunhofer Institute for Chemical Technology (ICT).” Available: https://www.ict.fraunhofer.de/en.html. [Accessed: 31-May-2017].

[44] G. Pisano, “The evolution of science-based business: innovating how we innovate,” *Industrial and Corporate Change*, vol. 19, no. 2, pp. 465–482, 2010.

[45] E. Maine, S. Lubik, and E. Garnsey, “Process-based vs. product-based innovation: Value creation by nanotech ventures,” *Technovation*, vol. 32, no. 3, pp. 179–192, 2012.

[46] E. Maine and P. Seegopaul, “Accelerating advanced-materials commercialization,” *Nature Materials*, vol. 15, no. 5, pp. 487–491, 2016.

[47] R. Harms, Y. Marinakis, and S. T. Walsh, “Lean startup for materials ventures and other science-based ventures: under what conditions is it useful?,” *Translational Materials Research*, vol. 2, p. 035001, 2015.

[48] A. P. Chatzimichali and K. D. Potter, “From composite material technologies to composite products: a cross-sectorial reflection on technology transitions and production capability,” *Translational Materials Research*, vol. 2, p. 026001, 2015.

[49] G. Pisano and W. Shih, “Does America really need manufacturing?,” *Harvard Business Review*, vol. 90, no. 3, pp. 94–102, Mar. 2012.

[50] W. Shih and M. Piersen, “Modularity in Design and Manufacturing: Application to Commercial Aircraft. Case No. 612-035,” Harvard Buisness School Publishing, Boston, MA, 9-612-035, 2012.

[51] E. R. Fuchs, “Global Manufacturing and the Future of Technology,” *Science*, vol. 345, no. 6196, pp. 519–520, 2014.

[52] M. E. Porter, *Competitive advantage: Creating and Sustaining Superior Performance*. New York, NY: Free Press, 1985.

[53] T. Jenkins, “Innovation Canada: A Call to Action,” Ottawa, Canada, 2011.

[54] Industry Canada, “The 2009 Survey of Innovation and Business Strategy (SIBS),” Ottawa, Canada, 2011.

[55] L. R. Reif, “A better way to deliver innovation to the world,” *The Washington Post*, 22-May-2015.

[56] H. W. Chesbrough, *Open innovation: The new imperative for creating and profiting from technology*. Boston, MA: Harvard Business Press, 2006.

[57] M. O’Driscoll, “Design for manufacture,” *Journal of Materials Processing Technology*, vol. 122, no. 2–3, pp. 318–321, Mar. 2002.

[58] J. W. Hermann, C. Joyce, S. K. Gupta, C. C. Hayes, K. Ishii, K. David, S. P. A, and W. H. Hood, “New Directions in Design for Manufacturing,” in *ASME 2004 International Design Engineering Technical Conferences and Computers and Information in Engineering Conference*, 2004, pp. 853–861.

[59] I. D. Graham, J. Logan, M. B. Harrison, S. E. Straus, J. Tetroe, W. Caswell, and N. Robinson, “Lost in knowledge translation: Time for a map?,” *Journal of Continuing Education in the Health Professions*, vol. 26, no. 1, pp. 13–24, 2006.

[60] S. E. Straus, J. Tetroe, and I. D. Graham, “Defining knowledge translation,” *Journal of the Canadian Medical Association*, vol. 181, no. 3–4, pp. 165–168, 2009.

[61] B. J. Hicks, S. J. Culley, R. D. Allen, and G. Mullineux, “A framework for the requirements of capturing, storing and reusing information and knowledge in engineering design,” *International Journal of Information Management*, vol. 22, no. 4, pp. 263–280, 2002.

[62] T. R. Gruber, “A translation approach to portable ontology specifications,” *Knowledge Acquisition*, vol. 5, no. 2, pp. 199–220, 1993.

[63] J. M. Wing, “Computational thinking,” *Communications of the ACM*, vol. 49, no. 3. pp. 33–35, 2006.

[64] J. M. Wing, “Computational thinking and thinking about computing,” *Philosophical Transactions of the Royal Society A: Mathematical, Physical and Engineering Sciences*, vol. 366, no. 1881. pp. 3717–3725, 2008.

[65] I. Sim, P. Gorman, R. A. Greenes, R. B. Haynes, B. Kaplan, H. Lehmann, and P. C. Tang, “Clinical Decision Support Systems for the Practice of Evidence-based Medicine,” *Journal of the American Medical Informatics Association*, vol. 8, no. 6, pp. 527–534, 2001.

[66] J. Kung, R. R. Miller, and P. A. Mackowiak, “Failure of Clinical Practice Guidelines to Meet Institute of Medicine Standards,” *Archives of Internal Medicine*, vol. 172, no. 21, pp. 1628–1633, 2012.

[67] B. Succar, “Building information modelling framework: A research and delivery foundation for industry stakeholders,” *Automation in Construction*, vol. 18, no. 3, pp. 357–375, 2009.

[68] J. E. Taylor and P. G. Bernstein, “Paradigm Trajectories of Building Information Modeling Practice in Project Networks,” *Journal of Management in Engineering*, vol. 25, no. 2, pp. 69–76, 2009.

[69] W. J. C. Verhagen and R. Curran, “Ontological Modelling of the Aerospace Composite Manufacturing Domain,” in *Improving Complex Systems Today*, D. D. Frey, S. Fukuda, and G. Rock, Eds. Springer, London, 2011, pp. 215–222.

[70] W. J. C. Verhagen, P. B. Garcia, P. Mariot, J.-P. Cotton, D. Ruiz, R. Redon, and R. Curran, “Knowledge-based cost modelling of composite wing structures,” *International Journal of Computer Integrated Manufacturing*, vol. 25, no. 4–5, pp. 368–383, 2012.

[71] W. J. C. Verhagen, P. Bermell-Garcia, R. E. C. van Dijk, and R. Curran, “A critical review of Knowledge-Based Engineering: An identification of research challenges,” *Advanced Engineering Informatics*, vol. 26, no. 1, pp. 5–15, Jan. 2012.

[72] V. Premkumar, S. Krishnamurty, J. C. Wileden, and I. R. Grosse, “A semantic knowledge management system for laminated composites,” *Advanced Engineering Informatics*, vol. 28, no. 1, pp. 91–101, Jan. 2014.

[73] D. Paul, L. Kelly, V. Venkayya, and T. Hess, “Evolution of U.S. Military Aircraft Structures Technology,” *Journal of Aircraft*, vol. 39, no. 1, pp. 18–29, 2002.

[74] W. Il Lee, A. C. Loos, and G. S. Springer, “Heat of Reaction, Degree of Cure, and Viscosity of Hercules 3501-6 Resin,” *Journal of Composite Materials*, vol. 16, no. 6, pp. 510–520, 1982.

[75] A. C. Loos and G. S. Springer, “Curing of Epoxy Matrix Composites,” *Journal of Composite Materials*, vol. 17, no. 2, pp. 135–169, 1983.

[76] A. Loos and G. Springer, “Calculation of Cure Process Variables During Cure of Graphite/Epoxy Composites,” in *Composite Materials: Quality Assurance and Processing*, no. STP28542S, C. Browning, Ed. West Conshohocken, PA: ASTM International, 1983, pp. 110–118.

[77] J. C. Halpin, J. L. Kardos, and M. P. Dudukovic, “Processing science: an approach for prepreg composite systems,” *Pure and Applied Chemistry*, vol. 55, no. 5, 1983.

[78] R. A. Brand, G. G. Brown, and E. L. McKague, “Processing Science of Epoxy Resin Composites. Report No. AFWAL-TR-83-4124,” Air Force Wright Aeronautical Laboratories, WPAFB, OH, AD-B083 264, 1984.

[79] J. M. Griffith, F. C. Campbell, and A. R. Mallow, “Effect of Tool Design on Autoclave Heat-up Rates,” in *SME Composites in Manufacturing 7 Conference and Exposition*, 1987, p. 14.

[80] F. Campbell, *Manufacturing Processes for Advanced Composites*. Elsevier Ltd., 2004.

[81] A. Maffezzoli, J. Kenny, and L. Nicolais, “Welding of PEEK/carbon fiber composite laminates,” *SAMPE Journal*, vol. 25, pp. 35–40, 1989.

[82] H.-T. Wu and B. Joseph, “Knowledge Based Control of Autoclave Curing of Composites,” *Sampe Journal*, vol. 26, no. 6, pp. 39–54, 1990.

[83] T. A. Bogetti and J. Gillespie, John W., “Cure Simulation of Thick Thermosetting Composites. Report No. ADA224885,” Army Ballistic Research Laboratory, Aberdeen Proving Ground, MD, 1990.

[84] T. A. Bogetti and J. W. Gillespie, “Two-Dimensional Cure Simulation of Thick Thermosetting Composites,” *Journal of Composite Materials*, vol. 25, no. 3, pp. 239–273, 1991.

[85] T. A. Bogetti and J. W. Gillespie, “Process-Induced Stress and Deformation in Thick-Section Thermoset Composite Laminates,” *Journal of Composite Materials*, vol. 26, no. 5, pp. 626–660, 1992.

[86] G. M. Martinez, “Fast cures for thick laminated organic matrix composites,” *Chemical Engineering Science*, vol. 46, no. 2, pp. 439–450, 1991.

[87] S. C. Mantell and G. S. Springer, “Manufacturing Process Models for Thermoplastic Composites,” *Journal of Composite Materials*, vol. 26, no. 16, pp. 2348–2377, Jan. 1992.

[88] P. Ciriscioli, G. Springer, and W. Lee, “An expert system for autoclave curing of composites,” *Journal of Composite*, vol. 25, no. 12, pp. 1542–1587, 1991.

[89] P. R. Ciriscioli, Q. Qiuling Wang, and G. S. Springer, “Autoclave Curing - Comparisons of Model and Test Results,” *Journal of Composite Materials*, vol. 26, no. 1, pp. 90–102, 1992.

[90] T. E. Twardowski, S. E. Lin, and P. H. Geil, “Curing in Thick Composite Laminates: Experiment and Simulation,” *Journal of Composite Materials*, vol. 27, no. 3, pp. 216–250, 1993.

[91] G. D. Smith and A. Poursartip, “A Comparison of Two Resin Flow Models for Laminate Processing,” *Journal of Composite Materials*, vol. 27, no. 17, pp. 1695–1711, 1993.

[92] M. Telikicherla, M. Altan, and F. Lai, “Autoclave curing of thermosetting composites: process modeling for the cure assembly,” *International Communications in Heat and Mass Transfer*, vol. 21, no. 6. pp. 785–797, 1994.

[93] M. Hojjati and S. V. Hoa, “Curing simulation of thick thermosetting composites,” *Composites Manufacturing*, vol. 5, no. 3, pp. 159–169, 1994.

[94] M. Hojjati, “Curing of Thick Thermosetting Composites: Experiment, Simulation, and Scaling. PhD thesis,” Concordia University, 1994.

[95] B. Joseph and F. Hanratty, “Predictive control of quality in a batch manufacturing process using artificial neural network models,” *Industrial & engineering chemistry research*, vol. 32, no. 9, pp. 1951–1961, 1993.

[96] B. Joseph, F. W. Hanratty, and J. L. Kardos, “Model Based Control of Voids and Product Thickness during Autoclave Curing of Carbon/Epoxy Composite Laminates,” *Journal of Composite Materials*, vol. 29, no. 8, pp. 1000–1024, 1995.

[97] C. Kim, H. Teng, C. L. Tucker, and S. R. White, “The Continuous Cuing Process for Thermoset Polymer Composites. Part 1: Modeling and Demonstration,” *Journal of Composite Materials*, vol. 29, no. 9, pp. 1222–1253, 1995.

[98] C. Kim and S. R. White, “The Continuous Curing Process for Thermoset Polymer Composites. Part 2: Experimental Results for a Graphite/Epoxy Laminate,” *Journal of Composite Materials*, vol. 30, no. 5, pp. 627–647, 1996.

[99] A. Johnston, P. Hubert, G. Fernlund, R. Vaziri, and A. Poursartip, "Process Modeling of Composite Structures Employing a Virtual Autoclave Concept," *Science and Engineering of Composite Materials*, vol. 5, no. 3–4, pp. 235–252, 1996.

[100] A. Johnston, "An integrated model of the development of process-induced deformation in autoclave processing of composite structures. PhD thesis," The University of British Columbia, Vancouver, 1997.

[101] A. Johnston, P. Hubert, R. Vaziri, and A. Poursartip, "An Investigation of Autoclave Convective Heat Transfer," in *Design and Manufacturing of Composites, Proceedings of the Second Joint Canada-Japan Workshop on Composites*, 1998, pp. 106–113.

[102] L. B. Ilcewicz, P. J. Smith, C. T. Hanson, T. H. Walker, S. L. Metschan, G. E. Mabson, K. S. Wilden, B. W. Flynn, D. B. Scholz, D. R. Polland, H. G. Fredrikson, J. T. Olson, and B. F. Backman, "Advanced Technology Composite Fuselage - Program Overview (ATCAS). Report No. NASA-CR-4734," NASA Langley Research Center, Hampton, VA, 97X10233, 1997.

[103] K. S. Wilden, C. G. Harris, B. W. Flynn, M. G. Gessel, D. B. Scholz, S. Stawski, and V. Winston, "Advanced Technology Composite Fuselage - Manufacturing (ATCAS). Report No. NASA-CR-4735," NASA Langley Research Center, Hampton, VA, 97X10235, 1997.

[104] M. M. Thomas, B. Joseph, and J. L. Kardos, "Experimental characterization of autoclave-cured glass-epoxy composite laminates: Cure cycle effects upon thickness, void content, and related phenomena," *Polymer Composites*, vol. 18, no. 3, pp. 283–299, Jun. 1997.

[105] V. K. Pillai, A. N. Beris, and P. S. Dhurjati, "Implementation of Model-Based Optimal Temperature Profiles for Autoclave Curing of Composites Using a Knowledge-Based System," *Industrial & Engineering Chemistry Research*, vol. 33, no. 10, pp. 2443–2452, Oct. 1994.

[106] V. Pillai, A. N. Beris, and P. Dhurjati, "Heuristics guided optimization of a batch autoclave curing process," *Computers & Chemical Engineering*, vol. 20, no. 3, pp. 275–294, 1996.

[107] V. Pillai, A. N. Beris, and P. Dhurjati, "Intelligent Curing of Thick Composites Using a Knowledge-Based System," *Journal of Composite Materials*, vol. 31, no. 1, pp. 22–51, 1997.

[108] J. S. Kim and D. G. Lee, "Development of an Autoclave Cure Cycle with Cooling and Reheating Steps for Thick Thermoset Composite Laminates," *Journal of Composite Materials*, vol. 31, no. 22, pp. 2264–2282, 1997.

[109] Y. Kim and S. White, "Viscoelastic analysis of processing-induced residual stresses in thick composite laminates," *Mechanics of Composite Materials And Structures*, vol. 4, no. 4, pp. 361–387, 1997.

[110] S. R. White and Y. K. Kim, "Process-induced Residual Stress Analysis of AS4/3501-6 Composite Material," *Mechanics of Advanced Materials and Structures*, vol. 5, no. 2, pp. 153–186, 1998.

[111] S. C. Joshi, X. L. Liu, and Y. C. Lam, "A numerical approach to the modeling of polymer curing in fibre-reinforced composites," *Composites Science and Technology*, vol. 59, no. 7, pp. 1003–1013, 1999.

[112] D. C. Blest, B. R. Duffy, S. McKee, and A. K. Zulkifle, “Curing simulation of thermoset composites,” *Composites Part A: Applied Science and Manufacturing*, vol. 30, no. 11, pp. 1289–1309, 1999.

[113] M. I. Naji and S. V. Hoa, “Curing of Thick Angle-Bend Thermoset Composite Part: Curing Cycle Effect on Thickness Variation and Fiber Volume Fraction,” *Journal of Reinforced Plastics and Composites*, vol. 18, no. 8, pp. 702–723, 1999.

[114] M. I. Naji and S. V. Hoa, “Curing of Thick Angle-Bend Thermoset Composite Part: Curing Process Modification for Uniform Thickness and Uniform Fiber Volume Fraction Distribution,” *Journal of Composite Materials*, vol. 34, no. 20, pp. 1710–1755, 2000.

[115] Z. L. Yang and S. Lee, “Optimized Curing of Thick Section Composite Laminates,” *Materials and Manufacturing Processes*, vol. 16, no. 4, pp. 541–560, 2001.

[116] D. J. Michaud, “Simulation-based design optimization and control of thick composite laminate manufactured by resin transfer molding. PhD thesis,” University of Delaware, 2000.

[117] D. J. Michaud, A. N. Beris, and P. S. Dhurjati, “Thick-Sectioned RTM Composite Manufacturing: Part I - In Situ Cure Model Parameter Identification and Sensing,” *Journal of Composite Materials*, vol. 36, no. 10, pp. 1175–1200, May 2002.

[118] D. J. Michaud, A. N. Beris, and P. S. Dhurjati, “Thick-Sectioned RTM Composite Manufacturing, Part II. Robust Cure Cycle Optimization and Control,” *Journal of Composite Materials*, vol. 36, no. 10, pp. 1201–1231, May 2002.

[119] J. H. Oh and D. G. Lee, “Cure Cycle for Thick Glass/Epoxy Composite Laminates,” *Journal of Composite Materials*, vol. 36, no. 1, pp. 19–45, 2002.

[120] M. Li, Q. Zhu, P. H. Geubelle, and C. L. Tucker III, “Optimal curing for thermoset matrix composites: Thermochemical considerations,” *Polymer Composites*, vol. 22, no. 1, pp. 118–131, 2001.

[121] M. Li and C. L. Tucker III, “Optimal Curing of Thermoset Matrix Composites: Thermochemical and Consolidation Considerations,” *Polymer Composites*, vol. 23, no. 5, pp. 739–757, 2002.

[122] V. Antonucci, M. Giordano, S. Inserraimparato, and L. Nicolais, “Analysis of heat transfer in autoclave technology,” *Polymer Composites*, vol. 22, no. 5, pp. 613–620, Oct. 2001.

[123] V. Antonucci, M. Giordano, S. I. Imparato, and L. Nicolais, “Autoclave manufacturing of thick composites,” *Polymer Composites*, vol. 23, no. 5, pp. 902–910, 2002.

[124] V. Antonucci, M. Giordano, K.-T. Hsiao, and S. G. Advani, “A methodology to reduce thermal gradients due to the exothermic reactions in composites processing,” *International Journal of Heat and Mass Transfer*, vol. 45, no. 8, pp. 1675–1684, 2002.

[125] G. L. Hahn, “Accelerated Insertion of Materials - Composites (AIM-C) Methodology. Document No. ADA511880 (2004P0020 V_1.2.0),” Boeing Phantom Works, St. Louis, MO, 2004.

[126] G. L. Hahn, K. M. Nelson, and C. R. Saff, “Accelerated Insertion of Materials - Composites,” in *33rd International SAMPE Technical Conference*, 2001, p. 11.

[127] J. Griffith, J. Madsen, T. Chung, E. Barnes, and J. Kirk, "Overview of the Accelerated Insertion of Materials - Composites (AIM-C) Producibility Module Development. Document No. ADA513514," *SAMPE Technical Conference*. Boeing Phantom Works, Long Beach, CA, 2002.

[128] J. M. Griffith, "New Material Transition From an OEM Perspective. Document No. ADA511695," *High Temple Workshop 24, 2-5 February*. Boeing Phantom Works, Sacramento, CA, p. 15, 2004.

[129] K. M. Nelson, "Accelerated Insertion of Materials - Composites: Overview. Document No. ADA513551," *SAMPE ISSE 2002*. Boeing Phantom Works, Long Beach, CA, 2002.

[130] K. M. Nelson, "Accelerated Insertion of Materials – Composites. Document No. ADA514496." Boeing Phantom Works, Penn State University, 2002.

[131] V. A. F. Costa and A. C. M. Sousa, "Modeling of flow and thermo-kinetics during the cure of thick laminated composites," *International Journal of Thermal Sciences*, vol. 42, no. 1, pp. 15–22, 2003.

[132] D. Shin and H. Hahn, "Compaction of thick composites: simulation and experiment," *Polymer Composites*, vol. 25, no. 1, pp. 49–59, 2004.

[133] S. Parthasarathy, S. C. Mantell, and K. A. Stelson, "Estimation, control and optimization of curing in thick-sectioned composite parts," *Journal of Dynamic Systems, Measurement, and Control (Transactions of the ASME)*, vol. 126, no. 4, pp. 824–833, 2004.

[134] K. M. Nelson, "University of Washington Chemical Engineering Leadership Series Lecture. Publicly released Boeing information: 12-00855-EOT." The Boeing Company, 2012.

[135] D. Van Ee and A. Poursartip, "NCAMP Hexply Material Properties Database for use with COMPRO CCA and RAVEN. Version 0.9," Convergent Manufacturing Technologies Inc., Vancouver, Canada, 2009.

[136] N. Ersoy, K. Potter, M. R. Wisnom, and M. J. Clegg, "An experimental method to study the frictional processes during composites manufacturing," *Composites Part A: Applied Science and Manufacturing*, vol. 36, no. 11, pp. 1536–1544, 2005.

[137] N. Ersoy, K. Potter, M. R. Wisnom, and M. J. Clegg, "Development of spring-in angle during cure of a thermosetting composite," *Composites Part A: Applied Science and Manufacturing*, vol. 36, no. 12, pp. 1700–1706, 2005.

[138] E. Ruiz and F. Trochu, "Numerical analysis of cure temperature and internal stresses in thin and thick RTM parts," *Composites Part A: Applied Science and Manufacturing*, vol. 36, no. 6, pp. 806–826, 2005.

[139] E. Ruiz and F. Trochu, "Thermomechanical Properties during Cure of Glass-Polyester RTM Composites: Elastic and Viscoelastic Modeling," *Journal of Composite Materials*, vol. 39, no. 10, pp. 881–916, 2005.

[140] Z.-S. Guo, S. Du, and B. Zhang, "Temperature field of thick thermoset composite laminates during cure process," *Composites Science and Technology*, vol. 65, no. 3–4, pp. 517–523, 2005.

[141] A. Rasekh, R. Vaziri, and A. Poursartip, "Simple Techniques for Thermal Analysis of the Processing of Composite Structures," in *Proceedings of 36th International SAMPE Technical Conference*, 2004, p. 11.

[142] A. Rasekh, “Efficient Methods for Non-Linear Thermochemical Analysis of Composite Structures Undergoing Autoclave Processing. PhD thesis,” The University of British Columbia, Vancouver, 2007.

[143] D. Dykeman and A. Poursartip, “Process Maps for Design of Cure Cycles for Thermoset Matrix Composite Materials,” in *Proceedings of 36th International SAMPE Technical Conference*, 2004, p. 9.

[144] D. Dykeman, “Minimizing Uncertainty in Cure Modeling for Composites Manufacturing. PhD thesis,” The University of British Columbia, Vancouver, 2008.

[145] T. Shimizu, J. C. Kotlik, A. R. A. Arafath, and A. Poursartip, “Evaluation of Temperature Profiles in Thick Composite Parts During Autoclave Processing,” in *Proceedings of 23rd ASC Technical Conference*, 2008, p. 17.

[146] A. Bebamzadeh, “Efficient Finite Element Response Sensititvity Analysis and Applications in Composites Manufacturing. PhD thesis,” The University of British Columbia, Vancouver, 2009.

[147] A. Bebamzadeh, T. Haukaas, R. Vaziri, A. Poursartip, and G. Fernlund, “Application of Response Sensitivity in Composite Processing,” *Journal of Composite Materials*, vol. 44, no. 15, pp. 1821–1840, 2010.

[148] N. Slesinger, T. Shimizu, A. R. A. Arafath, and A. Poursartip, “Heat Transfer Coefficient Distribution Inside an Autoclave,” in *Proceedings of ICCM-17 Conference*, 2009, p. 10.

[149] N. A. Slesinger, G. Fernlund, and A. Poursartip, “Development of a Test Method to Validate Cure Kinetics Models Used in Process Simulation,” in *Proceedings of SAMPE Technical Conference*, 2010, p. 15.

[150] N. A. Slesinger, “Thermal Modeling Validation Techniques for Thermoset Polymer Matrix Composites. MASc thesis,” The University of British Columbia, Vancouver, 2010.

[151] T. W. Secord, S. C. Mantell, and K. A. Stelson, “Scaling Analysis and a Critical Thickness Criterion for Thermosetting Composites,” *Journal of Manufacturing Science and Engineering*, vol. 133, no. 1, p. 011005, 2011.

[152] J. H. Panchal, S. R. Kalidindi, and D. L. McDowell, “Key computational modeling issues in Integrated Computational Materials Engineering,” *Computer-Aided Design*, vol. 45, no. 1, pp. 4–25, 2013.

[153] D. L. McDowell and S. R. Kalidindi, “The materials innovation ecosystem: A key enabler for the Materials Genome Initiative,” *MRS Bulletin*, vol. 41, no. 04, pp. 326–337, 2016.

[154] L. R. Liou, S. P. Engelstad, T. Harrington, R. Koon, and K. Kendig, “Integrated computational methods for composites materials (ICM2): Lessons learned from integration planning and feasibility demonstrations,” in *CAMX Conference Proceedings*, 2014, p. 13.

[155] S. P. Engelstad, R. W. Koon, J. E. Action, J. M. Riga, A. M. Wass, D. Robbins, R. W. Dalgarno, A. R. Arafath, and A. Poursartip, “Integrated Computational Materials Enigneering for Airframe Composite Structure Applications,” in *56th AIAA/ASCE/AHS/ASC Structures, Structural Dynamics, and Materials Conference*, 2015, p. 0198.

[156] J. Dustin, R. Dalgarno, and M. Hockemeyer, “Lessons Learned from the Development of a Structural Finite Element Progressive Failure Simulation for Integration into the ICM2 Framework,” in *57th AIAA/ASCE/AHS/ASC Structures, Structural Dynamics, and Materials Conference*, 2016, p. 1171.

[157] B. Koon, S. Engelstad, J. Action, R. Dalgarno, M. Maiaru, N. Riga, and C. Lynam, “Integrated Computational Methods for Composite Materials (ICM2): Process and Micromechanics Modeling for Airframe Applications,” in *Proceedings of SAMPE Technical Conference*, 2016, p. 19.

[158] S. Srinivasan, J. M. Riga, R. W. Koon, and T. Harrington, “Design, Integrated Computational Multi-Scale Modeling for Efficient Composite Material and Process,” in *Proceedings of SAMPE Technical Conference*, 2017, p. 15.

[159] R. Thorpe, C. Lynam, A. R. Arafath, and A. Poursartip, “TRUST: Efficient and Effective Materials Characterization for Process Simulation,” in *Proceedings of SAMPE Technical Conference*, 2014.

[160] Convergent Manufacturing Technologies Inc. (CMT Inc.), “Software and Hardware.” Available: http://www.convergent.ca/products/. [Accessed: 16-Oct-2017].

[161] T. S. Mesogitis, A. A. Skordos, and A. C. Long, “Uncertainty in the manufacturing of fibrous thermosetting composites: A review,” *Composites Part A: Applied Science and Manufacturing*, vol. 57, pp. 67–75, 2014.

[162] T. S. Mesogitis, A. A. Skordos, and A. C. Long, “Stochastic simulation of the influence of cure kinetics uncertainty on composites cure,” *Composites Science and Technology*, vol. 110, pp. 145–151, 2015.

[163] T. Mesogitis, A. Skordos, and A. Long, “Stochastic heat transfer simulation of the cure of advanced composites,” *Journal of Composite Materials*, vol. 50, no. 21, pp. 2971–2986, 2016.

[164] S. Mamani and S. V. Hoa, “Temperature Measurement in Autoclave Manufacturing Process for Thick Glass/epoxy Composite Laminate,” in *Proceedings of the International Workshop on Mechanical Behavior of Thick Composites*, 2016, p. 8.

[165] X. Wen, “Manufacturing and Fatigue Behavior of Thick Glass/Epoxy Composite Beams. MASc thesis,” Concordia University, 2016.

[166] M. Gude, R. Schirner, M. Muller, N. Weckend, M. Andrich, and A. Langkamp, “Experimental-numerical test strategy for evaluation of curing simulation of complex-shaped composite structures,” *Materialwissenschaft und Werkstofftechnik*, vol. 47, no. 11, pp. 1072–1086, 2016.

[167] T. A. Weber, J.-C. Arent, L. Münch, M. Duhovic, and J. M. Balvers, “A fast method for the generation of boundary conditions for thermal autoclave simulation,” *Composites Part A: Applied Science and Manufacturing*, vol. 88, pp. 216–225, 2016.

[168] C. Hunt, J. Kratz, and I. K. Partridge, “Cure path dependency of mode I fracture toughness in thermoplastic particle interleaf toughened prepreg laminates,” *Composites Part A: Applied Science and Manufacturing*, vol. 87, pp. 109–114, 2016.

[169] K. Gordnian, R. Vaziri, and A. Poursartip, “Crystallization and Melt Kinetics for Process Modelling of PEEK Matrix Composites,” in *Proceedings of SAMPE Technical Conference*, 2017, p. 16.

[170] K. Gordnian, “Crystallization and Thermo-Viscoelastic Modelling of Polymer Composites. PhD thesis,” The University of British Columbia, Vancouver, 2017.

[171] L. Ma, S. R. Athreya, R. Mehta, D. Barpanda, and A. Shafi, “Numerical modeling and experimental validation of nonisothermal resin infusion and cure processes in large composites,” *Journal of Reinforced Plastics and Composites*, vol. 36, no. 10, pp. 780–794, 2017.

[172] M. Shafi, F. Aguirre, E. Trottier, and S. Falcone-Potts, “Rheokinetic modeling of fusion bonded epoxy powder coatings at standard and low application temperature,” in *International Conference on Pipeline Protection, 18*, 2009, pp. 81–91.

[173] P. Shah, V. Halls, J. Zheng, and R. Batra, “Optimal cure cycle parameters for minimizing residual stresses in fiber-reinforced polymer composite laminates,” *Journal of Composite Materials*, p. 002199831771431, 2017.

[174] J. P. H. Belnoue, T. Mesogitis, O. J. Nixon-Pearson, J. Kratz, D. S. Ivanov, I. K. Partridge, K. D. Potter, and S. R. Hallett, “Understanding and predicting defect formation in automated fibre placement pre-preg laminates,” *Composites Part A: Applied Science and Manufacturing*, vol. 102, pp. 196–206, 2017.

[175] N. Adamovic, P. Asinari, G. Goldbeck, A. Hashibon, K. Hermansson, D. Hristova-Bogaerds, R. Koopmans, T. Verbrugge, and E. Wimmer, “European Materials Modelling Council,” in *Proceedings of the 4th World Congress on Integrated Computational Materials Engineering (ICME 2017)*, 2017, pp. 79–92.

[176] Information Technology for European Advancement (ITEA), “A new Interface Standard for Integrated Virtual Material Modelling in Manufacturing Industry (ITEA3 Project: 16010).” Available: https://itea3.org/project/vmap.html. [Accessed: 01-Feb-2018].

[177] J. Park, N. Zobeiry, and A. Poursartip, “Tooling Materials and Their Effect on Surface Thermal Gradients,” in *SAMPE Conference Proceedings*, 2017, p. 15.

[178] J. Park, “Simulation and Experimental Determination of Convective Heat Transfer Boundary Conditions for Thermal Processing of Composite Structures. MASc thesis in preparation,” The University of British Columbia, Vancouver, 2018.

[179] N. Zobeiry, J. Park, and A. Poursartip, “An IR Thermography Based Method for the Evaluation of the Thermal Response of Tooling for Composites Manufacturing. Manuscript submitted,” 2018.

[180] T. L. Bergman, A. S. Lavine, F. P. Incropera, and D. P. DeWitt, *Fundamentals of Heat and Mass Transfer*, 7th ed. John Wiley & Sons, 2011.

[181] Convergent Manufacturing Technologies Inc. (CMT Inc.), “COMPRO Simulation Software Model Documentation V1.5.8.” 2017.

[182] S. Vyazovkin and C. A. Wight, “Model-free and model-fitting approaches to kinetic analysis of isothermal and nonisothermal data,” *Thermochimica Acta*, vol. 340–341, pp. 53–68, Dec. 1999.

[183] A. Floyd, Private Communication. CMT Inc., 2017.

[184] W. L. Oberkampf, S. M. DeLand, B. M. Rutherford, K. V. Diegert, and K. F. Alvin, “Error and uncertainty in modeling and simulation,” *Reliability Engineering & System Safety*, vol. 75, no. 3, pp. 333–357, 2002.

[185] C. J. Roy and W. L. Oberkampf, “A comprehensive framework for verification, validation, and uncertainty quantification in scientific computing,” *Computer Methods in Applied Mechanics and Engineering*, vol. 200, no. 25–28, pp. 2131–2144, Jun. 2011.

[186] G. Fernlund, “Risk reduction in composites processing using prototype data, process simulation, and Bayesian statistics,” *Composites Part A: Applied Science and Manufacturing*, vol. 41, no. 2, pp. 295–303, 2010.

[187] K. Potter, C. Langer, B. Hodgkiss, and S. Lamb, “Sources of variability in uncured aerospace grade unidirectional carbon fibre epoxy preimpregnate,” *Composites Part A: Applied Science and Manufacturing*, vol. 38, no. 3, pp. 905–916, 2007.

[188] K. Potter, “Understanding the Origins of Defects and Variability in Composites Manufacture,” in *Proceedings of ICCM-17 Conference*, 2009.

[189] D. M. Crowley, C. Ward, and K. Potter, “A Status of Acceptance Criteria and Process Requirements in Advanced Composites Manufacturing, and Whether They are Fit for Purpose,” in *SAE Technical Paper 2013-01-2144*, 2013, p. 10.

[190] G. B. Olson, “Computational Design of Hierarchically Structured Materials,” *Science*, vol. 277, no. 5330, pp. 1237–1242, 1997.

[191] C. J. Kuehmann and G. B. Olson, “Computational materials design and engineering,” *Materials Science and Technology*, vol. 25, no. 4, pp. 472–478, 2009.

[192] CMH-17, *Polymer Matrix Composites Materials Usage, Design and Analysis*, Volume 3G. Warrendale, PA: SAE International, 2012.

[193] C. Ashforth and L. Ilcewicz, “Certification and Compliance Considerations for Aircraft Products with Composite Materials,” in *Comprehensive Composite Materials II*, Vol 3., A. Poursartip, Ed. Elsevier, 2018, pp. 1–25.

[194] M. Ashby, “Physical modelling of materials problems,” *Materials Science and Technology*, vol. 8, pp. 102–111, 1992.

[195] S. G. Advani and E. M. Sozer, “Model Simplifications and Solutions,” in *Process Modeling in Composites Manufacturing*, 2nd ed., Boca Raton, FL: CRC Press, 2011, p. 614.

[196] W. D. Callister and D. G. Rethwisch, *Materials science and engineering: an introduction*, 9th ed. John Wiley and Sons Inc., 2014.

[197] A. R. A. Arafath, G. Fernlund, and A. Poursartip, “Gas transport in prepregs: model and permeability experiments,” in *Proceedings of ICCM-17 Conference*, 2009, p. 10.

[198] M. Lane, A. Poursartip, G. Fernlund, K. Willden, and K. Nelson, “Robust Processing of Composite Structures,” in *SAMPE Conference Proceedings*, 2010, p. 12.

[199] Zhan-Sheng Guo, Ling Liu, Bo-Ming Zhang, and Shanyi Du, “Critical Void Content for Thermoset Composite Laminates,” *Journal of Composite Materials*, vol. 43, no. 17, pp. 1775–1790, Aug. 2009.

[200] L. K. Grunenfelder and S. R. Nutt, “Void formation in composite prepregs – Effect of dissolved moisture,” *Composites Science and Technology*, vol. 70, no. 16, pp. 2304–2309, 2010.

[201] T. Centea and P. Hubert, “Modelling the effect of material properties and process parameters on tow impregnation in out-of-autoclave prepregs,” *Composites Part A: Applied Science and Manufacturing*, vol. 43, no. 9, pp. 1505–1513, Sep. 2012.

[202] L. Farhang, “Void Evolution during Processing of Out-of-Autoclave Prepreg Laminates. PhD thesis,” The University of British Columbia, Vancouver, 2014.

[203] J. J. Gangloff, W. R. Hwang, and S. G. Advani, “Characterization of bubble mobility in channel flow with fibrous porous media walls,” *International Journal of Multiphase Flow*, vol. 60, pp. 76–86, 2014.

[204] H. Bedayat, M. Roy, A. Forghani, C. Hickmott, F. Palmieri, B. Grimsley, B. Coxon, G. Fernlund, and A. Poursartip, “An Efficient Modelling Approach for Prediction of Porosity Severity in Composite Structures,” in *Proceedings of SAMPE Technical Conference*, 2017, p. 9.

[205] C. Mobuchon, C. Keulen, K. Hsiao, G. Fernlund, and A. Poursartip, “Development of a structured approach to porosity management in composites manufacturing,” in *SAMPE Conference Proceedings*, 2014, p. 12.

[206] C. Rigard, “Process Selection and Optimization for Out of Autoclave Prepreg Structures,” in *CAMX Conference Proceedings*, 2015, p. 12.

[207] G. Fernlund, J. Wells, L. Fahrang, J. Kay, and A. Poursartip, “Causes and remedies for porosity in composite manufacturing,” *IOP Conference Series: Materials Science and Engineering*, vol. 139, no. 1, p. 012002, Jul. 2016.

[208] S. R. Kalidindi, “Data science and cyberinfrastructure: critical enablers for accelerated development of hierarchical materials,” *International Materials Reviews*, vol. 60, no. 3, pp. 150–168, 2015.

[209] E. Popova, T. M. Rodgers, X. Gong, A. Cecen, J. D. Madison, and S. R. Kalidindi, “Process-Structure Linkages Using a Data Science Approach: Application to Simulated Additive Manufacturing Data,” *Integrating Materials and Manufacturing Innovation*, vol. 6, no. 1, pp. 54–68, 2017.

[210] A. Forghani, C. Hickmott, H. Bedayat, C. Wohl, B. Grimsley, B. Coxon, and A. Poursartip, “A Physics-based Modelling Framework for Simulation of Prepreg Tack in AFP Process,” in *Proceedings of SAMPE Technical Conference*, 2017, p. 10.

[211] G. Fernlund and A. Floyd, “Process analysis and tool compensation for a complex composite panel,” in *Proceedings of 22nd ASC Technical Conference*, 2007, p. 12.

[212] J. Cao, R. Akkerman, P. Boisse, J. Chen, H. S. Cheng, E. F. de Graaf, J. L. Gorczyca, P. Harrison, G. Hivet, J. Launay, W. Lee, L. Liu, S. V. Lomov, A. Long, E. de Luycker, F. Morestin, J. Padvoiskis, X. Q. Peng, J. Sherwood, T. Stoilova, X. M. Tao, I. Verpoest, A. Willems, J. Wiggers, T. X. Yu, and B. Zhu, “Characterization of mechanical behavior of woven fabrics: Experimental methods and benchmark results,” *Composites Part A: Applied Science and Manufacturing*, vol. 39, no. 6, pp. 1037–1053, 2008.

[213] J. S. Lightfoot, M. R. Wisnom, and K. Potter, “A new mechanism for the formation of ply wrinkles due to shear between plies,” *Composites Part A: Applied Science and Manufacturing*, vol. 49, pp. 139–147, Jun. 2013.

[214] J. Lightfoot, M. Wisnom, and K. Potter, “Defects in woven preforms: formation mechanisms and the effects of laminate design and layup protocol,” *Composites Part A: Applied Science and Manufacturing*, vol. 51, pp. 99–107, 2013.

[215] L. D. Bloom, J. Wang, and K. D. Potter, “Damage progression and defect sensitivity: An experimental study of representative wrinkles in tension,” *Composites Part B: Engineering*, vol. 45, no. 1, pp. 449–458, 2013.

[216] T. J. Dodwell, R. Butler, and G. W. Hunt, “Out-of-plane ply wrinkling defects during consolidation over an external radius,” *Composites Science and Technology*, vol. 105, pp. 151–159, 2014.

[217] A. Stewart, K. Farnand, G. Fernlund, and A. Poursartip, “Experimental Study into the Parameters Affecting the Architecture of Waviness and Wrinkling in Prepreg Systems,” in *proceedings of CANCOM2015 Conference*, 2015, p. 8.

[218] K. Farnand, “Process-induced wrinkling and waviness in prepreg charge-forming. MASc thesis,” The University of British Columbia, Vancouver, 2016.

[219] S. A. Niaki, A. Forghani, R. Vaziri, and A. Poursartip, “A two-phase integrated flow-stress process model for composites with application to highly compressible phases,” *Mechanics of Materials*, vol. 109, pp. 51–66, Jun. 2017.

[220] S. A. Niaki, A. Forghani, R. Vaziri, and A. Poursartip, “A three-phase integrated flow-stress model for processing of composites,” *Mechanics of Materials*, vol. 117, pp. 152–164, Feb. 2018.

[221] G. Marsh, “Composites get in deep with new-generation engine,” *Materials Today*, 22-Dec-2006.

[222] B. Harris, “A perspective view of composite materials development,” *Materials & Design*, vol. 12, no. 5, pp. 259–272, 1991.

[223] T. Lean, “RB211 - Big Fan, Big Engine, Big Problems, Bigger Success,” 2012. Available: http://britishlibrary.typepad.co.uk/oralhistoryofscience/2012/05/. [Accessed: 06-Nov-2015].

[224] P. Eremenko, “Formal Model-Based Design & Manufacture: A Template for Managing Complexity in Large-Scale Cyber-Physical Systems,” *11th Annual Conference on Systems Engineering Research*. Atlanta, GA, 2013.

[225] W. F. Lyons, “How Boeing Manages Innovation,” *WBTOI Unmanned Aerial Systems Open Innovation Forum*. WBT - Open Innovation, Stillwater, OK, 2014.

[226] G. Warwick, “NASA-Led Consortium Will Bring Science To Art Of Composites,” *AviationWeek*, 27-Apr-2015.

[227] P. D. Soden, A. S. Kaddour, and M. J. Hinton, “Recommendations for designers and researchers resulting from the world-wide failure exercise,” in *Failure Criteria in Fibre-Reinforced-Polymer Composites*, vol. 64, no. 3–4, Elsevier, 2004, pp. 1223–1251.

[228] M. Freisthler, “Acceptance of Composite Speficiations and Design Values Developed using NCAMP process. FAA Memo No. AIR100-2010-120-003.” Federal Aviation Administration, Washington, D.C., 2010.

[229] B. R. Pipes, G. Klimeck, and M. R. Pipes, “The Composite Materials Manufacturing HUB-Crowd Sourcing as the Norm,” in *Proceedings of Composites 2012*, 2011.

[230] Anonymous, Private Communication. 2014.

[231] T. Centea and S. R. Nutt, “Manufacturing cost relationships for vacuum bag-only prepreg processing,” *Journal of Composite Materials*, vol. 50, no. 17, pp. 2305–2321, 2016.

[232] K. M. Nelson, T. Wu, and C. Lin, “Airflow in Autoclaves,” Patent US2016/0348976A1, 2016.

[233] Y. Kondo, K. Tanimoto, Y. Takeuchi, and Y. Yanase, “Autoclave and Method for Heat Curing Molded Material,” Patent US9586345B2, 2017.

[234] N. Odagiri, S. Suzue, H. Kishi, T. Nakae, and A. Matsusaki, “Fiber Reinforced Composite Materials Having Resin Practice Inter-layer Zones,” Patent US5028478A, 1991.

[235] H. Kishi, A. Ozaki, and N. Odagiri, “Prepreg and Composite,” Patent US5413847A, 1995.

[236] A. Arafath, A. McKee, P.-Y. Lavertu, R. Thorpe, C. Lynam, G. Fernlund, and A. Poursartip, “CCMRD 9.2 Dimensional Control for Large Complex Aerospace Structures Phase 2. Final Report,” Vancouver, Canada, 2015.

[237] K. Nelson, Private Communication. Boeing-UW MSE310, 2017.

[238] Convergent Manufacturing Technologies Inc. (CMT Inc.), “RAVEN Simulation Software V3.9.2.11692.” 2017.

[239] Convergent Manufacturing Technologies Inc. (CMT Inc.), “COMPRO Simulation Software Plug-in for ABAQUS CAE V1.12.11702.” 2017.

[240] K. Nelson, Private Communication. The Boeing Company, 2016.

[241] Hexcel Corporation, “HexPly 8552 Product Data Sheet (EU). FTA-072-AG16,” 2016. Available: http://www.hexcel.com/. [Accessed: 17-Sep-2017].

[242] Toray Composite Materials America Inc., “3900 Prepreg System (Rev 5),” 2018. Available: https://www.toraycma.com/. [Accessed: 17-Apr-2018].

[243] A. McKee, Private Communication. CCMRD Project 9.2, 2016.

[244] J. Mijovic and J. Wijaya, “Effect of Graphine Fiber and Epoxy Matrix Physical Properties on the Temperature Profile Inside Their Composite During Cure,” *SAMPE Journal*, vol. 25, no. 1, pp. 35–39, 1989.

[245] A. Poursartip, G. Fernlund, and R. Courdji, “Issues in Developing and Applying Process Models to Aid in Composites Manufacturing,” *9th International Conference on Flow Processes in Composite Materials*. Montreal, Canada, 2008.

[246] Abaris Training Resources Inc., “Thermocouples.,” *NetComposites Now*. Available: http://netcomposites.com/guide-tools/guide/repair/thermocouples/. [Accessed: 24-Feb-2017].

[247] Convergent Manufacturing Technologies Inc. (CMT Inc.), “KERMODE Data and Model Fitting Software V1.0.3.10040.” 2016.

Appendices

Appendix A Thermal Management Studies of Thick Thermoset Composites

This appendix contains the further details and synthesis of the thermal management studies of thick thermoset composites identified in the scientific literature and presented in Section 2.3, including:

- An overview of the studies reported
- Details of the science base (model complexity, material models and boundary conditions)
- Reported CK models used in the studies identified
- Details of the technology base (simulation: process modelling and process control)
- A summary of these studies terms of the ETPM factory ontology
- A summary of ETPM thermal management attributes for these studies

A.1 Definition of thick composites

The definition of what constitutes a 'thick' composites part in the scientific literature is somewhat arbitrary with few studies quantifying specific thickness values. For instance, Twardowski *et al* [90] specify 'thick composites' as laminates thicker than 50 mm. In studies examining thick-sectioned RTM manufactured composites, Michaud [116] describes 'thick' laminates as 'not strictly based based on the physical thickness but in the problems that arise in controlling the internal temperatures of the composite'. In proposing a model-based control method for cure optimization, Parthasarathy *et al* [133] defines 'thick-sectioned parts' as those with thicknesses

greater than 5 mm. Work by Wen [165], investigating thick thermoset composite laminates for aerospace (rotorcraft) applications, describe laminates thicker than 6 mm as 'significantly thick'.

Several researchers have used scaling analysis to distinguish 'thin' and 'thick' laminates from a science based standpoint. For example, work by Berglund and Kenny [25] describe and quantify three thermal processing scenarios: 1) isothermal conditions (thin); 2) non-isothermal conditions (thick); and 3) adiabatic conditions. As the thickness of a laminate increases beyond a critical value, there is an imbalance between the heat generated and the thermal diffusivity of the material. For the carbon/epoxy materials investigated, $h_{is} < 1$ mm and $h_{ad} > 10$ mm, where h_{is} is the laminate half-thickness for the isothermal condition and h_{ad} is the laminate half-thickness for the adiabatic condition.

Secord *et al* [151] propose two dimensionless parameters, a modified Damköhler number (Da^*) and dimensionless rise time ($\bar{t}_{rise}$), to establish a 'critical thickness criterion' with regard to controlling the temperature overshoot for thermoset composites, where Da^* is based on the Damköhler number (Da), a ratio of the conduction time scale to the reaction time scale. Both Da^* and $\bar{t}_{rise}$ dimensionless parameters include material properties, cure kinetics, and part thickness terms. A critical 'composite thickness' is reached when $Da^* = 1$. In this approach, through-thickness heat transfer and prescribed temperature boundary conditions are assumed for both ramp (non-isothermal) and hold (isothermal) cure conditions. From the analysis performed, it is observed that 'thin' laminates do not necessarily imply 'small thicknesses or ply counts'.

Analytical closed-form equations developed by Rasekh *et al* [141,142] can be used to describe the thermal behaviour of composites parts and tools in three scenarios: 1) transient steady-state response during a ramp (temperature lags in composite parts and tools, see Equation (2-3)); 2) steady-state response during a hold with no temperature overshoot (relevant for thermally massive tools at intermediate holds); and 3) the steady-state response during a hold with temperature overshoot (of interest for composite parts where the exotherm due to internal heat generation is significant, refer to Equation (2-4)). In this approach, through-thickness heat transfer and constant convective heat transfer coefficient boundary conditions are assumed. Differences in 'thin' and 'thick' parts are described qualitatively. It is suggested that for thin parts, it is sufficient to consider the thermal response of the tool in terms of tool material selection and tool plate thickness. For thick parts, on the other hand, is it necessary to consider the thermal response of both parts and tools.

A.2 Summary of thick laminate studies reported in the scientific literature

In most cases, the motivation for these studies identified in the literature was to investigate the difficulties associated with processing thick thermoset composites. These issues can arise due to: 1) internal heat generation that cannot be sufficiently dissipated to maintain isothermal conditions, given the low thermal diffusivity of the composite material; and 2) the development of large thermal gradients and variation in the degree of cure (DOC) that can lead to non-uniform curing. These issues can also contribute to material degradation, undesirable part quality and reductions in mechanical performance.

Table A-1: Overview of studies reported from literature review of thick thermoset composites.

Principal investigators	Material system[a]	Laminate thickness (mm)	Science[b]	Technology[b]	Practice[b]	Remarks[c]	Ref.
Loos & Springer	CFRP	1.9 mm, 3.8 mm, 7.8 mm	TM			Cure cycle design criteria proposed	[74,75]
Bogetti & Gillespie	GFRP	13.8 mm, 18.5 mm, 25.4 mm, 33.9 mm, 50.8 mm, 76.2 mm	TM, RSDM				[83–85]
Martinez	CFRP	24.9 mm		TM			[86]
Ciriscioli *et al*	CFRP	2.6 mm, 8.6 mm, 10 mm, 34.9 mm		TM			[88,89]
Twardowski *et al*	GFRP CFRP	50 mm	TM			Thick composites (≥ 50 mm)	[90]
Telikicherla *et al*	CFRP	0.95 mm, 1.9 mm, 3.8 mm, 5.7 mm	TM				[92]
Hojjati &Hoa	CFRP	25 mm, 35mm, 50 mm, 60 mm, 80 mm, 100 mm, 150 mm, 300 mm	TM, MDM				[93,94]
Joseph *et al*	CFRP	19 mm, 33.8 mm, 16.8 mm		TM, QM		Revised cure cycle design criteria	[95,96]
Kim *et al*	GFRP CFRP	50 mm 100 mm	TM, QM				[97,98]
Johnston *et al*	CFRP/core	28.2 mm	TM, QM, RSDM				[99–101]
Thomas *et al*	GFRP	5.3 mm	QM	QM			[104]
Pillai *et al*	GFRP	25.4 mm	TM, QM, RSDM	TM, QM, RSDM			[105–107]
Kim & Lee	CFRP	15 mm, 30 mm	TM	TM			[108]
Kim & White	CFRP	25.4 mm, 75 mm	RSDM				[109,110]
Joshi *et al*	CFRP	23.1 mm	TM				[111]
Blest *et al*	CFRP	7.8 mm	TM				[112]
Naji & Hoa	CFRP	8 mm	QM				[113,114]
Yang & Lee	CFRP	12.5mm ,25 mm, 50 mm 12.5 mm		TM			[115]
Michaud *et al*	GFRP	25.4 mm	TM	TM		Thick composites (> 20 mm) RTM process	[117,118]
Oh & Lee	GFRP	20 mm	TM	TM			[119]
Li *et al*	resin	2.0 mm, 40 mm		TM			[120,121]
Antonucci *et al* (1)	CFRP	30 mm	TM				[122,123]
Antonucci *et al* (2)	GFRP	10 mm, 13.5 mm, 6.8 mm		TM		RTM process	[124]

Table continued on next page

Table A-1 continued

Principal investigators	Material system[a]	Laminate thickness (mm)	Science[b]	Technology[b]	Practice[b]	Remarks[c]	Ref.
AIM-C	CFRP	17.8 mm 22.4 mm, 89 mm, 127 mm			TM		[129,130]
Costa & Sousa	CFRP	10mm, 12.5mm, 36.5 mm, 50 mm	TM, MDM, QM				[131]
Shin & Hahn	CFRP	30 mm, 50 mm	TM, QM				[132]
Parthasarathy *et al*	GFRP	4.8 mm, 5.4 mm, 14.4 mm, 21.6 mm	TM	TM			[133]
Ruiz & Trochu	GFRP	3mm, 15 mm	TM, RSDM	TM, RSDM		RTM (automotive)	[138,139]
Guo *et al*	CFRP	20 mm	TM				[140]
Shimizu *et al*	CFRP	38.4 mm	TM				[145]
Slesinger *et al*	CFRP	7.5 mm, 11.7 mm, 14.7mm	TM				[149,150]
Mamani & Hoa	GFRP	18.3 mm	TM				[164]
Gude *et al*	CFRP	100 mm	TM,			RTM (aerospace OOA)	[166]
Ma *et al*	GFRP	76.2 mm	TM, MDM, QM			VARTM (wind energy)	[171,172]
Shah *et al*	CFRP	1.2 mm, 12 mm 36.5 mm	TM, RSDM	TM, RSDM			[173]
Belnoue *et al*	CFRP	18 mm	TM, MDM, QM			CK validation for AFP/wrinkling study	[174]

[a] CFRP: Carbon Fibre Reinforced Polymer; GFRP: Glass Fibre Reinforced Polymer
[b] TM: Thermal Management; MDM: Material Deposition Management; QM: Quality Management; RSDM: Residual Stress & Dimensional Control Management
[c] RTM: Resin Transfer Moulding; OOA: Out-of-Autoclave; VARTM: Vacuum Assisted Resin Transfer Moulding; CK: Cure Kinetics; AFP: Automated Fibre Placement

Table A-2: Overview of studies reported from literature review of thick thermoset composites with respect to thermal management science base[a,b].

Principal investigators	Material system	Heat transfer		Resin cure kinetics		Boundary condition	Remarks	Ref.
		energy eqn.	tool inc.	CK model	model valided			
Loos & Springer	CFRP	1D		ck1	x	prescribed temp.		[74,75]
Bogetti & Gillespie	GFRP	1D, 2D		ck1 ck2	x	insulated prescribed temp. effective HTC	Influence of tooling & consumables at laminate surface is considered using a generalized BC formulation	[83–85]
Martinez	CFRP	1D	x	ck1	x	prescribed temp.		[86]
Ciriscioli *et al*	CFRP	1D		ck1 ck3		prescribed temp.	Use of Loos–Springer (1983) CURE code	[88,89]
Twardowski *et al*	GFRP CFRP	1D		ck1		prescribed temp.	Validity of CK model used is questioned	[90]
Telikicherla *et al*	CFRP	2D	x	ck1		effective HTCs	Heat transfer study	[92]
Hojjati & Hoa	CFRP	1D, 2D		ck1		prescribed temp.		[93,94]
Joseph *et al*	CFRP	1D		ck1		insulated (top) prescribed temp. (bottom)		[95,96]
Kim *et al*	GFRP CFRP	1D		ck2		inner: prescribed temp. outer: effective HTC		[97,98]
Johnston *et al*	CFRP/core	1D, 2D	x	ck4	x	effective HTC	HTC determined by measurement	[99–101]
Thomas *et al*	GFRP						Use of Joseph *et al* (1993) strategy CK model not specified	[104]
Pillai *et al*	GFRP	1D	x	ck2		effective HTC		[105–107]
Kim & Lee	CFRP	1D	x	ck5	x	effective HTC	Effective HTC based on Bogetti (1991)	[108]
Kim & White	CFRP	2D		ck1		prescribed temp.		[109,110]
Joshi *et al*	CFRP	1D, 3D	x	ck6		effective HTC	HTC from Vodicka (1994)	[111]
Blest *et al*	CFRP	2D		ck1		prescribed temp.		[112]
Naji & Hoa	CFRP	2D		ck1		effective HTC (top & edge) prescribed temp. (bottom)		[113,114]
Yang & Lee	CFRP	2D		ck1				[115]
Michaud *et al*	GFRP	1D	x	ck7	x	effective HTC		[117,118]
Oh & Lee	GFRP	3D	x	ck5	x	effective HTC	HTC from 3D FE model based on Joshi (1999)	[119]
Li *et al*	resin	1D	x	ck2		effective HTC	HTC arbitrarily specified	[120,121]

Table continued on next page

Table A-2 continued

Principal investigators	Material system	Heat transfer		Resin cure kinetics		Boundary condition	Remarks	Ref.
		energy eqn.	tool inc.	CK model	model valided			
Antonucci *et al* (1)	CFRP	1D	x	ck8		effective HTC	HTC estimated from experimental data	[122,123]
Antonucci *et al* (2)	GFRP	1D	x	ck9		prescribed temp.		[124]
AIM-C	CFRP	2D	x			effective HTC	Use of COMPRO-2D FE code CK model not specified	[129,130]
Costa & Sousa	CFRP	3D		ck1		prescribed temp.	Revised CK parameters used Model developed considers effect of consumables	[131]
Shin & Hahn	CFRP	1D		ck1		prescribed temp.	Influence of bleeder considered in model development	[132]
Parthasarathy *et al*	GFRP	1D		ck2		prescribed temp.		[133]
Ruiz & Trochu	GFRP	1D		ck10	x	prescribed temp.		[138,139]
Guo *et al*	CFRP	1D	x	ck11	x	effective HTC	HTC from Lee (2002)	[140]
Shimizu *et al*	CFRP	1D	x	ck12		effective HTC	HTC back-calculated from experimental data	[145]
Slesinger *et al*	CFRP	1D	x	ck12 ck13	x	prescribed temp.	Use of RAVEN software	[149,150]
Mamani & Hoa	GFRP	1D	x	ck14		effective HTC	HTC taken from Lee (2002)	[164]
Gude *et al*	CFRP	3D	x	ck15	x	effective HTC	HTC determined by measurement & validated numerically	[166]
Ma *et al*	GFRP	3D		ck16		effective HTC	HTC arbitrarily specified	[171]
Shah *et al*	CFRP	3D		ck1		prescribed temp. effective HTC	Prescribed temperature for comparative study HTC arbitrarily specified for optimization study	[173]
Belnoue *et al*	CFRP	1D	x	ck17	x	effective HTC	CK model validation for AFP/wrinkling study	[174]

[a] Details of the cure kinetics models used in these studies are summarized in Table A-3.
[b] CK: Cure Kinetics; BC: Boundary Condition; HTC: Heat Transfer Coefficient; FE: Finite Element

Table A-3: Cure kinetics models reported from literature review of thick thermoset composites (see Table A-2).

CK model	Model form	Parameters		Reference
		α	degree of cure	
		β	'isothermal' degree of cure	
		K_i	Arrhenius factor	
		A_i	pre-exponential coefficient	
		ΔE_i	activation energy	
		R	gas constant	
		T	absolute temperature	
ck1	$K_i = A_i e^{-\Delta E_i/RT}$ $\frac{d\alpha}{dt} = \begin{cases} (K_1 + K_2\alpha)(1-\alpha)(B-\alpha) & \alpha \le 0.3 \\ K_3(1-\alpha) & \alpha > 0.3 \end{cases}$	B	constant	[74]
ck2	$\frac{d\alpha}{dt} = A_i e^{-\Delta E_i/RT} \alpha^{m_i} (1-\alpha)^{n_i}$	m_i, n_i	exponents	[83,84]
ck3	$K_i = A_i e^{-\Delta E_i/RT}$ $\frac{d\alpha}{dt} = \frac{H_T}{H_U}(K_1 + K_2\beta^a)(B-\beta)^b(1-\beta^d)^c$ $\beta = \frac{H_U}{H_T}\int_0^t \frac{d\alpha}{dt} dt$	H_T H_U B a,b,c,d	isothermal heat of reaction ultimate heat of reaction constant exponents	[89]
ck4	$K = Ae^{-\Delta E/RT}$ $\frac{d\alpha}{dt} = \frac{K\alpha^m(1-\alpha)^n}{1+e^{C(\alpha-\alpha_{C0}-\alpha_{CT}T)}}$	m,n C α_{C0} α_{CT}	exponents diffusion constant "critical" degree of cure (T = 0 K) constant to account for increasing α_{C0}	[100]
ck5	$K_i = A_i e^{-\Delta E_i/RT}$ $\frac{d\alpha}{dt} = \frac{H_T}{H_U}(K_1 + K_2\beta^m)(1-\beta)^n$	H_T H_U m,n	isothermal heat of reaction ultimate heat of reaction exponents	[108,119]
ck6	$\frac{d\alpha}{dt} = \begin{cases} A_1(1-\alpha)^{m_1} e^{-\Delta E_1/RT} & \alpha \le \alpha_c \\ A_2(1-\alpha)^{m2} e^{-\Delta E_2/RT} & \alpha > \alpha_c \end{cases}$	m_i α_c	exponent critical degree of cure	[111]

Table continued on next page

Table A-3 continued

ck7	$K = Ae^{-\Delta E/RT}$ $\frac{d\alpha}{dt} = K\alpha^m \left(\alpha_{max} - \alpha\right)^{2-m}$	m α_{max}	exponent maximum degree of cure relationship	[117]
ck8	$K_i = A_i e^{-\Delta E_i/RT}$ $\frac{d\alpha}{dt} = \left(K_1 + K_2\alpha\right)\left(1-\alpha\right)^m + K_1\left(1-\alpha\right)^n$	m,n	exponents	[123]
ck9	$K_d = A_d e^{-\Delta E_d/RT}$ $K_p = A_{p0} e^{-\Delta E_{p0}/RT}\left(1 - \frac{\alpha}{\alpha_f}\right)^m$ $\frac{d\alpha}{dt} = K_p\left(1-\alpha\right)\left[R\right]$ $\frac{d\left[R\right]}{dt} = 2fK_d\left[I\right]$ $\frac{d\left[I\right]}{dt} = -K_d\left[I\right]$	α_f m f	final degree of cure exponent constant	[124]
ck10	$\frac{d\alpha}{dt} = K_1\left(T\right)K_2\left(\alpha\right)K_3\left(\alpha,T\right)K_4\left(I_d\right)$ $K_1\left(T\right) = Ae^{-\Delta E\left(\frac{T_{ref}}{T}-1\right)}$ $K_2\left(\alpha\right) = \sum_{i=0}^{s} a_i \cdot \alpha^i$ $K_3\left(\alpha,T\right) = \left(\alpha_{\max} - \alpha\right)^n$ $K_4\left(I_d\right) = \begin{cases} 0 & \text{if } I_d > 0 \\ 1 & \text{if } I_d \le 0 \end{cases}$	K_1(T) $K_2(\alpha)$ $K_3(\alpha, T)$ $K_4(I_d)$ α_{max} I_d a,s n	Arrhenius factor rate of conversion fitting a polynomial of degree s termination of kinetic reaction at α_{max} weight function of I_d accounting for inhibitor decomposition maximum degree of cure relationship induction time constants exponent	[138,139]

Table continued on next page

Table A-3 continued

ck11	$K = Ae^{-\Delta E/RT}$ $\frac{d\alpha}{dt} = K\alpha^m (1-\alpha)^n$ $m = C_1 e^{-C_2 T}$ $n = C_3 e^{-C_4 T}$	C_i	constants	[140]
ck12	See Appendix E.2			
ck13	See Appendix E.3			[144]
ck14	$K_i = A_i e^{-\Delta E_i/RT}$ $\frac{d\alpha}{dt} = \left(K_1 + K_2\alpha^m\right)(1-\alpha)^n$	m,n	exponents	[164]
ck15	$K_i = A_i e^{-\Delta E_i/RT}$ $\frac{d\alpha}{dt} = K_1\alpha^{m_1}(1-\alpha)^{n_1} + K_2\alpha^{m_2}(1-\alpha)^{n_2}$	m_i,n_i	exponents	[166]
ck16	$K_i = A_i e^{-\Delta E_i/RT}$ $\frac{d\alpha}{dt} = \left(K_1 + K_2\alpha^m\right)(1-\alpha)^n$ $\ln \alpha_T = \frac{-C_1\left(T - T_g\right)}{C_2 + T - T_g}$ $\frac{T_g - T_{g0}}{T_{g\infty} - T_{g0}} = \frac{\lambda\alpha}{(1-\lambda) + \lambda\alpha}$	C_i m,n T_g T_{g0} $T_{g\infty}$	constants exponents glass transition temperature T_g at initial cure T_g at full cure	[172]
ck17	See Appendix E.1			[135]

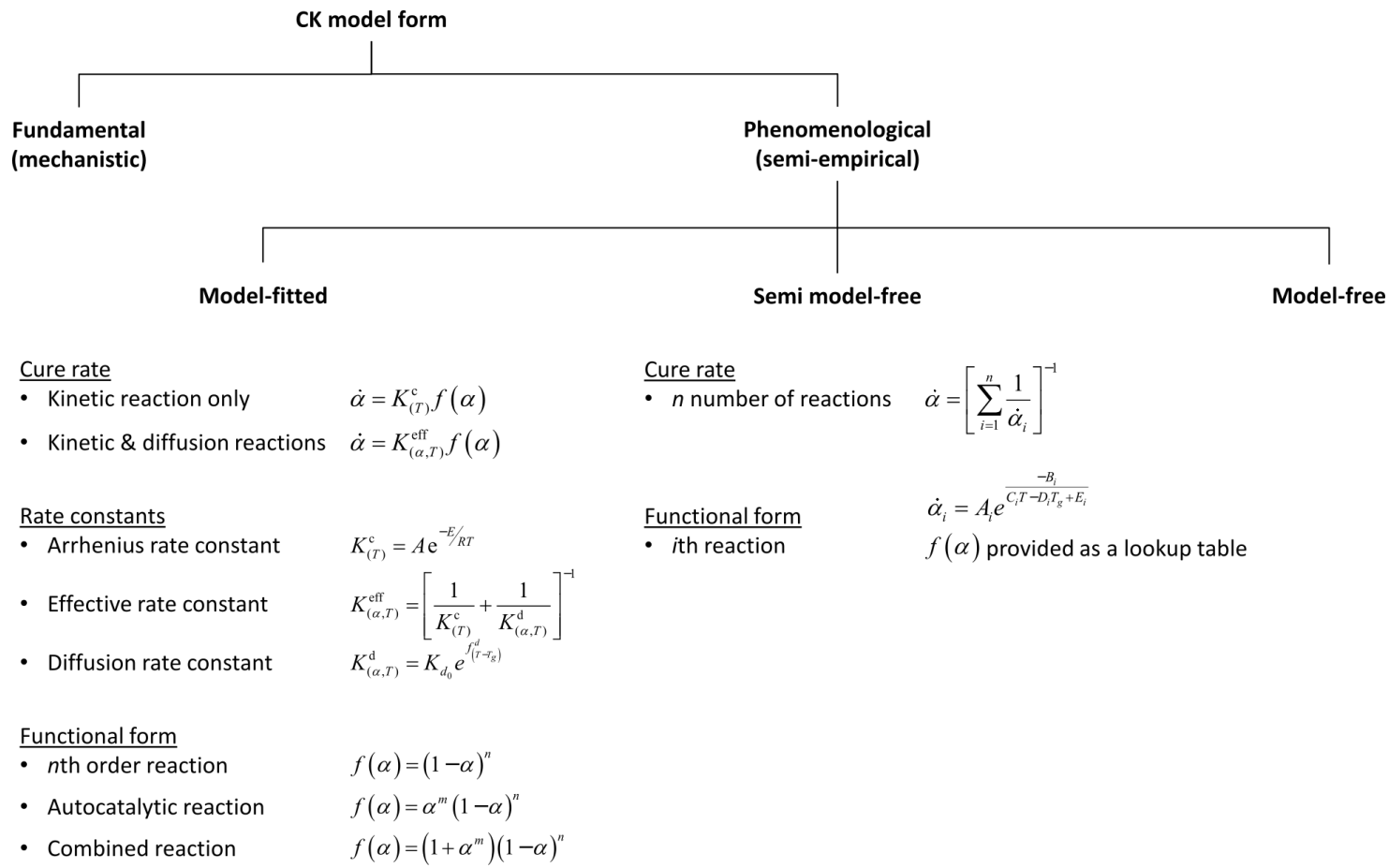

Figure A-1: General types of cure kinetics models developed for the thermal modelling of thermoset composites. Adapted from [100] (Johnston, 1997), [144] (Dykeman, 2008) and [181] (CMT Inc., 2017). CK: Cure Kinetics; $\dot{\alpha}$: cure rate; $f(\alpha)$: functional form.

Table A-4: Overview of studies reported from literature review of thick thermoset composites with respect to thermal management technology base.

Principal investigators	Material system	Simulation		Remarks	Ref.
		process modelling[a]	process control[b]		
Loos & Springer	CFRP	CURE code		Cure cycle design criteria proposed	[74,75]
Wu & Joseph	CFRP		QPA[c]	Autoclave control (expert-system) Method validated with simulated autoclave cure	[82]
Bogetti & Gillespie	GFRP	TGCURE code			[83–85]
Martinez	CFRP		user FD scheme	Predictive/adaptive control system for optimal cure schedules	[86]
Ciriscioli *et al*	CFRP	CURE code	SECURE code	Autoclave control (expert-system)	[88,89]
Twardowski *et al*	GFRP CFRP	user FD scheme			[90]
Telikicherla *et al*	CFRP	user FD scheme		Analysis based on Criscioli–Springer (1990)	[92]
Hojjati & Hoa	CFRP	user FD scheme		Simulation results in agreement with Twardowski (1993)	[93,94]
Joseph *et al*	CFRP	user FD scheme	SHMPC[d]	Autoclave control (model process control) Method validated with simulated data from Wu (1990) Revised cure cycle design criteria	[95,96]
Kim *et al*	GFRP CFRP	user FD scheme		Continuous cure method proposed Process model verified with experimental CFRP study	[97,98]
Johnston *et al*	CFRP/core	COMPRO 2D-FE code		Virtual autoclave concept proposed	[99–101]
Thomas *et al*	GFRP		SHMPC[d]	Method validated with experimental data	[104]
Pillai *et al*	GFRP		TGVCURE code	Autoclave control (model process control) Heuristics guided cure optimization Process model based on TGCURE code by Bogetti (1991)	[105–107]
Kim & Lee	CFRP	user FD scheme		Cure optimization	[108]
Kim & White	CFRP	user FD scheme			[109,110]
Joshi *et al*	CFRP	user subroutine with commercial FE (LUSAS)		Simulation results in agreement with Vodicka (1994) & CURE code predictions	[111]
Blest *et al*	CFRP	user FE method		Simulation results in agreement with Loos & Springer (1983)	[112]
Naji & Hoa	CFRP	user FD scheme			[113,114]
Yang & Lee	CFRP	CAHCD[e] code		Cure optimization	[115]
Michaud *et al*	GFRP		MULTICURE code	Autoclave control (model process control) Heuristics guided cure optimization Process model based on TGCURE code by Bogetti (1991)	[117,118]

Table continued on next page

Table A-4 continued

Principal investigators	Material system	Simulation		Remarks	Ref.
		process modelling[a]	process control[b]		
Oh & Lee	GFRP	user subroutine with commercial FE (ANSYS)		Cure optimization	[119]
Li *et al*	resin	user FE method		Cure optimization determined by DOT[f] software package	[120,121]
Antonucci *et al* (1)	CFRP	user FE method			[123]
Antonucci *et al* (2)	GFRP	user FE method		Cure optimization	[124]
AIM-C	CFRP	COMPRO 2D-FE code		Cure cycle evaluation & development	[129,130]
Costa & Sousa	CFRP	user FE method		Simulation results in agreement closed-form data from Dave (1987) & numerical predictions from Young (1996)	[131]
Shin & Hahn	CFRP	user FD scheme			[132]
Parathsarathy *et al*	GFRP	user FD scheme	user FD scheme	Autoclave control (model process control)	[133]
Ruiz & Trochu	GFRP	user FD scheme		Cure optimization determined by genetic algorithm	[138,139]
Guo *et al*	CFRP	user subroutine with commercial FE (ANSYS)			[140]
Shimizu *et al*	CFRP	COMPRO 2D-FE code		HTC back-calculation methods proposed	[145]
Slesinger *et al*	CFRP	RAVEN software		Thermal modelling validation techniques introduced	[149,150]
Mamani & Hoa	GFRP	user FD scheme			[164]
Gude *et al*	CFRP	PAM-RTM software		Thermal model inputs validated experimentally	[166]
Ma *et al*	GFRP	user subroutine with PAM-RTM software		Nonisothermal infusion & cure model validated experimentally	[171,172]
Shah *et al*	CFRP	COMPRO CCA code with commercial FE (ABAQUS)		Simulation results in agreement with numerical predictions from Costa (2003) & Carlone (2009) Cure optimization determined by genetic algorithm	[173]
Belnoue *et al*	CFRP	user subroutine with commercial FE (ABAQUS)		Novel multiscale modelling framework devised that includes a hyper-viscoelastic constitutive model	[174]

[a] FD: Finite Difference; FE: Finite Element
[b] AI: artificial intelligence (eg. machine learning, expert-systems, neural networks)
[c] QPA: qualitative process automation
[d] SHMPC: shrinking horizon model predictive control
[e] CAHCD: computer aided heating cycle design
[f] DOT: design optimization tool

Table A-5: Overview of thermal management studies of thick thermoset composites in the scientific literature based on ETPM factory ontology.

Principal investigators	Material system	Laminate thickness (mm)	Science[a]	Technology[a]	Practice[a]	Remarks	Ref.
Loos & Springer	CFRP	1.9 mm, 3.8 mm, 7.8 mm	(P, M)	(P, M)		Cure cycle design criteria proposed	[74,75]
Bogetti & Gillespie	GFRP	25.4 mm 13.8 mm, 18.5 mm, 25.4 mm, 33.9 mm, 50.8 mm, 76.2 mm	(P, M) (P, M)				[83,84] [85]
Martinez	CFRP	24.9 mm	(T, P, M)	(T, P, M)			[86]
Ciriscioli *et al*	CFRP	2.6 mm, 10 mm, 8.6 mm, 34.9 mm		(P, M)			[88,89]
Twardowski *et al*	GFRP CFRP	50 mm	(P, M)			Thick composites (≥ 50 mm)	[90]
Telikicherla *et al*	CFRP	0.95 mm, 1.9 mm, 3.8 mm, 5.7 mm	(T, P, M)				[92]
Hojjati & Hoa	CFRP	25 mm, 35mm, 50 mm, 60 mm, 80 mm, 100 mm, 150 mm, 300 mm	(P, M)				[93,94]
Kim *et al*	GFRP CFRP	50 mm 100 mm	(P, M)				[97,98]
Johnston *et al*	CFRP/core	28.2 mm	(E, T, P, M)				[99–101]
Joseph *et al*	CFRP	19 mm, 33.8 mm 16.8 mm		(P, M)		Revised cure cycle design criteria	[95,96]
Thomas *et al*	GFRP	5.3 mm	(P, M)	(P, M)			[104]
Pillai *et al*	GFRP	25.4 mm	(T, P, M)	(T, P, M)			[105–107]
Kim & Lee	CFRP	15 mm, 30 mm	(P, M)	(P, M)			[108]
Kim & White	CFRP	25.4 mm, 75 mm	(P) (M)				[109,110]
Joshi *et al*	CFRP	23.1 mm	(T, P, M)				[111]
Blest *et al*	CFRP	7.8 mm	(P, M)				[112]
Naji & Hoa	CFRP	8 mm,	(P, M)				[113,114]
Yang & Lee	CFRP	12.5 mm, 25 mm, 50 mm 12.5 mm	(P, M)				[115]
Michaud *et al*	GFRP	25.4 mm	(T, P, M)			Thick composites (> 20 mm) RTM process	[117,118]
Oh & Lee	GFRP	20 mm	(T, P, M)	(T, P, M)			[119]
Li *et al*	resin	2.0 mm, 40 mm	(T, P, M)	(T, P, M)			[120,121]

Table continued on next page

Table A-5 continued

Principal investigators	Material system	Laminate thickness (mm)	Science[a]	Technology[a]	Practice[a]	Remarks	Ref.
Antonucci *et al* (1)	CFRP	30 mm	(E, P, M)				[122,123]
Antonucci *et al* (2)	GFRP	6.8 mm, 10 mm, 13.5 mm	(T, P, M)			RTM process	[124]
AIM-C	CFRP	17.8 mm 22.4 mm, 89 mm, 127 mm			(E, T, P, M)		[129,130]
Costa & Sousa	CFRP	10mm, 12.5mm, 36.5 mm, 50 mm	(T, P, M)				[131]
Shin & Hahn	CFRP	30 mm, 50 mm	(T, P, M)				[132]
Parathsarathy *et al*	GFRP	4.8 mm, 5.4 mm, 14.4 mm	(P, M)	(P, M)			[133]
Ruiz & Trochu	GFRP	3mm, 15 mm	(P, M)	(P, M)		RTM (automotive)	[138,139]
Guo *et al*	CFRP	20 mm	(T, P, M)				[140]
Shimizu *et al*	CFRP	38.4 mm	(E, T, P, M)				[145]
Slesinger *et al*	CFRP	7.5 mm, 11.7 mm, 14.7mm	(E, T, P, M)				[149,150]
Mamani & Hoa	GFRP	18.3 mm	(T, P, M)				[164]
Gude *et al*	CFRP	100 mm	(E, T, P, M)			RTM (aerospace OOA)	[166]
Ma *et al*	GFRP	76.2 mm	(P, M)			VARTM (wind energy)	[171,172]
Shah *et al*	CFRP	1.2mm, 12 mm, 36.5 mm	(P, M)	(P) (M)			[173]
Belnoue *et al*	CFRP	18 mm	(E, T, P, M)			CK validation for AFP/wrinkling study	[174]

[a] ETPM: Equipment–Tool–Part–Material

Table A-6: Overview of studies of thick thermoset composites in the scientific literature based on the ETPM factory ontology with respect to thermal management.

Principal investigators	Equipment (E)	Tool & consumables (T)		Part (P)		Material & process (M)			Ref.
	heating system	geometry & thickness (mm)	consumables	geometry	thickness (mm)	material system		cycle[a]	
Loos & Springer	autoclave	tool plate	bleeder, edge dam	flat	1.9 mm, 3.8 mm, 7.8 mm	graphite/epoxy	AS/3501-6	1-hold 2-hold MRCC	[74,75]
Bogetti & Gillespie	autoclave	Al-alloy tool plate (6.4 mm)	bleeder, edge dam	flat	25.4 mm	glass/polyester	E-glass/4102	2-hold MRCC modified cure	[83,84]
	autoclave			flat	13.8 mm, 18.5 mm, 25.4 mm, 33.9 mm, 50.8 mm, 76.2 mm			2-hold 3-hold MRCC	[85]
Martinez	autoclave	G7 glass/silicone tool plate (12.7 mm)	bleeder, caul edge dam	flat	24.9 mm	graphite/epoxy	IM6/3506-1	1-hold 2-hold optimized cure	[86]
Ciriscioli *et al*	autoclave	Al-alloy tool plate (9.5 mm)	bleeder	flat	2.6 mm, 8.6 mm, 34.9 mm 10.0 mm	graphite/epoxy	T300/976 AS/3601-6	optimized cure	[88,89]
Twardowski *et al*	press	steel frame	bleeder, edge dam	flat	50 mm	glass/epoxy graphite/epoxy	3M Scotchply 1003 HyE 1676N AS4/3501-6	MRCC modified cure	[90]
Telikicherla *et al*	autoclave	tool plate	bleeder	flat	0.95 mm, 1.9 mm, 3.8 mm, 5.7 mm	graphite/epoxy	AS/3501-6	1-hold	[92]
Hojjati & Hoa	autoclave			flat	25 mm, 35mm, 50 mm, 60 mm, 80 mm, 100 mm, 150 mm, 300 mm	graphite/epoxy	AS/3501-6	2-hold MRCC 3-hold MRCC modified cure	[93]
	autoclave	Al-alloy tool plate	bleeder, edge dam	flat	38mm, 40mm, 45 mm	graphite/epoxy	AS/3501-6	3-hold MRCC	[94]
Kim *et al*	press	Al-alloy tool plate (7 mm)	bleeder, plunger	flat	100 mm	graphite/epoxy	AS4/3501-6	CCM cure	[97,98]
Johnston *et al*	industrial autoclave	Invar tool face plate (25.4 mm)	caul	panel	28.2 mm	carbon/epoxy core	AS4/8552 glass/phenolic core	3-hold MRCC 2-hold	[99–101]
Joseph *et al*	autoclave			flat	16.8mm, 19 mm, 33.8 mm	graphite/epoxy	AS4/3506-1	2-hold optimized cure	[95,96]
Thomas *et al*	press		silicone outer bag, bleeder, edge dam	flat	5.3 mm	glass/epoxy	E-glass/8551-7A	2-hold optimized cure	[104]
Pillai *et al*	autoclave	Al-alloy tool plate (6.4 mm)	bleeder, caul	flat	25.4 mm	glass/polyester	E-glass/4102	optimized cure	[105–107]
Kim & Lee	autoclave	Al-alloy tool plate	bleeder, edge dam	flat	15 mm, 30 mm	carbon/epoxy	USN150 prepreg	2-hold MRCC modified cure	[108]
Kim & White	autoclave			flat	25.4 mm, 75 mm	graphite/epoxy	AS/3501-6	2-hold MRCC	[109,110]
Joshi *et al*	autoclave	Al-alloy tool plate (13 mm)		flat	23.1 mm	graphite/epoxy	AS4/3501-6	1-hold	[111]
Blest *et al*	autoclave			flat	7.8 mm	graphite/epoxy	AS4/3501-6	1-hold	[112]

Table continued on next page

Table A-6 continued

Principal investigators	Equipment (E) heating system	Tool & consumables (T) geometry & thickness (mm)	consumables	Part (P) geometry	thickness (mm)	Material & process (M) material system		cycle[a]	Ref.
Naji & Hoa	autoclave	Al-alloy tool plate (25 mm)	bleeder, edge dam	L-shaped laminate	8 mm	graphite/epoxy	AS4/3501-6	2-hold MRCC 3-hold MRCC	[113,114]
Yang & Lee	autoclave			flat	12.5 mm, 25 mm, 50 mm 12.5 mm	graphite/epoxy	T300/3501-6 913C-HTA-5-34	2-hold MRCC optimized cure optimized cure	[115]
Michaud *et al*	press	Al-alloy matched tool (12.7 mm)		flat	25.4 mm	glass/vinyl-ester	E-glass/411-C50	1-hold	[117,118]
Li *et al*	press	Al-alloy matched tool (2 mm, 5 mm)		flat	2.0 mm, 40 mm	epoxy	EPON 862/W	optimized cure	[120,121]
Antonucci *et al* (1)	industrial autoclave	Al-alloy tool (RTM mould)	bleeder	flat	30 mm	carbon/epoxy		1-hold 2-hold	[123]
Antonucci *et al* (2)				flat	6.8 mm, 10 mm, 13.5 mm	glass/polyester		1-hold optimized cure	[124]
AIM-C	autoclave	CFRP, Invar, Al-alloy Invar tool (12.7 mm)		flat flat	17.8 mm 22.4 mm, 89 mm, 127 mm	carbon/epoxy	IM7/977-3 IM7/8552 IM7/977-3	MRCC optimized cure optimized cure	[129,130]
Costa & Sousa	autoclave	tool plate	bleeder	flat	10mm, 12.5mm, 36.5 mm, 50 mm	graphite/epoxy	AS4/3501-6	1-hold 3-hold optimized cure	[131]
Shin & Hahn	press	steel picture-frame	bleeder, caul edge dam	flat	30 mm, 50 mm	graphite/epoxy	AS4/3501-6	2-hold MRCC	[132]
Parthasarathy *et al*	press			flat	4.8 mm, 5.4 mm, 14.4 mm, 21.6 mm	glass/epoxy	E-glass/MXB7701	1-hold MRCC MPC cure	[133]
Ruiz & Trochu		Al-alloy tool plate (15 mm)		flat	3mm, 15 mm	glass/polyester	U101/T580-63 NCS 82620/ T580-63	1-hold optimized cure	[138,139]
Guo *et al*	autoclave	Al-alloy tool plate (35 mm)	bleeder, caul, edge dam	flat	20 mm	carbon/epoxy	T300/HD03	2-hold MRCC	[140]
Shimizu *et al*	autoclave	Al-alloy tool plate (25.4 mm)	edges insulated	flat	38.4 mm	carbon/epoxy	AS4/8552-1	1-hold 2-hold	[145]
Slesinger *et al*	autoclave	KE1204 RTV insulating bricks (16 mm)	edges insulated	flat	11.7 mm, 14.7mm 7.5 mm	carbon/epoxy	AS4/8552-1 T800H/3900-2	1-hold	[149,150]

Table continued on next page

Table A-6 continued

Principal investigators	Equipment (E)	Tool & consumables (T)		Part (P)		Material & process (M)			Ref.
	heating system	geometry & thickness (mm)	consumables	geometry	thickness (mm)	material system		cycle[a]	
Mamani & Hoa	autoclave	Al-alloy tool plate (50 mm)	bleeder, caul	flat	18.3 mm	glass/epoxy	S2-glass/E773	2-hold MRCC	[164]
Gude *et al*	oven	Al-alloy tool (RTM mould)		flat	100 mm	carbon/epoxy	GV300TFX/RTM6	1-hold	[166]
Ma *et al*	heated tool		infusion medium	flat	76.2 mm	glass/epoxy	E-LT2400-7P/780E+785H	2-hold	[171,172]
Shah *et al*				flat	36.5 mm 1.2 mm, 12 mm	graphite/epoxy	AS4/3501-6	3-hold 2-hold MRCC optimized cure	[173]
Belnoue *et al*	autoclave	Al-alloy tool plate (10 mm)		flat	18 mm	carbon/epoxy	IM7/8552	2-hold MRCC	[174]

[a] MRCC: Manufacturer Recommended Cure Cycle

Appendix B SME Qualitative Research Study Documentation

The research study protocol and methods and participant consent form for the qualitative industrial composites SME case studies presented in Section 3.2 are shown here.

B.1 Research study interview questions

Study:
Science based decision making strategies in composites manufacturing practice: An investigation of the impact and value creation for small and medium sized enterprise (SME) sized firms in Western Canada.

Research Method:
The primary research method used in this study will be expert interviews conducted by the principle investigator (PI) and faculty supervisor. Each interview is expected to last approximately 1-2 hours within an April to July 2016 time frame. The interview questions will reflect the research questions guiding this study and will invite research participants to comment on their experiences in using a science based approach to make decisions relating to technical problems and/or market needs in composites manufacturing. No personal information will be requested, except for their personal opinions and comments on composites manufacturing competitiveness (eg. cost, efficiency, quality). We are seeking research participants who are interested in discussing their technical and market decision making processes, how the use of a science based approach was useful in making these types of decisions and the value created in adopting this approach to solve their technical problems and/or market needs.

Interview Questions:
The following questions will be asked in interviews with research participants:

i) Please describe the technical problems and/or unmet market needs required you to make decisions and in what circumstances?

ii) On what basis or criteria were these technical and/or market decisions made?

iii) What aspects of the science based decision making approach were useful in order to make these technical and/or market decisions?

iv) What were the steps taken to resolve the given technical problem and/or unmet market need?
   a) Did this involve the introduction of a new innovative process?
   b) Did this require disrupting an existing process?

v) Were the outcomes of the technical and/or market decisions successful?
   a) If successful, how was value created?

vi) In what ways did a science based approach facilitate or alter your decision making process?

vii) Did the use of a science based decision making approach lower technical and/or market risk and uncertainty and in what way?

Contact for concerns about your rights as a research participant:
If you have any concerns about your treatment or rights as a research participant, please contact (director), The Office of Research Ethics at SFU. In all correspondence with ORE, please use the following study application number: (application number).

Contact for information about the study:
If you have any question or would like further information regarding this study, you may contact (principal investigator) and/or (faculty supervisor). Please be aware that email and the telephone are not considered to be confidential mediums.

B.2 Informed consent form

Study procedures:
Permission for your participation in this study will not be sought from your employer. Your participation will involve an interview of 1–2 hours within an April to July 2016 time frame, where you will be asked about your experiences in using a science based decision making approach to address technical problems and/or market needs in composites manufacturing.

Participants will be interviewed by (principal investigator) and/or (faculty supervisor) for this study. Interviews can be carried out by telephone and/or face-to-face meetings either at your company premises or an office at Simon Fraser University. If you do prefer to conduct a telephone interview, please post your written consent form to the postal address provided at the end of this form. Please be aware that email and the telephone are not considered to be confidential mediums. With your permission, the interview will be recorded and then transcribed to accurately record your comments and opinions. If you prefer the interview not to be recorded, written notes alone will be taken. The identity of the organization, interviewees, and the referrers, if any, will be anonymized in our publications for external communications.

Project outcomes:
Possible outcomes from this research study include: journal publications and/or case study exemplars. Draft copies of any publications for external communications will be provided to you for review.

Potential benefits:
The key benefit of this study is to better understand of how using a science based approach can improve composites manufacturing and design decision making in the presence of high technical and market risk and uncertainty. You may have the opportunity to express your opinions and comments regarding composites manufacturing competitiveness and trends in the composites industry.

Potential risks:
The risks to you as a research participant in this study are minimal. You will only be asked to discuss your own experiences with respect to technical and market decision making processes in composites manufacturing and how the use of a science based approach was useful in making these types of decisions. Refusal to participate or withdrawal/dropout after agreeing to participate will not have an adverse effect or consequences on your employment.

Confidentiality:
Any information that is obtained during this study will be kept confidential. No one other than the principal investigator and faculty supervisor for this study will have access to the information you provide in this study. Participant names will not appear on any documentation or in any resulting publications for external communications. Organizational names will not be attached to specific statements or information.

Interview tapes, consent forms and written notes will be stored in a locked filing cabinet at SFU for a minimum of three months after your interview. Interview tapes will be given numerical identifiers for transcription. Interview tapes will be erased immediately once transcription is complete and stored on a secured server administered by SFU. Written interview notes and any company documents that you may provide us will be masked of any identifying information, including company names and/or logos, before being scanned and stored on a secured server administered by SFU. These documents will be immediately destroyed once stored on a secure server administered by SFU. The data and information collected in this study may be used again and will be subject to the maintenance of confidentiality as stated above. UBC policy requires that the research data collected be retained for a minimum of five (5) years after publication in a UBC facility, after which all electronic and written data, including consent forms, will be disposed as per SFU policy.

Withdrawing your consent:
We will remove all information that could identify you or your organization from the data we have collected within three months of your interview and delete it permanently. You can withdraw your consent to participate for any reason and have your data immediately destroyed by contacting us within this time period. After this time, it is not possible to withdraw your consent to participate as we have no way of knowing which responses yours are. Additionally, you will not be able to withdraw consent once papers and publications have been submitted to publishers.

Reimbursements and Payments:
Please be advised that you will not be reimbursed for participating in this study.

In the event of future contact:
Please indicate your approval for future contact at the end of this consent form. If you do consent to future contact, any future contact by the principal investigator or faculty supervisor for this study will be done by email or telephone to arrange any follow up interviews or correspondence. Please be aware that email and the telephone are not considered to be confidential mediums.

Contact for information about the study:
If you have any question or would like further information regarding this study, you may contact (principal investigator) and/or (faculty supervisor). Please be aware that email and the telephone are not considered to be confidential mediums.

Contact for concerns about your rights as a research participant:
If you have any concerns about your treatment or rights as a research participant, please contact (Director) The Office of Research Ethics at SFU. In all correspondence with ORE, please use the following study application number: (application number).

Written consent:
Your signature on this form will signify that you have received a document which describes the procedures, whether there are possible risks and benefits of this research study, that you have received an adequate opportunity to consider the information in the documents describing the study and that you voluntarily agree to participate in the study.

As the research participant, I hereby agree to participate in the research study named above, I certify that I have read the requirements specified above and agreed to be interviewed. I understand the interview procedure to be used in this study and the personal risks and contributions of my participation as described above.

The participant and witness shall fill in this area. Please print legibly:

Participant Last Name	Participant First Name
Participant Contact Information:	
Please indicate if you approve of future contact (circle your response) YES / NO	
Participant Signature	Witness
Date (YYYY/MM/DD)	Date (YYYY/MM/DD)

If you prefer to conduct a telephone interview, please post your written consent form in an envelope marked confidential to the following postal address:

(Research Study Faculty Supervisor)

Mailing address and contact information

Application number

Appendix C Proposed Thermal Management Knowledge in Practice Document Topics

In this appendix, science based knowledge and design practice document topics for thermal management are proposed. Further details for selected thermal management topics are given as examples, including:

- Material screening and characterization
- Cure cycle development and evaluation

ETPM factory ontology scratchpad tools to systematically capture manufacturing scenarios using simulation based thinking are provided in C.2, including a decision tree (introduced in Section 4.3) and attribute canvas (introduced in Sections 5.2.1 and 5.3.1).

C.1 Positioning science based knowledge

The *Knowledge in Practice* framework, introduced in Chapter 4 (see Figure C-1) is intended to be an interface between open literature, and industrial specifications and design methods. This framework developed in this work is represented by two orthogonal manufacturing problems faced in industrial practice. Factory and producibility concepts are discussed in Section 4.2.1 and can be characterized using the ETPM factory ontology.

There are three structured layers:

- *Knowledge base* layer is intended to provide a science based understanding of manufacturing design choices and their response for given design problems (see Table C-1). Thermal management examples of this layer include knowing what resin cure kinetics is and how to

characterize it, understanding how the hold and ramp segments of cure cycles affect the temperature history of parts and tools, and knowing why the consideration of airflow uniformity, along with temperature uniformity, in autoclave and oven processing is important.

- *Design practice* layer is intended to provide engineers guidelines of the steps to consider and the traps to avoid, how to identify uncertainty, and knowing what knowledge is available to make informed decisions (see Table C-2). What to consider when specifying and qualifying an autoclave, how to develop a thermal profiling plan, how to assess apparent or real failures in an experimental thermal profile, and the steps to perform a thermal assessment using simulation are examples of thermal management design practice.

- *Case study* layer is intended to provide practical examples of knowledge use in practice (refer to Sections 5.2 and 5.3).

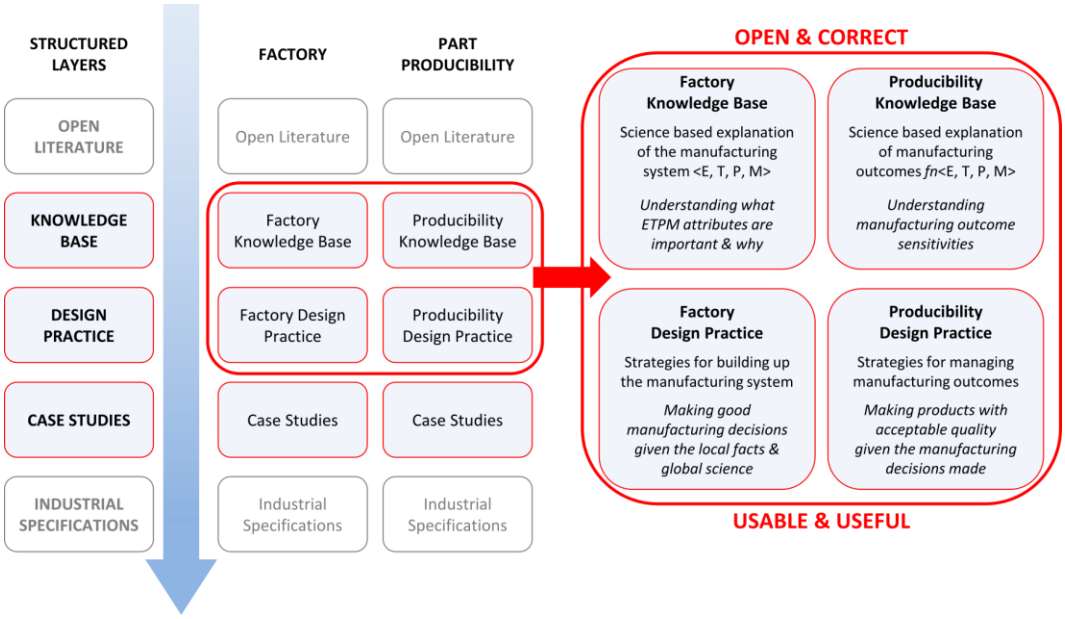

Figure C-1: The *Knowledge in Practice* framework is intended to act as an interface between open literature and industrial specifications and design methods. ETPM: Equipment–Tool–Part–Material; *fn:* function.

Table C-1: Proposed science based knowledge topics for thermal management.

Science based knowledge topics (KPD type[a,b]: Factory)
Equipment (E) • Understanding mechanisms of heat transfer (eg. conduction, convection, radiation): – The effect of gas pressure on heat transfer/HTC[c] – Thermal uniformity versus airflow uniformity • Sensors (limitations/trade-offs) – HTC/airflow (boundary conditions) (eg. visual inspection (tufting), calorimeters, heat flux sensors, IR[d] thermography, virtual: CFD[d], …) – Material point (outcomes) (eg. TCs[e], dielectric sensors, virtualTCs[e], …) • New approaches/techniques – Integrally heated tools – Quickstep concepts
Tool & consumables (T) • Tooling materials – Effects of thermal diffusivity (eg. standard existing/new materials, hybrids) – Evaluating new consumable materials (eg. thermal trade-offs) • Thermal ageing of tools
Part (P) …
Material & process (M) • Understanding thermosets – Cure: crosslinking (eg. DOC[f], gelation) & reactions (eg. cure kinetics, thermal diffusion) – Characteristics of esters, vinyl esters, epoxies, … • Understanding thermoplastics – Crystallization/melt kinetics (eg. DOX[f], lamellae structure) – Characteristics of PEEK[g], PEKK[g], … • Understanding important material properties for thermal management – C_p, T_g, k, … – Viscosity – Path dependent behaviour (eg. $T_g = f(\alpha, t, T)$) • Characterization instruments (measure) ▪ Limitations/trade-offs (eg. MDSC[h], TGA[h], TMA[h], rheometer, …) • Constitutive models/representations (model) ▪ Limitations/trade-offs (eg. semi-empirical: model fitted, 'semi model-free', …) ▪ Process maps • Understanding the characteristics of a cure cycle (process requirements) – The role of ramps (heat up/cool down) & holds (eg. intermediate/final hold) – Transient steady-state condition (eg. T distribution through-thickness) – Upper/lower bounds – What happens in key phases/regimes: ▪ Pre-gelation (resin: predominantly liquid phase) (eg. gelation $\alpha < \alpha_{gel}(t, T)$) ▪ Pre-solidification (resin: viscoelastic phase) (eg. vitrification $T_g > T(t, T)$)

Table continued on next page

Table C-1 continued

Science based knowledge topics (KPD type[a,b]: Factory)
Boundary conditions (E, T) • Understand airflow around one or more parts – Autoclave/oven loading with racks & multiple parts – Methods to determine HTC[c]/characterize airflow distribution – HTC[c] interaction effects (eg. effective top & bottom) • 2D heat flow (eg. edge effects, tool size effects, effect of uninsulated tools)
Material point response (*outcome*) (E, T, P, M) • Cure window robustness (probabilistic analysis) • Strategies to mitigate exotherm/thermal lag, achieve desired final DOC/DOX[f], …

[a] KPD: Knowledge in Practice Document
[b] ETPM: Equipment–Tool–Part–Material
[c] HTC: Heat Transfer Coefficient
[d] IR: Infrared; CFD: Computational Fluid Dynamics
[e] TC: Thermocouple
[f] DOC: Degree of Cure; DOX: Degree of Crystallization
[g] PEEK: Polyetheretherketone; PEKK: Polyetherketoneketone
[h] MDSC: Modulated Differential Scanning Calorimetry; TGA: Thermogravimetric Analysis; TMA: Thermomechanical Analysis

Table C-2: Proposed design practice topics for thermal management.

Design practice topics (KPD type[a,b]: Factory)

Equipment (E)
• Development/optimize
  – Autoclave specification
  ▪ Heating/cooling system, vacuum system
  Determination of representative thermal load
  Methods for evaluating parasitic thermal resistances (eg. wall, floor, rack)
  ▪ Fan capacity/power supply
  Methods for evaluating airflow behaviour (eg. pressurized/unpressurized)
  Strategies for managing airflow uniformity (eg. baffling/ducting)
  – Evaluating existing systems/recommendations for improvements

Tool & consumables (T)
• Development/optimize
  – Tool design
  ▪ Tool plate (skin) thickness
  ▪ Tool substructure geometry
  ▪ Welding/joining patterns
  – Qualification for new consumable materials
• Troubleshooting
  – Strategies for managing thermal hot/cold spots

Part (P)
• Development/optimize
  – Determination of representative proxy (eg. part family/charge)
  – Guidance on the design of representative parts
  – Identifying the zones/features of interest (size/complexity scaling)
  (eg. thin/thick solid laminate, sandwich, co-cured/co-bonded, pad-ups/zones)

Material & process (M)
• Development/optimize
  – Material qualification
  (material requirements for new materials/material substitution (equivalency))
  ▪ Assessment of thermal responsiveness relative to baselines
  ▪ Range of manufacturable thicknesses
  ▪ Discriminator tests/characterization protocols/methods (measure):
  Obtaining MDSC[c] data for cure kinetics (eg. nonisothermal, isothermal)
  Obtaining crystallization/melt data
  Viscosity measurements
  Thermal conductivity measurements
  ▪ Data fit/model fit procedures (model):
  Fitting baselines, determination of transitions (eg. reversing C_p signal)
  Model validation techniques
  – Process specifications (requirements)
  ▪ MRCC[d] determination
  ▪ Cure cycle evaluation/development relative to MRCC[d]
  Nominal/upper/lower bounds
  For two phase materials
  + For multiple phase materials (eg. interleaved/particle toughened materials)
  – Recommendations for improving existing M&P specifications (disrupt)

Table continued on next page

Table C-2 continued

Design practice topics (KPD type[a,b]: Producibility)
Boundary conditions (E, T) • Development/optimize – Thermal tool survey (measure) – Recommendations for improving existing specification requirements (disrupt) (eg. specify airflow requirements rather than thermal uniformity requirements) • Troubleshoot – Strategies to improve airflow uniformity (eg. introduce baffling/ducting)
Material point response (*outcome*) (E, T, P, M) • Thermal modelling practice – Validation of model inputs (material models/boundary conditions) – Determination of model complexity (‘right-sizing’ the problem) (eg. 1D drill point, 3D model with all thermal resistances explicitly modelled) • Development/optimize – Thermal assessment (model)/experimental thermal profile (measure)/ Conceptual design (eg. $((e)_w, (t)_x, (p)_y, (m)_z) = (1, 1, 1, 3,)$): ▪ Guidance as to whether design choices (manufacturing system) are likely to fall within/outside process requirements – Preliminary design/Trade Study (eg. $((e)_w, (t)_x, (p)_y, (m)_z) = (2, 2, 2, 3)$): ▪ Thermal profiling plan/documentation + What are the best practices for evaluating a representative charge? In-plane dimensions? What are the fewest thermocouples that can be instrumented? How should I insulate the tool to represent production? Where should the tool be placed in the autoclave to represent production? What cycle should be used? Analyzing results (eg. check acceptance of method, how to reduce/interpret the data) ▪ Determination of TC/sensor location (eg. part, tool, lead/lag/proxy) (eg. production scale part, part trim/edge band, proxy part (charge)) Detail design (eg. $((e)_w, (t)_x, (p)_y, (m)_z) = (3, 3, 3, 3)$): ▪ Validation of manufacturing choices (physical manufacturing system) • Troubleshoot – Production (eg. $[(e)_w, (t)_x, (p)_y, (m)_z] = [3, 3, 3, 3]$): – Apparent/real thermocouple (sensor) failure assessment – Cure cycle deviation (eg. bridging program, aborts) – Introduction of air gaps (eg. bag leaks, parts lifting off tools)

[a] KPD: Knowledge in Practice Document
[b] ETPM: Equipment–Tool–Part–Material; w, x, y, z: design-gate indices
An explanation of ETPM design states and design-gate indices is given in Section 4.2.4.
[c] MDSC: Modulated Differential Scanning Calorimetry
[d] MRCC: Manufacturer Recommended Cure Cycle

C.1.1 Material screening and characterization (subset of material qualification)

Table C-3: Material screening and characterization science based practice example.

	Material characterization: nominal
Open literature	*Fundamentals of material performance outcomes* (eg. importance of resin properties in compression & shear loading) *Fundamentals of material structure outcomes* • Thermoset cure, including T_g & DOC • For thermosets, including viscosity, viscoelasticity, … • For toughened thermosets, including effect of T_g, DOC, morphology, … • Tack behaviour (eg. what is it, how does fiber architecture, degree of impregnation, resin neat behaviour affect tack?) • Outgassing during cure • Measuring residual stress • …
Knowledge (Factory KPD[a])	*Understanding how material performance outcomes are tied to material constituents* (eg. neat resin, fibre architecture, other architectural features) • Identifying the state of the art in terms of how well it is understood to come together *Understanding the effect of process parameter outcomes on material structure & performance outcomes* • The response of the ETPM[b] system as a function of: – size scaling – production scaling • What is the rationale for the T_g+ 50 rule? Is it always applicable? How is any change in this rule tied to design approaches? • The relative effect of residual stress formation (eg. impact of residual stress on microcracking) • Sensitivity of specific structural elements (eg. stiffener configuration) to specific materials & outcomes • …
Practice (Factory KPD[a])	*How to define a 'good' material* • High level integration of many KPDs (eg. draws on KPD[a] for cure cycle development & others) • Managing: – outcomes (eg. tack, degree of impregnation) – size scaling issues (eg. laminate thickness, ply drops, other geometrical features) – production scaling issues (eg. compatibility with manufacturing processes: hand layup, AFP[c], …) • Managing compatibility with other materials and requirements • Balancing conflicting requirements *How to assess material performance* '*fatal-flaws*' • Managing sensitivities due to moisture, solvents, environments, fatigue, microcracking • Managing the effects of variation in cure cycle (nominal, upper & lower bounds) on outcomes

[a] KPD: Knowledge in Practice Document
[b] ETPM: Equipment–Tool–Part–Material
[c] AFP: Automated Fibre Placement

C.1.2 Cure cycle development and evaluation (subset of material qualification)

Table C-4: Cure cycle development and evaluation science based practice example.

	Cure cycle development for two phase material systems (eg. Hexcel AS4/8552)	**Cure cycle development for multiple phase material systems (eg. Toray T800H/3900-2)**
Open literature	*Fundamentals of thermoset response (cure management)* • Thermoset cure kinetics • T_g & DOC • Viscosity as a function of temperature & DOC • Prepreg morphology as a function of T & DOC (eg. permeability) • Outgassing during cure • Relationship between properties & structure in thermosets • …	Same as left + *Fundamentals of thermoplastic response (crystallization/melt management)* • Thermoplastic crystallization/melt kinetics • Miscibility of polymers • T_g of blends • Path dependencies (eg. phase separation/formation) • Relationship between properties & structure in blends and mixes • …
Knowledge (Factory KPD[a])	*Understanding cure in a part on a tool in a heating system* • Fundamentals of heat transfer from 1D to3D • The effects of ramps and holds in a cure cycle • The response of the ETPM[b] factory system: – size scaling – production scaling • …	Same as left
Practice (Factory KPD[a])	*How to design the nominal cycle: temperature, pressure, vacuum* • Managing outcomes: – process parameter (eg. cure cycle) – material structure (eg. viscosity, DOC) – material performance (eg. mechanical test results) • Managing issues relating to size scaling (eg. laminate thickness, ply drops, other features) • Managing compatibility with other materials & requirements • Balancing conflicting requirements *How to design the upper & lower bounds of the cycle specification* • At material level, managing the effects of variation in: – heat up/cool down rates – intermediate & final holds • At structural level, managing: – through-thickness variation effects – in-plane variation effects	Same as left + • Managing the additional effects of thermoplastic morphology on manufacturing & structural design outcomes – nominal cure cycle – upper (fast) & lower (slow) bounds

[a] KPD: Knowledge in Practice Document
[b] ETPM: Equipment–Tool–Part–Material

Table C-5: Manufacturer recommended cure cycle[a] for Hexcel AS4/552 and Toray T800H/3900-2.

	Hexcel AS4/8552[b]	**Toray T800H/3900-2[c]**
MRCC (nominal)	Heat at 1-3 °C/ min to 110 °C ± 5 °C Hold at 110 °C ± 5 °C for 60 min ± 5 min Heat at 1-3 °C/ min to 180 °C ± 5 °C Hold at 180 °C ± 5 °C for 120 min ± 5 min Cool at 2-5 °C/ min	Heat at 0.56-2.8 °C/ min to 180 °C ± 5 °C Heat at 0.17-2.8 °C/ min once part reaches 168 °C Hold at 180 °C ± 5 °C for 130 min ± 10 min Cool at 2.8 °C/ min (maximum rate)

[a] For autoclave cure of solid laminates (685-790 kPa/85-100 psig).
[b] From Hexcel HexPly 8552 product datasheet (EU version) [241] (Hexcel Corporation, 2016).
[c] From Section 4.1.2 [144] (Dykeman, 2008). Toray 3900 Prepreg System datasheet [242] (Toray, 2018).

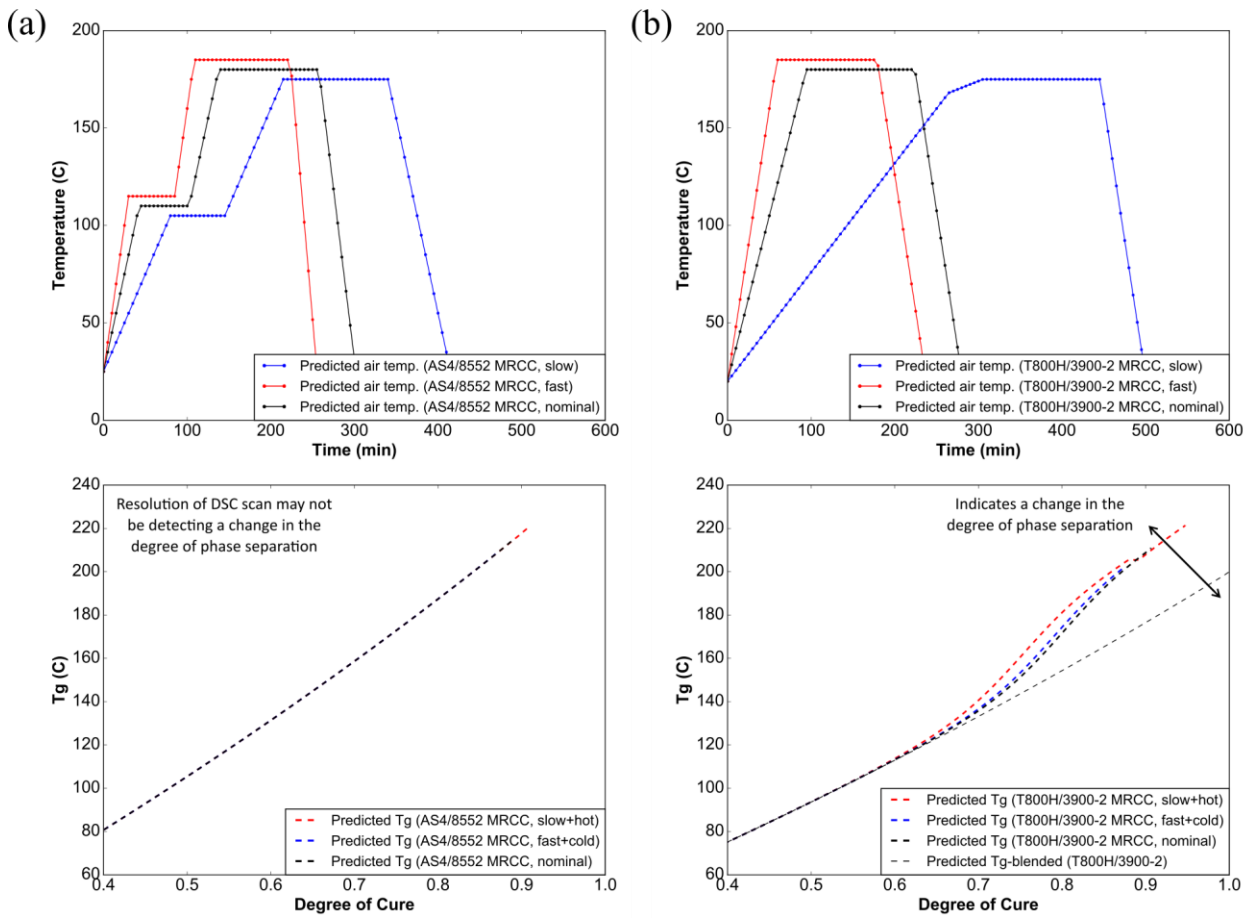

Figure C-2: Comparison of predicted RAVEN-1D MRCC processing envelopes. Temperature profile (T v t) and glass transition temperature versus cure advancement (T_g v α) plots shown for: (a) Hexcel AS4/8552 (example of a two phase material system) and (b) Toray T800H/3900-2 (example of a multiple phase material system). MRCC: Manufacturer Recommended Cure Cycle; α: Degree of Cure. Note: Evaluation performed using AS4/8552 NCAMP [135,238] **and T800H/3900-2 open literature** [144,238] **material models.**

C.2 ETPM factory ontology scratchpad

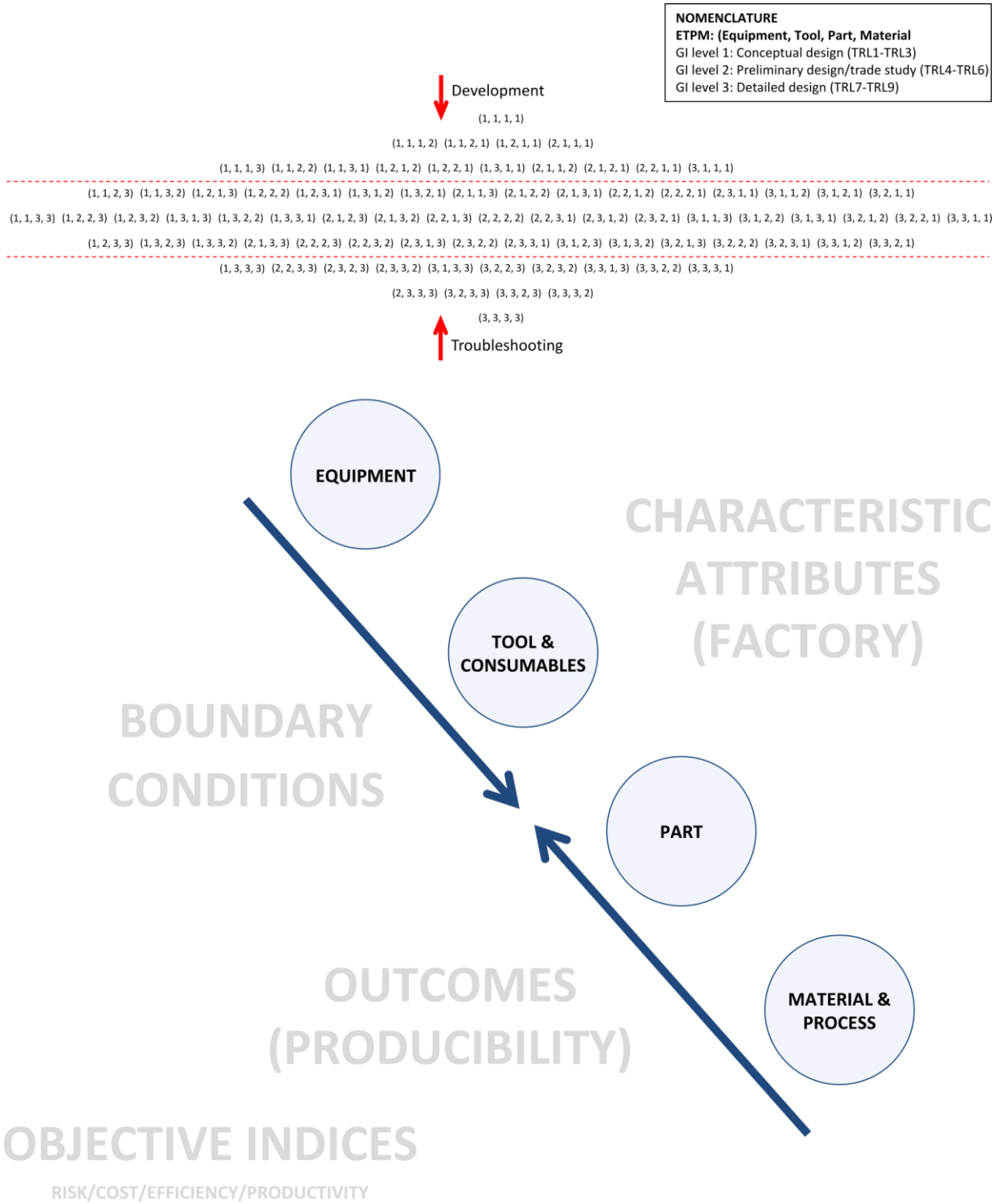

Figure C-3: ETPM decision tree and attribute canvas. These tools can be used to systematically capture manufacturing scenarios with simulation based thinking. GI: Design-gate Index.

Appendix D Thick Thermoset Composites Data Sets

This appendix contains summaries of the thick thermoset composites data sets presented in Chapter 5, including:

- Experimental setup and schematic of thermocouple locations
- Reported effective HTCs for original and revised analyses
- Summary of ETPM thermal management attributes
- Temperature plots showing experimental and predicted thermal responses

Material properties and material database input parameters used in all data sets are summarized in Appendix E. The method for back-calculating the effective HTCs for RAVEN-1D and COMPRO-3D thermal analyses is given in Appendix F.

D.1 Johnston and Hubert data set

The part considered in this data set is a thick panel with tapered core made with Hexcel AS4/8552 prepreg tape and glass/phenolic HRP 130 kg/m^3 honeycomb core. This part has intermediate geometric complexity due to the transition from a 28.2 mm laminate ('solid' zone) to a 23.7 mm honeycomb core with 2.2 mm thick facesheets ('sandwich' zone) [100].

For the cure cycle development and evaluation case study of a 28.2 mm thick panel with tapered core presented in Section 5.2.2, the modelling results for Cases II and III are given in D.1.5.

D.1.1 Experimental setup and schematic of thermocouple locations

(a)

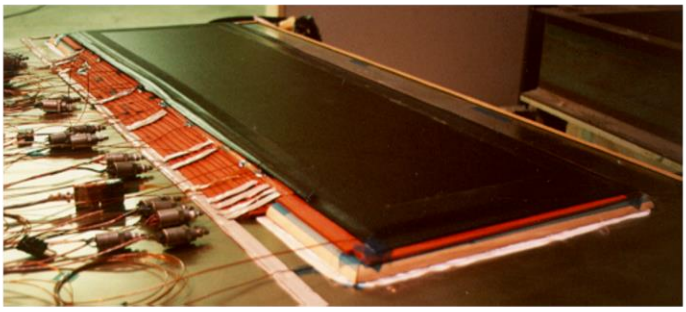

(b)

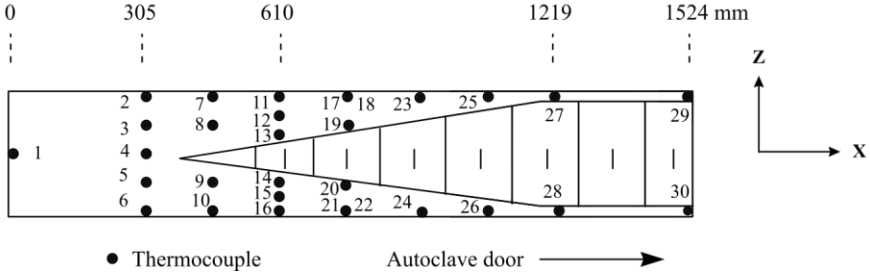

Figure D-1: Johnston and Hubert data set: (a) experimental setup prior to bagging[a] and (b) schematic of part and thermocouple locations (photo and schematic from [100] (Johnston, 1997)).

[a] This photo also shows the experimental setup (rubber edge dam and cylindrical pressure transducers) used to measure resin hydrostatic pressure during cure.

D.1.2 Reported effective heat transfer coefficients

Table D-1: Effective heat transfer coefficients for the Johnston and Hubert data set.

Analysis	Equivalent-1D HTC Low pressure (170 kPa/10 psig) top W/ (m^2 K)	Equivalent-1D HTC Low pressure (170 kPa/10 psig) bottom W/ (m^2 K)	Equivalent-1D HTC High pressure (375 kPa/40 psig) top W/ (m^2 K)	Equivalent-1D HTC High pressure (375 kPa/40 psig) bottom W/ (m^2 K)	Average equivalent-1D HTC top W/ (m^2 K)	Average equivalent-1D HTC bottom W/ (m^2 K)
Original[a] (~1995)	26	68	32	82	29	75
Revised[b,c] (2018)	10	40	20	70	15	55

[a] From Section 7.1.2 [100] (Johnston, 1997). Effective HTCs determined by direct temperature measurement.
[b] This analysis uses modified heat flux Method I' to back-calculate the effective HTCs, as described in Appendix F.2. Effective HTCs reported are calculated using all ramp cure cycle segments.
[c] Top HTC is back-calculated from part TC2. The thermal resistance of the rubber caul has been accounted for in the top HTC value, and thus the caul is omitted from the revised RAVEN-1D analysis. Bottom HTC value is back-calculated from part TC6. The Invar tool is assumed as a lumped mass. Although this would not necessarily be the case, no other thermocouple data is available.

D.1.3 Summary of ETPM thermal management attributes

Table D-2: ETPM[a] attribute definition for the Johnston and Hubert data set.

		Test[b]	Analysis[c]
Equipment	**(E)**	Autoclave: Industrial-A	h_{top_ave} = 15 W/ (m^2 K)
Tool	**(T)**	Invar tool z_{tool} = 25.4 mm	h_{bot_ave} = 55 W/ (m^2 K)
Part	**(P)**	Panel with tapered core (1524 mm x 457 mm) $z_{part\ (SOLID)}$ = 28.2 mm (152 ply) $z_{part\ (S/WICH)}$ = 2.2 mm (12 ply) / 23.8 mm (core) TC-4 (mid-laminate) TC-27 (upper facesheet)	RAVEN-1D drill point analysis [238] T4: mid (solid zone) T27: upper f/sheet (sandwich zone)
Material	**(M)**	AS4/8552 UD tape Glass/phenolic honeycomb core HRP (3/16-8.0) 3-hold cycle (110°C, 150 °C, 180 °C) Autoclave pressure: 375 kPa (40 psi)	AS4/8552 NCAMP material model Nominal aramid honeycomb (thermal only)

[a] ETPM: Equipment–Tool–Part–Material
[b] Experimental data from [100] (Johnston, 1997).
[c] HTCs reported from the revised HTC analysis using Method I', see Table D-1.

D.1.4 Temperature plots

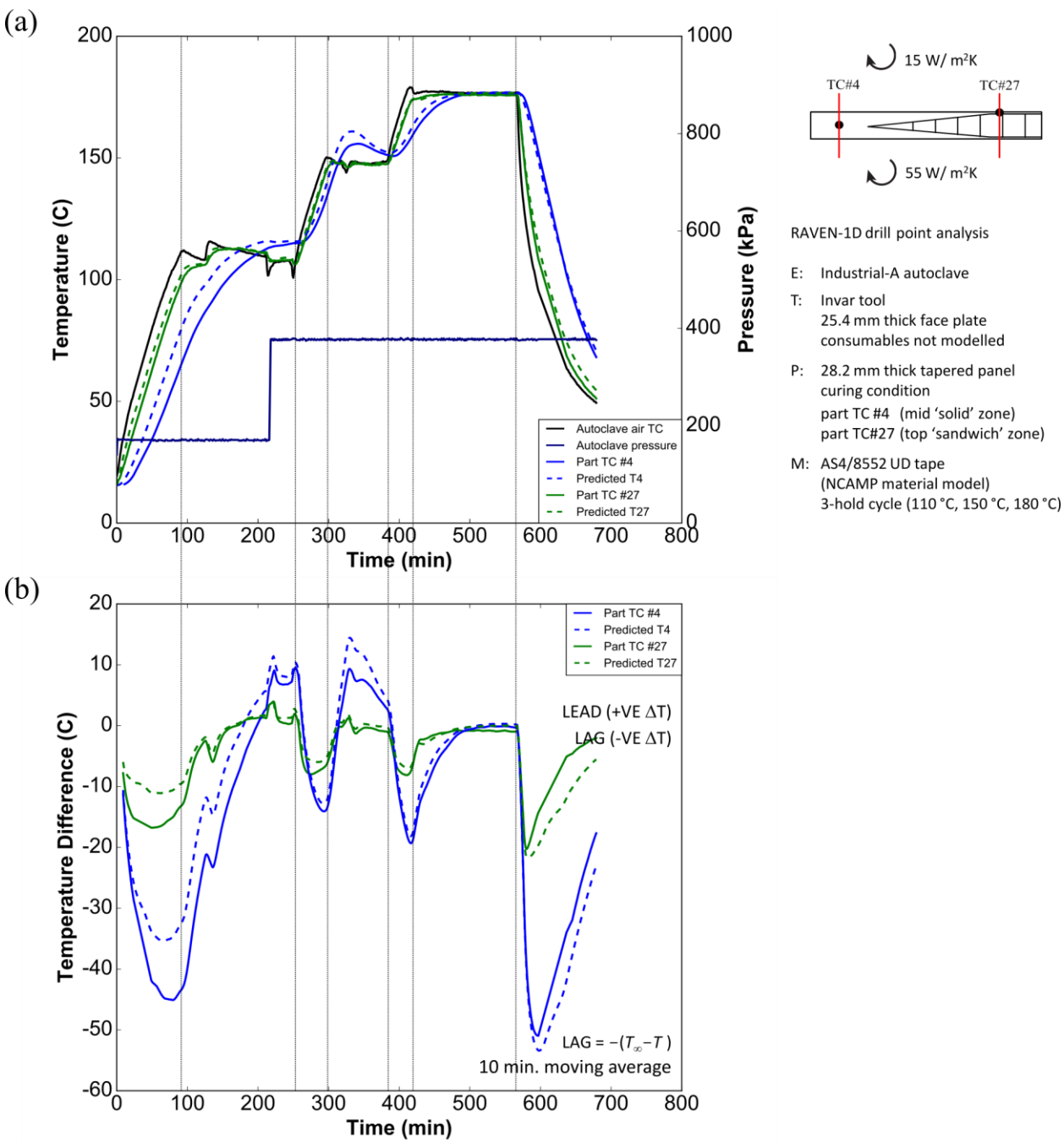

Figure D-2: Comparison of experimentally measured and predicted RAVEN-1D modelling results for the Johnston and Hubert data set (ATCAS: 28.2 mm thick panel with tapered core): (a) temperature profile (*T* v *t*) and (b) temperature difference with respect to the autoclave air temperature (Δ*T* v *t*). Experimental data from [100] (Johnston, 1997). ETPM: Equipment–Tool–Part–Material; TC: Thermocouple; UD: Unidirectional. Note: Vertical lines indicate heat up, hold and cool down cure cycle segments.

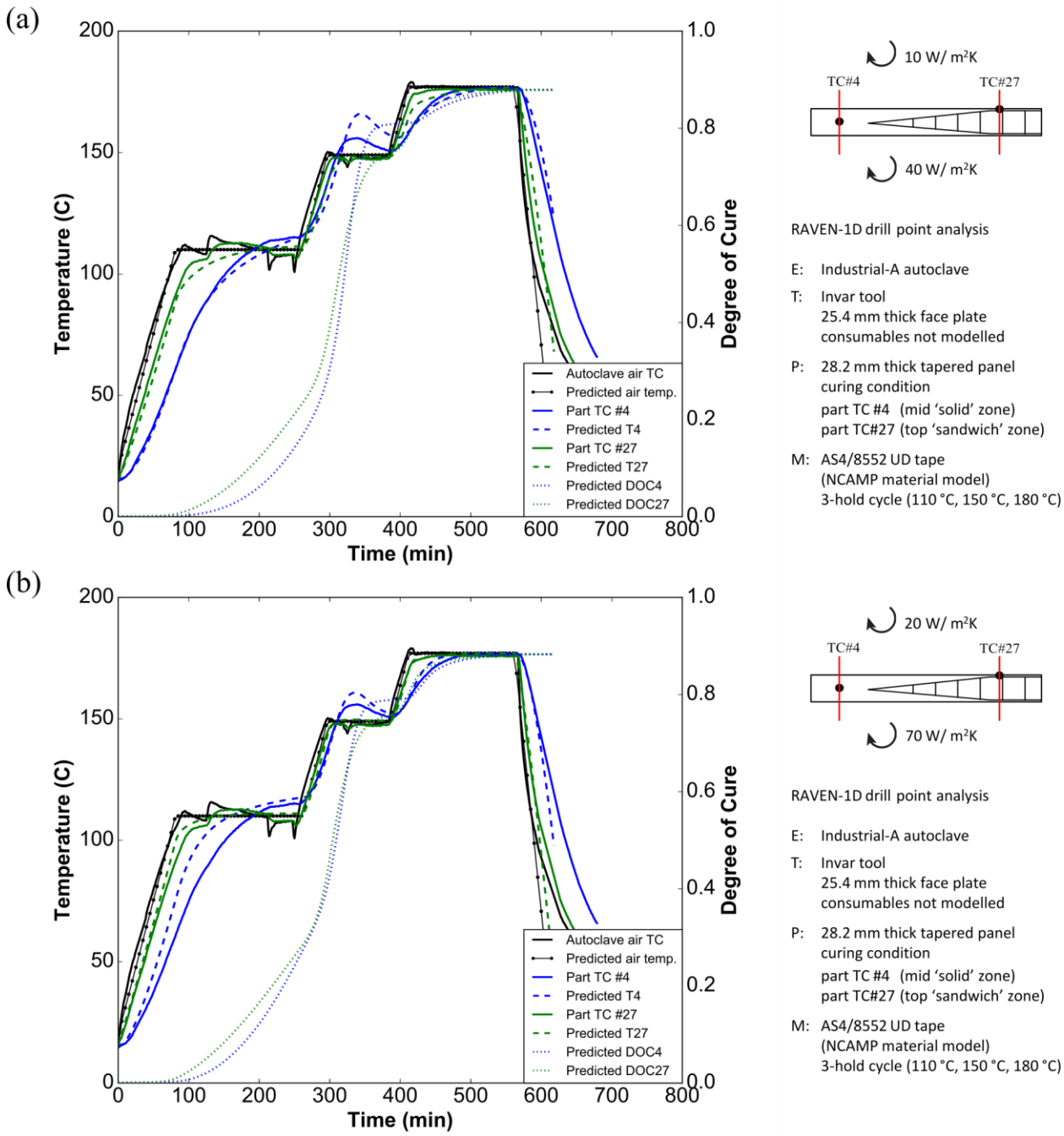

Figure D-3: Comparison of experimentally measured and predicted RAVEN-1D modelling results for the Johnston and Hubert data set (ATCAS: 28.2 mm thick panel with tapered core). The effect of low and high heat transfer: (a) low autoclave pressure (170 kPa/10 psig) and (b) high autoclave pressure (375 kPa/40 psig). Experimental data from [100] (Johnston, 1997). ETPM: Equipment–Tool–Part–Material; TC: Thermocouple; UD: Unidirectional; HTC: Heat Transfer Coefficient. Note: Revised effective HTCs are back-calculated from the experimental data and summarized in Table D-1.

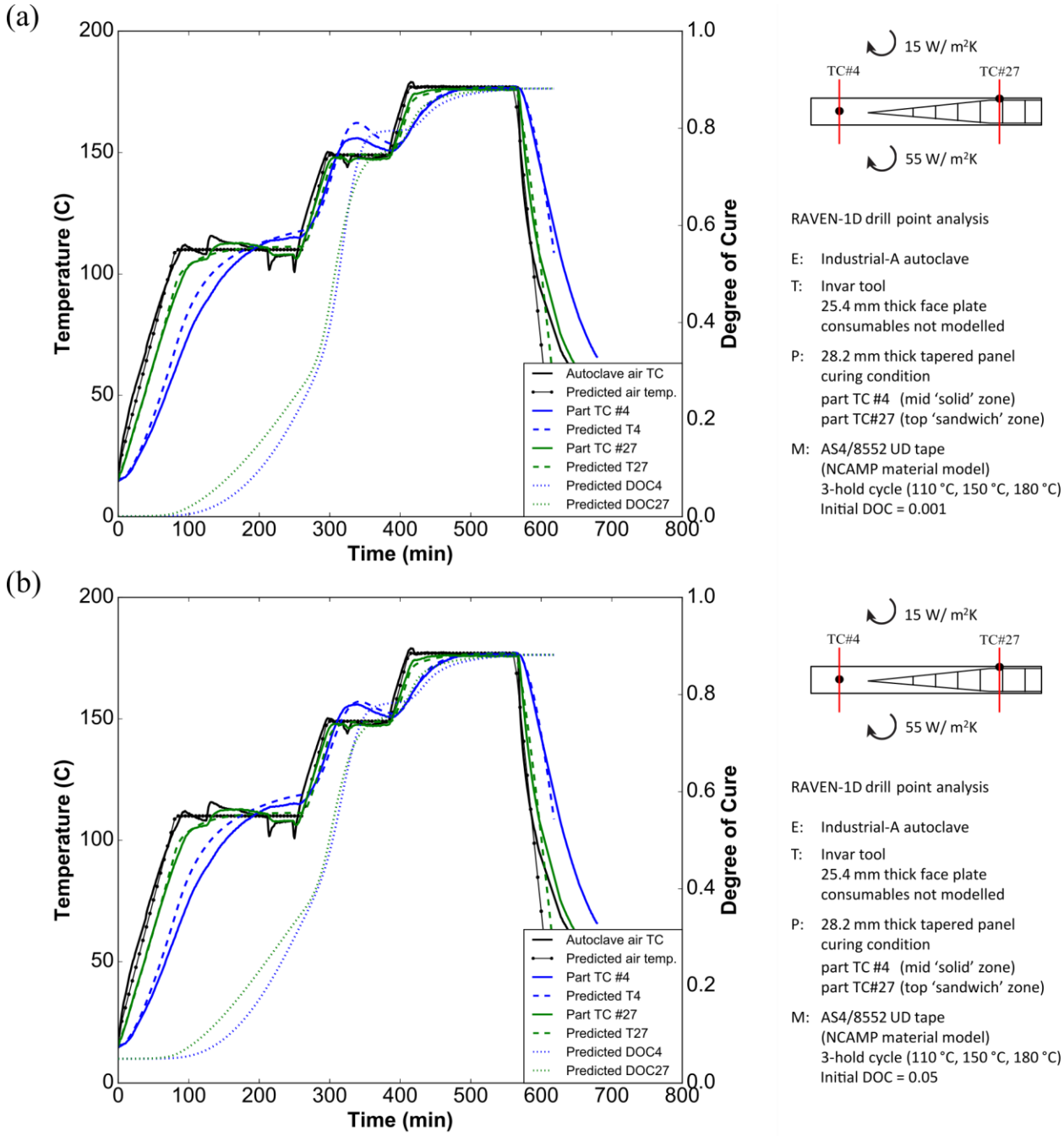

Figure D-4: Comparison of experimentally measured and predicted RAVEN-1D modelling results for the Johnston and Hubert data set (ATCAS: 28.2 mm thick panel with tapered core). AS4/8552 NCAMP material model initial DOC sensitivity: (a) α_i = 0.001 (default as per 8552 NCAMP CK model [135]) and (b) α_i = 0.05 (default as per the open literature 8552 CK model characterized by Johnston [100]). Experimental data from [100] (Johnston, 1997). ETPM: Equipment–Tool–Part–Material; TC: Thermocouple; UD: Unidirectional; DOC: Degree of Cure; α_i: initial degree of cure; CK: Cure Kinetics.

D.1.5 Case study: Panel with tapered core

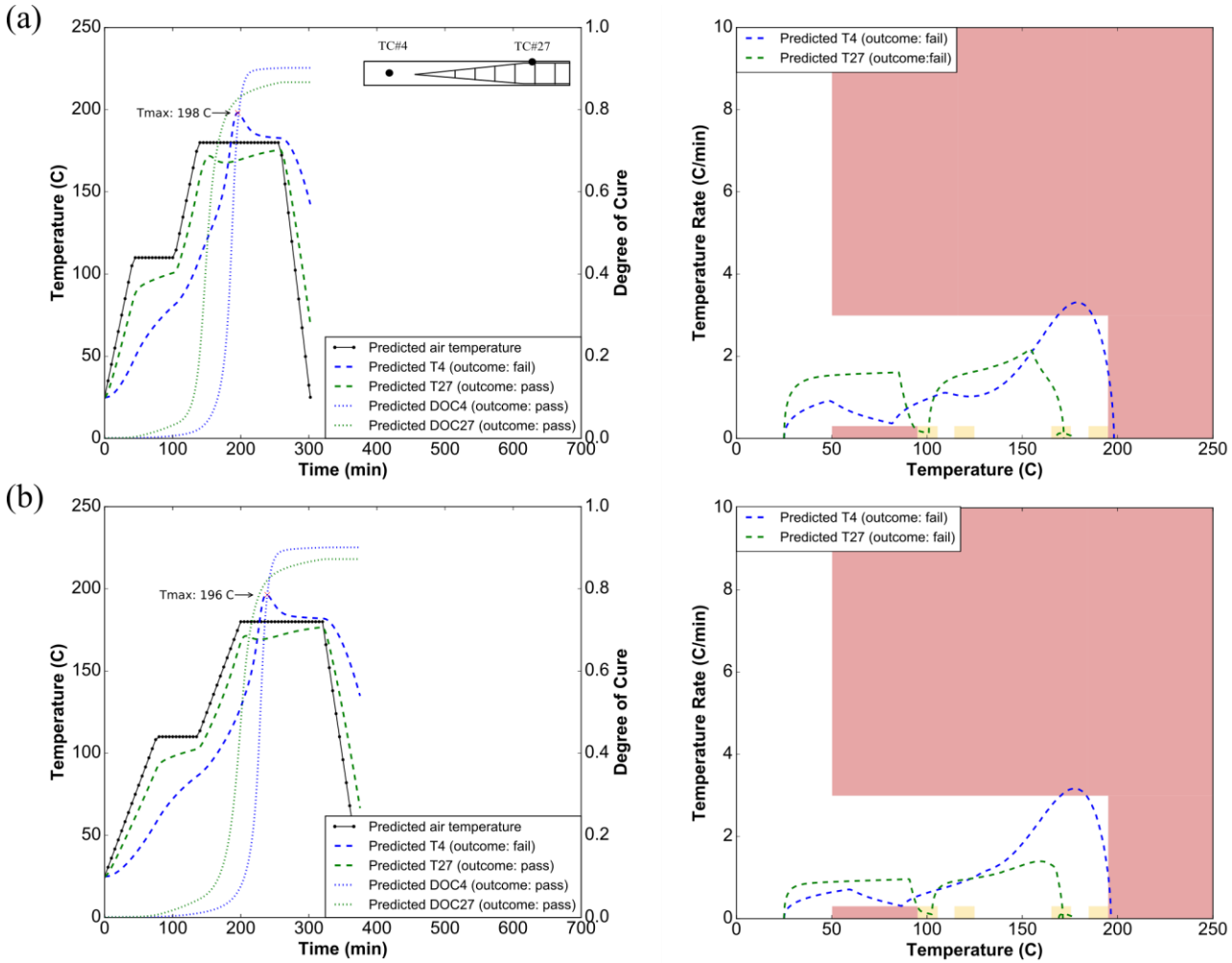

Figure D-5: Predicted RAVEN-1D modelling results for Case II (processing scenario: 25.4 mm thick Invar tool with closed substructure). Temperature profile (T v t) and temperature rate versus temperature ($\dot{T}$ v T) plots for: (a) nominal MRCC (overall outcome: fail) and (b) slow MRCC (overall outcome: fail). MRCC: Manufacturer Recommended Cure Cycle; TC: Thermocouple; DOC: Degree of Cure. Note: Cure cycle acceptance criteria are summarized in Table 5-5 (pass (unshaded), marginal (yellow), fail (red)).

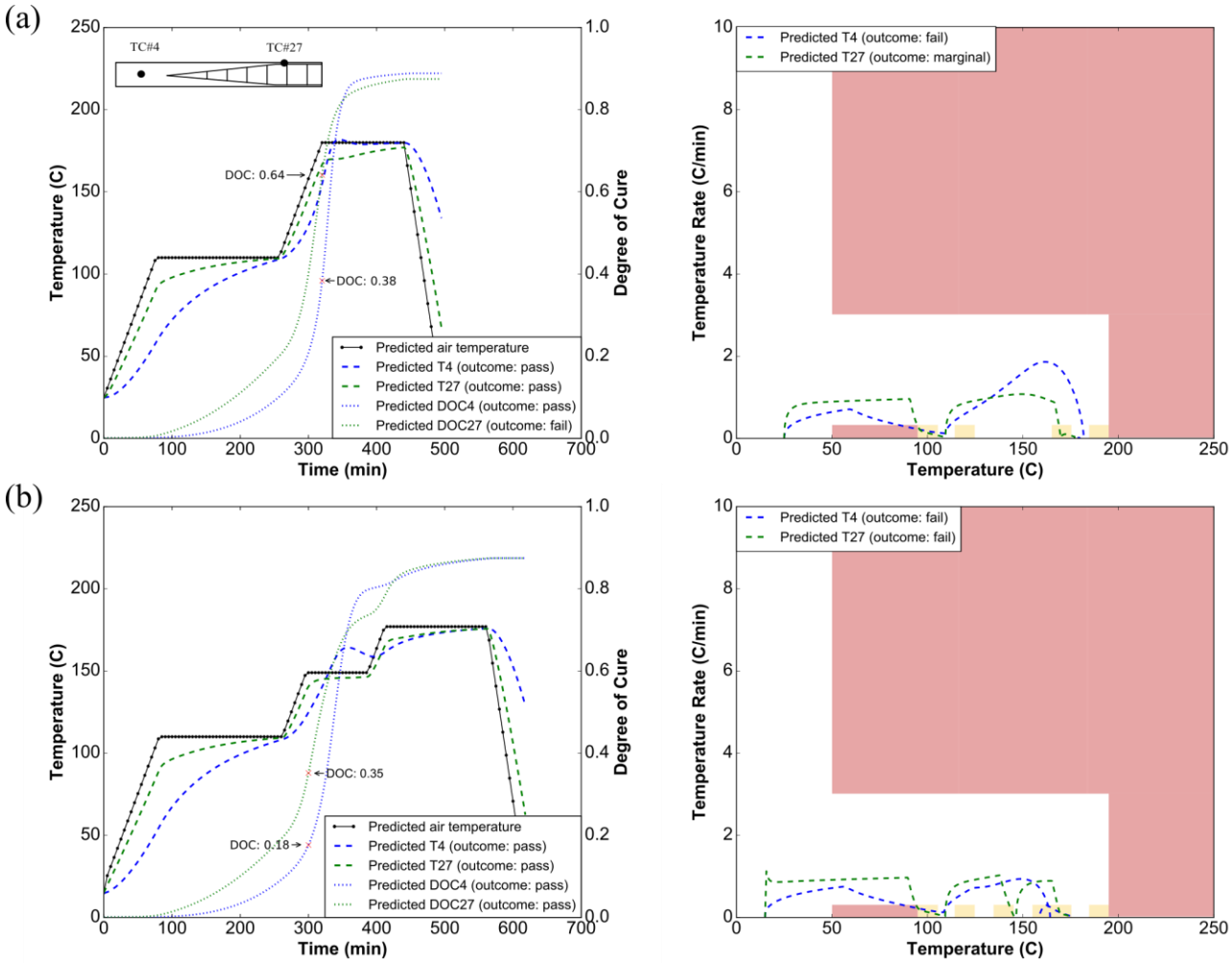

Figure D-6: Predicted RAVEN-1D modelling results for Case II (processing scenario: 25.4 mm thick Invar tool with closed substructure). Temperature profile (T v t) and temperature rate versus temperature ($\dot{T}$ v T) plots for: (a) extending the 110 °C hold (overall outcome: fail) and (b) introducing an intermediate 150 °C hold (overall outcome: fail). TC: Thermocouple; DOC: Degree of Cure. Note: Cure cycle acceptance criteria are summarized in Table 5-5 (pass (unshaded), marginal (yellow), fail (red)).

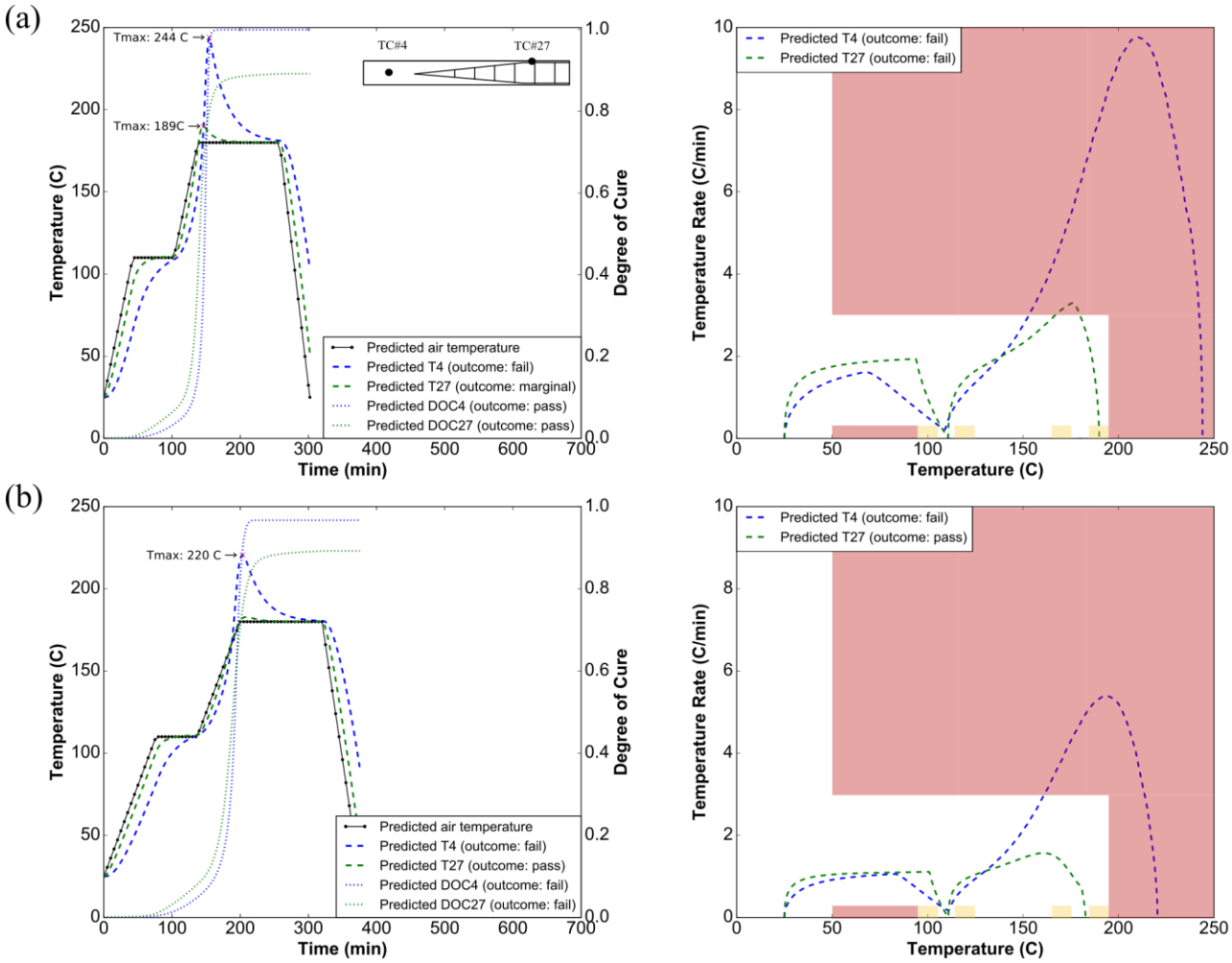

Figure D-7: Predicted RAVEN-1D modelling results for Case III (processing scenario: 9.5 mm thick Invar tool with open substructure). Temperature profile (T v t) and temperature rate versus temperature ($\dot{T}$ v T) plots for: (a) nominal MRCC (overall outcome: fail) and (b) slow MRCC (overall outcome: fail). MRCC: Manufacturer Recommended Cure Cycle; TC: Thermocouple; DOC: Degree of Cure. Note: Cure cycle acceptance criteria are summarized in Table 5-5 (pass (unshaded), marginal (yellow), fail (red)).

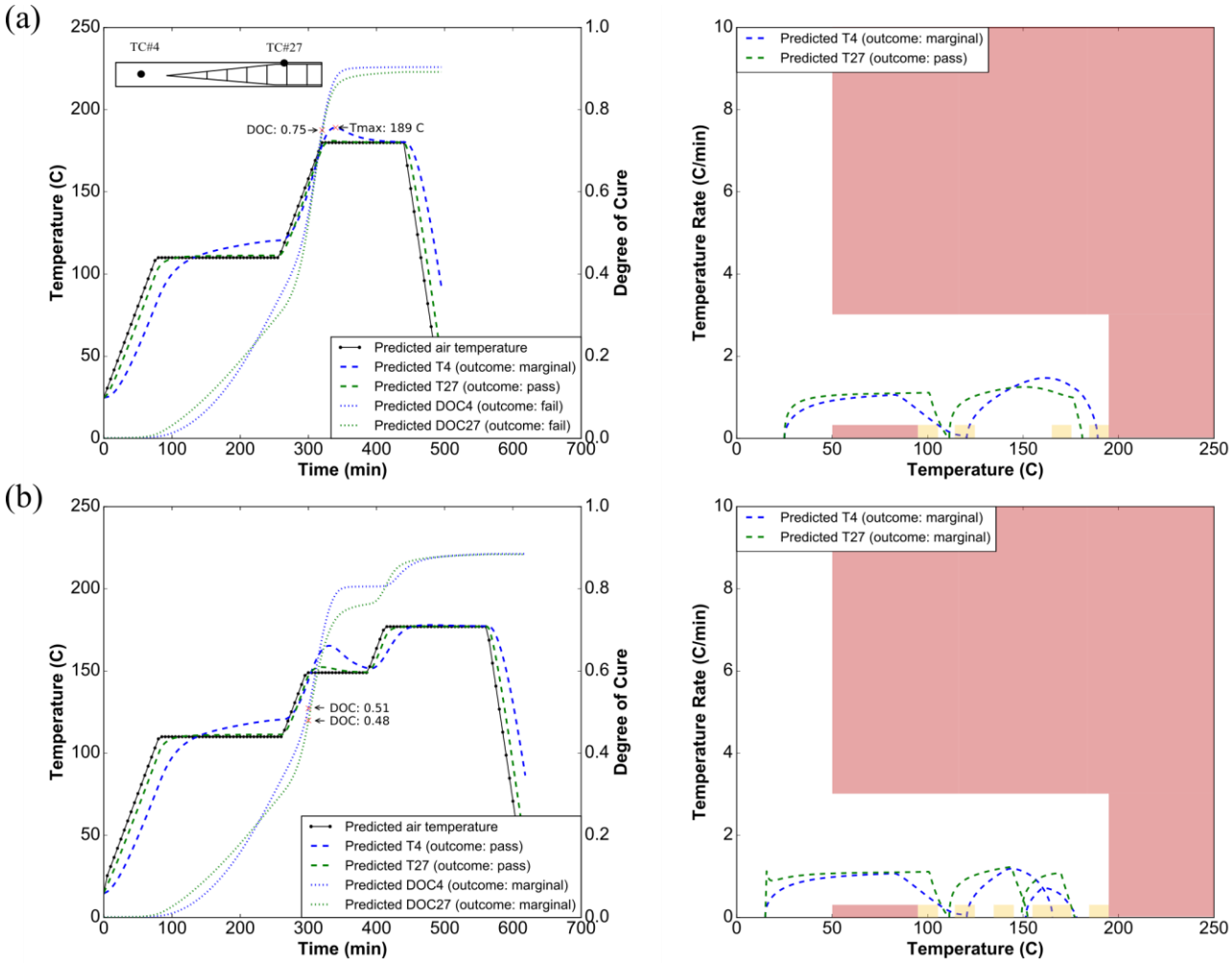

Figure D-8: Predicted RAVEN-1D modelling results for Case III (processing scenario: 9.5 mm thick Invar tool with open substructure). Temperature profile (T v t) and temperature rate versus temperature ($\dot{T}$ v T) plots for: (a) extending the 110 °C hold (overall outcome: marginal) and (b) introducing an intermediate 150 °C hold (overall outcome: marginal). TC: Thermocouple; DOC: Degree of Cure. Note: Cure cycle acceptance criteria are summarized in Table 5-5 (pass (unshaded), marginal (yellow), fail (red)).

D.2 Kotlik and Shimizu data set

A 38.4 mm thick laminate made with AS4/8552-1 prepreg tape is investigated in this data set. This part was instrumented with over 40 thermocouples to obtain detailed through-thickness temperature distributions for different processing conditions [145]. An unintentional bag leak was introduced into the experiment for TEST-C, TEST-D and TEST-E.

In addition to the work presented in Section 5.1.3 discussing thermal modelling uncertainties, a sensitivity study of reported heat transfer boundary conditions for this data set is given in D.2.5.

D.2.1 Experimental setup and schematic of thermocouple locations

(a)

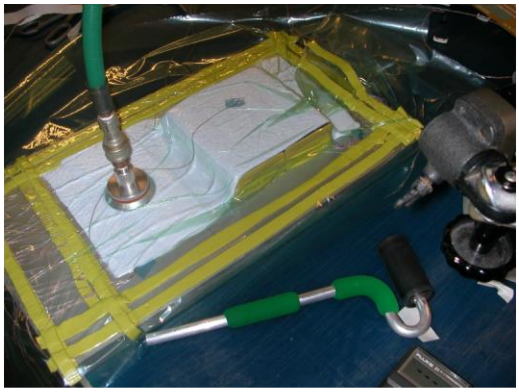

(b)

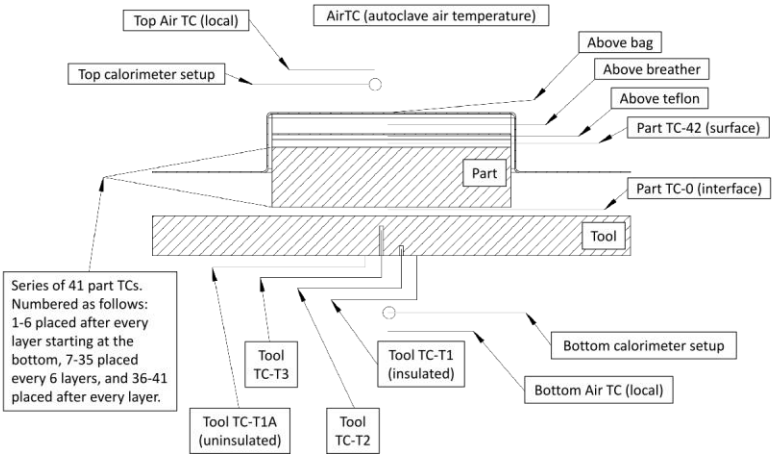

Figure D-9: Kotlik and Shimizu data set: (a) experimental setup and (b) schematic of thermocouple locations (photo and schematic from [145] (Shimizu *et al*, 2008)).

D.2.2 Reported effective heat transfer coefficients

Table D-3: Effective heat transfer coefficients for the Kotlik and Shimizu data set[a].

Analysis	HTC back-calc method[b,c]	Experiment	Equivalent-1D HTC		Equivalent-3D HTC (no tool substructure modelled)			Remarks
			top W/ (m^2 K)	bottom W/ (m^2 K)	top W/ (m^2 K)	tool top W/ (m^2 K)	tool bottom W/ (m^2 K)	
Original[d] (2008)	Method I	TEST-A	40-55	145-190				
		TEST-B	65-80	160-195				Consumables fill with resin
		TEST-C	5-10	100-120				Bag leak
		TEST-D	10	100-125				Bag leak
		TEST-E	5-10	115-135				Bag leak
Revised[e] (2018)	Method I	TEST-A	40-90	120-180	40-90	55-80	40-55	Cycle interruption during heat up Consumables fill with resin in latter stages of the cure cycle (eg. cool down)
		TEST-B	55-65	145-185	55-65	65-80	50-60	
		TEST-C	10	90-110				
		TEST-D	10	85-110				
		TEST-E	5	95-120				
Revised[e] (2018)	Method I'	TEST-A	75	160	75	70	50	
		TEST-B	65	160	65	70	55	
		TEST-C	15	100				
		TEST-D	15	95				
		TEST-E	15	95				

[a] Experimental data from [145] (Shimizu *et al*, 2008). TEST-A (curing, 2-hold cycle); TEST-B (cured, 2-hold cycle); TEST-C (cured, 1-hold cycle at 2.8 °C/ min); TEST-D (cured, 1-hold cycle at 1.7 °C/ min); TEST-E (cured, 1-hold cycle at 0.6 °C/ min).

[b] Method I is a heat flux based method from [145] (Shimizu *et al*, 2008). The distance to the adiabatic line from the part/tool interface ($L_{e\text{-}p}$) is computed using all through-thickness TCs and assuming a quadratic temperature distribution. The Al-alloy tool is assumed as a lumped mass.

[c] Method I' is a modified heat flux method, based on Method I, where two TCs are used to estimate $L_{e\text{-}p}$. Refer to Appendix F.2 & Appendix F.3.

[d] From [145] (Shimizu *et al*, 2008). The original analysis used TC-air (bottom) as the reference temperature (T_∞). Effective HTCs reported were calculated for the initial ramp cure cycle segment only.

[e] The revised analysis uses TC-AC as the reference temperature. Effective HTCs reported are an average calculated from all ramp cure cycle segments.

D.2.3 Summary of ETPM thermal management attributes

Table D-4: ETPM[a] attribute definition for the Kotlik and Shimizu data set (TEST-A, TEST-B).

		Test[b]	Analysis[c]
Equipment	**(E)**	Autoclave: UBC	$h_{\text{top (TEST-A)}}$ = 75 W/ (m^2 K) $h_{\text{top (TEST-B)}}$ = 65 W/ (m^2 K)
Tool	**(T)**	Al-alloy tool plate (535 mm x 305 mm) z_{tool} = 25.4 mm	$h_{\text{bot (TEST-A)}}$ = 160 W/ (m^2 K) $h_{\text{bot(TEST-B)}}$ = 160 W/ (m^2 K) $h_{\text{t-top (TEST-A)}}$ = 70 W/ (m^2 K) $h_{\text{t-bot (TEST-A)}}$ = 50 W/ (m^2 K)
Part	**(P)**	Flat laminate (152 mm x 152 mm) z_{part} = 38.4 mm (192 ply) [0/90] TC-0 (interface) to TC-42 (surface) TC-21 (mid)	RAVEN-1D drill point analysis [238] COMPRO-3D model (no tool substructure modelled) [239] T21: mid
Material	**(M)**	AS4/8552-1 UD tape Two-hold cycle (110 °C, 180 °C)	AS4/8552-1 preliminary material model

[a] ETPM: Equipment–Tool–Part–Material
[b] Experimental data from [145] (Shimizu *et al*, 2008).
[c] HTCs reported from the revised HTC analysis using Method I', see Table D-3.

Table D-5: ETPM[a] attribute definition for the Kotlik and Shimizu data set (TEST-C, TEST-D, TEST-E).

		Test[b]	Analysis[c]
Equipment	**(E)**	Autoclave: UBC	$h_{\text{top (TEST-C)}}$ = 15 W/ (m^2 K) $h_{\text{top (TEST-D)}}$ = 15 W/ (m^2 K) $h_{\text{top (TEST-E)}}$ = 15 W/ (m^2 K)
Tool	**(T)**	Al-alloy tool plate (535 mm x 305 mm) z_{tool} = 25.4 mm	$h_{\text{bot (TEST-C)}}$ = 100 W/ (m^2 K) $h_{\text{bot (TEST-D)}}$ = 95 W/ (m^2 K) $h_{\text{bot (TEST-E)}}$ = 95 W/ (m^2 K)
Part	**(P)**	Flat laminate (152 mm x 152 mm) z_{part} = 38.4 mm (192 ply) [0/90] TC-0 (interface) to TC-42 (surface) TC-21 (mid)	RAVEN-1D drill point analysis [238] T21: mid
Material	**(M)**	AS4/8552-1 UD tape One-hold cycle (120 °C)	Preliminary AS4/8552-1 material model

[a] ETPM: Equipment–Tool–Part–Material
[b] Experimental data from [145] (Shimizu *et al*, 2008).
[c] HTCs reported from the revised HTC analysis using Method I', see Table D-3.

D.2.4 Temperature plots

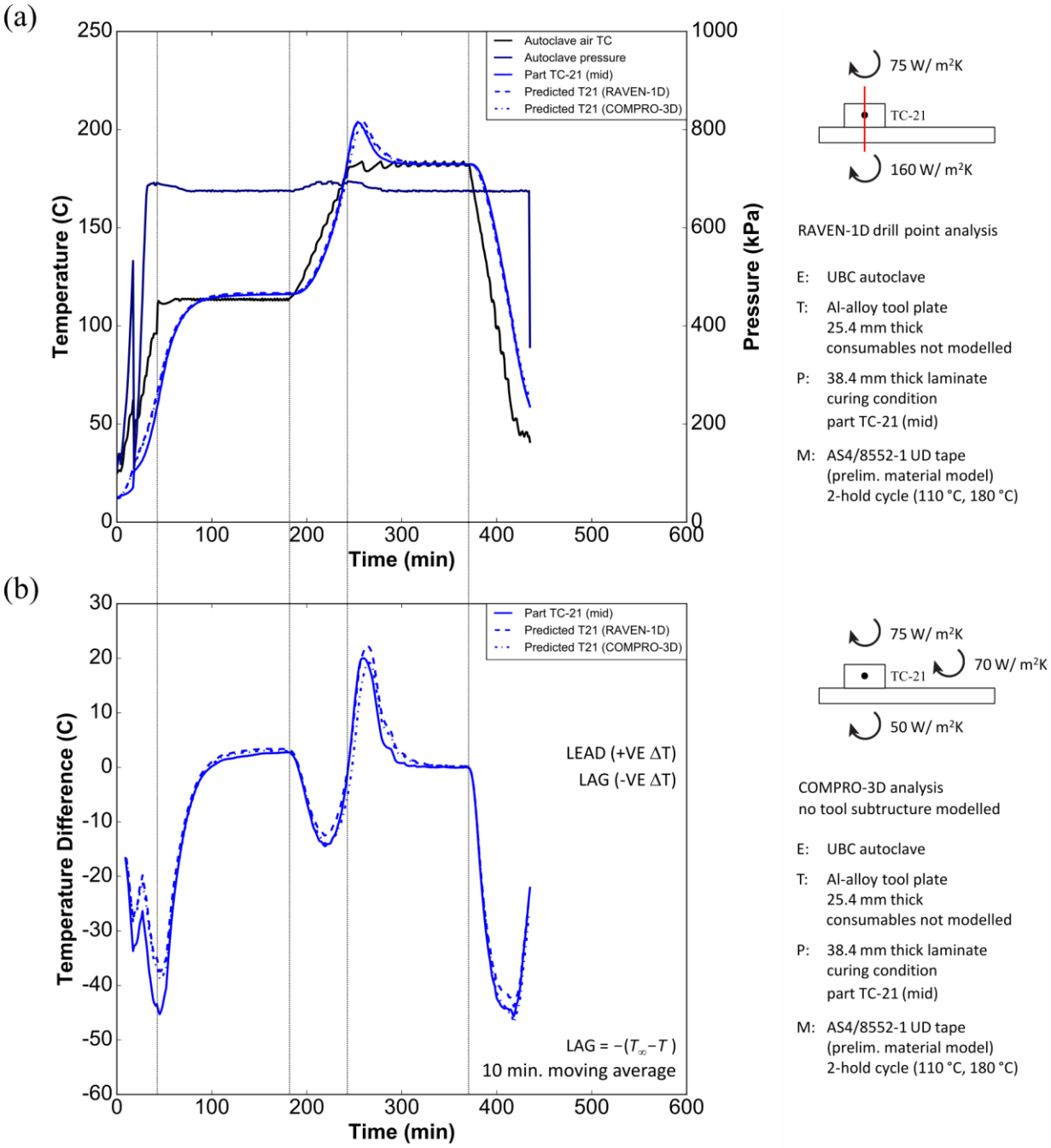

Figure D-10: Comparison of experimentally measured and predicted RAVEN-1D and COMPRO-3D modelling results for the Kotlik and Shimizu data set (TEST-A: 38.4 mm thick laminate, curing 2-hold cycle): (a) temperature profile (*T* v *t*) and (b) temperature difference with respect to the autoclave air temperature (Δ*T* v *t*). Experimental data from [145] (Shimizu *et al*, 2008). ETPM: Equipment–Tool–Part–Material; TC: Thermocouple; UD: Unidirectional. Note: Vertical lines indicate heat up, hold and cool down cure cycle segments.

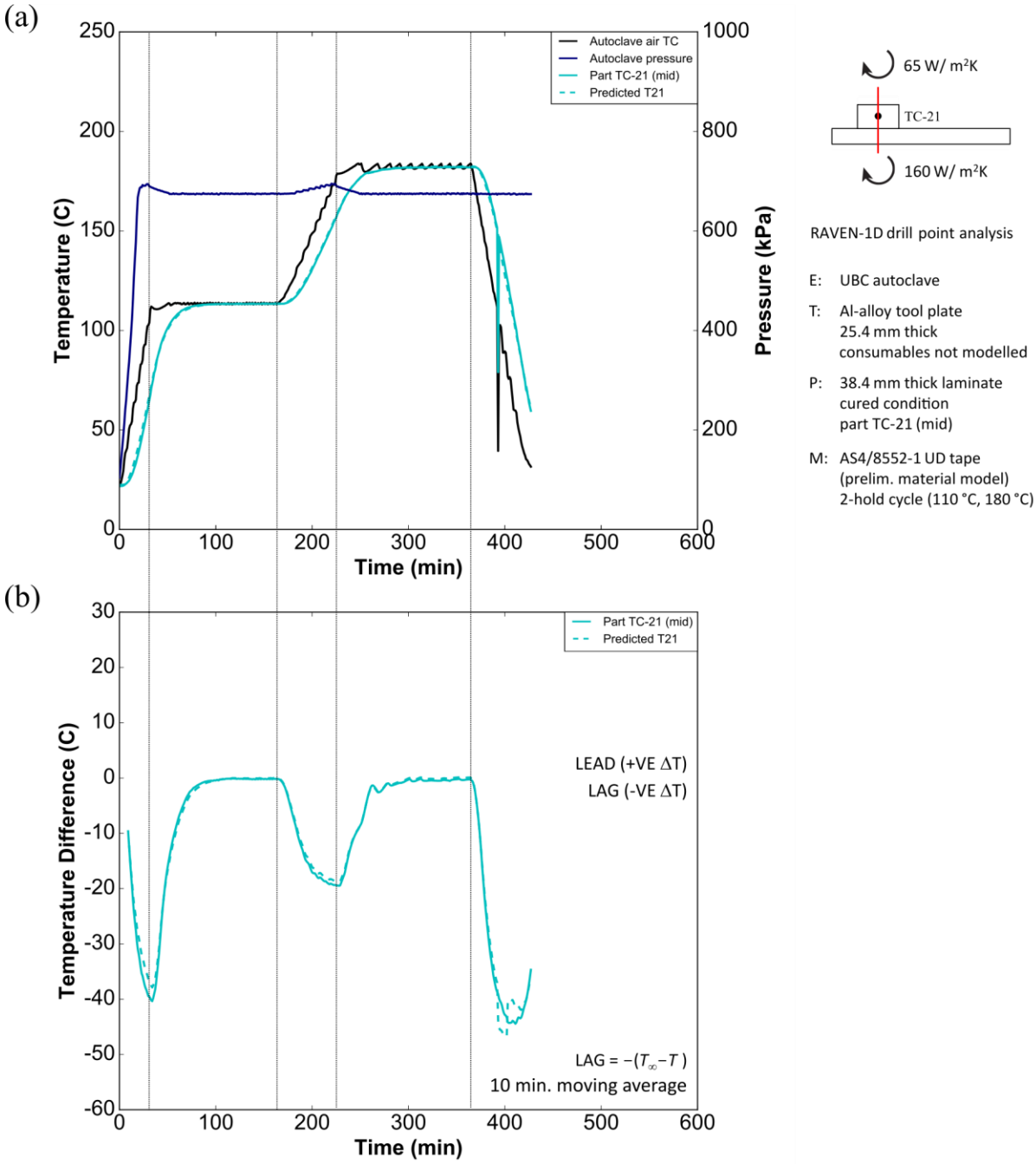

Figure D-11: Comparison of experimentally measured and predicted RAVEN-1D modelling results for the Kotlik and Shimizu data set (TEST-B: 38.4 mm thick laminate, cured 2-hold cycle): (a) temperature profile (*T* v *t*) and (b) temperature difference with respect to the autoclave air temperature (Δ*T* v *t*). Experimental data from [145] (Shimizu *et al*, 2008). ETPM: Equipment–Tool–Part–Material; TC: Thermocouple; UD: Unidirectional. Note: Vertical lines indicate heat up, hold and cool down cure cycle segments.

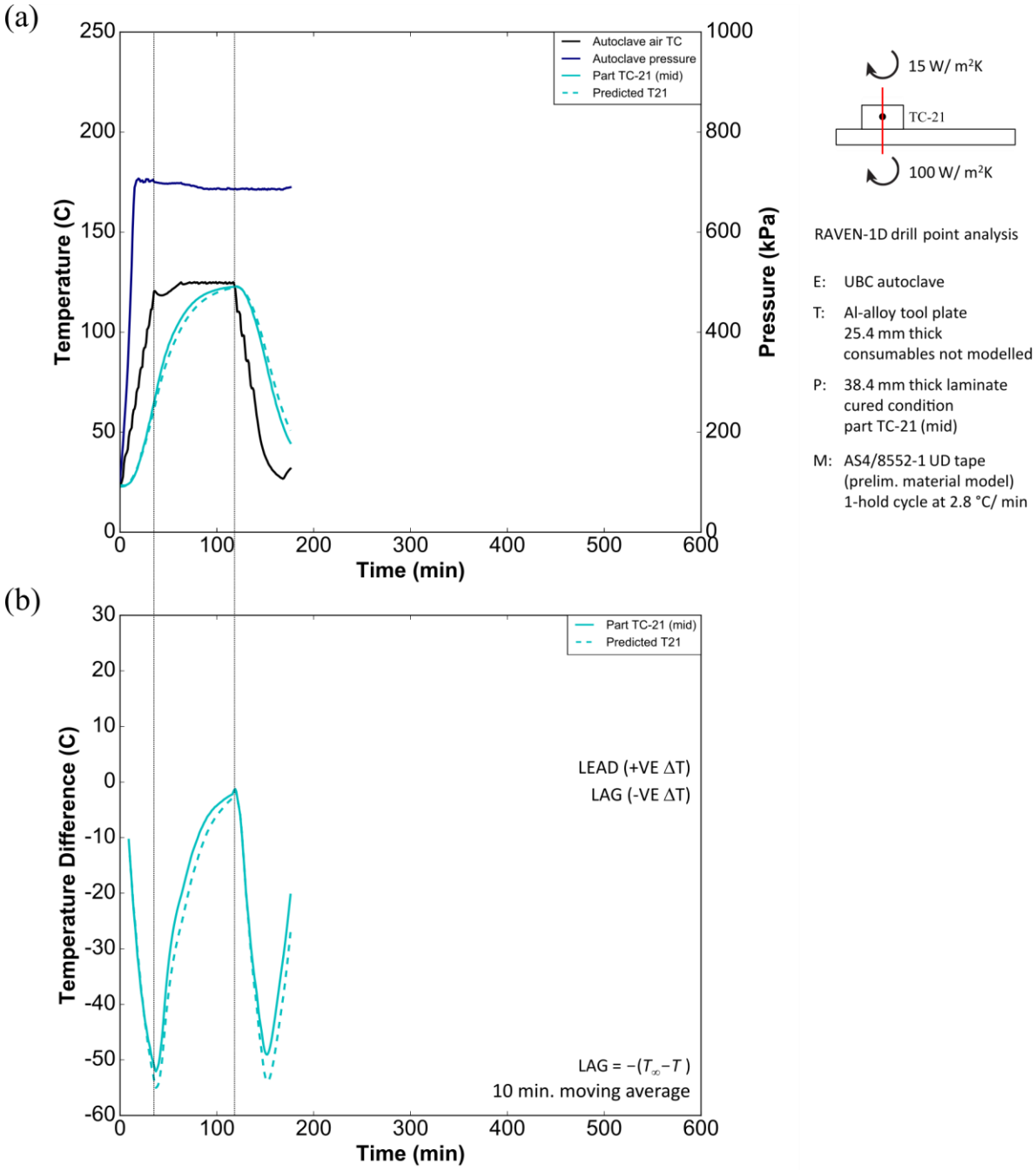

Figure D-12: Comparison of experimentally measured and predicted RAVEN-1D modelling results for the Kotlik and Shimizu data set (TEST-C: 38.4 mm thick laminate, cured 1-hold cycle at 2.8 °C /min): (a) temperature profile (*T* v *t*) and (b) temperature difference with respect to the autoclave air temperature (Δ*T* v t). Experimental data from [145] (Shimizu et al, 2008). ETPM: Equipment–Tool–Part–Material; TC: Thermocouple; UD: Unidirectional. Note: Unintentional bag leak introduced into experimental test setup. Vertical lines indicate heat up, hold and cool down cure cycle segments.

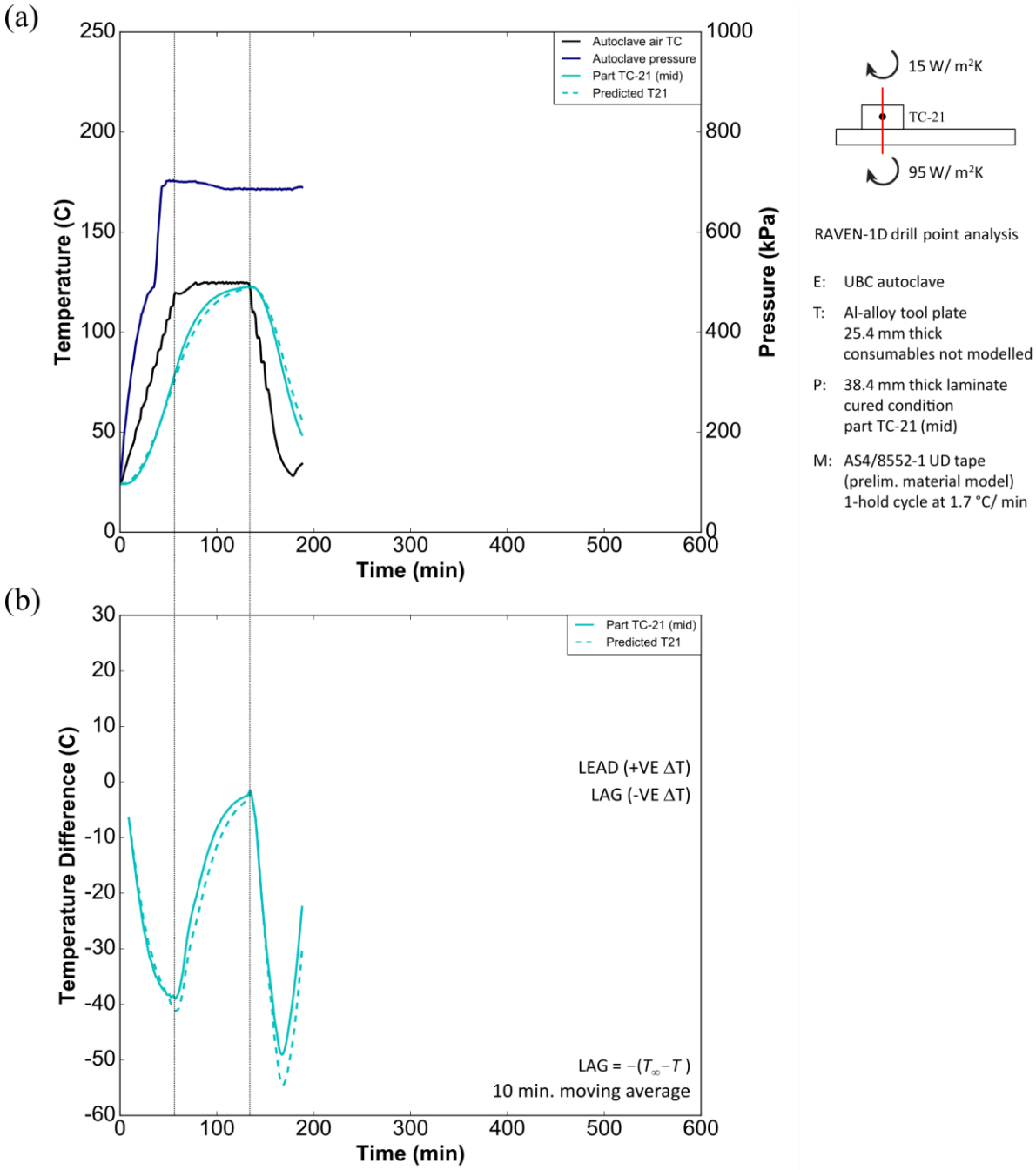

Figure D-13: Comparison of experimentally measured and predicted RAVEN-1D modelling results for the Kotlik and Shimizu data set (TEST-D: 38.4 mm thick laminate, cured 1-hold cycle at 1.7 °C /min): (a) temperature profile (*T* v *t*) and (b) temperature difference with respect to the autoclave air temperature (Δ*T* v *t*). Experimental data from [145] (Shimizu *et al*, 2008). ETPM: Equipment–Tool–Part–Material; TC: Thermocouple; UD: Unidirectional. Note: Unintentional bag leak introduced into experimental test setup. Vertical lines indicate heat up, hold and cool down cure cycle segments.

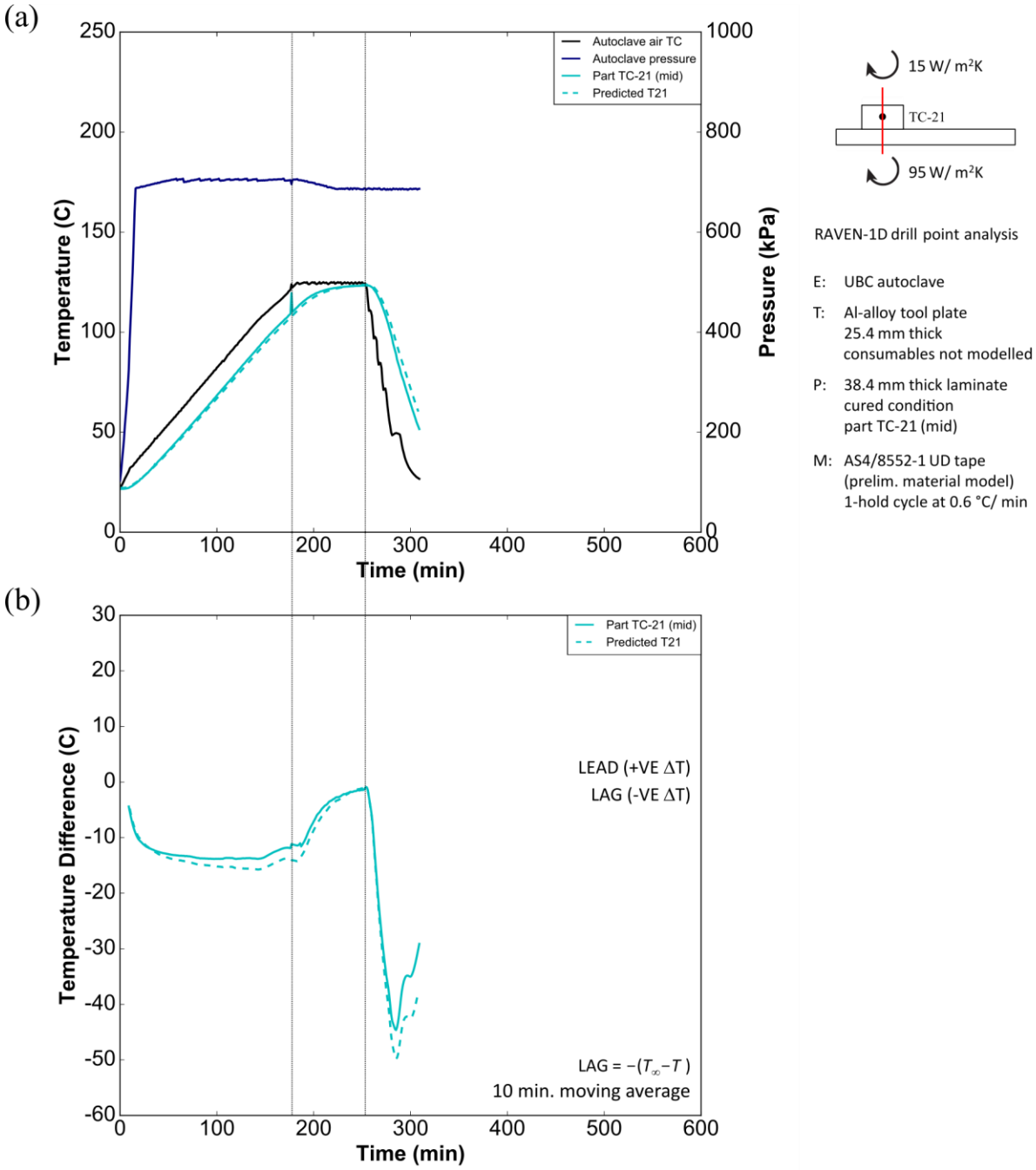

Figure D-14: Comparison of experimentally measured and predicted RAVEN-1D modelling results for the Kotlik and Shimizu data set (TEST-E: 38.4 mm thick laminate, cured 1-hold cycle at 0.6 °C /min): (a) temperature profile (*T* v *t*) and (b) temperature difference with respect to the autoclave air temperature (Δ*T* v *t*). Experimental data from [145] (Shimizu *et al*, 2008). ETPM: Equipment–Tool–Part–Material; TC: Thermocouple; UD: Unidirectional. Note: Unintentional bag leak introduced into experimental test setup. Vertical lines indicate heat up, hold and cool down cure cycle segments.

D.2.5 Case study: Effective heat transfer boundary condition sensitivity

A study investigating HTC sensitivity due to a reduction of experimental measurement points was performed that extends the preliminary analysis work performed by Shimizu *et al* [145]. In this current study, TEST-A and TEST-B are analyzed to compare HTC sensitivities for curing and cured laminates while TEST-B and TEST-C are analyzed to investigate HTC sensitivities given the presence of a bag leak. These experiments are nominally comparable during initial ramp and cool down cure cycle segments with heating and cooling rates of 2.8 °C/ min. It should be noted that TEST-A experienced a cure cycle interruption during the initial ramp segment.

Effective heat transfer coefficients are back calculated using the method given in Appendix F.2, and with measurement points spaced every 6 plies (33 part TCs), 12 plies (17 part TCs), 24 plies (9 part TCs), 48 plies (5 part TCs), 96 plies (3 part TCs) and top/bottom plies (2 part TCs). The results are summarized in Table D-6. Experimentally measured and RAVEN-1D predicted through-thickness temperature profiles are shown in Figure D-15 and Figure D-16 for the initial ramp segment when the autoclave air temperature reaches 110 °C, and Figure D-17 and Figure D-18 for the cool down segment when the autoclave air temperature reaches 60 °C.

Table D-6: Heat transfer boundary condition sensitivity due to a reduction of experimental measurement points for a 38.4 mm thick laminate[a,b,c]. Note: TEST-A experienced a cure cycle interruption during the initial ramp segment and an unintentional bag leak was introduced prior to TEST-C.

Through-thickness part TCs		TEST-A (curing) Equivalent-1D HTC		TEST-B (cured) Equivalent-1D HTC		TEST-C (cured) Equivalent-1D HTC	
Location (every *X* plies)	Total	top W/ (m^2 K)	bottom W/ (m^2 K)	top W/ (m^2 K)	bottom W/ (m^2 K)	top W/ (m^2 K)	bottom W/ (m^2 K)
6	33	38 (71)	122 (180)	64 (66)	147 (185)	9.2 (7.4)	109 (93)
12	17	37 (73)	124 (178)	62 (68)	149 (184)	11 (6.0)	107 (95)
24	9	36 (77)	125 (174)	63 (72)	149 (180)	12 (9.9)	105 (99)
48	5	31 (53)	132 (200)	69 (48)	145 (203)	14 (12)	104 (99)
96	3	28 (87)	140 (167)	85 (91)	135 (162)	10 (9.5)	121 (125)
top/bottom ply	2	55 (72)	151 (183)	74 (64)	163 (178)	18 (16)	95 (93)

[a] Based on experimental data from [145] (Shimizu *et al*, 2008).
Investigation of initial ramp and cool down cure cycle segments where TEST-A, TEST-B and TEST-C are nominally comparable. Heat up & cool down rate $\dot{T}$ = 2.8 °C/ min. Cool down HTC values shown in parentheses.

[b] The method for back-calculating effective HTCs is described in Appendix F.2.

[c] HTC values shown in grey are suspected to have been back calculated from TCs exhibiting apparent failures (TC-13 for TEST-A and TEST-B, and TC-21 for TEST-C). It should be noted that the TCs were reconnected given the part was rebagged prior to TEST-C.

The following observations are made, consistent with the work by Shimizu *et al* [145]:

- The effective top HTC for TEST-B (h_{top} = 64 W/ (m^2 K)) is higher than TEST-A (h_{top} = 38 W/ (m^2 K)) during the initial ramp segment and is attributed to the collapse/resin fill of the breather (see Figure D-15 (a)). The effective top HTC values are comparable during cool down (see Figure D-17 (a)).

- During the initial ramp, the effective top HTC for TEST-C (h_{top} = 9.2 W/ (m^2 K)) is significantly lower than for TEST-B (h_{top} = 64 W/ (m^2 K)) and is attributed to the presence of a bag leak. The effective bottom HTC for TEST-C (h_{bot} = 109 W/ (m^2 K)) is lower than for TEST-B (h_{bot} = 147 W/ (m^2 K)) and is due a reduction in the heat input into the top tool surface (bottom tool surface remains unchanged) for the bag leak case (see Figure D-15 (b)). These trends are also observed during cool down (see Figure D-17 (b)).

As shown in Figure D-15 and Figure D-17, the experimental through-thickness temperature profiles indicate apparent failures that are most likely due to mislabeled or misidentified thermocouples since adjacent measurement points appear inconsistent.

Nominally for curing and cured laminates, back calculated effective HTC values are relatively insensitive to the number of measurement points used in all cases investigated (see Figure D-16 and Figure D-18). The exceptions identified in Table D-6 are where the effective HTC values are computed for: 1) TEST-A and TEST-B using five measurement points; and 2) TEST-C using three measurement points. In these cases, the discrepancy in the back calculated HTC values can be attributed to an apparent thermocouple failure (TC-13 for TEST-A and TEST-B in Figure D-19 and TC-21 for TEST-C in Figure D-20). It is noted that the thermocouples were reconnected given that the part was rebagged prior to TEST-C.

Based on the results of this study, the following conclusions can be made:

- Cool down segments of parts or experiments using equivalent cured (inert) parts can be used to verify the baseline response and HTCs specified (see Figure D-17 (a)).
- Two measurement points, located at top/bottom plies, can provide reasonable estimates of effective HTC values (see Figure D-18 (a)).
- Recommendation that adjacent through-thickness thermocoupless are spaced no greater than 24 plies apart to ensure sufficient sensor redundancy.

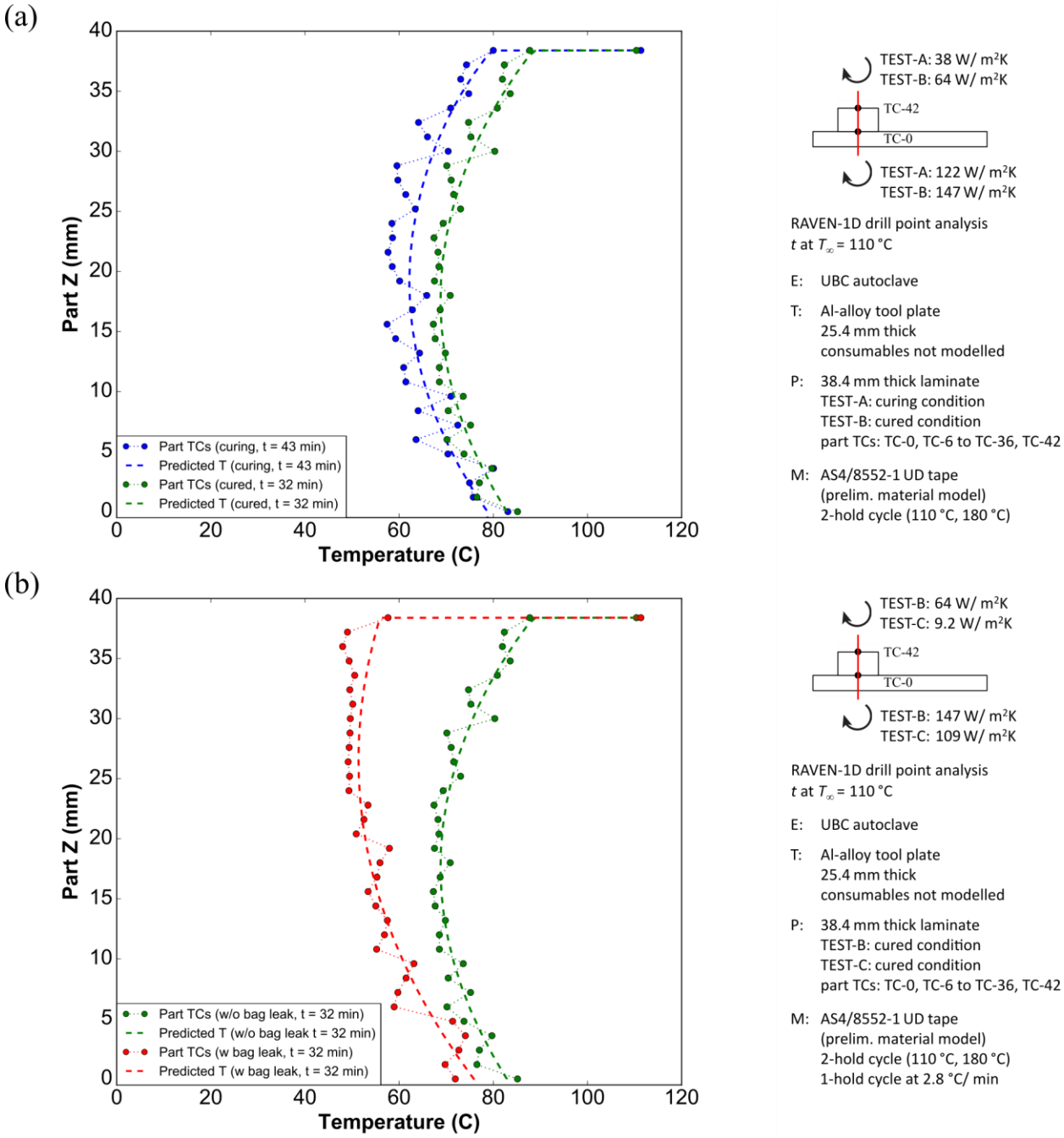

Figure D-15: Comparison of experimentally measured and predicted RAVEN-1D modelling results for a 38.4 mm thick laminate[a] (part TCs: TC-0 (interface, *z* = 0 mm), TC-6 to TC-36, TC-42 (surface, *z* = 38.4 mm). Through-thickness temperature profiles (*z* v *T*) of: (a) curing and cured laminate (experiment ID: TEST-A and TEST-B) and (b) laminate without bag leak and with bag leak (experiment ID: TEST-B and TEST-C). Experimental data from [145] (Shimizu *et al*, 2008). ETPM: Equipment–Tool–Part–Material; TC: Thermocouple; UD: Unidirectional. Note: Temperature profiles shown when the autoclave air temperature reaches 110 °C (initial ramp). Effective HTCs back calculated from 33 measurement points (spaced every six plies).

[a] TEST-A & TEST-B were run back-to-back in autoclave. TEST-A experienced a cure cycle interruption during the initial ramp segment. The part was rebagged & an unintentional bag leak introduced prior to TEST-C.

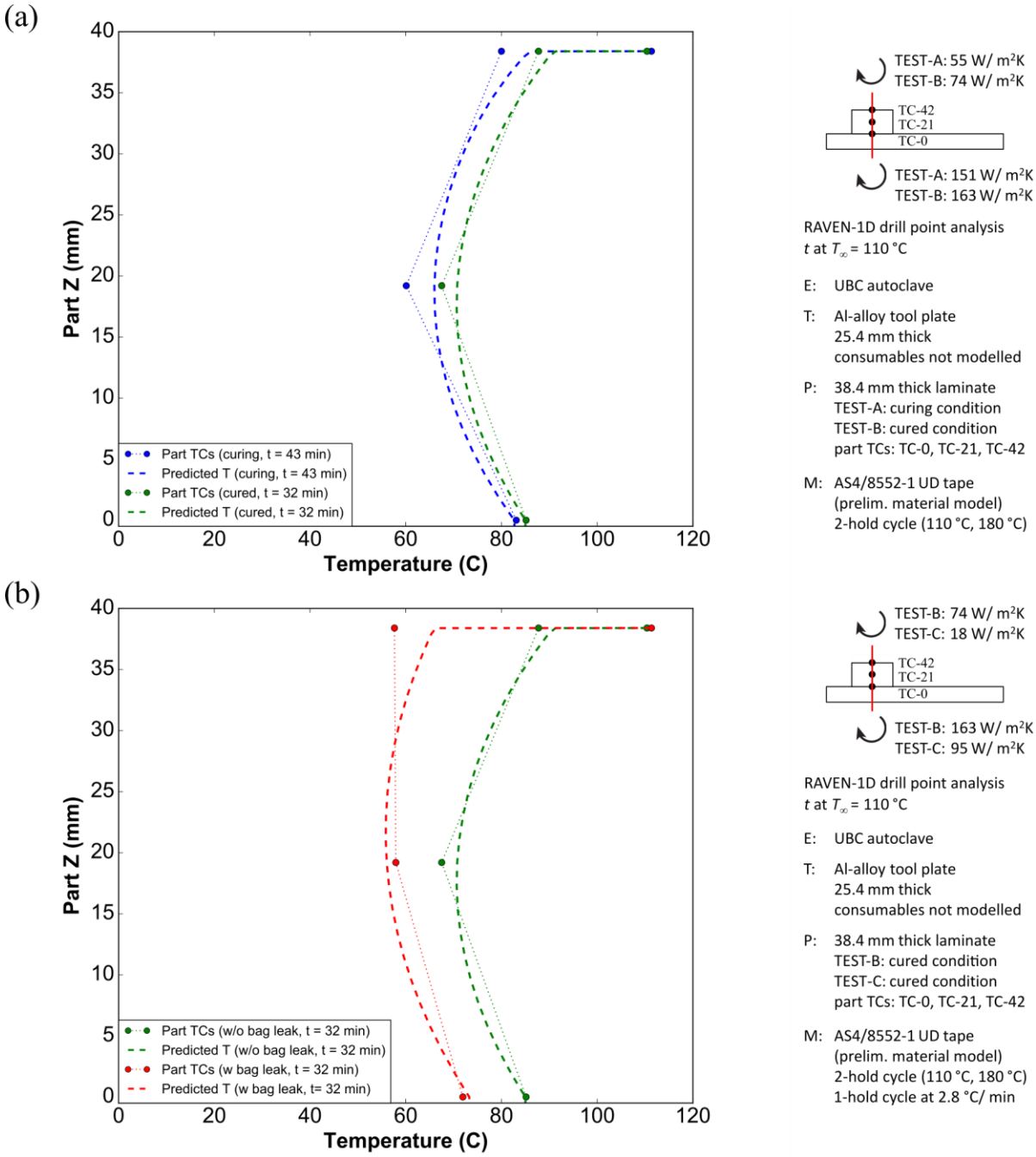

Figure D-16: Comparison of experimentally measured and predicted RAVEN-1D modelling results for a 38.4 mm thick laminate[a] (part TCs: TC-0 (interface, *z* = 0 mm), TC-21, TC-42 (surface, *z* = 38.4 mm). Through-thickness temperature profiles (*z* v *T*) of: (a) curing and cured laminate (experiment ID: TEST-A and TEST-B) and (b) laminate without bag leak and with bag leak (experiment ID: TEST-B and TEST-C). Experimental data from [145] (Shimizu *et al*, 2008). ETPM: Equipment–Tool–Part–Material; TC: Thermocouple; UD: Unidirectional. Note: Temperature profiles shown when the autoclave air temperature reaches 110 °C (initial ramp). Effective HTCs back calculated from two measurement points (top/bottom).

[a] TEST-A & TEST-B were run back-to-back in autoclave. TEST-A experienced a cure cycle interruption during the initial ramp segment. The part was rebagged & an unintentional bag leak introduced prior to TEST-C.

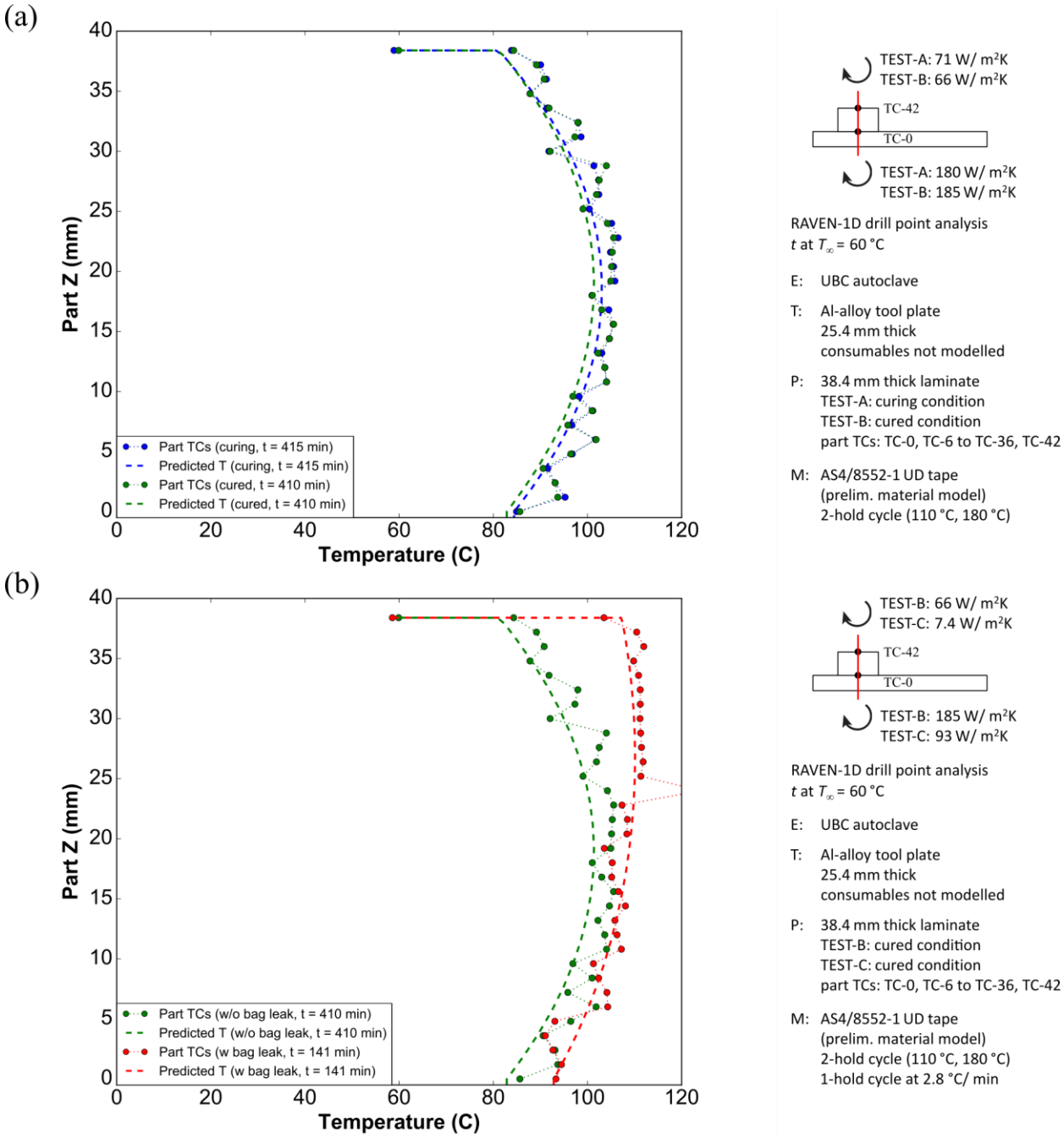

Figure D-17: Comparison of experimentally measured and predicted RAVEN-1D modelling results for a 38.4 mm thick laminate[a] (part TCs: TC-0 (interface, *z* = 0 mm), TC-6 to TC-36, TC-42 (surface, *z* = 38.4 mm). Through-thickness temperature profiles (*z* v *T*) of: (a) curing and cured laminate (experiment ID: TEST-A and TEST-B) and (b) laminate without bag leak and with bag leak (experiment ID: TEST-B and TEST-C). Experimental data from [145] (Shimizu *et al*, 2008). ETPM: Equipment–Tool–Part–Material; TC: Thermocouple; UD: Unidirectional. Note: Temperature profiles shown when the autoclave air temperature reaches 60 °C (cool down). Effective HTCs back calculated from 33 measurement points (spaced every six plies).

[a] TEST-A & TEST-B were run back-to-back in autoclave. The part was rebagged & an unintentional bag leak introduced prior to TEST-C.

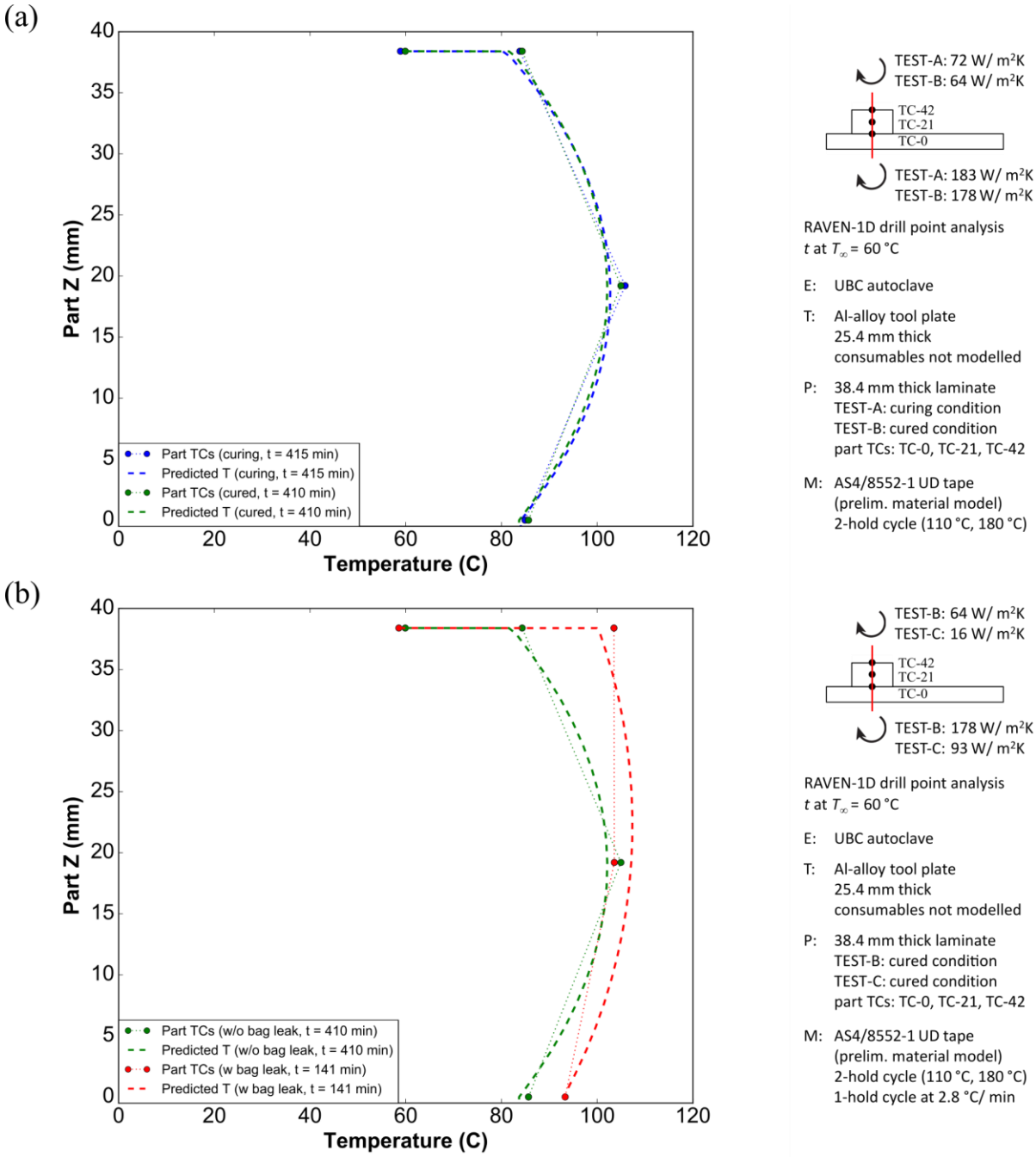

Figure D-18: Comparison of experimentally measured and predicted RAVEN-1D modelling results for a 38.4 mm thick laminate[a] (part TCs: TC-0 (interface, *z* = 0 mm), TC-21, TC-42 (surface, *z* = 38.4 mm). Through-thickness temperature profiles (*z* v *T*) of: (a) curing and cured laminate (experiment ID: TEST-A and TEST-B) and (b) laminate without bag leak and with bag leak (experiment ID: TEST-B and TEST-C). Experimental data from [145] (Shimizu *et al*, 2008). ETPM: Equipment–Tool–Part–Material; TC: Thermocouple; UD: Unidirectional. Note: Temperature profiles shown when the autoclave air temperature reaches 60 °C (cool down). Effective HTCs back calculated from two measurement points (top/bottom).

[a] TEST-A & TEST-B were run back-to-back in autoclave. The part was rebagged & an unintentional bag leak introduced prior to TEST-C.

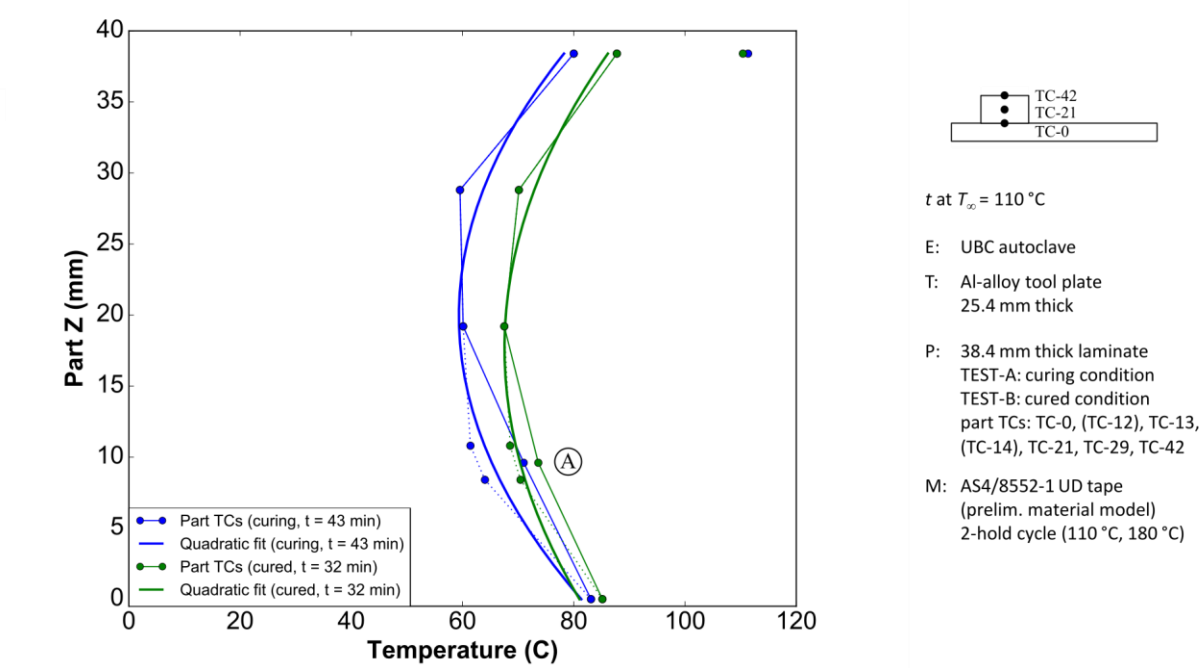

Figure D-19: Comparison of five measurement points (spaced every 48 plies) and quadratic data fit results from 33 measurement points (spaced every six plies) for a 38.4 mm thick laminate[a] (part TCs: TC-0 (interface, *z* = 0 mm), TC-13, TC-21, TC-29, TC-42 (surface, *z* = 38.4 mm). Through-thickness temperature profiles (*z* v *T*) of curing and cured laminate (experiment ID: TEST-A and TEST-B). Experimental data from [145] (Shimizu *et al*, 2008). ETPM: Equipment–Tool–Part–Material; TC: Thermocouple; UD: Unidirectional. Note: Temperature profiles shown when the autoclave air temperature reaches 110 °C (initial ramp). Adjacent TCs to TC-13 shown to highlight apparent TC failure at point A.

[a] TEST-A & TEST-B were run back-to-back in autoclave. TEST-A experienced a cure cycle interruption during the initial ramp segment.

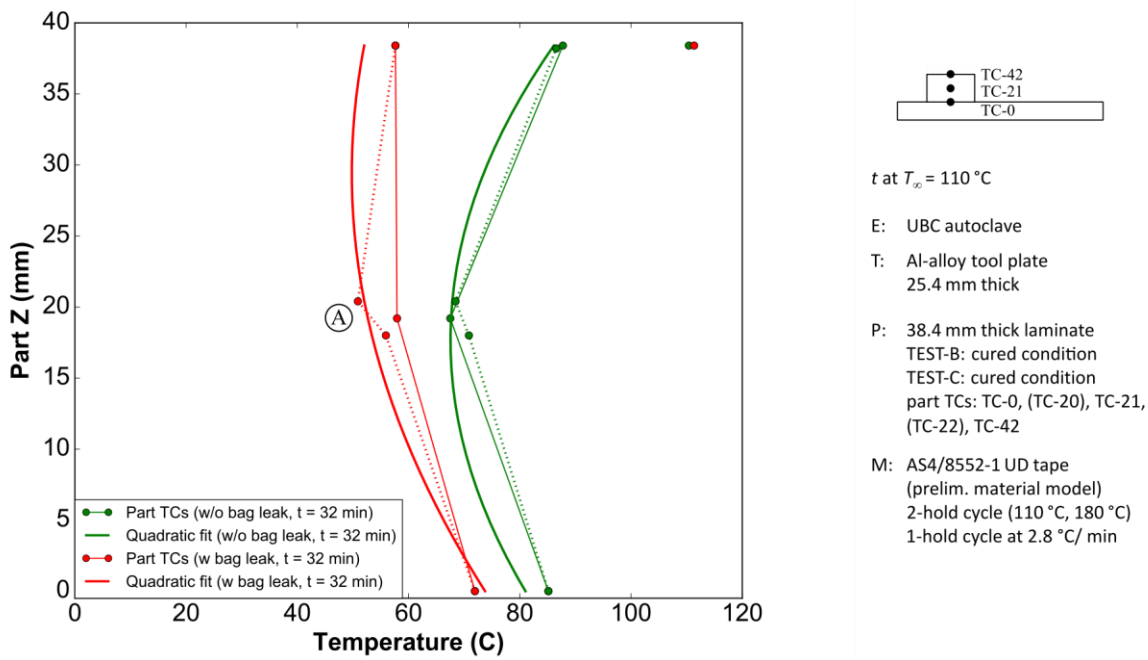

Figure D-20: Comparison of three measurement points (spaced every 96 plies) and quadratic data fit results from 33 measurement points (spaced every six plies) for a 38.4 mm thick laminate[a] (part TCs: TC-0 (interface, *z* = 0 mm), TC-21, TC-42 (surface, *z* = 38.4 mm). Through-thickness temperature profiles (*z* v *T*) of laminate without bag leak and with bag leak (experiment ID: TEST-B and TEST-C). Experimental data from [145] (Shimizu *et al*, 2008). ETPM: Equipment–Tool–Part–Material; TC: Thermocouple; UD: Unidirectional. Note: Temperature profiles shown when the autoclave air temperature reaches 110 °C (initial ramp). Adjacent TCs to TC-21 shown to highlight apparent TC failure at point A.

[a] The part was rebagged, thermocouples reconnected & an unintentional bag leak introduced prior to TEST-C.

D.3 Slesinger data set

This data set considers 11.7 mm and 14.7 mm thick laminates made with Hexcel AS4/8552-1 prepreg tape and a 7.5 mm thick laminate made with Toray T800H/3900-2 prepreg tape. All laminates are processed using insulating bricks, and in curing and cured conditions to enable thermochemical model validation [150]. These cases are a subset of the original experimental work performed.

D.3.1 Experimental setup and schematic of thermocouple locations

(a)

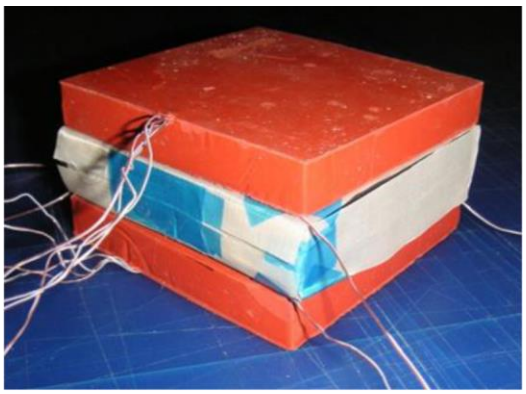

(b)

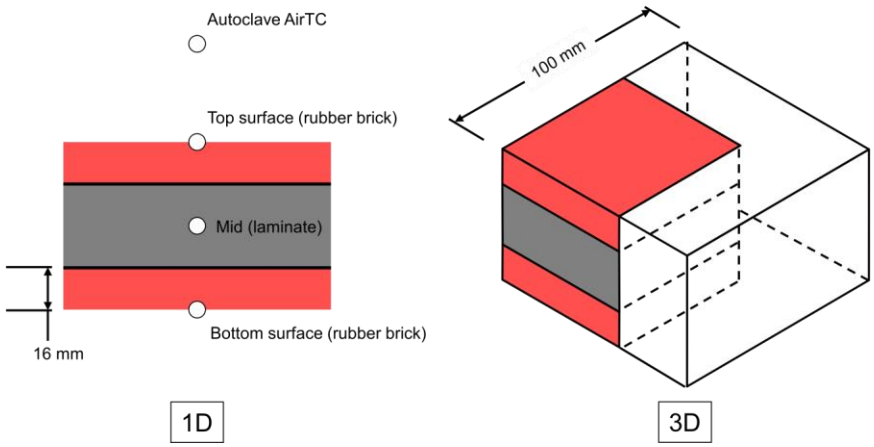

Figure D-21: Slesinger data set: (a) experimental setup prior to bagging and (b) schematic of thermocouple locations (photo and schematic from [150] (Slesinger, 2010)).

D.3.2 Summary of ETPM thermal management attributes

Table D-7: ETPM[a] attribute definition for the Slesinger data set.

		Test[b]	Analysis[c]
Equipment	**(E)**	Autoclave: UBC	
Tool	**(T)**	KE1204 RTV brick (100 mm x 100 mm) z_{tool} = 16.0 mm	
Part	**(P)**	Flat laminate (100 mm x 100 mm) $z_{part\ (AS4/8552\text{-}1)}$ = 11.7 mm (60 ply) $z_{part\ (AS4/8552\text{-}1)}$ = 14.7 mm (80 ply) $z_{part\ (T800H/3900\text{-}2)}$ = 7.5 mm (40 ply) TC (mid)	RAVEN-1D drill point analysis [238] T: mid
Material	**(M)**	AS4/8552-1 UD tape T800H/3900-2 UD tape Single-hold cycle (180 °C)	AS4/8552-1 preliminary material model T800H/3900-2 open lit. material model

[a] ETPM: Equipment–Tool–Part–Material

[b] Experimental data from [150] (Slesinger, 2010). AS4/8552-1 laminates: 20100225-60 (60 ply, curing); 20100226-60 (60 ply, cured), 20100225-80 (80 ply, curing); 20100226-80 (80 ply, cured); T800H/3900-2 laminate: 20100304-40 (40 ply, curing); 20100305-40 (40 ply, cured).

[c] Prescribed temperature boundary conditions are applied to the respective surface boundaries of the top and bottom insulating bricks.

D.3.3 Temperature plots

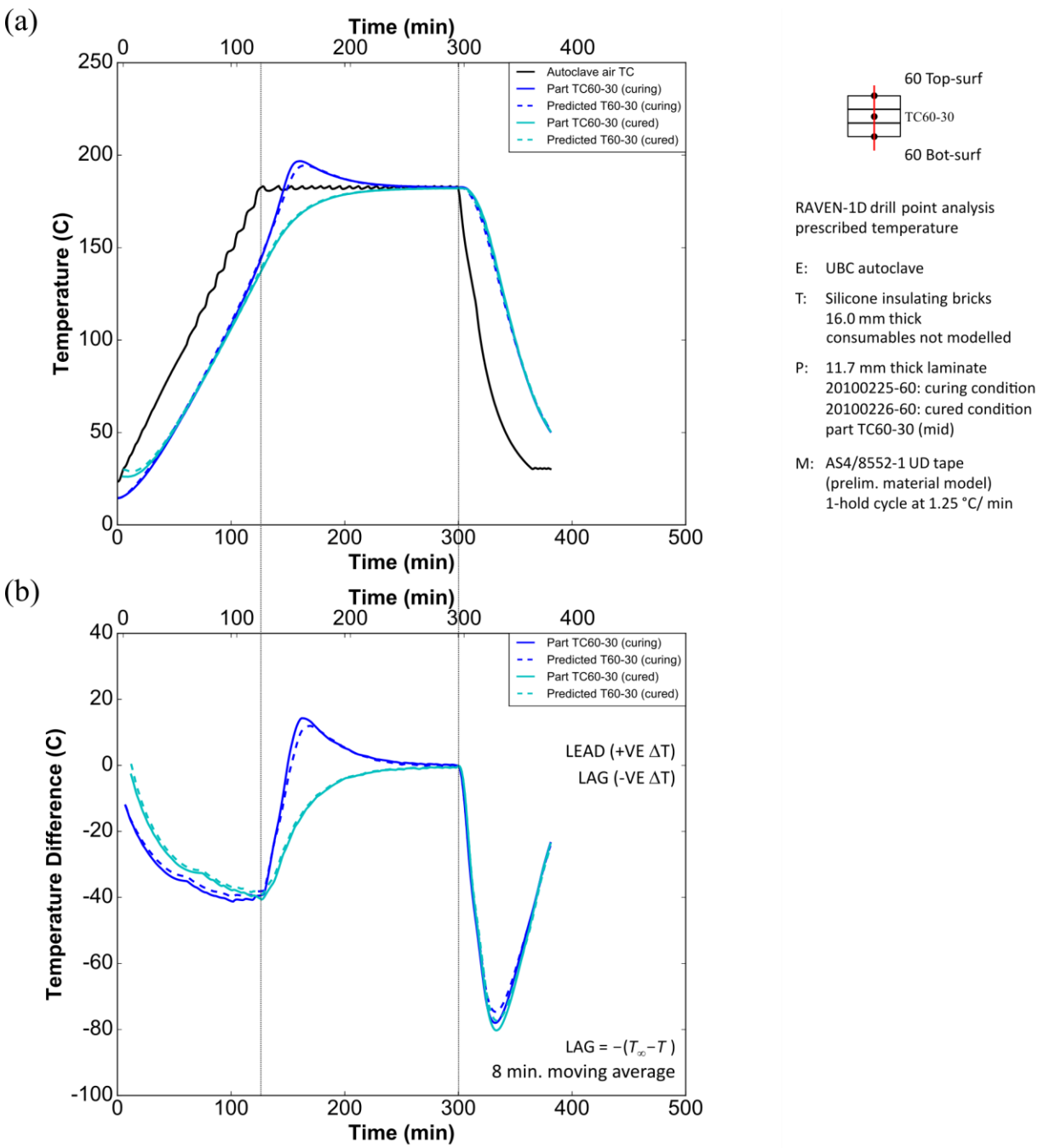

Figure D-22: Comparison of experimentally measured and predicted RAVEN-1D modelling results for the Slesinger data set (AS4/8552-1, 11.7 mm thick laminate): (a) temperature profile (*T* v *t*) and (b) temperature difference with respect to the autoclave air temperature (Δ*T* v *t*). Experimental data from [150] (Slesinger, 2010). ETPM: Equipment–Tool–Part–Material; TC: Thermocouple; UD: Unidirectional. Note: Vertical lines indicate heat up, hold and cool down cure cycle segments.

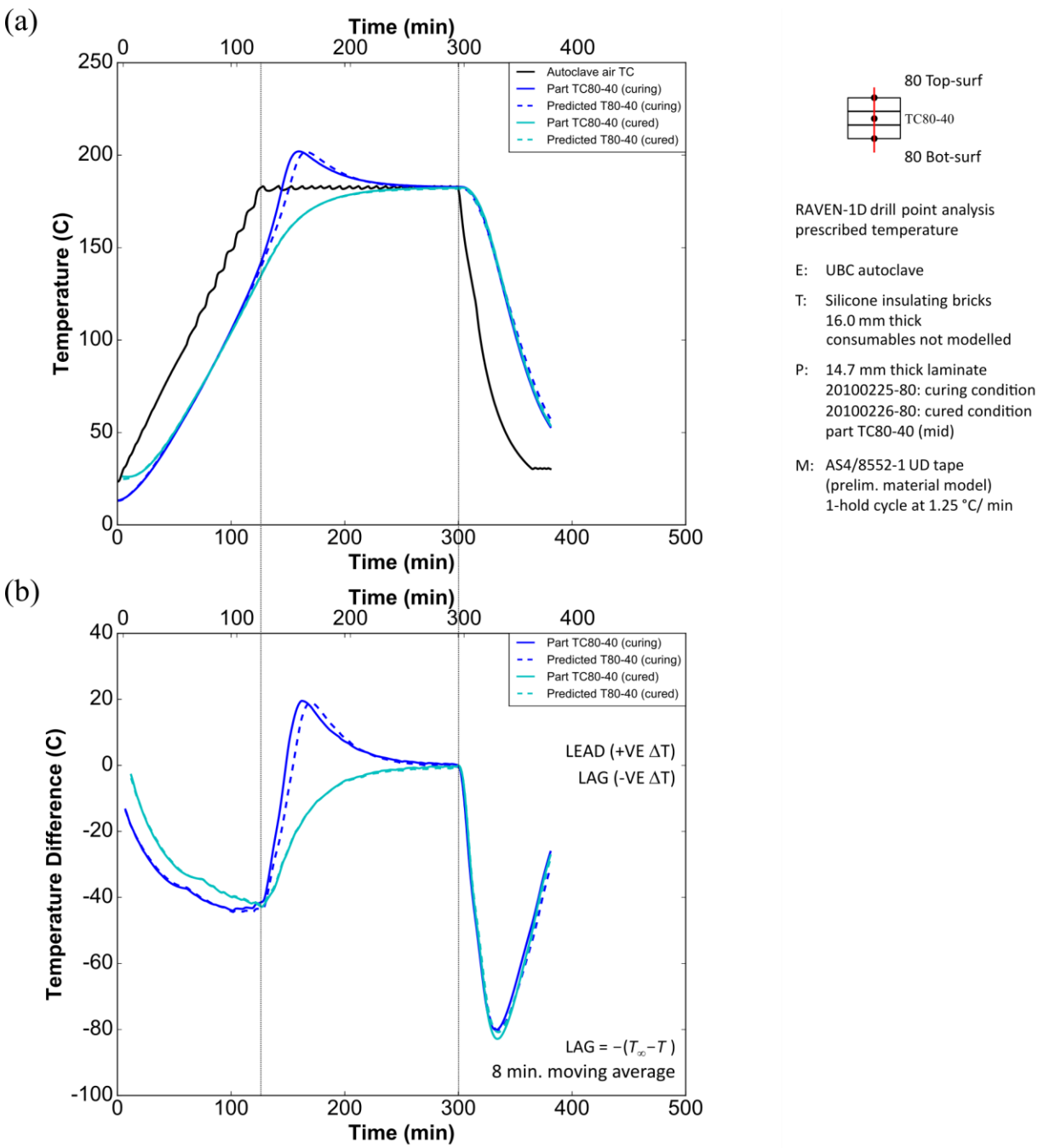

Figure D-23: Comparison of experimentally measured and predicted RAVEN-1D modelling results for the Slesinger data set (AS4/8552-1, 14.7 mm thick laminate): (a) temperature profile (*T* v *t*) and (b) temperature difference with respect to the autoclave air temperature (Δ*T* v *t*). Experimental data from [150] (Slesinger, 2010). ETPM: Equipment–Tool–Part–Material; TC: Thermocouple; UD: Unidirectional. Note: Vertical lines indicate heat up, hold and cool down cure cycle segments.

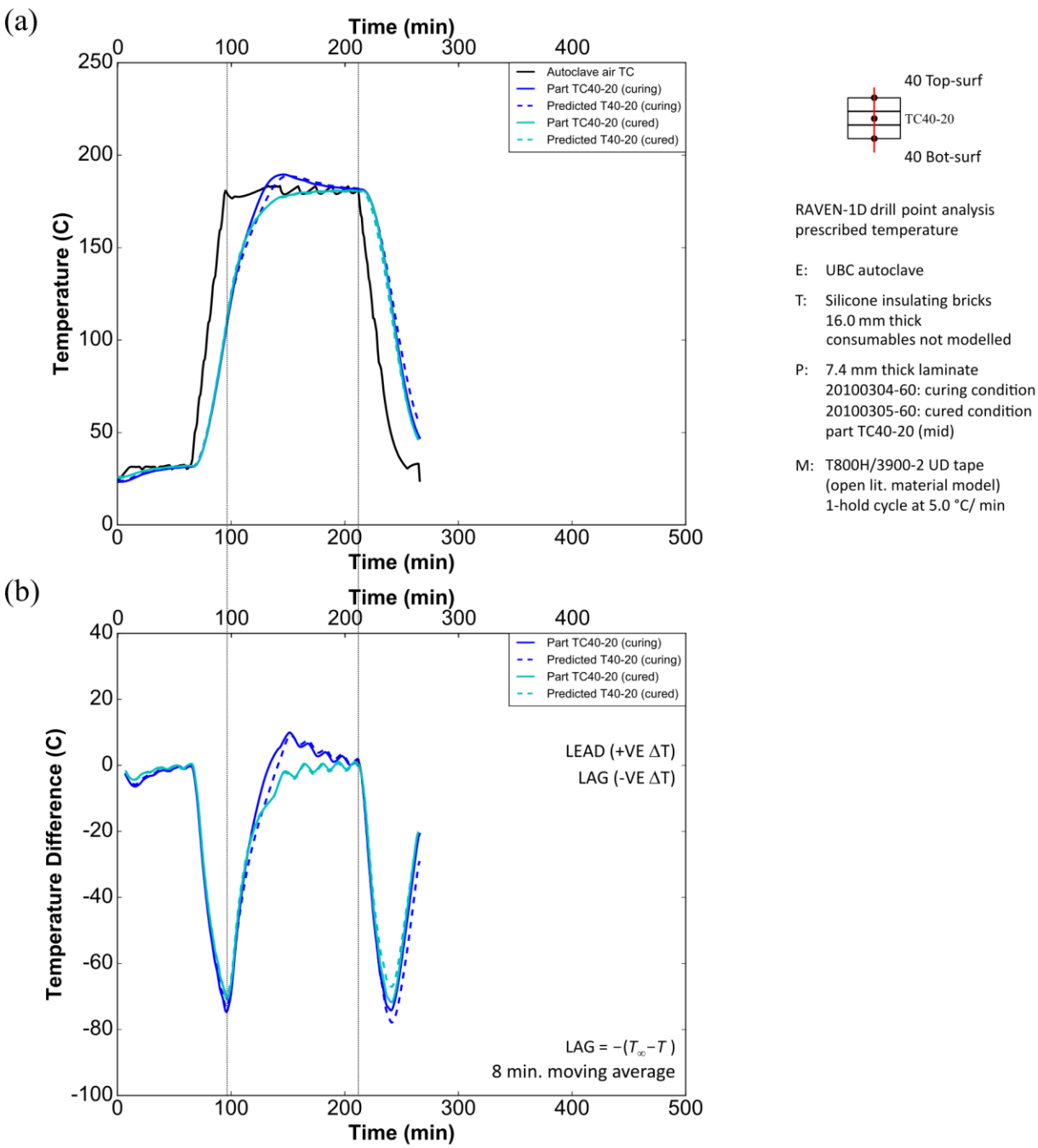

Figure D-24: Comparison of experimentally measured and predicted RAVEN-1D modelling results for the Slesinger data set (T800H/3900-2, 7.5 mm thick laminate): (a) temperature profile (*T* v *t*) and (b) temperature difference with respect to the autoclave air temperature (Δ*T* v *t*). Experimental data from [150] (Slesinger, 2010). ETPM: Equipment–Tool–Part–Material; TC: Thermocouple; UD: Unidirectional. Note: Vertical lines indicate heat up, hold and cool down cure cycle segments.

D.4 CCMRD9.2 data set

Two cases are considered in this data set. 3.1 mm thick C-shaped laminates processed on a family of identical small-scale Invar, Al-alloy and CFRP tools, and a 12.4 mm thick C-shaped laminate processed on a small-scale Invar tool [236]. All parts are made with Toray T800H/3900-2 prepreg tape. These cases represent a subset of the original experimental work performed.

In addition to the work presented in Section 5.3.3 investigating real thermocouple failures, the science based evaluation of apparent thermocouple failures is given in D.4.5.

Additional modelling results for a 12.4 mm thick C-shaped laminate are presented in D.4.6.

D.4.1 Experimental setup and schematic of thermocouple locations

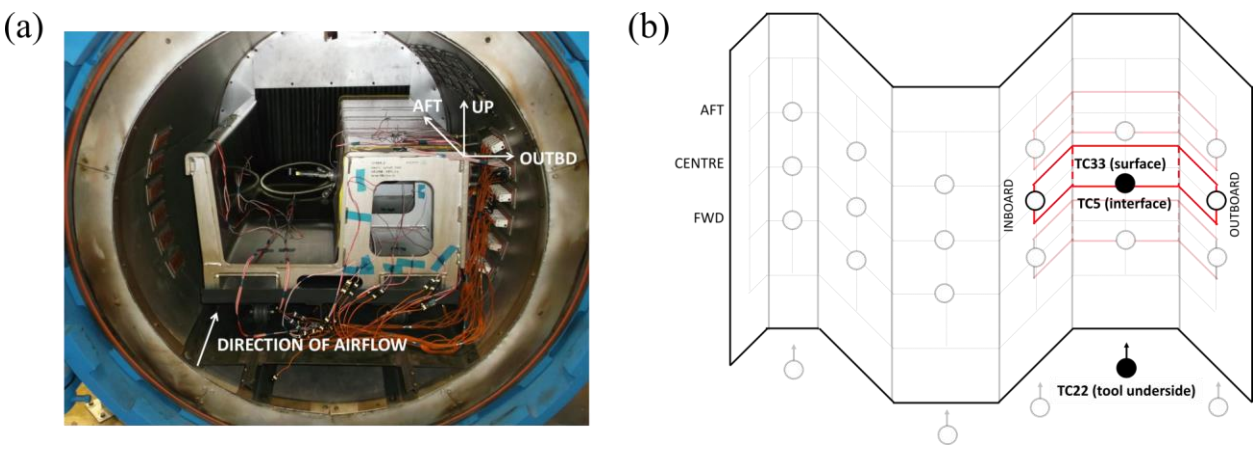

Figure D-25: CCMRD9.2 data set: (a) representative experimental setup and (b) schematic of thermocouple locations for 12.4 mm thick C-shaped laminate (photo and schematic courtesy of CCMRD [236]).

D.4.2 Reported effective heat transfer coefficients

Table D-8: Effective heat transfer coefficients for the CCMRD9.2 data set (12.4 mm thick C-shaped laminate)[a].

Analysis		Equivalent-1D HTC top W/ (m^2 K)	Equivalent-1D HTC bottom W/ (m^2 K)	HTC distribution top W/ (m^2 K)	HTC distribution bottom W/ (m^2 K)
Original[a] (~2015)		60	40		
Revised[b,c] (2018)	tool only (ave)	30	40		
	tool & part (low)	40	80		
	tool & part (high)	50	75		
Park[d] (2018)				60	45

[a] From [236] (Arafath *et al*, 2015). Part ID: CCM9.2-077 (Invar tool).
Effective HTCs were iteratively calibrated using RAVEN to match thermocouple data [236].
[b] Modified heat flux Method I' is used to back-calculate the effective HTCs, described in Appendix F.2.
Effective HTC values are back-calculated from tool TC22.
[c] Low HTC value (unpressurized) back-calculated at t = 30 min. High HTC value (pressuried) back-calculated at 70 min < t < 90 min.
[d] From [178] Park (2018). Convective HTC distribution based on CFD analysis. Average HTC values from sample points taken near part TCs TC33 & TC5 model locations at t = 120 min (see Figure D-33).

D.4.3 Summary of ETPM thermal management attributes

Table D-9: ETPM[a] attribute definition for the CCMRD9.2 data set (3.1 mm thick C-shaped laminate).

		Test[b]
Equipment	**(E)**	Autoclave: UBC
Tool	**(T)**	Invar, Al-alloy and CFRP (small-scale tools)[c] z_{tool} = 12.7 mm TC (tool underside)
Part	**(P)**	C-shaped laminate (300 mm (web) x 150 mm (flange) x 100 mm) 20 mm (fillet radius) z_{part} = 3.1 mm (16 ply) TC-5 (surface)
Material	**(M)**	T800H/3900-2 UD tape Single-hold cycle (180 °C)

[a] ETPM: Equipment–Tool–Part–Material
[b] Experimental data from [236] (Arafath *et al*, 2015). Part ID: CCM9.2-043 (Invar tool), CCM9.2-052 (Invar tool, repeat); CCM9.2-028 (Al-alloy tool); CCM9.2-031 (CFRP tool).
[c] This is a nominal face plate thickness. The measured face plate thickness of the CFRP tool is 8.8 mm.

Refer to Table 5-7 for details of the 12.4 mm thick C-shaped laminate (Part ID: CCM9.2-077).

D.4.4 Temperature plots

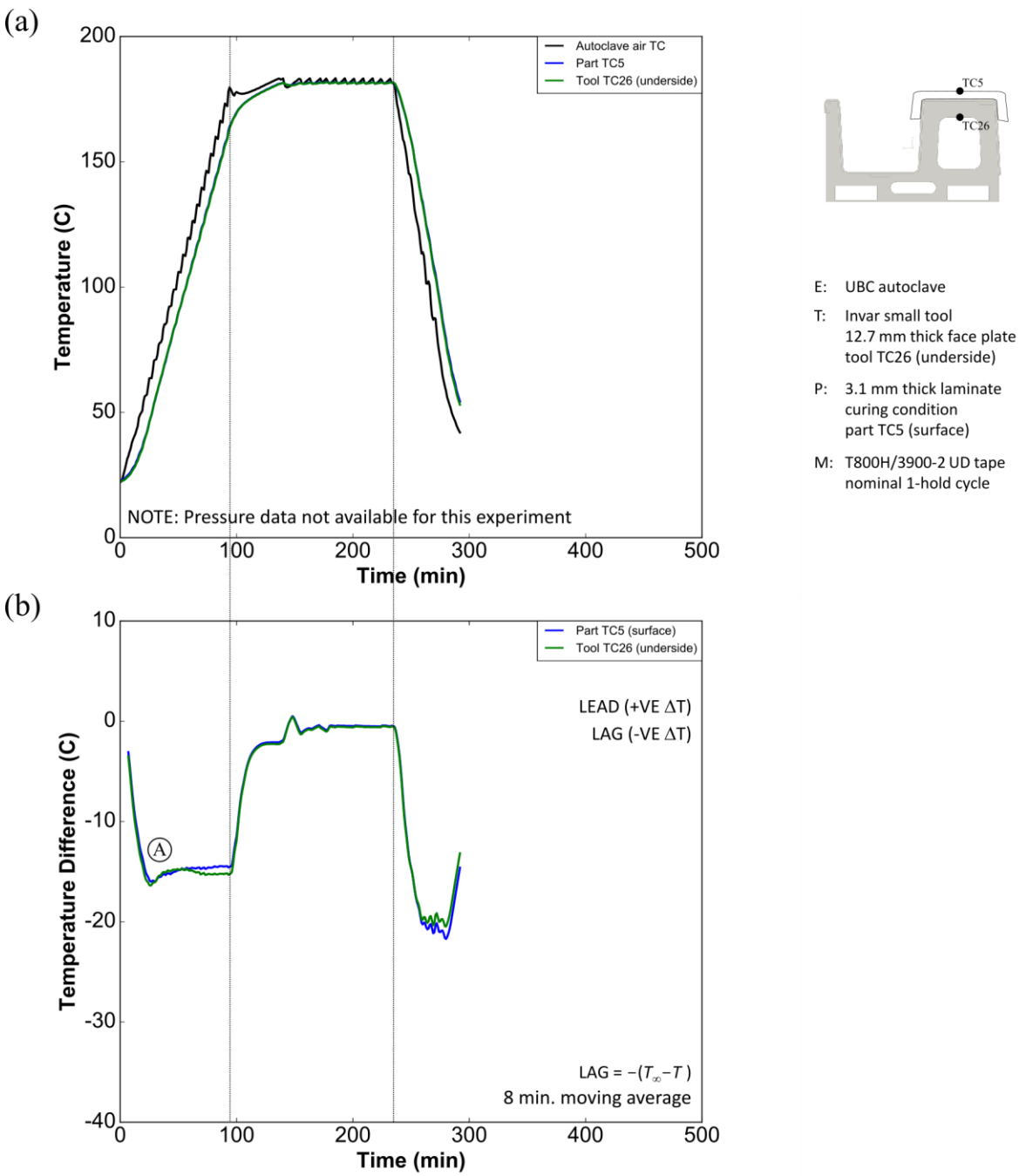

Figure D-26: Experimentally measured results for the CCMRD9.2 data set (3.1 mm thick C-shaped laminate, Invar tool (part ID: CCM9.2-043)): (a) temperature profile (*T* v *t*) and (b) temperature difference with respect to the autoclave air temperature (Δ*T* v *t*). Experimental data from [236] (Arafath *et al*, 2015). ETPM: Equipment–Tool–Part–Material; TC: Thermocouple; UD: Unidirectional. Note: Perturbation in temperature difference (< 1.5 °C TC limit of error) observed at approximately *t* = 30 min at point A due to autoclave pressurization (inferred from other experiments). Vertical lines indicate heat up, hold and cool down cure cycle segments.

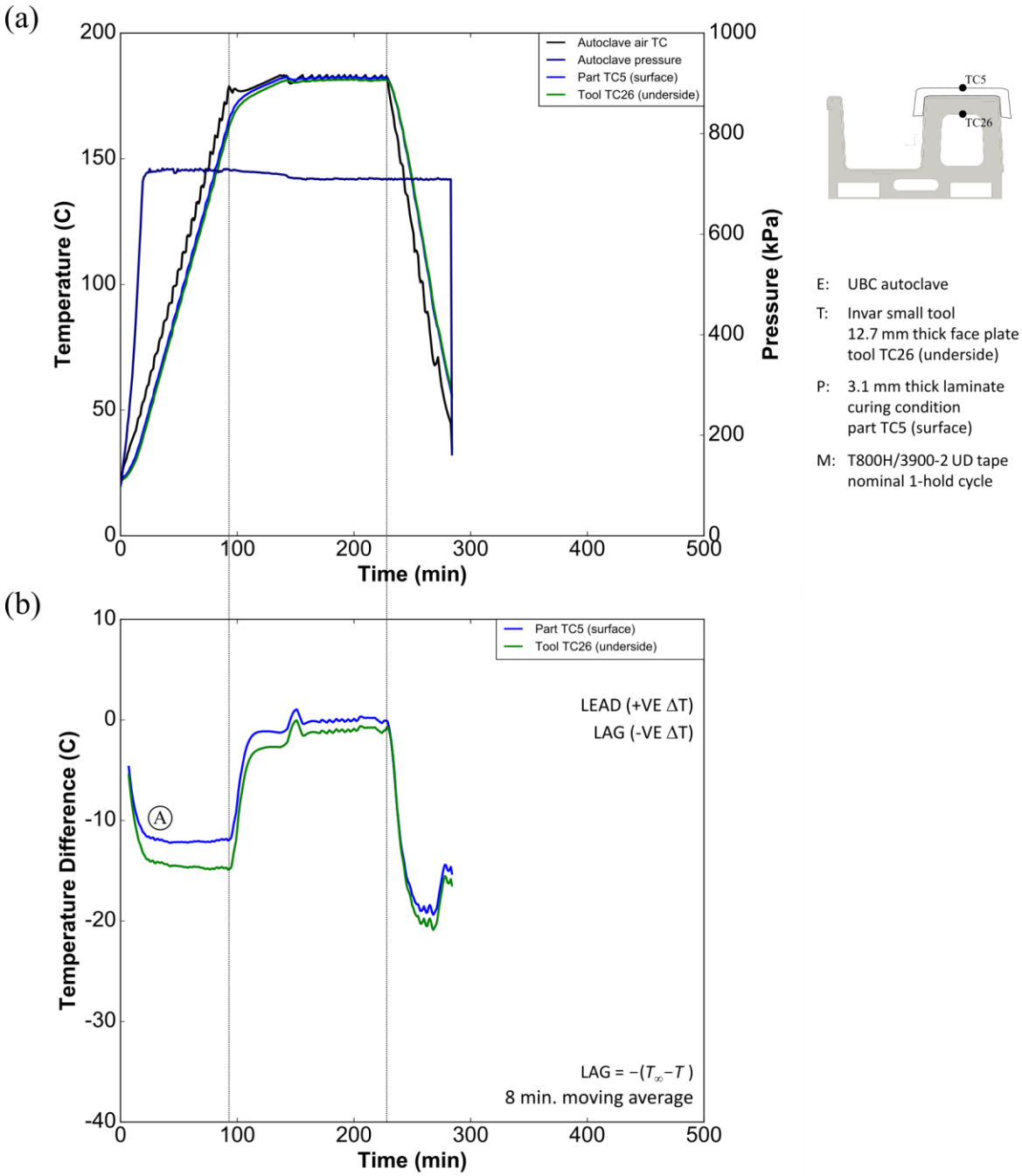

Figure D-27: Experimentally measured results for the CCMRD9.2 data set (3.1 mm thick C-shaped laminate, Invar tool (part ID: CCM9.2-052)): (a) temperature profile (*T* v *t*) and (b) temperature difference with respect to the autoclave air temperature (Δ*T* v *t*). Experimental data from [236] (Arafath *et al*, 2015). ETPM: Equipment–Tool–Part–Material; TC: Thermocouple; UD: Unidirectional. Note: Perturbation in temperature difference not observed at approximately *t* = 30 min at point A due to autoclave pressurization. Vertical lines indicate heat up, hold and cool down cure cycle segments.

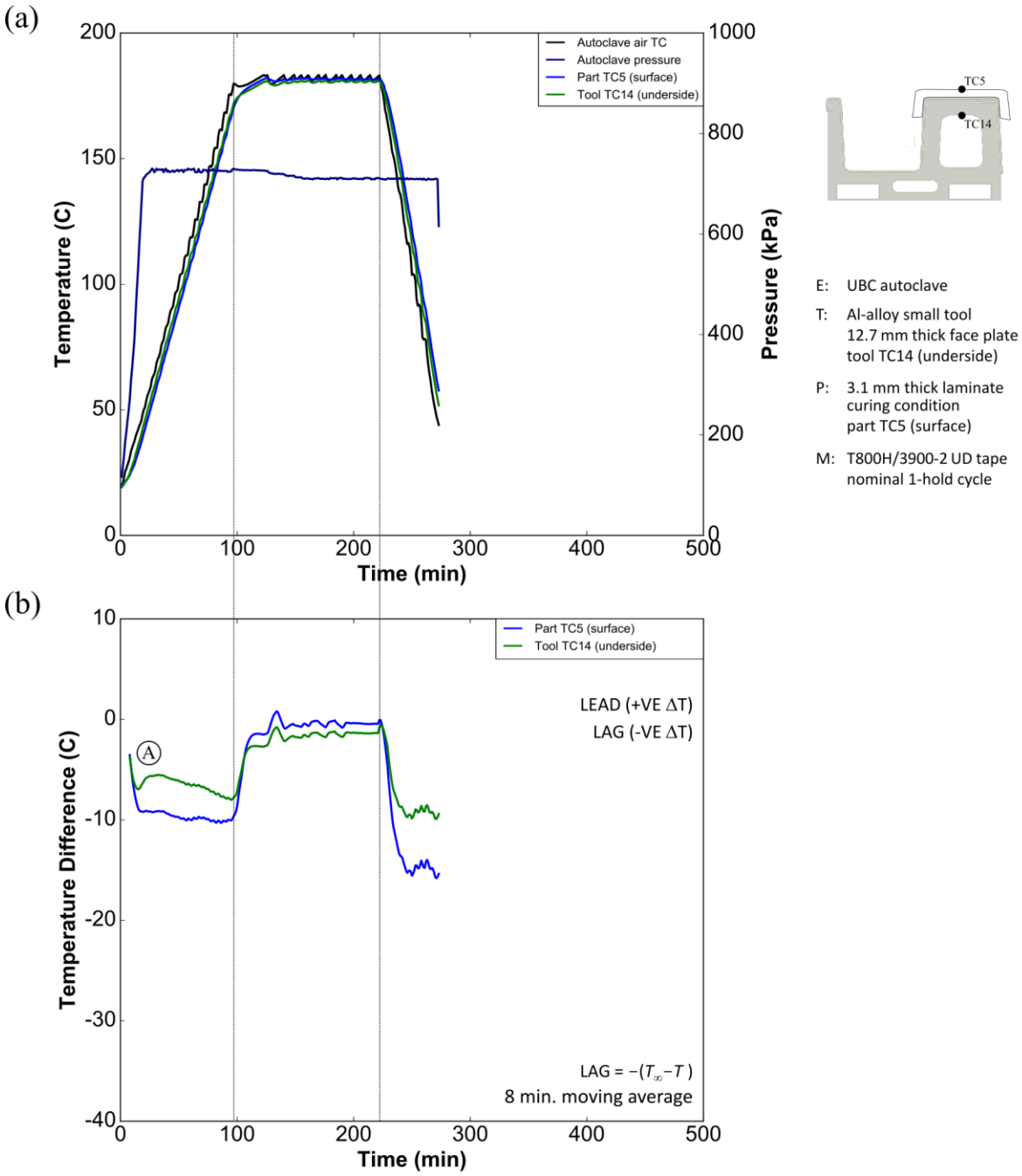

Figure D-28: Experimentally measured results for the CCMRD9.2 data set (3.1 mm thick C-shaped laminate, Al-alloy tool (part ID: CCM9.2-028)): (a) temperature profile (*T* v *t*) and (b) temperature difference with respect to the autoclave air temperature (Δ*T* v *t*). Experimental data from [236] (Arafath *et al*, 2015). ETPM: Equipment–Tool–Part–Material; TC: Thermocouple; UD: Unidirectional. Note: Perturbation in temperature difference (< 1.5 °C TC limit of error at the tool underside surface) observed at approximately *t* = 30 min at point A due to autoclave pressurization. Vertical lines indicate heat up, hold and cool down cure cycle segments.

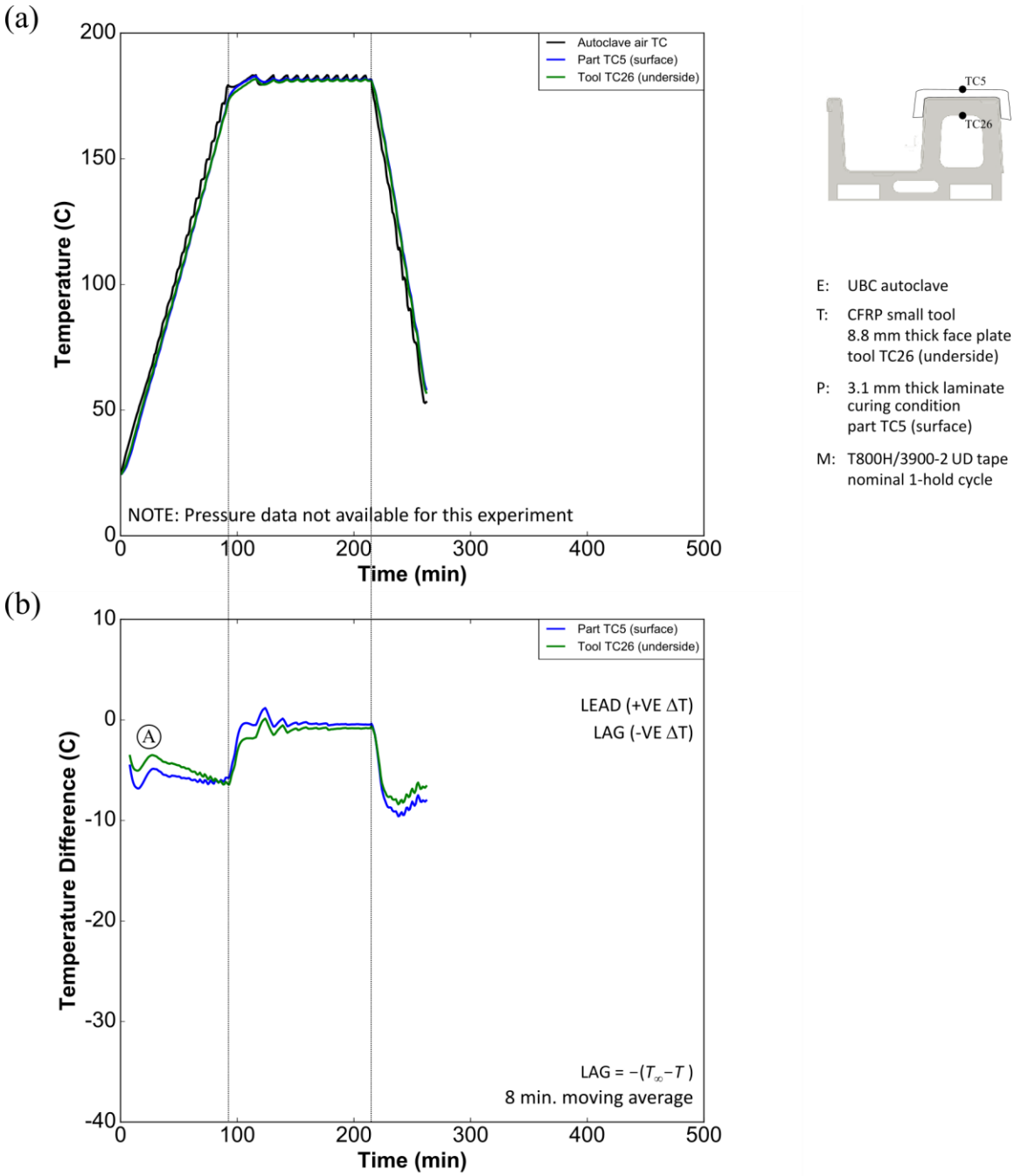

Figure D-29: Experimentally measured results for the CCMRD9.2 data set (3.1 mm thick C-shaped laminate, CFRP tool (part ID: CCM9.2-031)): (a) temperature profile (*T* v *t*) and (b) temperature difference with respect to the autoclave air temperature (Δ*T* v *t*). Experimental data from [236] (Arafath *et al*, 2015). ETPM: Equipment–Tool–Part–Material; TC: Thermocouple; UD: Unidirectional. Note: Perturbation in temperature difference (> 1.5 °C TC limit of error at the part surface) observed at approximately *t* = 30 min at point A due to autoclave pressurization (inferred from other experiments). Vertical lines indicate heat up, hold and cool down cure cycle segments.

D.4.4.1 Cursory analysis of experimentally measured temperature results

Experimentally measured thermcouple data from [236] (Arafath *et al*, 2015), shown as temperature profile (T v t) and temperature difference with respect to the autoclave air temperature (ΔT v t) plots, for 3.1 mm thick T800H/3900-2 C-shaped laminates processed on Invar, Al-alloy and CFRP tools are presented. These plots indicate some rather interesting and, in some cases obvious, observations. Complementary work by Park [178] provides a detailed analysis of these observed effects.

Firstly, the experimental data shows a consistent correlation between thermal lag (ΔT) and overall tool thermal mass ($m.C_p$). Based on the underside tool surface temperature, the Invar tool is the least thermally responsive with an approximate thermal lag ΔT_{Invar} = -14.5 °C (see Figure D-26 (b) and Figure D-27 (b)) compared to the respective Al-alloy and CFRP tools, $\Delta T_{Al\text{-}alloy}$ = -8.0 °C (see Figure D-28 (b)) and ΔT_{CFRP} = -6.4 °C (see Figure D-29 (b)). It should be noted that the tools were purposefully positioned in the same location in the autoclave to minimize the effect of autoclave airflow variations [243]. Secondly, there is neglible temperature difference (within the typical ±1.5 °C limits of thermocouple accuracy) between the part surface and tool underside surface thermocouples on the 180 °C hold.

Further insights during the heat up segment of the cure cycle require careful interpretation of the ΔT v t plots. Firstly, due to autoclave pressurization while heating, a perturbation in thermal lag is observed in the Al-alloy and CFRP tools at approximately t = 30 min. The Invar tool appears insensitive to this effect. It is also noted that the sensitivity of this change is more apparent at the

part surface than at the tool underside surface. Secondly, it is observed that for the Invar tool, the part thermal response leads the tool; for the Al-alloy tool, the part thermal response lags the tool, and for the CFRP tool, the part and tool thermal responses are the same. This is attributed to tool size effects resulting from the curing of small and thin parts on relatively large and uninsulated tools. Tool size effects have previously been reported in work by Shimizu *et al* [145].

Differences in the thermal lag measured on the tool underside surface for the respective 3.1 mm thick and 12.4 mm thick C-shaped laminates processed on the Invar tool are observed. This difference is approximately 3.7 °C, with $\Delta T_{\text{Invar (CCM9.2-043 \& 052)}}$ = -14.5 °C (see Figure D-26 (b) and Figure D-27 (b)) compared to $\Delta T_{\text{Invar (CCM9.2-077)}}$ = -18.2 °C (see Figure 5-16 (b)) at the tool underside surface. Given the airflow characteristics of the UBC autoclave are known, one possible explanation for this discrepancy is the position of the tool in the autoclave. It is known that the tool was positioned closer to the autoclave door, where the airflow is poor, for the 12.4 mm thick C-shaped laminate [150,243].

D.4.5 Case study: Invar, Al-alloy and CFRP tools

Apparent failures are caused by faulty sensors or sensors that provide invalid measurements. For example, apparent thermocouple failures include: 1) noisy signals and sudden spikes in temperature; 2) unusually high heating/cooling rates; 3) shortened cure cycles (indicating faulty lagging TCs); 4) thermocouple signals that fail to 'damp out' temperature modulation (indicating poorly insulated TCs and/or TCs that are not measuring the true surface part/tool temperature); and 5) thermcouple calibration.

In this case study, experimentally measured temperature data from [236] (Arafath *et al*, 2015) for three geometrically identical Invar, Al-alloy and CFRP tools with a nominal tool plate thickness of 12.7 mm (Figure D-30) are investigated. The details of the experiments analyzed are given in Table D-10. To assess this tool TC data, we first calculate an estimated temperature difference at the tool surface for these tools for a range of HTC values and heating rate of 1.7 °C/ min.

According to Rasekh [142] an approximate closed-form expression for the transient steady-state temperature difference at the slab surface, assuming symmetric boundary conditions, is:

$$\Delta T_{\mathrm{ss}} = -\left(T_{\infty} - T_{\mathrm{s}}\right) = -\dot{T}\,\frac{L^2}{a}\left(\frac{1}{Bi}\right) = -\dot{T}\,\frac{\rho C_{\mathrm{p}} L}{h} \qquad \text{(D-1)}$$

where in Equation (D-1), T_{∞} is the autoclave air temperature, $\dot{T}$ is the heating rate, a is the thermal diffusivity of the slab, L is the slab half-thickness, Bi is the Biot number (hL/k), ρ is the density, C_{p} is the specific heat capacity, h is the convective heat transfer coefficient and k is the thermal conductivity.

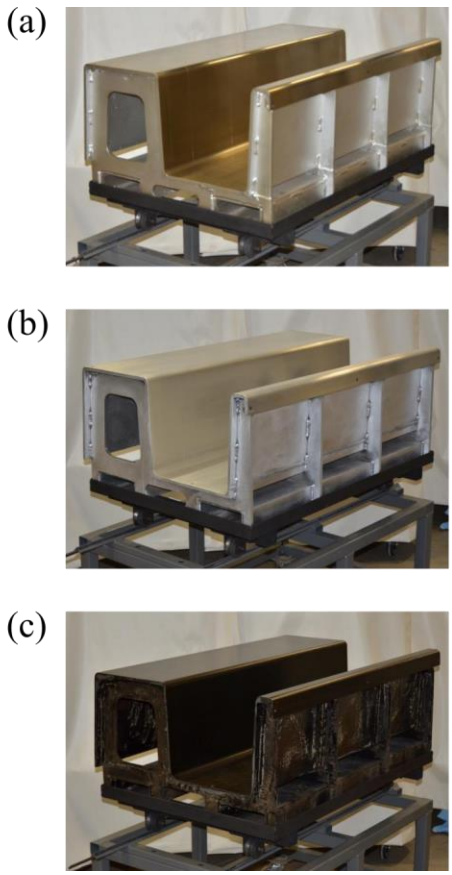

Figure D-30: Family of small-scale tools fabricated from: (a) Invar 36 (Invar), (b) 6061-T6 aluminum alloy (Al-alloy) and (c) composite (CFRP) (photo courtesy of CRN). Note: These tools are nominally geometrically identical (overall dimensions: 1200 mm (length), 800 mm (width), 480 mm (height)).

Table D-10: ETPM[a] attribute definition for a family of nominally geometrically identical small-scale tools.

		Test[b]
Equipment	**(E)**	Autoclave: UBC
Tool	**(T)**	Invar, Al-alloy and CFRP (small-scale tools)[c] z_{tool} = 12.7 mm
Part	**(P)**	N/A
Material	**(M)**	Single-hold cycle (180 °C)

[a] ETPM: Equipment–Tool–Part–Material
[b] Experimental data from [236] (Arafath *et al*, 2015).
CCM9.2-042-043-044 (Invar); CCM9.2-033-034-035 (Al-alloy); CCM9.2-030-031-032 (CFRP).
[c] This is a nominal face plate thickness. The measured face plate thickness of the CFRP tool is 8.8 mm.

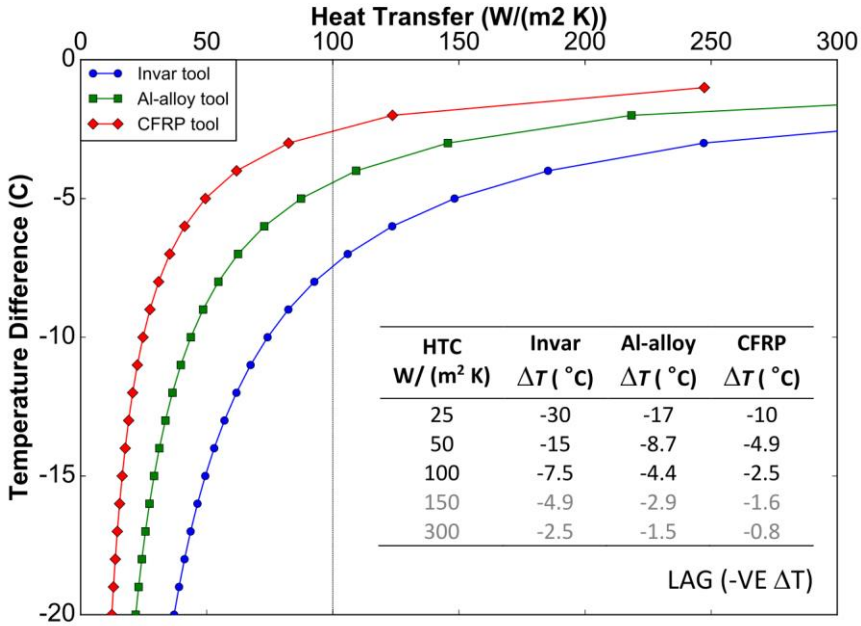

Figure D-31: Estimated temperature difference at the tool surface with respect to the autoclave air temperature (ΔT v h) for small-scale Invar, Al-alloy and CFRP tools[a,b]. h: heat transfer coefficient; ΔT: temperature difference. Note: Vertical line indicates typical upper heat transfer limit for autoclave cure (very high impinging airflow). Temperature difference values shown in grey are unlikely to be achieved in autoclave cure.

[a] Estimated temperature difference calculated with Equation (D-1) from [142] (Rasekh, 2007), and based on a tool plate thickness z = 12.7 mm & nominal heat up rate $\dot{T}$ = 1.7 °C/ min.

[b] The thermophysical properties for Invar, Al-alloy & CFRP are given in Appendix E.4.

The estimated ΔT results shown in Figure D-31 indicate that for a typical upper heat transfer limit for autoclave cure (h = 100 W/ (m^2 K) for very high impinging airflow) [29], the thermal lag in each of these tools with respect to the autoclave air temperature is: ΔT_{Invar} = -7.5 °C, $\Delta T_{\text{Al-alloy}}$ = -4.4 °C and ΔT_{CFRP} = -2.5 °C. Thus, we would expect to see thermal differences greater than these estimated values in experimentally measured temperature data.

Experimentally measured temperature results for insulated tool TCs located on topside and underside tool surfaces are shown as temperature profile (T v t) plots for these respective tools in Figure D-32. By inspection, tool TC15 (topside) appears to provide valid topside tool surface temperature measurements during the heat up segment of the cure cycle in all three cases. The experimental temperature data shows consistent trends between thermal lag (ΔT) and the overall tool thermal mass ($m.C_p$), with measured topside tool surface temperature differences: ΔT_{Invar} = -6.6 °C (see Figure D-32 (a)), $\Delta T_{\text{Al-alloy}}$ = -5.3 °C (see Figure D-32 (b)) and ΔT_{CFRP} = -4.0 °C (see Figure D-32 (c)).

Apparent failures are observed in tool TC31 (underside) temperature measurements for the Invar and CFRP tools (point A). In these cases, tool TC31 indicates an unreasonably high heating rate and effective HTC value (see Figure D-31). For the Invar tool, the measured underside tool surface temperature difference ΔT_{Invar} = -2.1 °C corresponds to h = 350 W/ (m^2 K) and for the CFRP tool, the measured underside tool surface temperature difference ΔT_{CFRP} = -1.6 °C corresponds to h = 155 W/ (m^2 K). The thermocouple signal also fails to dampen the modulated temperature. These factors suggest that this tool TC is providing invalid underside tool surface measurements.

These experimentally measured results highlight that tool thermocouple installation and surface temperature measurement are non-trivial activities.

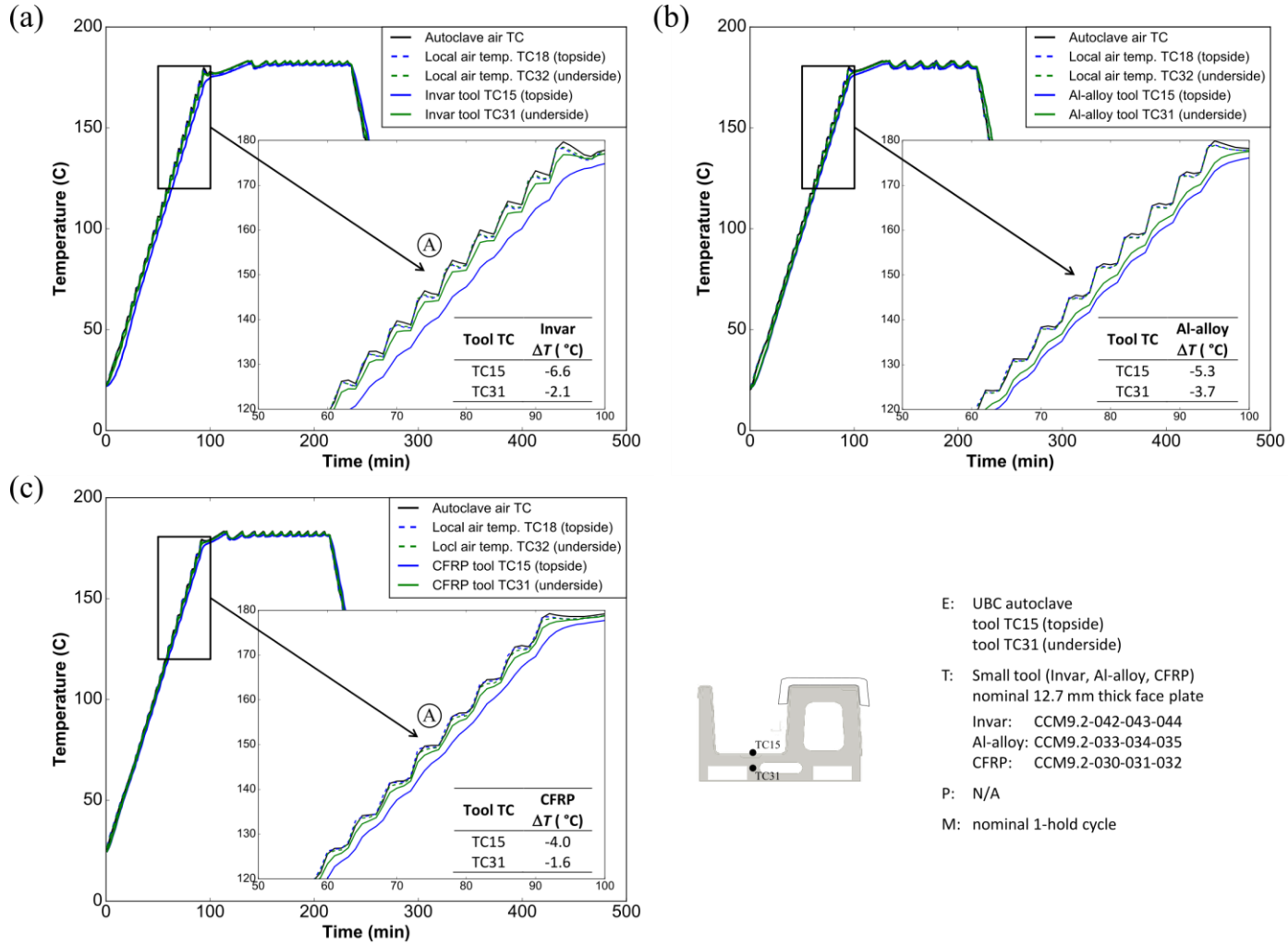

Figure D-32: Experimentally measured results for a family of small-scale tools comparing thermocouples located on the tool topside (TC15) and underside (TC31) surfaces. Temperature profiles (*T* v *t*) of: (a) Invar tool (experiment ID: CCM9.2-042-043-044), (b) Al-alloy tool (experiment ID: CCM9.2-033-034-035) and (c) CFRP tool (experiment ID: CCM9.2-030-031-032). Experimental data from [236] (Arafath *et al*, 2015). ETPM: Equipment–Tool–Part–Material; TC: Thermocouple; Δ*T*: temperature difference. Note: Apparent thermocouple failures observed in Invar and CFRP tools in heat up at point A.

D.4.6 Case study: 12.4 mm thick C-shaped laminate COMPRO-3D analysis (with CFD based HTC distribution)

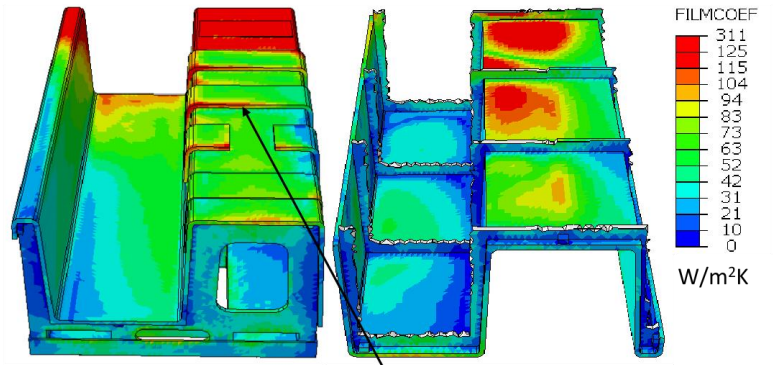

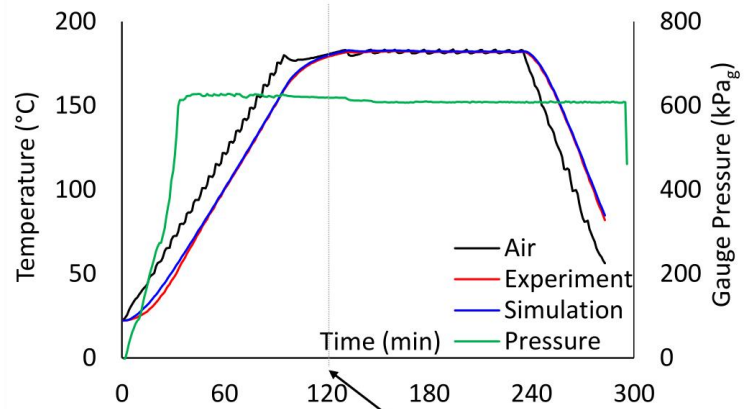

Near TC5 and TC33

Sample	h_{top}	h_{bot}
1	51.13	45.14
2	52.98	46.11
3	69.73	40.33
4	63.88	48.95
5	65.97	51.78
AVG	60.8	46.5

Laminate edges go up to 100 W/ (m²K)
It is very local to the (modeled) sharp laminate edge and likely not representative of real experiment

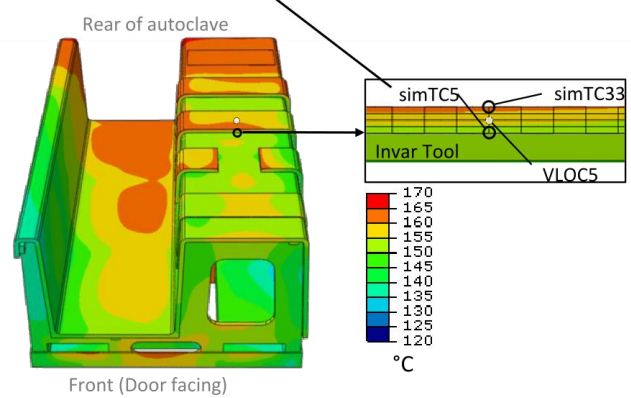

Substructure HTCs vary from approx. 20-40 W/ (m²K)
Local highs up to 60 W/ (m²K) , lows down to 15 W/ (m²K)

Figure D-33: HTC distribution and location for the CCMRD9.2 data set (12.4 mm thick C-shaped laminate, Invar tool (part ID: CCM9.2-077)). Experimental data from [236] (Arafath *et al*, 2015) and predicted CFD data from [178] Park (2018). TC: Thermocouple; HTC: Heat Transfer Coefficient. Note: HTC distribution based on CFD analysis that does not consider thermal resistances due to consumables/bagging.

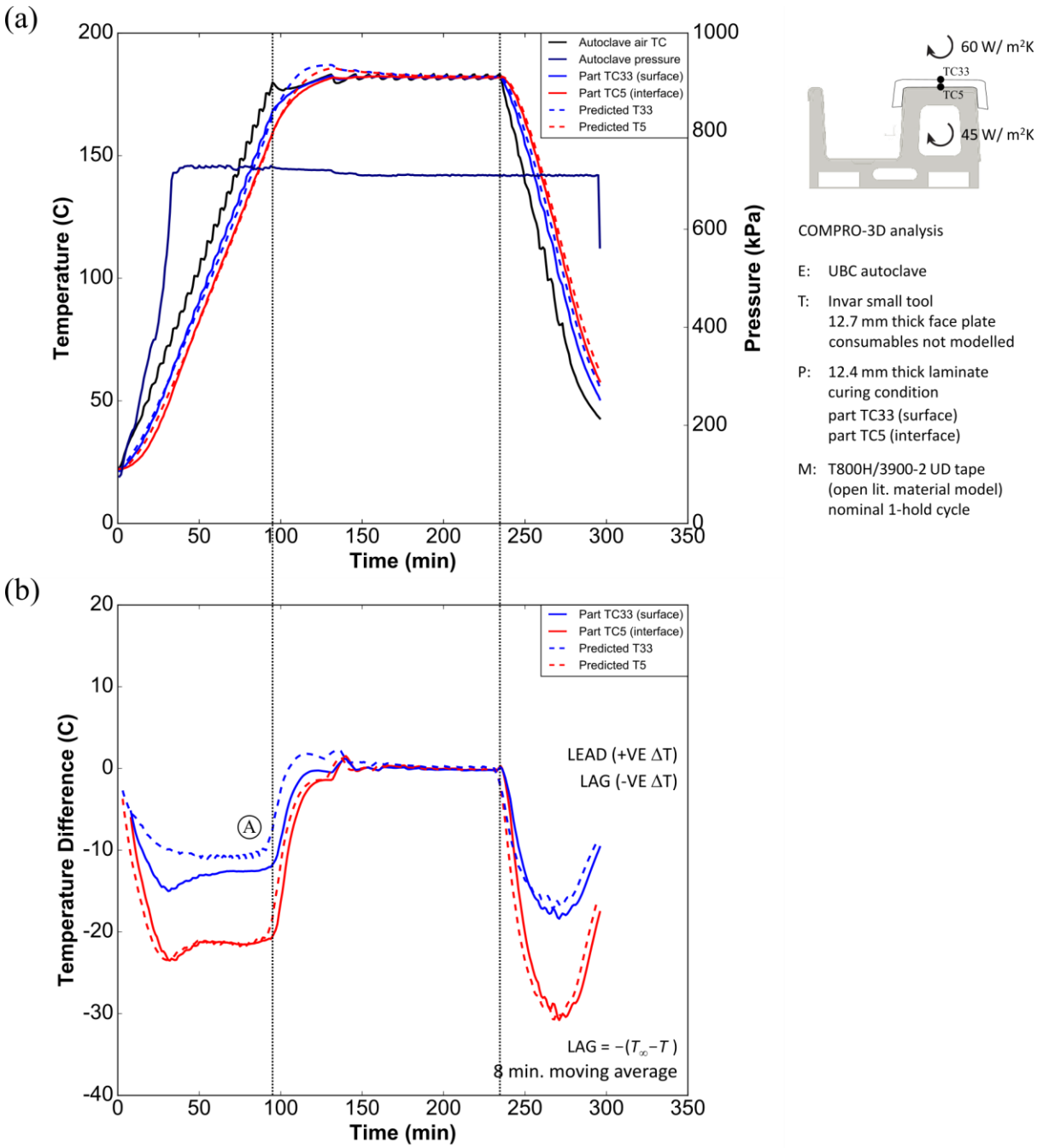

Figure D-34: Experimentally measured and predicted COMPRO-3D modelling results for a 12.4 mm thick C-shaped laminate (part ID: CCM9.2-077) comparing part thermocouples TC33 (surface) and TC5 (interface): (a) temperature profile (*T* v *t*) and (b) temperature difference with respect to the autoclave air temperature (Δ*T* v *t*). Experimental data from [236] (Arafath *et al*, 2015) and predicted modelling data from [178] Park (2018). ETPM: Equipment–Tool–Part–Material; TC: Thermocouple; UD: Unidirectional. Note: Temperature difference in heat up underpredicted at the part surface at point A. HTC distribution based on CFD analysis that does not consider thermal resistances due to consumables/bagging. Vertical lines indicate heat up, hold and cool down cure cycle segments.

A COMPRO-3D analysis was performed for this experiment, as shown in Figure D-33, that uses convective HTC distributions as heat transfer boundary condition inputs [178] (Park, 2018).

The predicted COMPRO-3D modelling results show excellent agreement with the experimental temperature data in Figure D-34. In the temperature difference plot shown in Figure D-34 (b), the model underpredicts the thermal lag at the part surface (T33) during the heat up segment of the cure cycle (point A). This observation is attributed to the applied HTC distribution boundary condition inputs as they do not account for thermal resistances due to consumables/bagging. As an aside, it should be noted that as the consumables collapse and fill with resin, the heat transfer at T33 is expected in increase, and thus an improvement in the COMPRO-3D model prediction is seen (eg. comparison of the model predictions during heat up versus cool down). The effect of the consumables on heat transfer has previously been reported in work by Shimizu *et al* [145]. However, more importantly, the COMPRO-3D model shows that no exotherm is predicted at the on the 180 °C hold. This indicates that tool size effects are significant for this experiment. Tool size effects are not accounted for in the RAVEN-1D model predictions presented in Section 5.3.3.

D.5 Boeing-UW data set

Five cases are considered in this data set. Laminates 6.4 mm and 19.1 mm thick, made with Toray T800H/3900-2 prepreg tape, are instrumented to investigate in-plane temperature distributions (MSE-2015). Laminates 12.7 mm and 25.4 mm thick, made with Toray T800H/3900-2 prepreg tape, and a 33 mm thick panel with septum, made with Toray T800H/3900-2 prepreg tape and honeycomb core, are instrumented to investigate through-thickness temperature distributions (MSE-2016).

Material model uncertainties relating to first-order thermal effects are discussed in Section 5.1.2. The results of a preliminary study investigating second-order effects, resin thermal conductivity sensitivity, for 12.7 mm thick and 25.4 mm thick T800H/3900-2 laminates is presented in D.5.5.

In addition to the work presented in Section 5.3.4 discussing the implications of thermocouples located on the edge of parts, experimentally measured data showing thermal edge effects is presented in D.5.6.

D.5.1 Experimental setup and schematic of thermocouple locations

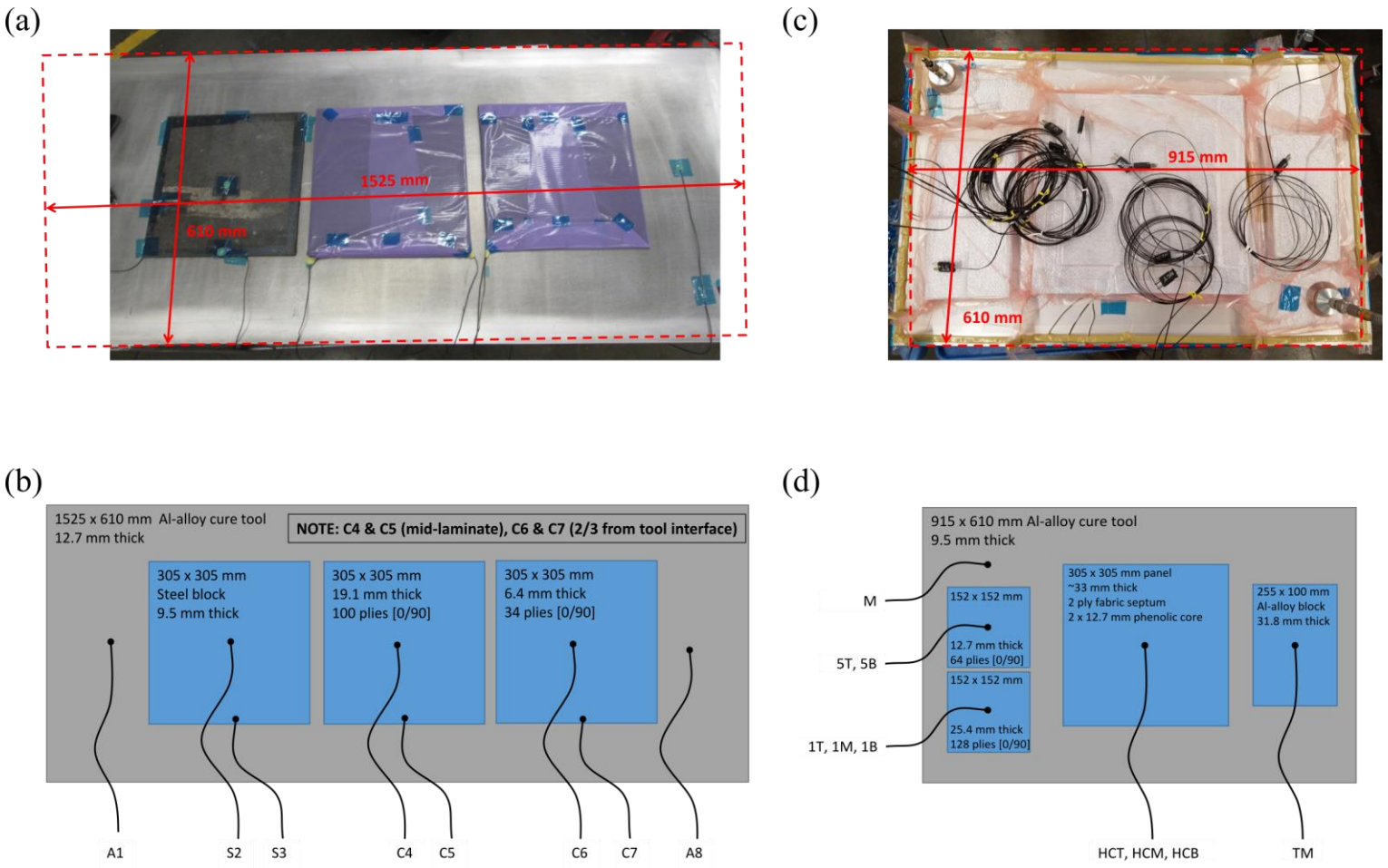

Figure D-35: Boeing-UW data set. MSE-2015 (experiments 20151028-001 & 20151109-002): (a) representative experimental setup and (b) schematic of thermocouple locations and MSE-2016 (experiment 20161017-001): (c) experimental setup and (d) schematic of thermocouple locations (photos courtesy of Karl Nelson [237]).

D.5.2 Reported effective heat transfer coefficients

Table D-11: Effective heat transfer coefficients for the Boeing-UW data set[a].

Analysis	Experiment		Equivalent-1D HTC		Equivalent-3D HTC (no tool substructure modelled)		
			top W/ (m^2 K)	bottom W/ (m^2 K)	top W/ (m^2 K)	tool top W/ (m^2 K)	tool bottom W/ (m^2 K)
Original[b] (2018)	20151028-001-1	tool & steel block (exp)[c]	35	150	35	85	75
	20151028-001-2	tool & steel block (exp)[c]	40	170	40	95	85
	20151109-002	tool only[d]	45	45		45	45
		tool & steel block (exp)[c]	30	95	30	50	45
		tool & steel block (syn)[e]	30	60			
		tool & steel block (syn)[f]	30	75	30	45	40
	20161017-001	tool & Al-alloy block (exp)[g]	40	100	40	35	30

[a] Experimental data from [237] (Boeing-UW, 2017). MSE-2015: 20151028-001-1 (curing, industrial autoclave B); 200151028-001-2 (cured, industrial autoclave B); 20151109-002: (curing, industrial autoclave C); MSE-2016: 20161017-001 (curing, industrial autoclave D).

[b] Modified heat flux Method I' is used to back-calculate the effective HTCs, as described in Appendix F.2 & Appendix F.3. Effective HTC values reported are an average calculated using all ramp cure cycle segments. The Al-alloy tool is assumed as a lumped mass.

[c] Top HTC value is back-calculated from calorimeter TC-S2. Bottom HTC value is back-calculated from tool TC-A1. Steel block (calorimeter) dimensions are: z_{block} = 9.5 mm (305 mm x 305 mm).

[d] Tool only HTCs are back-calculated from tool TC-A1.

[e] Synthetic HTCs are back-calculated using predicted RAVEN-1D data.

[f] Synthetic HTCs are back-calculated using predicted COMPRO-3D data.

[g] Top HTC value is back-calculated from calorimeter TC-TM. Bottom HTC value is back-calculated from tool TC-M. Al-alloy block (calorimeter) dimensions are: z_{block} = 31.8 mm (255 mm x 100 mm).

D.5.3 Summary of ETPM thermal management attributes

Table D-12: ETPM[a] attribute definition for the Boeing-UW data set (Experiment 20151028-001).

		Test[b]	Analysis
Equipment	**(E)**	Autoclave: Industrial-B	$h_{top\ (CURING)}$ = 35 W/ (m^2 K) $h_{top\ (CURED)}$ = 40 W/ (m^2 K)
Tool	**(T)**	Al-alloy tool plate (1525 mm x 610 mm) z_{tool} = 12.7 mm TC-A1 (tool surface) Steel calorimeter (305 mm x 305 mm) z_{block} = 9.5 mm TC-S2 (top-centre)	$h_{bot\ (CURING)}$ = 150 W/ (m^2 K) $h_{bot\ (CURED)}$ = 170 W/ (m^2 K)
Part	**(P)**	Flat laminate (305 mm x 305 mm) $z_{part\ (THIN)}$ = 6.4 mm (34 ply) [0/90] $z_{part\ (THICK)}$ = 19.1 mm (100 ply) [0/90] TC-C4 (mid-centre), TC-C5 (mid-edge)	RAVEN-1D drill point analysis [238] T4: mid
Material	**(M)**	T800H/3900-2 UD tape Single-hold cycle (180 °C)	T800H/3900-2 open lit. material model

[a] ETPM: Equipment–Tool–Part–Material
[b] Experimental data from [237] (Boeing-UW, 2017).

Table D-13: ETPM[a] attribute definition for the Boeing-UW data set (Experiment 20151109-002).

		Test[b]	Analysis
Equipment	**(E)**	Autoclave: Industrial-C	h_{top} = 30 W/ (m^2 K)
Tool	**(T)**	Al-alloy tool plate (1525 mm x 610 mm) z_{tool} = 12.7 mm TC-A1 (tool surface) Steel calorimeter (305 mm x 305 mm) z_{block} = 9.5 mm TC-S2 (top-centre)	h_{bot} = 95 W/ (m^2 K) $h_{t\text{-}top}$ = 50 W/ (m^2 K) $h_{t\text{-}bot}$ = 45 W/ (m^2 K)
Part	**(P)**	Flat laminate (305 mm x 305 mm) $z_{part\ (THIN)}$ = 6.4 mm (34 ply) [0/90] $z_{part\ (THICK)}$ = 19.1 mm (100 ply) [0/90] TC-C6 (mid-centre) TC-C4 (mid-centre), TC-C5 (mid-edge)	RAVEN-1D drill point analysis [238] COMPRO-3D model (no tool substructure modelled) [239] T6: 2/3 from part/tool interface T4: mid
Material	**(M)**	T800H/3900-2 UD tape Single-hold cycle (180 °C)	T800H/3900-2 open lit. material model

[a] ETPM: Equipment–Tool–Part–Material
[b] Experimental data from [237] (Boeing-UW, 2017).

Table D-14: ETPM[a] attribute definition for the Boeing-UW data set (Experiment 20161017-001).

		Test[b]	Analysis
Equipment	**(E)**	Autoclave: Industrial-D	h_{top} = 40 W/ (m^2 K)
Tool	**(T)**	Al-alloy tool plate (915 mm x 610 mm) z_{tool} = 9.5 mm TC-M (tool surface) Al-alloy calorimeter (255 mm x 100 mm) z_{block} = 31.8 mm TC-TM (top-centre)	h_{bot} = 100 W/ (m^2 K) $h_{t\text{-}top}$ = 35 W/ (m^2 K) $h_{t\text{-}bot}$ = 30 W/ (m^2 K)
Part	**(P)**	Flat laminate (152 mm x 152 mm) $z_{part\ (THIN)}$ = 12.7 mm (64 ply) [0/90] $z_{part\ (THICK)}$ = 25.4 mm (128 ply) [0/90] Panel with septum (305 x 305 mm) $z_{part\ (PANEL)}$ = 3.4 mm (18 ply) / = 12.7 mm (core) / = 0.762 mm (2 ply septum) TC-5T (surface), TC-5B (interface) TC-1M (mid-laminate) TC-HCM (mid-septum)	RAVEN-1D drill point analysis [238] COMPRO-3D model (no tool substructure modelled) [239] T5T: surface, T5B: interface T1M: mid THCM: mid
Material	**(M)**	T800H/3900-2 UD tape Aramid honeycomb core Single-hold cycle (180 °C)	T800H/3900-2 open lit. material model Nominal aramid honeycomb (thermal only)

[a] ETPM: Equipment–Tool–Part–Material
[b] Experimental data from [237] (Boeing-UW, 2017).

D.5.4 Temperature plots

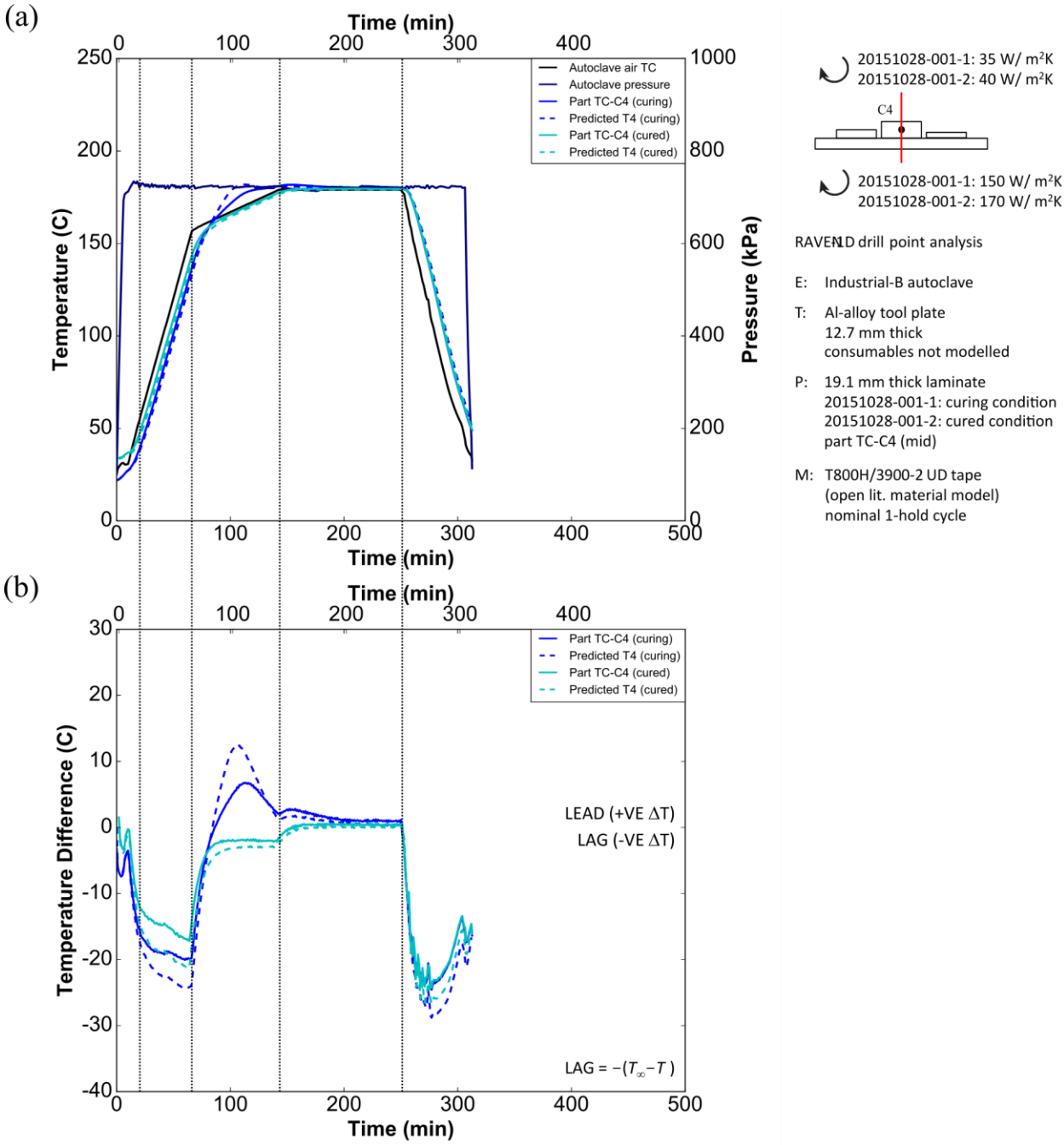

Figure D-36: Comparison of experimentally measured and predicted RAVEN-1D modelling results for the Boeing-UW data set (Experiment 20151028-001: 19.1 mm thick laminate): (a) temperature profile (*T* v *t*) and (b) temperature difference with respect to the autoclave air temperature (Δ*T* v *t*). Experimental data from [237] (Boeing-UW, 2017). ETPM: Equipment–Tool–Part–Material; TC: Thermocouple; UD: Unidirectional. Note: Experiments run back-to-back in autoclave. Vertical lines indicate heat up, hold and cool down cure cycle segments.

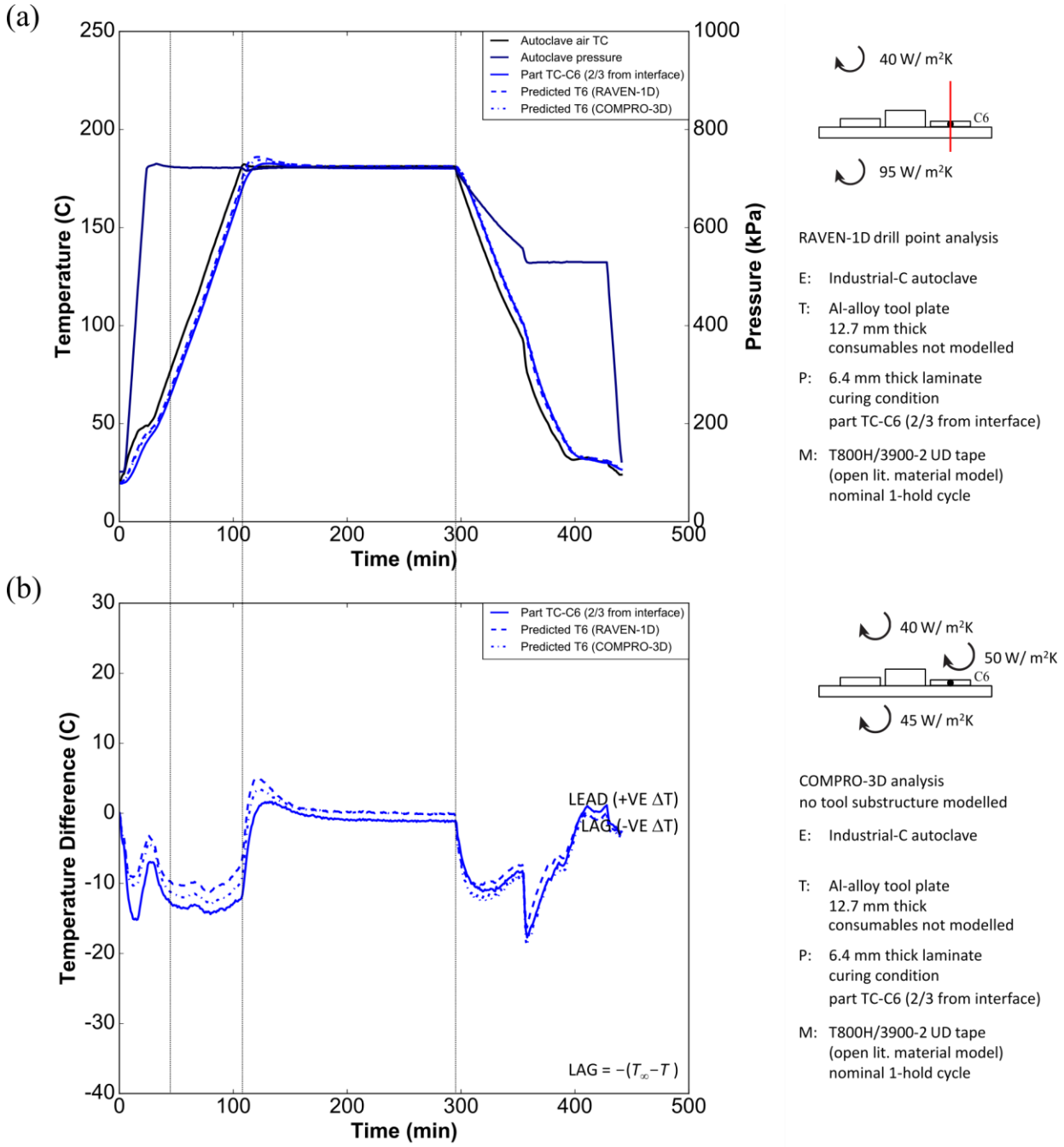

Figure D-37: Comparison of experimentally measured and predicted RAVEN-1D and COMPRO-3D modelling results for the Boeing-UW data set (Experiment 20151109-002: 6.4 mm thick laminate): (a) temperature profile (*T* v *t*) and (b) temperature difference with respect to the autoclave air temperature (Δ*T* v *t*). Experimental data from [237] (Boeing-UW, 2017). ETPM: Equipment–Tool–Part–Material; TC: Thermocouple; UD: Unidirectional. Note: Vertical lines indicate heat up, hold and cool down cure cycle segments.

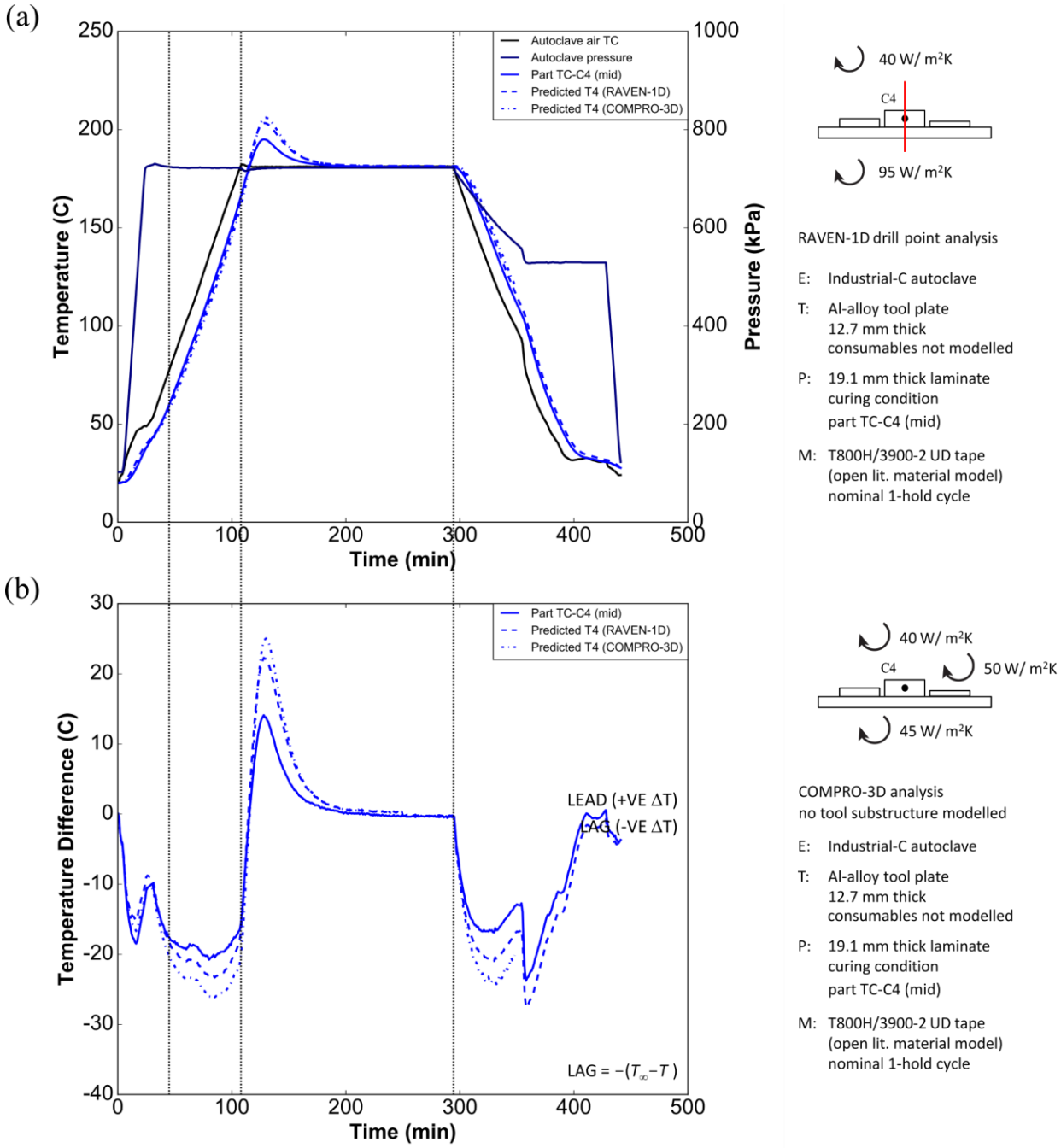

Figure D-38: Comparison of experimentally measured and predicted RAVEN-1D and COMPRO-3D modelling results for the Boeing-UW data set (Experiment 20151109-002: 19.1 mm thick laminate): (a) temperature profile (*T* v *t*) and (b) temperature difference with respect to the autoclave air temperature (Δ*T* v *t*). Experimental data from [237] (Boeing-UW, 2017). ETPM: Equipment–Tool–Part–Material; TC: Thermocouple; UD: Unidirectional. Note: Vertical lines indicate heat up, hold and cool down cure cycle segments.

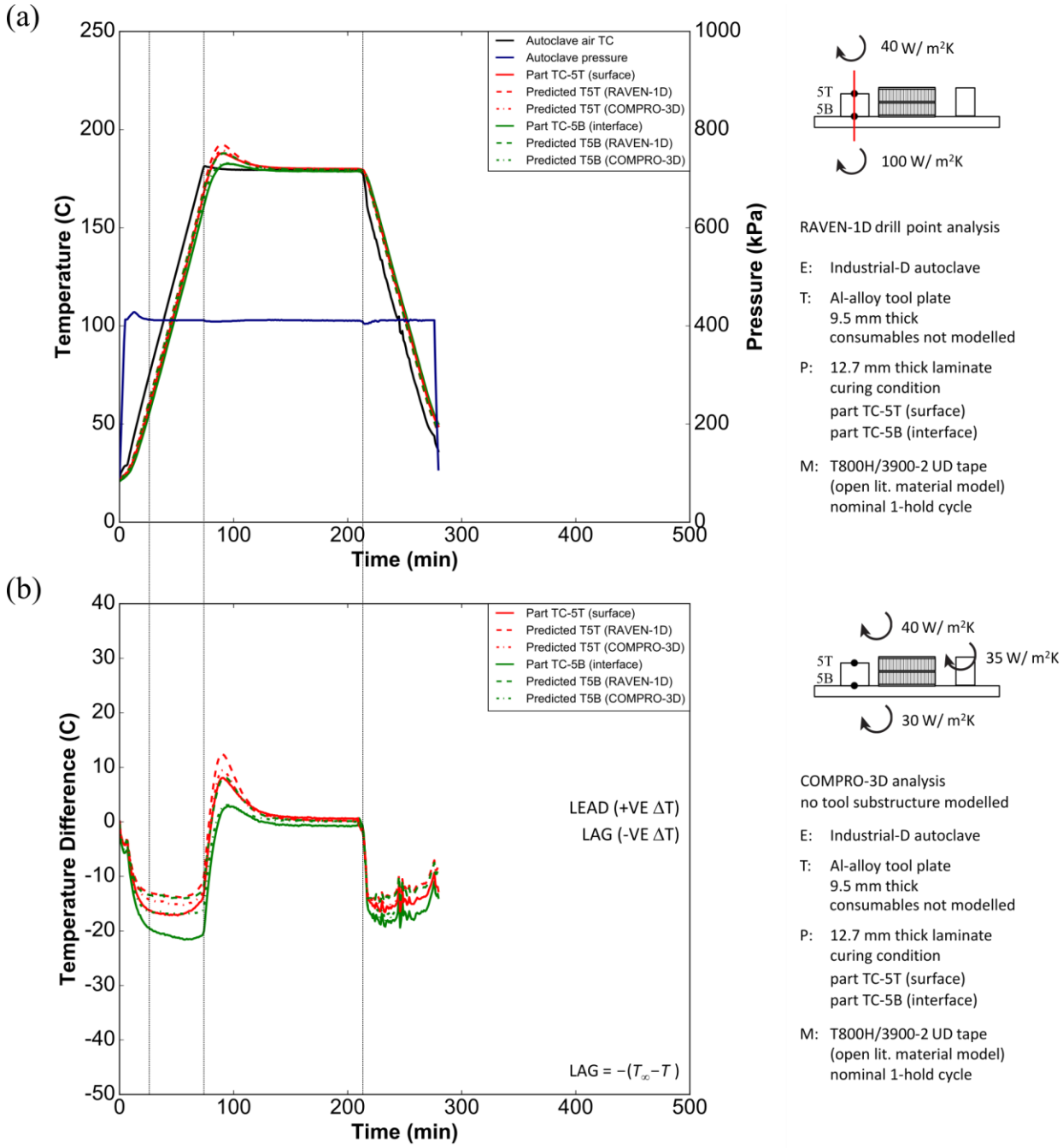

Figure D-39: Comparison of experimentally measured and predicted RAVEN-1D and COMPRO-3D modelling results for the Boeing-UW data set (Experiment 20161017-001: 12.7 mm thick laminate): (a) temperature profile (*T* v *t*) and (b) temperature difference with respect to the autoclave air temperature (Δ*T* v *t*). Experimental data from [237] (Boeing-UW, 2017). ETPM: Equipment–Tool–Part–Material; TC: Thermocouple; UD: Unidirectional. Note: Autoclave pressurized to 410 kPa/45 psig to prevent 'core crush'. Vertical lines indicate heat up, hold and cool down cure cycle segments.

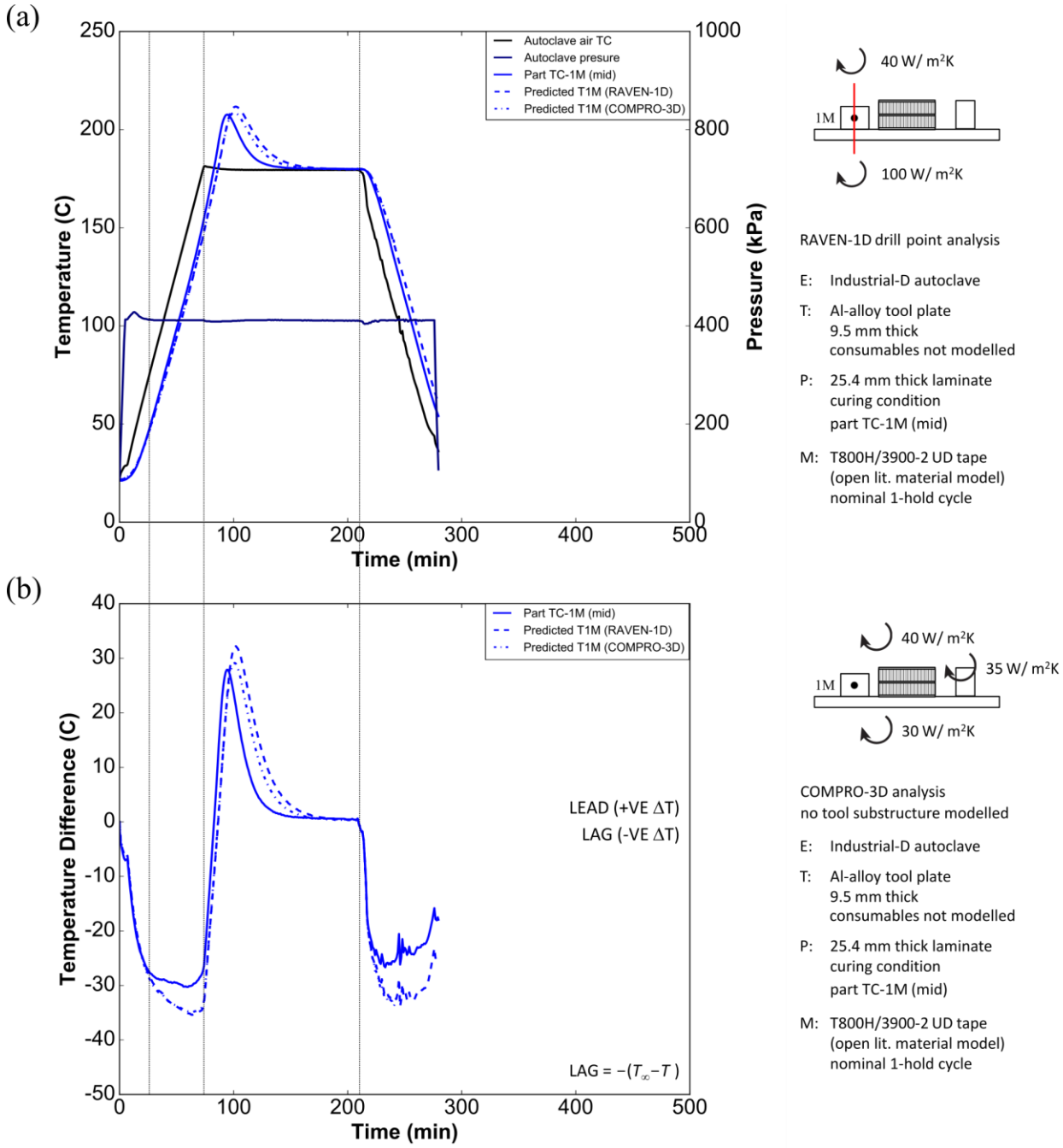

Figure D-40: Comparison of experimentally measured and predicted RAVEN-1D and COMPRO-3D modelling results for the Boeing-UW data set (Experiment 20161017-001: 25.4 mm thick laminate): (a) temperature profile (*T* v *t*) and (b) temperature difference with respect to the autoclave air temperature (Δ*T* v *t*). Experimental data from [237] (Boeing-UW, 2017). ETPM: Equipment–Tool–Part–Material; TC: Thermocouple; UD: Unidirectional. Note: Autoclave pressurized to 410 kPa/45 psig to prevent 'core crush'. Vertical lines indicate heat up, hold and cool down cure cycle segments.

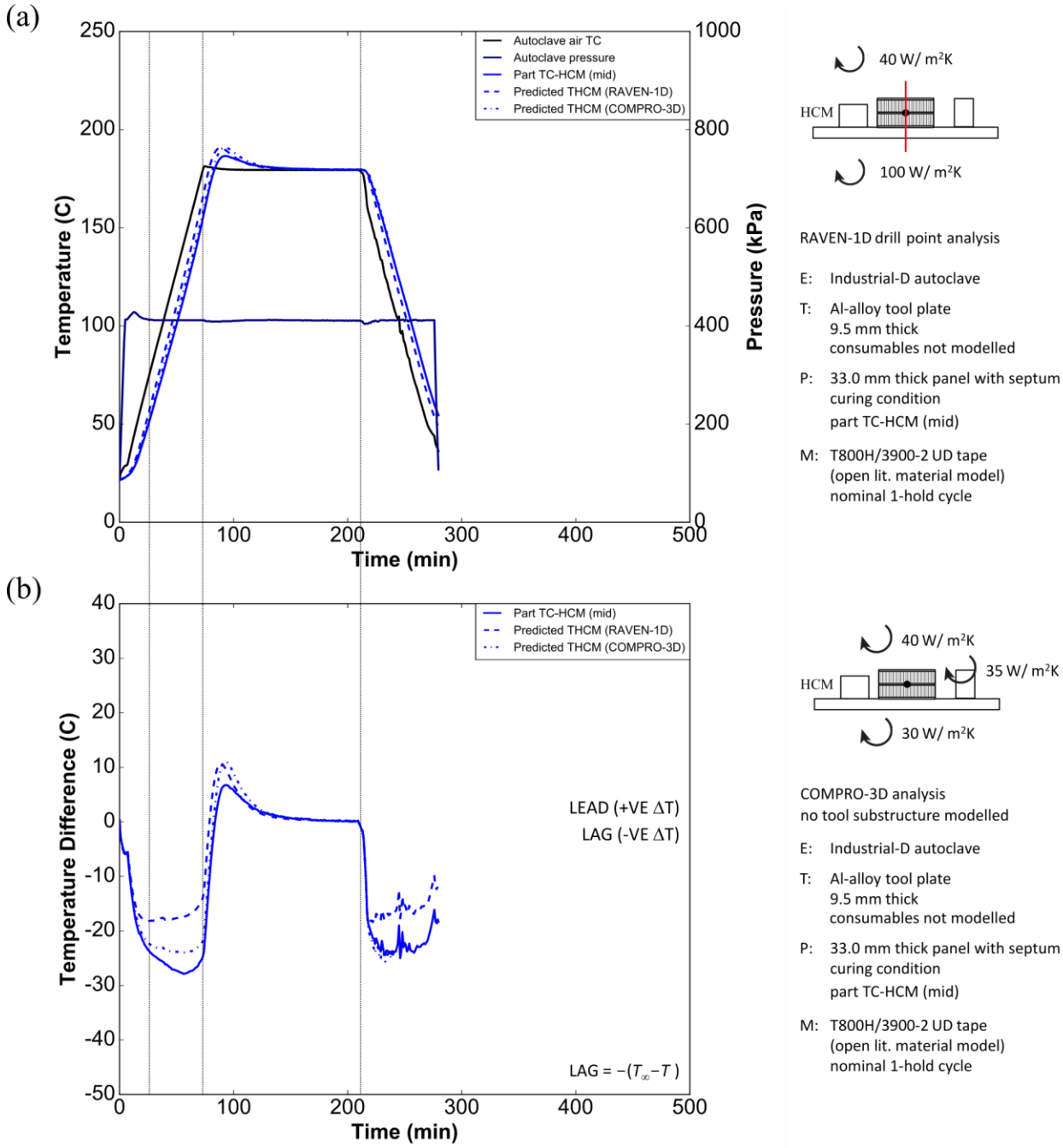

Figure D-41: Comparison of experimentally measured and predicted RAVEN-1D and COMPRO-3D modelling results for the Boeing-UW data set (Experiment 20161017-001: 33.0 mm thick panel with septum): (a) temperature profile (*T* v *t*) and (b) temperature difference with respect to the autoclave air temperature (Δ*T* v *t*). Experimental data from [237] (Boeing-UW, 2017). ETPM: Equipment–Tool–Part–Material; TC: Thermocouple; UD: Unidirectional. Note: Autoclave pressurized to 410 kPa/45 psig to prevent 'core crush'. Vertical lines indicate heat up, hold and cool down cure cycle segments.

D.5.5 Case study: Thermal conductivity sensitivity

As the gauge thickness of production scale composites parts increases, the sensitivity of changes in resin thermophysical properties may be large enough to have a significant influence on thermochemical response. Work by Mijovic and Wijaya [244] and Twardowski *et al* [90] have shown that changes in these properties, particularly in the neat resin thermal conductivity, can significantly influence the temperature profile of thick curing laminates.

These properties are assumed to be constant in a majority of models. To verify this assumption, Twardowski *et al* [90] performed a numerical sensitivity study of resin properties and their influence on the thermal response for thick AS4/3501-6 laminates. Combined variations of up to -40%, +40% and +80% were applied to specific heat capacity, density, and resin thermal conductivity property values respectively. It was concluded from this work that 'changes in the resin properties at gelation (eg. $\alpha = 0.5$) are relatively unimportant'.

With protocols established by Dykeman [144] to minimize uncertainties in cure kinetics model characterization, we now have high confidence in developing and validating cure kinetics and specific heat capacity models (eg. [135,150]). Second-order resin property effects, such as thermal conductivity, should be revisited to reconfirm that current assumptions remain valid.

In this work, a preliminary sensitivity study of resin thermal conductivity was performed to investigate its influence on the thermal response for 12.7 mm thick and 25.4 mm thick T800H/3900-2 laminates processed on a 9.5 mm thick Al-alloy tool plate. This study is a comparative analysis given that tool size effects significantly influence the thermal response of

the 12.7 mm thick laminate (see Figure D-39), and influence the thermal response of the 25.4 mm thick laminate to a lesser extent (see Figure D-40).

The in-plane dimensions of these laminates are 152 mm x 152 mm. Part TCs were installed at the surface (TC-5T) and interface (TC-5B) for the 12.7 mm thick laminate, and at the surface (TC-1T), mid-laminate (TC-1M) and interface (TC-1B) for the 25.4 mm thick laminate. All models were run using the open literature T800H/3900-2 material model. It should be noted that in this material model, the thermal conductivity model has not been characterized and assumes a constant value, with k_r = 0.167 W/ (m K) [238]. Where k_r is the resin thermal conductivity.

Predicted RAVEN-1D and COMPRO-3D modelling results for the 25.4 mm thick laminate, shown in in Figure D-40, indicate that while tool size effects appear to influence the severity of the exotherm, both models overpredict the thermal lag during the heat up and cool down segments of the cure cycle. Based on Equation (2-3), this suggests that the resin thermal conductivity value specified in the material model is low.

The results of the preliminary thermal conductivity sensitivity study are shown in Figure D-43. RAVEN-1D drill points were run using:

- Nominal 'non lumped' thermal conductivity model (k_r = 0.167 W/ (m K)) [238]
- Modified 'non-lumped' thermal conductivity model $k_r = f(\alpha, T)$ and k_{r0} = 0.167 W/ (m K)
- Modified 'non-lumped' thermal conductivity model $k_r = f(\alpha, T)$ and k_{r0} = 0.251 W/ (m K)

For both laminates investigated, gelation (eg. α = 0.5) occurs at approximately t = 90 min.

Based on the results of this preliminary study, the following conclusions can be made:

- For the 12.7 mm thick laminate, the temperature profile and DOC are insensitive to changes in the resin thermal conductivity (see Figure D-42). It is noted that tool size effects for this experiment are significant.

- Tool size effects are significant to a lesser extent for the 25.4 mm thick laminate. Comparatively, a +50% difference in resin thermal conductivity results in a 6 °C decrease in the predicted peak exotherm temperature. The timing of this peak temperature occurs 5 minutes earlier in the cure. DOC is insensitive to changes in resin thermal conductivity (see Figure D-43 (a)). During heat up, a +50% difference in resin thermal conductivity results in a 4.5 °C reduction in the thermal lag, while during cool down a 5.0 °C reduction in thermal lag is observed (see Figure D-43 (b)).

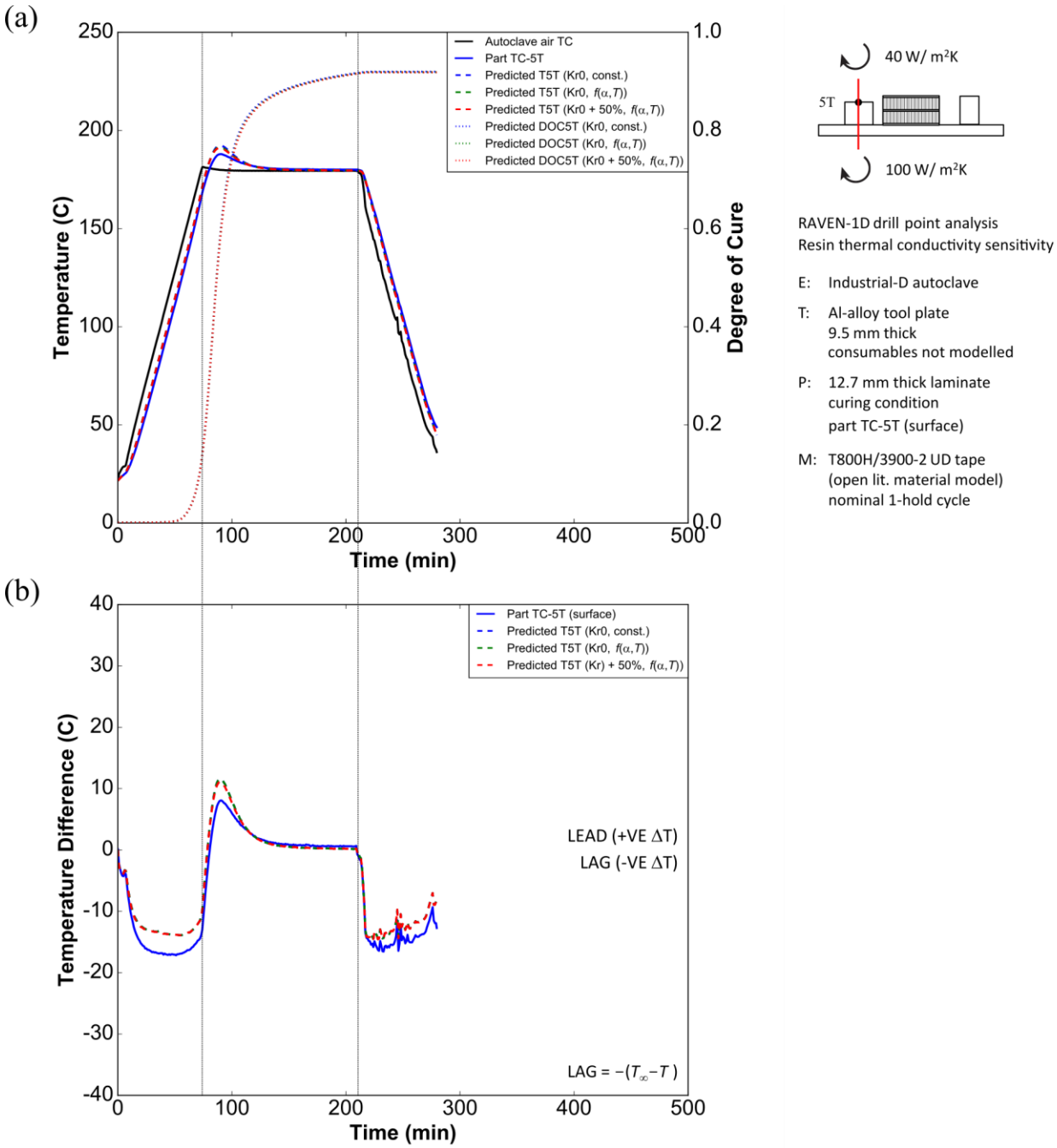

Figure D-42: Comparison of experimentally measured and predicted RAVEN-1D modelling results for a 12.7 mm thick laminate (experiment ID: 20161017-001): (a) temperature profile (*T* v *t*) and (b) temperature difference with respect to the autoclave air temperature (Δ*T* v *t*). Experimental data from [237] (Boeing-UW, 2017). ETPM: Equipment–Tool–Part–Material; TC: Thermocouple; UD: Unidirectional. Note: Tool size effects are significant for this experiment. The resin thermal conductivity sensitivity study is a comparative analysis. Autoclave pressurized to 410 kPa/45 psig to prevent 'core crush'. Vertical lines indicate heat up, hold and cool down cure cycle segments.

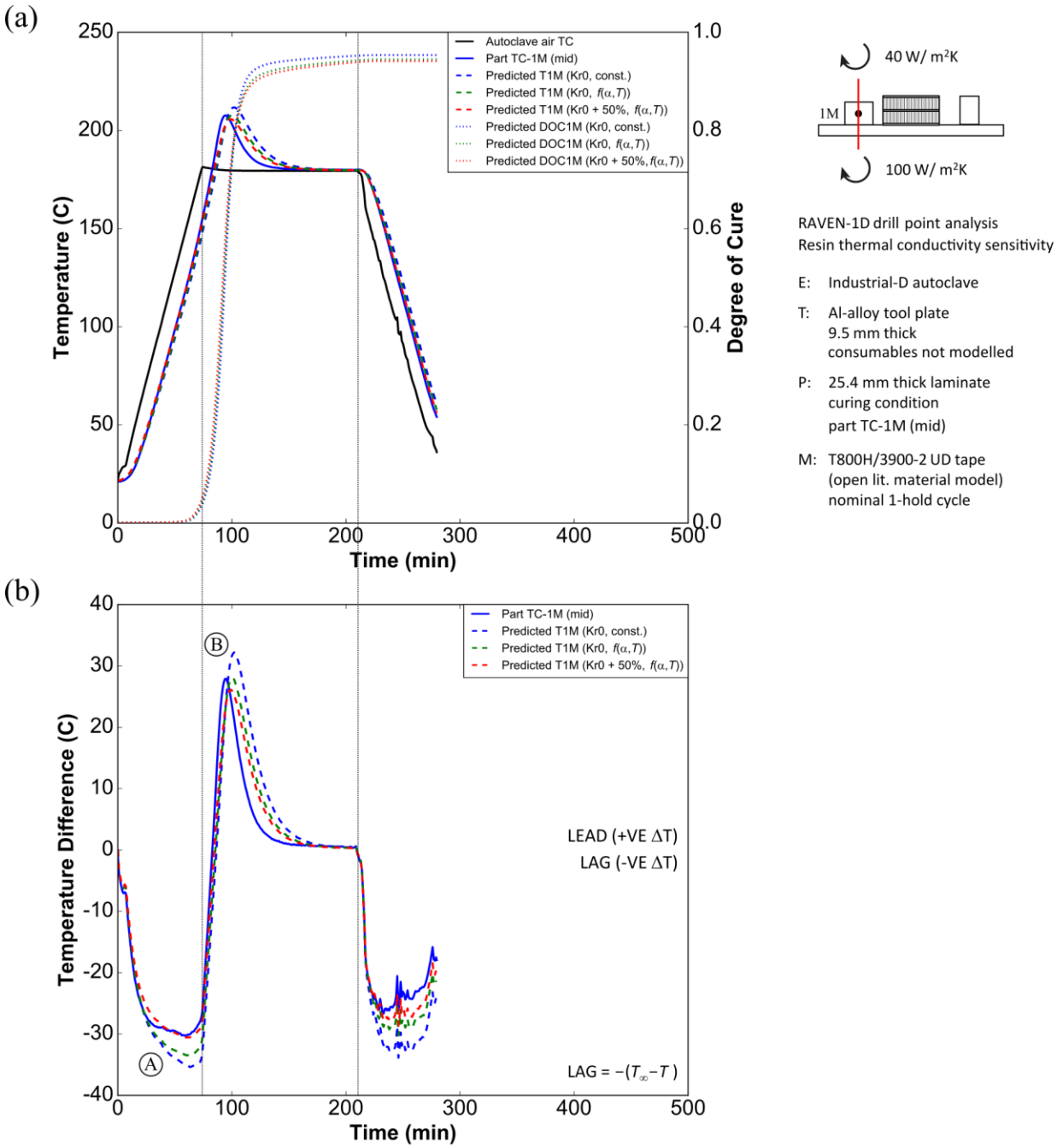

Figure D-43: Comparison of experimentally measured and predicted RAVEN-1D modelling results for a 25.4 mm thick laminate (experiment ID: 20161017-001): (a) temperature profile (*T* v *t*) and (b) temperature difference with respect to the autoclave air temperature (Δ*T* v *t*). Experimental data from [237] (Boeing-UW, 2017). ETPM: Equipment–Tool–Part–Material; TC: Thermocouple; UD: Unidirectional. Note: Temperature difference in heat up and cool down overpredicted at point A and temperature overshoot overpredicted at point B. Tool size effects are significant to a lesser extent in this experiment. The resin thermal conductivity sensitivity study is a comparative analysis. Autoclave pressurized to 410 kPa/45 psig to prevent 'core crush'. Vertical lines indicate heat up, hold and cool down cure cycle segments.

D.5.6 Case study: Thermal edge effects

Preliminary work by Rasekh investigated the limitations of the 1D closed-form equations developed due to edge and tool size effects [142]. From Rasekh [142], based on an infinite plate ($x >> L$) with a constant convective heat transfer and assuming an error of 2%, the maximum distance from the edge to avoid edge effects for a CFRP laminate ($k_z/k_x = 0.01$), is:

$$x = 20 \cdot L \tag{D-2}$$

where in Equation (D-2), x is the in-plane thickness coordinate, L is the slab half-thickness and k_z/k_x is the ratio of through-thickness thermal conductivity to in-plane thermal conductivity.

Recent work by Zobeiry (2017) extends the capability of the closed-form equations originally proposed by Rasekh to account for these 2D effects with non-symmetric convective heat transfer. Initial verification has been performed using simple FE models.

Courdji *et al* [245] demonstrated, using manufacturing similation, edge and tool size effects for a representative AS4/8552 spar geometry ranging in thickness from 3.2 mm to 25.4 mm. This work investigated the validity of RAVEN-1D drill point analyses compared with a more complex COMPRO-3D model (with tool plate and substructure modelled) given changes in part thickness and tooling material. The predicted COMPRO-3D results showed observable differences in the temperature profiles at the web centre versus the flange edge. The RAVEN-1D analyses, on the other hand, correlated reasonably well with the COMPRO-3D model at the web centre, the temperature profiles at the flange edge were overpredicted.

In this work, the analysis of experimentally measured data from [237] (Boeing-UW, 2017) was performed. Temperature profile (T v t) and temperature difference with respect to the autoclave air temperature (ΔT v t) plots, for 19.1 mm thick T800H/3900-2 laminates processed on a 12.7 mm thick Al-alloy tool plate in two different autoclaves are shown in Figure D-44 and Figure D-45. The in-plane dimensions of these laminates are 305 mm x 305 mm, and part TCs were installed mid-laminate at the centre (TC-C4) and edge (TC-C5).

This experimentally measured data shows that the temperature profiles at the centre and edge of the laminates are observably different. This difference is due to the capacity of the tool to contribute heat to the laminate (during heat up) and to act as a heat sink (during the hold), where:

- During heat up, the edge of the laminate is hotter than at the centre. This difference is 2.4 °C for the laminate cured in industrial autoclave B (see Figure D-44 (b)) and 2.3 °C for the laminate cured in industrial autoclave C (see Figure D-45 (b)).

- At the hold, where the exotherm occurs, the peak temperature on the edge of the laminate is cooler than at the centre. The peak temperature difference is 1.9 °C for the laminate cured in industrial autoclave B (see Figure D-44 (a)) and 3.5 °C for the laminate cured in industrial autoclave C (see Figure D-45 (a)).

These trends are consistent with observations from practical experience, relating specifically to thermal management for composites repair, where 'TCs naturally read cooler very near the edge rather than near the middle' [246]. Empirically it is recommended that thermocouples be installed greater than 50 mm (2 inches) from the edge [246].

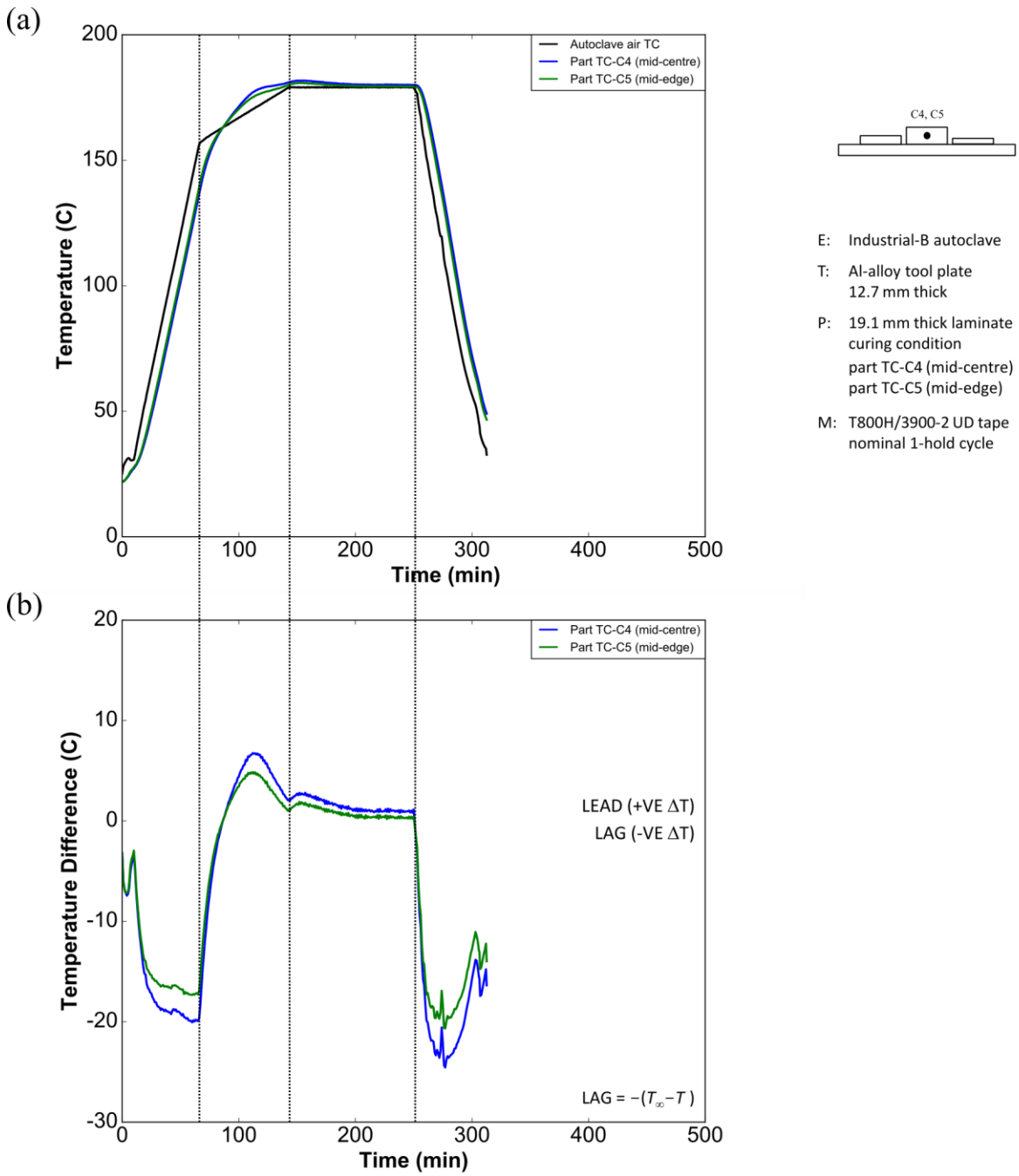

Figure D-44: Experimentally measured results for a 19.1 mm thick laminate comparing mid-laminate thermocouples located at the centre (TC-C4) and edge (TC-C5). Curing laminate in industrial autoclave B (experiment ID: 20151028-001-1): (a) temperature profile (*T* v *t*) and (b) temperature difference with respect to the autoclave air temperature (Δ*T* v *t*). Experimental data from [237] (Boeing-UW, 2017). ETPM: Equipment–Tool–Part–Material; TC: Thermocouple; UD: Unidirectional. Note: Vertical lines indicate heat up, hold and cool down cure cycle segments.

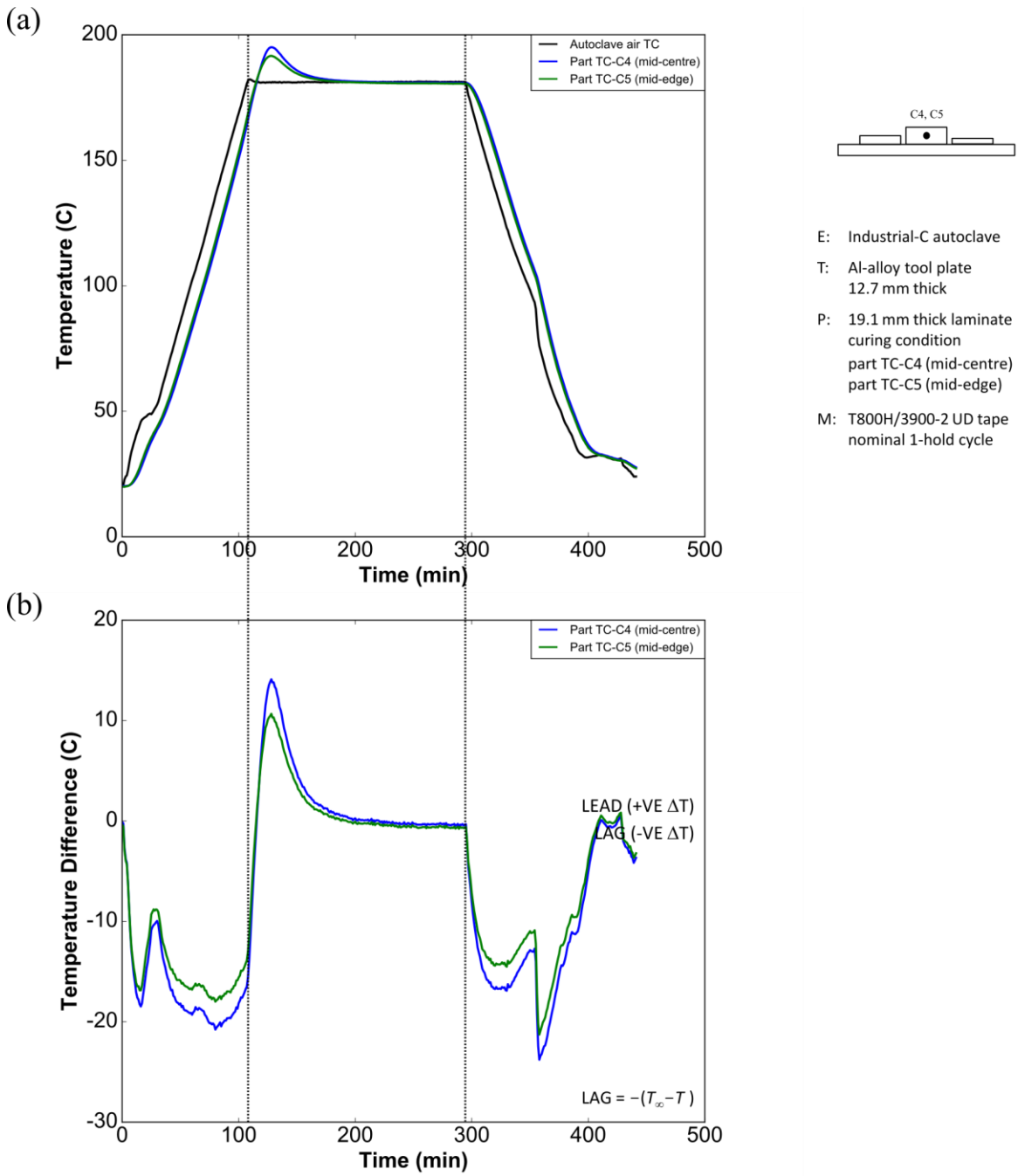

Figure D-45: Experimentally measured results for a 19.1 mm thick laminate comparing mid-laminate thermocouples located at the centre (TC-C4) and edge (TC-C5). Curing laminate in industrial autoclave C (experiment ID: 20151109-002): (a) temperature profile (*T* v *t*) and (b) temperature difference (Δ*T* v *t*). Experimental data from [237] (Boeing-UW, 2017). ETPM: Equipment–Tool–Part–Material; TC: Thermocouple; UD: Unidirectional. Note: Vertical lines indicate heat up, hold and cool down cure cycle segments.

Appendix E Material Properties and Material Database Input Parameters

This appendix summarizes the material properties used in the case studies in Chapter 5 and the thick composite laminate data set analyses in Appendix D. Also provided are the details of the preliminary cure kinetics characterization for the Hexcel 8552-1 resin system.

E.1 Properties of Hexcel AS4/8552 unidirectional prepreg

Cure kinetics model for Hexcel 8552 (CCA ck15) [181].

$$\dot{\alpha} = \left(\frac{1}{\dot{\alpha}_k} - \frac{1}{\dot{\alpha}_d} \right)^{-1}$$

$$\dot{\alpha}_k = \left(\frac{1}{\dot{\alpha}_{c1}} + \frac{1}{\dot{\alpha}_{i2} + \dot{\alpha}_{c2}} \right)^{-1} + \dot{\alpha}_e$$

$$\dot{\alpha}_i = k_{0_i} e^{-\frac{E_{a_i}}{RT}} (1-\alpha)^{l_i} \left(\frac{1}{r} - \alpha \right)^{m_i} \left(\alpha^{n_{2_i}} + b_i \right)^{n_i}$$

$$\dot{\alpha}_d = k_{d_0} e^{-\frac{B}{a_f (T - T_g) + b_f}} \tag{E-1}$$

$$a_f = \begin{cases} a_1 & T_g < T_{g_{a1}} \\ S_a T_g + C_a & T_{g_{a1}} < T_g < T_{g_{a2}} \\ a_2 & T_{g_{a2}} < T_g \end{cases} \quad \begin{cases} S_a = \dfrac{a_2 - a_1}{T_{g_{a2}} - T_{g_{a1}}} \\ C_a = a_2 - S_a T_{g_{a2}} \end{cases}$$

$$b_f = \begin{cases} b_1 & T_g < T_{g_{b1}} \\ S_a T_g + C_b & T_{g_{b1}} < T_g < T_{g_{b2}} \\ b_2 & T_{g_{b2}} < T_g \end{cases} \quad \begin{cases} S_a = \dfrac{b_2 - b_1}{T_{g_{b2}} - T_{g_{b1}}} \\ C_b = b_2 - S_a T_{g_{b2}} \end{cases}$$

$$T_g = T_{g0} + \frac{\lambda \alpha \left(T_{g\infty} - T_{g0} \right)}{1 - (1 - \lambda) \alpha}$$

Specific heat capacity model for Hexcel 8552 (CCA cp3) [181].

$$
\begin{aligned}
C_p &= C_{p_r} + \frac{C_{p_g} - C_{p_r}}{1 + e^{k\left[\left(T - T_g\right) - \Delta T_c\right]}} \\
C_{p_i} &= \left(1 - \alpha\right) C_{p_{i0}} + \alpha C_{p_{i\infty}} \quad i = r, g \\
C_{p_{ij}} &= s_{ij} T + c_{ij} \quad i = r, g \text{ and } j = 0, \infty
\end{aligned}
\tag{E-2}
$$

Table E-1: Hexcel AS4/8552 materials database input parameters used for the Johnston and Hubert data set (refer to Appendix D.1).

Property	Parameter	Value				Units
Fibre volume fraction[a]	V_f	0.57				
Cure kinetics[b] Equation (E-1)		$\dot{\alpha}_{c1}$	$\dot{\alpha}_{i2}$	$\dot{\alpha}_{c2}$	$\dot{\alpha}_e$	
	HR	600000				J/ kg
	k_0	153900.5	1000	1000	3.963E+11	1/ s
	E_a	64929.5	0.0	0.0	133168.3	J/ mol
	l	2.347	0.0	0.0	1.029	
	r	1.0	1.0	1.0	1.0	
	m	0.0	0.0	0.0	0.0	
	n_2	1.0	0.0	0.0	1.0	
	b	0.1594	1.0	1.0	0.0	
	n	1.413	0.0	0.0	5.586	
	k_{d_0}	4.0				1/ s
	B	0.21				
	a_1	4.8E-04				1/ °C
	a_2	4.8E-04				1/ °C
	$T_{g_{a1}}$	0.0				°C
	$T_{g_{a2}}$	100.0				°C
	b_1	0.021				
	b_2	0.031				
	$T_{g_{b1}}$	120.0				°C
	$T_{g_{b2}}$	195.0				°C
	T_{g0}	-7.0				°C
	$T_{g\infty}$	250.0				°C
	λ	0.78				
	α_{init}	0.001				

Table continued on next page

Table E-1 continued

Property	Parameter	Value	Units
Resin specific heat capacity[b] Equation (E-2)	s_{g0}	3.775	J/ (kg K^2)
	c_{g0}	730.0	J/ (kg K)
	$s_{g\infty}$	3.40	J/ (kg K^2)
	$c_{g\infty}$	830.0	J/ (kg K)
	s_{r0}	3.27	J/ (kg K^2)
	c_{r0}	1088.0	J/ (kg K)
	$s_{r\infty}$	2.0	J/ (kg K^2)
	$c_{r\infty}$	1350.0	J/ (kg K)
	k	0.278	1/ °C
	ΔT_c	-1.5	°C
Fibre specific heat capacity[a]	C_{pf}	$750+\left(T\times 2.05/^{\circ}\mathrm{C}\right)$	J/ (kg K)
Density[a]	ρ_{f}	1.79E+03	kg/ m^3
	ρ_{r}	1.30E+03	
Thermal conductivity[a]	$k_{11\mathrm{f}}$	$7.69+\left(T\times 1.56\times 10^{-2}/^{\circ}\mathrm{C}\right)$	W/ (m K)
	$k_{33\mathrm{f}}$	$2.4+\left(T\times 5.07\times 10^{-3}/^{\circ}\mathrm{C}\right)$	
	$k_{11\mathrm{r}}=k_{33\mathrm{r}}$	$0.148+\left(T\times 3.43\times 10^{-4}/^{\circ}\mathrm{C}\right)+\left(\alpha\times 6.07\times 10^{-2}\right)$	

[a] From Table C.11 [100] (Johnston, 1997).
[b] From Hexcel 8552 NCAMP materials database characterization binder [135] (Van Ee *et al*, 2009).

E.2 Properties of Hexcel AS4/8552-1 unidirectional prepreg

Cure kinetics model for Hexcel 8552-1 (CCA ck24) [181].

$$\frac{1}{\dot{\alpha}}=\sum_{i=1}^{n}\frac{1}{\dot{\alpha}_i}$$
$$\dot{\alpha}_i=A_i e^{\frac{-B_i}{C_i T-D_i T_g+E_i}} \qquad \text{(E-3)}$$
$$T_g=T_{g0}+\frac{\lambda\alpha\left(T_{g\infty}-T_{g0}\right)}{1-\left(1-\lambda\right)\alpha}$$

Table E-2: AS4/8552-1 preliminary materials database input parameters for the Kotlik and Shimizu (refer Appendix D.2) and Slesinger (refer Appendix D.3) data sets.

Property	Parameter	Value				Units
Fibre volume fraction[a]	V_f	0.57				
Cure kinetics Equation (E-3)	HR	520377				J/ kg
	T_{g0}	2.4 °				°C
	$T_{g\infty}$	250.0				°C
	λ	0.78				
	α_{init}	0.001				
	Reaction	A	B	C	D	E
	1	–	–	1	0	0
	2	3E+06	0.35	0.00025	0.00025	–
Resin specific heat capacity[b] Equation (E-2)	s_{g0}	3.775				J/ (kg K^2)
	c_{g0}	730.0				J/ (kg K)
	$s_{g\infty}$	3.40				J/ (kg K^2)
	$c_{g\infty}$	830.0				J/ (kg K)
	s_{r0}	3.27				J/ (kg K^2)
	c_{r0}	1088.0				J/ (kg K)
	$s_{r\infty}$	2.0				J/ (kg K^2)
	$c_{r\infty}$	1350.0				J/ (kg K)
	k	0.278				1/ °C
	ΔT_c	-1.5				°C
Fibre specific heat capacity[a]	C_{pf}	$750+\left(T\times 2.05\,/^{\circ}\mathrm{C}\right)$				J/ (kg K)
Density[a]	ρ_f	1.79E+03				kg/ m^3
	ρ_r	1.30E+03				
Thermal conductivity[a]	k_{11f}	$7.69+\left(T\times 1.56\times 10^{-2}\,/^{\circ}\mathrm{C}\right)$				W/ (m K)
	k_{33f}	$2.4+\left(T\times 5.07\times 10^{-3}\,/^{\circ}\mathrm{C}\right)$				
	$k_{11r} = k_{33r}$	$0.148+\left(T\times 3.43\times 10^{-4}\,/^{\circ}\mathrm{C}\right)+\left(\alpha\times 6.07\times 10^{-2}\right)$				

[a] From Table C.11 [100] (Johnston, 1997).

[b] From Hexcel 8552 NCAMP materials database characterization binder [135] (Van Ee *et al*, 2009). All thermophysical material properties were assumed to be comparable to the Hexcel 8552 resin system.

E.2.1 Preliminary Cure Kinetics Characterization

A preliminary materials characterization for Hexcel 8552-1 was performed using samples of Hexcel IM7/8552-1 prepreg material received on August 2016 (CRN material source #127). This material was manufactured in 2014. An 8552-1 CK model was developed to compare to a baseline Hexcel 8552 NCAMP CK model developed by CMT Inc. for the NCAMP program [135]. NIAR granted permission for the release of the 8552 NCAMP DSC data by CMT Inc. in May 2016. The preliminary Hexcel AS4/8552-1 materials database was specifically developed for use in the Kotlik and Shimizu data set summarized in Table 5-1 and in Appendix D.2.

DSC tests were performed and analyzed by Janna Fabris at The University of British Columbia. The KERMODE data and model fitting software package V1.0.3 [247] was used to perform preliminary data and model fits of the cure kinetics model based on the experimental data collected. The CCA 'semi model-free' cure kinetics model ck24 was used to compute the resin cure kinetics. The mathematical form of this model is shown in Equation (E-3) [181]. All other thermophysical properties, such as specific heat capacity, fibre volume fraction and density and thermal conductivity were not characterized. Given that the 8552-1 resin system is a derivative of the 8552 resin system, these material properties were assumed to be comparable to those characterized for the 8552 NCAMP materials database.

The preliminary cure kinetics model input parameters are summarized in Table E-2. The DSC protocols used are based on Dykeman [144] and the best practices developed by CMT Inc. for the NCAMP program [135].

E.2.1.1 Experimental Data

The data came from modulated DSC tests using a TA Discovery Instrument. Samples of IM7/8552-1 prepreg, approximately 11mg to 22 mg, were evaluated in normal aluminum sample pans and the thermal analysis was run using a nitrogen purge of 50 ml/ min. The test matrix used in this study was based on the cure cycle for the Kotlik and Shimizu experiment TEST-A, as reported in Table 5-1 and Appendix D.2. Overall, a total of 21 tests were performed (11 nonisothermal, 6 isothermal tests and 4 interrupted isothermal tests) which were used to fit the cure kinetics model. These tests consisted of nonisothermal tests ranging from 1 °C/ min to 5 °C/ min, at 1 °C/ min increments and isothermal tests at 110 °C, 120 °C, 150 °C and 180 °C. Residual scans of the isothermal and interrupted isothermal tests were performed at 4 °C/ min. These DSC tests are summarized in Table E-3. Heat flow data for the 8552-1 resin system was deconvoluted from the IM7/8552-1 prepreg samples using the KERMODE data and model fitting software and assuming a nominal V_f.

Table E-3: Summary of DSC tests used in the preliminary cure kinetics characterization of Hexcel 8552-1.

Test name	Batch	Mass (mg)	Ramp rate (°C /min)	Hold temp (°C)	Hold time (min)
127-MDYN-01CPM-01	DSC Oct 2016	16.05	1.0		
127-MDYN-01CPM-02	DSC Oct 2016	14.67	1.0		
127-MDYN-01CPM-03	DSC Nov 2016[a]	20.50	1.0		
127-MDYN-02CPM-01	DSC Oct 2016	14.06	2.0		
127-MDYN-02CPM-02	DSC Oct 2016	16.97	2.0		
127-MDYN-03CPM-01	DSC Oct 2016	12.93	3.0		
127-MDYN-03CPM-02	DSC Oct 2016	15.75	3.0		
127-MDYN-04CPM-01	DSC Oct 2016	16.16	4.0		
127-MDYN-04CPM-02	DSC Oct 2016	16.17	4.0		
127-MDYN-05CPM-01	DSC Oct 2016	17.60	5.0		
127-MDYN-05CPM-02	DSC Oct 2016	16.59	5.0		
127-MISO-110C-03	DSC Nov 2016	21.61		110	1080
127-MISO-150C-01	DSC Oct 2016	11.48		150	360
127-MISO-180C-01	DSC Oct 2016	15.54		180	180
127-MISO-180C-02	DSC Oct 2016	16.51		180	180
127-MISO-180C-06	DSC Nov 2016[a]	20.54		180	180
127-MISO-180C-07	DSC Nov 2016[a,b]	18.41		180	180
127-MISO-110C-INT240-01	DSC Oct 2016	13.03		110	240
127-MISO-110C-INT540-01	DSC Oct 2016	14.21		110	540
127-MISO-110C-INT540-02	DSC Oct 2016	15.56		110	540
127-MISO-120C-INT480-01	DSC Oct 2016	15.27		120	480

[a] Tests performed using TA Q2000 instrument to confirm the TA Discovery DSC test results.
[b] Residual scan performed at 2 °C/ min.

E.2.1.2 Data-fit Analysis

The nonreversing heat flow component of temperature modulated DSC tests was used to determine the baselines for all DSC tests. Linear baselines were used in this study for all nonisothermal tests and for all isothermal and residual scans of these isothermal tests. Example baselines are shown in Figure E-1. Once the baselines were established, the heat of reaction (HR) for each test was computed. Total HRs for the nonisothermal and isothermal tests are shown in Figure E-2 and Figure E-3 respectively. The total HR is the HR measured at each segment of the DSC test. DSC data for the Hexcel 8552 NCAMP materials database are shown here for comparison. This experimental data was provided by CMT Inc. on behalf of NIAR [135].

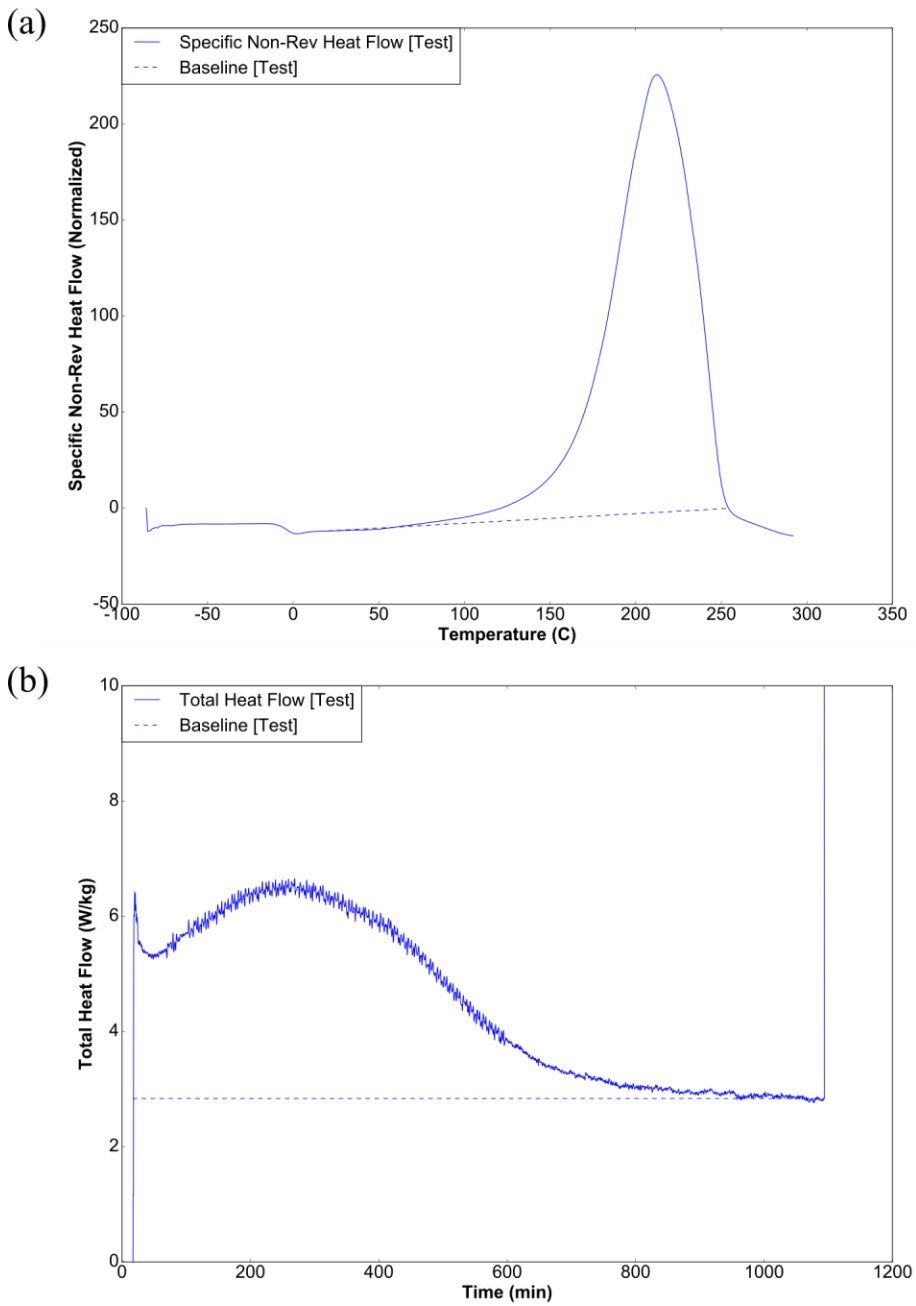

Figure E-1: Linear baseline examples for DSC tests: (a) baseline for nonisothermal DSC test and residual scans of isothermal tests (4 °C/ min nonisothermal scan) and (b) baseline for isothermal DSC tests (110 °C isothermal scan). Experimental data from Hexcel 8552-1 preliminary cure kinetics characterization.

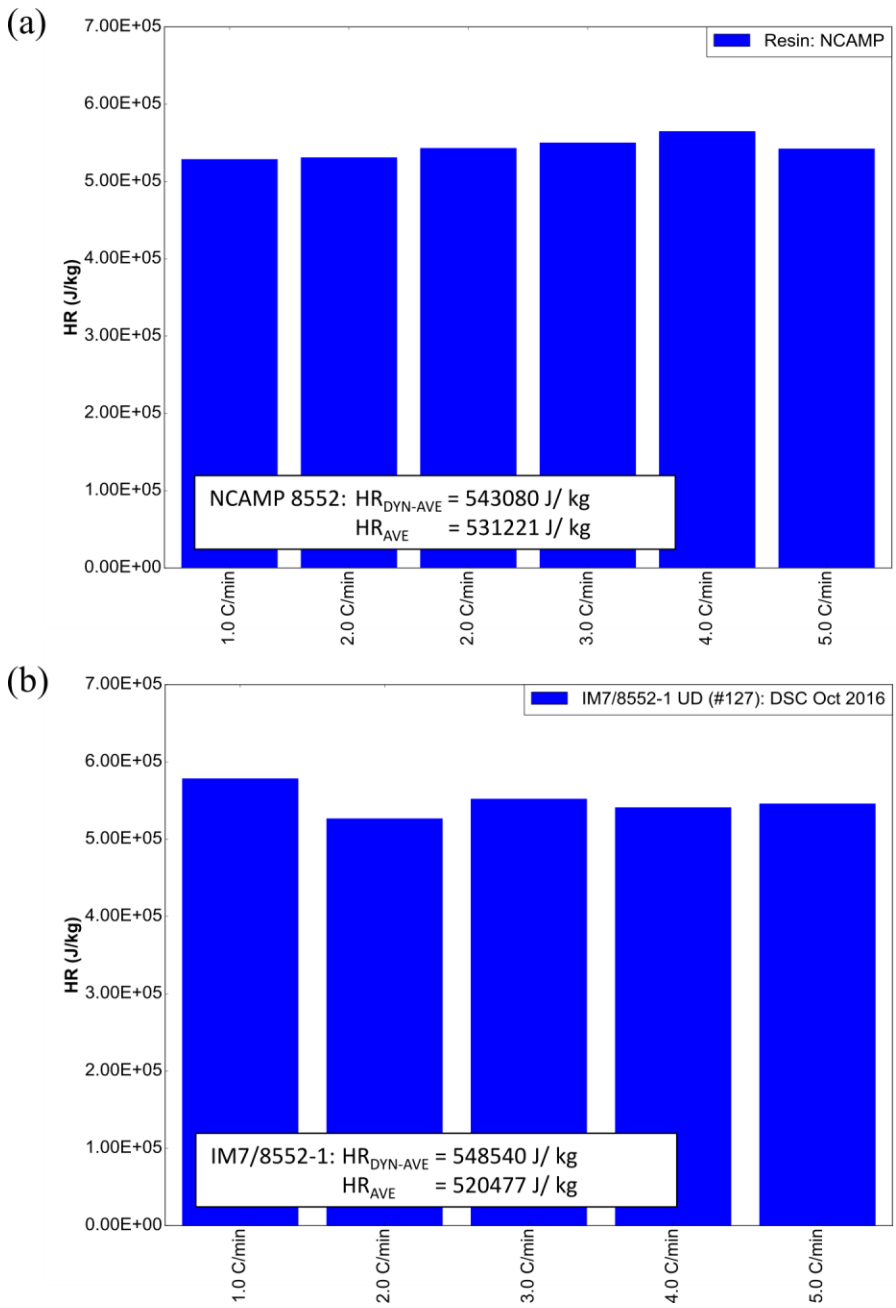

Figure E-2: Comparison of heat of reaction for nonisothermal DSC tests: (a) experimental data, used with permission, from Hexcel 8552 NCAMP material model database [135] (Van Ee *et al*, 2009) and (b) experimental data from Hexcel 8552-1 preliminary cure kinetics characterization. Note: Linear baselines were used for the cases shown.

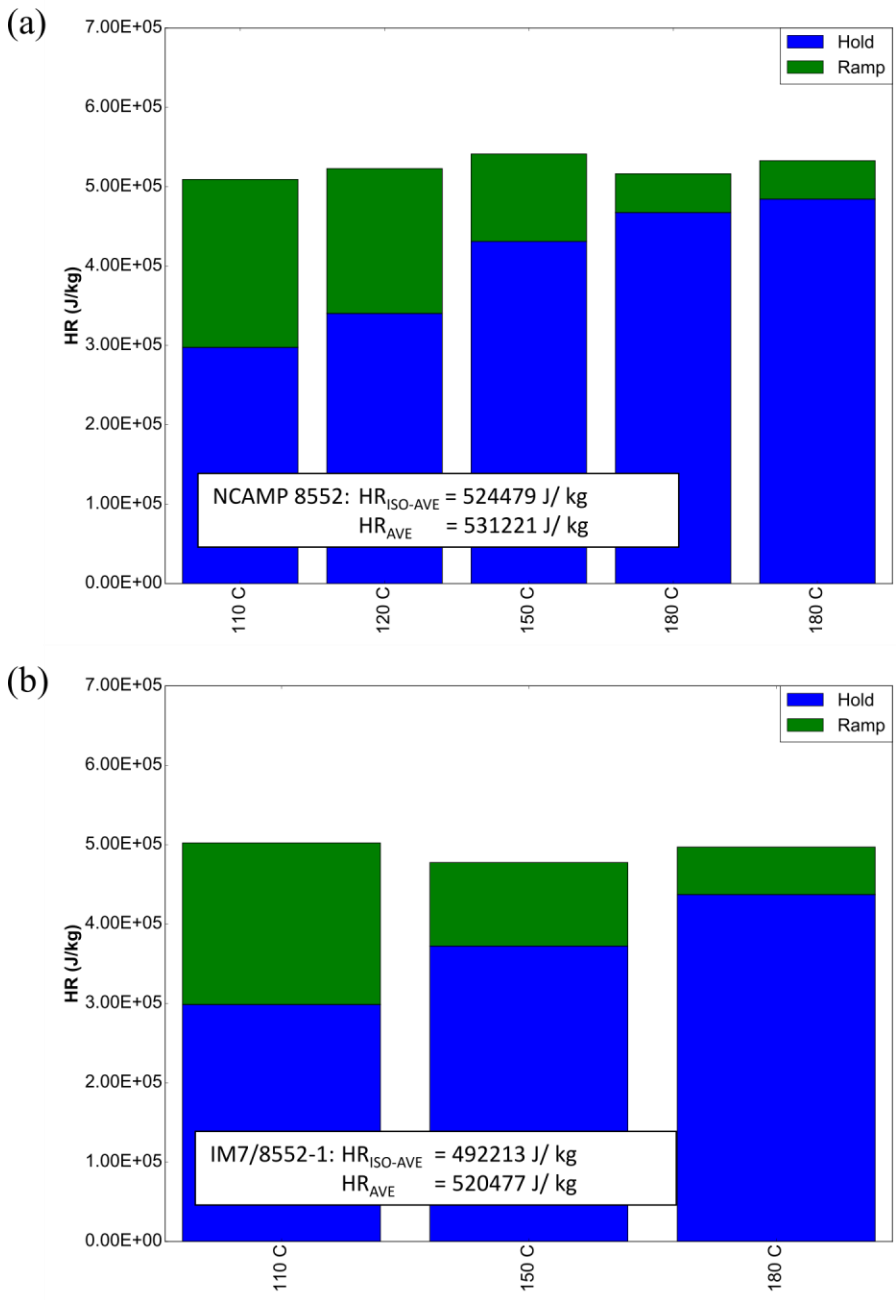

Figure E-3: Comparison of heat of reaction for isothermal DSC tests: (a) experimental data from the Hexcel 8552 NCAMP material model database [135] (Van Ee *et al*, 2009) and (b) experimental data from Hexcel 8552-1 preliminary cure kinetics characterization. Note: NCAMP DSC data used with permission (NIAR, 2016). Linear baselines were used for the cases shown.

Based on the values measured in the nonisothermal and isothermal tests, the following values for the 8552-1 resin system were computed:

$$HR_{DYN\text{-}AVE} = 548540 \text{ J/ kg}$$
$$HR_{ISO\text{-}AVE} = 492213 \text{ J/ kg}$$
$$HR_{AVE} = 520377 \text{ J/ kg}$$

The difference in the nonisothermal and isothermal values can be attributed to both the error in the HR measurement in the ramp and hold segments of the DSC tests and in using total heat flow and reversing heat flow signals.

With the baseline heat flow and total HR known, DOC was determined by reanalyzing the heat flow data. The resin cure rate was computed by considering the DOC as a function of time.

Cure kinetics model ck24 requires the glass transition temperature (T_g) of the material. The T_g is computed using the empirical DiBenedetto relationship. The model was fit to T_g data determined using the reversing heat flow component of temperature modulated DSC tests. The half-height method was used to determine the T_g transition when the material vitrifies and devitrifies from glassy and rubbery states. Nonisothermal tests were used to determine the initial T_g (T_{g0}) and isothermal and interrupted isothermal tests were used to determine the post hold T_g to enable model fitting. The final T_g ($T_{g\infty}$) was not characterized. T_g data for the 180 ºC isothermal tests were omitted from subsequent analysis due to the difficulty in detecting a post hold T_g. The signal washout observed in these tests was attributed to the high residual scan rate used in this study. The DiBenedetto equation was initially fitted using the parameters determined for the 8552 NCAMP T_g model. The T_g results and final DiBenedetto fit are shown in Figure E-4.

The T_g data and model for the 8552 NCAMP materials database are also shown here for comparison. This experimental data was provided by CMT Inc. on behalf of NIAR [135].

E.2.1.3 Model-fit Analysis

The cure kinetics model ck24 parameters were fit to the experimental DSC data. This model computes the cure rate using an inverse sum of n reactions. The first reaction (n = 1) is known as the kinetic term and the second reaction (n = 2) is known as the diffusion term. In this study, KERMODE data and model fitting software was used to first auto-fit reaction 1 A and B terms to the nonisothermal data. A linear fit was then used to fit the reaction 2 E term to the isothermal data. All other terms were defined as constants. The quality of the model-fit to the DSC test data is shown in Figure E-5 where comparisons of the DOC and cure rate from the experimental data and model predictions have been made. This preliminary cure kinetics model is valid within the following range of temperatures:

Nonisothermal	$-90\ °C < T < 275\ °C$ $1\ °C/\ min < \dot{T} < 5\ °C/\ min$
Isothermal	$110\ °C < T < 180\ °C$

An isothermal process map was generated using RAVEN simulation software V3.9.2.11692 [238] and is shown in Figure E-6. The isothermal process map for the 8552 NCAMP material model is also shown here for comparison. These process maps indicate that the 8552-1 resin system material derivative is more thermally latent than the 8552 resin system.

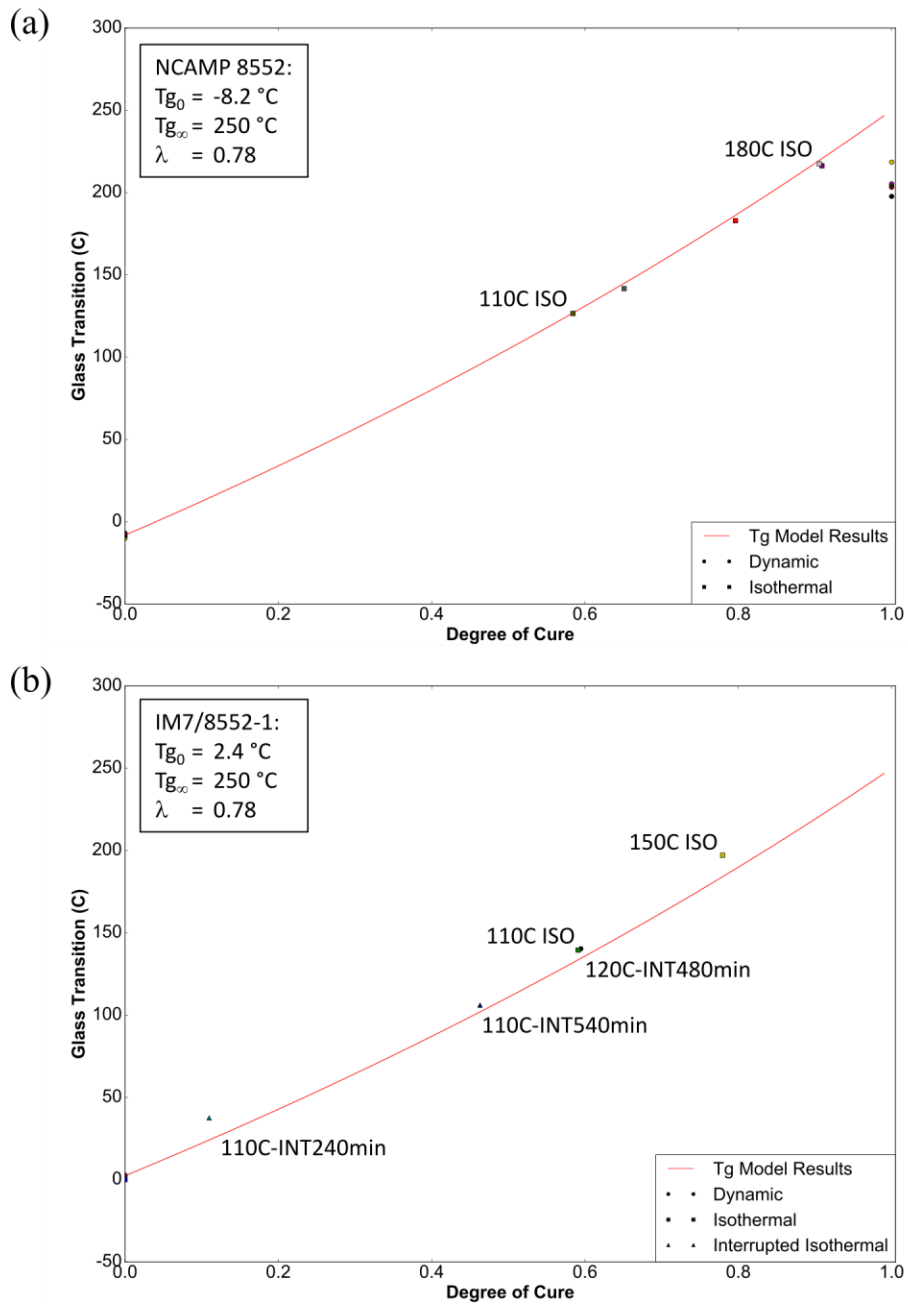

Figure E-4: Comparison of T_g versus α and the DiBenedetto model fit based on nonisothermal, isothermal and interrupted isothermal DSC tests: (a) experimental T_g data and model from Hexcel 8552 NCAMP material model database [135] (Van Ee *et al*, 2009) and (b) experimental T_g data and model from Hexcel 8552-1 preliminary cure kinetics characterization. Note: NCAMP DSC data used with permission (NIAR, 2016). Linear baselines were used for the cases shown.

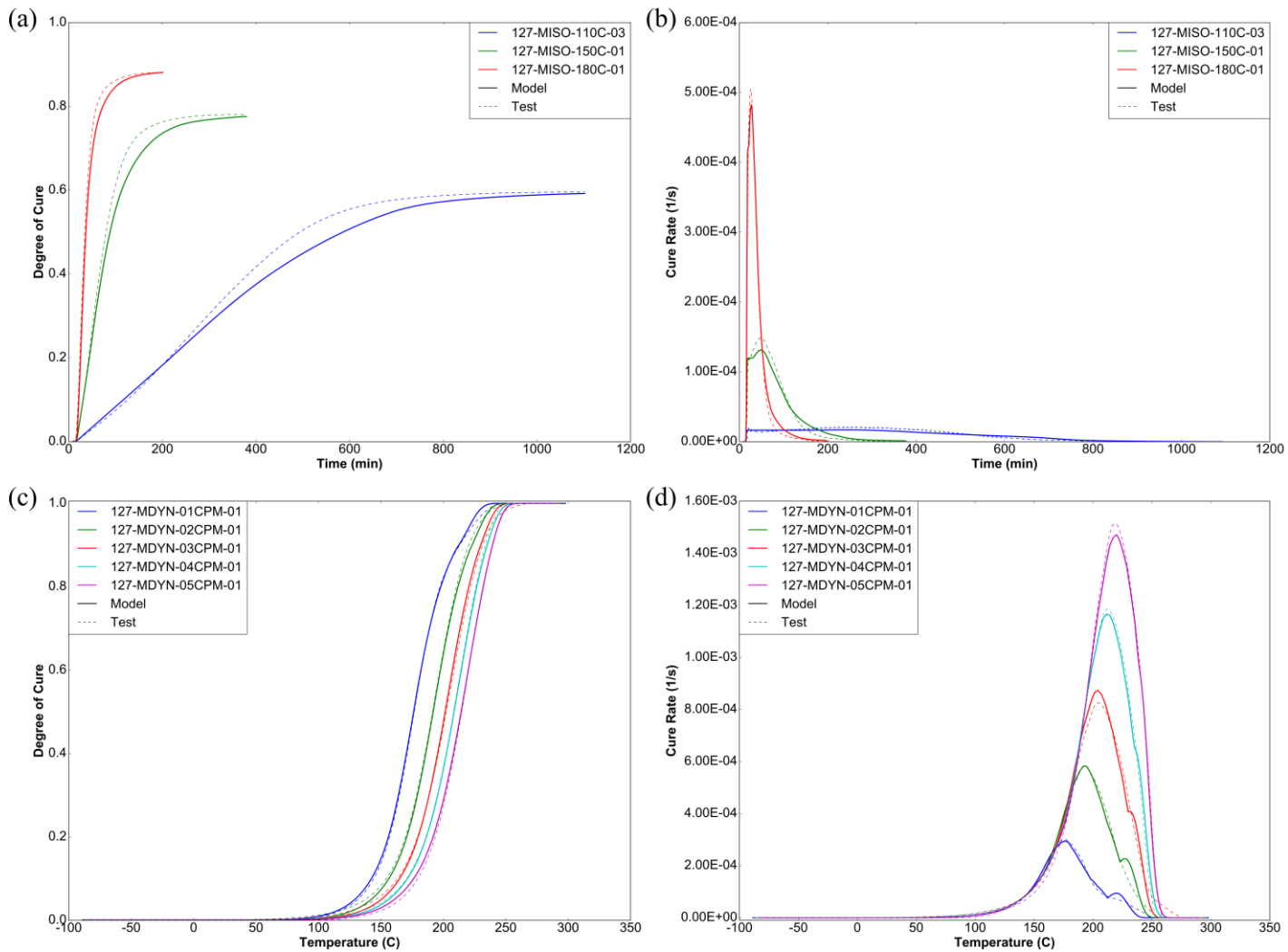

Figure E-5: Comparisons of DOC and cure rate from experimental data and model predictions for Hexcel 8552-1 preliminary cure kinetics characterization: (a) DOC for isothermal DSC tests, (b) cure rate for isothermal DSC tests, (c) DOC for nonisothermal DSC tests and (d) cure rate for nonisothermal DSC tests.

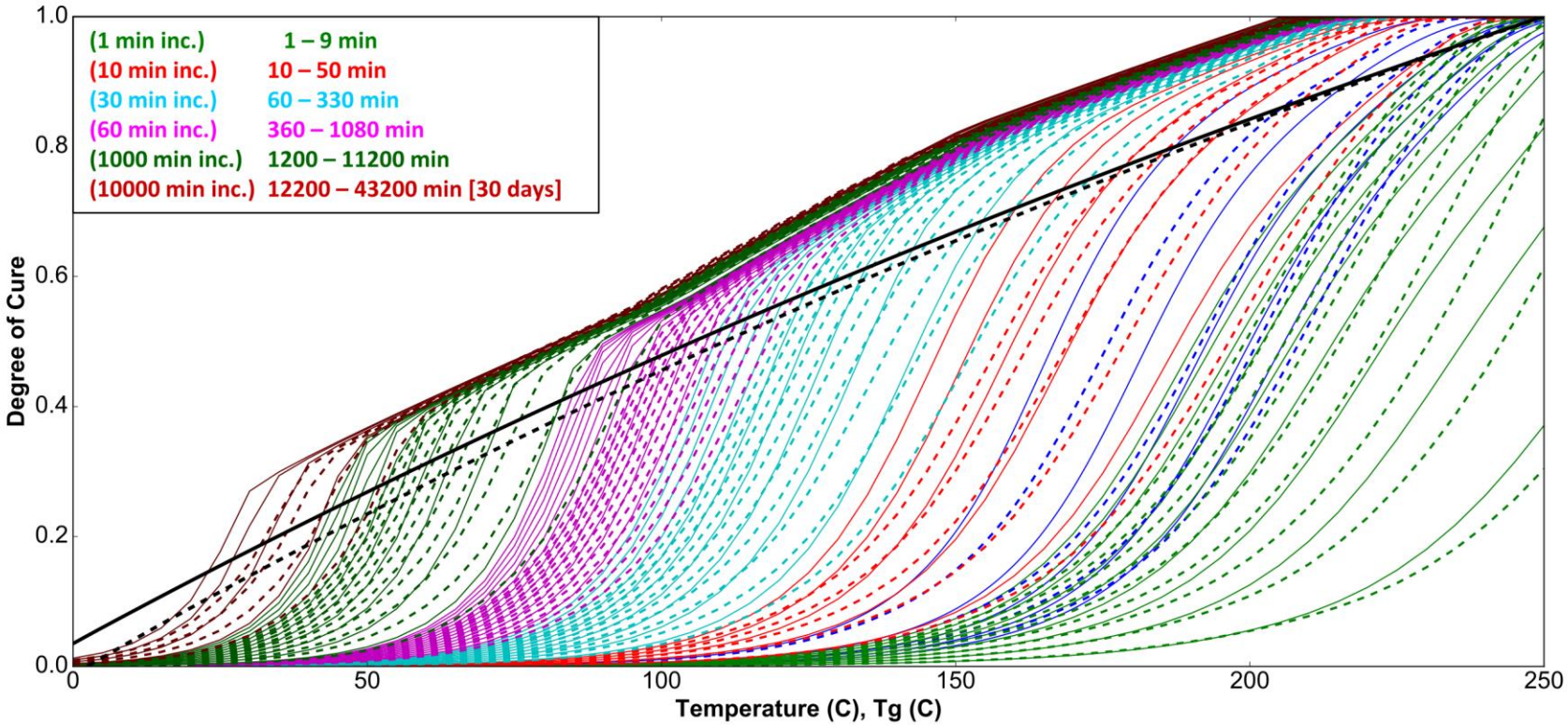

Figure E-6: RAVEN generated cure versus temperature (α v T) process maps for Hexcel AS4/8552 (NCAMP material model) with isochronals shown as solid lines and Hexcel AS4/8552-1 (preliminary material model) with isochronals shown as dashed lines. Note: The glass transition temperature (T_g) is shown in black.

E.3 Properties of Toray T800H/3900-2 unidirectional prepreg

Cure kinetics model for Toray 3900-2 (CCA ck17) [144,181].

$$\dot{\alpha} = k_1\left(\alpha^{m_1}\right)\left(1-\alpha\right)^{n_1} + k_2\left(\alpha^{m_2}\right)\left(1-\alpha\right)^{n_2} + k_3\left(\alpha^{m_3}\right)\left(1-\alpha\right)^{n_3}$$

$$k_i = \left(\frac{1}{k_{Ci}} + \frac{1}{k_{d_i}}\right)^{-1}$$

$$k_{Ci} = a_{Ci} e^{-\frac{e_{Ci}}{RT}}$$

$$\begin{cases} a_{C1} = a_{C1f1} \\ e_{C1} = e_{C1f1} & \text{if } T > T_C \\ a_{C1} = a_{C1f2}\log\alpha + a_{C1f3} \\ e_{C1} = e_{C1f2} & \text{if } \alpha > \alpha_{crit} \\ a_{C1} = a_{C1f4} \\ e_{C1} = e_{C1f3} & \text{if } \alpha > \alpha_{crit} \end{cases}$$

$$k_{d_{1,2}} = \begin{cases} A_{d_{1,2}} e^{-\left(\frac{E_{d_{1,2}}}{RT} + \frac{b_{1,2}}{a_f\left(T-T_g\right)+f_g}\right)} & \left(T-T_g\right) \geq T_{g_{d_{1,2}}} \\ 1E-99 & \left(T-T_g\right) < T_{g_{d_{1,2}}} \end{cases} \qquad \text{(E-4)}$$

$$k_{d_3} = \begin{cases} A_{d_3} e^{-\frac{b_3}{a_f\left(T-T_g\right)+f_g}} & \left(T-T_g\right) \geq T_{g_{d_3}} \\ 1E-99 & \left(T-T_g\right) < T_{g_{d_3}} \end{cases}$$

$$T_g = T_{g0} + \frac{\lambda\alpha\left(T_{g\infty} - T_{g0}\right)}{1-\left(1-\lambda\right)\alpha} + \frac{D}{1+e^{\left[-F\left(\alpha-\alpha_{crit}\right)\right]}}$$

$$\alpha_{crit} = \begin{cases} \alpha_{C1}T + \alpha_{C2} & \dot{T} < \dot{T}_C \\ \alpha_{C1}T + \alpha_{C2} + \frac{\alpha_{C3}}{\dot{T}} & \dot{T} > \dot{T}_C \end{cases}$$

$$\alpha_{crit} = \begin{cases} \alpha_{crit_{\max}} & \alpha_{crit} > \alpha_{crit_{\max}} \\ \alpha_{crit_{\min}} & \alpha_{crit} < \alpha_{crit_{\min}} \end{cases}$$

Lumped specific heat capacity model for Toray 3900-2 (CCA cp3) [181].

$$C_p = C_{p_r} + \frac{C_{p_g} - C_{p_r}}{1 + e^{k\left[\left(T - T_g\right) - \Delta T_c\right]}}$$
$$C_{p_i} = \left(1 - \alpha\right) C_{p_{i0}} + \alpha C_{p_{i\infty}} \quad i = r, g \tag{E-5}$$
$$C_{p_{ij}} = s_{ij} T + c_{ij} \quad i = r, g \text{ and } j = 0, \infty$$

Table E-4: T800H/3900-2 materials database input parameters used for the Slesinger (refer to Appendix D.3), CCMRD9.2 (refer to Appendix D.4) and Boeing-UW (refer to Appendix D.5) data sets.

Property	Parameter	Value	Units
Fibre volume fraction[a]	V_f	0.572	
Cure kinetics[b] Equation (E-4)	HR	457000	J/ kg
	α_{C1}	0.0025	
	α_{C2}	-0.3329	
	$\dot{T}_C$	0.0001	°C/ min
	α_{C3}	-0.00017	
	$\alpha_{crit_{max}}$	0.675	
	$\alpha_{crit_{min}}$	1.0	
	D	35.0	
	F	25.0	
	T_{g0}	8.8	°C
	$T_{g\infty}$	200.0	°C
	λ	0.8	
	T_C	124.0	°C
	α_{C1f1}	14240	
	e_{C1f1}	66435	
	α_{C1f2}	34378	
	α_{C1f3}	229563	
	e_{C1f2}	73300	
	$\alpha_{C1_{min}}$	50000	
	α_{C1f4}	113881	
	e_{C1f3}	73300	
	a_{C2}	473684	
	e_{C2}	73063	
	a_{C3}	1.50E+09	
	e_{C3}	115624	

Table continued on next page

Table E-4 continued

Property	Parameter	Value	Units
Cure kinetics (continued)	α_{crit}	0.035	
	$A_{d_{1,2}}$	4.00E+12	
	$E_{d_{1,2}}$	60000	
	$b_{1,2}$	0.52	
	$T_{g_{d1,2}}$	-50.0	
	A_{d_3}	1.50E+09	
	b_3	0.7	
	$T_{g_{d3}}$	-50.0	
	a_f	0.00008	
	f_g	0.025	
	m_1	0.0	
	n_1	1.0	
	m_2	1.0	
	n_2	2.5	
	m_3	2.91	
	n_3	0.83	
	α_{init}	0.001	
Resin specific heat capacity[b] Equation (E-5)	s_{g0}	4.23	J/ (kg K^2)
	c_{g0}	903	J/ (kg K)
	$s_{g\infty}$	3.08	J/ (kg K^2)
	$c_{g\infty}$	1002	J/ (kg K)
	s_{r0}	2.5	J/ (kg K^2)
	c_{r0}	1227	J/ (kg K)
	$s_{r\infty}$	1.78	J/ (kg K^2)
	$c_{r\infty}$	1363	J/ (kg K)
	k	0.124	1/ °C
	ΔT_c	3.632	°C
Fibre specific heat capacity[a]	C_{pf}	$750 + \left(T \times 2.05 / {}^{\circ}\mathrm{C}\right)$	J/ (kg K)
Density[a]	ρ_{f}	1.81E+03	kg/ m^3
	ρ_{r}	1.30E+03	
Thermal conductivity[a]	$k_{11\mathrm{f}}$	35	W/ (m K)
	$k_{33\mathrm{f}}$	5	
	$k_{11\mathrm{r}} = k_{33\mathrm{r}}$	0.167	
	$k_{11\mathrm{r\text{-}high}} = k_{33\mathrm{r\text{-}high}}$	0.251	

[a] From CCA T800H/3900-2 material data files [238] (CMT Inc., 2017).
[b] From Section 5.2.6 and Appendix E [144] (Dykeman, 2008).

E.4 Thermophysical material properties

Table E-5: Thermophysical material property input parameters used in the thick composite laminate data sets (refer to Appendix D).

	Density (ρ) (kg/ m^3)	**Specific heat capacity (C_p) (J/ (kg K))**	**Thermal conductivity (k_z) (W/ (m K))**
Invar[a]	8000	515	11.0
Al-alloy[a]	2710	896	167
Composite (CFRP)[a]	1580	870	0.69
CFRP (curing)[b] CFRP (cured)[b]	1580	1245 1068	–
Steel[a]	7860	465	51.9
Glass/phenolic core (HRP-3/16-8.0)[c]	128	1250	0.0971

[a] Typical properties from Table 1 [141] (Raskeh *et al*, 2004) and Table 2-1 [142] (Rasekh, 2007).
[b] From [145] (Shimizu *et al*, 2008). These parameters are used in back-calculating effective HTCs.
[c] 3/16-inch cell, 8 lb/ ft^3 glass/phenolic honeycomb core. From Table C.9 [100] (Johnston, 1997).

Appendix F Effective Heat Transfer Coefficient Back-calculation Method

In this appendix, the method for back-calculating equivalent-1D and equivalent-3D (no tool substructure modelled) heat transfer coefficients is given. These methods were used to compute the effective heat transfer coefficients reported in Chapter 5 and Appendix D.

F.1 Closed-form solution with asymmetric boundary conditions

From Rasekh [142], and assuming the heat generation due to resin cure is negligible, the transient steady-state temperature difference of a homogeneous slab with asymmetric boundary conditions at the top and bottom surfaces is given as follows:

$$\begin{aligned} \Delta T_{\mathrm{ss}} &= -\left(T_{\infty} - T_{\mathrm{s}}\right) = -\dot{T}\,\frac{L_e^2}{a}\left(\frac{1}{2} - \frac{1}{2}\zeta_e^2 + \frac{1}{Bi_e}\right) \\ &\text{if } Bi_{\mathrm{e}} = \frac{h_{\mathrm{top}} L_{\mathrm{e}}}{k} \quad L_{\mathrm{e}} = L\left(1-\delta\right) \\ &\text{if } Bi_{\mathrm{e}} = \frac{h_{\mathrm{bot}} L_{\mathrm{e}}}{k} \quad L_{\mathrm{e}} = L\left(1-\delta\right) \end{aligned} \tag{F-1}$$

where in Equation (F-1), T_{∞} is the autoclave air temperature, $\dot{T}$ is the heating rate, a is the thermal diffusivity of the slab, L_{e} is the effective slab half-thickness, ζ_{e} is the non-dimensional through-thickness coordinate ($-1 \leq \zeta_{\mathrm{e}} \leq 1$) with origin at the adiabatic line δ, Bi_{e} is the effective Biot number and h is the heat transfer coefficient. As shown in Equation (F-1), the through-thickness temperature distribution of the slab is a quadratic function of the non-dimensional through-thickness coordinate.

F.2 Equivalent-1D heat transfer boundary conditions

Equivalent-1D heat transfer coefficient values are determined for use as effective heat transfer boundary condition inputs in RAVEN-1D analyses.

F.2.1 Heat flux approach: Method I

Method I is a heat flux based approach originally proposed by Shimizu *et al* [145] (see Figure F-1). As discussed in Appendix F.1, this method also assumes a transient steady-state condition and quadratic through-thickness temperature distribution. The method described here was used to confirm the original effective heat transfer coefficients reported for the Kotlik and Shimizu data set in Appendix D.2.

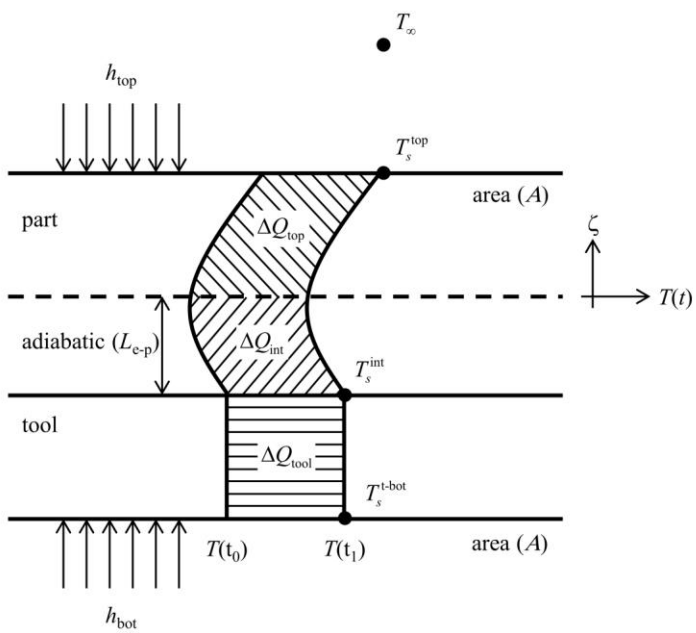

Figure F-1: Calculation of equivalent-1D heat transfer coefficient. Adapted from [145] (Shimizu *et al*, 2008).

The heat equation for Method I is approximated using the rectangular integration rule:

$$\Delta Q = \sum_{i=1}^{n} \rho C_{\mathrm{p}} L_{\mathrm{e}} \Delta T_{\mathrm{i}} \Delta \zeta_{\mathrm{i}} A \tag{F-2}$$

where in Equation (F-2), the subscript i represents a measurement point from the slab surface (i = 1) to the adiabatic line ($i = n$), ρ is the density, C_{p} is the specific heat capacity, ΔT_{i} is the change in temperature at the measurement point, $\Delta\zeta_{\mathrm{i}}$ is the distance between adjacent measurement points, and ζ is the non-dimensional through-thickness coordinate.

From Equation (2-6) and Equation (F-2), the effective heat transfer coefficient is:

$$\begin{gathered} h = \frac{\sum_{i=1}^{n} \rho C_{\mathrm{p}} L_{\mathrm{e}} \Delta T_{\mathrm{i}} \Delta \zeta_{\mathrm{i}}}{\Delta T_{\mathrm{s}} \cdot \Delta t} \\ T(\zeta) = a\zeta^2 + b\zeta + c \\ \text{if } \frac{dT}{d\zeta} = 0 \quad L_{\text{e-p}} = \frac{-b}{2a} \end{gathered} \tag{F-3}$$

where in Equation (F-3), a, b, c are quadratic function constants and the adiabatic line is defined by $dT/d\zeta = 0$.

The equivalent-1D heat transfer coefficients are given in Equation (F-4):

$$\begin{gathered} h_{\mathrm{top}} = \frac{\Delta Q_{\mathrm{top}}}{A \cdot \Delta T_{\mathrm{s}} \cdot \Delta t} \\ h_{\mathrm{bot}} = \frac{\Delta Q_{\mathrm{int}} + \Delta Q_{\mathrm{tool}}}{A \cdot \Delta T_{\mathrm{s}} \cdot \Delta t} \end{gathered} \tag{F-4}$$

F.2.2 Modified heat flux approach: Method I'

Method I is most accurate if a large number of through-thickness temperature data points are available. However, for many of the data sets presented in Chapter 5 and Appendix D, fewer than three data points were measured for any given drill point (eg. part surface (top), part/tool interface (interface), tool underside surface (bottom)). Given this reduction in the number of available measurement points, Method I' is a modified heat flux based approach that has been developed for use in all revised heat transfer coefficient analyses reported in Chapter 5 and Appendix D. This method is based on Method I with the heat equation approximated by Equation (F-2) and equivalent-1D heat transfer coefficients given by Equation (F-4). However, the adiabatic line is estimated using two surface measurement points rather than assuming a quadratic temperature distribution. The effective heat transfer coefficient is then computed as follows:

$$h = \dot{T}\,\frac{\rho C_{\mathrm{p}} L_{\mathrm{e}}}{\Delta T_{\mathrm{ss}}}$$
$$L_{\text{e-p}} = 2L \cdot \frac{\Delta T_{\mathrm{s}}^{\mathrm{top}}}{\Delta T_{\mathrm{s}}^{\mathrm{top}} + \Delta T_{\mathrm{s}}^{\mathrm{int}}} \tag{F-5}$$

where in Equation (F-5), T_{s} is the slab (laminate) surface temperature.

F.3 Equivalent-3D heat transfer boundary conditions (no tool substructure modelled)

Equivalent-3D (no tool substructure modelled) heat transfer coefficient values are determined for use as effective heat transfer boundary condition inputs in COMPRO-3D thermal analyses where only the tool plate has been modelled.

In cases where tool size effects exist (see Figure F-2), the equivalent-1D bottom heat transfer coefficient can be artificially higher than expected. As given by Equation (F-6), by taking the basic definition for the heat transfer coefficient and maintaining the same heat gained/lost, we can adjust for an equivalent-3D heat transfer coefficient in accounting for the heat transfer area of the tool plate surface boundaries.

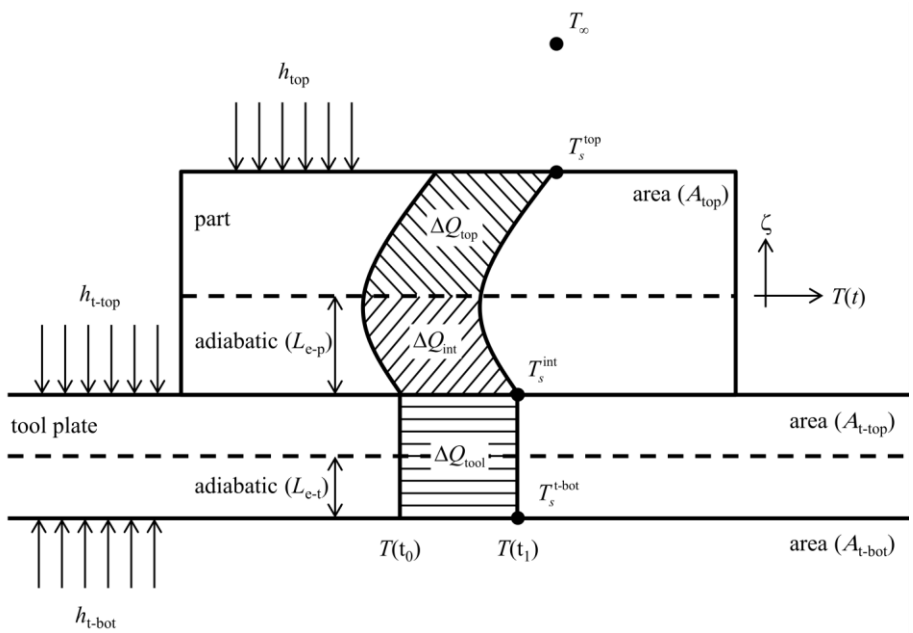

Figure F-2: Calculation of equivalent-3D heat transfer coefficient (no tool substructure modelled).

This approach requires that the tool face plate dimensions are known. The methods for approximating the heat equation and estimating the adiabatic line are the same as those described for Method I'.

$$\text{if } \frac{\Delta Q}{\Delta t} = h(\downarrow)\cdot A(\uparrow)\cdot \Delta T_{ss} \quad h = \dot{T}\,\frac{\rho C_p L_{\mathrm{e}}}{\Delta T_{\mathrm{s}}}$$

$$L_{\text{e-p}} = 2L\cdot\frac{\Delta T_{\mathrm{s}}^{\mathrm{top}}}{\Delta T_{\mathrm{s}}^{\mathrm{top}} + \Delta T_{\mathrm{s}}^{\mathrm{int}}} \tag{F-6}$$

$$L_{\text{e-t}} = 2L\cdot\frac{\Delta T_{\mathrm{s}}^{\mathrm{int}}}{\Delta T_{\mathrm{s}}^{\mathrm{int}} + \Delta T_{\mathrm{s}}^{\mathrm{bot}}}$$

The equivalent-3D (no tool substructure modelled) heat transfer coefficients are given in Equation (F-7):

$$h_{\mathrm{top}} = \frac{\Delta Q_{\mathrm{top}}}{A_{\mathrm{top}}\cdot\Delta T_{\mathrm{s}}\cdot\Delta t}$$

$$h_{\text{t-top}} = \frac{\Delta Q_{\mathrm{int}}}{A_{\mathrm{top}}\cdot\Delta \mathrm{T}_{\mathrm{s}}\cdot\Delta t}\left(\frac{A_{\mathrm{top}}}{A_{\text{t-top}}}\right) + \left(1-\frac{L_{\text{e-t}}}{2L_{\mathrm{t}}}\right)\cdot\frac{\Delta Q_{\mathrm{tool}}}{A_{\text{t-bot}}\cdot\Delta T_{\mathrm{s}}\cdot\Delta t}\left(\frac{A_{\text{t-bot}}}{A_{\text{t-top}}}\right) \tag{F-7}$$

$$h_{\text{t-bot}} = \frac{L_{\text{e-t}}}{2L_{\mathrm{t}}}\cdot\frac{\Delta Q_{\mathrm{tool}}}{A_{\text{t-bot}}\cdot\Delta T_{\mathrm{s}}\cdot\Delta t}$$

where the location of the tool plate effective thickness, $L_{\text{e-t}}$, determines the distribution of heat to the top and bottom tool plate surfaces. For instance, if the tool plate is considered a lumped mass, then a 50/50 heat distribution split is assumed since $L_{\text{e-t}} = L_{\mathrm{t}}$.